

University College London

**Search for endoderm genes
involved in early patterning of
vertebrates**

Rita Matos Dias de Sousa Nunes

Thesis submitted for the degree of Doctor of Philosophy

2004

UMI Number: U602567

All rights reserved

INFORMATION TO ALL USERS

The quality of this reproduction is dependent upon the quality of the copy submitted.

In the unlikely event that the author did not send a complete manuscript and there are missing pages, these will be noted. Also, if material had to be removed, a note will indicate the deletion.



UMI U602567

Published by ProQuest LLC 2014. Copyright in the Dissertation held by the Author.
Microform Edition © ProQuest LLC.

All rights reserved. This work is protected against
unauthorized copying under Title 17, United States Code.



ProQuest LLC
789 East Eisenhower Parkway
P.O. Box 1346
Ann Arbor, MI 48106-1346

This work was carried out at the National Institute for Medical Research, Mill Hill, London, U.K., in the Divisions of Mammalian Development and Developmental Biology. Rita Sousa-Nunes is a student of the Gulbenkian Ph.D. Program in Biology and Medicine and was supported by the Portuguese Foundation for Science and Technology and the European Social Fund in the context of the *III Quadro Comunitário de Apoio*, The Calouste Gulbenkian Foundation and the Medical Research Council.

To my parents

Acknowledgements

I dearly acknowledge Rosa Beddington, who drew me here and who will always remain a source of inspiration to me. I thank: Robb Krumlauf, for taking me as his student in my second year and offering me his insight. Derek Stemple, for guiding me in my final years, for his brilliance, enthusiasm and... entertainment. Alex Gould, my constant second-supervisor, for accompanying me throughout and being so supportive whenever I turned to him. Josh Brickman, Sally Dunwoodie, Amer Rana and Ross Kettleborough, for all their work on the mouse screen. Jim Smith, for his crucial role in putting together the paper concerning this screen. The Beddington, Krumlauf and Stemple lab members, for teaching me so much. I am particularly indebted to Nobue Itasaki, Shankar Srinivas, Ben Feldman and Isabel Campos for discussions, reagents and instruction. Kamala Maruthainer, Ian Harragan, Liz Hirst, and all the staff in Dunkin Green and Laidlaw Green, for technical assistance. My collaborators Lisa Cooper, Paul Martin and Marcus Fruttiger, for their help and interest. The NIMR, in particular the past and present developmental biology community, for making it such an exciting place to work. My funding agencies, for making this possible. My friends scattered in many places, for the richness and joy they bring to my life. My friends in London, who shared day-to-day chores as well as delights. My Portuguese and British families, for always being home, sweet home, to me. In a special way, to my parents, for their unconditional affection. Steve, for so much love.

Abstract

In addition to giving rise to the gut, the endoderm plays a crucial role in embryonic axis determination. The murine extra-embryonic endoderm is thought to provide an early positional cue defining the antero-posterior axis of the embryo. The axial mesendoderm, which emanates from the gastrula organizer, populates the midline of the embryo and patterns it in all three axes. Later, maintenance and refinement of the antero-posterior axis of the brain requires the embryonic endoderm (reviewed in Martinez-Barbera and Beddington, 2001).

Genes expressed in the endoderm are responsible for imparting it with its patterning properties. It is therefore useful to identify the expression profile of the endoderm. To this end, a cDNA library was made from 7.5 days *post-coitum* mouse endoderm (Harrison *et al.*, 1995). Many clones from this library were sequenced and constitute a set of expression sequence tags (ESTs). I screened these ESTs *in silico* for non-essential molecules whose role in embryonic patterning had not been determined. I then screened clones obeying these criteria by whole-mount *in situ* hybridisation on 6.5 – 9.5 dpc mouse embryos. Restricted expression was displayed by 18 % of the clones (from the total of my work and that of two other students). The restricted expression patterns encountered are presented.

One of the restricted genes I encountered in the mouse *in situ* hybridisation screen was that encoding the serum and glucocorticoid-regulated kinase (*Sgk*). I was very interested in the expression pattern of *Sgk* since it was asymmetric in the visceral endoderm at the onset of gastrulation. *Sgk* expression presented other interesting features, such as being exclusively expressed in angioblasts at 9.5 dpc. I constructed a targeting vector in order to analyse *Sgk* function in mouse by a loss-of-function approach. I targeted embryonic stem (ES) cells with this construct and recovered neomycin-resistant clones. One of these is possibly a clone where homologous recombination took place at the *Sgk* locus.

I cloned zebrafish orthologues of some of the restrictedly expressed endoderm genes. I functionally screened these genes in zebrafish by a loss-of-function approach, using

antisense morpholino oligonucleotides (MOs). I uncovered several molecules required for proper early embryonic development, one of which I studied in more detail. This was Nop seven-associated protein 2 (Nsa2), a eukaryotic protein involved in ribosome biogenesis (Harnpicharnchai *et al.*, 2001). Zebrafish *nsa2* morphants have slowed epiboly and early patterning defects. Furthermore, *nsa2* morphant cells gradually die by apoptosis. A smaller embryo develops from surviving *nsa2* morphant cells during the first day of development, after which presumably all cells die. The phenotype of *nsa2* zebrafish morphants is analogous to that of morphants for the ribosomal proteins RpL19 and RpS5, which when mutated in fly cause the *Minute* phenotype. I describe the zebrafish *Minute* phenotype and hypothesize that *nsa2* is likely to be a *Minute*.

Publications

The work described in this thesis contributed to the following publications:

Avner, P., Bruls, T., Poras, I., Eley, L., Gas, S., Ruiz, P., Wiles, M. V., **Sousa-Nunes, R.**, Kettleborough, R., Rana, A., Morissette, J., Bentley, L., Goldsworthy, M., Haynes, A., Herbert, E., Southam, L., Lehrach, H., Weissenbach, J., Manenti, G., Rodriguez-Tome, P., Beddington, R., Dunwoodie, S. and Cox, R. D. (2001) "A radiation hybrid transcript map of the mouse genome", *Nat Genet* **29**(2), 194-200.

Sousa-Nunes, R.*, Rana, A.*, Kettleborough, R.*, Brickman, J. M., Clements, M., Forrest, A., Grimmond, S., Avner, P., Smith, J. C., Dunwoodie, S. L. and Beddington, R. S. P. (2003) "Characterising embryonic gene expression patterns in the mouse using non-redundant sequence-based selection", *Genome Res*, **13**(12), 2609-20.

* These authors contributed equally to this work

Sousa-Nunes, R., Hirst, E. M. and Stemple, D. L., "The zebrafish *Minute* phenotype", manuscript in preparation.

Table of Contents

Acknowledgements.....	iv
Abstract.....	v
Publications.....	vi
List of Figures.....	xiii
List of Tables.....	xvii
Abbreviations.....	xviii

Chapter 1 General Introduction

1.1 Model organisms and conservation of developmental processes.....	3
1.2 Vertebrate embryology from egg to gastrula.....	5
1.2.1 Generalities.....	5
1.2.2 Frog.....	9
1.2.3 Fish.....	10
1.2.4 Chick.....	12
1.2.5 Mouse.....	14
1.3 Vertebrate morphogenetic movements during gastrulation.....	21
1.3.1 Vertebrate fate maps.....	21
1.3.2 Morphogenetic movements converge in the phylotypic stage.....	24
1.3.3 Epiboly.....	24
1.3.4 Cell internalisation.....	27
1.3.5 Convergence and extension.....	28
1.3.6 Mouse embryo turning.....	28
1.4 Early molecular events in vertebrate axes specification and germ-layer formation.....	29
1.4.1 Maternal dorsal determinants are present in fish and frog.....	29
1.4.2 Downstream of β -catenin.....	33

1.4.3	Mesoderm induction.....	36
1.4.4	Endoderm induction.....	41
1.4.5	Neural induction.....	46
1.4.6	The AVE and patterning of the early mouse embryo.....	49
1.4.7	Molecular pathways mediating vertebrate gastrulation movements.....	53
1.5	Aims and thesis outline.....	55

Chapter 2 Materials and Methods

2.1	Bioinformatics and genomics.....	59
2.1.1	General software used.....	59
2.1.2	Selection of mouse endoderm library clones to screen.....	59
2.1.3	Identification of zebrafish orthologues of mouse proteins.....	59
2.1.4	Oligonucleotide design.....	60
2.1.4.1	Primers.....	60
2.1.4.2	Antisense morpholino oligonucleotides (MOs).....	61
2.2	Embryo manipulation.....	62
2.2.1	Embryo collection.....	62
2.2.1.1	Mouse embryo harvest.....	62
2.2.1.2	Zebrafish embryo collection.....	62
2.2.2	Paraffin-embedded embryo sectioning.....	63
2.2.3	Embryo/tissue stainings.....	63
2.2.3.1	Whole-mount <i>in situ</i> hybridisation.....	63
2.2.3.2	<i>In situ</i> hybridisation on paraffin-embedded tissue sections.....	64
2.2.3.3	Whole-mount terminal deoxy-nucleotidyl transferase-mediated dUTP nick end labelling (TUNEL).....	66
2.2.4	Mouse embryo wound-healing protocol.....	66
2.2.5	Zebrafish embryo injections.....	66
2.2.6	Zebrafish embryo incubation with cycloheximide.....	67
2.2.7	Embryo photographing.....	67
2.2.8	Transmission electron microscopy (TEM).....	68

2.3 Molecular biology	68
2.3.1 Plasmid transformation of competent bacteria.....	68
2.3.2 Purification of plasmid DNA.....	69
2.3.3 Nucleic acid spectrophotometric quantification.....	70
2.3.4 Agarose gel electrophoresis.....	70
2.3.5 Gel extraction of DNA.....	71
2.3.6 Phenol:chloroform extraction of nucleic acids.....	71
2.3.7 Ethanol precipitation of nucleic acids.....	71
2.3.8 Lambda bacteriophage growth.....	72
2.3.9 Purification of bacteriophage DNA from liquid cultures.....	72
2.3.10 Purification of genomic DNA from 96-well plates.....	73
2.3.11 Restriction digestion of DNA.....	73
2.3.12 Automatic sequencing of plasmid DNA.....	74
2.3.13 ³² P-labelled DNA probe synthesis.....	75
2.3.14 ³² P-end-labelled DNA oligonucleotide probe synthesis.....	75
2.3.15 Bacteriophage plaque hybridisation with DNA probe.....	76
2.3.16 Southern analysis of genomic DNA.....	77
2.3.17 Cloning of DNA fragments prepared by restriction digest.....	78
2.3.18 Cloning of PCR products.....	78
2.3.19 Total RNA purification.....	78
2.3.20 mRNA purification from total RNA.....	79
2.3.21 Reverse transcriptase (RT)-PCR.....	79
2.3.22 Rapid amplification of cDNA ends (RACE).....	81
2.3.23 Riboprobe synthesis.....	82
2.3.24 MO column-purification.....	84
2.4 ES cell manipulation	88
2.4.1 Production of buffalo rat liver (BRL) cell conditioned medium.....	88
2.4.2 ES cell thawing, expansion and freezing.....	89
2.4.3 ES cell electroporation with targeting vector.....	90
2.4.4 ES cell antibiotic resistance selection.....	90
2.4.5 Resistant ES cell colony picking and culture.....	90

Chapter 3 Whole-mount *in situ* hybridisation screen of a mouse endoderm library

3.1 Introduction to the <i>in situ</i> hybridisation screen of the endoderm library	93
3.1.1 Organism gene counts.....	93
3.1.2 Gene expression profiling.....	94
3.1.3 Mouse endoderm cDNA library.....	95
3.2 Results of the <i>in situ</i> hybridisation screen of the endoderm library	96
3.2.1 Sequence-based clone selection.....	96
3.2.2 Expression analysis.....	97
3.2.3 Brief description of 12 restricted expression patterns.....	104
3.2.4 Synexpression and co-expression groups.....	107
3.3 Discussion of the <i>in situ</i> hybridisation screen of the endoderm library	108
3.3.1 Overview.....	108
3.3.2 Efficiency of novel strategy for cDNA selection.....	109
3.3.3 Perspectives.....	112

Chapter 4 Functional analysis of mouse *Sgk*

4.1 Literature review on <i>Sgk</i>	114
4.1.1 <i>Sgk</i> expression.....	114
4.1.2 <i>Sgk</i> protein and mRNA structure.....	116
4.1.3 <i>Sgk</i> transcriptional regulation.....	117
4.1.4 <i>Sgk</i> post-translational regulation.....	120
4.1.5 Subcellular localisation of <i>Sgk</i>	122
4.1.6 Downstream of <i>Sgk</i>	123
4.1.7 Biological roles of <i>Sgk</i>	124
4.1.8 <i>Sgk</i> family members.....	126

4.2 Results of the functional analysis of mouse <i>Sgk</i>	128
4.2.1 Further characterisation of mouse <i>Sgk</i> expression.....	128
4.2.2 Groundwork for the differentiation of ES cells into endothelial cells.....	134
4.2.3 Is <i>Sgk</i> upregulated during embryonic wound-healing?.....	136
4.2.4 Isolation and characterisation of mouse <i>Sgk</i> genomic DNA.....	136
4.2.5 Construction of <i>Sgk</i> targeting vector.....	139
4.2.6 Targeting of <i>Sgk</i> in ES cells.....	144
4.2.7 Zebrafish <i>sgk</i>	146
4.3 Discussion of the functional analysis of mouse <i>Sgk</i>	149
4.3.1 Regulation of <i>Sgk</i> expression.....	149
4.3.2 <i>Sgk</i> targeting strategy.....	150
4.3.3 Is there a role for <i>Sgk</i> in embryonic patterning?.....	150

Chapter 5 Functional screen of endoderm library genes with restricted expression

5.1 Introduction to the functional screen of endoderm library genes	154
5.1.1 Selection of clones to screen.....	154
5.1.2 Use of MOs	155
5.2 Results and discussion of the functional screen	157
5.2.1 Search for zebrafish orthologues of mouse genes.....	157
5.2.2 Expression of screened zebrafish molecules.....	162
5.2.3 Early phenotypes of zebrafish morphants screened	171

Chapter 6 Functional analysis of zebrafish *nsa2*

6.1 Introduction to the functional analysis of zebrafish <i>nsa2</i>	185
6.1.1 <i>Nsa2</i> is required for ribosome biogenesis.....	185
6.1.2 Ribosome biogenesis in brief.....	186
6.1.3 Mutations in ribosomal proteins lead to the <i>Minute</i> phenotype in flies....	187

6.1.4	<i>Minute</i> growth rates.....	189
6.1.5	Some <i>Minute</i> phenotypes arise by maternal effect.....	190
6.1.6	<i>Minute</i> cell proliferation and cell size.....	190
6.1.7	<i>Minute</i> morphological defects.....	192
6.1.8	Competition between <i>Minute</i> and wild-type cells.....	194
6.2	Results of the functional analysis of zebrafish <i>nsa2</i>	194
6.2.1	Nsa2 is highly conserved among eukaryotes.....	194
6.2.2	In zebrafish as in mouse, <i>nsa2</i> is mainly expressed in endodermal and mesodermal derivatives.....	196
6.2.3	Depletion of zebrafish Nsa2 slows DEL epiboly.....	197
6.2.4	Embryos lacking <i>nsa2</i> have patterning defects.....	201
6.2.5	The epiboly phenotype of <i>nsa2</i> is analogous to that of <i>Minute</i> ribosomal proteins.....	207
6.2.6	Loss of Nsa2 and <i>Minute</i> Rps produce similar morphological defects.....	211
6.2.7	Is the fly orthologue of <i>nsa2</i> a <i>Minute</i> ?.....	216
6.2.8	Phenotypes of <i>nsa2</i> morphant cells.....	218
6.2.8.1	Cells morphant for <i>nsa2</i> undergo apoptosis.....	218
6.2.8.2	TEM study of <i>nsa2</i> morphant cells of the epiboly-stage zebrafish embryo.....	220
6.3	Discussion of the functional analysis of zebrafish <i>nsa2</i>	224
	References	232

Appendices

Appendix 1	Widespread and ubiquitous mouse endoderm clones.....	300
Appendix 2	Protocol for differentiation of ES cells into endothelial cells.....	307
Appendix 3	cDNA and protein sequences of zebrafish orthologues of restricted mouse endoderm genes.....	313

List of Figures

Fig. 1.1	Zygotes of four vertebrate model organisms.....	6
Fig. 1.2	Blastulae of four vertebrate model organisms.....	8
Fig. 1.3	Mouse embryonic development from blastocyst to gastrula.....	18
Fig. 1.4	Fate maps of four vertebrate model organisms at gastrula stage.....	22
Fig. 1.5	Comparison between the patterning of four vertebrate model organisms at early gastrula stage.....	23
Fig. 1.6	The vertebrate phylotypic stage.....	25
Fig. 1.7	Gastrulation movements of vertebrate embryos.....	26
Fig. 1.8	One strategy employed by the organizer to promote dorsal fates is to inhibit ventralising activities.....	35
Fig. 1.9	In vertebrates, early dorsalisating signals act through β -catenin and converge in the activation of the Nodal pathway.....	37
Fig. 3.1	Restricted expression patterns found in whole-mount <i>in situ</i> hybridisation screen of mouse endoderm library.....	98
Fig. 4.1	<i>Sgk</i> is expressed strongly in the VE and weakly in the nascent mesoderm of the egg-cylinder stage mouse embryo.....	129
Fig. 4.2	At 5.5 dpc, mouse <i>Sgk</i> expression is transiting from symmetric to asymmetric.....	130
Fig. 4.3	<i>Sgk</i> is expressed in sites of embryonic angiogenesis.....	131
Fig. 4.4	<i>Sgk</i> expression in the vasculature is very dynamic.....	132
Fig. 4.5	Sites of <i>Sgk</i> expression in the 11.5 – 13.5 dpc mouse embryo.....	133
Fig. 4.6	RT-PCR of <i>Oct4</i> , <i>Sgk</i> and <i>Gapdh</i> performed on whole RNA obtained from 9.5 dpc mouse embryos or each of two ES cell lines.....	135
Fig. 4.7	Map of mouse <i>Sgk</i> genomic clone.....	138
Fig. 4.8	Construction of <i>Sgk</i> targeting vector.....	140
Fig. 4.9	<i>Sgk</i> targeting with construct used in this investigation.....	143
Fig. 4.10	Southern analysis of ES cells targeted with <i>Sgk</i> targeting vector.....	145
Fig. 4.11	Expression of zebrafish <i>sgk-1 a</i> at 24 hpf.....	147
Fig. 4.12	Alignment of mouse and zebrafish <i>Sgk-1</i> proteins.....	148
Fig. 5.1	Restricted expression patterns found in zebrafish screen.....	164
Fig. 5.2	Early phenotype of <i>14-3-3</i> ϵ zebrafish morphants.....	172
Fig. 5.3	Early phenotype of <i>embigin</i> zebrafish morphants.....	174

Fig. 5.4	Early phenotype of <i>claudin b</i> zebrafish morphants.....	175
Fig. 5.5	Early phenotype of Module A <i>pancortins</i> zebrafish morphants.....	177
Fig. 5.6	Early phenotype of <i>sp120 / hnrpu</i> zebrafish morphants.....	179
Fig. 5.7	Early phenotype of novel gene ' <i>p7822b53</i> ' zebrafish morphants.....	181
Fig. 6.1	Putative Nsa2 proteins are present throughout the eukaryota.....	195
Fig. 6.2	Expression of <i>nsa2</i> during early zebrafish development.....	196
Fig. 6.3	Zebrafish <i>nsa2</i> cDNA sequence and regions targeted by MOs in this investigation.....	197
Fig. 6.4	Zebrafish embryos morphant for <i>nsa2</i> have uncoupled EVL, DEL and YSL epiboly	198
Fig. 6.5	Zebrafish embryos morphant for <i>nsa2</i> show DEL epiboly delay relative to controls	199
Fig. 6.6	Progression of DEL epiboly of zebrafish embryos morphant for <i>nsa2</i> compared with that of epiboly mutants.....	200
Fig. 6.7	Progression of DEL epiboly of zebrafish embryos morphant for <i>nsa2</i> specifically in the YSL compared with that of completely morphant embryos.....	201
Fig. 6.8	Zebrafish embryos morphant for <i>nsa2</i> present a variety of distorted shapes at late gastrulation stages.....	202
Fig. 6.9	Expression of <i>gsc</i> is reduced in <i>nsa2</i> morphant embryos relative to controls	204
Fig. 6.10	Expression of <i>axial</i> is enhanced in <i>nsa2</i> morphant embryos relative to controls	205
Fig. 6.11	Expression of <i>bhikhari</i> extends further anteriorly in <i>nsa2</i> morphants than in controls.....	206
Fig. 6.12	The ventral domain of <i>swr</i> expression is upregulated in early <i>nsa2</i> morphants whereas the organizer domain of expression is not.....	208
Fig. 6.13	DEL epiboly is more delayed than cell internalisation in <i>nsa2</i> morphants....	209
Fig. 6.14	Progression of DEL epiboly of zebrafish embryos morphant for ribosomal proteins compared with that of <i>nsa2</i> morphants.....	210
Fig. 6.15	Progression of DEL epiboly of zebrafish embryos morphant for <i>cop α</i> compared with that of <i>nsa2</i> morphants.....	211
Fig. 6.16	Zebrafish embryos morphant for <i>nsa2</i> , <i>RpS5</i> and <i>RpL19</i> present analogous morphological phenotypes.....	212
Fig. 6.17	Zebrafish embryos injected with 5 ng of <i>nsa2</i> , <i>RpS5</i> or <i>RpL19</i> MO are smaller than controls	214
Fig. 6.18	Region of <i>Drosophila melanogaster</i> genome to which the <i>Minute</i> mutation <i>M(2)31A</i> has been mapped.....	216
Fig. 6.19	Genomic locus of <i>Drosophila melanogaster</i> <i>RpS27A</i> and <i>nsa2/Ip259</i>	217

Fig. 6.20 Cells morphant for <i>nsa2</i> die by apoptosis.....	219
Fig. 6.21 Zebrafish cells morphant for <i>nsa2</i> lise and cell debris attach to plasma membrane of living cells.....	221
Fig. 6.22 Zebrafish <i>nsa2</i> morphant cell debris attach to plasma membrane of the YSL, impairing contact between the DEL and the YSL.....	222
Fig. 6.23 Zebrafish cells morphant for <i>nsa2</i> are less orderly arranged in the lateral regions of the embryo and have larger intercellular spaces than controls.....	223
Fig. 6.24 Close to the leading edge of epiboly, less cell lysis of <i>nsa2</i> morphant cells is observed relative to other regions of the embryo but cells are highly vacuolated.....	224
Fig. 6.25 Not only the plasma membranes but also the intracellular membranes of <i>nsa2</i> morphant DEL cells have altered appearance relative to controls.....	226
Fig. 6.26 The surface layer of the yolk cell, over which cells migrate during epiboly, is thinner and smoother in <i>nsa2</i> morphants than in controls.....	227

List of Tables

Table 2.1 Parameters entered in <i>Primer3</i> for primer design.....	60
Table 2.2 MOs used in this investigation.....	61
Table 2.3 Primers used in this investigation for RT-PCR.....	80
Table 2.4 Primers used in this investigation for 5' RACE.....	83
Table 2.5 Preparation of zebrafish antisense riboprobes used in this investigation.....	85
Table 2.6 Primers used in this investigation to isolate templates for riboprobe synthesis.....	87
Table 3.1 Identity of endoderm library cDNAs with restricted expression patterns...	102
Table 3.2 Co-expression groups found in endoderm library screen.....	108
Table 3.3 Frequency of restrictedly expressed cDNAs identified in different expression screens.....	111
Table 4.1 Exon and intron size, and exon-intron boundary sequences of mouse <i>Sgk</i> .	137
Table 5.1 Steps in searching for zebrafish orthologues of selected mouse endoderm library genes.....	158
Table 6.1 Complementation test between <i>RpS27A</i> ⁰⁴⁸²⁰ , <i>RpS27A</i> ^{mf31} , <i>RpS27A</i> ^P / <i>nsa2</i> ^P / <i>Ip259</i> ^P and <i>M(2)31A</i> in <i>Drosophila melanogaster</i>	218
Table A.1 Identity of endoderm library cDNAs with widespread or ubiquitous expression.....	300

Abbreviations

ADE	anterior definitive endoderm
ALK	activin receptor-like kinase
AMV	avian myeloblastosis virus
AP	Activating Protein
APS	ammonium persulfate
ATP	adenosine 5'-triphosphate
AVE	anterior visceral endoderm
BBA	benzyl-benzoate: benzyl alcohol (2:1)
BCIP	X-phosphate/5-Bromo-4-chloro-3-indolyl-phosphate
BMK	big mitogen-activated protein kinase
BMP	bone morphogenetic protein
BRL	buffalo rat liver
BSA	bovine serum albumin
CaMKK	Ca ²⁺ and calmodulin-dependent protein kinase kinase
CIP	calf intestinal phosphatase
CMF PBS	Ca ²⁺ and Mg ²⁺ free PBS
CNS	central nervous system
<i>cre</i>	cyclisation recombination gene (from bacteriophage P1)
CRE	cAMP-regulatory element
CREB	CRE binding protein
DAB	diaminobenzidine
DEL	deep cell layer
DEPC	diethyl-pyrocabonate
DIG	digoxigenin
dpc	days post- <i>coitum</i>
DMEM	Dulbecco's modified Eagle's medium
DMSO	dimethylsulphoxide
dCTP	deoxy-cytidine 5'-triphosphate
dNTP	deoxy-nucleotide triphosphate
Dsh	dishevelled
DTT	dithiothritol
dUTP	deoxy-uracil triphosphate
EB	embryoid body
EDTA	ethylene-diamine-tetra-acetate
EGF	epidermal growth factor
EMS	ethyl methanesulfonate
ENaC	epithelial sodium channel

EPO	erythropoietin
ERK	extracellular signal-regulated kinase
ES	embryonic stem
ESQ	ES cell quality FCS
ESQD	ESQ batches selected to promote EB differentiation
EST	expressed sequence tag
EtOH	ethanol
EVL	enveloping layer
FBS	foetal bovine serum
FCS	foetal calf serum
FGF	fibroblast growth factor
Flk	foetal liver kinase
Fnk	FGF-induced kinase
FSH	follicle-stimulating hormone
Fz	frizzled
β-gal	β-galactosidase
GBP	Gsk3-binding protein
Gsc	goosecoid
Gsk	glycogen synthase kinase
GR	glucocorticoid receptor
GRE	glucocorticoid-response element
GTP	guanidine 5'-triphosphate
hbFGF	human basic fibroblast growth factor
HEPES	N-2-hydroxyethylpiperazine-N'-2-ethanesulfonic acid
HH	Hamburger-Hamilton stage
HMG	high mobility group
Hnf3β	hepatocyte nuclear factor 3β
hpf	hours post-fertilisation
Hyb	hybridisation buffer
ICM	inner cell mass
IL	interleukin
IMAGE	Integrated Molecular Analysis of Genomes and their Expression
IMDM	Iscove's modified Eagle's medium
IPTG	isopropylthio-β-D-galactosidase
IP3	phosphatidylinositol 3
LEF	lymphoid enhancer factor
LIF	laekemia inhibiting factor
loxP	locus of X-over of P1
MAP	mitogen-activated protein

MBT	mid-blastula transition
MC	methylcellulose
MeOH	methanol
MPC	magnetic particle concentrator
MTG	monothioglycerol
MO	antisense morpholino oligonucleotide
NaOAc	sodium acetate
NBT	4-nitro blue tetrazolium chloride
Nedd	neural precursor cell-expressed developmentally down-regulated
NLS	nuclear localisation signal
<i>ntl</i>	<i>no tail</i> (zebrafish <i>brachyury</i>)
OD	optical density
ORF	open reading frame
PBS	phosphate buffer saline
PBT	PBS with 0.1% Tween-20
PBTr	PBS with 0.1% TritonX
PCR	polymerase chain reaction
PDGF	platelet-derived growth factor
PDK	phosphoinositide-dependent protein kinase
PECAM	platelet endothelial cell adhesion molecule
PEG	polyethylene glycol
PFA	<i>para</i> -formaldehyde
PI	phosphoinositide
PI3K	phosphatidylinositol 3'-kinase
PIP₃	phosphatidylinositol 3,4,5-trisphosphate
PKA	cyclic adenosine monophosphate-regulated kinase
PKC	Ca ²⁺ -regulated kinase
PMZ	posterior marginal zone
Prk	proliferation-related kinase
PX	Phox homology domain
RA	Retinoic Acid
RACE	rapid amplification of cDNA ends
Rp	ribosomal protein
RT	reverse transcriptase / transcription
S6K	ribosomal protein S6 kinase
SAPK	stress-activated protein kinase
SDS	sodium dodecyl sulphate
SEP	sperm entry point
Sgk	serum and glucocorticoid-induced kinase

SGKL	SGK-like
Snk	serum-induced kinase
TAE	TRIS, acetate, EDTA
TAP	tobacco acid pyrophosphatase
TBE	TRIS borate, EDTA buffer
TCF	T-cell factor
TE	TRIS EDTA
TEM	transmission electron microscopy
TEMED	N, N, N', N'-tetramethyl-ethylenediamine
TGF	transforming growth factor
Tie	tyrosine kinase with immunoglobulin and EGF homologous domains
Tm	melting temperature
TPA	tetradecanoylphorbol acetate
TRIS	tris(hydroxymethyl)methylamine
TTP	thymidine 5'-triphosphate
TUNEL	terminal deoxy-nucleotidyl transferase-mediated dUTP nick end labelling
UTR	untranslated region
UV	ultraviolet
VE	visceral endoderm
VE-cadherin	vascular endothelial cadherin
VEGF	vascular endothelial growth factor
VSMC	vascular smooth muscle cell
Wg	wingless
Wnt	wingless and Int homologue
X-Gal	5-bromo-4-chloro-3-indolyl- β -D-galactosidase
YSL	yolk syncitial layer

Chapter 1

General Introduction

Chapter 1

General Introduction

- 1.1 Model organisms and conservation of developmental processes**
 - 1.2 Vertebrate embryology from egg to gastrula**
 - 1.2.1 Generalities**
 - 1.2.2 Frog**
 - 1.2.3 Fish**
 - 1.2.4 Chick**
 - 1.2.5 Mouse**
 - 1.3 Vertebrate morphogenetic movements during gastrulation**
 - 1.3.1 Vertebrate fate maps**
 - 1.3.2 Morphogenetic movements converge in the phylotypic stage**
 - 1.3.3 Epiboly**
 - 1.3.4 Cell internalisation**
 - 1.3.5 Convergence and extension**
 - 1.3.6 Mouse embryo turning**
 - 1.4 Early molecular events in vertebrate axes specification and germ-layer formation**
 - 1.4.1 Maternal dorsal determinants are present in fish and frog**
 - 1.4.2 Downstream of β -catenin**
 - 1.4.3 Mesoderm induction**
 - 1.4.4 Endoderm induction**
 - 1.4.5 Neural induction**
 - 1.4.6 The AVE and patterning of the early mouse embryo**
 - 1.4.7 Molecular pathways mediating vertebrate gastrulation movements**
 - 1.5 Aims and thesis outline**
-

The most influential study ever performed in experimental embryology was the one published in 1924 by Hans Spemann and Hilde Mangold (Spemann and Mangold, 1924). Using differences in pigmentation between two species of salamanders, they showed that the dorsal region of one gastrula embryo, when grafted to a ventral or lateral location of another, could induce the formation of a complete second embryonic axis. Pigmentation differences allowed them to observe that the majority of the secondary axis was made up from cells of the host organism rather than from the graft. The active region, which comprises the dorsal lip of the blastopore, was named organizer. Since the organizer was first described in amphibia, functional equivalents have been identified in every major vertebrate taxon. For example, the embryonic shield in teleost fish (Oppenheimer, 1936c; Shih and Fraser, 1996; Saude *et al.*, 2000), Henson's node in avians (Waddington, 1932) and the node in mammals (Beddington,

1994; Knoetgen *et al.*, 2000). The cellular and molecular basis of organizer formation and function remain the object of intense investigation.

1.1 Model organisms and conservation of developmental processes

Despite the recognition of the conservation of fundamental cellular processes, such as DNA replication and cell division, transcription and translation, the remarkable diversity among animal species led to the widely held notion that the basic molecular machinery and processes governing animal development must be divergent. This was largely overturned throughout the last two decades as a result of application of classical mutational genetics and modern molecular biology to the study of developing model organisms.

The genetic screens of Christiane Nusslein-Volhard and Eric Wieschaus (Nusslein-Volhard and Wieschaus, 1980) and the analysis of homeosis by Ed Lewis (Lewis, 1978) marked the beginning of a new era in developmental biology. Identified genes could be grouped according to related phenotypes, which in turn obeyed strict hierarchical relationships. In addition to generating a conceptual framework to explain how a homogenous population of cells can acquire domains of distinct fates, these studies led to the discovery that molecules and processes controlling development are conserved among metazoa.

Drosophila melanogaster was an already prominent model for the study of heredity and evolution, and it naturally became a model also for the new discipline of developmental genetics. Modern genetic and molecular methods rapidly took over from the biochemical ones in their application to animals traditionally used for embryological studies. On the one hand, the fly is small, has a short generation time and only 4 chromosomes, so its genetic amenability has been used over and over again in the recovery of mutations affecting development. On the other hand, the classical embryological models, frog and chick, have large embryos, suitable for transplantation and tissue recombination, which had already yielded intriguing results. In addition, as vertebrates, they have the attraction of being evolutionarily closer to humans than the fly. This has naturally been the main incentive for the pursuit of mouse development,

even if the mammalian embryo is the least accessible of all, gestating inside the mother. Two other species, the nematode worm *Caenorhabditis elegans* and the teleost fish *Danio rerio* (zebrafish), have become well established as model organisms for developmental genetic studies. *C. elegans* has an even shorter life cycle than that of the fly (3 days from egg to egg), has a small and traceable number of cells, occurs as self-fertile hermaphrodites in addition to males which can cross-fertilise the former, is transparent from embryo to adult, and profits from the easiest possible way of stock maintenance by larvæ freezing. Zebrafish have a short and productive breeding cycle and transparent embryos. These properties combined to make zebrafish suitable for mutagenesis screens of the sort performed with *Drosophila* and so it was the first vertebrate in which this was done in large-scale (Driever *et al.*, 1996; Haffter and Nusslein-Volhard, 1996).

Biologists will forever be short of having a detailed account of the developmental genetics of the ten million species of animals known (Alberts *et al.*, 2002). However, the embryology of numerous other animal species has been studied and, combined with detailed molecular understanding, this has allowed evolutionary biologists to discern some of the molecular basis of diversity. Scientists are still assessing the degree of conservation among metazoan species. It cannot be ruled out that some developmental processes are indeed evolutionarily divergent, but the great conservation that has emerged as the main theme of developmental biology is at times motivation enough for persistent endeavours to look for a particular mechanism in a species where it has not been found.

Early development, from oogenesis up to and including gastrulation, is one of the areas in developmental biology where the notion of conservation has been most challenged. It has not been considered useful to pursue analogies between invertebrate and vertebrate early development. Nonetheless, there is an example of striking analogy between the molecular mechanism used by arthropods and vertebrates in a fundamental patterning process such as the generation of a dorso-ventral axis. There remains some dispute, however, as to whether this reflects homology of the process, *i. e.*, continuity by descent or convergent evolution (reviewed in De Robertis and Sasai, 1996). Also, as we now enter an era of understanding the effects of patterning on cellular behaviour, vertebrate developmental biologists will surely look closer at simpler organisms for

lessons in cell biology applicable to early development. For example, evidence is now emerging that the molecular pathway implicated in cell movements of gastrulation in vertebrates is the planar cell polarity pathway (Heisenberg *et al.*, 2000), first discovered in *Drosophila* as the basis for bristle orientation (for reviews see Heisenberg and Tada, 2002 and Tada *et al.*, 2002).

In this thesis, I will describe my work on mouse and zebrafish early development. Given the premise that many developmental processes are likely to be conserved, it is appropriate to compare the four most widely used vertebrate model organisms with respect to the topic in question. The central goal was to identify new molecules involved in early patterning, with the hope of contributing to the understanding of antero-posterior and dorso-ventral axes formation. I therefore start by reviewing literature concerning the early patterning of the most popular vertebrate model organisms (Fig. 1.1), presenting a comparative analysis and the highlighting of unresolved issues.

1.2 Vertebrate embryology from egg to gastrula

1.2.1 Generalities

Most eggs contain yolk for nutrition of the embryo. The yolk can be intermixed with cytoplasm, as in amphibia where every cell inherits yolk in its cytoplasm; but when the amount of yolk is very large, it can become segregated into a special compartment, either before or after fertilisation, as with chicken or zebrafish embryos, respectively. Independently of the yolk, the nucleus is positioned towards one end of the egg, limiting the loss of cytoplasm to the polar bodies during meiosis (Gardner, 1999a). It is from this end, which is organelle-rich and thus metabolically active, that the polar bodies are extruded. This end of the zygote is known as the animal pole, and the opposite is known as the vegetal pole (Fig. 1.1).

The morphology of the first cell divisions in an embryo is correlated with the amount and distribution of yolk because the cleavage furrow is greatly delayed in yolk-rich regions (reviewed in Gilbert, 2000). In telolecithal embryos, where yolk and cytoplasm are separated, as with teleost fish and birds, the yolk mass does not cleave at all and the

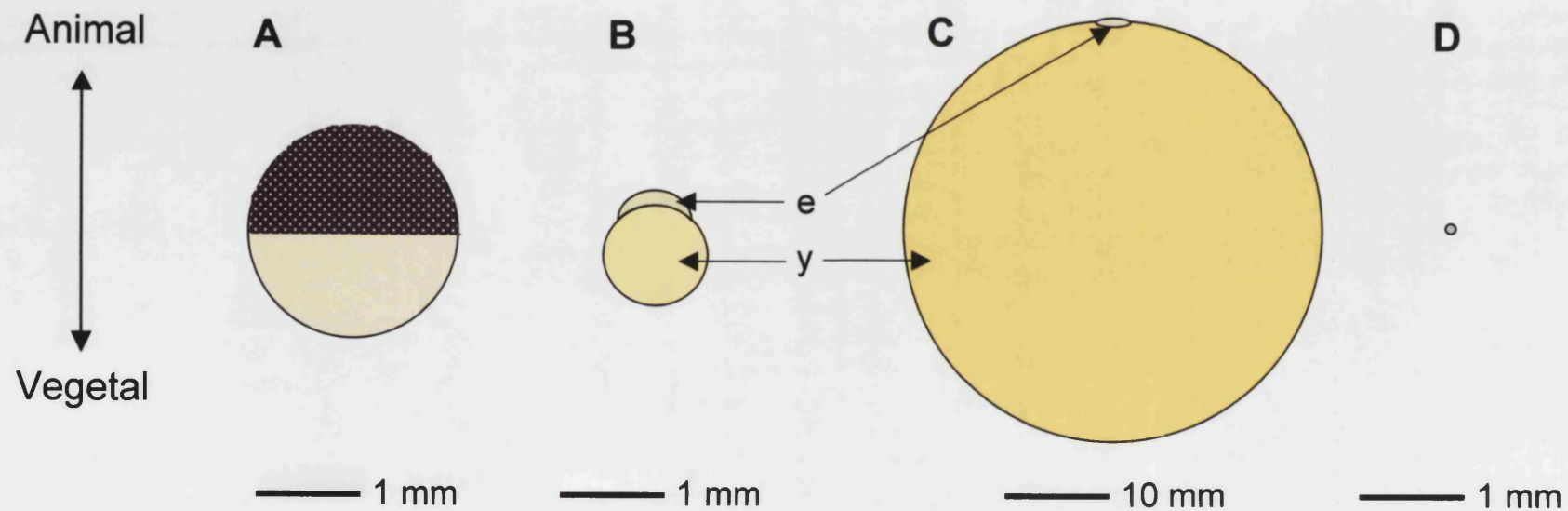


Fig. 1.1 Zygotes of four vertebrate model organisms. Schematics of **A**, *Xenopus laevis* (frog); **B**, *Danio rerio* (zebrafish); **C**, *Gallus gallus* (chick); **D**, *Mus musculus* (mouse) zygotes, oriented with the animal pole upward. **A**, **B** and **D** are shown at the same magnification whereas **C** is shown at a 10 x lower magnification than the others. In fish and chick (**B** and **C**), embryo and yolk are segregated from each other and the two compartments are labelled **e** and **y**, respectively. With the exception of chick, information on sizes was taken from Wolpert *et. al.*, 1998.

embryo develops from a flat disc of cells on top of the yolk mass. Such cell divisions are said to be meroblastic and the flat mass of embryonic cells is referred to as the blastodisc or blastoderm. In mesolecithal embryos, where the yolk is mingled with cytoplasm, as with amphibians, or in isolecithal embryos, where the yolk is evenly distributed or absent, as with mammals, furrows extend through the entire egg in what is called a holoblastic cleavage.

In embryos that undergo meroblastic cleavages the cells of the embryo remain in contact with the yolk for a few divisions. In the early fish embryo, the cells are surrounded by a plasma membrane but there are wide cytoplasmic bridges linking them to the yolk. In the chick embryo, up to the 64-cell stage newly formed cells are not surrounded by a plasma membrane but, rather, open directly to the yolk; these are called open cells (reviewed in Bellairs, 1993). In animals that undergo holoblastic cleavages, adhesion of cells to the hyaline layer, a transparent surface coat secreted by the embryos shortly after fertilisation, as well as osmotic pressure created by secretion of proteins into the extracellular medium, causes the formation of a fluid-filled cavity in the animal region of the embryo (reviewed in Gilbert, 2000). This is called the blastocoel and the embryos are said to be at the blastula stage at the time it forms. In animals that undergo meroblastic cleavages, a thin cavity is present between the blastoderm and the yolk at blastula stage (Fig. 1.2).

During cleavage cell divisions, cells employ a rapid cell-cycle, consisting of alternating S and M phases, with no gap phases and no cell growth. There is no change in the overall volume of the embryo; instead, the initial content of the zygote becomes partitioned into smaller cells. Cells resulting from cleavage divisions are called blastomeres. Cleavage divisions are usually synchronous within a species. When cell-cycles acquire gap phases, however, synchrony is lost. This cell-cycle transition, termed mid-blastula transition (MBT), often correlates with the onset of zygotic transcription (Wylie, 1972; Newport and Kirschner, 1982a; Newport and Kirschner, 1982b; Sawicki *et al.*, 1982; Kane and Kimmel, 1993). One mechanism thought to control this transition is the nuclear-to-cytoplasmic volume ratio in the blastomeres. In frog embryos, its onset has been altered experimentally by adding or removing nuclei thus altering the ratio between the two volumes (Newport and Kirschner, 1982a and Newport and Kirschner, 1982b).

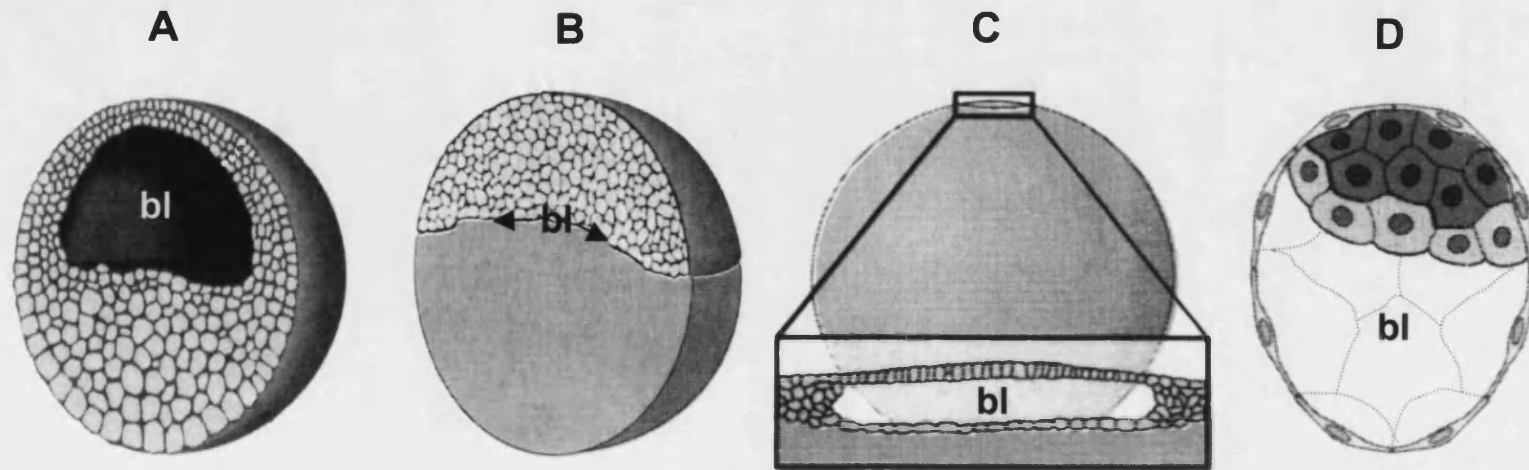


Fig. 1.2 Blastulae of four vertebrate model organisms. Schematics of sagittal sections through **A**, frog; **B**, zebrafish; **C**, chick; **D**, mouse embryos at blastula stage. **A - C**, animal pole is upward; **D**, proximal is upward; **bl**, blastocoel. Adapted from Tam and Quinlan, 1996, and Wolpert *et. al.*, 1998.

1.2.2 Frog

Fertilisation in *Xenopus laevis* begins when a sperm enters the egg in the pigmented animal hemisphere. Microtubule growth from the sperm aster leads the outer, cortical, region of the egg to rotate by 30° relative to the central yolky core, which remains stationary due to gravity (Ancel and Vintemberger, 1948; Vincent *et al.*, 1986; Scharf *et al.*, 1986; Vincent and Gerhart, 1987; Elinson and Rowning, 1988; Scharf *et al.*, 1989). This process is called cortical rotation and occurs before the zygote undergoes its first cleavage. Cortical rotation has its maximal effect at a point directly opposite the sperm entry point (SEP) and displaces a set of cortical-located patterning molecules as well as a set of organelles (Ubbels, 1977; Kirschner *et al.*, 1980; Rowning *et al.*, 1997), while leaving other, deeper, proteins and mRNAs unaffected (see below). The region of maximal cortical rotation, opposite the SEP, marks the future dorsal side of the embryo and dorsal determinant molecules are concentrated in this region.

When cortical rotation is impaired, for example by ultraviolet (UV) irradiation, the three germ-layers still form but the mesoderm consists only of the ventral type, such as lateral plate mesoderm and blood, and the ectoderm gives rise solely to epidermis rather than to epidermis and nervous system. The resulting embryo is totally devoid of dorsal structures and consists of radially symmetric ventral tissue around a gut (Gerhart *et al.*, 1989). In contrast, if a *Xenopus* zygote is manually tilted or centrifuged gently in opposite directions sequentially before the first cell division, cortical rotation can occur for a second time and a double axis will become apparent in the later embryo (Scharf and Gerhart, 1980; Black and Gerhart, 1986). Removal of vegetal pole cytoplasm before cortical rotation blocks formation of dorsal structures and its injection into another embryo induces an ectopic axis in the recipient (Sakai, 1996; Kikkawa *et al.*, 1996). Thus, dorsal determinants are normally resident in the vegetal region and are shifted dorsally by cortical rotation (Fujisue *et al.*, 1993; Yuge *et al.*, 1990; Holowacz and Elinson, 1993; Sakai, 1996; Kageura, 1997; Kikkawa *et al.*, 1996).

As amphibian embryos undergo holoblastic cleavage, cytoplasmic determinants become segregated into individual cells. In *Xenopus laevis*, the first two cleavages are meridional with respect to the animal-vegetal axis and at right angles to each other but the third cleavage is equatorial. Therefore, from the eight-cell stage onwards the

embryo has distinct animal and vegetal blastomeres. In the early 1970s, Pieter Nieuwkoop showed that transplantation of dorsal-vegetal blastomeres of a 32-cell stage embryo could induce a complete second axis in a host without contributing to axial tissues (Nieuwkoop, 1973). These dorsal-vegetal blastomeres would contain the dorsal determinants displaced by cortical rotation and this region has since been called the Nieuwkoop centre. Thus, as a model of dorsal determination, cortical rotation generates the Nieuwkoop centre; then the Nieuwkoop centre induces the dorsal organizer in the overlying blastomeres (reviewed in Moon and Kimelman, 1998). Supporting this notion, 32-cell embryos in which two dorsal-marginal and two dorsal-animal blastomeres are removed will develop a normal axis, demonstrating that a Nieuwkoop centre is sufficient to dorsalise an embryo in the absence of normal organizer precursor cells (Kageura, 1995). The simplicity of this model is very attractive, but it does not fully explain all the data. Later experiments showed that Nieuwkoop activity is broadly distributed over the dorsal side of the embryo, reaching as far as the upper animal hemisphere. Indeed, it is greatest in the dorsal-vegetal cells that lie just below the equator, the traditional Nieuwkoop centre, but significant levels of activity are also present in cells that will populate the organizer itself (Kageura, 1990). In addition, embryos in which the two dorsal-vegetal blastomeres are removed at the 32-cell stage are able to develop an axis, although gut development is impaired (Kageura, 1995). The broad distribution of dorsalising activity and its presence in organizer precursor cells calls into question the existence of a separate Nieuwkoop centre for normal organizer formation and raises the possibility that the organizer may arise directly from dorsal determinants localised during cortical rotation. Alternatively, Nieuwkoop centre and prospective organizer may cooperate or act redundantly to ensure organizer formation (reviewed in Moon and Kimelman, 1998 and Kodjabachian and Lemaire, 1998).

1.2.3 Fish

In teleost fish, sperm enter the egg through a specialised structure at the animal pole, called the micropyle. Yolk and cytoplasm are intermixed in the egg but soon after fertilisation most cytoplasm is shifted to the animal pole, while a thin layer of subcortical cytoplasm covers the entire surface of the yolk. In fish there is no correlation between the first division planes and the dorso-ventral axis (Clapp, 1891; Oppenheimer, 1936a; Kimmel and Warga, 1987; Abdelilah *et al.*, 1994; Helde *et al.*,

1994; Wacker *et al.*, 1994). Moreover, removal of single *Fundulus* blastomeres up to the four-cell stage does not affect development (Morgan, 1895; Hoadley, 1928; cited in Jesuthasan and Stahle, 1997).

In zebrafish, starting at about 40 min after fertilisation at 28 °C, the cytoplasm undergoes regular cleavages every 15 min. After ten such cleavages, MBT takes place and, as zygotic transcription begins, three distinct embryonic compartments/lineages form. The outermost cells differentiate into a protective layer, first called the enveloping layer (EVL) and later called the periderm. Marginal blastomeres, still connected to the yolk cell via large cytoplasmic bridges, open up to and formally become part of the yolk cell, generating a syncytium called the yolk syncytial layer (YSL) (Kimmel and Law, 1985a; Kimmel and Law, 1985b). Both the EVL and the YSL are extraembryonic lineages. The remaining blastomeres, called the deep cell layer (DEL), are destined to form the embryo-proper (Kimmel and Law, 1985c). YSL nuclei undergo several more cell divisions before becoming post-mitotic (Kane *et al.*, 1992). These nuclei are initially restricted to the rim of the upper part of the yolk (external YSL) but spread to also populate the centre of the upper yolk (internal YSL), underlying the entire blastoderm (reviewed in Sakaguchi *et al.*, 2002). At the time of YSL formation, gap junctions between the yolk and overlying marginal blastomeres are eliminated, hindering the free translocation of large proteins between the two compartments (Kimmel and Law, 1985).

There are several lines of evidence demonstrating that dorsal determinants are segregated within the yolk during early teleost development. When the vegetal half of the yolk cell is removed shortly after fertilisation or even after a few cell divisions, fish embryos later display dorsal deficiencies (Tung *et al.*, 1945; Mizuno *et al.*, 1997; Yamaha *et al.*, 1998; Mizuno *et al.*, 1999a; Mizuno *et al.*, 1999b; Ober and Schulte-Merker, 1999; Aanstad, 1999). The severity of the ventralised phenotype was observed to decrease gradually with increasing the time of contact between the blastoderm and the yolk such that most embryos develop normally when vegetal yolk is removed after the four- or eight-cell stages (Mizuno *et al.*, 1999b). Earlier experiments had already shown there is a critical stage before which yolk removal results in total absence of dorsal/axial structures and after which embryos are able to form an axis (Oppenheimer, 1936a). Younger blastodiscs require a larger fraction of adhering yolk to develop

normally (Tung *et al.*, 1945). Furthermore, when young blastodiscs are transplanted onto gastrula stage yolk cells that have been marked on the dorsal side, it can be observed that embryos develop with a dorso-ventral axis determined by the yolk cell (Long, 1983). Finally, a gastrula stage yolk transplanted to the animal pole of a host blastoderm is able to induce dorsal and mesodermal molecular markers in the host (Mizuno *et al.*, 1996).

Within the yolk cell, is the YSL required for inducing the dorsal organizer? As with the amphibian Nieuwkoop centre, there is debate over this issue. The dorsal YSL is able to specify dorsal deep cell fates but when YSL transcripts are eliminated, dorsal fates are unaffected, although ventro-lateral mesoderm specification is impaired (Chen and Kimelman, 2000).

No cortical rotation has been reported for fish. However, in zebrafish, cytoplasmic streaming, also a microtubule-dependent process, is capable of transporting substances from the yolk into blastomeres up to the 128-cell stage (Jesuthasan and Stahle, 1997). Following fertilisation, microtubules begin to organise in the vegetal pole as parallel arrays, becoming disorganised near the equator. After the first cleavage, equatorial cortical microtubules gradually extend and become aligned with the animal-vegetal axis (Jesuthasan and Stahle, 1997). Disruption of microtubules prior to the first cleavage causes cytoplasmic streaming to cease and the resulting embryos display dorsal deficits later in development (Strahle and Jesuthasan, 1993; Jesuthasan and Stahle, 1997). How the dorsal bias is imposed is not yet known.

1.2.4 Chick

At the time the chicken egg is laid, it is at the blastula stage. In chick blastulae the posterior is morphologically recognisable by the presence of a transparent crescent-shaped region on one side of the blastodisc, called Koller's sickle. Early chicken development up to the blastula stage is obscured by its intrauterine location. A few studies, however, suggest that maternal, yolk-localised antero-posterior patterning cues become asymmetrically positioned by gravity. While the egg descends the oviduct, peristalsis of the uterine wall causes the outer, albumin-rich, layers of the conceptus to rotate on the long axis while the yolk remains stationary but slightly oblique in the

direction of rotation (Kochav and Eyal-Giladi, 1971; Callebaut, 1993a; Callebaut, 1993b). The side of the embryo that is tilted upward is gradually specified to become posterior-dorsal and bias towards this fate can be imposed by experimentally tilting embryos of this stage (Vintemberger and Clavert, 1960; Kochav and Eyal-Giladi, 1971; reviewed in Gerhart and Kirschner, 1997). When blastoderms are cultured in isolation so, without yolk, they will form an axis only if harvested after stage VII (Eyal-Giladi and Kochav, 1976), suggesting need for vegetal cytoplasmic determinants to reach the animal pole in order for radial symmetry to be broken in the blastoderm. Stage VI-VII is thus thought to be the time they reach the blastoderm in a chick embryo. Tilting is accompanied by a subtle sliding of the embryo towards the anterior, as seen by a minute shear zone left behind in the posterior (Callebaut, 1987; Callebaut, 1993b; Callebaut, 1993a; Callebaut and Van Nueten, 1994). This movement is reminiscent of cortical rotation in the frog. In both cases a superficial layer moves in an anterior direction relative to a deep layer with, presumably, accompanying redistribution of cytoplasm in a large yolky cell (reviewed in Bachvarova, 1999).

Despite the interuterine cues, antero-posterior patterning is not irreversibly established until stage 2 HH, when the primitive streak becomes visible, defining the onset of gastrulation. Prior to gastrulation, the chick blastoderm can be cut into posterior, lateral and anterior quadrants, each of which can develop into an embryo with a complete axis. The different quadrants differ in their ability to regulate in this way, though, where posterior quadrants have a very high regulative capacity and anterior quadrants have a very low one (Spratt and Haas, 1960). If pieces of posterior Koller's sickle, called the posterior marginal zone (PMZ), are ectopically positioned on all quadrants of a developing embryo, only a single, normal embryo develops (Spratt and Haas, 1960). The latter experiment shows that the blastodisc has the ability to suppress supranumerary axes. The PMZ has been proposed to be the avian Nieuwkoop centre: when transplanted to another part of the marginal zone, it induces a complete embryonic axis without making a cellular contribution to the induced structures; and when removed, the embryo can initiate axis formation from another part of the remaining marginal zone known to possess, albeit weaker, Nieuwkoop activity (Skromne and Stern, 2001).

Extraembryonic cell lineages are set aside very early in avian development. Adaptation to land engendered the evolution of several tissue layers in order to protect the embryo from desiccation among other things. Birds, reptiles and mammals are classified as amniote vertebrates, which means they are supported by four kinds of specialised extraembryonic membranes, the yolk sac, the amnion, the allantoic membrane and the chorion (reviewed in Gerhart and Kirschner, 1997 and Gilbert, 2000). As in fish, avian extraembryonic lineages are set aside around MBT. Initially scattered clumps of cells found in the thin blastocoelic cavity are thought to shed from the overlying epithelial layer (Eyal-Giladi and Kochav, 1976) and are called primary hypoblast (Stern, 1990). The centre of the epithelium becomes a translucent monolayer, the *area pellucida*, surrounded by a bilayered opaque ring, the *area opaca*. The border between the two areas is known as the marginal zone. Sections show that the PMZ is actually bilayered as well. The epithelial monolayer is called epiblast and will mainly give rise to the embryo-proper. The lateral marginal zone together with the *area opaca* will give rise to extraembryonic tissues other than the yolk sac. Slightly later, at stage XIV (Eyal-Giladi and Kochav, 1976) / HH 2 (Hamburger and Hamilton, 1992), another deep layer starts to form, mainly by migration of cells from the PMZ but also from ingression of cells from the posterior epiblast. This tissue forms in an anterior-to-posterior direction, displacing the primary hypoblast anteriorly and eventually coming to lie under the entire *area pellucida*. This is the secondary hypoblast or hypoblast proper, which will give rise to the yolk sac. At approximately this time, gastrulation begins, defined by the appearance of a dark triangle with its base in the PMZ and its apex in the epiblast. In this triangular area, a groove develops which is the primitive streak. The traditional view, based on the PMZ transplantation and removal experiments described above, is that the primitive streak is induced by the underlying PMZ / hypoblast (reviewed in Eyal-Giladi, 1997). However, this view has been challenged by the finding that a few scattered cells found in the pre-streak stage epiblast contribute to both endoderm and mesoderm (Stern, 1990; Stern and Canning, 1990).

1.2.5 Mouse

Mouse zygotes from which substantial fractions of either animal, vegetal or meridional cytoplasm have been removed three to five hours prior to the first cleavage can develop into healthy and fertile adults (Zernicka-Goetz, 1998). Moreover, after centrifugation

(Mulnard and Puissant, 1984) or high-speed swirling of cytoplasm by an electrically controlled glass probe (Evsikov *et al.*, 1994) development proceeds normally. It has been argued, however, that no assessment was made of whether scrambling effects were cortical as well as central, or whether the egg might have reversed to its original polarity prior to the first cell division (Gardner, 1999b). The cytoplasmic stratification caused by the centrifugation performed, however, was determined to last for at least 8 h.

Very recently, attention turned from highly invasive procedures to the observation of what happens in normal, unperturbed, mouse embryo development. Sperm can enter the mouse egg at any point of its surface, with the exception of an area above the metaphase II spindle (Piotrowska and Zernicka-Goetz, 2001). The first cleavage plane of the zygote is meridional with respect to the animal-vegetal axis of the zygote. Whether the orientation of this initial cleavage about the animal-vegetal axis is somehow regulated or whether it is random is still subject of controversy. Recent studies reach opposing conclusions. Using either lectin-treated fluorescent microspheres as a long-lasting means of labelling the SEP, or direct fluorescent labelling of the sperm, one group finds that the first cleavage plane is usually located close to the SEP (Piotrowska and Zernicka-Goetz, 2001; Plusa *et al.*, 2002b). By removing, transplanting or duplicating the animal or vegetal poles of the mouse egg, this group further showed that the site of the last meiotic division, in the animal pole, contains, or correlates with, a cue that orients the plane of the initial cleavage (Plusa *et al.*, 2002a). A correlation between SEP inheritance and subsequent cleavage was also shown by this group, whereby the blastomere that inherits the SEP usually divides earlier (Piotrowska and Zernicka-Goetz, 2001; Piotrowska *et al.*, 2001). Another group, using injection of small oil drops into the *zona pellucida* as a means to landmark the embryo, finds that the plane of first cleavage is random with respect to the SEP (Davies and Gardner, 2002).

To address whether an early distinction exists between the extraembryonic trophectoderm lineage and the embryonic inner cell mass (ICM) lineage, two-cell stage fate mapping experiments have been done. In several studies, marking of single cells of the two-cell stage embryo revealed disproportionate contribution of the early dividing blastomeres to the ICM (Kelly *et al.*, 1978; Graham and Deussen, 1978; Balakier and Pedersen, 1982; Surani and Barton, 1984). However, in one very recent study this bias

was not observed (Fujimori *et al.*, 2003). Concern about the perturbation to cleavage timing caused by intracellular microinjection of lineage tracers led to the repetition of the two-cell lineage tracing experiment using the membrane-soluble dyes DiI, DiD and DiO or the use of oil droplets on the *zona pellucida* to mark early blastomeres. A reciprocal fate bias of the two-cell blastomeres was again found (Piotrowska and Zernicka-Goetz, 2001; Gardner, 2001). The embryonic part of the blastocyst, the ICM, consists predominantly of the progeny of the blastomere that divides first (Piotrowska *et al.*, 2001). One possibility is that the early cell division imparts an advantage that allows cells in one lineage to initiate a developmental program earlier than the other. Alternatively, sperm entry may promote some other developmental process influencing the fate of the cell (Piotrowska *et al.*, 2001).

These studies suggest that the early mouse zygote may be prepatterned but this is difficult to reconcile with results obtained in many previous experiments. The capacity to generate correct pattern after blastomere disaggregation, aggregation or rearrangement, has been used to argue against the existence of cytoplasmic determinants in mammalian eggs. Blastomeres isolated at the 16-cell stage and reaggregated in groups of 16 cells can form blastocysts that undergo normal post-implantation development when transferred to pseudopregnant recipients (Ziomek *et al.*, 1982). Chimeras have been generated from up to four eight-cell embryos, that regulate to normal size by gastrulation (Rands, 1986) without segregation of blastomeres (Garner and McLaren, 1974), and develop into apparently normal mice (Petters and Markert, 1980). Individual blastomeres from two-, four- and eight-cell embryos have been observed to give rise to relatively normal blastocysts (Tarkowski, 1959; Tarkowski and Wroblewska, 1967; Rossant, 1976; Tojo and Ogita, 1984; Pierce *et al.*, 1997). It is not known, however, if all blastomeres isolated from a single embryo have the same capacity, the only example other than monozygotic twins being a report of bovine monozygotic quadruplets (Johnson *et al.*, 1995).

By the eight-cell stage, mammalian embryos undergo compaction, during which cells maximise surface contact between each other and become polarised, with apical, external, and basolateral, internal, domains. Asymmetric divisions, along the apico-basal axis, of each of these cells leads to the generation of distinct cell types in the 16-cell stage embryo: outer, trophoctoderm lineage cells, which are polarised in the same

way as the eight-cell blastomeres were; and inner, ICM lineage cells, which are round and appear to be apolar (reviewed in Gilbert, 2000). Following disaggregation, eight-cell or outer 16-cell blastomeres retain several traces of their polarity, such as asymmetric distribution of organelles, actin, tubulin and microtubule-organising centres, whereas the internal 16-cell blastomeres remain apparently apolar (reviewed in Johnson *et al.*, 1986). This feature has been exploited to show that subsequent division planes are not fixed but, rather, depend upon the cellular context. The plane of division adopted will indicate cell fate. If two 16-cell stage polar blastomeres are cultured in contact with each other, they will in most cases divide asymmetrically, *i. e.*, equatorially with respect to their axis of polarity, and give rise to one polar and one apolar daughter cell. If a polar blastomere is cultured in contact with an apolar one, the former envelopes the latter and its division will in most cases be symmetrical, *i. e.*, meridional, giving rise to two polar daughter cells, while the apolar blastomere will give rise to two apolar daughters. If two apolar blastomeres are cultured in contact with each other, at least one of them will generate a polar daughter cell and the polar-plus-apolar cell behaviour ensues (Johnson and Ziomek, 1983). When several of these cells are present, polar ones always wrap around an apolar cell core and there seems to be a constraint on the ratio of inside to outside cells (Fleming, 1987).

Cavitation takes place at 3.5 days *post-coitum* (dpc) in the mouse, when a critical number of polar blastomeres wrapped around an apolar core is attained. ICM cells remain attached to one part of the trophoctoderm and detach from the other, while the blastocoel forms; the embryo is at the blastula stage and is called a blastocyst. What determines which part of the trophoctoderm will remain attached to the ICM is not known but this relationship controls subsequent cell fate decisions within the trophoctoderm. Those trophoctoderm cells in contact with the ICM will differentiate into polar trophoctoderm, pushing the ICM into the blastocoel and forming the egg-cylinder, whereas remaining trophoctoderm will differentiate into the polytenic mural lineage, responsible for implantation into the uterus (Fig. 1.3). The embryo-proper forms from the distal portion of the egg-cylinder and is derived entirely from the ICM. However, not all the ICM gives rise to the embryo-proper: the portion of the ICM in contact with the blastocoel differentiates into another extraembryonic tissue called primitive endoderm. The primitive endoderm gives rise to the parietal endoderm, which by egg-cylinder stages lines the mural trophoctoderm, and the visceral endoderm (VE),

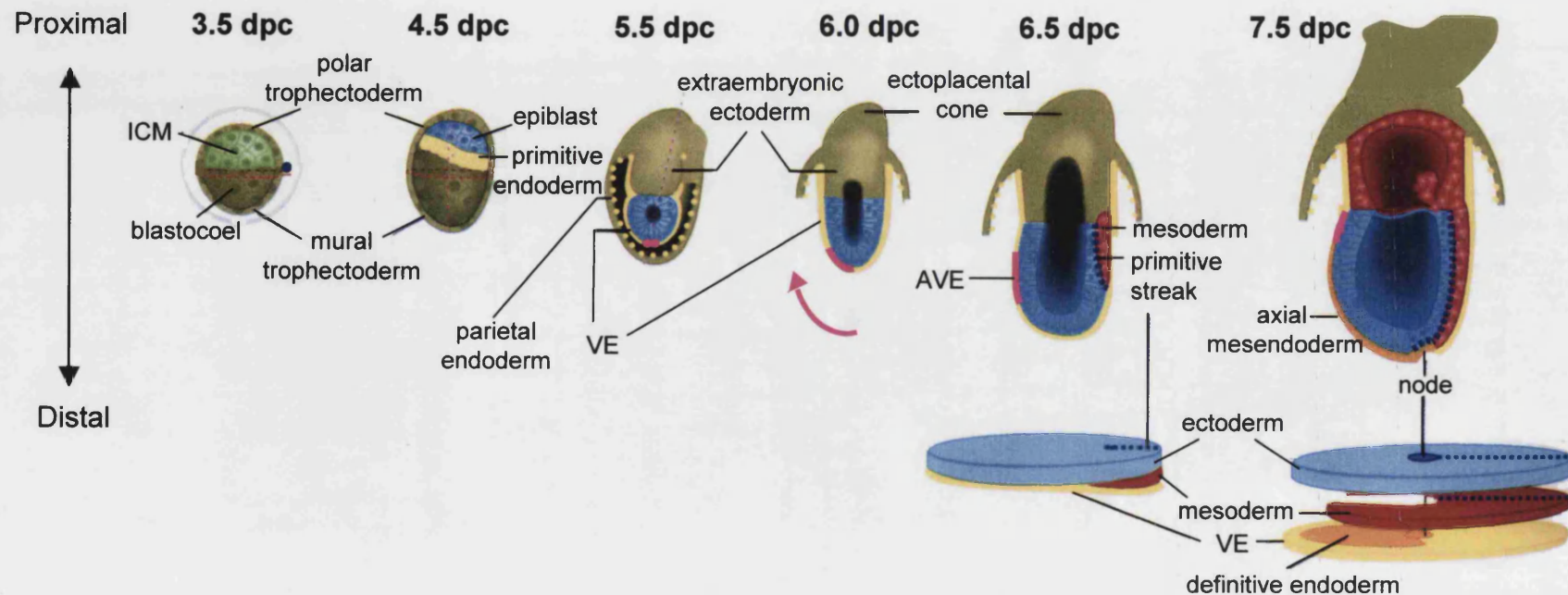


Fig. 1.3 Mouse embryonic development from blastocyst to gastrula. The second polar body is sometimes seen still tethered to the early blastocyst, marking the animal pole; this is represented by •. Running through the plane outlined by the red dashed line in the blastocyst schematics is their axis of bilateral symmetry. The pink arrow depicted at 6.0 dpc indicates the movement of the AVE population of cells (in pink), from a distal position, at 5.5 dpc, to an anterior location, at 6.5 dpc. The three germ-layers are shown as flattened sheets below the 6.5 and 7.5 dpc embryo schematics in order to highlight their extent and facilitate comparison with other species. See text for further explanations. Adapted from Beddington and Robertson, 1999.

which by egg-cylinder stages surrounds both the epiblast – the embryo-proper – in the distal half of the egg-cylinder, as well as the extraembryonic ectoderm, in the proximal half, which is derived from the polar trophoctoderm. At egg-cylinder stages, the mural trophoctoderm cells have ceased to undergo cytokinesis and become polytenic, being named trophoblast giant cells.

If the mouse zygote were to contain molecular determinants that would promote development in a stereotypical way, it would be expected that its polarity would correlate with that of blastocyst, egg-cylinder and the embryonic axes. The blastocyst has an obvious axis of polarity that runs between the ICM and the blastocoel. In this orientation, it is called the embryonic-abembryonic or the proximo-distal axis and it will correspond to the dorso-ventral axis of the future embryo. A top view of the embryonic-abembryonic axis reveals that the blastocyst is not radially symmetric but, rather, bilaterally symmetric, with a long and a short diameter (Smith, 1980; Gardner, 1990), as had long been observed for the rat (Huber, 1915; referred to in Gardner, 1999b). The animal-vegetal axis of the blastocyst, when recognizable by the presence of a polar body tethered by a thin cytoplasmic bridge, is usually aligned with the greater diameter of the blastocyst and orthogonal to the embryonic-abembryonic axis (Gardner, 1997).

There is some evidence that the axes of the mouse blastocyst predict the embryonic axes. When blastocyst stage primitive endoderm cells in proximity to the polar body are labelled they are found to contribute progeny predominantly to the distal half of the egg-cylinder. In contrast, progeny of primitive endoderm labelled away from the polar body becomes localised to the proximal half (Weber *et al.*, 1999). This raises the possibility that the animal-vegetal axis of the blastocyst is translated into the distal-proximal axis of the egg-cylinder. Shortly after, at approximately 5.0 dpc, the distal-proximal axis of the egg-cylinder is translated into the antero-posterior axis of the embryo, as distal VE cells move to what will be the anterior of the conceptus (Thomas, 1998). This movement of distal VE cells to the anterior, forming the so-called AVE, has been postulated to be part of the global movement of the VE revealed by the primitive endoderm labelling experiments described above. However, recent observations indicate that distal VE cells move actively and independently of surrounding VE cells (Srinivas, 2004). Approximately 24 h after the formation of the

AVE, at 6.5 dpc, an indentation is formed on the opposite side of the embryo (posterior). The indentation is called primitive streak as in the chick, and its appearance marks the onset of gastrulation.

What has been lacking for an assessment of the existence of axial patterning cues in the mouse zygote is the long-term labelling of the progeny of early blastomeres, up to post-implantation stages, when the embryonic axes are clearly observable. This has very recently been accomplished by genetic labelling of one of the two- and four-cell stage blastomeres using the β -galactosidase (β -gal) reporter gene activated by the Cre-loxP system. In 35/37 cases, single blastomeres of the two-cell stage embryo contribute uniformly to all embryonic lineages and extraembryonic ectoderm displaying no clear predominance at any level of any of the embryonic axes. However, in one case, labelled cells were found exclusively in the extraembryonic ectoderm and in another, no labelled cells were found in the extraembryonic ectoderm. More embryos belonging to the latter categories were found when single blastomeres of the four-cell stage embryo were labelled: 16/54 and 4/54, respectively (Fujimori *et al.*, 2003). The issue of whether the progeny of particular blastomeres of the two- or four-cell stage embryo, with identifiable animal-vegetal positions, showed a bias in the contribution to particular lineages or regions of the embryo was not addressed in this study. Delivery of the Cre protein to the desired blastomere was performed by injection so arguments concerning perturbation of normal development can still be raised. Also, when injecting Cre protein into zygotes, or even when crossing wild-type females to males ubiquitously expressing Cre and β -gal, only few X-gal-positive cells were detected later in the parietal endoderm and none were ever detected in the primitive endoderm or VE, revealing lack of promoter activity in these tissues. This is particularly disappointing and precludes a definite argument against prepattern of the mouse zygote since the VE is known to grow in a clonally coherent manner – as opposed to other tissues, which undergo extensive cell mixing (Gardner, 1984; Lawson and Pederson, 1987) – and is known to possess early axial patterning cues, features that are likely related (see Section 1.4.6, below).

1.3 Vertebrate morphogenetic movements during gastrulation

Gastrulation consists of a series of cell movements during which the three classically defined germ layers are specified and arranged spatially, with the ectoderm on the outside, the endoderm on the inside and the mesoderm in between. The germ layers generate embryonic tissues gradually, following stereotypical and hierarchical commitment steps. The ectoderm will ultimately give rise to the skin, neural crest and central nervous system; the mesoderm to muscle, cartilage, bone, reproductive organs, kidneys, blood vessels and blood cells; and the endoderm will give rise to the gut and its derivative structures, liver, pancreas and lungs.

1.3.1 Vertebrate fate maps

The fate of distinct regions of the germ layers generated during gastrulation is established very early in most embryos. Despite the rather different topologies of the model organisms at gastrula stages, some degree of similarity between the relative positions of regions with similar fates and/or expressing orthologous molecules can be noted (Figs. 1.4 and 1.5, respectively). The depiction of a fate map does not mean that cells are irreversibly committed to a particular fate but, rather, that cells in specific locations will normally adopt a particular fate. It should also be noted that a fate map is not a lineage map nor, conversely, are cells of the same lineage necessarily committed to the same fate.

Fate mapping as well as molecular marker analyses show that in frog and fish the endoderm and mesoderm are specified prior to internalisation whereas in chick and mouse, the internal germ-layers are specified as they emanate from the streak (Tam and Beddington, 1987; Dale and Slack, 1987; Wetts and Fraser, 1989; Kimmel *et al.*, 1990; Warga and Kimmel, 1990; Schoenwolf *et al.*, 1992; Psychoyos and Stern, 1996; David and Rosa, 2001; Horb and Slack, 2001). In the zebrafish, progenitors of mesoderm and endoderm co-localise in the equatorial region of the blastoderm (Warga and Nusslein-Volhard, 1999) and are collectively called mesendoderm. In the frog blastula, the region fated to become ectoderm is the animal pole, prospective endoderm is in the vegetal pole and prospective mesoderm lies at the equator, or marginal zone, between two other prospective germ layers.

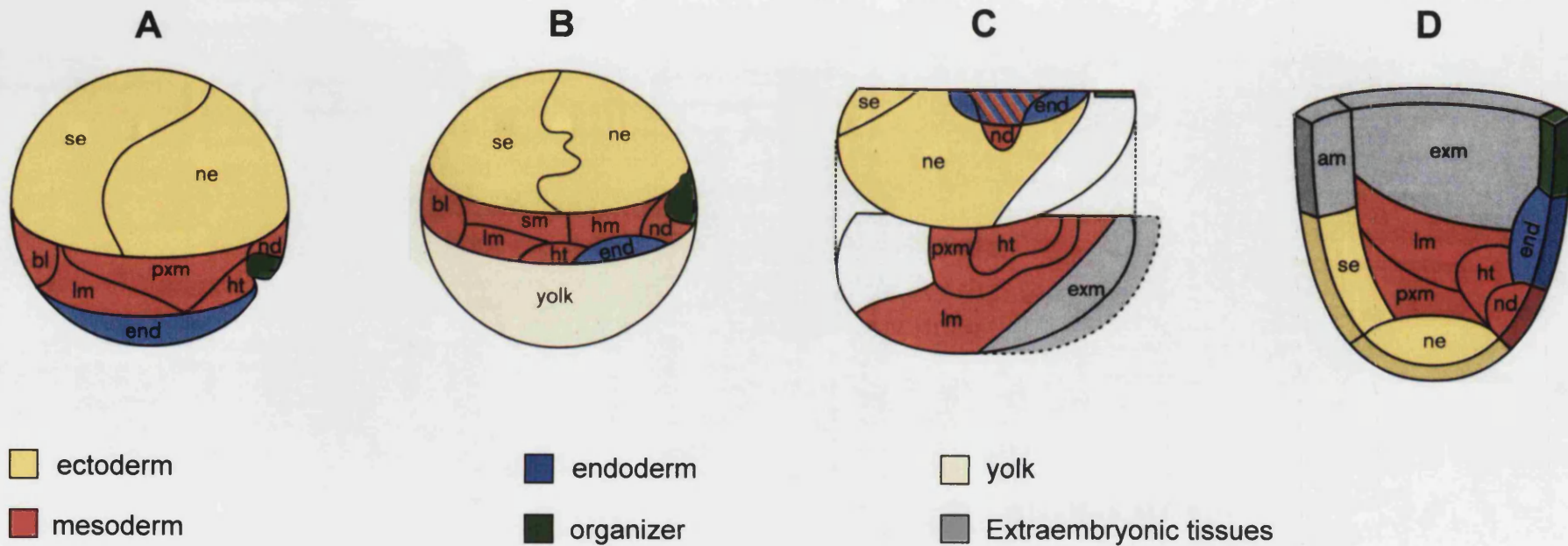


Fig. 1.4 Fate maps of four vertebrate model organisms at early gastrula stage. A, frog; B, zebrafish; C, chick schematics oriented with the animal pole upward; D, mouse schematic oriented with proximal upward. In representing the chick embryo, two separate images of a blastoderm are shown to indicate germ-layer precursors with overlapping distributions. **ne**, neuroectoderm; **fb**, forebrain; **mb**, midbrain; **hb**, hindbrain; **sc**, spinal cord; **se**, surface ectoderm; **pxm**, paraxial mesoderm; **hm**, head mesoderm; **sm**, somites; **lm**, lateral mesoderm; **nd**, notochord; **ht**, heart; **bl**, blood; **end**, gut endoderm; **am**, amnion ectoderm; **exm**, extraembryonic mesoderm. The organizer cells themselves give rise to the notochord and prechordal plate, midline mesoderm tissues that are essential for correct patterning namely of the ventral neural tube. Adapted from Tam and Quinlan, 1996.

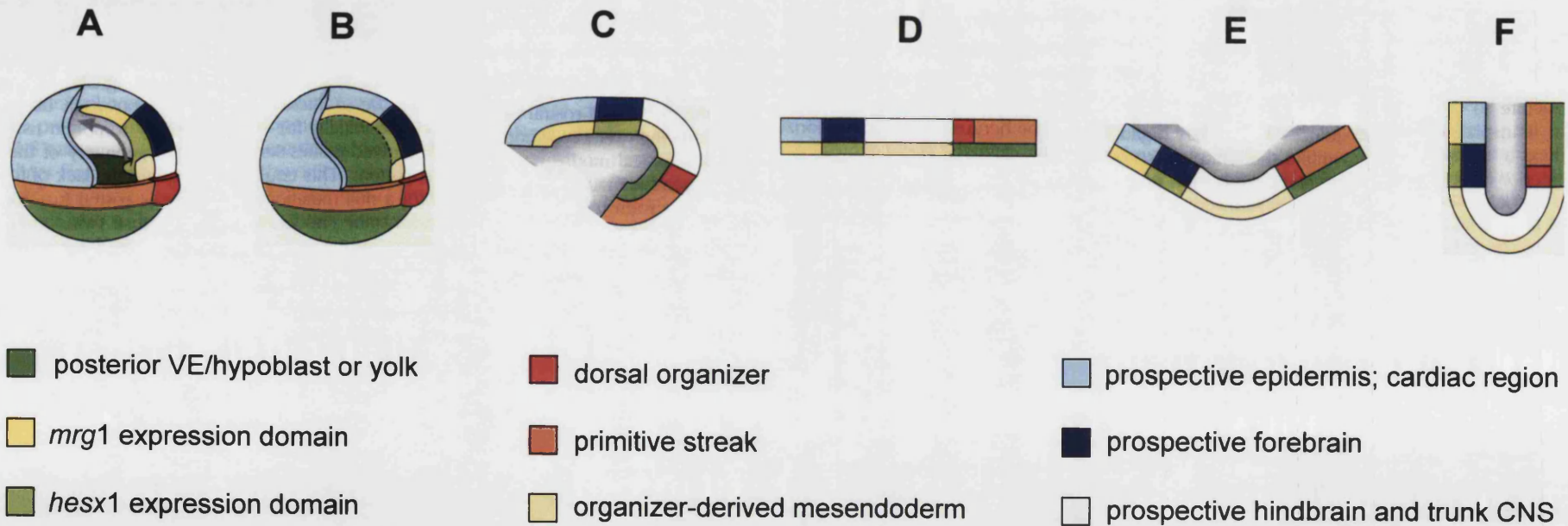


Fig. 1.5 Comparison between the patterning of four vertebrate model organisms at early gastrula stage. Schematics of **A**, frog; **B**, zebrafish; **C**, conceptual unrolling of zebrafish blastoderm; **D**, chick; **E**, conceptual folding up of chick blastoderm with epiblast on the inside; **F**, mouse. Adapted from Beddington and Robertson, 1998.

1.3.2 Morphogenetic movements converge in the phylotypic stage

Morphogenetic movements are highly reproducible within each class of vertebrates and different classes share strategies in order to bring cells that were on the outside of the embryo to the inside, to generate migratory cells and to extend an originally circular, convex or spherical mass of cells. The specific topology of the blastula and the way the embryo obtains nutrition determine the gastrulation movements of a species. Vertebrate embryos display great morphological variation at the blastula stage but by the end of gastrulation they assume a common morphology, often referred to as the phylotypic stage (Sander, 1983) (Fig. 1.6). This presumably reflects a constraint on the relative positions of tissues as they form, for proper cellular interactions and appropriate development thereafter.

The morphogenetic movements that occur during gastrulation were first described extensively for amphibians. Work in teleosts uncovered similarities and differences between gastrulation cell movements in the two classes of vertebrates. Due to accessibility and size, the morphogenetic movements of amphibians and teleosts have been studied in the most detail. A comparison of the gastrulation movements in the four most common vertebrate model organisms is presented next.

1.3.3 Epiboly

In zebrafish, morphogenetic movements start when the yolk cell bulges in an animal direction and pushes the DEL cells up and from the centre to the periphery. This is radial intercalation and it initiates the thinning and spreading of the blastoderm over the yolk cell in an animal-to-vegetal direction, in a process called epiboly (Fig. 1.7 A, Epiboly). Teleost epiboly takes place until the whole yolk cell is engulfed by embryo-proper. Epiboly is thought to be driven by shortening of cortical microtubules all around the yolk cell, which moves external YSL nuclei towards the vegetal pole. The external YSL is attached to the EVL and thus presumably tows it along, as well as the DEL in between the two (Warga and Kimmel, 1990; Strahle and Jesuthasan, 1993; Solnica-Krezel and Driever, 1994). In *Fundulus* embryos, when the blastoderm is removed, the YSL autonomously carries on its vegetal-ward movement (Trinkaus, 1951). There is no evidence for an active role of the deep cells in teleost epiboly (reviewed in Kane and Adams, 2002).

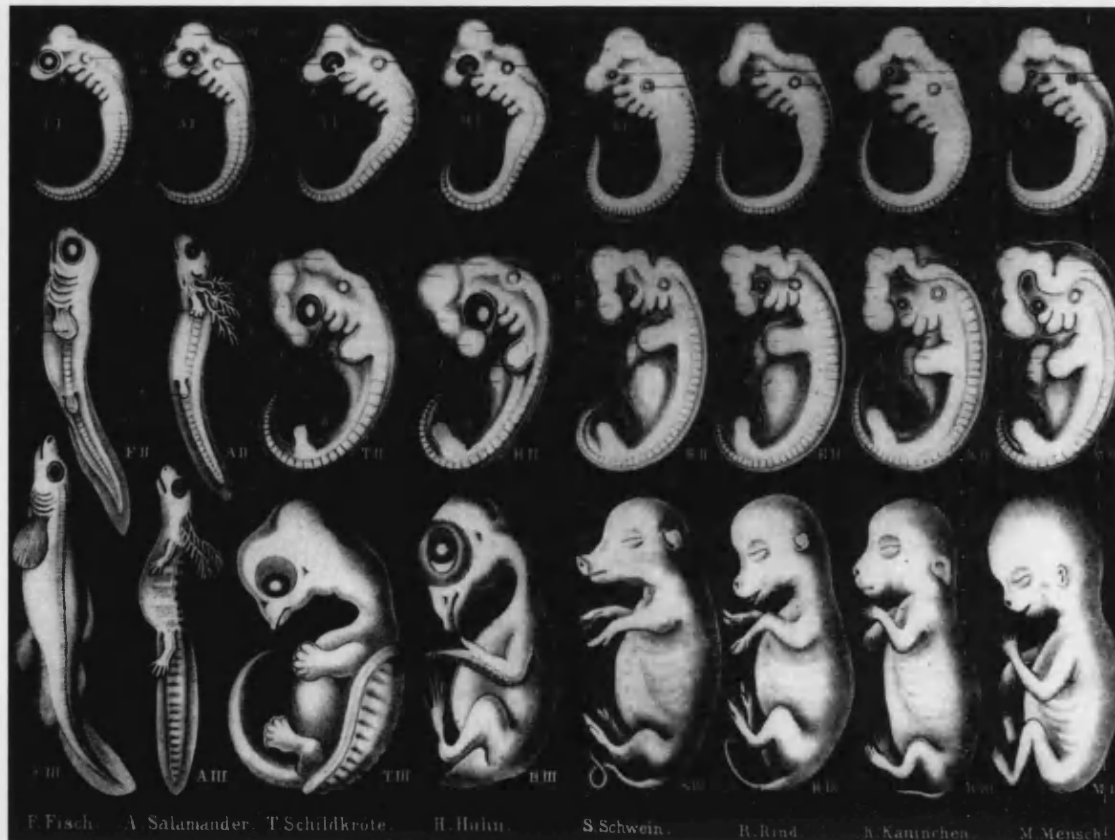


Fig. 1.6 **The vertebrate phylotypic stage.** Plates 4 and 5 from 18917d.25 by Haeckel, 1874; Bodleian Library, University of Oxford. Three different stages in the development of a species are depicted from top to bottom; the organisms are, from left to right: fish, salamander, turtle, chicken, pig, cow, rabbit and human. The top row represents a stage at which the vertebrate body plan is clearly discernable and analogous between different species. Reproduced from Richardson *et al.*, 1997.

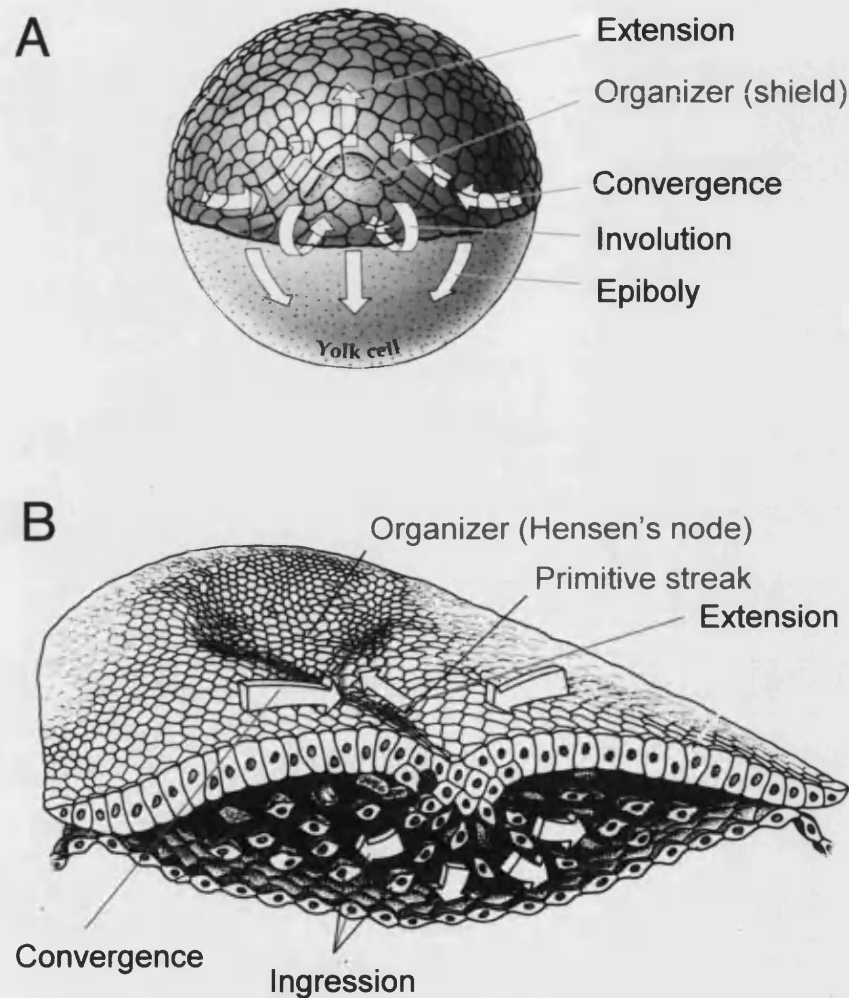


Fig. 1.7 Morphogenetic movements during vertebrate gastrulation. **A**, Schematic of zebrafish gastrulation movements; **B**, Schematic of chick gastrulation movements. In black are written the name of the gastrulation movements whereas in grey are labelled the organizer and primitive streak. Gastrulation movements are analogous throughout the Vertebrata but are particularly similar between fish and frog, and between chick and mouse. Epiboly is less prominent in the frog than in the fish since there is no acellular yolk to cover up with blastoderm. In mouse, gastrulation movements take place in a cupped-shape embryo rather than in a flat one as in chick. Adapted from Walbot and Holder, 1987, and Gilbert and Raunio, 1997. See text for description.

Epiboly also occurs in frog embryos although they have no EVL or YSL. Frog epiboly is thought to be driven entirely by radial intercalation (Keller, 1980). Whether epiboly occurs in avians and mammals is a topic of debate. Those that advocate epiboly in avians consider it to be driven by a ring of cells called the zone of juncture, which outlines the *zona opaca*, that move in an analogous way to the YSL (Arendt and Nubler-Jung, 1999); in mammals, trophoctoderm expansion has been suggested to be the homologous morphogenetic movement to epiboly but is not at all clear whether these two cell movements are evolutionarily related (reviewed in Kane and Adams, 2002).

1.3.4 Cell internalisation

At approximately 50% epiboly in zebrafish, another morphogenetic movement is initiated. Mesendodermal cells at the blastoderm margin move inward ultimately to form the bilayered structure known as the germ ring (Fig. 1.7 A, Involution). The inner layer is called the hypoblast while the outer layer is called the epiblast. There is a temporary pause in epiboly as the inward movement begins but once epiboly resumes new cells at the blastoderm rim become specified as mesendoderm and become internalised (reviewed in Kimmel *et al.*, 1995; Solnica-Krezel *et al.*, 1995; Kane and Adams, 2002). It is unclear whether hypoblast formation in teleosts involves the coordinate internalisation of a sheet of cells – involution – or whether it results from the independent internalisation of individual cells – ingression (reviewed in Kane and Adams, 2002). Traditionally, the movement has been called involution and it is homologous to that of amphibians.

In frogs, gastrulation starts by the appearance of the so-called bottle cells, a group of cells whose apical constriction and invagination generates the blastopore lip (Rhumbler, 1902). Morphological analyses, however, suggest that initiation of gastrulation movements takes place in the deep marginal zone rather than in the superficial layer, of which the bottle cells are part (Keller, 1981). Prospective endoderm is moved inside, just beneath the blastocoel roof, pulled by the deep mesodermal cells, forming a cavity called the archaenteron. As involution proceeds, mesodermal precursors are also pulled inside the embryo, between the forming endoderm and ectoderm. Cells of the dorsal-most marginal zone involute first, followed by lateral and ventral marginal cells.

In both chicken and mouse the homologous movement involves an epithelial-to-mesenchymal transition of epiblast cells, which individually internalise at the primitive streak (Fig. 1.7 B, Ingression). This is called ingression and as it takes place endoderm displaces the hypoblast or VE and mesoderm moves between the epiblast and the hypoblast or VE. As cells delaminate, they move laterally, making way for newly ingressing cells. The streak elongates in an anterior direction as new cells ingress in its most anterior portion. The anterior tip of the streak becomes morphologically distinct, forming in chick a circular thickening of cells called Hensen's node and in mice a bilayered depression known as the node. At this stage, node-derived cells give rise to the axial mesendoderm structures, notochord and prechordal plate. In mice, some cells emerge proximally from the posterior of the streak, which become extraembryonic mesoderm; cells emerging from the intermediate streak form lateral plate and paraxial mesoderm. Eventually, in both chicken and mice, the node starts to regress, moving in an anterior-to-posterior direction, depositing somitic, intermediate and lateral mesodermal precursors (reviewed in Hogan *et al.*, 1994; Bellairs and Osmond, 1998; Beddington and Robertson, 1999; Gilbert, 2000).

1.3.5 Convergence and extension

In the zebrafish, germ-ring cells in both the hypoblast and the epiblast converge to the future dorsal side of the embryo, forming a local thickening called the embryonic shield, which is the dorsal organizer (Fig. 1.7 A, Convergence). As with frog embryos, while cells converge towards the midline they undergo medio-lateral intercalation. This results in the extension of the embryo along the antero-posterior axis, perpendicular to the movement of individual cells (Fig. 1.7 A, Extension). This coordinated cell movement is denominated convergence-extension (reviewed in Gilbert, 2000; Sive *et al.*, 2000). Convergence-extension is thought to occur also in birds and mammals, although being rather more difficult to visualise directly given the small size of gastrula-stage cells in these Classes of organisms (Fig. 1.7 B, Convergence and Extension).

With organizer formation and convergence-extension, the dorso-ventral and antero-posterior axes as well as, consequently, the left-right embryonic axis, are defined.

1.3.6 Mouse embryo turning

The cup-shaped mouse embryo is unusual, even among mammalian embryos, in that the endoderm is formed on the outside and the ectoderm on the inside. Following gastrulation, at 8.5 dpc, this tissue topology is reversed to the normal endoderm-on-the-inside, ectoderm-on-the-outside by the process of turning (see Kaufman, 1992 for figure and description).

1.4 Early molecular events in vertebrate axes specification and germ-layer formation

In the previous sections, attention was focused on the dynamics of embryonic morphogenesis, highlighting regions or tissues responsible for early pattern generation. In this section I will review our understanding of the molecular basis of those early morphogenetic and patterning events, which lead to dorsoventral and antero-posterior axes specification. Due to space restrictions I will not touch upon the issue of left-right specification. At the same time as the embryonic axis become specified, the internal germ layers, mesoderm and endoderm, are formed, and cells of the ectoderm commit to either an epidermal or a neural fate. The molecular cues underlying mesoderm, endoderm and neural induction will be discussed but, again owing to space restrictions, I will not dwell upon molecular interactions between the formed germ-layers nor upon fine patterning within them. Although aiming for a comparative review, due to the extent of the literature, I emphasise zebrafish and mouse studies as they are the basis of the work described in this thesis, but I also make frequent reference to frog research as much of our understanding draws from it.

1.4.1 Maternal dorsal determinants are present in fish and frog

Embryological experiments in frog and fish reveal the existence of vegetal-located maternal patterning cues that move dorsally where they impart dorsal character to this region of the embryo. Teleost and amphibian eggs do contain vegetally localised maternal mRNAs and proteins. In frog, these include *Vgl* mRNA and protein, *VegT / Antipodean / Xombi / Brat* mRNA and Dishevelled (Dsh) protein (Melton, 1987; Tannahill and Melton, 1989; Dale *et al.*, 1989; Kloc *et al.*, 1993; Ku and Melton, 1993;

Stennard *et al.*, 1996; Zhang and King, 1996; Lustig *et al.*, 1996; Miller *et al.*, 1999; Wessely and De Robertis, 2000).

Vg1, a member of the Transforming Growth Factor β (TGF β) superfamily of growth factors, was the first molecule associated with Nieuwkoop activity. Vg1 protein is synthesised as an inactive precursor that is cleaved into a mature, active, form that can completely rescue UV-ventralised embryos (Thomsen and Melton, 1993), induce secondary axes when overexpressed (Dale *et al.*, 1993) and induce dorsal mesoderm in animal pole explants (animal caps) (Thomsen and Melton, 1993; Dale *et al.*, 1993; Kessler and Melton, 1995). Expression of mutant Vg1 ligands impairs normal endodermal development and dorsal mesoderm induction *in vivo* (Joseph and Melton, 1998). A true loss-of-function of Vg1 has not been reported. Vg1 is not the endogenous dorsal determinant, however. Firstly, Vg1 remains vegetal throughout cleavage stages, rather than becoming dorsally restricted, as does the Nieuwkoop activity. Secondly, endogenous mature Vg1 protein remains to be detected in embryos (Tannahill and Melton, 1989; Dale *et al.*, 1989).

VegT, a member of the T-box family of transcriptional regulators, is not the endogenous dorsal determinant either since it is not able to induce a secondary axis in embryos when overexpressed (Stennard *et al.*, 1996). At low doses VegT can induce endoderm as well as ventral mesoderm, and at high doses it can induce pan-mesodermal markers (Stennard *et al.*, 1996; Lustig *et al.*, 1996; (Horb and Thomsen, 1997)). VegT antisense-depleted embryos lack endoderm (Zhang *et al.*, 1998a). Given that VegT is a transcription factor, lack of VegT protein is presumed to be manifest after the onset of zygotic transcription, at MBT. Indeed, VegT depleted embryos do develop normally up to blastula stage in morphology and timing (Zhang *et al.*, 1998a). Yet, there is an earlier effect of VegT mRNA depletion: it causes dispersion of vegetal mRNAs, namely that of *Vg1*, implicating it in vegetal transcript localisation (Heasman *et al.*, 2001). This effect is specific to the loss of mRNA and not protein since injection of an antisense morpholino oligonucleotide (MO) against VegT does not cause transcript dispersion (Heasman *et al.*, 2001).

The closest zebrafish homologue of *VegT* is the *T-box-containing gene 16* (*Tbx16*), also called *spadetail*, *spt* (Ruvinsky *et al.*, 1998; Griffin *et al.*, 1998). Expression of

spadetail is only zygotic and mutant analysis also dismisses it as implicated in early dorso-ventral patterning. No T-box gene with an analogous role to *VegT* has been identified in other classes of vertebrates.

Following cortical rotation in frog, Dsh, as well as two other intracellular components of the Wnt signalling pathway that are initially evenly distributed, β -catenin and glycogen synthase kinase 3 β (Gsk3 β), become differentially enriched dorso-ventrally. Dsh and β -catenin are displaced dorsally (Larabell *et al.*, 1997; Rowning *et al.*, 1997; Miller *et al.*, 1999) whereas Gsk3 β , a negative regulator of β -catenin, is depleted dorsally (Dominguez and Green, 2000). The timing, location and magnitude of Gsk3 β depletion are coincident with those of endogenous β -catenin accumulation (Dominguez and Green, 2000). Blocking cortical rotation by UV-irradiation results in vegetal pole accumulation of nuclear β -catenin (Schneider *et al.*, 1996; Larabell *et al.*, 1997) and abolishes dorsal depletion of Gsk3 β (Dominguez and Green, 2000). Overexpression of *Dsh* or *β -catenin* in *Xenopus* embryos induces a complete secondary axis (Sokol *et al.*, 1995; Funayama *et al.*, 1995) and so does expression of dominant-negative *Gsk3 β* (Dominguez *et al.*, 1995; Pierce and Kimelman, 1995; He *et al.*, 1995; Kimelman and Pierce, 1996).

What has proved difficult to determine is which is/are the endogenous dorsal determinant(s), since the assays through which dorsal activity has been demonstrated are usually quite artificial. There are molecules other than those mentioned that can dorsalise the embryo when overexpressed but which are ruled out as endogenous dorsalising factor(s) given that they are not expressed at the right time and/or place. This is the case for the homeobox transcriptional regulators Goosecoid (Gsc) and Siamois, as well as the secreted molecules Activin β B, Noggin, Wnt1, Wnt2b, Wnt8 and Wnt8b (McMahon and Moon, 1989; Thomsen *et al.*, 1990; Cho *et al.*, 1991; Sokol *et al.*, 1991; Smith and Harland, 1991; Smith and Harland, 1992; Cui *et al.*, 1995; Lemaire *et al.*, 1995; Landesman and Sokol, 1997). Then, there are maternal molecules that are widespread throughout early development and that when overexpressed also induce a secondary axis. Examples include the *Xenopus* homologue of the mammalian immunosuppressant *Fkbp* (Nishinakamura *et al.*, 1997), the protooncogene homologue *Xski* (Amaravadi *et al.*, 1997) as well as Smad7 and Smad8, intracellular transducers of signalling by Bone Morphogenetic Proteins (BMPs) (Casellas and Brivanlou, 1998; Nakayama *et al.*, 1998).

Highlighting the caution with which overexpression results should be interpreted, the ability of ectopic Smad7 to dorsalise *Xenopus* embryos is concentration-dependent. Xsmad7 acts as a dorsalising factor when overexpressed at moderate levels and represses endogenous axis formation when overexpressed at higher levels (Casellas and Brivanlou, 1998). Loss-of-function experiments provide the only strong assessment of the requirement of a molecule for a given process. Depletion of β -catenin with antisense oligonucleotides blocks the formation of the endogenous dorsal axis in *Xenopus* embryos (Heasman *et al.*, 1994; Heasman *et al.*, 2000). This established β -catenin as the earliest dorsal determinant known.

Gain and loss of β -catenin function in other organisms corroborate the notion that it is conserved as an early dorsal determinant in vertebrates. In zebrafish, dorsal nuclear β -catenin is first seen in the YSL but is soon followed by the dorsal blastomeres (Schneider *et al.*, 1996). What causes dorsal accumulation of β -catenin in zebrafish is not known but it presumably is the unknown vegetal-located dorsal determinant postulated by embryological experiments. Overexpression of β -catenin also induces a secondary axis in zebrafish (Kelly *et al.*, 1995). In the pre-streak chick embryo, β -catenin protein starts by being present in a radially symmetric fashion. Nuclear β -catenin is found all around the blastoderm, in the area opaca and marginal zone, and cytoplasmic but not nuclear β -catenin is found in the central part of the blastoderm (Roeser *et al.*, 1999). However, with the formation of Koller's sickle and the hypoblast, preceding streak formation and expression of organizer genes, cells containing nuclear β -catenin accumulate in the midline directly anterior of the sickle (Izpisua-Belmonte *et al.*, 1993; Ruiz i Altaba *et al.*, 1995; Streit *et al.*, 1998; Roeser *et al.*, 1999). Ectopic expression of processed cVg1 in chick embryos only results in secondary axis induction when it overlaps with the domain of nuclear β -catenin expression (Shah *et al.*, 1997). β -catenin-null mouse embryos fail to form the antero-posterior axis by 5.5 dpc. They retain the bilayered structure of the early egg-cylinder, with correct proximal-distal polarity, but simply continue to grow rather than undergoing morphogenetic change. These embryos never express primitive streak and mesoderm markers and no mesoderm or head structures are generated (Haegel *et al.*, 1995; Huelsken *et al.*, 2000). Concordantly, mouse embryos mutant for *Axin / Fused*, which encodes a protein that promotes β -catenin degradation, develop axial duplications (Zeng *et al.*, 1997).

1.4.2 Downstream of β -catenin

Since β -catenin is the earliest endogenous dorsal determinant known, a major issue in understanding dorsal specification is the identity of its targets, in cooperation with the high mobility group (HMG) transcription factors of the lymphoid enhancer factor (LEF) / T-cell factor (TCF) family (Behrens *et al.*, 1996; Huber *et al.*, 1996; Molenaar *et al.*, 1996; Miller and Moon, 1996; He *et al.*, 1998; Tetsu and McCormick, 1999; reviewed in Polakis, 1999; Daniels *et al.*, 2001).

In *Xenopus*, β -catenin directly promotes transcription of the organizer genes *Siamois* and *Twin* (Heasman *et al.*, 1994; Kelly *et al.*, 1995; Brannon and Kimelman, 1996; Wylie *et al.*, 1996; Carnac *et al.*, 1996; Brannon *et al.*, 1997; Fagotto *et al.*, 1997; Laurent *et al.*, 1997). *Siamois* and *Twin* are homeodomain-containing transcriptional activators that are structurally closely related and expressed in a similar manner, in dorsal vegetal and equatorial cells shortly after MBT. They are likely to control the same target genes and to be functionally redundant (Lemaire *et al.*, 1995; Carnac *et al.*, 1996; Brannon and Kimelman, 1996; Brannon *et al.*, 1997; Fan and Sokol, 1997; Kessler, 1997; Laurent *et al.*, 1997). Overexpression of dominant-negative *Siamois* suggests requirement of the endogenous protein for axis formation (Fan and Sokol, 1997; Kessler, 1997) but no loss-of-function of *Siamois* nor that of *Twin* has yet been reported.

No *Siamois* or *Twin* orthologues have been identified in other species although functionally analogous genes may exist. In zebrafish, another homeobox-containing gene called *bozozok* (*boz*) / *dharma* / *nieuwkoid* (Solnica-Krezel *et al.*, 1996) is a direct target of β -catenin. The *boz* gene is expressed at the sites of β -catenin accumulation, that is, dorsal YSL and dorsal blastomeres (Koos and Ho, 1998; Yamanaka *et al.*, 1998), its expression follows that of β -catenin when the latter is enhanced or reduced artificially (Ober and Schulte-Merker, 1999; Shimizu *et al.*, 2000; Yamanaka *et al.*, 1998) and is dependent on TCF binding sites (Ryu *et al.*, 2001). However, unlike *Siamois* or *Twin*, which can induce complete secondary axes in *Xenopus* (but not in zebrafish, Sumoy *et al.*, 1999), overexpression of *boz* in zebrafish has weak axis-inducing activity (Lemaire *et al.*, 1995; Koos and Ho, 1998; Yamanaka *et al.*, 1998). Also unlike *Siamois* or *Twin*, *boz* is a transcriptional repressor (Solnica-Krezel and

Driever, 2001). The *boz* mutation has variable penetrance and expressivity but even strong mutants, which lack prechordal plate and notochord as well as having a variety of head defects, have a less severe phenotype than β -catenin-depleted embryos and possess some organizer activity since a neural axis is induced (Fekany *et al.*, 1999; reviewed in Solnica-Krezel and Driever, 2001). No *boz* orthologues have been identified in other species.

The expression pattern of *boz* and its function directly downstream of β -catenin implicate Boz as a component of the Nieuwkoop centre (Solnica-Krezel and Driever, 2001). As such, Boz should promote the expression of organizer genes, even if, as a transcriptional repressor, it does so by antagonising ventral genes (reviewed in Solnica-Krezel and Driever, 2001; Schier, 2001). This is indeed the case, as seen by altered gene expression in *boz* mutants. According to how their expression is affected in *boz* embryos, genes can be grouped into one of four classes (Solnica-Krezel, 2001 #538}. The expression of most organizer genes is reduced or eliminated from blastula throughout gastrulation in *boz* embryos. These include the transcriptional regulators *goosecoid* (*gsc*), *floating-head* (*flh*, the zebrafish orthologue of *Xnot*, Talbot *et al.*, 1995), *lim1* and *foxa2 / hmf3 β* (called *axial* in zebrafish, Strahle *et al.*, 1993), and the secreted BMP antagonist *noggin1* (Solnica-Krezel *et al.*, 1996; Fekany *et al.*, 1999; Koos and Ho, 1999; Sirotkin *et al.*, 2000a). There are organizer genes whose expression is more severely reduced at blastula and early gastrula stages than at late gastrula stages. This is the case for another BMP antagonist, *chordin* (*chordino*, *din*, in zebrafish, Schulte-Merker *et al.*, 1997; Koos and Ho, 1999; Shimizu *et al.*, 2000; Fekany-Lee *et al.*, 2000). There are organizer genes whose induction is independent of Boz but whose maintenance during gastrulation depends on Boz. These include the two zebrafish nodals, called *squint* (*sqt*) and *cyclops* (*cyc*) (Feldman *et al.*, 1998; Sampath *et al.*, 1998), members of the TGF β superfamily of proteins, as well as the gene coding for the Wnt antagonist *dkk1* (Sampath *et al.*, 1998; Hashimoto *et al.*, 2000; Shimizu *et al.*, 2000; Sirotkin *et al.*, 2000a). Finally, there are nonaxial mesoderm genes whose absence from the dorsal side of the embryo also depends upon Boz. These include the secreted factors *bmp2b* (*swirl*, *swr*, in zebrafish, Kishimoto *et al.*, 1997) and *bmp4*, consistent with Boz induction of Bmp antagonists mentioned above, and *wnt8*, as well as the transcription regulators *tbx6* and *tbx16 / spt* (Griffin *et al.*, 1998), *vox* and *vent* (Koos and Ho, 1999; Fekany-Lee *et al.*, 2000; Melby *et al.*, 2000). Surprisingly,

though, *bmp2b* has a small domain of expression in the organizer (Kishimoto *et al.*, 1997), whose function is not known.

So, a main strategy employed by the organizer to promote dorsal fates involves inhibition of ventral fates. This is accomplished by direct inhibition of *bmp* genes, promotion of the expression of Bmp antagonists, as well as by direct inhibition of *wnt* genes and promotion of the expression of genes coding for Wnt antagonists (Fig. 1.8). In addition to *Dkk1*, Wnt signalling antagonists in the organizer include *Frzb*, a secreted molecule which competes with the structurally similar Wnt receptors (Frizzled, Fz) sequestering Wnts (Leyns *et al.*, 1997; Moon *et al.*, 1997; Wang *et al.*, 1997), and Cerberus, a secreted cysteine knot superfamily member that multivalently binds to Nodals, BMPs and Wnts, antagonising their activity (Bouwmeester *et al.*, 1996; Piccolo *et al.*, 1999).

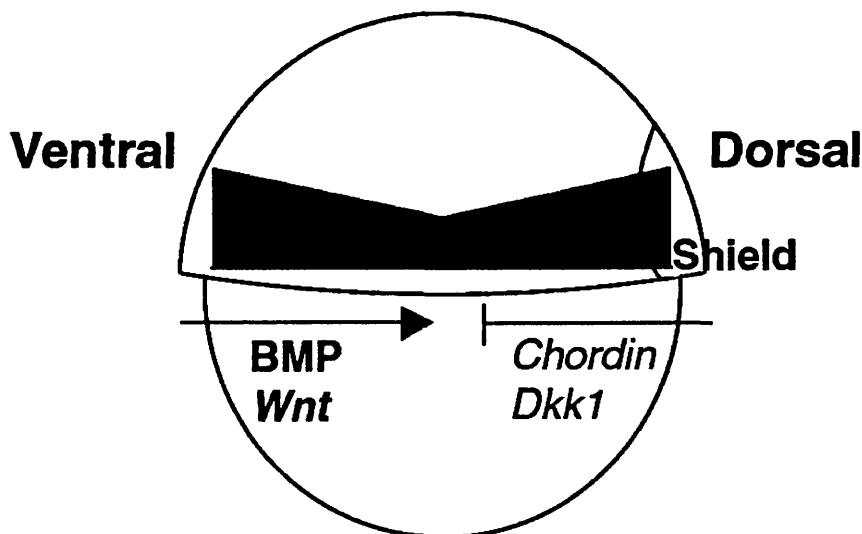


Fig. 1.8 One strategy employed by the organizer to promote dorsal fates is to inhibit ventralising activities. Schematic of a zebrafish embryo at gastrula stage. BMP and Wnt signals from the ventral side of the embryo are antagonised by factors expressed within the shield region. Thus, a gradient of signals is created, allowing varying fates to be specified in an activity-level dependent fashion. Picture kindly provided by K. A. Thomas.

Another theme in organizer formation is that the genes downstream of β -catenin are subject to complex regulation. A complex regulatory network might reflect the distinction between induction and maintenance phases of gene expression but it probably also accounts for the high redundancy observed between organizer gene functions, making gastrulation a very well protected process.

1.4.3 Mesoderm induction

The immediate steps in the genetic cascade downstream of β -catenin appear to be evolutionarily very plastic. However, these divergent steps soon converge, as most organizer genes are conserved throughout vertebrate classes. This is in accordance with the results of heterospecific transplantation experiments, which have long suggested evolutionary conservation of the signals that emanate from the organizer and induce axis formation (Oppenheimer, 1936b; Kintner and Dodd, 1991; Blum *et al.*, 1992; Hatta and Takahashi, 1996; Knoetgen *et al.*, 1999; Knoetgen *et al.*, 2000). A molecular pathway that is at the pivotal point of convergence in organizer formation is the Nodal signalling pathway (Fig. 1.9). Nodals are involved in both of the organizer main functions: dorsal specification and induction of the internal germ-layers, mesoderm and endoderm (reviewed in Harland and Gerhart, 1997; Heasman, 1997).

Xenopus blastulae animal pole explants (animal caps) differentiate into ectodermal derivatives in the absence of growth factors. However, in combination with vegetal explants, mesoderm is induced at the interface between the two. One manifestation of mesoderm induction is animal cap extension, due to convergence and extension-like movements that can occur *in vitro*. The first protein shown to be able to induce mesoderm (blood and muscle) was a member of the Fibroblast Growth Factor (FGF) family (Slack *et al.*, 1987), which is enhanced in its muscle-inducing activity by TGF β (Kimelman and Kirschner, 1987). Pursuit of endogenous members of these growth factor families followed, in search for the endogenous mesoderm inducer(s). These studies led to the identification of the already-mentioned Vg1 as well as Activin, another member of the TGF β superfamily (Smith *et al.*, 1990; van den Eijnden-Van Raaij *et al.*, 1990; Thomsen *et al.*, 1990; Thomsen and Melton, 1993; Dale *et al.*, 1993; Kessler and Melton, 1995).

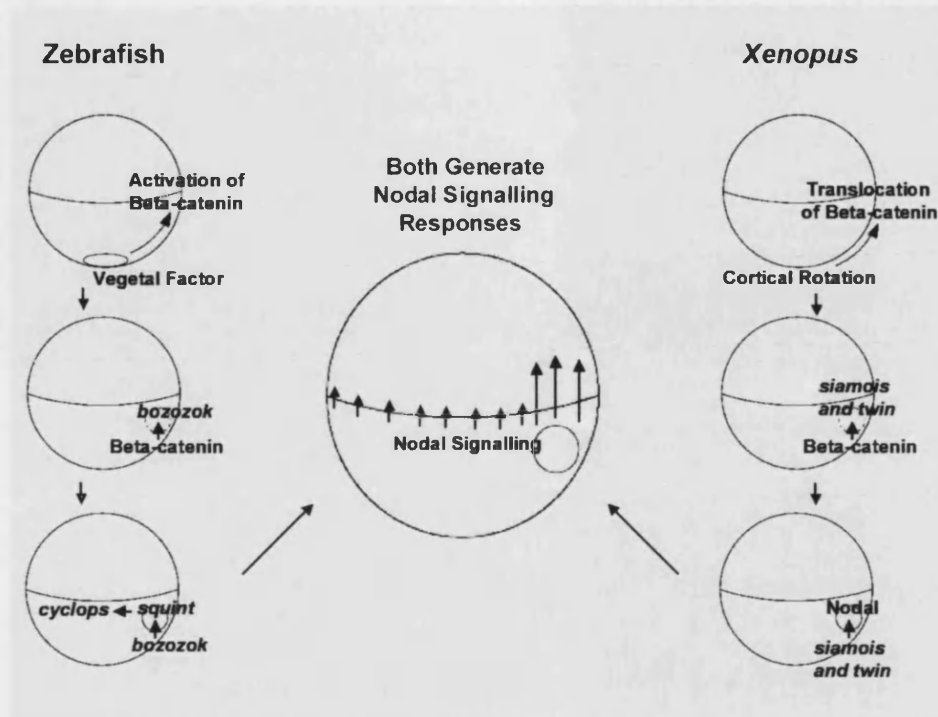


Fig. 1.9 In vertebrates, early dorsalising signals act through β -catenin and converge in the activation of the Nodal pathway. Schematics of pre-gastrula fish and frog embryos, where β -catenin is the earliest dorsal determinant known. Early β -catenin target genes are divergent between the two classes of animals (*bozozok* in zebrafish; *Siamois* and *Twin* in *Xenopus*) but produce the same outcome of inducing the Nodal signalling pathway. Picture kindly provided by K. A. Thomas.

Activins signal by binding to one of two so-called type II receptors, ActRIIA and ActRIIB, which then heterodimerise with and phosphorylate one of the so-called type I receptors / Activin receptor-Like Kinases, ALK1, 4 or 5, responsible for the activation of downstream transducers (reviewed in Moustakas *et al.*, 2001). Overexpression of dominant-negative Activin in fish as well as dominant-negative (truncated) forms of Activin receptors blocks mesoderm formation in *Xenopus* (Hemmati-Brivanlou and Melton, 1992; Schulte-Merker *et al.*, 1994; Wittbrodt and Rosa, 1994; Dyson and Gurdon, 1997; Chang *et al.*, 1997). Targeted disruption of murine *ALK4* results in egg-cylinder disorganisation and arrest prior to gastrulation (Gu *et al.*, 1998). Chimeric analysis shows that *ALK4*-null ES cells can contribute to mesoderm suggesting that *ALK4* is not essential for mesoderm induction (Gu *et al.*, 1998). Nonetheless, primitive streak formation is impaired in these chimeras (Gu *et al.*, 1998). Disruption of *ActRIIA*

results in late skeletal and endocrinological phenotypes, and that of *ActRIIB* results in antero-posterior defects at segmentation stages as well as laterality defects (Matzuk *et al.*, 1995a; Oh and Li, 1997). Composite *ActRIIA* and *ActRIIB* mutants, however, arrest at egg-cylinder stage but chimeric analysis showing requirement for these receptors for mesoderm formation was not reported (Song *et al.*, 1999). A role for Activin as the endogenous mesoderm inducer was questioned mainly by the fact that mice mutant for both *Activin β A* and *Activin β B* undergo unperturbed gastrulation, forming mesoderm normally (Matzuk *et al.*, 1995b). The accumulating disparate evidence concerning the role of Activins as endogenous mesoderm inducers was resolved by the finding that other molecules signal through the Activin receptors. This is the case for Vg1 and Nodals (Schulte-Merker *et al.*, 1994; Yamashita *et al.*, 1995; Hemmati-Brivanlou and Thomsen, 1995; Meno *et al.*, 1999).

Nodal was first identified in the mouse by positional cloning of a mutation that results in lack of a primitive streak and near-total depletion of mesoderm (Zhou *et al.*, 1993; Conlon *et al.*, 1994). In the mouse, chimeras can be generated with embryonic and extraembryonic tissues of different genotypes. This is possible because when ICM-derived, embryonic stem (ES), cells are injected into a blastocyst they mainly populate the ICM, from which the embryo-proper is derived, and not the extraembryonic tissues (Beddington and Robertson, 1989). This allowed the demonstration that it was lack of Nodal signalling in the epiblast, and not in the VE, that was required for primitive streak formation (whereas lack of Nodal signalling specifically in the VE led to impairment of antero-posterior development, Varlet *et al.*, 1997; see section below). In zebrafish, while mutants for either *cyc* or *sqt* have some mesodermal defects, *cyc;sqt* double mutants lack all head and trunk mesoderm as well as endoderm (Hatta *et al.*, 1991; Heisenberg and Nusslein-Volhard, 1997; Feldman *et al.*, 1998).

The phenotype of *cyc;sqt* double mutant fish is identical to that of maternal and zygotic (MZ) mutant embryos for the Nodal co-receptor, One-eyed pinhead (Oep), related to mammalian Cripto and Cryptic, as well as to the *Xenopus* FGF Receptor Ligand 1 (FRL-1) (Zhang *et al.*, 1998b; Gritsman *et al.*, 1999). Oep is essential for Nodal signalling in fish since overexpression of Nodals in MZ-*oep* embryos has no effect (Gritsman *et al.*, 1999). *Cripto*-null mouse embryos fail to form a streak and are totally devoid of embryonic mesoderm and endoderm (Ding *et al.*, 1998). However, in

contrast with what is observed in fish, *Cripto* loss-of-function does not phenocopy *Nodal* loss-of-function in the mouse. Mouse *Cryptic*, despite being expressed in the node, axial mesendoderm, and nascent mesoderm (Shen *et al.*, 1997), is not essential for the establishment of the antero-posterior and dorso-ventral axes (but it is required for normal left-right development; Gaio *et al.*, 1999).

In *Xenopus*, Nodals signal through ActRIIA and B, and specifically through ALK4 / ActRI β and ALK7 (reviewed in Whitman, 2001; Oh *et al.*, 2002). The phenotype of mouse embryos depleted from both type II receptors, as well as that of *ALK4*-null embryos, was discussed above. Depletion of ALK4 / TARAM-A (Tar; Renucci *et al.*, 1996) in zebrafish has not been reported but TARAM-A can rescue some phenotypes of *oep* embryos, suggesting the existence of ALK4-dependent and ALK4-independent Nodal signalling (Peyrieras *et al.*, 1998).

Nodal signalling is transduced intracellularly by the ubiquitously-expressed members of the Smad family of transcriptional regulators (reviewed in Moustakas *et al.*, 2001). Smads can also mediate BMP signalling but the only Smad thought to be common to the two pathways is Smad4, which oligomerises with Smads specific for either Nodal or BMP signalling (reviewed in Moustakas *et al.*, 2001). The Nodal-specific Smad mediators are Smad2 and 3 that, after being directly phosphorylated by active type I receptors (R-Smads), can oligomerise with Smad4, translocate into the nucleus and act as transcriptional regulators (reviewed in Whitman, 2001). Mouse embryos devoid of *Smad2* fail to form a streak and any embryonic mesoderm (Nomura and Li, 1998; Waldrip *et al.*, 1998; Weinstein *et al.*, 1998). In contrast to *Nodal*-null embryos, however, *Smad2*-null embryos express many dorso-posterior markers, some of which are even expanded (Brennan *et al.*, 2001). *Smad3*-null mice do not present an early embryonic phenotype (Zhu *et al.*, 1998; Datto *et al.*, 1999). *Smad4*-null embryos have reduced cell proliferation, which results in growth retardation, do not express mesodermal markers, do not gastrulate and show abnormal VE development (Sirard *et al.*, 1998). However, chimeras in which the epiblast is mainly of the *Smad4*-null genotype and the VE is wild-type have restored mesoderm formation (Sirard *et al.*, 1998). Although disruption of *Smad4* impairs both Nodal and BMP signalling, this analysis allows for some reflection on Nodal signalling. *Nodal* is required in the epiblast for mesodermal gene expression (Varlet *et al.*, 1997) but neither *Smad2*, 3 or 4

are required in the epiblast for that gene expression (Sirard *et al.*, 1998; Zhu *et al.*, 1998; Datto *et al.*, 1999; Brennan *et al.*, 2001). This suggests that these three Smads are not the only intracellular Nodal transducers, either there remaining other Smads to be identified or there being a Smad-independent mechanism of transducing Nodal signalling (reviewed in Whitman, 2001).

Context-specificity of Nodal signalling is conferred by the transcriptional partners of the Smads (reviewed in Derynck *et al.*, 1998; Massague and Wotton, 2000). The first of these to be identified and one that is important in the context of mesoderm formation is the winged helix transcriptional regulator FoxH1 / Fast, called *Schmalspur* in zebrafish (Huang *et al.*, 1995; Chen *et al.*, 1996; Labbe *et al.*, 1998; Pogoda *et al.*, 2000; Sirotkin *et al.*, 2000b; reviewed in Whitman, 2001). FoxH1 only activates transcription when associated with Smads and can form complexes with receptor-activated Smad2 or Smad3 (Labbe *et al.*, 1998; Yeo *et al.*, 1999). Deletion of the mouse *FoxH1* results in patterning defects of the anterior primitive streak and consequent failure to form the node, prechordal mesoderm, notochord and definitive endoderm (Hoodless *et al.*, 2001). The *schmalspur* mutant phenotype includes lack of floorplate, reduced prechordal plate and ventral forebrain defects (Brand *et al.*, 1996). However, this phenotype is not as strong as that of *cyc;sqt* or *MZoep* embryos, which means there are *schmalspur*-independent effectors of Nodal signalling. The mouse *FoxH1* phenotype is very similar to that of another member of the winged helix family of transcriptional regulator, that of *FoxA2* (formerly known as *Hnf3 β*) (Dufort *et al.*, 1998) and in fact, *FoxA2* expression is dependent upon FoxH1 (Hoodless *et al.*, 2001).

At least in zebrafish, Nodals can function as morphogens, that is, they can act directly in a concentration dependent manner over many cell diameters, generating different responses in cells with varying distance from the source of the signal. Thus, a point source of Nodal can activate Nodal-target genes in distant cells, even if the intervening cells are unable to transduce Nodal signals (Chen and Schier, 2001). This confirms that Nodals act directly and not via a relay mechanism whereby they induce local production of a second signal. Despite the sequence similarity between the Nodal ligands, *Cyc* and *Sqt*, it is only *Sqt* that has long-distance activity. In contrast, *Cyc* appears able to only activate gene expression in neighbouring cells. The biochemical basis of this difference in activity is not understood. It is likely that Nodals will function as morphogens in

other animals and indeed Gurdon and other workers have extensively documented how TGF β proteins can function in concentration dependent manner in *Xenopus* embryos (reviewed in McDowell and Gurdon, 1999).

Nodal signalling induces expression of both agonists (ligands) and antagonists, which restrict Nodal signalling in time and/or range. The divergent Lefty family of TGF β s antagonise Nodal signalling probably through competition for the same receptor (Meno *et al.*, 1999; Bisgrove *et al.*, 1999; Thisse and Thisse, 1999). Overexpression of *lefty1* or *lefty2* in zebrafish leads to a phenotype analogous to that of *cyc,sqt* double-mutants or MZ *oep* embryos (Meno *et al.*, 1999; Bisgrove *et al.*, 1999; Thisse and Thisse, 1999). Depletion of Lefty2 in zebrafish using MOs has no obvious phenotype whereas depletion of Lefty1 by the same means causes aberrations during somitogenesis, including laterality defects (Agathon *et al.*, 2001; Feldman *et al.*, 2002). Depletion of both Lefty1 and Lefty2 results in excess Nodal signalling, excess cell internalisation and excess mesoderm production at the expense of ectoderm (Feldman *et al.*, 2002). In mice, mutants for *Lefty2* have an enlarged streak and produce excess mesoderm whereas *Lefty1* mice produce mesoderm normally but present laterality defects (Meno *et al.*, 1998; Meno *et al.*, 1999). The phenotype of *Lefty2*-null mice can be partially rescued by reducing Nodal levels through heterozygosity (Meno *et al.*, 1999). Another Nodal antagonist is Cerberus but deletion of the mouse *Cerberus* orthologue, *Cerberus-like* or *Cerberus-related*, results in no obvious phenotype (Simpson *et al.*, 1999; Shawlot *et al.*, 2000; Belo *et al.*, 2000).

Mouse *Nodal* embryos, as well as fish *cyc,sqt* double-mutants and MZ-*oep* mutants still form posterior mesoderm (Conlon *et al.*, 1994; Feldman *et al.*, 1998; Gritsman *et al.*, 1999). This means that another, as yet uncharacterised, mesoderm inducing factor exists. Candidate molecules for posterior mesoderm inducing signals are FGFs and BMPs (reviewed in Altmann and Brivanlou, 2001).

1.4.4 Endoderm induction

Endoderm formation is tightly coupled to that of mesoderm, both in time and space. In addition, in all vertebrate classes at least a portion of the endoderm and mesoderm are specified initially as a common progenitor population, which has been named mesendoderm (reviewed Shivdasani, 2002). Impairment of endoderm formation often

results in mesoderm expansion and, conversely, endoderm expansion occurs mainly at the expense of mesoderm (Henry and Melton, 1998; Yasuo and Lemaire, 1999; Kikuchi *et al.*, 2001). It is therefore not surprising that some of the molecules implicated in the induction of the two internal germ-layers appear to be shared by the two processes, namely the Nodal signalling pathway.

In the frog, the molecule thought to be at the top of the molecular cascade directing formation of endoderm is the maternal T-box-containing transcriptional regulator VegT. VegT transcripts are localised in the vegetal hemisphere of the egg and early frog embryo and this corresponds to the prospective endoderm (Lustig *et al.*, 1996; Stennard *et al.*, 1996; Zhang and King, 1996; Horb and Thomsen, 1997). When ectopically expressed in animal caps, VegT can induce endoderm (Horb and Thomsen, 1997) and frog embryos depleted of VegT totally lack endoderm as well as most mesoderm (Zhang *et al.*, 1998a; Xanthos *et al.*, 2001).

In other species, VegT-related genes with an equivalent function in endoderm induction have not been found. In zebrafish, *Tbx16 / spt* is only expressed zygotically and although the existent *spt* mutations are likely to be null alleles, *spt* embryos form endoderm (Griffin *et al.*, 1998) and both *Tbx6* and *Eomesodermin* have been implicated in mesoderm rather than endoderm specification in zebrafish and mouse (Hug *et al.*, 1997; Chapman and Papaioannou, 1998; Russ *et al.*, 2000).

Downstream of VegT in the frog, mediation of endoderm induction by secreted factors is suggested by the observation that cellular disaggregation reduces induction of the endoderm markers *Sox17* and *Mix.1* in animal caps (Clements *et al.*, 1999; Yasuo and Lemaire, 1999). These secreted factors might be the Nodals, which are believed to be VegT targets (Hemmati-Brivanlou and Melton, 1994; McKendry *et al.*, 1997; Kofron *et al.*, 1999; Clements *et al.*, 1999; Osada and Wright, 1999; Yasuo and Lemaire, 1999; Hyde and Old, 2000; Chang and Hemmati-Brivanlou, 2000; Xanthos *et al.*, 2001). Furthermore, several endoderm markers lie downstream of Nodal signalling. This is the case for *Mix.2*, *Mixer*, *Sox17* and *Gata5*, which are FoxH1 targets.

Genetic analyses in zebrafish clearly implicate Nodal signalling in endoderm induction. Zebrafish *cyc; sqt* or MZ *oep* mutants lack all endoderm in addition to lacking nearly all

mesoderm (Feldman *et al.*, 1998; Gritsman *et al.*, 1999). In the mouse, several mutations in the Nodal signalling pathway cause developmental arrest at the egg-cylinder stage prior to primitive streak formation (see previous section). Although these results are consistent with a role of Nodal signalling in endoderm induction in mammals, these mutants have not been analysed specifically for this issue. This will require further studies on chimeric embryos and/or conditional targeted mutation analyses.

In agreement with Nodal signalling driving endoderm formation, expression of constitutively active *TARAM-A* in zebrafish causes marginal or central blastomeres to acquire an endodermal fate (Peyrieras *et al.*, 1998). However, constitutively active *TARAM-A* can also induce mesodermal fates (see above) and it is not clear what the local cues are that direct cells preferentially into one of the two responses by this one reagent (Renucci *et al.*, 1996). It has been suggested that dosage of Nodal signalling regulates the discrimination between endoderm and mesoderm in zebrafish embryos, where high levels of Nodal signalling are required for endoderm formation, lower levels being required for that of mesoderm (Schier *et al.*, 1997; Feldman *et al.*, 1998; Thisse and Thisse, 1999; Thisse *et al.*, 2000; Aoki *et al.*, 2002; reviewed in Warga and Stainier, 2002). Fate mapping shows that endoderm progenitors lie in the two most marginal tiers of cells whereas mesoderm progenitors extend further anteriorly, well in agreement with the action of *Sqt* as a morphogen (reviewed in Warga and Stainier, 2002). Zebrafish embryos mutant singly for *cyc*, *sqt* or zygotic *oep*, or expressing a dominant-negative *TARAM-A* have a greater loss of endoderm than of mesoderm (Schier *et al.*, 1997; Warga and Nusslein-Volhard, 1999; Aoki *et al.*, 2002). Furthermore, embryos overexpressing low levels of the Nodal antagonist *lefty1* are mainly depleted of endoderm and anterior mesoderm whereas those overexpressing high levels of *lefty1* are additionally depleted of the remainder of the mesoderm (Thisse *et al.*, 2000). Nonetheless, these effects could reflect a timing rather than a dosage issue given that the fates which are most affected by reduction of Nodal levels are also those adopted by the first cells to internalise (Thisse *et al.*, 2000; Aoki *et al.*, 2002).

Other zebrafish mutants that have impaired endoderm development turned out to contain mutations in genes that are targets of Nodal signalling. These consist of *casanova* (*cas*), a gene closely related to *Sox17* (Dickmeis *et al.*, 2001; Sakaguchi *et al.*,

2001; Kikuchi *et al.*, 2001), *bonnie and clyde* (*bon*), a *mixer*-like homeobox gene (Kikuchi *et al.*, 2000), and *faust* (*fau*), *gata5* (Reiter *et al.*, 1999).

All three genes, *cas*, *bon* and *fau*, initiate expression simultaneously at dome stage, where they are restricted to deep marginal cells. The extent of their expression differs in the vegetal-animal direction, with *bon / mixer* being the broadest and *cas* being expressed in only a subset of the *fau / gata5*-expressing cells. Whereas *fau*-expressing cells comprise endoderm and mesoderm progenitors, the subset that also express *cas* has been hypothesised to be the ones fated to become endoderm. All three genes are also expressed in the YSL during high and sphere stages (Alexander and Stainier, 1999; Dickmeis *et al.*, 2001}; Sakaguchi *et al.*, 2001; Kikuchi *et al.*, 2001).

Cas, Fau / Gata5 and Bon / Mixer occupy high positions in the pathway leading to endoderm formation, directly downstream of Nodal signalling (Poulain and Lepage, 2002). In zebrafish, expression of the genes coding for these transcription factors precedes that of other endoderm markers such as *sox17* and *axial / foxA2*, which are only expressed in internalised cells, and *gata4*, expressed only after gastrulation (Reiter *et al.*, 2001).

How do *fau*, *bon* and *cas* relate to each other in the genetic cascade that controls endoderm formation? Several lines of evidence suggest that *fau* and *bon* act in parallel. First, *fau* and *bon* are expressed in reciprocal mutants; second, the *fau;bon* phenotype is more severe than that of either single mutants, with the development of very little or no endoderm; third, *fau* overexpression can still lead to endoderm expansion in *bon* mutants (Reiter *et al.*, 2001). Whether *cas* acts in parallel to or downstream of *fau* and *bon* is still object of debate. On one hand, *cas* mutants fail to maintain *fau* expression but on the other hand they have normal *bon* expression (Alexander *et al.*, 1999). Furthermore, *fau* or *bon* overexpression has very little effect on *cas* mutants, as judged by *sox17* expression, arguing that Cas function lies between Fau and/or Bon and *sox17* but, then again, a few *sox17* cells are sometimes induced in these embryos (Alexander and Stainier, 1999; Reiter *et al.*, 2001). Finally, *cas* overexpression in *bon* or *fau* mutants leads to expansion of endodermal markers (Kikuchi *et al.*, 2001).

In the mouse a single member of the *Mix / Bix* family of homeobox genes is known. It is called (murine) *Mix-like1* (*Mixl1* or *Mml1*) and it is expressed in the VE, primitive

streak and nascent mesoderm of the early mouse embryo (Pearce and Evans, 1999; Robb *et al.*, 2000). *Mixl1*-null embryos display a variety of morphological defects and arrest at early somite stages. Significantly, however, the defects include absence of heart tube and gut, deficient paraxial mesoderm as well as an expansion of midline mesoderm; in addition, *Mixl1*-null cells can contribute to all embryonic structures but the hindgut (Hart *et al.*, 2002). Expression of early definitive endoderm markers such as *Cer1* and *Sox17* indicates that endoderm induction takes place but is severely reduced in *Mixl1*-null embryos (Hart *et al.*, 2002).

Murine *Gata5* is first expressed in the developing heart and subsequently in the lungs, vasculature and genitourinary system. *Gata5*-null mice are viable and fertile although females exhibit pronounced genitourinary abnormalities (Molkentin *et al.*, 2000). It is possible that another Gata factor assumes the role of fish *Gata5* in endoderm formation. There are six GATA factors in the mouse and these can be grouped into two classes according to their expression pattern and sequence. *Gata1* – *3* are expressed predominantly in hematopoietic cell lineages and are required for their differentiation; *Gata3* is also required for nervous system development (Pevny *et al.*, 1991; Tsai *et al.*, 1994; Pevny *et al.*, 1995; Pandolfi *et al.*, 1995; Ting *et al.*, 1996; Shivdasani *et al.*, 1997). *Gata4* – *6* are expressed in several distinct sites but all are expressed in the cardiovascular system (Arceci *et al.*, 1993; Kelley *et al.*, 1993; Laverriere *et al.*, 1994; Morrisey *et al.*, 1996; Morrisey *et al.*, 1997). *Gata4*-null mice die at 8 dpc from impaired ventral morphogenesis that prevents the formation of the heart tube (Kuo *et al.*, 1997; Molkentin *et al.*, 1997), whereas *Gata6* mutant embryos die before gastrulation from defects in the VE (Morrisey *et al.*, 1998; Koutsourakis *et al.*, 1999). Therefore, if a GATA factor is conserved throughout vertebrate evolution as an obligate player in endoderm formation, *Gata6* seems the strongest candidate but it might also be that two or more family members, especially of the *Gata4* – *6* subfamily, act redundantly in this process.

Sox17-null mouse embryos are specifically deficient in gut endoderm. Mid- and hindgut endoderm induction is greatly reduced and the few progenitors fail to expand whereas prospective foregut endoderm undergoes massive apoptosis after an initial period of normal specification (Kanai-Azuma *et al.*, 2002).

1.4.5 Neural induction

Neural induction, the early commitment of ectodermal cells to a neural fate, takes place as the organizer forms and for a long time embryologists held the view that the organizer directed close-by ectodermal cells to become neural. It was postulated that, by default, ectodermal cells would form epidermis and that a signal(s) from the organizer diverted them from the default route (reviewed in Hamburger, 1988). *Xenopus* animal cap explants indeed differentiate into epidermis in the absence of any growth factors. However, when these explants are dissociated into single cells these adopt a neural rather than an epidermal fate (Grunz and Tacke, 1989; Sato and Sargent, 1989; Godsave and Slack, 1991). The new hypothesis became that the ectoderm, by default, commits to neurectoderm and that diversion into an epidermal fate requires a signal(s) that is resident in the ectoderm and that is diluted out by cell dissociation.

The discovery that BMPs can divert dissociated animal cap cells from a neural to an epidermal fate (Wilson and Hemmati-Brivanlou, 1995; Suzuki *et al.*, 1997) led to the formulation of the Neural Default model. According to this model, ectodermal cells adopt a neural fate unless exposed to BMPs; BMP antagonists are direct neural inducers; one function of the organizer is to secrete BMP antagonists in order to suppress the BMP signals that originate in the ventral side of the embryo (see Fig. 1.8), thus promoting / allowing neural commitment on the dorsal side (Hemmati-Brivanlou and Melton, 1997). Indeed, overexpression of several components of BMP signalling pathway induces epidermis in dissociated animal cap cells and BMP antagonists or overexpression of dominant-negative versions of some components of the pathway repress epidermal differentiation in intact animal caps (Sasai *et al.*, 1995; Suzuki *et al.*, 1995; Xu *et al.*, 1995; Hawley *et al.*, 1995; Onichtchouk *et al.*, 1998; reviewed in Weinstein and Hemmati-Brivanlou, 1999). Furthermore, the organizer-expressed BMP antagonists Noggin, Chordin, Follistatin and Cerberus (Piccolo *et al.*, 1996; Zimmerman *et al.*, 1996; Fainsod *et al.*, 1997; Piccolo *et al.*, 1999) induce neural fates in animal cap explants in a direct manner, that is, without inducing mesoderm (Lamb *et al.*, 1993; Hemmati-Brivanlou *et al.*, 1994; Sasai *et al.*, 1995; Bouwmeester *et al.*, 1996; Hansen *et al.*, 1997).

The Neural Default model does not accommodate all the information available

concerning neural induction. Mouse embryos devoid of the hepatocyte nuclear factor 3 β (HNF3 β) do not form an organizer (Ang and Rossant, 1994; Weinstein *et al.*, 1994) and, despite the absence of organizer-secreted BMP antagonists such as Chordin and Noggin, still develop a neural tube with correct antero-posterior patterning (Klingensmith *et al.*, 1999). Mice mutant for *Cerebrus-like*, *Noggin* and *Chordin;Noggin* double-mutants undergo neural induction (McMahon *et al.*, 1998; Simpson *et al.*, 1999; Shawlot *et al.*, 2000; Belo *et al.*, 2000; Bachiller *et al.*, 2000). In zebrafish, the gastrula ectoderm in the ventral-vegetal quadrant adopts neural fates, despite being a region with high levels of BMPs (Kudoh *et al.*, 2003). In the chick, misexpression of BMP antagonists in the *area opaca* margin (extraembryonic epiblast), a region where node transplants are able to induce a complete secondary axis (Storey *et al.*, 1992), does not induce ectopic neural commitment and misexpression of BMPs does not repress endogenous neural induction, despite inhibiting primitive streak formation (Streit *et al.*, 1998). One possibility is that BMP antagonists play a role in the maintenance, rather than in the induction, of the neurectoderm. When a chick node is transplanted onto the *area opaca* margin for 5 h, a period of time insufficient to induce a neural plate, and is then replaced by Chordin-secreting cells, expression of the pan-neural marker *Sox3* is stabilised in the host tissue (Streit *et al.*, 1998).

In vitro studies of embryonic stem (ES) cells, which are cell lines derived from the ICM of mouse blastocysts and have the potential to differentiate into all embryonic and adult cell types (reviewed in Keller, 1995), show that these cells can undergo neural conversion in the absence of serum or any growth factor addition to the culture medium, whether in multicellular aggregates, in single cell suspension, or in adherent monoculture (Wiles and Johansson, 1999; Tropepe *et al.*, 2001; Ying *et al.*, 2003). In the most recent of these studies the Neural Default model was addressed by the addition of BMP antagonists to the culture medium. ES cell differentiation along neural fates was insensitive to Noggin but was suppressed by the presence of BMP4 (Ying *et al.*, 2003). These results suggest that, although exogenous BMP signals stimulate ES cell differentiation into non-neural fates, endogenous BMP signalling in these cultures does not obstruct neural conversion (Ying *et al.*, 2003).

As for positive neural inducers, FGF signalling is emerging as required for neural induction in planaria, fish, frog and chick (Launay *et al.*, 1996; Streit *et al.*, 2000;

Wilson *et al.*, 2000; Cebria *et al.*, 2002; Kudoh *et al.*, 2003). ES cell differentiation studies are in agreement with this view, since addition of FGF4 to a chemically defined culture medium increases neural conversion, and since administration of a pharmacological inhibitor of FGF receptor tyrosine kinases (Mohammadi *et al.*, 1997) eliminates it without a discernible effect on cell viability or proliferation (Ying *et al.*, 2003).

A subject of debate is whether neural induction predisposes an unpatterned neurectoderm to antero-posterior signals that then regionalise it or whether neural induction inherently carries antero-posterior information (Chapman *et al.*, 2003; reviewed in Foley and Stern, 2001). The first of these models goes back to Nieuwkoop. When testing the capacity of neurectoderm to induce antero-posterior pattern in naïve ectoderm, Nieuwkoop inserted pieces of naïve ectoderm perpendicularly into the presumptive neural plate of early amphibian gastrulae at different antero-posterior levels. While the proximal portion of the graft always conformed with the host in antero-posterior value, the distal portion always exhibited the character of the most anterior neural tissue. To explain these results he proposed the Activation-Transformation model, according to which the axial mesoderm produces an initial, activator, signal, that induces anterior neurectoderm in the overlying ectoderm; and then, a second, transformer, signal, present in the mesoderm with an antero-posterior gradient with the highest level in the posterior, posteriorises the neurectoderm in an accordingly graded fashion, giving rise to all intermediate values between the most anterior and the most posterior neural tissue (Nieuwkoop, 1952). More recently, the molecular translation of the Activation-Transformation model states that BMP inhibitors would be the activator signal(s) and that FGFs, Wnts and Retinoic Acid (RA) are the signals responsible for posteriorising the neurectoderm. Experimental support for this model has been obtained mainly with *Xenopus* animal caps, where the neural markers induced by BMP inhibitors are anterior ones, and where the combination of BMP inhibitors with FGFs, Wnts or RA can elicit posterior neural markers (e.g., Lamb *et al.*, 1993; Kengaku and Okamoto, 1993; Hemmati-Brivanlou *et al.*, 1994; Sasai *et al.*, 1994; Cox and Hemmati-Brivanlou, 1995; Lamb and Harland, 1995; McGrew *et al.*, 1995; Kengaku and Okamoto, 1995; Blumberg *et al.*, 1997; Domingos *et al.*, 2001; Kudoh *et al.*, 2002; reviewed in Conlon, 1995; Sasai and De Robertis, 1997).

The notion that the organizer necessarily induces anterior neural tissue has been challenged mainly by transplantation studies in zebrafish, which advocate that the epiblast possesses antero-posterior pattern that is independent of dorso-ventral pattern. Transplantation suggests that the zebrafish germ-ring, that is, non-axial mesendoderm, confers antero-posterior pattern to the overlying epiblast (Woo and Fraser, 1997). The antero-posterior specification of the epiblast is uncovered by organizer transplantation onto the ventral side of a wild-type host with variation of the latitude where the organizer is placed. Organizer grafts close to the margin (vegetal location) are not able to induce the most anterior neural markers, whereas grafts further away from the margin (animal location) are. Therefore, distance to the margin reflects the antero-posterior competence of the epiblast, where the vegetal epiblast is posterior and the animal epiblast is anterior, which cannot be overridden by signals present in the organizer (Koshida *et al.*, 1998). Furthermore, the antero-posterior pattern of the secondary axes induced by organizer grafts in ventralised host embryos, advocate independence between antero-posterior and dorso-ventral patterning (Koshida *et al.*, 1998). Antero-posterior pre-patterning of the epiblast is consistent with the fact that the antero-posterior polarity of the secondary axis induced by organizer transplant in any species is always reproducible, with the anterior ends of ectopic and host axes facing each other.

1.4.6 The AVE and patterning of the early mouse embryo

The study of early mouse development has brought forth a new set of ideas concerning neural and anterior induction as well as organizer formation and function. It was long known that the outcome of organizer transplantation in several species is dependent on the stage of both donor and host tissues. A complete secondary axis is induced in the frog, fish or chick when the organizer is transplanted early enough, meaning at early gastrula, onto gastrula-stage hosts. When a late gastrula from these species is used as donor, organizer transplants result in an incomplete secondary axis, which is anteriorly truncated (Spemann, 1931; Waddington, 1932; Saude *et al.*, 2000). The mouse, however, has been a puzzle since, no matter how early the donor gastrula, the secondary axis induced by transplant of its node or node precursor cells, called the early gastrula organizer (EGO), is invariably incomplete, lacking the fore- and midbrains (Beddington, 1994; Tam *et al.*, 1997). This suggests requirement for a tissue other than the node for induction and/or maintenance of the mammalian anterior neural plate.

It has since been shown that the AVE, an extraembryonic tissue, is required for complete anterior patterning of the mouse axes. As already mentioned, the AVE is a group of VE cells that migrate from the distal tip of the egg cylinder to the prospective anterior side of the conceptus 24 h prior to gastrulation, where they come to underlie the future neural plate. The first hint as to the importance of the AVE came from the observation of asymmetric gene expression in the VE as early as 24 h prior to gastrulation (5.5 dpc), which demonstrated antero-posterior polarity in this tissue way before primitive streak formation revealed morphological polarity (at 6.5 dpc). The homeobox-containing gene *Hex* was observed to be expressed on the side of the VE opposite to that where the primitive streak would form (Thomas *et al.*, 1998). Since, other VE transcripts were found to be specific to the AVE, such as *VE-1 antigen*, *Lim1*, *Hesx1*, *Gsc*, *Cerberus-like*, *Hnf3 β* , *Otx2* and *fgf8* (Sasaki and Hogan, 1993; Simeone *et al.*, 1993; Ang *et al.*, 1994; Rosenquist and Martin, 1995; Shawlot and Behringer, 1995; Crossley and Martin, 1995; Wakamiya *et al.*, 1997; Belo *et al.*, 1997; Rhinn *et al.*, 1998; Tam and Steiner, 1999). Interestingly, some of these genes, for example, *Lim1*, *Gsc* and *Hnf3 β* , are also expressed in the mouse node.

Hex remains the earliest AVE marker. By blastocyst stage, *Hex* is expressed in the VE-precursor cells, called the primitive endoderm. As the embryo grows, this resolves into distal VE expression at 5.0 dpc. As distal cells move anteriorly, so does *Hex* expression move with them (Thomas, 1998). On the other hand, early primitive streak markers such as the T-box family founder *T* or *Brachyury*, are expressed in a ring of cells in the proximal epiblast at the onset of gastrulation. As the streak forms and elongates, *T* expression moves posterior-distally (Wilkinson *et al.*, 1990). It thus seems that the expression of AVE and primitive streak markers move in a somewhat complementary fashion: distal-proximally on the anterior *versus* proximal-distally on the posterior. This is in agreement with the proposed global movement of the VE (Weber *et al.*, 1999).

The first experiment assessing the requirement of the AVE for patterning of the early embryo was its removal. AVE removal at the beginning of gastrulation prevents or diminishes the expression of forebrain markers in the adjacent anterior ectoderm but does not affect gene expression in more caudal neurectoderm (Thomas and Beddington, 1996). Genetic experiments subsequently showed a requirement for the expression of a number of genes specifically in the VE for anterior neurectoderm formation. Mouse

mutants for *Hnf3 β* , *Otx2* (*Drosophila orthodenticle* homologue) or *Lim1* were known to lack the anterior neural plate (Ang and Rossant, 1994; Acampora *et al.*, 1995; Shawlot and Behringer, 1995). With the emergence of the AVE model, it was shown that it is the lack of these gene products specifically in the VE that is the primary cause for the anterior truncation phenotypes. Chimeras generated by injection of wild-type ES cells into mutant blastocysts show that *Otx2*, *Nodal*, *Lim1* and *Hnf3 β* are required specifically in the VE for correct anterior neurectoderm patterning (Varlet *et al.*, 1997; Filosa *et al.*, 1997; Rhinn *et al.*, 1998; Dufort *et al.*, 1998; Shawlot *et al.*, 1999).

The AVE is able to induce forebrain markers when transplanted into an ectopic location. This was shown by transplanting pre-streak stage rabbit AVE onto chick epiblast (Knoetgen *et al.*, 1999). However, the AVE is not an organizer in the classical sense since it is not able to alter gene expression in neighbouring tissues in such a complete way that whatever those tissues were fated to become they will coordinately assume the fate and morphology imposed by the organizer (as is the case of the Spemann organizer and of the Zone of Polarising Activity in the limb, for example). Transplant of the AVE is not able to induce the formation of a head but the AVE is required to form a head in the mouse. It is noteworthy that the visceral endoderm grows in a clonally coherent manner, as opposed to the epiblast, where extensive cell mixing occurs (Gardner, 1984; Lawson and Pederson, 1987). The former type of growth would seem a requirement for a tissue that is to carry patterning information, especially in an organism where patterning occurs in concomitance with ample cell proliferation, as is the case for mammalian embryos.

Transplantation of the AVE along with the EGO onto a mouse host does result in the induction of a complete secondary axis (Tam and Steiner, 1999). This indeed suggests that antero-posterior patterning activity is subdivided into two disunited regions of the mammalian embryo, the AVE and the node. Surprisingly, however, rabbit and mouse nodes have been transplanted onto chick ectoderm, resulting in the induction of complete secondary axes (Knoetgen *et al.*, 2000). These experiments highlight the importance of assessing the molecular nature and topology of the responding / host tissue as well as of the donor graft.

It is still not clear whether the properties of the AVE allocated to this tissue after mammals evolved as a distinct class from birds or when amniotes separated from

anamniotes, or whether the unique topology of the mouse embryo allowed for the discovery of two distinct antero-posterior signalling centres that also exist as such in other vertebrates, possibly lying in closer proximity. It has been argued that the chick anterior hypoblast, the amphibian deep mesendoderm – the cells that line the blastocoel floor – and the fish dorsal YSL are the equivalents of the mammalian AVE (Beddington and Robertson, 1998). According to this idea, the dorsal-central location of anteriorising signals in these other species would allow them to act upon the ventral region of the embryos onto which organizers are transplanted, explaining why a complete secondary axis is obtained (Thomas *et al.*, 1997). Indeed, the anterior hypoblast, the deep mesendoderm and the dorsal YSL express AVE markers (Bouwmeester *et al.*, 1996; Yamanaka *et al.*, 1998; Yatskievych *et al.*, 1999; Jones *et al.*, 1999; Zorn *et al.*, 1999) and it has been shown that the frog deep mesendoderm cells possess anterior signalling ability (Jones *et al.*, 1999). In addition, it has been suggested that the anterior migration of *Xenopus* deep mesendoderm and of the chick anterior hypoblast could be the equivalent of the anterior migration of mouse distal VE cells (Arendt and Nubler-Jung, 1999).

Chick hypoblast removal, unlike mouse AVE removal, does not prevent forebrain marker expression (Knoetgen *et al.*, 1999). Furthermore, anterior hypoblast transplantation is not able to stably induce neurectoderm. However, anterior hypoblast does induce transient expression of the early neural markers *Sox3* and *Otx2* (Foley *et al.*, 2000), which is in accordance with a model where the AVE / anterior hypoblast is responsible for initiating anterior character in the embryonic ectoderm, after which the anterior definitive endoderm (ADE) and the axial mesendoderm take over in its maintenance (reviewed in Martinez-Barbera and Beddington, 2001). In *Hex* null mice, it is lack of the later, definitive endoderm, expression domain that is responsible for the observed forebrain truncations, rather than lack of the AVE domain of expression (Martinez-Barbera *et al.*, 2000). In *Hex* mutant mice, the most anterior early forebrain markers are induced but are not maintained (Martinez-Barbera *et al.*, 2000). In mice mutant for the novel conserved gene *Arkadia*, which possess a primitive streak but lack a node, both the ADE and the axial mesendoderm are markedly reduced while AVE marker expression and location are normal. *Arkadia* mutant embryos initiate anterior neurectoderm marker expression but fail to maintain it (Episkopu *et al.*, 2001). In chick, removal of the head process-stage ADE results in embryos that lack induction

or maintenance of regionalisation within the forebrain, rather than in loss of the most anterior neurectoderm markers (Withington *et al.*, 2001). Although non-identical, the results from both mouse and chick argue for a role of the early ADE in patterning of the anterior neurectoderm.

The role mainly advocated for the chick anterior hypoblast has been a mechanical one, of moving prospective forebrain cells away from posteriorising signals emitted by the classical organizer (Foley *et al.*, 2000). This is in accordance with the results obtained decades ago by Waddington. When the hypoblast was rotated 90° relative to the epiblast, the primitive streak curved towards the anterior hypoblast (Waddington, 1932), showing an influence of the hypoblast on the movement of the overlying epiblast. On the other hand, the AVE has been mainly ascribed a patterning role in the mouse. In the mouse, *Fgf8* and *Otx2*, as well as the widely expressed *Nodal* co-receptor-encoding gene *Cripto*, are required for the anteriorward displacement of the AVE from the distal tip (Ding *et al.*, 1998; Sun *et al.*, 1999; Perea-Gomez *et al.*, 2001a). Mouse mutants for these genes retain AVE markers in a distal position and primitive streak markers are either absent or retained as proximal. In *Otx2* mutants it appears that the proximal expression of posterior markers, typical of early wild-type gastrulae, extends further anteriorly than in younger wild-type embryos, suggesting a role for the AVE in restricting posterior character in the mouse embryo (Perea-Gomez *et al.*, 2001a; reviewed in Perea-Gomez *et al.*, 2001b). Future work should show if both tissues exert both actions with the ultimate goal of separating anterior and posterior influences.

1.4.7 Molecular pathways mediating vertebrate gastrulation movements

Although a great deal has been learnt about the signalling pathways that specify cell fate during early development, we still know very little about the pathways that regulate cell movement and shape the embryo. In the large-scale genetic screens performed on zebrafish, mutants with impaired epiboly, cell internalisation and convergent-extension movements were isolated. The cloning of the epiboly mutants has not yet been reported. Analyses of the behaviour of MZ-*oep* cells as well as cells overexpressing *lefties* has demonstrated the requirement for Nodal signalling in cell internalisation and the requirement for Nodal antagonists in order to suppress excess of this cell movement (Carmany-Rampey and Schier, 2001; Feldman, 2002). As for convergence-extension, cloning of *silberblick* (*slb*, Heisenberg and Nusslein-Volhard, 1997), a mutant with a

shorter and wider body axis, implicated Wnt11 in this cell movement (Heisenberg *et al.*, 2000).

From overexpression studies in *Xenopus*, it was known that not all Wnt signalling proteins are able to efficiently induce axis formation (Du *et al.*, 1995). The members of the so-called Wnt5a class of Wnts, Wnt4, Wnt5, Wnt5a and Wnt11, do not have axis-inducing activity and appear not to signal through β -catenin but, rather, through Jun N-terminal kinase (JNK), in a pathway similar to the *Drosophila* Planar Cell Polarity pathway, often termed the non-canonical Wnt signalling pathway (Du *et al.*, 1995).

The hypothesis that the non-canonical or planar cell polarity Wnt signalling pathway mediates vertebrate convergence-extension has been supported by data showing that vertebrate homologues of other components of the pathway play a role during gastrulation movements. These include Fz, Dsh, small GTPases, rho kinase 2 (Rok2), Prickle, Strabismus / van Gogh / Trilobite and Widerborst (Carreira-Barbosa *et al.*, 2003; Habas *et al.*, 2003; reviewed in Wallingford *et al.*, 2002; Tada *et al.*, 2002).

Although all of these genes are implicated in regulating cell movements, it is unclear if they function in a single linear pathway. For instance, both Prickle and Trilobite / Strabismus are required for neuronal migration, whereas there is no indication of a requirement for Wnt11 or proteins involved in the reception of the Wnt11 signal in this process. We also have much to learn regarding how this (and other) pathway(s) actually influence cell dynamics. Wnt11 functions in a non-cell-autonomous fashion to regulate cell movements in mesoderm and ectoderm (Heisenberg *et al.*, 2000). Related studies in *Xenopus* showed that a dominant negative form of Wnt11 is able to block Activin induced elongation of animal cap explants (Tada and Smith, 2000). Although it is a challenge to quantify cell morphologies in 3 dimensions over time, this approach is now technically feasible and has shown that Wnt11 is required for polarised outgrowth of processes in the direction of cell movement (Ullrich *et al.*, 2003). Wnt11 is not, however, required for polarised cell movement, instead it appears to ensure movement is efficient and free of errors. This suggests that other signalling pathways are likely to influence the overall directionality of gastrulation cell movements. In support of this, several studies have implicated other genes / pathways in promoting gastrulation cell movements. For instance, a PI3 kinase pathway possibly involving Stat3 affects the

migratory behaviours of axial mesendodermal cells (Montero *et al.*, 2003; Yamashita *et al.*, 2002), and the Robo / Slit pathway may be important for the dorsalward movement of gastrulating cells (Yeo *et al.*, 2001).

1.5 Aims and thesis outline

The aim of my project was to search for new molecules involved in the early patterning of the vertebrate embryo. In particular, I aimed at exploring the Beddington Endoderm cDNA library (Harrison *et al.*, 1995) for genes expressed either in the definitive or visceral endoderm, node and/or axial mesendoderm that had not previously been characterised in an early developmental context. The results are presented in four chapters, which are outlined next.

The first results chapter, Chapter 3, delineates the screening of the endoderm library by whole-mount *in situ* hybridisation in early-to-mid-gestation mouse embryos. A new, sequence-based, approach to clone selection was used and its effectiveness in leading to restricted expression patterns is compared with that of random selection from parent, subtracted and normalised libraries (performed by others).

Chapter 4 describes in further detail *Sgk*, a gene selected from the above screen for loss-of-function analysis in the mouse embryo. Mouse genomic DNA encompassing *Sgk* was isolated and used to generate an *Sgk*-targeting vector, which was transfected into embryonic stem cells (ES). ES cells successfully transfected were selected and screened for the rare event of homologous recombination. At this point I learnt about the phenotype of *Sgk*-null mice from others. This was not a developmental phenotype but, rather, a renal physiological phenotype and I stopped the task of generating *Sgk*-null mice myself.

I next performed a small-scale loss-of-function screen of zebrafish orthologues of mouse genes chosen from the first screen, using antisense morpholino oligonucleotides (MOs). This is reported in Chapter 5. I isolated zebrafish orthologues of the chosen genes making use of ongoing zebrafish expression sequence tag (EST) and genome sequencing projects and, when necessary, performed rapid amplification of cDNA ends

(RACE) in order to obtain 5' end sequence. The expression patterns of mouse and fish orthologues are compared, and the MO phenotypes, assessed usually up to 30 h, are briefly described.

Chapter 6 consists of the functional analysis of *Nsa2*, a gene isolated from the zebrafish screen, which is required for proper epiboly and embryo survival up to 24h. At the beginning of my analysis of *Nsa2* there was no structural or functional information on this gene in any species. During the course of my work the product of the yeast orthologue of this gene was designated Nsa2, for Nop seven associated protein 2, where Nop7 is a nucleolar protein involved in ribosome biogenesis. Nsa2 itself was shown to be involved in ribosome biogenesis. I discuss my own results concerning zebrafish *Nsa2* in the light of its ascribed function.

Each chapter of results starts with a short specific introduction to the topic of study, which is followed by the results obtained concerning that topic, and ends with a discussion of those results.

Chapter 2

Materials and Methods

Chapter 2

Materials and Methods

- 2.1 Bioinformatics and genomics**
 - 2.1.1 General software used**
 - 2.1.2 Selection of mouse endoderm library clones to screen**
 - 2.1.3 Identification of zebrafish orthologues of mouse proteins**
 - 2.1.4 Oligonucleotide design**
 - 2.1.4.1 Primers**
 - 2.1.4.2 Antisense morpholino oligonucleotides (MOs)**

- 2.2 Embryo manipulation**
 - 2.2.1 Embryo collection**
 - 2.2.1.1 Mouse embryo harvest**
 - 2.2.1.2 Zebrafish embryo collection**
 - 2.2.2 Paraffin-embedded embryo sectioning**
 - 2.2.3 Embryo/tissue stainings**
 - 2.2.3.1 Whole-mount *in situ* hybridisation**
 - 2.2.3.2 *In situ* hybridisation on paraffin-embedded tissue sections**
 - 2.2.3.3 Whole-mount terminal deoxy-nucleotidyl transferase-mediated dUTP nick end labelling (TUNEL)**
 - 2.2.4 Mouse embryo wound-healing protocol**
 - 2.2.5 Zebrafish embryo injections**
 - 2.2.6 Zebrafish embryo incubation with cycloheximide**
 - 2.2.7 Embryo photographing**
 - 2.2.8 Transmission electron microscopy (TEM)**

- 2.3 Molecular biology**
 - 2.3.1 Plasmid transformation of competent bacteria**
 - 2.3.2 Purification of plasmid DNA**
 - 2.3.3 Nucleic acid spectrophotometric quantification**
 - 2.3.4 Agarose gel electrophoresis**
 - 2.3.5 Gel extraction of DNA**
 - 2.3.6 Phenol:chloroform extraction of nucleic acids**
 - 2.3.7 Ethanol precipitation of nucleic acids**
 - 2.3.8 Lambda bacteriophage growth**
 - 2.3.9 Purification of bacteriophage DNA from liquid cultures**
 - 2.3.10 Purification of genomic DNA from 96-well plates**
 - 2.3.11 Restriction digestion of DNA**
 - 2.3.12 Automatic sequencing of plasmid DNA**
 - 2.3.13 ³²P-labelled DNA probe synthesis**
 - 2.3.14 ³²P-end-labelled DNA oligonucleotide probe synthesis**
 - 2.3.15 Bacteriophage plaque hybridisation with DNA probe**
 - 2.3.16 Southern analysis of genomic DNA**
 - 2.3.17 Cloning of DNA fragments prepared by restriction digest**
 - 2.3.18 Cloning of PCR products**
 - 2.3.19 Total RNA purification**
 - 2.3.20 mRNA purification from total RNA**
 - 2.3.21 Reverse transcriptase (RT)-PCR**
 - 2.3.22 Rapid amplification of cDNA ends (RACE)**
 - 2.3.23 Riboprobe synthesis**
 - 2.3.24 MO column-purification**

- 2.4 ES cell manipulation**
 - 2.4.1 Production of buffalo rat liver (BRL) cell conditioned medium**
 - 2.4.2 ES cell thawing, expansion and freezing**

- 2.4.3 ES cell electroporation with targeting vector
 - 2.4.4 ES cell antibiotic resistance selection
 - 2.4.5 Resistant ES cell colony picking and culture
-

2.1 Bioinformatics and genomics

2.1.1 General software used

All manipulations of DNA sequences were performed with Sequencher, DNASTrider, DNASTAR or SoftBerry software (see below for the latter). Protein alignments were performed with the Clustal method in MegAlign (DNASTAR) or MacVector.

2.1.2 Selection of mouse endoderm library clones to screen

Clustered sequences were compared to the publicly available sequence databases using the gapped BLAST algorithms (Altschul *et al.*, 1997) accessed via the internet at <http://www.ncbi.nlm.gov/BLAST/>. Clones that matched genes or domains belonging to one of the following categories: transcriptional regulators and proteins involved in chromatin structure, splicing factors and proteins involved in RNA binding and transport, signalling molecules (extracellular, intracellular or transmembrane proteins), cell-cycle regulators, cytoskeleton, extracellular matrix components, and genes implicated in human disease were selected for performing whole-mount *in situ* hybridisation. In addition, clones that matched ESTs found in other species, most of which were human or murine (uncharacterized mammalian ESTs), and some of which spanned invertebrate to vertebrate species (presumably, conserved open reading frames) were also selected, as well as clones which did not match anything in the databases. Selected clones were picked from 384 plates and sequenced in order to confirm their identity.

2.1.3 Identification of zebrafish orthologues of mouse proteins

Zebrafish ESTs corresponding to orthologues of mouse genes were sought by name in the nucleotide databases or by using the mouse sequence as the query for TBLASTN at <http://www.ncbi.nlm.gov/BLAST/>. Sequences were clustered using Sequencher software. When available, ESTs were ordered to obtain DNA templates for riboprobe

synthesis (from the Integrated Molecular Analysis of Genomes and their Expression, IMAGE or Resource Center/Primary Database, RZPD).

Zebrafish genomic clones containing exons corresponding to desired orthologues were sought by probing the Ensembl Trace Server with the mouse protein using the SSAHA algorithm, at <http://trace.ensembl.org/>. Sequences found were clustered using Sequencher software. Cluster consensus sequences were used to probe the protein databases using the blastx algorithm, at <http://www.ncbi.nlm.gov/BLAST/>, in order to confirm their coding for the desired protein. In this way, exons sequence could be identified but to this end I also used the SoftBerry FGENESH gene-finder algorithm (Salamov and Solovyev, 2000), available at <http://www.softberry.com/berry.phtml>.

2.1.4 Oligonucleotide design

2.1.4.1 Primers

Primers for sequencing or performing rapid amplification of cDNA ends (RACE) were designed either manually or using the program *Primer3* (Rozen and Skaletsky, 2000), available at http://www-genome.wi.mit.edu/cgi-bin/primer/primer3_www.cgi (Table 2.1), from regions where reliable DNA sequence was available. Both methods worked equally well. When designed manually, primers were between 18 and 23 nts in length and aimed at having a melting temperature T_m of 60 °C according to the following simplified rule: each C or G contributes 4 °C to the T_m and each A or T contributes 2 °C to the T_m .

Table 2.1 Parameters entered in *Primer3* for primer design

		Minimum	Optimum	Maximum
Sequencing	Length	18 nt	20 nt	27 nt
	T _m	57 °C	60 °C	63 °C
	G/C content	20%	50%	80%
RACE	Length	23 nt	25 nt	27 nt
	T _m	70 °C	72 °C	75 °C
	G/C content	50%	60%	70%

2.1.4.2 Antisense morpholino oligonucleotides (MOs)

To disrupt mRNA translation *in vivo*, MOs were designed to target the region around the first codon (most frequently) or the 5' untranslated region (UTR). The translation start site of zebrafish genes was identified by alignment of orthologous protein sequences belonging to several species and by looking in the cDNA for a Kozak consensus sequence in the identified region (Kozak, 1987). MOs were designed and synthesised by GeneTools LLC using sequence I provided. All MOs were 25-mers of approximately 50% G/C content, with less than 36% G content, no more than two consecutive Gs, and forming no more than 4 contiguous internal paired bases. The MOs used in this investigation are indicated in Table 2.2.

Table 2.2 MOs used in this investigation

Target mRNA	MO
None (Control MO)*	CCTCTTACCTCAGTTACAATTTATA
<i>sgk</i> MO1	CTGTAGTTTTCCACTCTGGGCCCA
<i>sgk</i> MO2	CTCGTCTCCGTTTAGATTGTCATGG
<i>14-3-3 ε</i>	TCCCGGTCACCCATGTTGGAGAGCG
<i>embigin</i>	ATGTATTTCCGATGTCTGCCTGCA
<i>lztr-1</i>	GACGGTCAAACGCCACCATAGTGTG
<i>claudin b</i>	CCGGTTGATGCCATGCTTTTTTCG
<i>pancortin</i> Module A	CTGCATCTCGCGCCGCGCTCGCTC
<i>pancortin</i> Module B (genomic [#])	CGATCTTCAGCAAAGGCACCGACAT
<i>calcyphosine</i> (genomic [#])	GCGATGTACCTGCCATCCTCCACC
<i>sp120</i>	TCTTGTCGATTTAGCGTAGATGGTC
<i>nsa2</i> MO1	GCATCTTAATCGTCTTCTTCATCTG
<i>nsa2</i> MO2	AAGTGTTTATGGAGCTACCAGGTGT
novel p7822b53	TCACCAGAATCCATGACACCTTCAA
<i>RpS5</i>	GTGCAGCCTCCCAATCTTCAGCCAT
<i>RpL19</i>	GAGCATACTCATGGCTGGTGGTCAG

* Designed by GeneTools LLC

[#] Designed from genomic rather than expressed sequence

2.2 Embryo manipulation

2.2.1 Embryo collection

2.2.1.1 Mouse embryo harvest

5.5 – 13.5 dpc wild-type mouse (*Mus musculus*) embryos for staining procedures were collected from either C57BL6 x DBA or C57BL6 x C57BL6 matings. Noon on the day of vaginal plug detection was considered 0.5 dpc. All extraembryonic membranes were removed in M2 medium (Hogan *et al.*, 1994) plus 10% foetal calf serum (FCS). Embryos were fixed overnight (O/N) in 4% *para*-formaldehyde (PFA) in phosphate buffer saline (PBS: 137 mM NaCl, 2.7 mM KCl, 4.3 mM Na₂HPO₄·7H₂O, 1.4 mM KH₂PO₄) at 4 °C, after which they were dehydrated in increasing concentrations of methanol (MeOH) in PBS (25 – 100%). Dehydrated embryos were stored in 100% MeOH at -20 °C until used.

2.2.1.2 Zebrafish embryo collection

Zebrafish (*Danio rerio*) female and male pairs were placed in tanks together in the evening preceding the desired collection day. Eggs are usually laid and fertilised the following morning shortly after the lights come on in the mating room. Embryos were collected in Embryo Water (0.03 g/l Red Sea Salt, 2 mg/l methylene blue) shortly after having been laid. Embryos were raised from the day of collection up to 3 days at 25 °C – 32 °C (usually 28 °C) in Embryo Water or in 0.3 – 1x Danieau's solution (1x: 58 mM NaCl, 0.7 mM KCl, 0.4 mM MgSO₄, 0.6 mM Ca(NO₃)₂, 5 mM HEPES (pH 7.6)). Embryos were staged according to the morphological criteria provided in Kimmel *et al.*, 1995. Zebrafish embryos collected for staining procedures were fixed at least O/N in 4% PFA in PBS at 4 °C. Embryos 24 hours post fertilisation (hpf) or older were dechorionated prior to fixation whereas embryos younger than 24 hpf were dechorionated after fixation and before dehydration. Following fixation, embryos were dehydrated in increasing concentrations of MeOH in PBS. Dehydrated embryos were stored in 100% MeOH at -20 °C until used.

2.2.2 Paraffin-embedded embryo sectioning

Prior to or after having been subject to whole-mount *in situ* hybridisation, embryos/tissues were dehydrated in increasing concentrations of EtOH in PBS. Once washed twice in 100% EtOH, embryos/tissues were cleared in HistoClear (National Diagnostics) for at least 40 min at 56 °C. Cleared embryos/tissues were subsequently washed several times in paraffin (at least 2 h in total), also at 56 °C, and finally oriented at room temperature paraffin while the latter set. Embedded embryos were placed for 2 h at 4 °C prior to sectioning. Sections 10 µm thick were cut using a microtome (Jung CM3000, Leica Instruments GmbH), and placed to dry O/N on water-covered positively charged glass slides (Superfrost Plus, BDH) on a warm table. Slides containing attached sections were kept in a covered box at 4 °C until used.

2.2.3 Embryo/tissue stainings

2.2.3.1 Whole-mount *in situ* hybridisation

Mouse embryos were rehydrated in decreasing concentrations of MeOH in PBS. Once in PBS, 7.5 and 9.5 dpc embryos were pierced with a glass needle in regions likely to trap probe. Whole-mount *in situ* hybridisation of mouse embryos was performed according to a classical protocol (Wilkinson, 1992), using the hybridisation conditions of Rosen and Beddington, 1993, with the following modifications: proteinase K (10 mg/ml) treatment was 5 min for 6.5 – 7.5 dpc embryos, 12 min for 8.5 – 9.5 dpc embryos and 20 - 30 min for 10.5 – 13.5 dpc embryos; embryo powder was omitted from the procedure. Embryos were processed in baskets with mesh bases (Costar) applied to 12-well plates: 7.5 dpc or younger in 12 µm pore meshes and 8.5 dpc or older in 74 µm pore meshes. After staining, embryos were post-fixed in 4 % PFA, 0.1% glutaraldehyde in PBS for 1 h at room temperature and stored in 0.4% PFA at 4 °C. Stained mouse embryos were photographed in 0.1% Tween 20 in PBS (PBT) on 1% agarose-coated dishes.

Zebrafish embryos were rehydrated in decreasing concentrations of MeOH in PBT. Whole-mount *in situ* hybridisation of zebrafish embryos was performed using a modification of a standard protocol (Thisse and Thisse, 1998). Embryos were washed 5 times in PBT, 5 min each. Embryos older than 24 hpf were digested with 10 µg/ml proteinase K for 15 min, washed twice in PBT and refixed in 4% PFA in PBT for

20 min at room temperature, then. Embryos were then transferred to hybridisation buffer (Hyb: 50% formamide, 5x SSC (0.75 M NaCl, 75 mM Na₃Citrate.2H₂O (pH 7.0)), 500 µg/ml type VI torulae yeast RNA, 50 µg/ml heparin, 0.1% Tween-20, 9 mM citric acid (pH 6.0-6.5)) for 2-5 hours at 68 °C. The Hyb was then replaced with Hyb containing 1 µg/ml of digoxigenin (DIG)-labelled riboprobe and the embryos were incubated at 68 °C O/N. The first washes of the following day were done at the hybridisation temperature with preheated solutions: 75% Hyb / 2x SSC; 50% Hyb / 2x SSC; 25% Hyb / 2x SSC; 100% SSC for 15 min each, and two washes with 0.2x SSC for 30 min each. Next, a series of washes was performed at room temperature: 75% 0.2x SSC / PBT; 50% 0.2x SSC / PBT; 25% 0.2x SSC / PBT and 100% PBT for 10 min each. The embryos were blocked in 2 mg/ml BSA, 2 % heat-inactivated goat or sheep serum in PBT for several hours, after which they were incubated with alkaline-phosphatase-conjugated anti-DIG Fab fragments diluted 1:2500 in blocking solution at 4 °C, O/N. The following day embryos were washed with PBT at least 8 times, for 15 min each. The embryos were then rinsed 3 times for 5 min each in NTMT buffer (0.1 M tris(hydroxymethyl)methylamine (TRIS)-HCl pH 9.5; 50 mM MgCl₂; 0.1 M NaCl; 0.1% Tween 20). Detection was performed using NBT / BCIP (112.5 µl of 100 mg/ml NBT in 70% dimethyl-formamide and 175 µl of 100 mg/ml BCIP in 70% of dimethyl-formamide, in 50 ml of NTMT). After stopping the reaction with 100% PBS (pH 5.5), embryos were refixed in 4% PFA in PBS. Stained zebrafish embryos younger than 24 hpf were dehydrated in increasing concentrations of MeOH in PBT and two final washes in 100% MeOH. These were then cleared in a fresh 2:1 mixture of benzyl-benzoate:benzyl alcohol (BBA) and mounted in a 10:1 mixture of Canada Balsam : methyl-salicylate. As soon as embryos were in BBA their exposure to light was kept to a minimum to avoid the yolk turning red. For storage, these embryos were rehydrated in decreasing concentrations of MeOH in PBT, two final washes in PBT, and finally placed in 0.4% PFA in PBT at 4 °C. 24 hpf or older embryos were placed straight into 80% glycerol in PBT, which was both the clearing and mounting solution. These embryos were stored in 80% glycerol at 4 °C.

2.2.3.2 *In situ* hybridisation on paraffin-embedded tissue sections

In situ hybridisation on paraffin-embedded mouse tissue sections was carried out either in slide boxes or Coplin jars. Slides containing tissue sections were de-waxed by

washing 3 times in HistoClear (National Diagnostics), 5 min each, followed by 2 washes in ethanol (EtOH). Tissue was bleached and dehydrated by incubating with gentle shaking in 6% H₂O₂ in MeOH for 2.5 – 3 h at room temperature. Slides were rehydrated in MeOH/PBT series: 75%, 50%, 25%, 5 min each, and finally 3 times in PBT. Tissue was digested for 15 min at room temperature by incubating with 12.5 µg/ml proteinase K in PBT, in slide box. When slides are incubated flat in slide boxes, 300 µl solution / slide is enough to cover tissue. Digestion was stopped by washing twice in 2 mg/ml glycine in PBT. Slides were refixed in slide box for 20 – 30 min at room temperature, in 4% PFA (fresh), 0.2% glutaraldehyde in PBS, followed by 2 washes in PBT. Hybridisation mix (Sections Hyb: 50 % formamide, 5x SSC, 50 µg/ml heparin, 50 µg/ml tRNA) was added to slides and these were covered with coverslip or parafilm (note that the latter shrinks at the high temperature). Pre-hybridisation was carried out in humidified slide box for at least 1 h at 70 °C. Sections Hyb was then replaced with Sections Hyb containing previously denatured (80 °C for 2 min; ice for 5 min) DIG-labelled riboprobe, slides were covered as before, and hybridised in humidified slide box O/N at 70 °C. The following day, slides were washed twice for 30 min each in pre-heated 50 % Formamide, 5x SSC (pH 4.5 – 5.2), 1% SDS, at 70 °C; and twice again for 30 min each in pre-heated 50% Formamide, 5x SSC (pH 4.5 – 5.2), at 65 °C. Slides were washed in fresh MAB (100 mM maleic acid, 150 mM NaCl, pH 7.5), 3 times for 5 min each at room temperature. Blocking was performed for at least 2 h at room temperature in slide box, with 2 % Blocking Reagent (Boehringer; dissolve hot) in MAB (no serum). Blocking solution was then replaced with 1:2000 anti-DIG antibody in blocking solution and slides were incubated for 2 h at room temperature in slide box. Slides were washed with gentle shaking in MABT (MAB, 0.1% Tween-20), 3 times, 20 min each, at room temperature, followed by washing in NTMT, 3 times 5 min each. Detection was performed using NBT / BCIP (112.5 µl of 100 mg/ml NBT in 70% dimethyl-formamide and 175 µl of 100 mg/ml BCIP in 70% of dimethyl-formamide, in 50 ml of NTMT). Detection reaction was carried out in light-tight slide box and was left to take place for at least O/N (when left longer, slides were checked occasionally to ensure they were not drying out and more developing solution was added when necessary). After stopping the reaction with 10 mM EDTA in PBS, slides were refixed in MEMFA (0.1 M MOPS (pH 7.4), 2 mM EGTA, 1 mM MgSO₄, 37% formaldehyde), for 1 h at room temperature. Slides were then washed in PBS and mounted with Aquamount (MERCK).

2.2.3.3 Whole-mount terminal deoxy-nucleotidyl transferase-mediated dUTP nick end labelling (TUNEL)

Zebrafish embryos were rehydrated, washed and, for embryos older than 24 hpf, digested with proteinase K followed by post-fixation with 4% PFA in PBS, as for whole-mount *in situ* hybridisation. Embryos older than 24 hpf were then subject to endogenous alkaline phosphatase inactivation, by incubation with pre-chilled (-20 °C) EtOH:glacial acetic acid (2:1) for 10 min at -20 °C. Specialised reagents subsequently used were those of ApopTag kit (Intergen). All embryos were incubated in 75 µl Equilibration Buffer for 1 h at room temperature and then incubated in at least 50 µl working strength TdT enzyme (prepared fresh by mixing Reaction Buffer:TdT enzyme 2:1 + 0.3% TritonX-100) O/N at 37 °C. The following day, the reaction was stopped by washing embryos in working strength Stop/Wash Buffer (Stop/Wash Buffer:water 1:17) for 3 h at 37 °C. Blocking was performed by incubation in 2 mg/ml BSA, 5% goat serum in PBT for at least 1 h at room temperature, after which embryos were incubated with alkaline-phosphatase-conjugated anti-DIG Fab fragments diluted 1:2500 in blocking solution at 4 °C, O/N. Subsequent washes, detection and mounting were performed as for whole-mount *in situ* hybridisation.

2.2.4 Mouse embryo wound-healing protocol

For wound healing experiments, performed by Dr. Lisa Cooper in Prof. Paul Martin's Lab, 11.5 dpc mouse embryos were recovered according to Martin and Cockroft, 1999 from CD1 x CD1 matings. Living embryos were immediately wounded by hind limb-bud amputation as well as flank incision and healing was allowed to take place for 30 min, 3 h, 6 h or 12 h by culturing the embryos under the conditions described in Martin and Cockroft, 1999. Whole-mount *in situ* hybridisation of wounded embryos was performed as described above with *Sgk* or *Krox24* (positive control) riboprobes.

2.2.5 Zebrafish embryo injections

Injection needles were prepared by pulling 1.0 mm filament-containing borosilicate glass capillaries (World Precision Instruments, item no. 1B100F-4) with a vertical pipette puller (David Kopf Instruments, Model 720), cutting the edge with a razor blade, and calibrating under the microscope with micrometer. The injection system consisted

of a needle holder (World Precision Instruments), carried by a 3-axis micromanipulator (Narishige, MN-153), connected to a foot-pedal-controlled pressure injector (World Precision Instruments, Pneumatic PicoPump PV 820).

Prior to microinjection, MOs were usually diluted to desired concentration in MO Buffer (1:4 25 mg/ml phenol red : 5 mM HEPES (pH 7.2), 200 mM KCl). In general, a volume of 1.4 nl, containing 10 ng of the desired solution, was injected through the chorion of zebrafish embryos up to the 8-cell stage, targeting the whole embryo and extraembryonic tissues. In a few experiments where the YSL was targeted, embryos were injected at 4 hpf, a stage when blastoderm cells have detached from the YSL (Cooper and D'Amico, 1996; see also Cooper and D'Amico, 2001). By injecting the yolk cell just below the blastoderm, in the centre of the YSL, the latter can be targeted specifically, as seen by a thin layer of phenol red (constituent of the MO buffer described above) lying just beneath the blastoderm. For injection, embryos were aligned on the side of a glass slide in a glass petri dish, with just enough Embryo Water to ensure their hydration.

2.2.6 Zebrafish embryo incubation with cycloheximide

Prior to incubation with cycloheximide, live zebrafish embryos were dechorionated in 1x Danieau's Solution on 2% agarose in 1x Danieau's Solution-coated dishes. At the chosen stages, dechorionated embryos were incubated with desired concentration of cycloheximide in 1x Danieau's Solution.

2.2.7 Embryo photographing

Low-power photographs of embryos were taken using a Nikon camera-coupled Nikon dissecting microscope, using tungsten film (Kodak 64T). Images acquired through the former were digitised using a Polaroid SprintScan 35 scanner. High-power Nomarski or fluorescent images of live or fixed embryos as well as images of tissue sections were obtained using a Zeiss Axiophot microscope fitted with a Kodak DCS420 digital camera. Images were treated with AdobePhotoshop. Living zebrafish embryos were photographed in 3% methylcellulose (Sigma).

2.2.8 Transmission electron microscopy (TEM)

Whole zebrafish embryos were dechorionated manually and fixed overnight with 2% glutaraldehyde, 2% paraformaldehyde in 0.1M sodium cacodylate buffer (pH 7.2) (SCB). The following day, embryos were washed for 10 min in SCB and postfixed for 1 h in 1% osmium tetroxide in SCB. They were washed again with SCB and stained *en bloc* with 1% aqueous uranyl acetate for 1 h. The samples were then dehydrated through a graded ethanol series, followed by 2 changes of propylene oxide over 20 min and embedded in Epon resin (Agar Scientific). 50 nm ultra thin sections were cut and mounted on pioloform coated slot grids and stained with 1% aqueous uranyl acetate for 15 min, followed by Reynold's lead citrate for 7 min. Sections were visualised in a Jeol 1200 EX electron microscope.

2.3 Molecular biology

2.3.1 Plasmid transformation of competent bacteria

TOP10 chemically competent bacteria (Invitrogen) were used for heat-shock transformation of plasmid DNA. 2 μ l of DNA solution were added to 25 μ l cells and incubated on ice for 5 min. Cells were then heat-shocked at 42 °C for 30 s and 250 μ l of SOC (2% tryptone, 0.5% yeast extract, 10 mM NaCl, 2.5 mM KCl, 10 mM MgCl₂, 20 mM glucose) medium was added. An aliquot of the culture was spread onto a selective L-Broth (LB: 1% w/v bacto-tryptone, 0.5% w/v bacto-yeast extract, 1% w/v NaCl) + agar (L-agar) plate (e.g., 100 mg/ml of ampicillin in L-agar) previously treated with 40 μ l of 20 mg/ml in dimethylformimide 5-bromo-4-chloro-3-indolyl- β -D-galactosidase (X-Gal) and, if the bacteria so require, 40 μ l of 200 mg/ml isopropylthio- β -D-galactosidase (IPTG). Plates were incubated O/N at 37 °C.

TOP10 electrocompetent bacteria (Invitrogen) were used for electroporation of plasmid DNA. Up to 2 μ l of DNA solution was added to 20 μ l of cells thawed on ice and immediately transferred to a pre-cooled 0.1 cm electroporation chamber. Cells were electro-shocked at 1.8 kV, 25 μ F and 200 Ω . 1 ml of warm SOC medium was immediately added to the electroporated cells. The mixture was transferred to a plastic tube and incubated with shaking at 37 °C for 1 hour. Cells were plated as described for chemical transformation.

2.3.2 Purification of plasmid DNA

For all plasmid preparations, Qiagen Spin kits (Mini or Midi Prep) were used as recommended. For a small-scale plasmid preparation, 2 ml bacterial cultures were grown O/N at 37 °C in selective LB medium with vigorous shaking. 1.5 ml culture was transferred to a 1.5 ml microcentrifuge tube and spun for 20 s at ~10,000 x g on a bench centrifuge. The supernatant was removed completely and the pellet resuspended in 250 µl of Resuspension Buffer (10 mM EDTA, 50 mM TRIS-HCl (pH 8.0), 100 µg/ml RNase A). 250 µl of Lysis Buffer (0.2 M NaOH, 1% SDS) were added, mixed and the tubes left for 5 min at room temperature to allow alkaline lysis of the cells. Lysis solution was then neutralised by adding 350 µl of ice-cold Neutralisation Buffer (3 M KOAc (pH 5.5)) and mixed by carefully inverting the tube a few times, followed by 10 min incubation on ice. The tube was spun for 15 min at room temperature and the supernatant was transferred into a fresh microcentrifuge tube containing a mini column and spun for 1 min at ~10,000 x g on a bench centrifuge. Column was washed with 750 µl of Wash Solution and DNA was finally eluted with 30 - 50 µl of sterile water by spinning at ~10,000 x g on a bench centrifuge.

For a medium scale plasmid preparation, 25 ml bacteria culture were grown O/N at 37 °C in selective LB medium with vigorous shaking. Culture were transferred to 30 ml polycarbonate tubes (Nalgene) and spun for 15 min at 6,000 x g in a Sorvall SS-34 rotor at 4 °C in a Sorvall RC5C centrifuge. The supernatant was removed completely and the pellet resuspended in 4 ml of Resuspension Buffer (10 mM EDTA, 50 mM TRIS-HCl (pH 8.0), 100µg/ml RNase A). 4 ml of Lysis Buffer (0.2 M NaOH, 1% SDS) were added, mixed and the tubes left for 5 min at room temperature to allow alkaline lysis of the cells. Lysis solution was then neutralised by adding 4 ml of ice-cold Neutralisation Buffer (3 M KOAc (pH 5.5)) and mixed by carefully inverting the tube a few times, followed by 15 min incubation on ice. Tube was spun for 30 min at 20,000 x g in a Sorvall SS-34 rotor at 4 °C in a Sorvall RC5C centrifuge. Supernatants were transferred into Qiagen-tip 100 columns previously equilibrated with 4 ml of Equilibration Buffer (750 mM NaCl, 50 mM MOPS (pH 7.0), 15% isopropanol, 0.15% Triton X-100). Columns were washed with 2 x 10 ml of Wash Solution (1.0 M NaCl, 50 mM MOPS (pH 7.0), 15% isopropanol) and DNA was finally eluted with 200 µl of sterile water into 30 ml glass tubes (Corex). DNA was precipitated by adding 3.5 ml of isopropanol and centrifuging for 30 min at 15,000 x g in a Sorvall SS-34 rotor at 4 °C in a Sorvall RC5C

centrifuge. DNA pellets were washed with 2 ml of 70% EtOH and centrifuged for 10 min at 15,000 x g in a Sorvall SS-34 rotor at 4 °C in a Sorvall RC5C centrifuge. Pellets were air-dried for approximately 10 min and resuspended in 200 µl of sterile water.

2.3.3 Nucleic acid spectrophotometric quantification

Nucleic acid quantification was performed by spectrophotometry at $\lambda = 260$ nm, where an optic density (OD) unit corresponds to 50 µg/ml of double-stranded nucleic acid or to 35 µg/ml single-stranded nucleic acid. The ratio between the readings at $\lambda = 260$ nm and $\lambda = 280$ nm provided an estimate of the purity of the nucleic acid preparation (pure preparations of DNA should have OD_{260}/OD_{280} ratio of 1.8).

MOs were supplied lyophilised. Following solution and column-purification (see section 2.3.24), eluates were diluted 1/1000 in 0.1 N HCl and quantified by spectrophotometry at $\lambda = 265$ nm. MO concentration corresponds to the ratio between the OD and their molar extinction coefficient (ϵ), multiplied by their molecular weight (MW). Manufacturers provide ϵ and MW values for each MO synthesised.

2.3.4 Agarose gel electrophoresis

Nucleic acid concentration estimation, size determination and/or separation were performed by agarose gel electrophoresis. Gels were prepared by dissolving agarose in 0.5x TAE (20 mM TRIS acetate, 1 mM $Na_2EDTA \cdot 2H_2O$ (pH 8.5)) to a final concentration of 0.8 – 2% (w/v), depending on the expected size of the DNA fragments, and 0.5 mg/ml ethidium bromide. Nucleic acid samples were mixed with 6x gel loading buffer (6x TAE, 50% v/v glycerol, 0.25% w/v bromophenol blue) and, in the case of RNA, with RNase inhibitor. Electrophoresis was performed at 5 – 20 V/cm gel length until appropriate resolution was achieved. Ethidium bromide-stained nucleic acid was visualised using ultraviolet light ($\lambda \approx 302$ nm) and fragment size was estimated by comparison with the 1 kb ladder molecular weight markers (Gibco BRL) run in at least one of the gel lanes.

2.3.5 Gel extraction of DNA

For the extraction of DNA from agarose gels, the appropriate band was excised under long ultraviolet light ($\lambda \approx 365$ nm) with minimal amount of agarose. The QIAquick Gel Extraction Kit (Qiagen) was then used according to manufacturer's protocol. The 1% agarose slice containing the desired band(s) was weighed and using the correspondence 100 mg \approx 100 μ l, 3 volumes of Buffer QG (Qiagen) were added. Sample was incubated for 10 min at 50 °C, with occasional vortexing. After slice was completely dissolved, 1 gel volume of isopropanol was added if purifying DNA fragments < 500 bp or > 4 kb. Samples were loaded onto QIAquick spin columns (Qiagen) and spun for 1 min at \sim 10,000 x g on a bench centrifuge (MicroCentaur). No more than 800 μ l per column were loaded at a time. When sample volume exceeded 800 μ l, it was loaded and spun as many times as necessary on the same column. Flow-through was discarded and agarose traces were removed by adding 0.5 ml QG Buffer (Qiagen) and spinning for 1 min at \sim 10,000 x g. Flow-through was discarded and column was washed by adding 0.75 ml PE Buffer (Qiagen) and spinning for 1 min at \sim 10,000 x g. Flow-through was discarded and column was spun for 1 min more at \sim 10,000 x g. Flow-through was discarded and column was placed into fresh microfuge tube. DNA was eluted by adding 30 or 50 μ l of water and spinning for 1 min at \sim 10,000 x g.

2.3.6 Phenol:chloroform extraction of nucleic acids

To remove proteins from nucleic acid solutions, one volume of a 25:24:1 mixture of phenol : chloroform : isoamyl-alcohol (v/v/v) was added to the nucleic acid solution and mixed for 1 minute. After a 5 min centrifugation, the upper (aqueous) layer was transferred into a new microcentrifuge tube and extracted again with one volume of chloroform.

2.3.7 Ethanol precipitation of nucleic acids

EtOH precipitation of nucleic acids was carried out by adding 1/10 volume of 3 M sodium acetate (NaOAc) (pH 4.6) and 2.5 volumes of cold 100% EtOH to the nucleic acid solution. This mixture was left at -20 °C or -80 °C (depending on how much concern salt precipitation is for subsequent procedures) for approximately 20 min. 1 μ l

of 10 mg/ml tRNA was often used as a carrier to visualise the pellet formation. Centrifugation was carried out at 20,000 x g for 5 – 20 min, the DNA pellet was washed in 70% EtOH and spun again at the same speed for 5 min. After EtOH removal nucleic acid was left to air-dry at room temperature for approximately 10 min and resuspended in TE (1 mM EDTA, 10 mM TRIS.HCl (pH 8.0)) or distilled water.

2.3.8 Lambda bacteriophage growth

XL1-Blue bacteriophage host cells were grown in 10 mM MgSO₄, 0.2% maltose in LB at 37 °C until reaching O.D.₆₀₀ = 1.0. Cells were centrifuged down and resuspended to O.D.₆₀₀ = 0.5 in 10 mM MgSO₄. This cell suspension was used up to 1 week.

For phage growth in plates, phage suspension was mixed with bacterial suspension, combined with Top-agarose (0.7g agarose, 0.2 g MgSO₄·7H₂O, 100 ml LB), and plated on LB-agar plates to grow O/N. Success of phage culture in plates is assessed by confluency of plaques formed by bacterial lysis. An ideal culture generates a confluent, totally lysed, plate. Phage grown in plates were used for up to 1 week to inoculate XL1-Blue cells in liquid medium.

For phage growth in liquid medium, plaque plugs were punched with a Pasteur pipette from a confluent portion of the plate and added to a 50 ml tube containing 3 ml of the following solution: 0.5 ml host cells prepared as described above, 30 ml SM buffer (0.58 g NaCl, 0.20 g MgSO₄·7H₂O, 5 ml 1 M TRIS-HCl (pH 7.5), 0.5 ml 2% gelatin in water), 0.2% maltose (which can be kept at 4 °C for 4 – 5 days). This mix was shaken for at least 20 min at 37 °C, after which 12 ml of XL1-Blue Medium (500 ml LB, 15 ml 1 M TRIS (pH 7.4), 1.5 ml 1 M MgSO₄) were added. Culture was grown at 37 °C with shaking and monitored for lysis after 7 h. Lysis was recognised by solution clearing. Culture was shaken at 37 °C for up to 2 h more after clearing. Lysis was finalised by the addition of 0.5 ml of chloroform and culture was left for at least 30 min at 4 °C before DNA purification.

2.3.9 Purification of bacteriophage DNA from liquid cultures

1 – 2 ml phage lysate was kept for stock and remaining was poured into a 30 ml glass tube (Corex), avoiding the chloroform layer. Suspension was spun at 15,000 x g for

10 min after which supernatant was poured into a 50 ml tube containing 10 μ l of 10 mg/ml RNase and 10 μ l of 10 mg/ml DNase. Tube was mixed and incubated for 1 h at 37 °C with shaking. Equal volume of 20% polyethylene glycol (PEG), 2 M NaCl was added, mixed, and suspension left for at least 30 min at 4 °C. This suspension was then spun at 1000 \times g for 10 min and the supernatant discarded. In order to completely remove PEG, tube was spun again at 1000 \times g for 10 min and supernatant completely removed with a pipette. The pellet was resuspended in 0.5 ml of 10 mM TRIS (pH 7.4), 10 mM EDTA, the solution was transferred to a microfuge tube containing 0.5 ml of phenol and shaken intermittently for 5 – 10 min, then spun in a microfuge for 15 s. The aqueous (upper) layer was transferred to a fresh tube and DNA was precipitated with 1 ml of EtOH. The solution was spun for 2 – 5 min, the supernatant was aspirated, the pellet was resuspended in 250 μ l of 10 mM TRIS (pH 7.4), 0.1 mM EDTA and left at 4 °C for at least 30 min for DNA to disperse. A second precipitation was performed with 5 μ l of 3 M (pH 4.6) NaOAc, 600 μ l of EtOH and the pellet was washed with 500 μ l of 70% EtOH and left to dry at room temperature. Finally, the pellet was resuspended in 50 μ l of 10 mM TRIS (pH 7.4), 0.1 mM EDTA.

2.3.10 Purification of genomic DNA from 96-well plates

Genomic DNA was purified from ES cells grown in 96-well plates. Cells were washed twice with 100 μ l PBS / well. Lysis Buffer (10 mM TRIS (pH 7.5), 10 mM EDTA, 10 mM NaCl, 0.5% sarcosyl) + 1 mg/ml proteinase K was added at 50 μ l / well and plates were incubated in a humidified environment O/N at 55 °C. EtOH/salt solution (15% 5 M NaCl in EtOH, kept at –20 °C), was mixed thoroughly and added to plates, 100 μ l / well, with no mixing. Plates were incubated for 30 min at room temperature and then slowly inverted, allowing the EtOH/salt solution to drain and removing excess liquid by blotting plate on paper towels. The DNA was washed three times with 70% EtOH, 150 μ l / well. Each time, EtOH was removed by slowly inverting the plates and after final wash, plates were blotted on paper towels and left inverted to dry.

2.3.11 Restriction digestion of DNA

Restriction enzyme digests were performed at the recommended temperature for approximately 2 h (or O/N) using commercially supplied restriction enzymes and buffers (Boehringer Mannheim, Promega, New England Biolabs). The enzyme

component of the reaction never comprised more than 10% of the reaction volume. For multiple enzymatic digests, the most compatible buffer for all the enzymes used was chosen as long as all the enzymes were predicted to digest at least 75% of the DNA in those conditions; when enzymes required incompatible buffers, one digest was done at a time and the DNA was either phenol/chloroform extracted and precipitated or gel extracted between digests. When multiple digests with restriction sites in close proximity were performed, the enzyme with worse performance close to DNA ends was used first.

2.3.12 Automatic sequencing of plasmid DNA

DNA sequencing was performed using the ABI PRISM Big Dye Terminator Cycle Sequencing Ready Reaction kit (Applied Biosystems) and an ABI 377 automatic sequencer. Samples were prepared essentially according to the manufacturers instructions. Each reaction contained 1 – 2 µg of plasmid DNA (in 5 µl), 8 µl H₂O, 3 µl 5x CSA buffer, 2 µl 1.6 pmol/µl primer and 2 µl Big Dye Terminator reaction mix. Labelled product was amplified using the following polymerase chain reaction (PCR) program:

35 cycles of: 96 °C for 30 s
50 °C for 15 s
60 °C for 4 min

The product was precipitated by adding 60 µl EtOH (cold) and 2 µl 3 M NaOAc (pH 4.6), incubating 10 min on ice and centrifuging for 30 min at ~10,000 x g in a bench centrifuge at 4 °C. The pellet was washed with 250 µl 70% EtOH and spun for 5 min at ~10,000 x g in a bench centrifuge at 4 °C. After EtOH removal, the DNA was left to air-dry at room temperature for approximately 10 min and resuspended in 4 µl Sequencing Buffer (5:1 deionised formamide : 25 mM EDTA (pH 8.0) with 50 mg/ml Dextran Blue). Samples were kept at 4 °C for up to several days until loading on the gel. For the gel, 18 g urea were mixed with 5 ml 10x TRIS borate EDTA (TBE) buffer (0.89 M TRIS borate (pH 8.3), 20 mM Na₂EDTA), 5 ml of Long ranger Gel solution and the volume made up to 50 ml with distilled water. The mix was stirred and filtered through 0.4 µm pore membrane and left at 4 °C for up to a few hours until use.

Glass plates were washed with warm water, rinsed with distilled water, left to dry and

assembled with spacers in between. They were then clamped to the frame with which to mount on the sequencing machine and tilted slightly, ready for pouring. Just prior to pouring, 250 μ l of fresh 10% ammonium persulfate (APS) and 50 μ l N, N, N', N'-tetramethyl-ethylenediamine (TEMED) were added to the gel mix. The mix was poured between the plates with the aid of a syringe, with constant tapping so as to ensure steady gel progression with no bubbles. Back of plastic comb was inserted at the top of the gel to create chamber for subsequent loading and this region of the gel was very tightly clamped. Gels were left to polymerise for at least 2 h (O/N at a maximum, for which gel edges were covered with plastic film to avoid drying). 36-well paper combs (PE Biosystems) were used for loading, which was performed with duck-bill tips (2 μ l / well). Running buffer consisted of 1x TBE.

2.3.13 32 P-labelled DNA probe synthesis

Where possible, all steps were performed on ice. 28 μ l aqueous solution containing 15 – 25 ng linearised DNA template were mixed with 5 μ l of Random Primers (DNA Labelling System, Invitrogen). This mix was denatured for 5 min at 95 °C and spun briefly. 10 μ l Labelling Buffer (DNA Labelling System, Invitrogen), 5 μ l 32 P deoxycytidine 5'-triphosphate (dCTP) (\approx 1.85 MBq), 2 μ l Klenow (DNA Labelling System, Invitrogen) were added, mixed carefully and the whole mixture was spun briefly. Mix was incubated for 10 min at 37 °C, after which reaction was stopped with 2.5 μ l 0.5 M EDTA, 47.5 μ l TE. Meanwhile, a spin column was prepared: 1ml syringe stopped with glass wool filled with Sephadex-G50 was spun at 150 x g for 5 min. The reaction was pipetted onto spin column and spun at 150 x g for 5 min. To quantify the radioactivity, 1 μ l of probe was added to scintillation fluid and labelling intensity was measured on a scintillation counter (Beckman LS6000IC). The remaining probe was denatured for 5 min at 95 °C and left on ice for 2 min before adding to Pre-Hyb (1 – 1.5 x 10⁶ counts/ml).

2.3.14 32 P end-labelled DNA oligonucleotide probe synthesis

1 μ l containing 5 ng DNA was mixed with 10 μ l water, 1.5 μ l 10x T4 polynucleotide protein kinase buffer, 2.2 μ l 32 P- γ adenosine 5'-triphosphate (ATP), 0.3 μ l T4 polynucleotide protein kinase. Mix was incubated for 30 min at 37 °C.

2.3.15 Bacteriophage plaque hybridisation with DNA probe

Mouse *Sgk* genomic clones were isolated from a Stratagene mouse genomic library cloned into Lambda FixTM II. In order to plate library, eight 22 x 22 cm² plates (NUNC) were poured with LB-agar and left for 2 days to harden and dry completely. 2 µl library (phage suspension) were diluted in 1 ml SM Buffer. 8 aliquots of 36 µl of this were mixed with 8 aliquots of 1.2 ml of XL1-Blue host cells prepared as described in section 2.3.8 and incubated for 15 min at 37 °C. Each of these mixes was combined with 22 ml 40 °C Top-Agarose and pour onto one of the LB-agar plate previously prepared and preheated at 37 °C. We aimed at plating 150,000 pfu/plate. Plates were incubated for 8 – 9 h at 37 °C, after which they were kept at 4 °C.

For library plaque-lifting, sixteen 22 x 22 cm² positively charged nylon membranes (HybondTM-N+) were cut (2 per plate). Membranes were carefully placed on top of plaqued plate and left transferring for: 2 min for the first membrane and 4 min for the duplicate. Each membrane was unequivocally identified on the back and exact correspondence between membrane and plate orientation was achieved by piercing a distinct number of holes in each corner of the membrane through to the agar and marking these sites on the back of the plate. Membranes were submerged face-up in Denaturing Solution (1.5 M NaCl, 0.5 M NaOH) for 2 min, placed in Neutralising Solution (1.5 NaCl, 0.5 M TRIS-HCl (pH 8.0)) for 5 min and rinsed in Rinsing Solution (0.2 M TRIS-HCl (pH 7.5), 2 x SSC) for 30 s. Membranes were left to dry at room temperature, face-up on filter paper (Whatmann). DNA was crosslinked to membranes (Stratagene crosslinker). When not used immediately, filters were stored at 4 °C between filter paper.

Membranes were prehybridised for at least 2 h at 65 °C in PreHyb (7% SDS, 1% BSA, 1 mM EDTA, 0.5 M sodium phosphate buffer (pH 7.2)), inside rotating hybridisation bottles (Hybaid). After adding the radioactive DNA probe, membranes were left to hybridise O/N at 65 °C. The next day, membranes were washed at 65°C with preheated solutions. First, a low stringency wash with 0.5 x SSC, 0.1% SDS for 20 min; and next, 2 – 3 high stringency washes with 0.2 x SSC + 0.1% SDS for approximately 20 min each (decided upon scanning filters with Geiger-counter). Membranes were left to dry at room temperature, face-up on filter paper. Once dry, the membranes were enclosed

in plastic wrap (Saran) and placed in developing cassette with film. After developing, film was lined up with membranes to label it with the positions of landmark holes. Putative positive clones were determined by comparison between the two duplicate films.

For the secondary screening, landmark labels on film were lined up with the dots on the back of the plates and the site of the putative positive clones was marked on the back of the plate. Agarose “windows” corresponding to putative positive clones were cut and placed in 1 ml SM Buffer supplemented with 20 µl chloroform. This was vortexed for 10 min and left for at least 2 h in rotating carousel at room temperature. In 15 ml tubes, 3 different concentrations of phage suspension in SM Buffer were added to 300 µl of O.D.₆₀₀ = 0.5 host cells, aiming for an ideal 1000 pfu. These mixes were incubated for 15 min at 37 °C, after which they were combined with 3 ml 48 °C Top-agarose. Whole mix was poured onto LB plates and left to harden at room temperature for 10 min. Plates were incubated inverted for 8 – 9 h at 37 °C; then placed at 4 °C. The plate with the most appropriate plaque concentration was chosen to carry out screening, as before. Up to quaternary screening was performed in order to obtain plates containing solely a positive clone.

The probe used to screen this library was the mouse *Sgk* cDNA fragment identified in the endoderm library, linearised with *Sal* I and labelled with ³²P-dCTP.

2.3.16 Southern analysis of genomic DNA

Lambda DNA was subject to various single and double digestions. Fragments were separated on a 0.8% agarose gel and transferred to a nylon filter (HybondTM-N+). Filters were probed with a ³²P-labelled DNA probe. Hybridisation solution consisted of Amersham Rapid-Hyb Buffer. Hybridisation was performed O/N at 50 °C in rotating bottles. The following day, filters were washed at room temperature in 5x SSC, 0.1% SDS, covered with plastic wrap and exposed at least O/N to X-ray films in cassettes at –80 °C. Between probing with different probes, filters were stripped with 0.4 N NaOH at 45 °C for 30 min and washed in 0.1x SSC, 0.1% SDS, 0.2 M TRIS (pH 7.5) at 45 °C for 15 min.

DNA fragments used as templates for probes used for Southern analysis are described in Chapter 4 (see Fig. 4.9).

2.3.17 Cloning of DNA fragments prepared by restriction digest

Cloning reactions of restriction digest products contained a molar ratio of $\geq 3:1$ of insert : vector, whenever possible, in a total volume of 10 μ l. Fresh or gel-extracted digest products were EtOH-precipitated before mixed with 1 μ l of 10x DNA ligase buffer and 1 μ l of 10x DNA ligase. Mix was incubated O/N at 16 °C. 2 – 10 μ l of the ligation reaction were then transformed into competent bacteria as described above.

2.3.18 Cloning of PCR products

The cloning of PCR products was performed using the TOPO TA Cloning kit (Invitrogen). The cloning reaction consisted of the following: 4 μ l fresh or gel extracted PCR product, 1 μ l of 1.2 M NaCl solution and 0.5 μ l pCR II-TOPO vector (which contains covalently bound topoisomerase I for fast cloning). These were mixed gently and incubated for 5 min at room temperature. 2 μ l of this reaction were then transformed into competent bacteria as described above.

2.3.19 Total RNA purification

Embryos, tissues or cells for RNA purification were either fresh or quick-frozen for 10-15 min in dry-ice and stored at -80 °C. TRIzol reagent (GibcoBRL) was used for total RNA purification, essentially according to manufacturer's instructions. 1 ml TRIzol Reagent was added to approximately 100 μ l of embryos, tissues or cells and these were triturated thoroughly in homogeniser and/or by passing suspension several times through needle or pipette tip. 200 μ l chloroform were added and mixture was left for 3 min at room temperature. Samples were centrifuged at 12,000 x g for 15 min at 4 °C. The aqueous (upper) phase was transferred to fresh tube and 0.5 ml isopropanol was added. The mixture was left for 10 min at room temperature and then centrifuged at 12,000 x g for 10 min at 4 °C. The pellet was washed by adding 1 ml of 70 % EtOH and vortexing. The suspension was centrifuged at 7,500 x g for 5 min at 4 °C and the pellet was left to dry at room temperature for approximately 10 min. The dry pellet was resuspended in water and placed at 55 °C to dissolve completely when necessary. The

RNA solution was then subject to DNase treatment for 1 – 2 h at 37 °C. RNA was extracted by adding equal volume of acid phenol (pH 4.5) : chloroform (1:1), vortexing vigorously and centrifuging at 12,000 x g for 15 min at 4 °C. The aqueous phase (approximately 100 µl) was transferred to fresh tube and 200 µl EtOH + 10 µl 3 M NaOAc (pH 4.5) were added. The RNA was left to precipitate for 30 min at –80 °C and then centrifuged at 12,000 x g for 15 min at 4 °C. The pellet was washed with 70% EtOH and spun at 12,000 x g for 5 min at 4 °C and left to dry at room temperature for approximately 10 min. The pellet was resuspended in water and placed at 55 °C to dissolve completely when necessary. Finally, 1 µl RNA solution was analysed by gel electrophoresis, with 0.5 µl RNase Inhibitor.

2.3.20 mRNA purification from total RNA

Poly-T-coated Dynabeads (Dynal) were resuspended by placing tube in roller O/N at 4 °C. The concentration of total RNA was adjusted to 75 µg / 100 µl with 10 mM TRIS-HCl (50 – 250 ng mRNA should be obtained per 75 µg total RNA) and the solution was heated to 65 °C for 2 min and placed on ice. Dynabeads were washed by pipetting into microfuge tube, placing on the Dynal magnetic particle concentrator (MPC) for 30 s, discarding supernatant, removing tube from MPC, resuspending beads in 100 µl Binding Buffer (Dynal), and repeating this once. The 100 µl of RNA solution were added to resuspended 100 µl resuspended Dynabeads and mixed thoroughly by placing tube in roller for 3 – 5 min at room temperature. The tube was then placed on MPC for at least 30 s (until solution is clear) and the supernatant was discarded. The Dynabeads were washed twice with 200 µl Washing Buffer B (Dynal), with complete removal of the supernatant between washes. The mRNA was eluted from the Dynabeads by adding 5 – 20 µl of 10 mM TRIS-HCl, heating to 65 – 80 °C for 2 min, placing tube immediately on MPC, and immediately recovering RNA-containing supernatant into fresh tube.

2.3.21 Reverse transcriptase (RT)-PCR

First strand cDNA was synthesised from total RNA template using random hexamer primers and superscript reverse transcriptase (GibcoBRL). To this end 20 µl aqueous reactions were prepared, containing 1 µg of RNA, 1 µl 0.1 mg/ml primer mix, 4 µl 5x RTase buffer, 1 µl 20 mM dithiothritol (DTT), 0.5 µl RNase inhibitor, 2 µl 5 mM dNTP

mix and 0.25 μ l RT. A negative control devoid of RT was also prepared. Reactions were allowed to proceed at 42 °C for 30 min, after which cDNAs were used directly as templates for PCRs with specific primers for *Sgk*, *Oct4* or *Gapdh* (Table 2.3). RT-PCR primers for *Oct4* were manually designed and kindly provided by Dr. Ariel Avilion. RT-PCR primers for glyceraldehyde 3-phosphate dehydrogenase (*Gapdh*), as well as for *Sgk* were designed using *Primer3* software (see above).

Table 2.3 Primers used in this investigation for RT-PCR

cDNA	Forward Primer	Reverse Primer
<i>Sgk</i>	GCCAAGTCCCTCTCAACAAA	CAGGAAAGGGTGCTTCACAT
<i>Oct4</i>	GACAACAATGAGAACCTTCAGGAG	CTGAGTAGAGTGTGGTGAAGTGG
<i>Gapdh</i>	CCCACTAACATCAAATGGGG	CCTTCCACAATGCCAAAGTT

PCR was performed on 20 μ l aqueous reactions, containing 2 μ l cDNA template prepared as described above, 2 μ l 0.05 mg/ml of each of the gene-specific primers, 2.5 μ l 10x Taq DNA polymerase buffer, 0.5 mM dNTP mix, 0.1 10 μ C/ μ l ³²P dATP and 0.25 μ l 5 U/ μ l Taq DNA polymerase. PCR program was as follows:

93 °C for 2.5 min
 25 cycles of: 94 °C for 1 min
 55 °C for 1 min
 72 °C for 1 min
 Ended by 1x: 72 °C for 5 min

PCR products were analysed by non-denaturing polyacrylamide gel electrophoresis. 60 ml gels were prepared with 6% polyacrilamide in 1x TBE, 0.1% APS. Just before pouring, 120 μ l of the polymerising agent TEMED were added and gel was allowed to polymerise for at least 2 h. Buffer consisted of 1x TBE. Gels were pre-run for 15 – 20 min at 12 – 14 W, loaded, and then run at 12 W for approximately 2 h. After running, gel was fixed for 20 min in 25% MeOH, 10% acetic acid, dried for 2 h in gel dryer (Savant), and exposed to X-ray films in cassettes at -80 °C.

2.3.22 Rapid amplification of cDNA ends (RACE)

RACE PCRs were performed using cDNAs synthesised by the GeneRacer cDNA amplification kit (Invitrogen). mRNA was purified total RNA purified from pooled zebrafish embryos of the following stages: sphere, 50% epiboly, 11-13 somite, 40 h and 4 days (a volume of 100 μ l of embryos of each stage). Non-mRNA or truncated mRNA species were dephosphorylated by treatment with calf intestinal phosphatase (CIP). The reaction consisted of 0.2 μ l mRNA (containing 200 ng mRNA), 1 μ l 10x CIP buffer, 1 μ l 40 U/ μ l RNaseOUT, 1 μ l 10 U/ μ l CIP made up to 10 μ l with water. The reaction was allowed to proceed at 50 °C for 1 h, after which RNA was phenol-chloroform-extracted and ethanol-precipitated with the aid of 2 μ l 10 mg/ml glycogen. The pellet was resuspended in 7 μ l water, after which the 5' cap structure was removed from full-length mRNA. This reaction consisted of 7 μ l dephosphorylated mRNA, 1 μ l 10x tobacco acid pyrophosphatase (TAP) buffer, 1 μ l 40 U/ μ l RNaseOUT and 1 μ l 0.5 U/ μ l TAP. Reaction was allowed to proceed at 37 °C for 1 h, after which RNA was phenol-chloroform-extracted and ethanol-precipitated with the aid of 2 μ l 10 mg/ml glycogen. The pellet was resuspended in 7 μ l water, after which the GeneRacer 5' RNA oligonucleotide (CGACUGGAGCACGAGGACACUGACAUGGACUGAAGGAG UAGAAA) was ligated to the 5' end of decapped mRNA. Decapped mRNA was heated at 65 °C for 5 min to relax secondary structure and left to rest on ice for 2 min. Subsequently, the RNA was mixed with 1 μ l 10x ligase buffer, 1 μ l 10 mM ATP, 1 μ l RNaseOUT and 1 μ l T4 RNA ligase. The reaction was allowed to proceed at 37 °C for 1 h, after which RNA was phenol-chloroform-extracted and ethanol-precipitated with the aid of 2 μ l 10 mg/ml glycogen. The pellet was resuspended in 10 μ l water, after which it was reverse transcribed using either the GeneRacer Oligo dT primer or a random primer mix. RNA template (10 μ l) was mixed with 50 μ M primers (1 μ l) and heated at 65 °C for 5 min to relax secondary structure, after which they were left to rest on ice for 2 min. Subsequently, 2 μ l 10x RT buffer, 1 μ l 5 U/ μ l avian myeloblastosis virus (AMV) RT, 1 μ l RNaseOUT and 4 μ l water were added to this mix. Reaction was allowed to proceed at 42 °C for 1 h, after which AMV-RT was heat-inactivated at 85 °C for 15 min. The cDNA thus prepared was stored at -20 °C and used directly for 5' RACE.

RACE reactions were performed by nested PCR. The GeneRacer 5' end primer (CGACTGGAGCACGAGGACTGA) and a gene-specific primer (GSP 1), designed by us using Primer3 software (see above), were used in a first round of PCR, for 15 cycles. The product of this round of PCR was diluted 1/40 and 5 μ l of this dilution were used as template for the second round of PCR. In the latter, the GeneRacer 5' end nested primer (GGACTGACATGGACTGAAGGAGTA) and a second, nested, gene-specific primer (GSP 2) were used for 25 cycles. The GSP primers used in this investigation for 5' RACE are indicated in Table 2.4.

Each PCR reaction consisted of the following: 5 μ l DNA template, 5 μ l 10x buffer, 36 μ l water, 1 μ l 10 mM dNTP mix, 1 μ l 10 μ M each primer and 1 μ l Taq polymerase. A touchdown PCR program was used to increase specificity of the reaction. The standard PCR program used was as follows:

	94 °C for 3 min
5 cycles of:	94 °C for 30 s
	72 °C for 4 min*
5 cycles of:	94 °C for 30 s
	70 °C for 4 min*
15 or 25 cycles of:	94 °C for 30 s
	68 °C for 4 min*

*Extension time was varied according to the expected length of the PCR product, with a minimum of 2 min and adding 1 min more for each kb of predicted product (e.g. 3 min for a 1 kb product, 4 min for a 2 kb product, etc.).

2.3.23 Riboprobe synthesis

Template (plasmid) DNA was linearised for 2 h after which 1/4 of initial volume of enzyme was added and left to digest for 1 h more. In all cases, digoxigenin (DIG)-labeled deoxy-uracil triphosphate (dUTP) (Boehringer Mannheim) was incorporated during RNA transcription, following manufacturer's instructions. After synthesis, riboprobes were treated with 20 U DNase I (Boehringer Mannheim) at 37 °C for 15 min to remove DNA template and were purified by size-exclusion chromatography through a DEPC water column (Clonatech Chroma Spin-100). All riboprobes were electrophoresed on a 1% agarose gel to check size and integrity prior to use. All

Table 2.4 Primers used in this investigation for 5' RACE

cDNA RACEd	Gene-specific primer 1	Gene-specific primer 2 (nested primer)
ptp(r) σ	GTTTCCAGCGGTGGGAAGACAATGG	TGGGTCCACCATCGCTACTGTCCTG
embigin	ACCAGTTCCAGGTGTTTGGCATGTG	CCAATGTAGCTCACCACAGGCTTGTCC
lztr-1	TGACGCTTCAATGTACTGAACGCAGAGC	CTGCTGCATGGAACAGCCTTCCACTT
sp120	CTCGGCCTTCAACCCCTTGTCAGAG	TGCCGCTTCTTTAGCTCGTCCTTCA
Rho GEF 16	ATCAGAAGCGGCAGACGGGTGACTC	TGCATGGGTAAGAAGGAGAGCA
liv-1-related	TGATGCACCATCACTTTCCGGATGC	ATCTGGTACAGGAGGGCAGGGCACA
novel p7822b53	GACAGCACCAAACGGTGAAGCTGGA	TGATGCTCTTCACAACACGGCTGGA

riboprobes were denatured (at 80 °C for 2 min, followed by 5 min on ice) prior to adding to Hyb solution. Mouse riboprobes were added to Hyb immediately prior to use and this Hyb was discarded after use. Zebrafish riboprobes were added to Hyb shortly after synthesis and were stored in this way. For zebrafish *in situ* hybridisations, the same riboprobe-containing Hyb solution was used several times. In all cases, riboprobes were stored at -20 °C

Mouse endoderm library cDNAs are in a pSPORT1. To prepare antisense riboprobes, these plasmids were linearised with *Sal* I and transcribed with SP6 RNA polymerase. Zebrafish cDNAs used as templates to prepare antisense riboprobes are indicated in Table 2.5, along with the restriction enzyme used to linearise plasmid and RNA polymerase used to transcribe cDNA. Templates consisted of EST cDNAs, 5'RACE products, ordinary PCR products or Stemple Lab stock plasmids obtained from a variety of sources. In the cases where templates were isolated by 5'RACE or ordinary PCR, they were cloned into pCR II TOPO. Primers used to PCR riboprobe templates, other than by 5'RACE are indicated in Table 2.6. The zebrafish sequences determined in this investigation are presented in Appendix 3.

2.3.24 MO column-purification

MOs were supplied lyophilised (approximately 300 nmole) and resuspended in 60 µl of DEPC water. Concern about MO purity led to the standard procedure of column-purification of MO suspension using Micro-spin G-25 diethyl-pyrocabonate (DEPC) water columns (Amersham Pharmacia). Columns were pre-spun at 750 x g for 2 min in a bench-top centrifuge. 50 µl MO solution were loaded onto a column and spun at 750 x g for 2 min in a bench centrifuge (MSE MicroCentaur). The first eluate is the most concentrated one; it was quantified spectrophotometrically and diluted in MO Buffer (containing phenol red) to the desired concentration prior to injection. A second eluate was also recovered from the columns by adding 50 µl of DEPC water and spinning at 750 x g for 2 min in a bench centrifuge (MSE MicroCentaur). Note: MOs precipitate out of solution even when stored at -20 °C. Therefore, when using a MO solution for a period of months, it is advisable to re-evaluate regularly its real concentration by spectrophotometry.

Table 2.5 Preparation of zebrafish antisense riboprobes used in this investigation

cDNA	Template origin	Template size (bp)	Vector	Linearisation	RNA polymerase
<i>ptp(r)</i> σ	PCR product	1677	pCR II TOPO	<i>Not</i> I	SP6
<i>14-3-3</i> ϵ	EST fk44f04	480	pSPORT1	<i>Eco</i> R I	SP6
<i>embigin</i>	5' RACE product	650	pCR II TOPO	<i>Spe</i> I	T7
<i>lztr-1</i>	EST fj94f07	710	pBK-CMV	<i>Bam</i> H I	T7
<i>claudin b</i>	EST fb01g12	1082	pBK-CMV	<i>Sal</i> I	T7
<i>claudin-like</i>	EST AGENCOURT_10693383	737	pCMV-SPORT6.1.ccdb	<i>Not</i> I	SP6
<i>pancortin</i> Module A	PCR product	350	pCR II TOPO	<i>Xho</i> I	SP6
<i>pancortin</i> Module B (EST)	PCR product	250	pCR II TOPO	<i>Xho</i> I	SP6
<i>pancortin</i> Module B (genomic)	PCR product	377	pCR II TOPO	<i>Xho</i> I	SP6
<i>pancortin</i> Module Y	PCR product	495	pCR II TOPO	<i>Xho</i> I	SP6
<i>pancortin</i> Module Z	PCR product	1090	pCR II TOPO	<i>Hind</i> III	T7
<i>calcyphosine</i> (EST)	EST fj05b10	626	pSPORT1	<i>Sac</i> II	SP6
<i>sp120 a</i>	EST fb39f08	1474	pSPORT1	<i>Sal</i> I	SP6
<i>sp120 b</i>	EST fb93d06	> 3500	pSPORT1	<i>Sal</i> I	SP6
<i>plu-1 a</i>	PCR product	890	pCR II TOPO	<i>Bam</i> H I	T7
<i>plu-1 b</i>	PCR product	930	pCR II TOPO	<i>Not</i> I	SP6
<i>nsa2</i>	EST fb52h05	1113	pSPORT1	<i>Sal</i> I	SP6
<i>transformer 2</i> β	EST fk31a01	1073	pBK-CMV	<i>Sal</i> I	T7
<i>rho GEF 16</i>	5' RACE product	520	pCR II TOPO	<i>Bam</i> H I	T7
<i>liv-1-related</i>	EST ZF637-2-000611	1733	pSPORT1	<i>Eco</i> R I	SP6
novel p7822b53	PCR product	940	pCR II TOPO	<i>Not</i> I	SP6

Table 2.5 (cont.)

cDNA	Template origin		Linearisation	RNA polymerase
flh	As in Talbot <i>et al.</i> , 1995	(Stemple Lab stock)	<i>EcoR</i> I	T7
fgf 8	As in Furthauer <i>et al.</i> , 1998	(Stemple Lab stock)	<i>Xba</i> I	T7
PapC	As in Yamamoto <i>et al.</i> , 1998	(Stemple Lab stock)	<i>Apa</i> I	T3
pax 2b	As in Krauss <i>et al.</i> , 1991	(Stemple Lab stock)	<i>BamH</i> I	T7
hgg1	As in Thisse <i>et al.</i> , 1994	(Stemple Lab stock)	<i>Xho</i> I	T3
gsc	As in Stachel <i>et al.</i> , 1993	(Stemple Lab stock)	<i>EcoR</i> I	T7
dbx1a	As in Fjose <i>et al.</i> , 1994	(Stemple Lab stock)	<i>Xba</i> I	T7
axial	As in Strahle <i>et al.</i> , 1993	(Stemple Lab stock)	<i>Sac</i> I	T3
eve1	As in Joly <i>et al.</i> , 1993	(Stemple Lab stock)	<i>EcoR</i> I	T7
bhikhari	As in Vogel and Gerster, 1999	(Stemple Lab stock)	<i>Pst</i> I	T7
bmp2b	As in Nikaido <i>et al.</i> 1997	(Stemple Lab stock)	<i>Xba</i> I	T7
ntl	As in Schulte-Merker <i>et al.</i> , 1992	(Stemple Lab stock)	<i>Xho</i> I	T7

Table 2.6 Primers used in this investigation to isolate templates for riboprobe synthesis

cDNA	Forward Primer	Reverse Primer
pancortins Module A	CTGCGTGACGCTCATCTAAC	GTGAGTTCCGTGCCCATC
pancortins Module B (ESTs)	TTGGTGGTCCTCCAGTTCTC	AGCAGTGACAGCGACACACT
pancortins Module B (genomic)	GCAGACTGCTCGGTTTTTCAT	GGTCAGTTTGGTGGTGTGGA
pancortins Module Y	GGCTAACTATAAAGACATGATAGGAGA	GGGAAAAGACTTTATTAGTTTATCGTT
pancortins Module Z	CCGTCCTGGAGGAGTACAAA	CCAAAGGATGGTCTTGTTCC
plu-1 a	TCCTACCTCACACCACCACA	GGAAGAGAAACCTGCTGCAC
plu-1 b	GCACTATTGCTCGCAGA	CCGAAACCTCCAGAAACGTA
novel p7822b53	GATGACGTCACTGCGAAGAA	ACACTAATGGCGTGGTCCTC

2.4 ES cell manipulation

2.4.1 Production of buffalo rat liver (BRL) cell conditioned medium

BRL cells were stored in cryovials submerged in liquid nitrogen. Each BRL cell vial was thawed into and grown in previously gelatinised 150 mm tissue culture dishes: dish surface was covered with 0.1% gelatine solution for at least 5 min, which was then replaced with medium in order for gelatine not to dry. BRL cells were cultured in E14.2 Medium (480 ml Dulbecco's modified Eagle's medium (DMEM) High glucose / no L-glutamine, 6 ml L-glutamine, 6 ml non-essential amino acids, 4.4 μ l β -mercaptoethanol) supplemented with 20% ES quality foetal calf serum (ESQ FCS). All FCS batches were tested for their ability to support normal ES cell growth at clonal densities according to Robertson, 1987.

To thaw BRL cells, cryovials were removed from liquid nitrogen and placed into ice with screw caps loosened. After a few minutes on ice, cryovials were placed at 37 °C to thaw completely. Cells were then transferred into a 15 ml tube and 9 ml of ES cell Complete Medium (1000 U/ml leukaemia inhibiting factor (LIF) in 3:2 BRL cell conditioned medium : E14.2 Medium supplemented with 20% ESQ FCS; see below for BRL conditioned medium) were slowly added while agitating the tube. Cells were spun-down at 250 x g for 5 min, resuspended in fresh medium and plated. Cells were incubated at 37 °C in a 95% humidified incubator with 7% CO₂ until reaching 80 – 90% confluency. At this stage, the medium was collected, filtered through a 0.2 μ m pore membrane and stored at -20°C. Cells were split 1:10 as follows: cells were washed with Ca²⁺ and Mg²⁺ free (CMF) PBS; 3 ml of 37 °C Trypsin/EDTA (0.25% Trypsin, 1 mM Na₂EDTA in CMF PBS (pH 7.5)) were added per 15 mm dish; cells were incubated in Trypsin/EDTA at 37°C for 5 min or slightly longer, until lifting from dish. This suspension was further triturated (approximately 6 times) with a P1000 tip in order to obtain a single cell suspension. Trypsin solution was neutralised by adding at least 5 times its volume of medium, and 9 x 1/10 cell suspension was plated in 9 new dishes.

The non-plated 1/10 cell suspension was spun at 250 x g for 5 min and resuspended in 1 ml of 90% foetal bovine serum (FBS), 10% dimethylsulphoxide (DMSO). This cell suspension was transferred to a cryovial, which was placed in a freezing pot (Nalgene)

containing isopropanol, O/N at -80°C . The following day, the cryovial was transferred from -80°C to liquid nitrogen.

The nine new plates were grown for 2 days, after which conditioned medium was collected and replaced by fresh medium. This process was repeated two more times, after which plates were discarded. As before, collected medium was filtered through a $0.2\ \mu\text{m}$ pore membrane and stored at -20°C .

2.4.2 ES cell thawing, expansion and freezing

ES cells used in this investigation were feeder-independent E14.2 cells (Fisher *et al.*, 1989). ES cells were stored in cryovials submerged in liquid nitrogen. Each ES cell vial was thawed into a $25\ \text{cm}^2$ tissue culture flask. Flasks or tissue culture dishes were always gelatinised prior to ES cell plating (see above section).

To thaw ES cells, cryovials were removed from liquid nitrogen and placed into ice with screw caps loosened. After a few minutes on ice, cryovials were placed at 37°C to thaw completely. Cells were then transferred into a 15 ml tube and 9 ml of ES cell Complete Medium were slowly added whilst agitating the tube. Cells were spun-down at $250 \times g$ for 5 min, resuspended in ES cell Complete Medium and plated. Cells were incubated at 37°C in a 95% humidified incubator with 7% CO_2 . ES cell Complete Medium was replaced daily until culture reached 70 - 80% confluency (3 - 4 days).

Medium was replaced 2 – 4 h prior to splitting ES cells. For splitting, medium was removed and cells washed with CMF PBS. 0.3 ml of 37°C Trypsin/EDTA was added per $25\ \text{cm}^2$ flask (or an accordingly higher volume for larger flasks or plates). Cells were incubated in Trypsin/EDTA at 37°C for 5 min or slightly longer, until lifting from dish. This suspension was further triturated (approximately 6 times) with a P1000 tip in order to obtain single cell suspension. Trypsin solution was neutralised by adding at least 5 times its volume of medium, and 1/6 – 1/4 cell suspension was plated per new flask, as needed.

To freeze, ES cells were spun-down at $250 \times g$ for 5 min, the supernatant was carefully aspirated and cells were resuspended at the approximate concentration of 5×10^6 cells/ml in 90% FBS, 10% DMSO. This cell suspension was transferred to a cryovial, which

was placed in a freezing pot (Nalgene) containing isopropanol, O/N at -80°C . The following day, the cryovial was transferred from -80°C to liquid nitrogen.

2.4.3 ES cell electroporation with targeting vector

For each ES cell transfection, around 3×10^7 cells should be used, that is, a well growing 75 cm^2 flask. Prior to electroporation, cells were washed in CMF PBS, trypsinised, washed again in CMF PBS, and resuspended in 0.8 ml DMEM. This cell suspension was then transferred to a 0.4 cm electroporation cuvette and mixed with 40 μg of linearised targeting vector suspended in 0.1 ml DMEM. Mixture was left to stand at room temperature for 20 min, after which it was subject to 2 electro-shocks: first, at 240 V, 500 μF for approximately 6 s; second, at 230 V, 500 μF for approximately 6 s. Cuvette was tapped and placed on ice for 20 min. Electroporated cells were then transferred to a 50 ml tube where 30 ml of ES cell Complete Medium was added. Cells were plated in 3 x 10 mm dishes.

2.4.4 ES cell antibiotic resistance selection

Positive selection is started the day following electroporation with the targeting vector. The positive selection cassette used in the *Sgk* targeting vector contained the neomycin-resistance gene, so cells were incubated in G418, at the concentration 200 $\mu\text{g}/\text{ml}$ ES cell Complete Medium. Cells were washed with CMF PBS daily and medium replaced by fresh one, until resistant colony picking had ended (12 days later).

2.4.5 Resistant ES cell colony picking and culture

Resistant ES cell colonies reached an adequate size for picking by 10 days of incubation in selection medium. Each colony was picked into an individual well of a round-bottomed non-gelatinised 96-well plate containing 25 μl Trypsin/EDTA / well. Prior to picking colonies, medium was replaced by 10 ml CMF PBS. Colonies were picked in CMF PBS outside the tissue-culture hood, using a microscope. Each colony was gently detached around the edges with a 10 μl tip, aspirated and transferred into a well containing Trypsin/EDTA. After picking 48 colonies (half of the 96-well plate), 75 μl medium were added to the first row of trypsinised colonies. These were triturated well and transferred to a flat-bottomed 96-well plate, previously gelatinised and containing

50 μ l of 200 μ g/ml G418 in ES cell Complete Medium / well. This process was repeated for the other three rows of trypsinised cells. The whole procedure was repeated until all colonies available in that day were picked. Colonies were picked during 2 days.

The cultures in the 96-well plates were fed daily until the majority was ready to split. Each clone was split into 2 wells of 48-well plates, one in each plate, in order to generate duplicate 48-well plates. A few cells were left in original 96-well plates and left to grow for subsequent preparation of genomic DNA. Clones in the 48-well plates were frozen individually in cryovials, when approximately 80% confluent.

Chapter 3

Whole-mount *in situ* hybridisation screen of a mouse endoderm library

Chapter 3

Whole-mount *in situ* hybridisation screen of a mouse endoderm library

- 3.1 Introduction to the *in situ* hybridisation screen of the endoderm library
 - 3.1.1 Organism gene counts
 - 3.1.2 Gene expression profiling
 - 3.1.3 Mouse endoderm cDNA library
 - 3.2 Results of the *in situ* hybridisation screen of the endoderm library
 - 3.2.1 Sequence-based clone selection
 - 3.2.2 Expression analysis
 - 3.2.3 Brief description of 12 restricted expression patterns
 - 3.2.4 Synexpression and co-expression groups
 - 3.3 Discussion of the *in situ* hybridisation screen of the endoderm library
 - 3.3.1 Overview
 - 3.3.2 Efficiency of novel strategy for cDNA selection
 - 3.3.3 Perspectives
-

3.1 Introduction to the *in situ* hybridisation screen of the endoderm library

3.1.1 Organism gene counts

The complete genomic sequences of several animal species have been or will soon be determined (The *C. elegans* genome consortium, 1998; Adams *et al.*, 2000; International Human Genome Sequencing Consortium, 2001; Venter *et al.*, 2001; Aparicio *et al.*, 2002; Carlton *et al.*, 2002; Dehal *et al.*, 2002; Gardner *et al.*, 2002; Mouse Genome Sequencing Consortium, 2002). Although the past decade taught us how similar patterning mechanisms can be between distantly related animals, we still appreciate big differences between a fly and a man, from morphology and physiology to behaviour. It was therefore expected that more genes might account for the greater complexity of a species over another. However, as far as current predictions go, this is not the case. Flies possess ~13,600 protein-coding genes, nemotodes ~19,000, the lower chordate *Ciona intestinalis* is estimated to have ~16,000, and mice and humans ~30,000 (The *C. elegans* genome consortium, 1998; Adams *et al.*, 2000; Venter *et al.*, 2001; International Human Genome Sequencing Consortium, 2001; Dehal *et al.*, 2002; Mouse Genome Sequencing Consortium, 2002).

Estimates of the number of protein-coding genes and gene products in a genome rely on prediction algorithms that are designed with all the existent knowledge about gene structure, as well as experimental evidence for the expression of these genes. For example, sequencing of multiple full-length-enriched cDNA libraries generated by the RIKEN Mouse Gene Encyclopedia Project contributed around 22,000 new exons and 1,200 new genes to the efforts of the mouse genome project (Mouse Genome Sequencing Consortium, 2002).

To resolve real genes and pseudogenes and to identify non-coding genes and splice variants, direct analysis of expressed genes is essential. For example, mammals use alternative splicing to produce, on average, significantly more proteins per gene than other genomes sequenced (International Human Genome Sequencing Consortium, 2001; Venter *et al.*, 2001; The FANTOM Consortium and the RIKEN Genome Exploration Research Group Phase I & II Team, 2002). This suggests a significant increase in the number of gene products generated by the genomes of increasingly complex organisms. Nonetheless, genomic and proteomic analyses, namely between humans and invertebrates, has shown that increased organism complexity is associated with a richer arrangement of pre-existing components, such as more domains per protein and novel combinations of domains (Baltimore, 2001).

3.1.2 Gene expression profiling

The generation of cDNA libraries and the sequencing of cDNA clone ends, called expressed sequence tags (ESTs), is a simple and effective way to evaluate the expression profile of tissues, organs or whole-organisms. Once an expressed gene is identified, it becomes important to elucidate its function. One approach is to describe the spatio-temporal profile of its expression as well as the phenotype caused by perturbation of this expression. Also, it has often been the expression pattern of a gene that has motivated endeavours for the elucidation of its function and/or been the first clue to the existence of a previously unsuspected structure or process. For example, the expression of *Hex* in the mouse AVE led to the recognition of a distinct molecular domain within the VE (Thomas, 1998); and in chick, it was the cyclic expression of *cHairy1* in the paraxial mesoderm that led to the recognition of a segmentation clock involved in somitogenesis (Palmeirim *et al.*, 1997).

Gene expression analysis can be performed in several ways, from reverse transcriptase-polymerase chain reaction (RT-PCR) to the recent technique of microarray hybridisation, but *in situ* hybridisation is the only method that provides spatial information. Many research groups have screened cDNA libraries from various model systems by whole-mount *in situ* hybridisation, following the temporal and spatial pattern of mRNA expression during embryogenesis. Libraries screened have either been unmanipulated ones (for example, Gawantka *et al.*, 1998), normalised (for example, Neidhardt *et al.*, 2000; Kudoh *et al.*, 2001) or libraries which have undergone subtractive hybridisation with another library in order to enrich for genes expressed differentially between the tissues from which the libraries were made (for example, Christiansen *et al.*, 2001; Neidhardt *et al.*, 2000). Although subtractive hybridisation greatly enriches for differentially expressed genes, and greatly reduces the number of essential genes screened, which by definition are ubiquitously expressed, it has the disadvantage of greatly enriching for clones that are expressed at high levels, at the expense of rare transcripts. This problem can be overcome by performing a normalisation prior to subtraction, which places the representation of rare transcripts on a par with high copy number ones, at the minor risk of loss of some clones.

Although there are many examples of developmentally important genes expressed in a widespread manner, restricted expression patterns may suggest a function, especially when associated with other pieces of information. For example, the combination of gene mapping with expression analysis has been the basis for defining candidate human disease genes (Ballabio, 1993; Reymond *et al.*, 2002).

3.1.3 Mouse endoderm cDNA library

The Beddington mouse endoderm cDNA library was generated from 7.5 dpc endoderm dissected manually from mouse embryos (Harrison *et al.*, 1995). At 7.5 dpc, the definitive endoderm is *in continuum* with the VE, the node and the axial mesendoderm. Hence, these three signalling centres are represented in the endoderm library. The endoderm library contains more than 5.8×10^5 independent clones of which approximately 10,000 have been randomly picked and gridded into 384-well plates using an automatic colony picker (Harrison *et al.*, 1995). Nearly 2000 of these clones have been partially sequenced, and the ESTs clustered, in collaboration with Dr.s A.

Forrest, S. Grimmond, P. Avner and H. Lehrach, based at the Institute of Molecular Bioscience, University of Queensland, Australia, Unité Génétique Moleculaire Murine, Institut Pasteur, Paris, France, and the Max-Planck Institute for Molecular Genetics, Berlin, Germany. Clustering of 1978 ESTs resulted in 1440 independent sequences.

I screened clones from this library by whole-mount *in situ* hybridisation to identify genes whose expression pattern suggested a role in early patterning. On the whole, I was looking for restricted expression patterns but, in particular, I was looking for genes with an asymmetric expression prior to or during the onset of gastrulation, especially in the VE, as well as genes expressed in the node and/or axial mesendoderm

3.2 Results of the *in situ* hybridisation screen of the endoderm library

I performed this screen with two other students (Kettleborough, 2002; Rana, 2003). I present the combined results of the three of us so that the screen is appreciated in its entirety. I will delineate my own contribution.

3.2.1 Sequence-based clone selection

We first compared 1440 independent mouse ESTs with the publicly available sequence databases using gapped BLAST algorithms (Altschul *et al.*, 1997). I performed one-third of these sequence comparisons. We found that 1317 of these sequences matched mouse ESTs and 123 did not. We found mouse orthologues of genes identified in other species, genes similar to others previously identified either in mouse or other species, clones containing a known domain, and clones which matched nothing in the current databases.

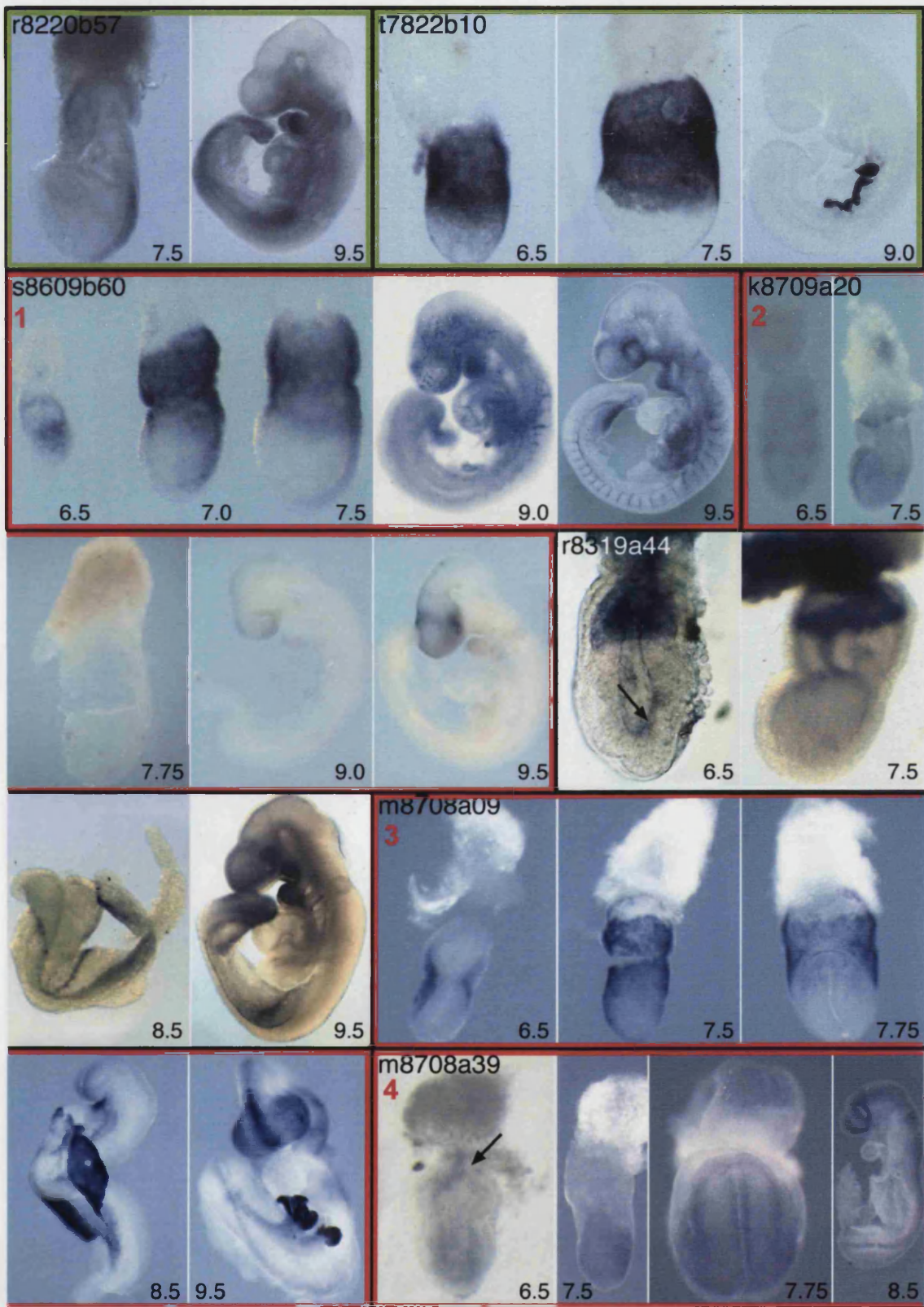
We excluded cDNAs predicted to be ubiquitously expressed, cDNAs representing genes already extensively studied in a developmental context and cDNAs representing the same gene. We selected clones that matched genes, or domains found in genes, belonging to one of the following categories: transcriptional regulators and proteins involved in chromatin structure, splicing factors and proteins involved in RNA binding and transport, components of signalling cascades, cell-cycle regulators, cytoskeleton

constituents, extracellular matrix components, and genes implicated in human disease. In addition, clones that matched uncharacterised ESTs found in other species and clones that did not match anything in the databases were also selected. With these criteria, 173 clones were selected for expression analysis and I selected 38 of these.

3.2.2 Expression analysis

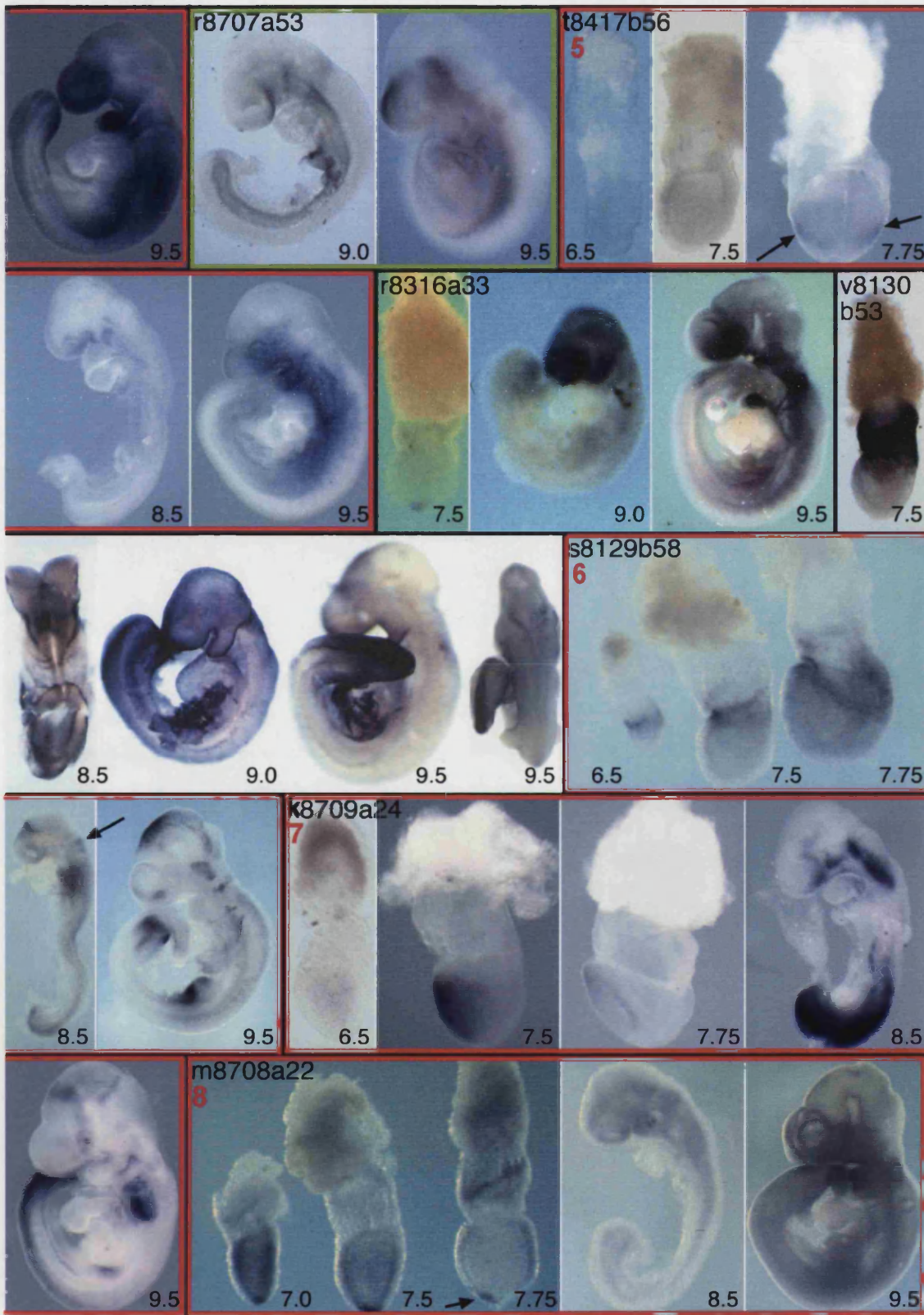
We performed whole-mount *in situ* hybridisation on 6.5 – 9.5 dpc mouse embryos with riboprobes derived from 160 of the 173 selected clones. The remainder 13 clones either did not grow, linearise, release insert or transcribe. The expression patterns obtained were classified subjectively as ubiquitous (64; 40 %) if similar levels of expression were observed in all tissues, widespread (57; 36 %) if expression was observed in several but not all tissues (frequently with different levels in different tissues), restricted (29; 18 %) if transcripts were detectable in just a few regions or tissues in at least one of the embryonic stages examined, and undetectable (10; 6 %) when no expression was observable at any of the stages examined.

The expression patterns of the 29 cDNAs classified as restricted, as well as two examples of widespread and one example of a ubiquitous expression pattern, are shown on Fig. 3.1. Details concerning the identification of the restricted clones are presented in Table 3.1 and details concerning the identity and expression classification of widespread and ubiquitous clones is presented in an Appendix to this Thesis. I identified 12 clones with restricted expression patterns. I depict and describe their expression at all stages examined. With the exception of *Sgk*, *mD2LIC* and *v8130b25*, these descriptions are based solely on the observation of whole-mount stained embryos; in some cases, confirmation and/or more detailed description of the tissues stained would require analysis of sections.



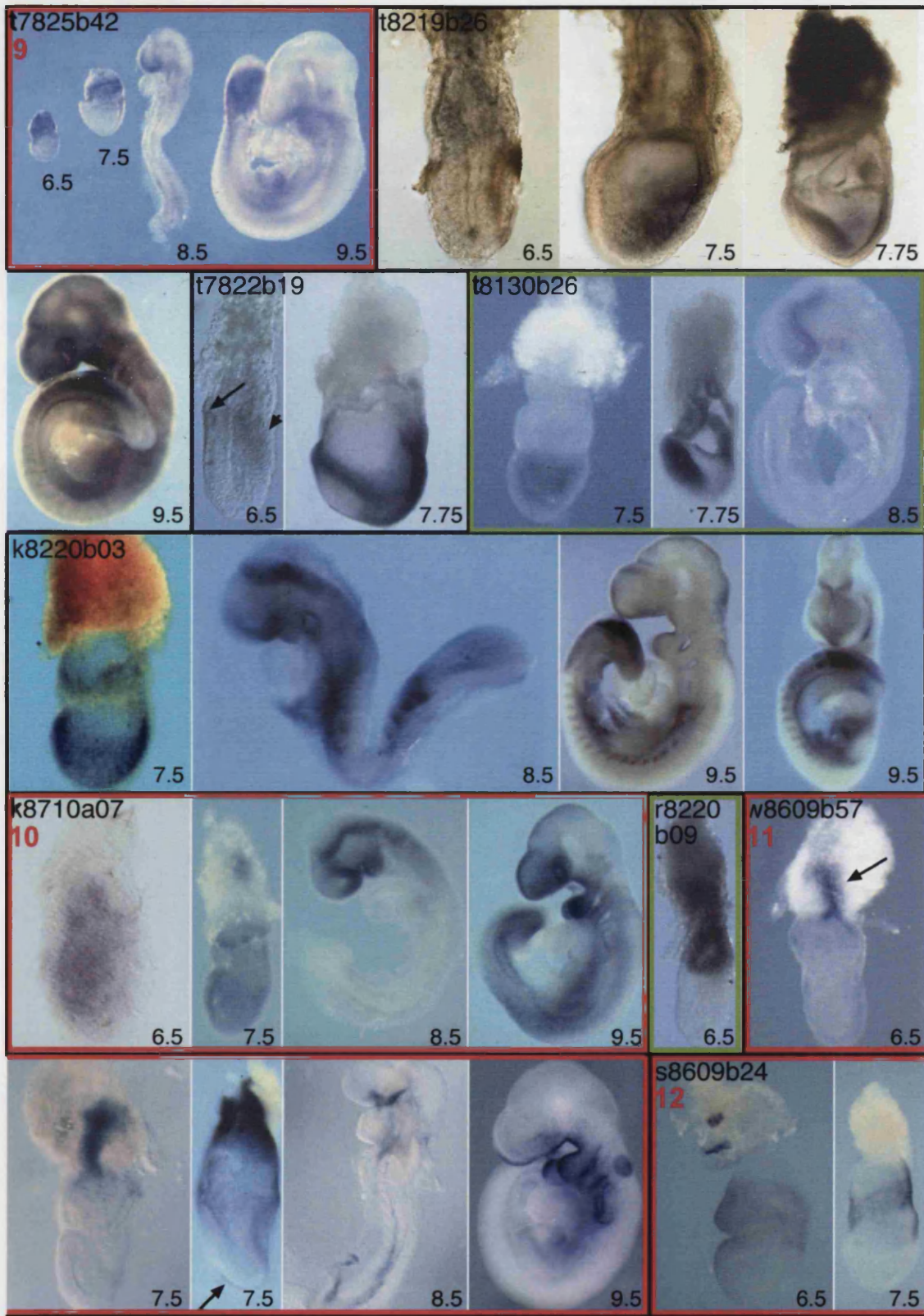
(continued on next page)

(Fig. 3.1 cont.)



(continued on next page)

(Fig. 3.1 cont.)



(continued on next page)

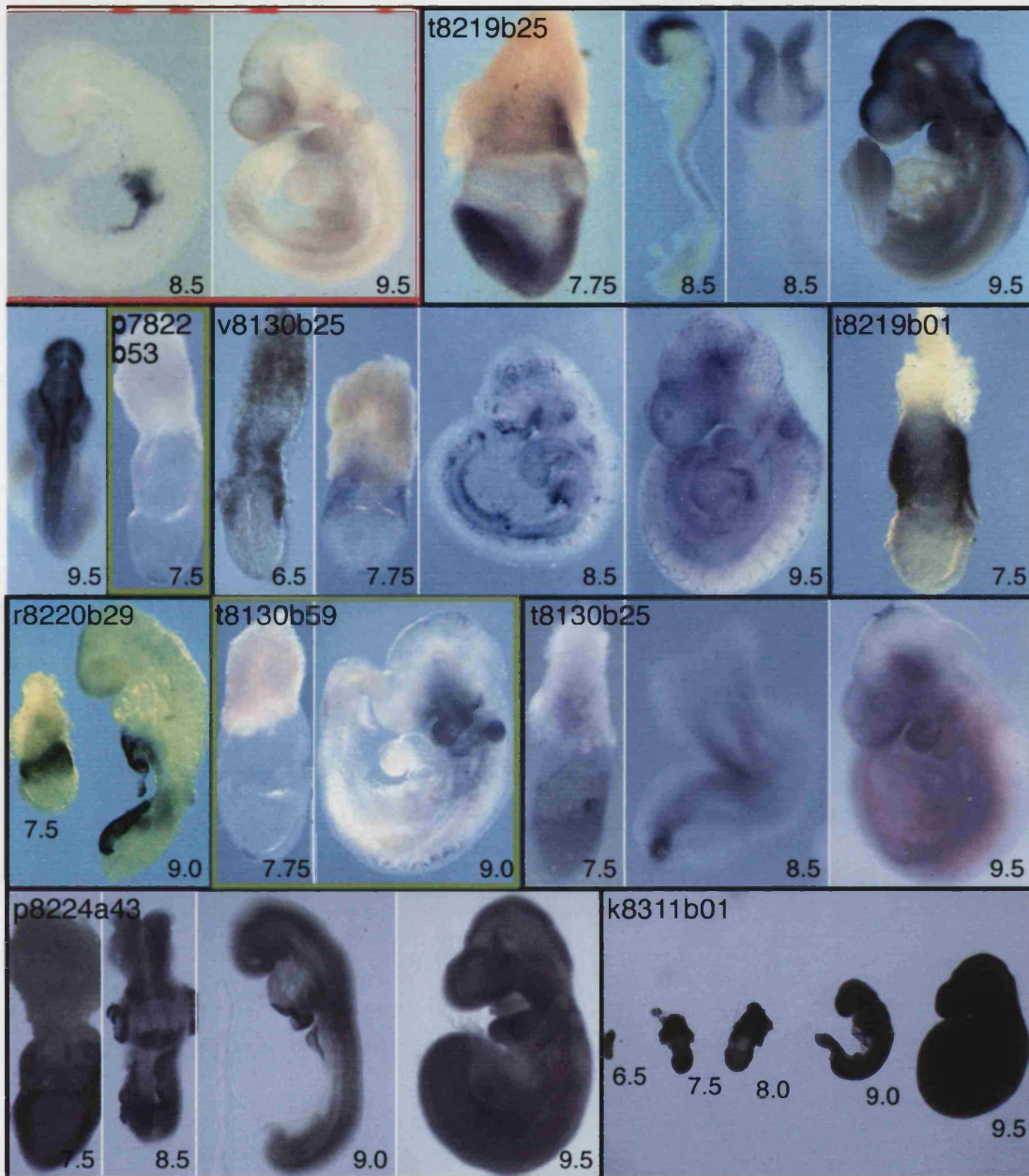


Fig. 3.1 Restricted expression patterns found in whole-mount *in situ* hybridisation screen of mouse endoderm library. Individual clones are outlined by black lines, in some cases carrying on to the next row; further outlined in red or green are clones selected for functional analysis in zebrafish; outlined and/or numbered in red are the clones I identified; the numbering in red matches that of the descriptions presented in the next section. On the top left of each clone composite is its sequence identifier. Clones are presented in the same order as they appear in Table 3.1. Staging (in dpc) is indicated below each embryo. 29 restricted expression patterns are shown, as well as two examples of widespread (t8130b25 and p8224a43) and one example of a ubiquitous one (k8311b01). I thank Dr. R. Kettleborough and Dr. A. Rana for contributing their pictures and Prof. J. C. Smith for the composition of this figure.

Table 3.1 Identity of endoderm library cDNAs with restricted expression patterns

Sequence ID	Frequency	Representative ID	Description
r8220b57	1	ENSMUSG00000005566	Transcription intermediary factor 1- β (Tif1- β); also known as Krip-1 or Kap-1
t7822b10	2	ENSMUSG00000013236	Protein-tyrosine phosphatase, receptor-type (EC 3.1.3.48)
s8609b60	2	ENSMUSG00000019970	Serum and glucocorticoid-regulated kinase (Sgk) (EC 2.7.1.)
k8709a20	2	ENSMUSG00000020849	14-3-3 protein epsilon (protein kinase C inhibitor protein-1)
r8319a44	2		14-3-3 protein sigma
m8708a09	4	ENSMUSG00000021728	Embigin; also known as Teratocarcinoma glycoprotein 70 (GP-70)
m8708a39	1	ENSMUSG00000022761	Leucine-zipper-like transcriptional regulator 1 (Lztr1)
r8707a53	3	ENSMUSG00000023906	Claudin-6
t8417b56	1	ENSMUSG0000002764	Neuronatin; also known as Peg5 (isoform 2)
r8316a33	1	ENSMUSG00000024253	Dynein 2 light intermediate chain
v8130b53	9	TC461859	Solute carrier family 2 (facilitated glucose transporter) member 3 (Slc2a3)
s8129b58	1	ENSMUSG00000026833	Pancortins 1 and/or 3
k8709a24	1	ENSMUSG00000031665	Sal-like 1 (Sall1)
m8708a22	1	ENSMUSG00000039676	Calcyphosine
t7825b42	3	TC511260	Sp120 (Hnrpu)
t8219b26	1	ENSMUSG00000032376	Ubiquitin specific protease 3 (Ubp7)

t7822b19	1	ENSMUSG00000021681	Paternally expressed gene 3 (Peg3)
t8130b26	1	ENSMUSG00000042142	Plu1 (Rb-binding protein 2 (Rb-BP2)-like)
k8220b03	1	ENSMUSG00000029381	Shroom (actin binding protein) (Shrm)
k8710a07	1	ENSMUSG00000021667	Nop seven associated protein 2 (Nsa2); also known as Lnr42, TINP1 or HCLG1
r8220b09	1	TC501397	Transformer 2 β (arg/ser-rich splice factor); also known as Silg41
w8609b57	1	ENSMUSG00000029032	Rho GEF 16; also known as Neuroblastoma
s8609b24	1	ENSMUSG00000039878	LIV-1 (estrogen-regulated)-related
t8219b25	1	TC488224	16% identity to human KIAA0802
p7822b53	1	ENSMUSG00000005505	Weakly similar to ring canal protein; contains BTB/POZ domain
v8130b25	1	ENSMUSG00000028162	
t8219b01	1		
r8220b29	1	TC469486	
t8130b59	1	TC503400	

The twenty-nine cDNAs with restricted patterns of expression are grouped into four categories (separated by dashed lines) based on gene description. From the top of the table, 20 are categorised as known genes, 4 are similar to known genes, 1 contains a known protein domain and 4 have no known motif. Headings represent (i) the sequence identification number; (ii) the number of times the sequence was isolated; (iii) the ENSEMBL gene number of the cDNA or its TIGR Cluster number; (iv) gene family.

3.2.3 Brief description of 12 restricted expression patterns

1 **s8609b60** At the onset of gastrulation, the serine/threonine protein kinase *Sgk* is strongly expressed in the VE overlying the nascent mesodermal wings and, more weakly, in the mesoderm itself. Transcripts are also detected in the VE overlying the extra-embryonic ectoderm. As gastrulation proceeds, the latter domain of expression becomes more robust, and in the embryo proper it is strongest in the regions juxtaposed to the streak. At 8.5 and 9.5 dpc *Sgk* transcripts are found in the vasculature as well as in the eye and branchial arches. The expression pattern of *Sgk* at 8.5 and 9.5 dpc has recently been described elsewhere (Lee *et al.*, 2001). Loss of function of this gene reduces the ability of mice to reduce Na⁺ excretion when subjected to dietary NaCl restriction (Wulff *et al.*, 2002).

2 **k8709a20** *14-3-3 epsilon*, which encodes a phospho serine/threonine-binding protein, is ubiquitously expressed at 6.5 dpc but is then down-regulated such that by 7.75 dpc transcripts are barely detectable. At 8.5 dpc weak expression occurs in the forebrain and heart. At 9.5 dpc, forebrain expression is prominent, along with strong expression in the midbrain and branchial arches. These observations complement work by McConnell *et al.*, 1995, where *14-3-3 epsilon* expression was analysed from 8.5 dpc and found to be high in the neural tissue by 12.5 dpc.

3 **m8708a09** At 6.5 dpc, *Embigin*, which encodes a transmembrane glycoprotein of the immunoglobulin superfamily, is strongly expressed in the VE at the junction between extra-embryonic and embryonic portions of the conceptus. By 7.5 dpc, expression occurs throughout the VE and, more weakly, in the definitive endoderm. At head-fold stages, *Embigin* transcription occurs in the ADE, with strong expression also detectable in the VE. At 8.5 dpc transcripts are present in the forebrain neuroepithelium the foregut diverticulum, and the yolk sac. By 9.5 dpc, expression is strong in forebrain neuroepithelium (especially in the dorsal midline), and also occurs in the mid- and hindbrain. Transcripts are also detectable in the branchial arches and the nephrogenic cord. The early expression pattern of this gene has been described in Shimono and Behringer, 1999 and later stages in Fan *et al.*, 1998.

4 m8708a39 At 6.5 dpc, the leucine-zipper transcriptional regulator *Lztr-1* is expressed in the epiblast and in extraembryonic ectoderm and/or endoderm adjacent to in the ectoplacental cone (arrow). At 7.5 dpc, although expression is widespread in the embryonic region, it is stronger posteriorly and down-regulated in the node. At head-fold stages *Lztr-1* expression is most prominent in the neural folds and nascent neural tube. At 9.5 dpc expression is high in the forebrain, branchial arches and limb buds.

5 t8417b56 At 6.5 dpc, the imprinted gene *Neuronatin* is expressed weakly in the embryonic half of the conceptus. By 7.0 dpc transcripts are present throughout the mesoderm and ectoderm and maximal expression is then seen in the posterior head-folds (arrows). At 8.5 to 9.5 dpc, *Neuronatin* expression is detectable in ventral forebrain, branchial arches and foregut diverticulum. Forebrain expression is more widespread at this time and expression also occurs throughout the trunk mesoderm. Expression of *Neuronatin* at 8.5 and 9.5 dpc has also been described in Wijnholds *et al.*, 1995, where expression in rhombomeres 3 and 5 was detected.

6 s8129b58 At the onset of gastrulation, *Pancortin -1* and/or *-3*, which encode putative endoplasmic reticulum-localised proteins that belong to the olfactomedin family of extracellular matrix proteins, is expressed at the junction between embryonic and extra-embryonic portions of the conceptus, with higher levels anteriorly. As gastrulation proceeds, expression occurs in the amnion and chorion and becomes widespread within the embryo proper. During somitogenesis, expression becomes restricted to rhombomere 4 (arrow), to the junction between the diencephalon and mesencephalon and to anterior and posterior portions of trunk mesenchyme. At 10 dpc spotty expression is detectable in the midbrain in what are presumed to be the earliest differentiating neurons. Expression also occurs in the olfactory placodes and in some cranial ganglia. Expression in limb buds is initially widespread but becomes restricted to posterior regions as development proceeds. Expression of the closely related genes *Noelin 1* and *2* at 10.5 dpc has recently been reported (Moreno and Bronner-Fraser, 2002). The expression pattern described is similar, though not identical, to that described here for 10 dpc embryos.

7 k8709a24 At egg cylinder stages *Sall1*, a vertebrate homologue of the *Drosophila* homeobox gene *spalt*, is expressed in the anterior and, more weakly, in the

posterior epiblast. At headfold stages, transcripts become restricted to anterior neural folds and at 8.5 dpc this expression resolves into ventral neural plate and neural groove. Weak expression is also seen in the branchial arch region and posterior trunk. At 9.5 dpc *Sall1* is expressed in the ventral forebrain, anterior midbrain, the midbrain/hindbrain boundary, branchial arch ectoderm, posterior trunk and, most prominently, in the mesonephros, presomitic mesoderm and newly-formed somites. *SALL1* is implicated in Townes-Brocks syndrome (Kohlhase *et al.*, 1998) and loss-of-function of murine *Sall1* indicates that this gene is required for ureteric bud invasion during kidney development (Nishinakamura *et al.*, 2001). Expression of *Sall1* at 7.5, 8.5 and 9.5 dpc has been reported in Buck *et al.*, 2001.

8 m8708a22 *Calcyphosine*, a gene encoding a calcium-binding protein of the calmodulin superfamily, is weakly expressed in extra-embryonic ectoderm at 6.5 dpc. At 7.0 dpc expression occurs throughout the extra-embryonic ectoderm and the epiblast, with maximal expression in the node. During elongation of the streak, highest expression is seen in axial mesendoderm (arrow). At 8.5 and 9.5 dpc expression is ubiquitous at low level.

9 t7825b42 At egg cylinder stages, the mouse heteronuclear riboprotein-encoding gene *Sp120* is most strongly expressed in the extra-embryonic half of the conceptus, with only weak expression in the embryonic half, mostly in the primitive streak. At 8.5 and 9.5 dpc, robust expression is seen in the tail bud, when transcripts are also present in the ventral forebrain, branchial arches and limb buds.

10 k8710a07 The ribosome biogenesis protein encoded by *Nsa2* is expressed throughout the epiblast and extraembryonic ectoderm at 6.5 dpc. At 7.5 dpc it continues to be expressed in all internal cell layers of the conceptus. By 8.5 and 9.5 dpc expression is strongest in the branchial arches and neural tube, particularly in the forebrain. Low-level expression also occurs throughout the lateral mesoderm.

11 w8609b57 At the onset of gastrulation, the guanine exchange factor *Rho GEF 16* is strongly expressed in a single domain comprising the most proximal region of the egg cylinder and a proximo-distal stripe within the ectoplacental cone (arrow). This domain persists during headfold stages, when the gene becomes weakly

expressed throughout the VE and strongly activated in the headfold pocket and notochord (arrow). At 8.5 dpc expression is strong in the notochord and ventral forebrain, with weak activation in the foregut diverticulum. By 9.5 dpc, epithelial expression extends from the ventral forebrain to the fourth branchial arch, with transcription also occurring in the otic vesicle.

12 s8609b24 At 6.5 dpc the unknown gene represented by s8609b24 is expressed in the VE. VE expression of this gene is absent from the most proximal region of the conceptus. At 7.5 dpc, expression persists in most of the VE and is still absent from its most proximal region. By 8.5 dpc, expression is confined to the yolk sac but by 9.5 dpc there is widespread, albeit weak, expression in the embryo proper, particularly in the forebrain, anterior midbrain, branchial arches and gut.

3.2.4 Synexpression and co-expression groups

The restricted expression patterns reveal a single group of genes with a similar expression pattern at all stages examined (6.5–9.5 dpc). This synexpression group (Niehrs and Pollet, 1999) comprises clones t8219b01, r8220b29 and t7822b10, all of which are expressed in the VE at 6.5 and 7.5 dpc and in the yolk sac at 8.5 and 9.5 dpc. Members of a synexpression group might be co-regulated and function in the same process but we do not have data to support this. Of the three, only t7822b10 has been described previously. It encodes a receptor-type protein tyrosine phosphatase termed *Ptpt9*, whose loss of function causes abnormalities of the central and peripheral nervous systems and of the neuroendocrine system (Elchebly *et al.*, 1999; Wallace *et al.*, 1999; Batt *et al.*, 2002). No known motifs have been identified in t8219b01 or r8220b29. *Ptpt9* is on chromosome 17 at 56.3 Mb, while t8219b01 maps to chromosome 8 at 61.5 Mb and r8220b29 to chromosome 5 at 130.7 Mb. The coordinated expression of the three genes is therefore unlikely to be a consequence of their genomic organisation.

In addition to the synexpression group, we have also identified three co-expression groups, all members of which are expressed in a particular tissue at a particular stage of development and which therefore may cooperate in the specification of the tissue in which they are expressed. Members of a co-expression group may also be expressed in other regions and their expression patterns at earlier and later stages may also diverge.

The co-expression groups comprise clones expressed in the tissues that constitute the 7.5 dpc mouse endoderm. We found 6 restricted clones expressed in the VE, 5 in the node and 2 in the gut endoderm (Table 3.2). One clone, v8130b25, belongs to all three co-expression groups.

Table 3.2 Co-expression groups found in endoderm library screen

Co-expression group	Clones
VE	s8609b60, m8708a09, v8130b53, t7825b42, s8609b24, v8130b24
Node	r8316a33, m8708a22, p7822b53, v8130b25, t8130b59
Gut Endoderm	r8707a53, v8130b25

3.3 Discussion of the *in situ* hybridisation screen of the endoderm library

3.3.1 Overview

Approximately 1.8 % of the Beddington Endoderm cDNA Library has been gridded and one-third of that sequenced. Of the sequences generated, two-thirds (1978 sequences) were of high quality and used for clustering, followed by our own analysis. We therefore explored ~0.4 % of the endoderm library. Clustering reduced the number of independent sequences to two-thirds of the original number (1440 clusters). This means that most transcripts are represented only once in the subset of the library analysed, but it also meant a significant reduction in the number of sequences to be analysed manually. Manual sequence comparisons reduced the number of clones to be analysed by *in situ* hybridisation by 88%. To minimise prejudice as to which might be essential genes, the majority of clones we excluded from our screen were those encoding energy metabolism enzymes and ribosomal proteins. A few transcripts belonging to these groups, however, show spatially restricted patterns of expression at some stage of embryonic development (see for example, Gawantka *et al.*, 1998).

Out of the 160 genes analysed by *in situ* hybridisation, 29 (18%) were restricted to particular tissues at least at one of the time points examined. Of these 29 restricted

clones, 22 (76%) were expressed in the cell types predicted to constitute the endoderm library and for which this screen was designed: VE, definitive endoderm, axial mesendoderm and node (see Table 3.2). Clones w8609b57, r8220b09, t8130b26, m8708a39, r8220b57, r8319a44, t8219b26 were undetected in tissues from which the library was made, which might be accounted for by low endoderm expression or by tissue contamination during the extremely difficult dissections required for library construction.

3.3.2 Efficiency of novel strategy for clone selection

The mouse embryo is less accessible than other, non-mammalian, vertebrate embryos. In addition, the early streak mouse embryo (200 – 300 μm long) is much smaller than other early streak embryos, rendering it unamenable to automatic whole-mount *in situ* hybridisation at present. It is thus impractical to perform a large-scale whole-mount *in situ* hybridisation screen on mouse embryos prior to organogenesis. We were particularly interested in the patterning events known to occur prior to or during gastrulation that establish the axes in the mammalian embryo. We therefore limited the number of whole-mount *in situ* hybridisation we would manually carry out on 6.5 – 9.5 dpc mouse embryos by a preliminary sequence analysis of clones identified as ESTs.

We chose non-redundant cDNAs and eliminated cDNAs already extensively studied in an embryological context. Consequently, our screen differed from related screens (Gawantka *et al.*, 1998; Neidhardt *et al.*, 2000; Christiansen *et al.*, 2001; Kudoh *et al.*, 2001) in that we only examined unique cDNAs that had not been characterised in the context of embryonic development. The restricted clones we found may constitute useful molecular markers for the tissues in which they are expressed and their expression patterns may provide hints as to their developmental functions. They represent genes with a variety of cellular functions as well as a few unknown genes and their study could generate insight into the mechanistics of patterning. Since this screen was undertaken, mutations in 7 of the 29 restricted genes presented here have been generated in the mouse by us or others (Hildebrand and Soriano, 1999; Li *et al.*, 1999; Elchebly *et al.*, 1999; Wallace *et al.*, 1999; Nishinakamura *et al.*, 2001; Wulff *et al.*, 2002; Batt *et al.*, 2002; Kettleborough, 2002; Rana, 2003). Each of these mutations

results in discernible phenotypes and one was found to be required for the establishment of the embryonic axes (Rana, 2003).

Our strategy proved successful in that the percentage of restricted expression patterns obtained (18%) was comparable to the highest obtained in previous whole-mount *in situ* hybridisation studies (18 % in Neidhardt *et al.*, 2000 when random clones were picked from a normalised library). In Table 3.3 I have compared our screen with other *in situ* hybridisation screens, emphasising the efficiency of discovery of restricted expression patterns. It is difficult to make direct comparisons because definitions of restricted may vary. Also, other screens have used different species at different stages, and we selected certain families of cDNAs to study. Nevertheless, screens using randomly selected cDNAs have tended to produce proportionately fewer restricted expression patterns than ours (Neidhardt *et al.*, 2000; Christiansen *et al.*, 2001; Kudoh *et al.*, 2001; Table 3.3). We distinguished between restricted and widespread expression patterns, as did Neidhardt and co-workers. In contrast, the 25% of differentially expressed genes reported by Gawantka and colleagues include all expressed clones that are non-ubiquitous. A similar percentage of restricted patterns to ours was obtained in the expression analysis of murine orthologues of the genes contained in human chromosome 21 at 9.5 dpc (Reymond *et al.*, 2002; Gitton *et al.*, 2002).

The similarity between the percentage of restricted clones obtained in our study and that by Neidhardt *et al.*, 2000 when using a normalised library is consistent with the similarity of the two approaches. Indeed, the strategy we used for clone selection is comparable to a normalisation since sequence clustering allowed us to assess the relative abundance of clones and sequence identity allowed us to reject presumably essential transcripts, both aims of a normalisation procedure. Our strategy presents a few advantages over a hybridisation-based normalisation. Our method precludes the loss of rare clones, saves material, especially important when tissue collection requires skilled embryo manipulation, and circumvents clone repetition.

Table 3.3 Frequency of restrictedly expressed cDNAs identified in different expression screens

Reference	Species	Stages screened	cDNA library	Library type	No. clones screened	Restricted cDNAs
This study	Mouse	6.5–9.5 dpc	7.5 dpc endoderm	Parent	160	18%
Neidhardt <i>et al.</i> , 2000	Mouse	9.5 dpc	9.5 dpc embryo	Parent	989	6%
Neidhardt <i>et al.</i> , 2000	Mouse	9.5 dpc	9.5 dpc embryo	Subtracted	3737	7%
Neidhardt <i>et al.</i> , 2000	Mouse	9.5 dpc	9.5 dpc embryo	Normalised	622	18%
Reymond <i>et al.</i> , 2002	Mouse	9.5 dpc	Murine orthologues of human chromosome 21 genes	—	158	21%
Reymond <i>et al.</i> , 2002	Mouse	10.5 dpc	<i>idem</i>	—	158	28%
Reymond <i>et al.</i> , 2002	Mouse	14.5 dpc (sections)	<i>idem</i>	—	158	42%
Gitton <i>et al.</i> , 2002	Mouse	9.5 dpc	<i>idem</i>	—	158	21%
Christiansen <i>et al.</i> , 2001	Chick	HH* 9–12	Hindbrain HH* 10–11	Subtracted	445	8%
Kudoh <i>et al.</i> , 2001	Zebrafish	Shield, 3 somites, 15 somites, 24 h	Early somitogenesis embryo	Normalised	2765	13%
Gawantka <i>et al.</i> , 1998	<i>X. laevis</i>	Stages 10+, 13, 30	Neurula stage embryo	Parent	1765	25% [†]

*Staging according to Hamburger and Hamilton, 1992.

[†]This figure is reduced to 16% if only unique cDNAs with a restricted expression pattern are considered.

3.3.3 Perspectives

The identification of mouse transcripts is incomplete as measured by the level of non-overlap between the output of gene prediction programs and the study of cDNA libraries (Mouse Genome Sequencing Consortium, 2002). We found 123 new mouse ESTs in the endoderm library and a few completely novel sequences that matched nothing in the currently available databases. Our work thus contributes to the efforts of many in the definition of the mouse genome and transcriptome, in addition to providing spatial information concerning the expression of 160 mouse transcripts during early stages of embryogenesis. The endoderm library provides a valuable source of ESTs that can be useful in future structural and functional genomic projects as well as expression profiling. Exploring 0.4% of the endoderm library we found 29 transcripts with restricted expression patterns, of which 4 (2.5%) constitute completely novel sequences. Extrapolating for the total library, this means that a few thousand more restricted genes, of which a few hundred completely novel ones, could still be found using this resource.

Chapter 4

Functional analysis of mouse *Sgk*

Chapter 4

Functional analysis of mouse *Sgk*

- 4.1 Literature review on *Sgk*
 - 4.1.1 *Sgk* expression
 - 4.1.2 *Sgk* protein and mRNA structure
 - 4.1.3 *Sgk* transcriptional regulation
 - 4.1.4 *Sgk* post-translational regulation
 - 4.1.5 Subcellular localisation of *Sgk*
 - 4.1.6 Downstream of *Sgk*
 - 4.1.7 Biological roles of *Sgk*
 - 4.1.8 *Sgk* family members
 - 4.2 Results of the functional analysis of mouse *Sgk*
 - 4.2.1 Further characterisation of mouse *Sgk* expression
 - 4.2.2 Groundwork for the differentiation of ES cells into endothelial cells
 - 4.2.3 Is *Sgk* upregulated during embryonic wound-healing?
 - 4.2.4 Isolation and characterisation of mouse *Sgk* genomic DNA
 - 4.2.5 Construction of *Sgk* targeting vector
 - 4.2.6 Targeting of *Sgk* in ES cells
 - 4.2.7 Zebrafish *sgk*
 - 4.3 Discussion of the functional analysis of mouse *Sgk*
 - 4.3.1 Regulation of *Sgk* expression
 - 4.3.2 *Sgk* targeting strategy
 - 4.3.3 Is there a role for *Sgk* in embryonic patterning?
-

4.1 Literature review on *Sgk*

From the 12 genes showing restricted expression that I isolated in the mouse endoderm screen, I selected *Sgk* (serum and glucocorticoid-regulated kinase) for functional analysis in the mouse. *Sgk* was interesting to us because of its asymmetric expression during early gastrulation. *Sgk* is expressed in the posterior and not in the anterior of the embryo at early streak stages. In addition, I was also interested in the restriction of *Sgk* expression to a single cell type, angioblasts, in the mid-gestation embryo.

4.1.1 *Sgk* expression

Sgk is found in numerous embryonic and adult cDNA libraries, as well as in many cell lines. Mouse embryonic libraries containing *Sgk* cDNA include one made from embryos as young as 2-cell stage. No *Sgk* expression has been detected in oocytes

(Alliston *et al.*, 1997). In the adult, *Sgk* mRNA has been detected by Northern analysis in all tissues examined in a variety of species, including shark, rat and human (Imaizumi *et al.*, 1994; Waldegger *et al.*, 1997; Waldegger *et al.*, 1998; Kobayashi *et al.*, 1999). *In situ* hybridisation shows that *Sgk* is not expressed in all cell types of each tissue, however. For example, in the brain, *Sgk* is expressed in most oligodendrocytes but only in a limited set of neurons (Imaizumi *et al.*, 1994; Warntges *et al.*, 2002); in the ovary, *Sgk* is selectively expressed in granulosa cells (Alliston *et al.*, 1997); in the pancreas, highest levels of *Sgk* transcripts are found in the acinar cells, followed by the ductal epithelial cells and are undetectable in the pancreatic islet cells (Klingel *et al.*, 2000); in the intestine, the vast majority of *Sgk* transcripts are detected in the apical villus enterocytes whereas none have been detected in the crypt cells (Waldegger *et al.*, 1999).

There are two reports concerning the embryonic expression of murine *Sgk*. One describes the overall expression of *Sgk* between 8.5 and 16.5 dpc (Lee *et al.*, 2001) and the other deals specifically with the localisation of transcript and protein during metanephrogenesis (Huber *et al.*, 2001). Lee *et al.*, 2001 describe expression of *Sgk* in the yolk sac of 8.5 dpc conceptuses, followed by expression in the heart chamber, intersomitic vessels, otic vesicles and lung buds between 9.5 and 12.5 dpc. Between 13.5 and 16.5 dpc *Sgk* transcripts are still detected in the heart and intersomitic vessels, and become apparent in the choroid plexus, bronchi and bronchioles, adrenal gland, liver, thymus and intestines (Lee *et al.*, 2001). Huber *et al.*, 2001 detect *Sgk* mRNA in the ureteric buds as well as in the adjacent mesenchymal cells that undergo condensation and mesenchyme-epithelial transition, in 15 dpc embryos. These condensations first constitute the so-called comma-shaped bodies that then develop into the s-shaped bodies and eventually form the segments of the nephron up to the collecting duct (reviewed in Horster *et al.*, 1999). In the metanephrogenic system, *Sgk* protein is undetectable at 14 dpc but at 16 dpc its localisation is consistent with the mRNA signals detected at 15 dpc. In addition, at 16 dpc *Sgk* is found in the loops of Henle and the maturing medullary collecting duct. At postnatal day 1, *Sgk* protein is still found in the latter domain, whereas it is down-regulated in the nephrogenic zone (Huber *et al.*, 2001).

4.1.2 *Sgk* protein and mRNA structure

Sgk is a 50 kDa protein that was initially classified as a serine/threonine protein kinase on the basis of its amino acid sequence. Protein kinases contain a large central catalytic domain of approximately 270 amino acid residues and which can be subdivided into 11 subdomains, and regulatory regions in the N- and/or C-termini (reviewed in Hanks *et al.*, 1988). The catalytic domain of *Sgk* contains all the essential features to make it a functional serine/threonine kinase, with a characteristic ATP-binding motif, downstream of which lies a conserved lysine (L127); with highly conserved motifs in subdomains VIb, VII and VIII; and a threonine in the activation loop (T256) (Webster *et al.*, 1993b). The catalytic domain of *Sgk* is mainly related to that of second-messenger-regulated kinases. In particular, it is most similar (45-55% identity) to the *Rac* protein kinases, the ribosomal protein S6 kinase (S6K), protein kinase C-zeta (PKC-zeta), PKB / AKT and cyclic adenosine monophosphate-dependent protein kinase (PKA) (Webster *et al.*, 1993b), rendering *Sgk* a member of the growth factor-activated AGC family of serine/threonine protein kinases (so-called because it includes PKA, PKG and PKC) (reviewed in Firestone *et al.*, 2003).

In addition to the similarity of their catalytic domains, AGC kinases have in common aspects of their regulation. Thus, many AGC kinases are activated by phosphatidylinositol 3,4,5-trisphosphate (PIP₃), by translocation to the plasma membrane, and by phosphorylation within a highly conserved motif in the activation loop and, sometimes, in another site some 160 residues C-terminal to the former (reviewed in Peterson and Schreiber, 1999). *Sgk* contains three phosphorylation sites: S78, in the N-terminal domain; the already mentioned T256, which lies within the activation loop; and S422, in the C-terminal domain (reviewed in Firestone *et al.*, 2003). The first of these sites has not yet been shown to be of functional significance but the other two have (see below).

The N-terminal region of *Sgk* bears no obvious similarity with any known protein but other regions contain several putative protein-protein interaction domains, including a PY motif (PPxY) and a nuclear localisation signal (NLS) set in the central (catalytic) portion of the protein, and a PDZ domain in the C-terminal region (Chun *et al.*, 2002; Maiyar *et al.*, 2003; Firestone *et al.*, 2003). Theoretical three-dimensional modelling of

the catalytic domain of *Sgk* with previously resolved structures of related kinases shows that the PY domain and the NLS lie in an external face of the protein, available for establishing interactions with molecular partners (Firestone *et al.*, 2003).

The 3' UTR of the *Sgk* transcript contains several AU-rich regions analogous to those implicated in destabilising short-lived mRNAs such as a few early-response oncogenes and cytokines (Webster *et al.*, 1993b). Indeed, rat *Sgk* mRNA has a half-life of approximately 20 min, placing it in the group of transcripts with the shortest observed turnover times (Webster *et al.*, 1993a). So, this gene product is prone to regulation by transcript stability. In addition, *Sgk* transcription itself is subject to complex regulation, an unusual feature for a protein kinase.

4.1.3 *Sgk* transcriptional regulation

Sgk was originally identified in a differential display using a rat mammary tumour cell line induced by the glucocorticoid dexamethasone (Webster *et al.*, 1993a; Webster *et al.*, 1993b). *Sgk* expression was found to be an immediate-early response to dexamethasone, as well as to serum (Webster *et al.*, 1993b; Webster *et al.*, 1993a).

Since its initial discovery, many more inducers of *Sgk* transcription have been identified, acting through a variety of molecular pathways, in a cell type-dependent manner, and with variable kinetics and duration. In many cell lines, cell shrinkage induces expression of *Sgk* and cell swelling halts its transcription. These include human hepatoma, pancreas carcinoma, macrophage and endothelial cell lines, mouse fibroblasts, mammary epithelial and neuroblastoma cell lines, and a canine kidney cell line (Waldegger *et al.*, 1997; Waldegger *et al.*, 1999; Bell *et al.*, 2000; Klingel *et al.*, 2000; Lang *et al.*, 2000; Warntges *et al.*, 2002). The distinct ways by which cell volume changes were induced in hepatoma cells, including both hyper- and isotonic conditions, suggest that *Sgk* is regulated by cell volume rather than by osmolarity and it was shown to be an immediate-early effect of volume change (Waldegger *et al.*, 1997). Excessive concentration of extracellular glucose, a condition found in patients suffering from diabetic nephropathy, also leads to *Sgk* upregulation (Lang *et al.*, 2000) and *Sgk* mRNA is increased in diabetic kidneys (Kumar *et al.*, 1999). *Sgk* transcription in hyperosmotic conditions appears to be mediated by the stress-activated protein kinase 2

(SAPK2)/p38 mitogen-activated protein kinase (MAPK) pathway since it is abolished in the presence of a SAPK2 inhibitor or of a kinase-dead MAP-kinase-kinase 3 (Bell *et al.*, 2000; Waldegger *et al.*, 2000). Surprisingly, however, in *Xenopus* A6 cells *Sgk* is induced by hypotonicity (Rozansky *et al.*, 2002).

TGF β 1, which also leads to renal cell hypertrophy (Fine *et al.*, 1985; Ling *et al.*, 1995; Sharma *et al.*, 1996), has been shown to lead to immediate-early upregulation of *Sgk* mRNA in intestinal, hepatocarcinoma macrophage and fibroblast cell lines and expression of both molecules is concordant in the intestine of both healthy subjects and patients with Crohn's disease (Waldegger *et al.*, 1999; Lang *et al.*, 2000).

The mineralocorticoid aldosterone, which controls body fluid homeostasis, namely blood pressure, also leads to immediate-early transcription of *Sgk* in the *Xenopus* A6 cell line, primary cultures of rabbit cortical collecting duct cells, rat kidneys and colon but not lungs (Chen *et al.*, 1999; Naray-Fejes-Toth *et al.*, 1999; Shigaev *et al.*, 2000; Brennan and Fuller, 2000). Aldosterone controls body fluid homeostasis mainly through the regulation of renal Na⁺ reabsorption, largely achieved by increasing the activity of the epithelial sodium channel (ENaC) (reviewed in Farman *et al.*, 2002). Aldosterone also induces *Sgk* expression in neonatal rat cardiac myocytes and fibroblasts. Interestingly, it does so exclusively via the glucocorticoid receptor rather than through the mineralocorticoid receptor, indicating that aldosterone can have glucocorticoid-like actions in the heart (Sheppard and Autelitano, 2002). Nonetheless, transgenic mice overexpressing the mineralocorticoid receptor in aldosterone target tissues shown a significant increased *Sgk* expression in those tissues (Le Menuet *et al.*, 2001).

Dehydration increases both *in situ* hybridisation and immunohistochemistry signals for *Sgk* in the temporal lobe and in hippocampal neurons of the rat brain (Warntges *et al.*, 2002). The effect of dehydration on *Sgk* regulation should not be mediated by aldosterone as this mineralocorticoid is decreased following water deprivation (Huang *et al.*, 1996).

Other immediate-early inducers of *Sgk* are the follicle-stimulating hormone (FSH), its mediator PKA, and forskolin, a PKA agonist that directly activates adenylyl cyclase in

primary granulosa cells (Alliston *et al.*, 1997; Gonzalez-Robayna *et al.*, 1999; Alliston *et al.*, 2000), several proinflammatory cytokines in human peripheral blood granulocytes (Cowling and Birnboim, 2000), FGF, platelet-derived growth factor (PDGF) and the tumour promoting phorbol ester tetradecanoylphorbol acetate (TPA) in a fibroblast cell line (Mizuno and Nishida, 2001), and amphetamine in the rat striatum (Gonzalez-Nicolini and McGinty, 2002). Transcriptional activation of *Sgk* by FGF, PDGF and TPA is mediated by the extracellular signal-regulated kinase (ERK) MAPK pathway since it is blocked by a specific MAPK-kinase inhibitor (Mizuno and Nishida, 2001). FSH activates the p38 MAPK in ovary granulosa cells via PKA (Maizels *et al.*, 1998) and specific inhibition of PKA, p38MAPK or of the phosphatidylinositol 3'-kinase (PI3K) pathway abolishes *Sgk* induction by FSH (Gonzalez-Robayna *et al.*, 2000).

Additional inducers of *Sgk* expression include the secreted factors carbachol and vasoactive intestinal polypeptide in the shark rectal gland (Waldegger *et al.*, 1998), several phorbol esters other than TPA and increased cytosolic Ca²⁺ concentration, in pancreatic cells (Klingel *et al.*, 2000), and heat shock, UV irradiation and oxidative stress induced by hydrogen peroxide, also through a p38/MAPK-dependent pathway, in murine mammary cells (Leong *et al.*, 2003). Central nervous system (CNS) injury induces *Sgk* expression in the oligodendrocytes surrounding the lesion, within 3 days and for at least 14 days (Imaizumi *et al.*, 1994; see also Hollister *et al.*, 1997).

Sgk transcription is not induced by just any stimulus, however. Heparin downregulates *Sgk* transcription in vascular smooth muscle cells (VSMCs) (Delmolino and Castellot, 1997), as does the protein kinase inhibitor staurosporine and the second messenger cAMP in pancreatic cells (Klingel *et al.*, 2000).

The immediate-early effect of many *Sgk* inducers means that they activate *Sgk* expression independently of *de novo* protein synthesis. Therefore, they either directly bind the gene regulatory elements or modulate factors already present in the cells, which in turn do so. Software analysis of the genomic sequence upstream of the *Sgk* transcriptional start site reveals numerous consensus transcription factor binding sites. These include binding sites for the cAMP regulatory element binding protein (CREB), Activating Proteins (AP)-1 and -2, Activating Transcription Factor 6, NF-κB, E2F,

STAT, p53, c-Rel, SMAD 3 and SMAD 4, FAST, Sp1 and Sp3, heat shock factors, retinoid X receptor, vitamin D receptor, glucocorticoid/mineralocorticoid/progesterone receptors, farnesoid receptor, peroxisome proliferator activator receptor and sterol regulatory element binding protein (Firestone *et al.*, 2003). Very few of these have been analysed functionally but, given the number of different *Sgk* inducers, it would not be surprising if many were found to be operational. There is a functional glucocorticoid responsive element (GRE) as well as a functional p53 binding site, and glucocorticoids and p53 can indeed induce *Sgk* transcription through these enhancers (Maiyar *et al.*, 1996; Itani *et al.*, 2002b). Activation of these two elements is probably interdependent as p53 represses dexamethasone-stimulated activation of the GRE and, conversely, activated glucocorticoid receptors suppress the transactivation function of p53, as seen with reporter constructs (Maiyar *et al.*, 1997). None of these elements mediate FSH/PKA/forskolin-induced *Sgk* transcription but another region of the *Sgk* promoter that does specifically binds the general transcriptional co-factors Sp1 and Sp3 (Maiyar *et al.*, 1996; Alliston *et al.*, 1997). Mutations in this region prevent Sp1/Sp3 binding and abolish PKA-mediated transactivation of reporter constructs (Maiyar *et al.*, 1997). The same region mediates *Sgk* transcription in response to hyperosmotic stress, via binding of Sp1 (Bell *et al.*, 2000). A putative AP-2 binding site has thus far failed to prove functional or even to bind AP-2 (Alliston *et al.*, 1997). No serum-responsive element has yet been uncovered.

4.1.4 *Sgk* post-translational regulation

In addition to regulation at the transcriptional level, *Sgk* protein is post-translationally regulated by phosphorylation. The enzymatic activity of *Sgk* has been shown to depend upon phosphorylation of the activation loop T256 and the C-terminal domain S422 (Park *et al.*, 1999; Kobayashi *et al.*, 1999). These two sites can be phosphorylated by the phosphoinositide-dependent protein kinase (PDK)-1, which is in turn directly activated by PI₃ kinase (reviewed in Storz and Toker, 2002; Cantley, 2002). *Sgk* phosphorylation by PDK1 requires interaction between *Sgk* and a pocket in the kinase domain of PDK1, called the PIF domain, which is a substrate recognition domain (Biondi *et al.*, 2001). In some contexts PDK-1 phosphorylation of *Sgk* can be promoted by the formation of a protein complex mediated by the Na⁺/H⁺ exchanger regulatory factor 2 (NHERF2/TKA-1/E3KARP). The PDZ domain of *Sgk* interacts with the first

PDZ domain of NHERF2 and the PIF domain of NHERF2 binds to the PIF-binding pocket of PDK-1, resulting in an Sgk-NHERF2-PDK-1 complex (Chun *et al.*, 2002).

Mutation of T256 and S422 to alanines (a non-polar amino acid) results in an enzymatically inactive Sgk, with a dominant-negative activity (Brunet *et al.*, 2001; Leong *et al.*, 2003). On the other hand, mutation of T256 to the negatively charged amino acid aspartate results in a constitutively active Sgk (Park *et al.*, 1999). Sgk can be further phosphorylated on S78 and can be phosphorylated by the big mitogen-activated protein kinase (BMK)1/Erk5, a member of the MAPK pathway (Hayashi *et al.*, 2001). Mutation of Sgk S78 to an alanine prevents cells of the human mammary epithelial cell line MCF10A to undergo growth factor-stimulated S phase entry (Hayashi *et al.*, 2001), implicating Sgk in mediating the previously reported requirement for BMK1 for this effect (Kato *et al.*, 1998). Unlike for T256 and S422, the effect of Sgk phosphorylation on S78 on the enzymatic activity of the protein has not yet been defined.

Many inducers of *Sgk* expression, result in the production of a hyperphosphorylated, catalytically active, protein. This has been demonstrated for serum, glucocorticoids, hyperosmotic conditions, insulin and insulin-like growth factor, heat shock, UV irradiation and oxidative stress (Buse *et al.*, 1999; Park *et al.*, 1999; Kobayashi and Cohen, 1999; Bell *et al.*, 2000; Perrotti *et al.*, 2001; Leong *et al.*, 2003; Firestone *et al.*, 2003). Heat shock, UV irradiation and oxidative stress have been shown to activate Sgk in conditions where PKB remains in its non-phosphorylated state (Leong *et al.*, 2003). This is a relevant point since a difficulty in establishing a link between the enzymatically active Sgk and a biological response is that many signals that produce hyperphosphorylated Sgk also result in the activation of the constitutively-expressed, structurally related, PKB (Brazil and Hemmings, 2001). Both proteins are phosphorylated by PDK-1 at analogous sites and both proteins share substrate recognition sites.

Another level of post-translational regulation of Sgk is achieved by ubiquitination. Several groups observed low levels of endogenous Sgk in several cell lines, as well as low levels of the protein following overexpression of full-length mRNA. Much higher levels of Sgk are observed with overexpression of a truncated transcript, lacking the codons for the first 60 amino acid residues, which mediate polyubiquitination of Sgk (Brickley *et al.*, 2002).

Finally, a few stimuli are known to modulate *Sgk* activity but the molecular mechanisms involved are often not known. In human embryonic kidney cells, insulin and insulin-like growth factor, working through PI3K, activate ectopically expressed *Sgk*, but not *Sgk* transcription (Park *et al.*, 1999; Kobayashi and Cohen, 1999). A PI3K-independent pathway, however, mediates insulin-mediated *Sgk* activation in Chinese hamster ovary cells. Treatment of cells with a cell-permeable Ca^{2+} chelator abolishes insulin-induced *Sgk* activation, whereas treatment with Ca^{2+} ionophores greatly increases it. This effect is insensitive to the PI3K inhibitor wortmannin, but is completely blocked by calmodulin inhibitors. Furthermore, *Sgk* was detected in direct association with the Ca^{2+} and calmodulin-dependent protein kinase kinase (CaMKK), suggestive of a Ca^{2+} -triggered signalling cascade in which an increased intracellular Ca^{2+} concentration directly stimulates *Sgk* through CaMKK (Imai *et al.*, 2003). Hepatocyte growth factor and Rac1, but not Rap1 (small guanine 5'-triphosphate (GTP)-binding proteins of the Rho family), as well as adhesion to immobilized fibronectin, induce activation of *Sgk* in MDCK cells (Shelly and Herrera, 2002).

4.1.5 Subcellular localisation of *Sgk*

The phosphorylation status of *Sgk* correlates with the intracellular localisation of the protein, in accordance with the proliferative conditions of cells. In mammary tumour cells exposed to glucocorticoids, which induce a G1 cell cycle arrest, *Sgk* is detected as a hypophosphorylated form and is seen by immunocytochemistry to localise mainly to perinuclear or cytoplasmic cellular compartments. In contrast, in highly proliferative serum-stimulated cells, the protein transiently assumes a hyperphosphorylated form and is located in the nucleus (Buse *et al.*, 1999). In synchronous cells, *Sgk* shuttles between the nucleus and the cytoplasm in synchrony with the cell cycle, where it is localised to the nucleus during S phase and is mainly cytoplasmic at the other stages (Buse *et al.*, 1999). This suggests that it might be important to make *Sgk* accessible or inaccessible to certain substrates at particular stages of the cell-cycle. It is probably not a particular subcellular localisation that influences proliferation, since forced retention of exogenous *Sgk* in either subcellular compartment suppresses growth and DNA synthesis of serum-stimulated cells (Buse *et al.*, 1999). It might therefore be the nuclear-cytoplasmic shuttling that is important for *Sgk* function under proliferative conditions. This may

mean that *Sgk* substrates necessary for cell-cycle progression lie both in the nucleus and the cytoplasm.

Within the cytoplasm, *Sgk* can be further compartmentalised, having been detected in the inner surface of the plasma membrane (Brickley *et al.*, 2002), a feature shared by many AGC kinases, as mentioned above; and in association with mitochondria, in response to hyperosmotic conditions, UV irradiation, heat shock and oxidative stress (Firestone *et al.*, 2003)

4.1.6 Downstream of *Sgk*

Three endogenous *Sgk* substrates have been identified. The first two were identified by a candidate approach, testing known substrates of the related PKB. One is the forkhead transcription factor FoxO3a, which upon phosphorylation is withdrawn from its role as a transcription factor by exiting the nucleus. *Sgk*, like PKB, can phosphorylate the three regulatory sites of FoxO3a but they differ in the efficiency with which they phosphorylate specific sites. Thus, *Sgk* preferentially phosphorylates S315 of FoxO3a whereas PKB preferentially phosphorylates S253. The third site, S32, is phosphorylated more efficiently by PKB than by *Sgk* (Brunet *et al.*, 2001). For a discussion on the possible significance of the differential phosphorylation of FoxO3a by these two kinases, see Brunet *et al.*, 2001.

A second *Sgk* substrate is the MAPK pathway mediator B-Raf, itself a protein kinase. B-Raf has several phosphorylation sites and its activity is both positively and negatively regulated by phosphorylation. *Sgk* phosphorylates B-Raf mainly on S364, which results B-Raf inhibition. Although PKB can phosphorylate B-Raf of the same serine, inhibition of B-Raf activity by *Sgk* phosphorylation is stronger than by PKB phosphorylation, which is probably due to a higher affinity of *Sgk*-B-Raf binding than that of PKB-B-Raf binding (Zhang *et al.*, 2001).

A third *Sgk* substrate is the ubiquitin ligase called neural precursor cell-expressed developmentally down-regulated (Nedd) 4-2. Following phosphorylation by *Sgk*, Nedd4-2 loses affinity for the ENaC, mediating body fluid homeostasis by aldosterone (reviewed in Farman *et al.*, 2002), leading to increased abundance of ENaC in the

plasma membrane (Debonneville *et al.*, 2001; Snyder *et al.*, 2002). Indeed, *Sgk* increases the activity of ENaC but not by direct phosphorylation (Chen *et al.*, 1999; Naray-Fejes-Toth *et al.*, 1999; Alvarez de la Rosa *et al.*, 1999; Loffing *et al.*, 2001). *Sgk* enzymatic activity, however, is necessary for ENaC-mediated Na⁺ transport (Faletti *et al.*, 2002). Expression of each of the three ENaC subunits is stimulated by glucocorticoids in parallel to that of *Sgk*, in a bronchiolar epithelial cell line (Itani *et al.*, 2002a). In addition to potentiating Na⁺ transport through the ENaC, *Sgk* synergises with other activators of this channel, mCAP1 – 3, resulting in a more than additive effect (Vuagniaux *et al.*, 2002). Several other ion channels may be substrates for *Sgk*, as they have been shown to be modulated by *Sgk* activity (Wagner *et al.*, 2000; Wagner *et al.*, 2001; Setiawan *et al.*, 2002; Yun *et al.*, 2002; Gamper *et al.*, 2002a; Gamper *et al.*, 2002b; Warntges *et al.*, 2002; Embark *et al.*, 2003; Boehmer *et al.*, 2003; Yoo *et al.*, 2003).

4.1.7 Biological roles of *Sgk*

Immediate-early transcriptional regulation of a protein kinase is unusual and, besides *Sgk*, is only known to occur with three other serine/threonine kinases: *Snk* (serum inducible kinase) (Simmons *et al.*, 1992), *Fnk* (FGF inducible kinase) (Donohue *et al.*, 1995) and *Prk* (proliferation related kinase) (Li *et al.*, 1996). All are rapidly transactivated in response to specific hormonal and environmental stimuli and their induction is often associated with increased cellular proliferation. However, *Sgk* is also transactivated during differentiation, such as that elicited by glucocorticoids, which induce a G1 cell cycle arrest. This sets *Sgk* apart from any other kinase. How *Sgk* might be implicated in cell proliferation as well as differentiation is not understood but its restriction to certain cell types argues against it being a general intermediate in a ubiquitous process.

The distinct cellular localisation of most *Sgk* in proliferating versus differentiated granulosa cells suggests that there are distinct *Sgk* functions under the two conditions. The state of *Sgk* phosphorylation is also distinct under the two conditions, where the hyperphosphorylated form is the main one found in proliferating cells (Buse *et al.*, 1999). The exact *Sgk* sites phosphorylated under these conditions have not been determined but another study has shown that *Sgk* phosphorylation at S78 is required for MCF10A cells to enter S phase in response to growth factors (Hayashi *et al.*, 2001).

The same cell type may use *Sgk* for mediating its proliferation and differentiation stages. Ovarian granulosa cells show a bi-phasic response to FSH, with an initial proliferative reaction, including transient induction of *Cyclin D2* mRNA, followed 24 – 48 h later by differentiation (reviewed in Richards, 1994). In the rat ovary, *Sgk* mRNA is detected exclusively in the granulosa cells. In cultured granulosa cells, *Sgk* mRNA is also induced in a bi-phasic manner, which parallels both stages of FSH action. Immediate-early *Sgk* transcript levels reach a maximum after 2 h of exposure of cells to FSH; levels then decrease but rise several hours later, being highest by 48 h (Alliston *et al.*, 1997). *Sgk* protein is mainly nuclear in the first phase and as granulosa cells differentiate, luteinise and cease dividing, *Sgk* becomes mainly cytoplasmic (Gonzalez-Robayna *et al.*, 1999). The same progression of *Sgk* compartmentalisation is observed *in vivo*, in ovaries of hypophysectomised rats, stimulated to differentiate by hormonal administration (Alliston *et al.*, 2000).

A role for *Sgk* in cell survival was demonstrated by the reduction of apoptosis levels of MCF10A cells in the absence of growth factors when *Sgk* was ectopically expressed. Protection from apoptosis was not observed when the kinase-dead versions of *Sgk* (K127M, T256A or S422A) were used (Mikosz *et al.*, 2001). This implicates the enzymatic activity of *Sgk* in mediating the known antiapoptotic role of glucocorticoid receptor activation in these cells (Moran *et al.*, 2000). *Sgk* enzymatic activity is also correlated with increased cell survival under several stress-inducing stimuli. Ectopic expression of wild-type or constitutively active *Sgk* protects mammary epithelial cells against stress-induced cell death, whereas that of the enzymatically inactive T256A/S422A *Sgk* mutant does not (Leong *et al.*, 2003).

The generation of *Sgk*-null mice has confirmed a role for *Sgk* in osmoregulation. *Sgk*-null mice fail the normal response of decreasing Na^+ excretion when subject to NaCl dietary restriction (Wulff *et al.*, 2002). Na^+ excretion is similar in wild-type and *Sgk*-null mice subject to a normal NaCl diet (Wulff *et al.*, 2002), which suggests *Sgk* mediates the response to osmotic stress rather than establishing normal osmotic balance. *Sgk* transactivation by systemic pathological triggers, such as in patients with diabetes, Crohn's disease or during dehydration, is consistent with a role in osmotic stress response. A role for *Sgk* in the physiological regulation of blood pressure has also been

suggested. The human *SGK* locus is linked to blood pressure phenotypes. Furthermore, significant interactions exist between each of two single nucleotide polymorphisms and blood pressure, as well between the single nucleotide polymorphisms themselves, which in combination enhance the effect observed with each individually (Busjahn *et al.*, 2002). The action of *Sgk* on blood pressure is possibly exerted by ENaC, which remains the only Na⁺ transport protein for which there is genetic evidence supporting its involvement in the genesis of both hypertension (Liddle's syndrome) and hypotension (pseudohypoaldosteronism type 1) (reviewed in Kamynina and Staub, 2002).

There are other possible roles for *Sgk*. Recently, *Sgk* mRNA was found to be upregulated in the dorsal hippocampus of rats that are fast learners in the Morris water maze task, when compared with slow learners. There is clear upregulation of *Sgk* in three areas of the fast learners' hippocampus (CA1, CA3 and dentate gyrus). Consistent with this, transfection of *Sgk* into the CA1 facilitates water maze performance, whereas transfection of S422A mutant *Sgk* impairs water maze performance. That learning and memory rather than sensory-motor abilities is affected is further supported by the fact that mutant *Sgk* transfection did not alter spatial learning when the platform was visible (Tsai *et al.*, 2002). This provides a substantial biochemical mechanism underlying glucocorticoid-induced memory facilitation (Tsai *et al.*, 2002). The fact that *Sgk* modulates the activity of several ion channels involved in neuronal excitability offers obvious molecular candidates to establish a link between *Sgk* activity and memory consolidation.

4.1.8 *Sgk* family members

Sgk was the first of three *Sgk* genes to be discovered in vertebrates. Since the finding of others, *Sgk* is often referred to as *Sgk*-1. *Sgk*-3 is also known as cytokine-independent survival kinase, CISK (Liu *et al.*, 2000) or SGK-like (SGKL) in humans. In addition, human *SGK*-2 and *SGK*-3 give rise to at least two splice variants (Kobayashi *et al.*, 1999). Analysis of the human proteins shows that SGK-1 and -3 are most similar in their catalytic domain (approximately 80% identical). The C-termini are the next most similar regions (44 – 68% identity) and the N-termini differ considerably (only approximately 25% identity in the best of cases, *i. e.*, between SGK-1 and -3, which present nearly no identity to SGK-2 in this region (Kobayashi *et al.*, 1999). In contrast

to the N-terminus of SGK-1, which contains no known motifs, the N-terminus of SGK-3 contains a Phox (PX) homology domain (Liu *et al.*, 2000). The function of the PX domain is not known but it has been implicated in cellular trafficking. PX domains can mediate interactions with phospholipids or with other proteins (Haft *et al.*, 1998).

The most structurally related family members, SGK-1 and -3, are also the ones that display the most similar expression profiles in a Northern analysis of adult tissues. *SGK-1* and -3 mRNAs are widely expressed in adult tissues, as opposed to that of *SGK-2*, which is significantly more restricted in adults (present mainly in the brain, liver, kidney and pancreas) (Kobayashi *et al.*, 1999). *Sgk-3* mRNA has been identified in a few cDNA libraries but much less frequently than that of *Sgk-1*. *Sgk-3* is expressed in the 7.5 dpc (Liu *et al.*, 2000) and 13.5 dpc mouse embryo (forelimb and testis cDNA libraries), but no spatial information has been published. There is no spatial information available for *Sgk-2* mRNA.

In contrast to *Sgk-1* mRNA, *Sgk-2* and -3 mRNAs are not induced by serum nor by dexamethasone in rat fibroblast or human hepatoma cell lines (Kobayashi *et al.*, 1999). *Sgk-2* and -3 can be phosphorylated and activated *in vitro* by PDK1, although with slower kinetics. Phosphorylation occurs in residues equivalent to the activation loop T256 of *Sgk-1*. Also like *Sgk-1*, the activities of *Sgk-2* and -3 are greatly increased in the presence of H₂O₂ but, in contrast to *Sgk-1*, this activation is only partially suppressed by PI3K inhibitors. In addition, *Sgk-2* and -3 are activated by the insulin-like growth factor-1 but less so than *Sgk-1*. Furthermore, the preferential consensus phosphorylation sites for *Sgk-2* and -3 are identical to those of *Sgk-1* (and PKB) (Kobayashi *et al.*, 1999).

Further characterisation of *Sgk-3* shows that it is activated by IL-3 in a PI3K-dependent manner and that it can block the apoptotic response that normally occurs upon IL-3 withdrawal. The latter phenomenon might be explained by the fact that *Sgk-3* can phosphorylate FoxO3a and the proapoptotic Bcl-2 family member Bad. Therefore, *Sgk-3*, like *Sgk-1*, appears to mediate cell survival (Liu *et al.*, 2000).

Sgk-3 has a distinct subcellular localization from *Sgk-1*. In embryonic kidney and COS cells, *Sgk-3* has been found to localise in endosomes and this localisation is strictly

dependent upon the PX domain (Liu *et al.*, 2000; Xu *et al.*, 2001; Virbasius *et al.*, 2001). The PX domain of Sgk-3 was shown to interact with PIP₂ and PIP₃ and mutation of this domain was shown to impair Sgk-3 activity and activation by the insulin-like growth factor-1 and by EGF (Xu *et al.*, 2001; Virbasius *et al.*, 2001).

There are *Sgk* orthologues in *Ciona intestinalis* and *C. elegans* as well as two homologous budding yeast genes, *YPK1* and *YKR2*. *YKR2* mutants present no obvious phenotype but *YPK1* mutants exhibit slow growth (Chen *et al.*, 1993). Double-mutants fail to grow in glucose-containing medium, a phenotype which can be complemented by rat *Sgk* (Casamayor *et al.*, 1999). The phosphorylation and intracellular localisation of Ypk1 is regulated by the intracellular levels of sphingolipids, via yeast kinases homologous to PDK1 (Pkh kinases) (Sun *et al.*, 2000). Yeast do not have PIP₂ or PIP₃ and it is thought that sphingolipid signalling might be their equivalent to the phosphoinositide pathway of metazoans. Concordantly, yeast Pkh kinases do not have the pleckstrin homology (PH) domain, which in PDK mediates its interaction with inositol phospholipids. So, *Sgk* and Ypk1 appear to be regulated in an analogous fashion (Sun *et al.*, 2000). Furthermore, overexpression of mammalian *Sgk* overcomes sphingolipid depletion in yeast (Sun *et al.*, 2000).

4.2 Results of the functional analysis of mouse *Sgk*

To understand a role for *Sgk* in early development I began a project to generate *Sgk*-null mice. In addition, I addressed the role of *Sgk* with a few other experiments. There were several questions I wanted to address: Is *Sgk* asymmetrically expressed as early as at 5.5 dpc? Is *Sgk* required for primitive streak formation and/or mesoderm induction? Does *Sgk* expression label some stem cell populations, namely endothelial stem cells / angioblasts? Is *Sgk* expression involved in angioblast or endothelial cell proliferation and/or differentiation?

4.1 Further characterisation of mouse *Sgk* expression

I have described *Sgk* expression during early gastrulation (clone s8609b60 in Fig. 3.1; section 3.2.3). At the onset of gastrulation *Sgk* is strongly expressed in the VE overlying the nascent mesodermal wings and, more weakly, in the mesoderm itself (Fig 4.1).

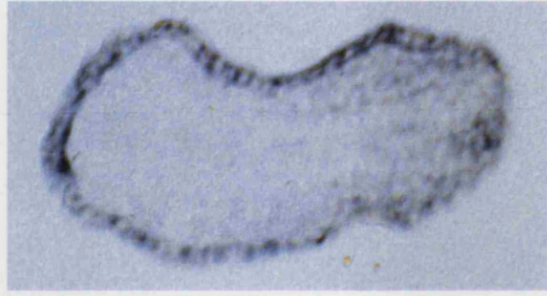


Fig. 4.1 *Sgk* is expressed strongly in the VE and weakly in the nascent mesoderm of the egg-cylinder stage mouse embryo. Transverse section of a 6.5 dpc mouse embryo at approximately the level of the extraembryonic-embryonic junction, following whole-mount *in situ* hybridisation with *Sgk* riboprobe. Anterior is to the left. Strong staining is visible in the VE and weaker staining is visible in the nascent mesoderm.

Whole-mount *in situ* hybridisation on 5.5 dpc embryos reveals *Sgk* mRNA in the VE and the epiblast on both the anterior and posterior of the conceptus (Fig. 4.2). In most cases, *Sgk* mRNA was symmetric at 5.5 dpc (Fig. 4.2, A-B) but in some cases staining did seem stronger on one of the sides of the pre-gastrula conceptuses (Fig. 4.2 C-D), presumably in the future posterior, as this is where staining is detected at 6.5 dpc. Therefore, *Sgk* is initially expressed symmetrically in the pre-gastrula mouse embryo, after which it is specifically down-regulated in the anterior.

At 8.5 and 9.5 dpc *Sgk* transcripts are found in the vasculature as well as in the eye and branchial arches. Both nascent capillary endothelial cells and blood cells are thought to derive from a common precursor called the hemangioblast. These cells derive from mesoderm that lies in close proximity to the endoderm, the splanchnopleura. They group into spheres, called blood islands, which then fuse to form primary capillaries. The outside cells of the blood islands give rise to the endothelial lineage, whose precursors are named angioblasts. The interior cells of the blood islands give rise to the hematopoietic lineages. The process of *de novo* blood vessel formation is called vasculogenesis. However, vasculature formation makes use of another process, termed angiogenesis, whereby already existent vessels branch and invade non-vascularised areas (reviewed in Risau and Flamme, 1995). In addition to being expressed in blood islands of the splanchnopleura, *Sgk* is expressed in the forming limb blood vessels,

where no endoderm is present (Fig. 4.3). This means that *Sgk* mRNA labels sites of both vasculogenesis and angiogenesis in the embryo.

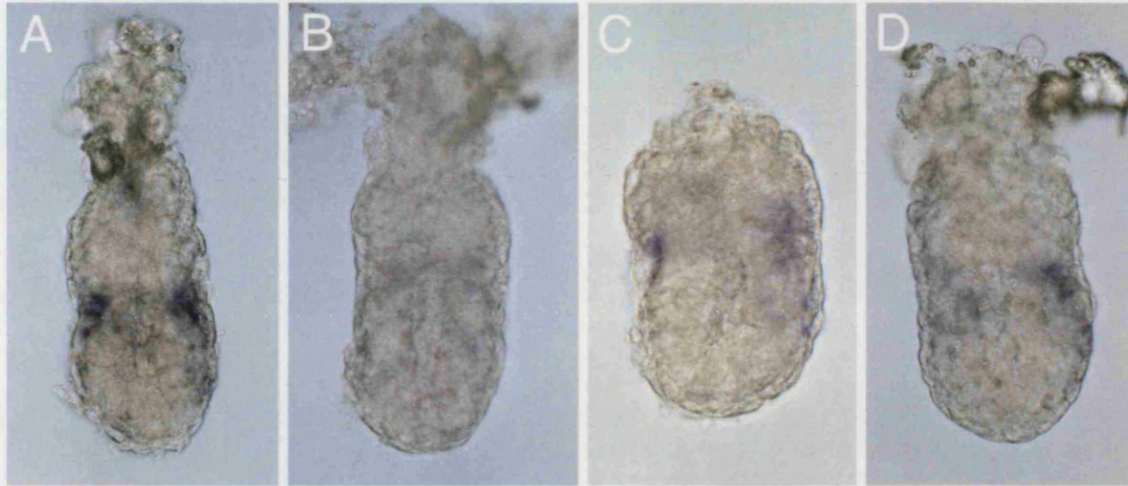


Fig. 4.2 At 5.5 dpc, mouse *Sgk* expression is transiting from symmetric to asymmetric. Whole-mount *in situ* hybridisation with *Sgk* riboprobe on four distinct 5.5 dpc mouse embryos: A – D.

In 10.5 – 13.5 dpc mouse embryos, whole-mount staining was indistinguishable from that obtained with a probe for the endothelial marker foetal liver kinase (*Flk*)-1, receptor for the vascular endothelial growth factor (VEGF). At these stages the vasculature has branched and refined considerably so the overall staining assumes a blurred aspect (data not shown). To assess whether *Sgk* is expressed throughout the vasculature or in a subtype of vessels, I collaborated with Dr. Marcus Fruttiger (University College London) who analysed *Sgk* expression in retinal vasculature preparations. The retinal vasculature is an excellent model for vascular development given that each contains a *continuum* of developmental stages ordered ontogenetically from the periphery to the centre. The retinal vasculature develops from the centre to the periphery. Hence, the centre contains the most mature vessels (reviewed in Fruttiger, 2002). The expression of *Sgk* in the retinal vasculature presents several unusual features (Fig. 4.4). *Sgk* expression is not uniform throughout development, unlike most blood vessel markers.

Ontological variation of *Sgk* expression in blood vessels is most apparent in arteries, where mRNA signals are high in the immature vessels and greatly down-regulated as the arteries mature. In general, expression of *Sgk* in mature veins is higher than in

mature arteries. Highest levels of *Sgk* expression are found in capillaries, rather than in any large vessel. This could be related to the higher levels observed in immature, capillary-like, arteries, compared to the mature vessel. In addition to labelling endothelial cells, *Sgk* is also seen in pericytes (VSMCs), the other cell type required to generate blood vessels. *Sgk* mRNA does not label all pericytes, however.

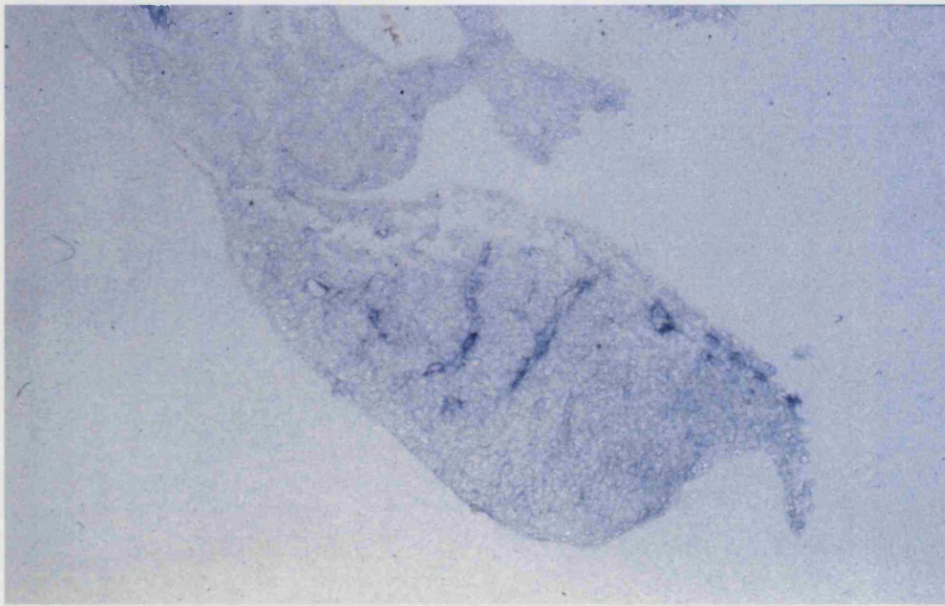


Fig. 4.3 *Sgk* is expressed in sites of embryonic angiogenesis. Transverse section of a 9.5 dpc mouse embryo at the level of the forelimb bud, following whole-mount *in situ* hybridisation with *Sgk* riboprobe. Staining is visible in blood islands and primary capillaries within the limb bud.

I performed *in situ* hybridisation on sections of 10.5 – 13.5 dpc mouse embryos. As expected, *Sgk* is visible in the forming vasculature but other sites of expression, such as the choroid plexus, Rathke's pouch, from which the pituitary is derived, the eye, the hair placodes of the whisker pads, and limb bud mesenchyme, are prominent (Fig. 4.5).

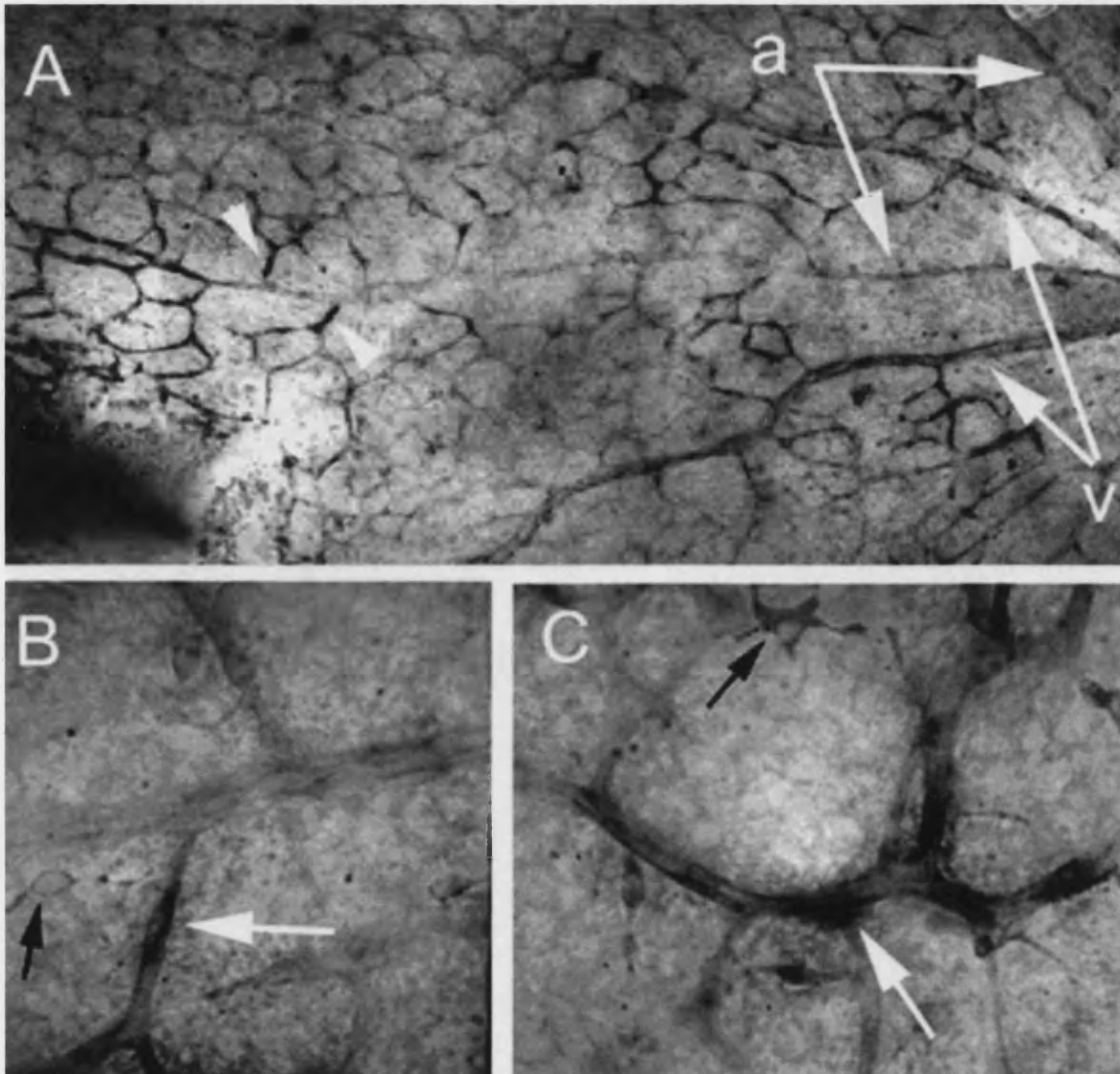


Fig. 4.4 *Sgk* expression in the vasculature is very dynamic. Transverse sections through the retina of a newborn mouse, following *in situ* hybridisation with *Sgk* riboprobe. In A, the centre of the retina is to the right and the periphery is to the left; 'a' arrows point at downregulation of *Sgk* expression in mature arteries and 'v' arrows point at high *Sgk* expression in mature veins; arrowhead points at a small capillary, the vascular structures where *Sgk* expression is highest. Note that *Sgk* is also strongly expressed in immature arteries. B and C are higher power images than A; black arrows point at background staining (in C it points at a macrophage), which can easily be distinguished from the real, darker, staining; white arrows point at *Sgk* expression in what appear to be pericytes.

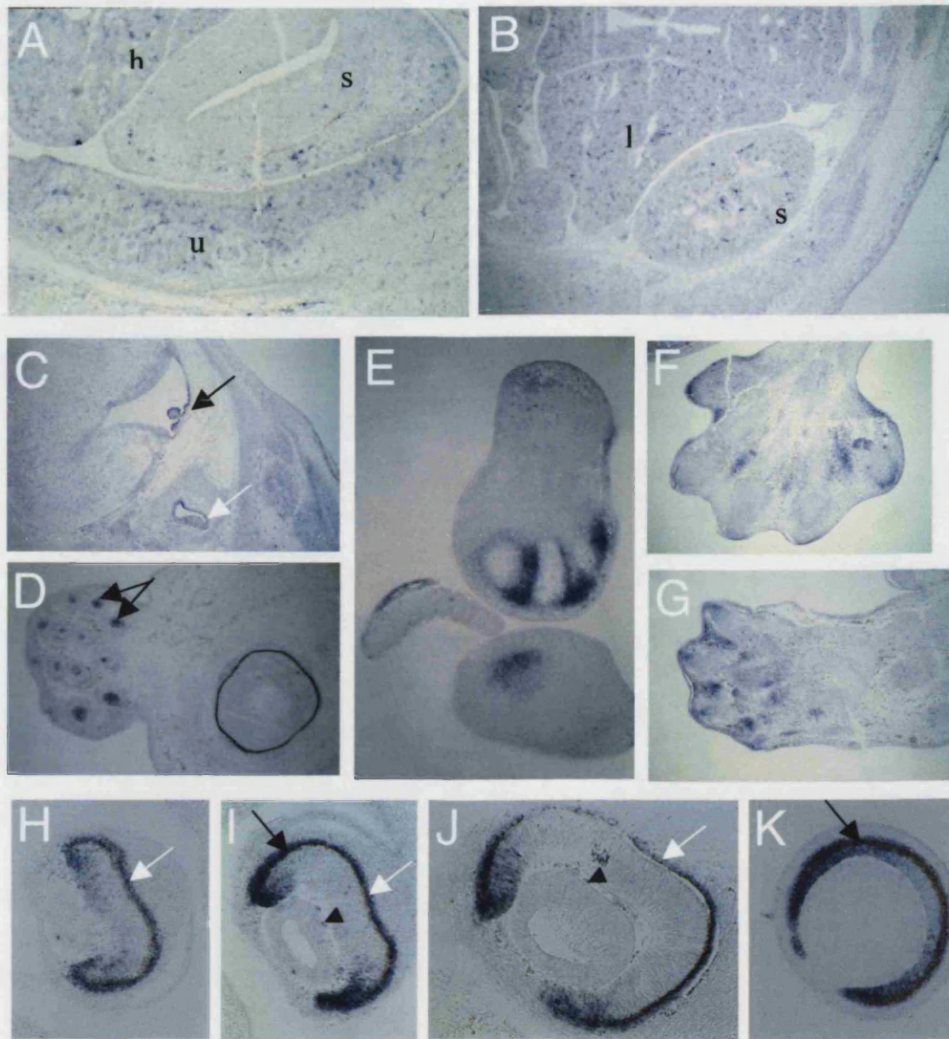


Fig. 4.5 Sites of *Sgk* expression in the 11.5 – 13.5 dpc mouse embryo. *In situ* hybridisation with *Sgk* riboprobe on parasagittal sections of 11.5 and 13.5 dpc mouse embryos. Anterior is to the left, except in E-G. **A** and **B** depict vasculature staining throughout the developing organs at 11.5 and 13.5 dpc, respectively; **h**, heart, **s**, stomach, **u**, urogenital ridge, **l**, liver. **C** is a section through the 13.5 dpc brain; **black arrow** points at *Sgk* expression in the choroid plexus; **white arrow** points at *Sgk* expression in Rathke's pouch. **D** is a section through the 13.5 dpc head; **black arrows** point at two of the whisker pad hair placodes stained. **E** is a section through 11.5 dpc limb buds, where the forelimb is at the top and the hindlimb at the bottom; **F** and **G** are sections through 13.5 dpc fore- and hindlimb buds, respectively; *Sgk* is expressed mainly in the interdigital areas and becomes more refined as development proceeds. **H – I** are sections through the 11.5 dpc eye and **J – K** are sections through the 13.5 dpc eye; **black arrows** point at the pigmented layer; **white arrows** point at the presumptive choroid and arrowhead points at the hyaloid plexus.

In the eye, *Sgk* is expressed in the retina and in one or two cell layers outlining exteriorly the pigmented layer, in what is probably the presumptive choroid, in addition to the vascular cells that accumulate between the lens and the retina constituting the hyaloid plexus. At 11.5 dpc *Sgk* expression in the retina is not uniform and detectable only in the periphery. At 13.5 dpc, retinal expression is also stronger in the periphery but central expression was also visible. Retinal expression appears biased towards the inner retinal layers (Fig. 4.5, H and I) although in some sections it spanned all cell layers (Fig. 4.5, K).

I performed whole-mount *in situ* hybridisation on 6.5 – 9.5 dpc mouse embryos with an *Sgk-2* antisense probe and no expression was detected (data not shown). Therefore, *Sgk-1* and *Sgk-2* are unlikely to be redundant during these stages of mouse development. *Sgk-3* is, however, the most likely candidate for redundancy. At the time of my study, however, no *Sgk-3* cDNA was available.

I was interested in determining the subcellular localisation of *Sgk* in the early embryonic tissues. To this end we established a collaboration with Dr. Gary Firestone (University of California at Berkeley) who sent us an anti-*Sgk* polyclonal antibody (Alliston *et al.*, 1997), which failed in whole-mount immunohistochemistry using a variety of fixation methods.

4.2.2 Groundwork for the differentiation of ES cells into endothelial cells

Sgk expression in angioblasts and endothelial cells provides us with an opportunity to study the role of this gene in a differentiation process since endothelial cells can be generated *in vitro* from ES cells. This differentiation takes place in a progressive fashion involving at least three steps, defined by the onset of expression of: 1) *Flk-1*; 2) platelet endothelial cell adhesion molecule (*PECAM*) and the tyrosine kinase with immunoglobulin and EGF homologous domains (*Tie*)-2; 3) vascular endothelial cadherin (*VE-cadherin*) and *Tie-1* (Vittet *et al.*, 1996). The order of endothelial cell transcript appearance upon *in vitro* ES cell differentiation recapitulates that of vasculogenesis *in vivo*.

I combined the endothelial-specific conditions defined in Vittet *et al.*, 1996 with the protocol for ES cell differentiation into hematopoietic lineages established by Dr. G. Keller (Keller *et al.*, 1993). The protocol (Appendix 2) is adequate for feeder-independent ES cells and is accomplished via the formation of embryoid bodies.

I performed RT-PCR on ES cells and detected high levels of *Sgk* transcript (Fig. 4.6), consistent with the presence of *Sgk* cDNA in a blastocyst cDNA library. Therefore, in addition to providing an opportunity to study the role of *Sgk* in endothelial differentiation, ES cells directly constitute a cell type in which to compare proliferation and apoptotic indexes of wild-type and *Sgk*^{-/-} cells.

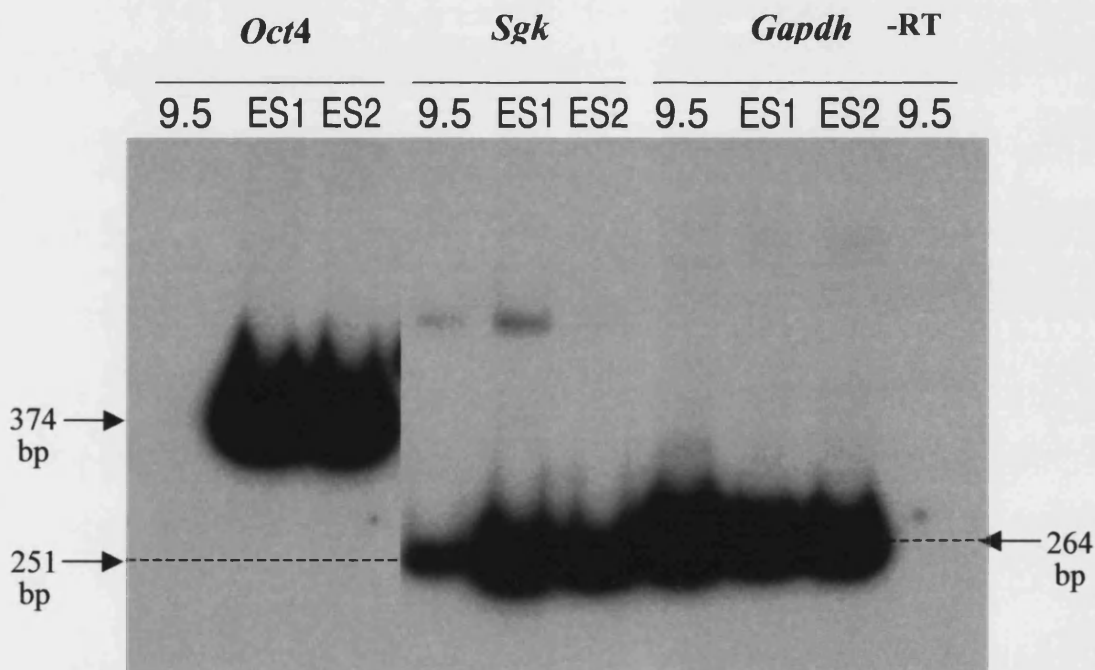


Fig. 4.6 RT-PCR of *Oct4*, *Sgk* and *Gapdh* performed on whole RNA obtained from 9.5 dpc mouse embryos or each of two ES cell lines. 9.5, 9.5 dpc mouse embryo; ES1, ES cell line 1; ES2, ES cell line 2. *Oct4* is positive control for ES cells and negative control for 9.5 dpc embryos; fragment size is 374 bp. *Gapdh* is loading control for all samples; fragment size is 264 bp. *Sgk* is expressed at high levels in ES cells; fragment size is 251 bp. -RT lane represents reaction mix in the absence of reverse transcriptase.

4.2.3 Is *Sgk* upregulated during embryonic healing?

The fact that *Sgk* mRNA is upregulated after cortical brain injury in adults (Imaizumi *et al.*, 1994), led us to ask whether *Sgk* is a general mediator of the wound healing response. I collaborated with Dr. Lisa Cooper in Prof. Paul Martin's lab in order to perform wound healing experiments directly on our system of interest, the mouse embryo.

No *Sgk* mRNA was detected by whole-mount *in situ* hybridisation in the wounds of 11.5 dpc embryos allowed to heal for 30 min, 3 h or 6 h (data not shown), in contrast to *Krox24* positive control mRNA (Grose *et al.*, 2002). Nonetheless, microarray analysis of mRNAs expressed in wound-healed mouse embryos compared to unwounded controls revealed an approximately two-fold increase in *Sgk* mRNA by 3 h after wounding, which was maintained up to 24 h (L. Cooper, personal communication). More experiments are needed to confirm the specificity and reproducibility of this result. In case the result is confirmed, further experiments are needed to address whether *Sgk* is required for the healing process and if, so, in which cells it is required.

4.2.4 Isolation and characterisation of mouse *Sgk* genomic DNA

I screened a mouse genomic bacteriophage (phage) lambda library (Stratagene) to isolate genomic clones containing *Sgk* and found three independent clones. Two of these clones contained both the 5' and 3' ends of the *Sgk* open reading frame (ORF). I used one of these, hereafter called *Sgk* genomic clone, for all subsequent work. This *Sgk* genomic clone contained an insert of approximately 12 kb that could be released from the vector with *Not* I or *Sal* I.

I mapped the insert of the *Sgk* genomic clone with restriction digests followed by Southern analysis probed with end-labelled DNA oligonucleotides that identified the 5' and 3' ends of the *Sgk* cDNA. A map displaying a few informative restriction sites found in the *Sgk* genomic clone is shown in Fig. 4.7. I used this map to design and construct an *Sgk* targeting vector. Additionally, as this was being carried out, I sequenced the *Sgk* genomic clone in order to aid the mapping and cloning process. The *Sgk* genomic sequence obtained is 99% identical to the sequence subsequently

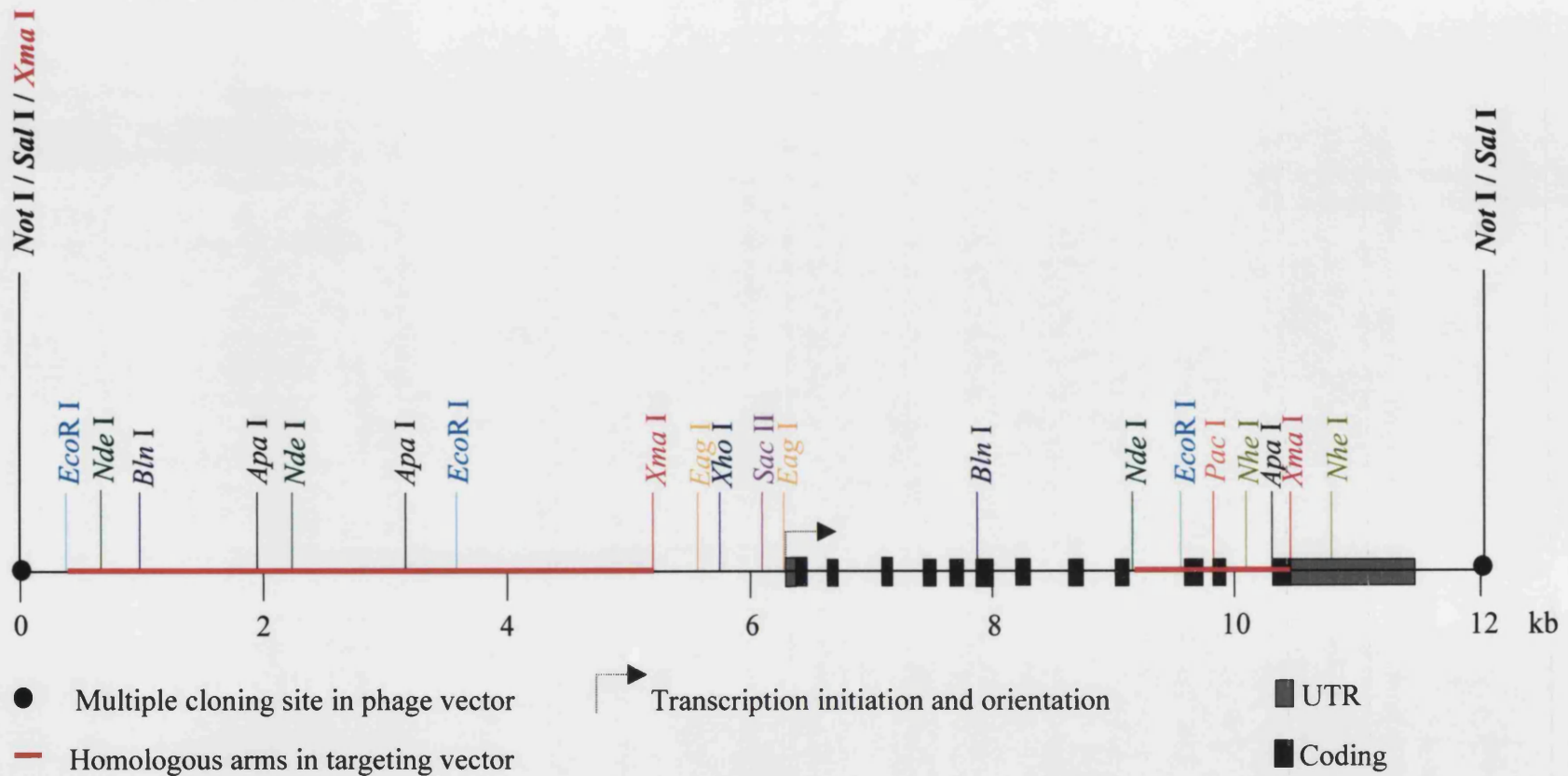


Fig. 4.7 **Map of mouse *Sgk* genomic clone.** Selected restriction sites, exon – intron structure of *Sgk* , and fragments chosen as homologous arms for *Sgk* targeting construct are shown. Each restriction enzyme and corresponding site is represented in a different colour. Boxes represent exons, wherein the 5' and 3'UTRs are depicted in grey and coding regions are depicted in black. Proportions are approximately correct.

published in the public database (Accession NT_039491.1) following completion of the mouse genome sequencing. In addition to *Not* I and *Sal* I, *Age* I, *Asc* I, *Bam*H I, *Fse* I, *Nco* I and *Pme* I sites are absent from the *Sgk* genomic clone. Comparison between *Sgk* cDNA and genomic sequences, refined with current knowledge on splice donor and acceptor sequences, allowed me to determine the genomic organisation of the gene (Fig. 4.7 and Table 4.1). Like the human gene, mouse *Sgk* contains 12 exons (Table 4.1, A – L), which span approximately 5 kb. The exon-intron organisation of mouse *Sgk* is identical to that of human *SGK* gene (Kobayashi *et al.*, 1999).

Table 4.1 Exon and intron size, and exon-intron boundary sequences of mouse *Sgk*

Exon	Exon length (bp)	Splice donor	Intron length (bp)	Splice acceptor
A	144 (68 are 5'UTR)	TC ATC Ggtgagt	140	ttatagCT TTT A
B	76	C AAA CAgtaatg	428	ccacagC GAC AA
C	76	CCT CCGgtaagt	243	ttctagCCA AGT
D	90	GGA AAGggcagt	123	atgactGGC AGT
E	99	AAA GAGgtaagg	113	tcctagGAG AAG
F	132	GGA GAGgtgagc	204	tcgcagCTG TTC
G	113	T TAT AGgtgagc	310	ctacagA GAC TT
H	124	CCT GAGgtaggc	241	tttcagTAT CTG
I	96	GGC CTGtgagta	414	ttccagCCC CCG
J	156	GAC TTTgtgagt	104	caacagATG GAG
K	90	AAT GTGgtaagt	410	taacagAGT GGG
L	1233 (1068 are 3'UTR)			

Capital letters refer to exonic sequences and lowercase letters to intronic sequences.

Codons are separated by a space.

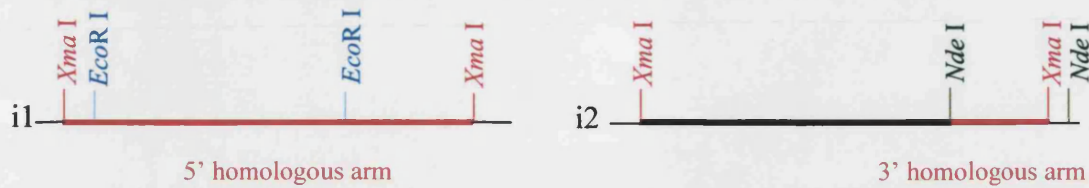
4.2.5 Construction of *Sgk* targeting vector

I aimed at generating a null *Sgk* allele. Leaving exons behind in the targeted locus after homologous recombination means that a portion of the coding region of the targeted gene might still be expressed. In many cases, however, a null allele is still generated due to disruption of the promoter or given that expressed sequences often result in nonsensical and/or severely truncated gene products. However, when possible, the most desirable approach is to remove most or the whole coding region of a gene. *Sgk* is a kinase and, as such, its catalytic domain is spread throughout a large portion of the protein. I aimed at removing the largest possible portion of the coding region in order to preclude possible dominant-negative effects from a putative truncated enzyme that might be generated otherwise. The steps involved in the construction of the *Sgk* targeting vector are described in Fig. 4.8

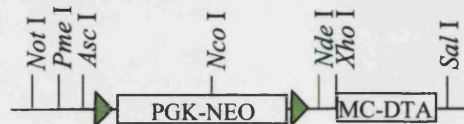
The fragments of genomic DNA chosen as homologous arms for the *Sgk* targeting construct were already highlighted in Fig. 4.7. The 5' homologous arm is an *EcoR* I – *Xma* I fragment (following partial digest of the genomic DNA with *EcoR* I) that spans 4.9 kb and the 3' homologous arm is an *Nde* I – *Xma* I fragment that spans 1.4 kb. In our strategy, 9 out of the 12 *Sgk* exons are removed and they contain the vast majority of the kinase domain. There were no convenient restriction sites to allow us to design the 3' homologous arm further downstream or even to make this arm longer in the 3' direction. Given that the 3' homologous arm is relatively short, it was important that the 5' homologous arm be as long as possible. The 5' arm was designed taking this into consideration along with the restriction map of the 5' genomic region, the aim of removing great part of the *Sgk* coding region and promoter, and the necessity of leaving genomic sequence upstream of the arm to probe for the homologous recombination event.

The rare homologous recombination event is best selected for by means of positive-negative selection scheme (Mansour *et al.*, 1988). The targeting vector must contain a positive selection gene, usually an antibiotic resistance gene, that selects for cells with a successfully integrated targeting vector; and a negative selection gene, coding for a lethal protein, that selects against random integration events rather than homologous recombination. Both selection genes should be linked to position-independent

A Two distinct *Xma* I fragments of approximately 5 kb were obtained from the *Sgk* genomic clone and cloned into intermediate vectors, i1 and i2. Each fragment contains one of the homologous arms. Fragment containing 3' homologous arm was cloned upstream of an *Nde* I site in the vector.



B MC-DTA was cloned into main vector containing floxed (\blacktriangleright) PGK-NEO, between *Xho* I and *Sal* I sites.



C 3' homologous arm was excised from i2 by *Nde* I and was cloned into the *Nde* I site in main vector



D *Xma* I insert was excised from i1 and subject to partial digestion with *Exo*R I. Resulting 4.9 kb fragment was cloned into an intermediate vector, i3, so as to be flanked upstream by a *Pme* I site and downstream by an *Asc* I site.



E 5' homologous arm was excised from i3 by *Pme* I and *Asc* I and cloned into corresponding sites in main vector, upstream of PGK-NEO.

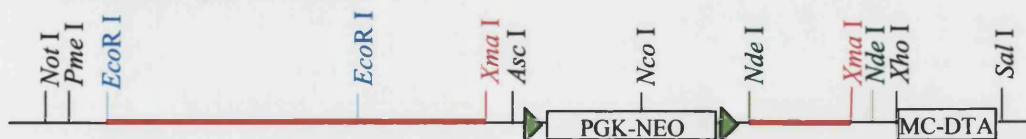


Fig. 4.8 Construction of *Sgk* targeting vector. Selected restriction sites are shown. All intermediate vectors and main vector backbone are pBSK-based. Targeting vector can be linearised with *Not* I and contains unique *Nco* I site that is absent from endogenous locus. PGK-NEO is positive selection gene and MC-DTA is negative selection gene. Insert proportions are approximately correct but size of *loxP* sites and of multiple cloning sites between inserts is exaggerated to allow their depiction or that of restriction sites.

promoters to assure their expression. In addition, each selection gene must hold a particular position within the targeting vector if it is to accomplish its role. Thus, the positive selection gene must reside between the homologous arms so that following homologous recombination it replaces the deleted genomic region and the negative selection gene must reside outside the homologous arms so that it is lost when homologous recombination takes place and is only left in the cases where random integration of the targeting vector occurs. When a reporter gene is used, it should be placed between the homologous arms so that it is expressed in homologous recombinants, hopefully under the control of the endogenous regulatory regions of the targeted gene (reviewed in Torres and Kuhn, 1995). For positive selection I used the Neomycin resistance cDNA under the control of the phosphoglycerate kinase promoter (PGK-NEO), and for negative selection I used the Diphtheria toxin A-chain cDNA downstream of the synthetic mutant polyoma enhanced HSVtk promoter (MC-DTA) (Fig. 4.8). Positive selection was achieved by exposing targeted cells to the antibiotic G418.

When homozygous null cells are to be generated from heterozygous cells, the PGK-NEO positive selection cassette has the added function of selecting for mitotic recombination events in the locus of interest upon increasing the concentration of selecting agent, since those cells with two copies of the antibiotic resistance gene will resist better to a great antibiotic insult than those with only one (Mortensen *et al.*, 1992). This avoids having to target the same locus twice, each with a different positive selection gene, when generating homozygous targeted cells.

The strong promoters used to drive expression of positive selection genes, such as the PGK promoter, have been found to account for phenotypes observed in some of the earliest targeting experiments performed. Therefore, it is now current practise to delete the positive selection gene from the genome of targeted cells once the desired targeting event has been confirmed. This can be achieved by flanking the positive selection cassette in the targeting vector with 34 bp sites from the bacteriophage P1, each called locus of X-over of P1 (*loxP*) sites, placed in the same orientation, which can subsequently be recognised and induced to recombine by the product of the P1 cyclisation recombination (*cre*) gene. Cre recognises *loxP* sites and induces their recombination. Recombination of the intrachromosomal *loxP* sites results in excision of

the positive selection cassette from the targeted locus. Excision of the “floxed” cassette can be achieved in cell culture, by expressing *cre* in targeted cells prior to their injection into blastocysts or, more commonly, *in vivo*, by crossing mice ubiquitously expressing the *cre* transgene with heterozygous carriers of the targeted allele. An identical result can be achieved by means of other recombination sites / recombinase pairs, but the Cre/LoxP system remains the most reliable for use in a mammalian context (reviewed in Torres and Kuhn, 1995). In the *Sgk* targeting vector constructed, PGK-NEO is flanked by *loxP* sites (Fig. 4.8).

Another consideration in the design of a targeting construct is that homologous recombination is most efficient between linear DNA (Bollag *et al.*, 1989; Hasty *et al.*, 1992). Therefore, the targeting vector must include a unique restriction site in the backbone with which to linearise the construct without disrupting any of its modules. The *Sgk* targeting vector I constructed can be linearised with *Not* I (Fig. 4.8).

Finally, the targeting event must remove or add a restriction site within the locus, in order for us to distinguish between endogenous and targeted loci. This means that there is a restriction site between the homologous arms of in the construct that is not present in the targeted locus or vice-versa. Homologous recombination events induced by my targeting vector in the *Sgk* locus can be recognised by digesting ES cell genomic DNA with *Nco* I, a site for which is introduced within the PGK-NEO cassette and which is absent from the region of the *Sgk* genomic locus targeted (Fig. 4.9). I tested *Nco* I in advance for its ability to digest mammalian genomic DNA and it proved successful.

Successful targeting of the *Sgk* locus should be visualised by a genomic probe flanking either of the homologous arms, as generating a smaller *Nco* I fragment than the endogenous locus (Fig. 4.9). A 5' genomic probe can be generated by excising the 320 bp *Xma* I – *Eco*R I fragment in the intermediary construct i1 (Fig. 4.8) and a 3' genomic probe can be generated by excising a 1.1 kb *Xma* I – *Not* I fragment containing the 3'UTR from an *Sgk* cDNA. Probes were tested for their ability to label a specific genomic fragment following genomic DNA digestion with *Nco* I and proved successful, labelling a fragment larger than 13 kb.

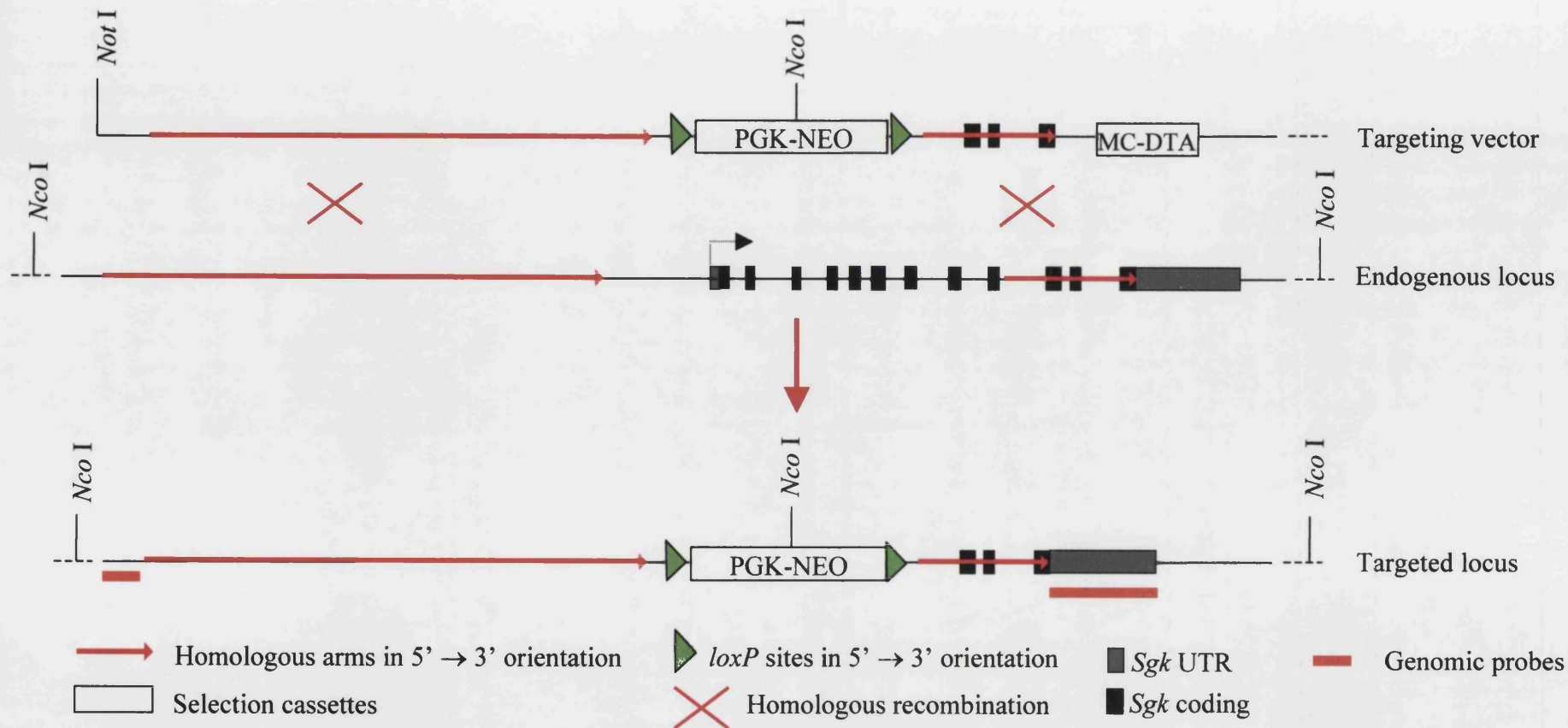


Fig. 4.9 *Sgk* targeting with construct used in this investigation. Following homologous recombination, the negative selection cassette MC-DTA is lost and an *Nco I* site is introduced in the targeted locus. Targeting event can be assessed by Southern analysis of genomic DNA digested with *Nco I*, probed with one of the genomic probes indicated. Insert proportions are approximately correct but size of *loxP* sites and of multiple cloning sites between inserts is exaggerated to allow their depiction or that of restriction sites.

4.2.6 Targeting of *Sgk* in ES cells

I electroporated 1.6×10^7 ES cells with 40 μg of linearised targeting vector and plated them into three 10 cm tissue culture dishes. Positive selection was started the following day by replacing ES cell medium with fresh one containing 200 $\mu\text{g/ml}$ G418. Positive selection was undertaken for 10 days. On the tenth day of selection, 96 G418-resistant clones were picked into 48-well plates. The following day, 32 more G418-resistant clones were picked, and the day after 4 more, bringing the total of putative positive clones up to 132. Picked clones were grown and split individually into duplicate 48-well plates, and a few cells of each seeded into 96-well plates in order to generate material for genomic DNA purification and analysis. Fresh duplicate clones were grown and frozen individually when appropriate.

Genomic DNA was prepared from each clone in the 96-well plates and digested with *Nco* I. 81 out of the 132 sample lanes analysed by agarose gel electrophoresis displayed clearly detectable genomic DNA whereas the remainder 51 lanes displayed weak or undetectable signal. Out of the 51 lanes where genomic DNA was weak or undetectable, 5 corresponded to clones that never grew in selection medium; the remainder 46 probably correspond to clones that grew comparatively slower and for which the material collected from the 96-well plate was insufficient for analysis. Since all clones picked were expanded into duplicate 48-well plates, one of the duplicate vials for each can be used to purify more genomic DNA.

Southern analysis of the *Nco* I genomic digests was performed using the 5' genomic probe. The results of this Southern analysis are depicted in Fig. 4.10. Results indicate that only 1 out of the 81 analysed samples may represent a successful targeting event (arrow in Fig. 4.10).

The next step would be to confirm the candidate positive clone with the 3' genomic probe and also to assay the remainder untested 46 clones by purifying a larger amount of genomic DNA from one of their frozen duplicates. If this were not positive, another round of targeting would be attempted.

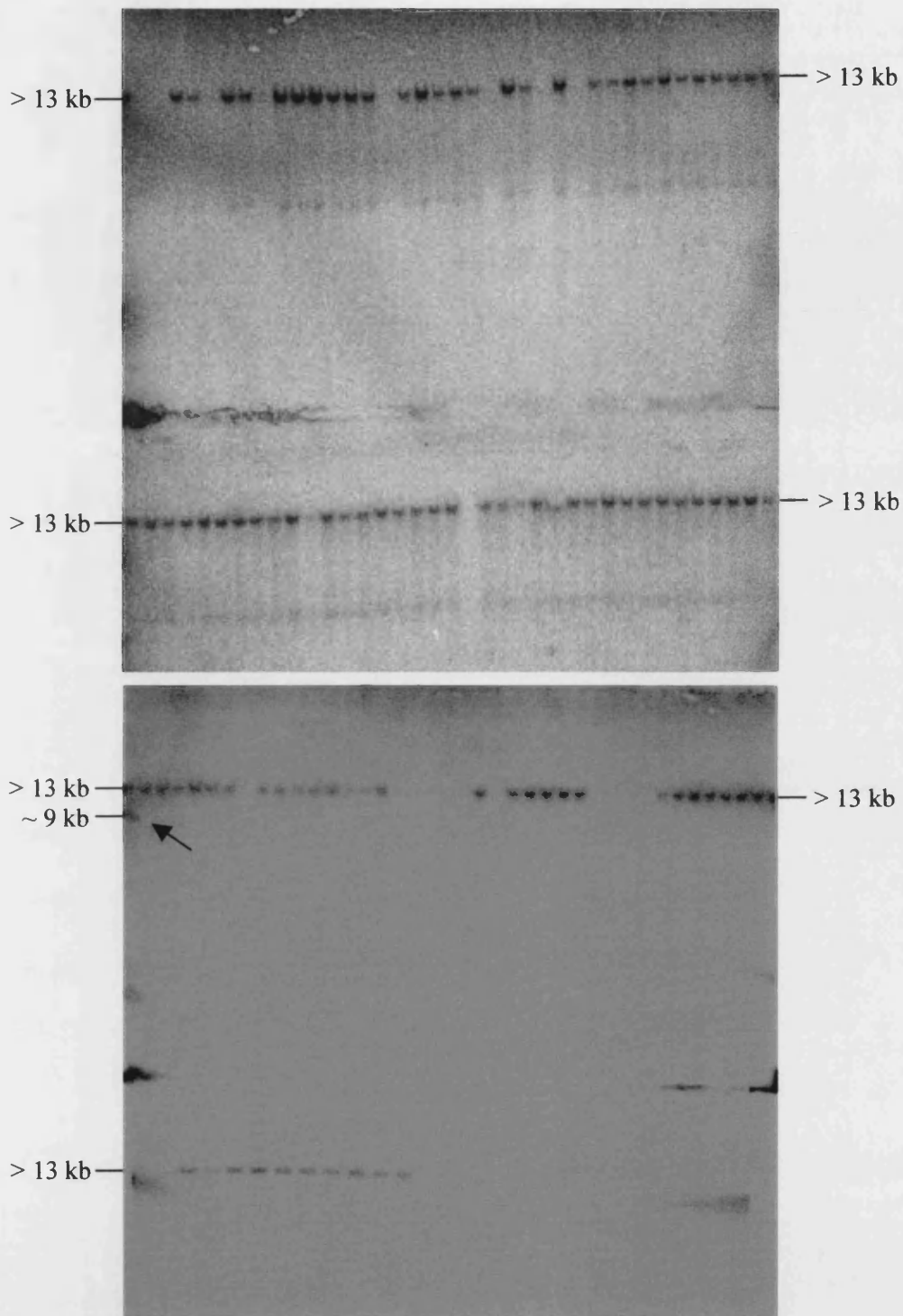


Fig. 4.10 Southern analysis of ES cells targeted with *Sgk* targeting vector. Genomic DNA was digested with *Nco* I. All lanes where DNA was visible display band at > 13 kb, which corresponds to endogenous *Sgk* locus. Arrow points at single lower molecular weight band that may represent a successful targeting event.

By this point I learnt that *Sgk* had been targeted by another group that was preparing a manuscript for publication. More importantly, I learnt that *Sgk* was not required for embryonic patterning. In the published *Sgk* knock-out, the first three exons and the last exon of *Sgk* were left intact but the remainder of the coding region, which contains the catalytic domain, was removed. This targeting strategy should result in a null allele (Wulff *et al.*, 2002). I accepted Dr. Derek Stemple's offer to perform a small-scale functional screen of the other endoderm library restricted clones in zebrafish, under his supervision.

4.2.7 Zebrafish *sgk*

I looked for a zebrafish orthologue of *Sgk* in order to compare its early expression with the murine one and to assess the embryonic phenotype of its depletion. At the time of this experiment, I found a single zebrafish *Sgk* orthologue but at the time of writing this thesis I detected another orthologue in the sequence database. I named the two zebrafish orthologues *Sgk-1 a* and *b*, respectively. Zebrafish *sgk-1 a* is strongly maternally expressed and is ubiquitous up to somite stages (data not shown). At 24 hpf, however, *sgk-1 a* expression becomes more restricted and is strong throughout the brain mesenchyme, the otic vesicles and pronephros (Fig. 4.11).

Fig. 4.12 shows the alignment between mouse *Sgk-1* and zebrafish *Sgk-1 a* and *b*. Zebrafish *Sgk-1 a* is indeed the closest to mouse *Sgk-1*, with 85.6% identity between the two proteins; zebrafish *Sgk-1 b* presents 67.8% identity to the mouse protein and 68.3% identity to zebrafish *Sgk-1 a*. The cDNA sequences of zebrafish *sgk-1 a* and *b* are shown in Appendix 3, where the sites targeted in *sgk-1 a* mRNA by the MOs used in this investigation are highlighted. Depletion of zebrafish *sgk-1 a* with 10 ng of either one of two distinct MOs did not cause any overt patterning defect up to 4 days of larval development.

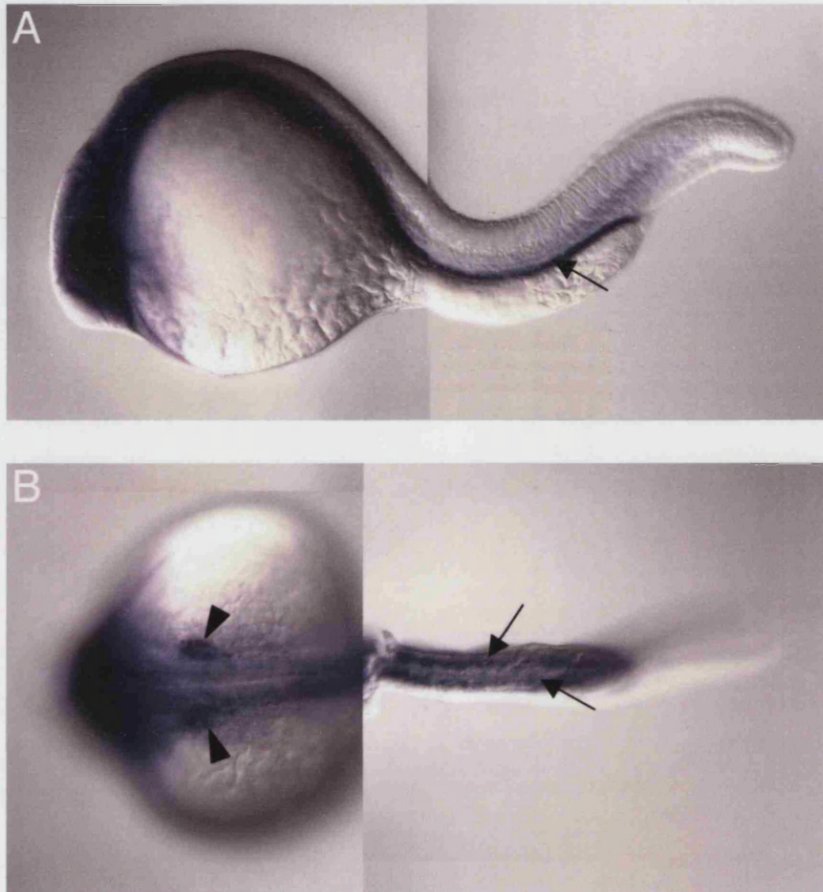


Fig. 4.11 Expression of zebrafish *sgk-1 a* at 24 hpf. **A**, side view; **B**, dorsal view at the level of the hindbrain and posterior trunk. Arrowheads point at expression in the otic vesicles and arrows point at expression in the pronephric ducts.

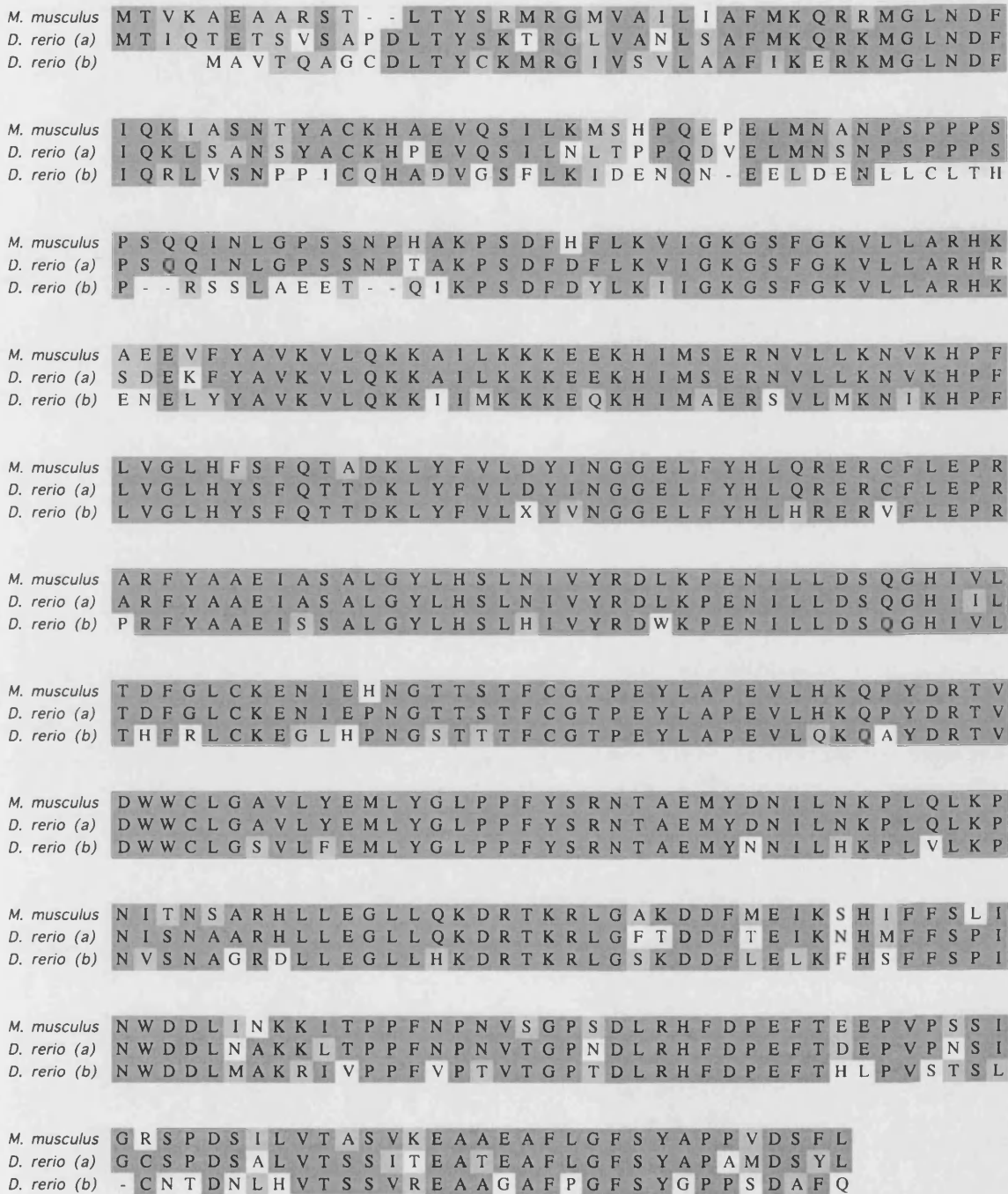


Fig. 4.12 Alignment between zebrafish *Sgk-1 a* and *b*, and mouse *Sgk-1* proteins. ■ Identical amino acids; ■ similar amino acids.

4.3 Discussion of the functional analysis of mouse *Sgk*

4.3.1 Regulation of *Sgk* expression

Sgk has a very interesting expression pattern at all stages examined, given that it is highly restricted within tissue domains in the early mouse embryo, within cell types in each tissue, and, unusually, displaying variability within the same cell type. The fact that the *Sgk* transcript has a short half-life allows for rapid regulation of its levels. We can only speculate on the significance of the restricted expression pattern of *Sgk* in the embryo given that *Sgk*-null mice do not hint at an embryonic role for *Sgk*. A few noteworthy points are discussed next.

Sgk is upregulated in the nascent mesoderm, which could reflect one or several of the dramatic changes in cellular properties associated with the epithelial-to-mesenchymal transition that occur during mesoderm induction. It would be interesting to know if and how cell volume is altered in this process, for example. The nascent angioblasts, where *Sgk* is highly upregulated, are also a population of cells that have undergone an epithelial-to-mesenchymal transition. Is this a recurrent theme in *Sgk* expression? Is there a role for *Sgk* in this process? If so, is it linked to the role of *Sgk* as a cell survival kinase? In other words, is an epithelial-to-mesenchymal transition a stressful event for a cell, as defined by molecular criteria?

Sgk mRNA levels are higher in the endothelial cells lining mature veins than in the endothelial cells lining mature arteries; and are higher in the endothelial cells lining small capillaries than in the endothelial cells lining large vessels. Do these differences correlate with variations in the osmotic pressure to which endothelial cells are subject during their development?

The differential expression of *Sgk* in the peripheral and central retina could reflect the fact that the former lags behind in development relative to the latter (Furukawa *et al.*, 1997). Namely, at 11.5 dpc of murine development there is higher cellular proliferation in the the retinal periphery than in the remainder of the retina (Burmeister *et al.*, 1996).

4.3.2 *Sgk* targeting strategy

In studying the function of *Sgk*, our main experimental goal was to generate and analyse *Sgk*-null mice. In the design of an *Sgk* targeting vector, several options were possible. Expression of *Sgk* in ES cells would allow the use a promoterless construct, which would be designed to place the positive selection gene in frame with the endogenous promoter after homologous recombination (promoter trap strategy). With such a construct the positive selection gene should only be expressed once homologous recombination took place, since random insertion events would only rarely place the selection gene in frame with another promoter. In order to adopt this strategy, the promoter of *Sgk* could not be part of the 5' homologous arm. The 5' UTR of *Sgk* is only 68 nts long and to have a 5' homologous arm of at least 1 kb in a promoter trap strategy would require leaving intact the first 4 exons, which I did not want, especially since the 3 last exons would be part of the 3' homologous arm. Moreover, a promoter trap method can only be applied safely to a gene that is expressed in all ES cells and not only in a subset of them, in order to assure colonisation of all lineages after injection into blastocysts, most importantly the germ-line. I did not test this.

Another decision to be made was whether a conventional or conditional targeting should be performed. I opted for the more simple conventional strategy since I was interested in the role of *Sgk* in early embryonic development.

In the design of my targeting vector I used both negative and positive selection cassettes. Only a small percentage of the cells containing random insertion of a construct containing a negative-selection gene actually express it, presumably due to position effects, so false positives are always encountered in this way (false positives occur less frequently in a promoter trap strategy).

4.3.3 Is there a role for *Sgk* in embryonic patterning?

Targeted mutation has so far failed to reveal a role for *Sgk* in embryonic patterning. Histological analysis of the skin, brain, skeletal muscle, heart, lung, liver, spleen, pancreas, intestine, colon, ovary, uterus, urinary bladder and kidney of born mice failed to reveal any phenotype for *Sgk* deletion in mice (Wulff *et al.*, 2002); and

morphological inspection of zebrafish larvae depleted of *Sgk* protein also failed to reveal any notorious patterning defect up to 4 days (data not shown). Nonetheless, a role for *Sgk* in osmoregulation was found by challenging *Sgk*-null mice with NaCl deprivation (Wulff *et al.*, 2002). This could mean that *Sgk*, with its highly sophisticated regulation that allows swift up- and downregulation, is engaged in adaptive responses to physiopathological triggers. This is in accord with *Sgk* induction and activation by many stress-inducing stimuli.

As with all genetic experiments, there is the possibility that another gene compensates for the loss of *Sgk* in targeted mice. This would likely be a gene encoding for a protein structurally and/or functionally related to *Sgk*, which might normally even display some functional redundancy with *Sgk* and be exacerbated in its absence. The most likely candidates are *Sgk*-2 and -3 and the PKB proteins. Between *Sgk*-2 and -3, the latter seems a stronger candidate for compensating *Sgk*-1 given their stronger similarity in terms of structure and expression profile (Kobayashi *et al.*, 1999). As for PKB, it shares the same consensus target recognition sequence with *Sgk* and at least two substrates, FoxO3a and B-Raf, are shared between the two kinases (Brunet *et al.*, 2001; Zhang *et al.*, 2001). Even if the phosphorylation efficiencies of *Sgk* and PKB at particular sites of particular targets differ, it would seem probable that one could take over the whole process if the other was missing. *PKB*-1- and *PKB*-2-null mice do not appear to have any developmental abnormalities. *PKB*-1-null mice exhibit growth retardation as early as foetuses, are smaller, are less able to survive genotoxic stress and at least a few of tissues are more susceptible to apoptosis (Chen *et al.*, 2001; Cho *et al.*, 2001b). *PKB*-2-null mice display an impaired response to insulin, in its ability to lower blood glucose levels (Cho *et al.*, 2001a). Targeted deletion of *PKB*-3 has not yet been reported. It seems appropriate to analyse the effect of the *PKB*-1 and -2 composite mutations, which is surely underway, but also that of each and both of the *PKB* mutations with that of *Sgk*. This might uncover redundant roles for these proteins, downstream of phosphoinositide signalling, in embryonic patterning.

The existence of more than one zebrafish *sgk*-1 implies that the MOs used in this investigation might have only partially depleted *Sgk*-1 activity in the early zebrafish embryo. We do not know if the activities of zebrafish *Sgk*-1 a and b are equivalent and, if so, whether they are redundant or spatially and/or temporally complementary;

alternatively, these activities could be co-regulatory or might have diverged into unrelated functions. With the availability of zebrafish ESTs representing *sgk-1 b* one can easily assess its expression pattern and with the availability of full-length sequence, one can design MOs to knock-down *Sgk-1 b* protein as well as *Sgk-1 a* and *b* together, and one can generate overexpression constructs. These experiments should allow the evaluation of whether zebrafish *sgk-1 a* and *b* are indeed redundant, complementary or functionally unrelated. The amenability of zebrafish to injection and multiple protein knocks-down could also prove very useful in assessing whether/which other proteins play a compensatory role when *Sgk* activity is absent. Namely, in testing the hypothesised compensatory role between several *Sgk* proteins and between *Sgks* and *PKBs*.

Chapter 5

Functional screen of endoderm library genes with restricted expression

Chapter 5

Functional screen of endoderm library genes with restricted expression

- 5.1 Introduction to the functional screen of endoderm library genes
 - 5.1.1 Selection of clones to screen
 - 5.1.2 Use of MOs
 - 5.2 Results and discussion of the functional screen
 - 5.2.1 Search for zebrafish orthologues of mouse genes
 - 5.2.2 Expression of screened zebrafish molecules
 - 5.2.3 Early phenotypes of zebrafish morphants screened
-

5.1 Introduction to the functional screen of endoderm library genes

5.1.1 Selection of clones to screen

Because of the time-consuming nature of generating targeted mutations in mice and the technical development of a rapid method for protein depletion in zebrafish, I decided to examine the function of some of the expression-restricted clones found in the whole-mount *in situ* hybridisation screen performed on mouse embryos.

Out of the 29 restricted clones identified in the whole-mount *in situ* hybridisation screen (Table 3.1), 7 have now been deleted in the mouse by targeted mutagenesis (Hildebrand and Soriano, 1999; Li *et al.*, 1999; Elchebly *et al.*, 1999; Wallace *et al.*, 1999; Nishinakamura *et al.*, 2001; Wulff *et al.*, 2002; Batt *et al.*, 2002; Kettleborough, 2002; Rana, 2003). Out of the remainder 22 genes, 5 are being analysed in *Xenopus tropicalis* by Dr. Amer Rana. I decided to identify zebrafish orthologues of the remaining 17 clones and to deplete zebrafish embryos of the corresponding proteins, using MOs (Nasevicius and Ekker, 2000).

The Zebrafish Genome Project has greatly advanced over the past year (<http://trace.ensembl.org/>). In addition, there are ~355,000 zebrafish ESTs published in GenBank. Taken together, these two sequence databases allow the rapid identification of zebrafish orthologues of known genes or genomic sequence for most genes.

Using the protein sequence from other species as a query, I obtained orthologous zebrafish sequences, which I assembled into contigs. I then compared the predicted zebrafish sequence to the non-redundant protein database using BLAST algorithms (<http://www.ncbi.nlm.gov/BLAST/>).

5.1.2 Use of MOs

MOs are oligonucleotides in which the sugar-phosphate backbone has been modified to include 6-membered morpholine rings instead of (deoxy)ribose and phosphorodiamides instead of phosphates. These modifications render the oligonucleotides non-ionic and, most importantly, resistant to nuclease degradation (Hudziak *et al.*, 1996). Therefore, MOs are extremely stable *in vivo*.

MOs have a high affinity for complementary RNA sequences (Stein *et al.*, 1997) and can reliably hybridise with target RNA sequences (reviewed in Summerton and Weller, 1997; Summerton, 1999). When bound to the region of translation initiation, MOs sterically prevent ribosome attachment to the mRNA and, consequently, inhibit translation. When bound to splice junctions, MOs prevent spliceosome attachment and, consequently, inhibit splicing.

MOs have been used to deplete gene products from cells in culture and have recently been successfully applied to deplete proteins from embryos of several species (Heasman *et al.*, 2000; Nasevicius and Ekker, 2000; Howard *et al.*, 2001; Kos *et al.*, 2001; Mellitzer *et al.*, 2002; Siddall *et al.*, 2002). It is in zebrafish that the MO methodology has become well established and even routine among developmental biologists. In July 2001, an entire issue of the journal *Genesis* reported many MO-phenocopies of known zebrafish mutations.

MOs are non-toxic so they display minimal unspecific activity and their excellent sequence specificity allows for predictable targeting (reviewed in Summerton, 1999). In the above-mentioned *Genesis* issue, the MO doses used, namely to phenocopy known mutations, were usually below 10 ng. This is the maximum dose of MO I have used in my studies.

Although MOs have been used mainly to target translation initiation sites, successful targeted inhibition of splicing has been reported for zebrafish (Draper *et al.*, 2001). This approach has a few specific applications or advantages. First, it can be used to selectively disrupt the protein product of a zygotic mRNA without affecting the product of the corresponding maternal transcript, which is already processed when deposited in the egg so will not be subject to splicing (Draper *et al.*, 2001). Second, it can be used to knock-down a specific product of a gene with multiple splice variants that share the initiation of translation site. Furthermore, in the absence of an antibody to confirm depletion of the product of the targeted mRNA, a MO-derived aberrant splice form can be detected by RT-PCR allowing the confirmation of the MO activity and the acknowledgement of the abnormal product generated (Draper *et al.*, 2001). Current knowledge does not yet allow us to predict the exact product generated by a splice MO. Blocking of a splice site might result in exon skipping but it might also result in the usage of a cryptic splice site that emerges in an intron or an exon. Nonetheless, as mentioned, the outcome can always be unequivocally assessed *a posteriori* by RT-PCR.

Considerations to take into account when designing a MO are the following: MOs are generally effective when designed to target anywhere in the 5' UTR or the first codon, up to approximately 20 bases downstream of it; MOs should have little or no self-complementarity, forming no more than 4 contiguous internal base pairing; MOs should have no more than 36% of G content or 3 consecutive Gs in order to dissolve well in aqueous solution; the longer the MO, the more efficient it should be so the maximum commercially available length, 25-mer, should be used whenever possible. When inhibiting a splicing event, targeting the splice donor has proved more successful than targeting the splice acceptor (www.gene-tools.com).

Controls that have been used for the analysis of a phenotype obtained by a MO, namely for the non-toxicity and specificity of the MO, are the following: injection of a standard control MO designed by Gene Tools LLC, which in the same concentration as the experimental MO should result in no observable phenotype; the use of another, non-overlapping, MO targeting the same transcript, which should result in a similar phenotype; the use of a MO targeting the exact same region as the first but with 4-5 mismatches, which should result in no observable phenotype; rescue of the MO phenotype by overexpression of an mRNA that is unsusceptible to the MO, coding for

the protein that is being downregulated. An easy way to achieve the latter is to design the MO to target the 5' UTR and to rescue with an RNA that does not comprise the targeted region. However, us and others have observed higher efficiency of targeting of particular mRNAs when the MO actually comprises the first codon than when it is far upstream of it so 5' UTR targeting might compromise MO efficacy in the first place. A laborious alternative would be to design a MO that does span the first codon but then introducing mismatches into the cDNA from which the RNA is synthesised so that it is not targeted by that MO. Far easier is the rescue with an orthologous RNA from another species. Nonetheless, it should be noted that the RNA overexpression itself might cause a phenotype and/or that the RNA need to be stable enough to be able to rescue, both which could preclude the interpretation of the rescue experiment. In the few cases where antibodies are available, they are the best way to assess the effectiveness of protein knock-down achieved.

5.2 Results and discussion of the functional screen

5.2.1 Search for zebrafish orthologues of mouse genes

The 17 mouse genes for which I tried to identify zebrafish orthologues or paralogs are outlined in red (found by me) or green (found by Dr. Kettleborough) in Fig. 3.1 and are indicated in Table 5.1. They consisted of: *tif1-β*, *ptp(r) σ*, *14-3-3 ε*, *embigin*, *lztr-1*, *claudin-6*, *neuronatin 2*, *pancortins* Modules A and B (the mouse clone identified as restricted in the whole-mount *in situ* hybridisation screen could belong to either of the isoforms AMZ/pancortin-3 or BMZ/pancortin-1), *calcyphosine*, *sp120*, *plu1*, *nsa2*, *transformer 2β*, *rho GEF 16*, *liv-1-related*, and two novel genes whose sequence identifiers in the Beddington endoderm cDNA library are p7822b53 and t8130b59.

In order to block translation of the corresponding mRNAs in zebrafish embryos, 5' end zebrafish sequence is necessary. Table 5.1 summarises the steps taken towards finding these sequences and, ultimately, designing the desired MOs.

Zebrafish orthologues or paralogs of 14 of the selected mouse genes were identified in the mRNA or EST databases. This was the case for *ptp(r) σ*, *14-3-3 ε*, *embigin*, *lztr-1*, *claudin b* and *claudin-like* (two paralogs of mouse *claudin-6*), *pancortin* Modules A

Table 5.1 Steps in searching for zebrafish orthologues of selected mouse endoderm library genes.

Mouse ID	Murine name	Zebrafish EST/cDNA [†]	Genomic sequence [°]	5' RACE** [§]	Notes	MO [§]
r8220b57	<i>tif1-β</i>	—	zfish41361-436f11.p1c	—	Sequence found could belong to any of several family members	N
t7822b10	<i>ptp(r) σ</i>	AJ311886	Z35723-a4160f03.p1c	Y	5' RACE from <i>ptp(r) σ</i> -specific sequence was unsuccessful; other sequence available could belong to any of several family members	N
k8709a20	<i>14-3-3 ε</i>	fd17b10	—	—	5' end from ESTs	Y
m8708a09	<i>embigin</i>	fk62a01	—	Y	5' RACE successful	Y
m8708a39	<i>lztr1</i>	fj89h04	Z35725-a6648a02.p1c zfishC-a1960e04.q1c	Y	5' RACE successful but recent ESTs reveal that protein is longer than previously thought so MO ordered does not block translation	Can order new
r8707a53	<i>claudin-6</i>	faa02a04 (<i>claudin b</i>)	—	—	5' end from ESTs	Y
	<i>idem</i>	ft84h10 (<i>claudin-like</i>)	—	—	5' end from ESTs	Can order
t8417b56	<i>neuronatin 2</i>	—	—	—	No zebrafish sequence found	N
s8129b58	<i>pancortin-1 (BMZ)</i>	—	z06s004714	—	5' end from genomic sequence	Y
	<i>idem</i>	fr67h12	—	—	5' end from ESTs	Can order
	<i>idem</i>	fd42d07	—	—	5' end from ESTs	Y

m8708a22	<i>calcyphosine</i>	—	zfishC-a1916g03.p1c	—	5' end from genomic sequence	Y
	<i>idem</i>	fj05b10	—	Y	5' RACE unsuccessful	N
t7825b42	<i>sp120</i>	fb55c01	—	Y	5' RACE successful	Y
	<i>idem</i>	(sp120 a) fb93d06	—	N	Can do 5' RACE	N
t8130b26	<i>plu1</i>	(sp120 b) fc44h11	—	—	Can do 5' RACE	N
	<i>idem</i>	(plu1 a) fp32a03	—	—	Can do 5' RACE	N
k8710a07	<i>nsa2</i>	(plu1 b) fb52h05	—	—	5' end from ESTs	Y
r8220b09	<i>transformer 2 β</i>	fk31a01	—	—	5' end from ESTs	Can order
w8609b57	<i>rho GEF 16</i>	fp38h09	—	Y	5' RACE successful but incomplete; 5' end from ESTs	Can order
s8609b24	<i>liv-1-related</i>	fc12g10	—	Y	5' RACE successful	Can order
p7822b53	Novel	fy23a03	—	Y	5' RACE successful	Y
t8130b59	Novel	—	—	—	No zebrafish sequence	N

† Only one EST/cDNA per gene is indicated, which contains the most upstream coding sequence found.

° Genomic clones are only indicated when they contain the most upstream coding sequence found and/or sequence used to design RACE primers.

* 5'-RACE was performed when sequence flanking the first codon was not found in EST or genomic databases.

— non-existent or non-applicable †Y, yes; N, no.

and B, *calcyphosine*, *sp120* a and b, *plu1* a and b (two paralogues of mouse *sp120* and *plu1* were found, which I named “a” and “b”, where “a” is the closest sequence), *nsa2*, *transformer 2 β* , *rho GEF 16*, *liv-1-related* and novel p7822b53 (Table 5.1, zebrafish EST/cDNA column). It is not surprising that more than one zebrafish paralog of a single mouse gene was found in a few cases given that teleosts underwent an ancient duplication of their genome. When a putative orthologous zebrafish sequence was found using the mouse protein as a TBLASTN query, it was translated and used as a query in the BLASTP algorithm in order to confirm the orthology.

There are several zebrafish paralogs of mouse Claudin-6 (for a phylogenetic tree see Kollmar *et al.*, 2001). The closest in sequence to mammalian Claudin-6 are zebrafish Claudin-a, Claudin-b and Claudin-like (there is currently some disorganisation as to the nomenclature of zebrafish Claudins).

The *pancortin* transcript present in the mouse endoderm library is not full-length and could represent either *pancortin-1* or *pancortin-3*. The rodent *pancortin* locus contains two alternative promoters that result in the production of two distinct first exons (called Modules A and B in Danielson *et al.*, 1994; see Nagano *et al.*, 1998 for alternative nomenclature). The second exon of rodent *pancortins* is common to all transcripts (called Module M in Danielson *et al.*, 1994; see Nagano *et al.*, 1998 for alternative nomenclature) and there are two possibilities for the third exon (called Modules Y and Z in Danielson *et al.*, 1994; see Nagano *et al.*, 1998 for alternative nomenclature), which arises by alternative splicing. Thus, the rodent *pancortin* locus generates the four transcripts: AMY (*pancortin-4*), AMZ (*pancortin-3*), BMY (*pancortin-2*) and BMZ (*pancortin-1*) (Danielson *et al.*, 1994). I endeavoured to target each of the zebrafish *pancortin* 5' ends (A and B).

Some of the EST sequences identified included the first codon, allowing for immediate design of a translation-inhibition MO. This was the case for *14-3-3 ϵ* , *claudin-b*, *pancortin* Modules A and B, *nsa2*, *transformer 2 β* and *rho GEF 16* (Table 5.1, Notes column).

For the genes for which the ESTs found did not include the first codon, or for which no ESTs had been found, zebrafish genomic sequence was searched with the mouse protein

using a TBLASTN algorithm. No zebrafish sequence was found for *neuronatin 2* or novel t8130b59. In the case of *tif1- β* , genomic sequence constituted the only zebrafish sequence found; in two cases, *pancortin* Module B and *calcyphosine*, the search of the genomic database allowed the identification of putative paralogs of the mouse genes distinct from the ones identified in the EST database; in two other cases, *ptp(r) σ* and *lztr-1*, the genomic sequence found lay upstream from the one identified with ESTs, although not containing the first codon, and was chosen for the design of 5'RACE primers (Table 5.1).

The cases where it was the genomic database that yielded sequence flanking the first codon were those of the alternative paralogs of the *pancortin* Module B and *calcyphosine* (Table 5.1, Notes column).

For most cases where sequence flanking the first codon was not found through *in silico* methods, 5'RACE was attempted. The only cDNA for which this approach was not attempted was *Tif-1 β* , given that the only sequence found could belong to any of several family members. 5'RACE could have been attempted in these circumstances, where the different isoforms hopefully obtained would have been distinguished by sequencing. However, since the zebrafish genome project was evolving fast I waited for *tif-1 β* -specific sequence to appear, which it did in the duration of my work.

5'RACE was attempted for *ptp(r) σ* , *embigin*, *lztr-1*, the *calcyphosine* paralog identified by ESTs, *sp120*, *rho GEF 16* and novel p7822b53. 5'RACEs were successful except for *ptp(r) σ* and the *calcyphosine* paralog identified by ESTs (Table 5.1, 5'RACE column). 5'RACE yielded sequence flanking the first codon of *embigin*, *sp120*, *liv-1-related* and novel p7822b53 (Table 5.1, 5'RACE column). For *lztr-1*, recent ESTs revealed that the mouse cDNA is longer than originally thought so the 5'RACE zebrafish sequence obtained was incomplete. The 5' end of the zebrafish ortholog was subsequently found in the EST database. For *rho GEF 16*, the 5'RACE sequence obtained was also incomplete but, used as a query for the EST database using the BLASTN algorithm, it also allowed the identification of the 5' end of this cDNA.

Given that the zebrafish genome project is underway at the minute, the *in silico* searches were performed regularly and up to the time when this study is being written. Some

sequences were only found recently hence 5'RACE can now be performed where it could not before and some MOs that can now be ordered have not been studied (Table 5.1).

The cDNA sequences I identified during this investigation are presented in Appendix 3, along with the alignment between the predicted protein sequences of mouse and zebrafish orthologues/paralogs. The target sites of 5'RACE primers as well as those of MOs are also indicated when appropriate.

5.2.2 Expression of screened zebrafish molecules

When available, ESTs were ordered with the purpose of obtaining cDNA templates from which to synthesise antisense riboprobes. When neither EST nor 5'RACE cDNAs were not available, PCR was performed in order to obtain templates for riboprobes. This was the case for *ptp(r)* σ , the *calcyphosine* and *pancortin* Module B paralogs identified in the genomic database, *plu1* a and b paralogs and novel p7822b53.

Furthermore, PCR was used to generate templates specific for the *pancortin* Modules A, B- ESTs, B-genomic, Y and Z, as a means to assess the expression pattern of specific isoforms of the gene. All these PCRs were successful with the exception of the *calcyphosine* paralog identified in the genomic database. Several attempts to isolate this cDNA, including the use of distinct primer pairs, failed. The template used was a mixture of cDNA purified from zebrafish embryos/larvae of various stages, between the 2-cell stage and 4 days. Other than technical difficulty, justifications for not isolating this cDNA could be that this *calcyphosine* isoform is not expressed at early stages of zebrafish development (up to 4 days; see Materials and Methods) or that the genomic sequence identified corresponds to a pseudogene.

The majority of genes analysed are expressed maternally. Ones that are not are the two isoforms of *pancortin* Module B, found in the EST or genomic databases, and possibly *pancortin* Module Z, *sp120* a, *sp120* b and novel p7822b53, which were detected at levels just above background (data not shown). Expression of the *pancortin* Module B isoform identified in the EST database was not detected prior to shield stage.

The vast majority of genes analysed are expressed ubiquitously or in a widespread manner at least up to early somite stages (data not shown), according to the definitions presented in Chapter 3, but by 24 hpf become restricted to a few tissues. Figure Fig. 5.1 depicts the noteworthy expression patterns encountered and a brief description follows. The descriptions are based solely on the observation of whole-mount stained embryos; in some cases, confirmation and/or more detailed description of the tissues stained requires analysis of sections.

Zebrafish *14-3-3 ε* is maternally and ubiquitously expressed up to 24 hpf. However, at the 16-cell stage, a very clear intracellular mRNA localisation pattern was observed, where transcripts are greatly enriched close to the membrane region where contacts are established between the outer and the inner blastomeres (Fig. 5.1, A and B). This is not observed at the 8-cell stage (data not shown). In *Xenopus Laevis*, *14-3-3 ε* mRNA has been reported to localise intracellularly to the animal half of vegetal cells (Bunney *et al.*, 2003). In the early mouse embryo, *14-3-3 ε* expression is also widespread but, unlike in fish, by 8.5 dpc, a stage comparable to zebrafish at 24 hpf, it becomes restricted to the forebrain, midbrain and branchial arches (Fig. 3.1, k8709a20).

Zebrafish *embigin* is maternal and ubiquitously expressed up to early somite stages, when it becomes downregulated in the trunk ectoderm (Fig. 5.1, C). Like mouse *embigin*, at late somite stages this transcript becomes restricted to the foregut primordium, and the head region (Fig. 5.1, D and Fig. 3.1, m8708a09).

Zebrafish *lztr-1* is maternal and ubiquitously expressed up to 24 hpf, when it becomes restricted to the head region, from forebrain to hindbrain (Fig. 5.1, E). This is analogous to the expression of mouse *lztr-1* at 8.5 dpc, although by 9.5 dpc the latter resolves to prominent expression specifically in the forebrain (Fig. 3.1, m8708a39). At 24 hpf, zebrafish *lztr-1* transcripts are also found in the trunk mesoderm (Fig. 5.1, E).

Fig. 5.1 **Restricted expression patterns found in zebrafish screen.** Expression patterns of individual genes are outlined in coloured line (either red or green); the colour of the outline is the same colour used to outline mouse orthologues in Fig. 3.1. In some cases pictures of a single clone carry on to the next row. The name of the gene whose expression is depicted is indicated within outlined box. Staging is indicated below each embryo. **A, C, D, E, F, J, L, M, P, Q, U, V, W, X, AA, AB, AC, AD, AE, AF,** are side views of the whole embryo; **B** is an animal view of the embryo depicted in **A**; **G, K, R** are frontal views of the embryos depicted in **F, J, Q,** respectively; **H** is a dorsal view of the head of the embryo depicted in **F**; **S, Y,** are dorsal views of the hindbrain of the embryos depicted in **Q, X,** respectively; **I, N, T** are dorsal views of the spinal cord of the embryos depicted in **F, M, Q,** respectively; **Z** is a dorsal view of the tail of the embryo depicted in **X**. **Arrows in A and B** point at *14-3-3 ε* mRNA enrichment in membrane region that establishes contact between the outer and inner blastomeres; **arrow in C** points at *embigin* mRNA downregulation in the ectoderm at early somite stage; **arrows in I, M, N, Q, T,** point at *pancortin* Module A, Module B (genomic) and Module Z mRNA enrichment in a subset of neurons/neuronal progenitors in the spinal cord; **arrow in J** points at *pancortin* Module B (EST) expression in the blood islands; **arrows in X, Z, AA,** point at *plu1 a* and *plu1 b* expression in the pronephric ducts; **arrows in S** point at *pancortin* Module Z expression in cranial ganglia; **arrows in Y** point at *plu1 a* expression in the otic vesicles; **arrow in AB** points at *transformer 2 β* in the ventral aspect of somites; **arrow in AE** points at exclusion of *rho GEF 16* mRNA from the ectoderm at early somite stage.

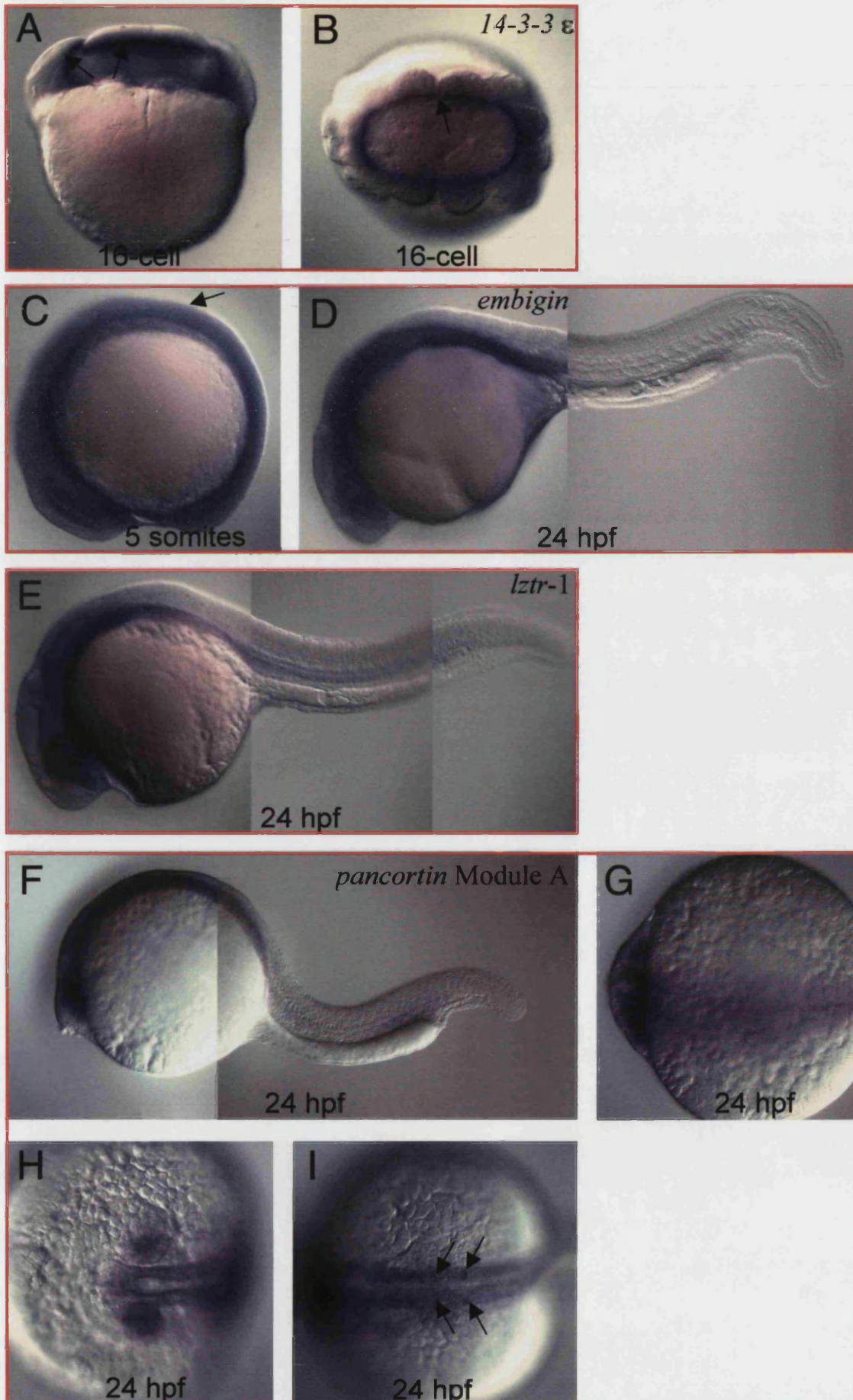
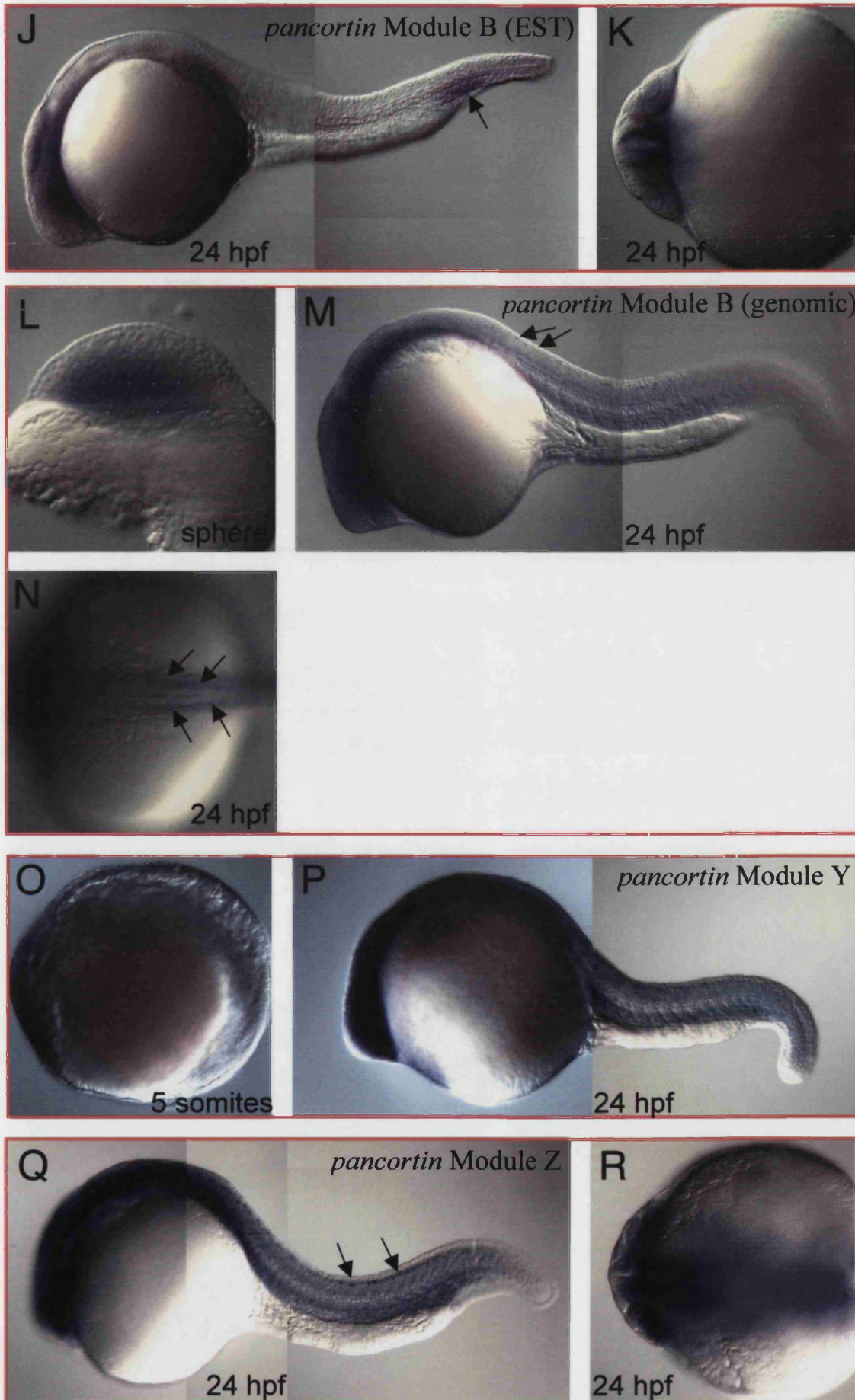
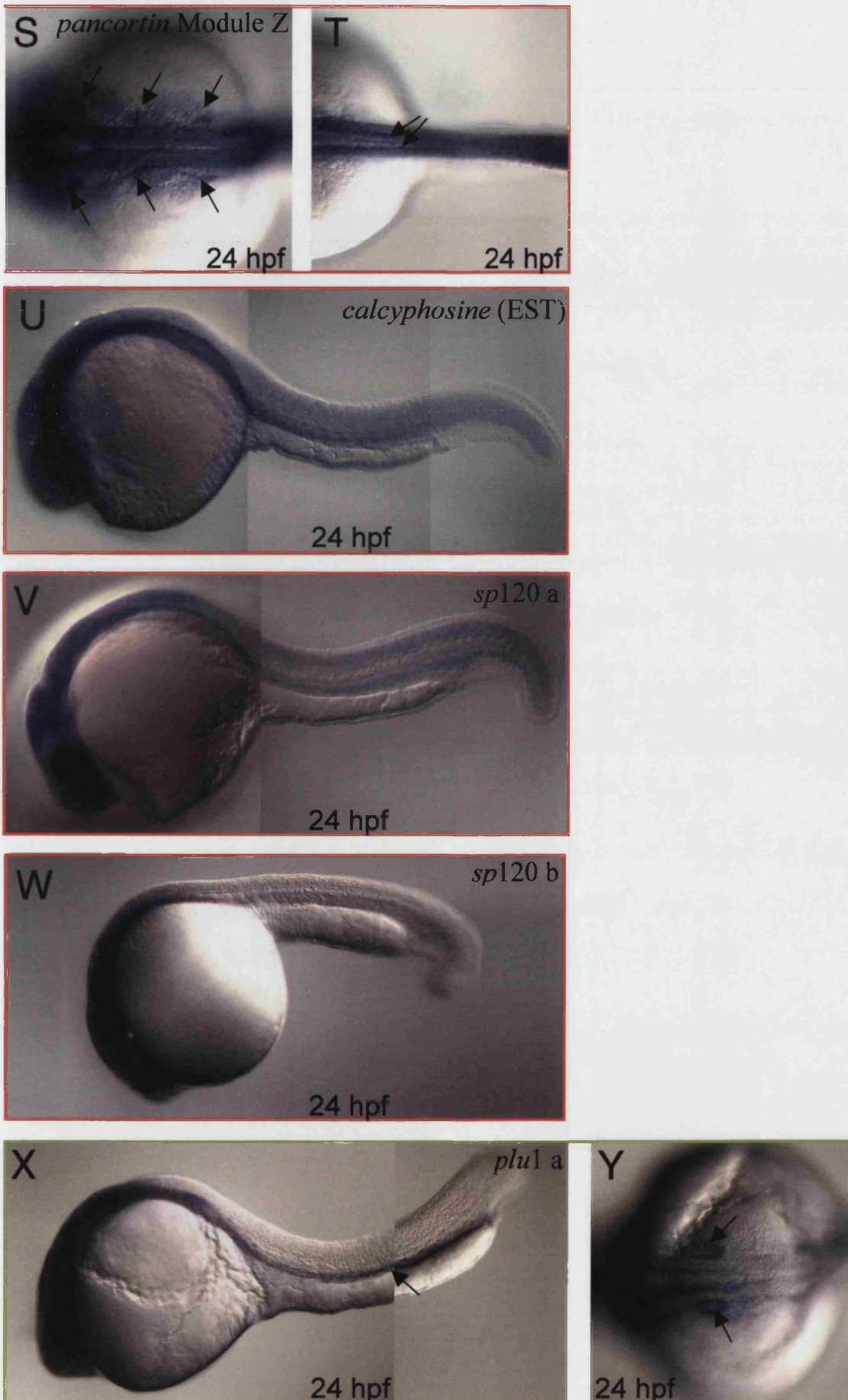


Fig. 5.1 (Continued on next page)



(Fig. 5.1 cont.; continued on next page)



(Fig. 5.1 cont.; continued on next page)

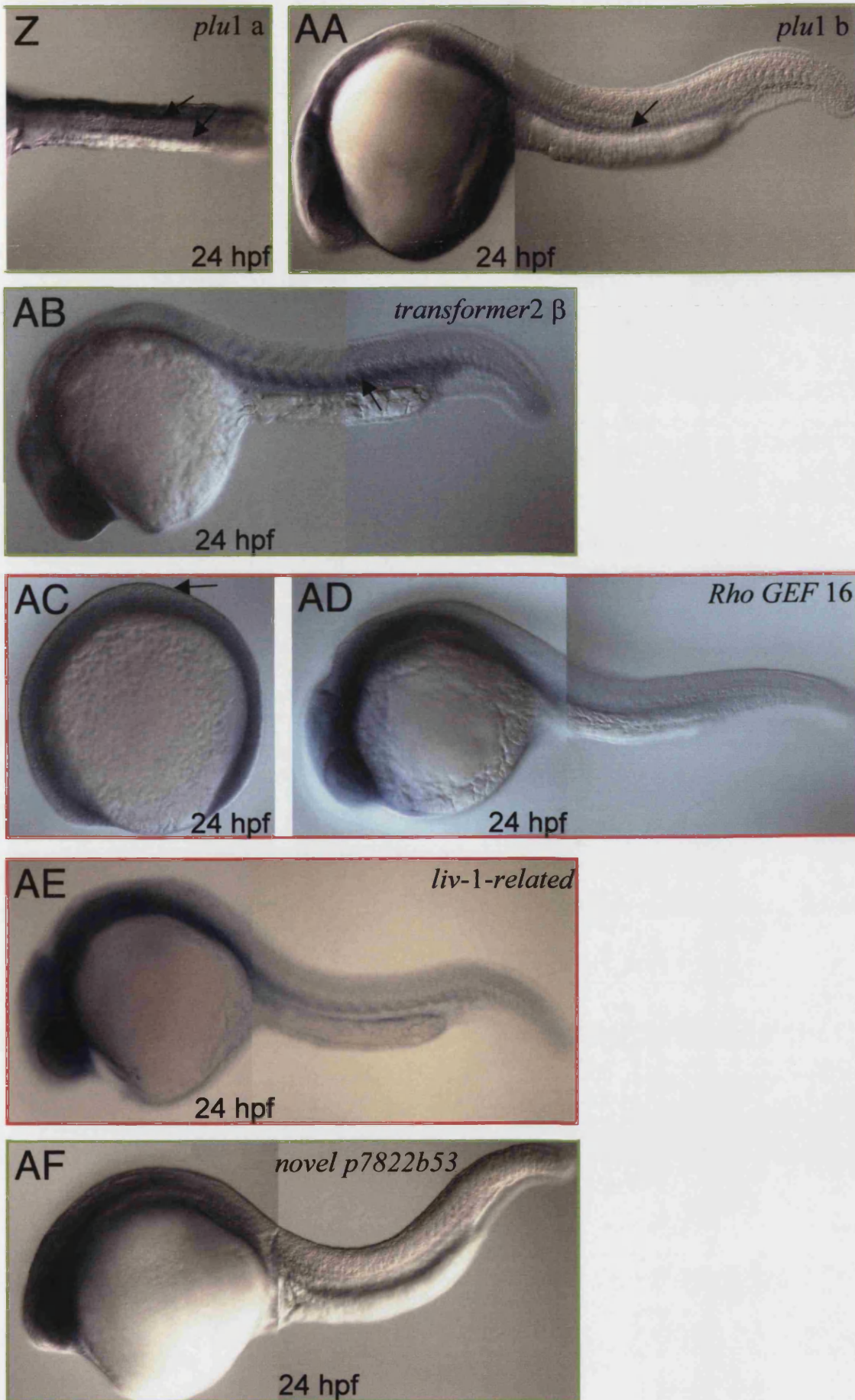


(Fig. 5.1 cont.)

The expression of zebrafish *pancortins* was analysed by using probes to specific mRNA modules, which can be alternatively spliced to generate several distinct transcripts. A riboprobe for module M was not used since this is common to mouse *pancortins* from 1 to 4. Furthermore, two distinct probes were used for module B, one derived from an EST and one obtained by PCR with primers designed from genomic sequence – Module B (EST) and Module B (genomic), respectively. Zygotic expression of the latter differed from that of all other *pancortin* modules in that it was not ubiquitous at sphere stage, being expressed solely in inner vegetally-located cells (Fig. 5.2, L). All modules are restrictedly expressed by 24 hpf with the main site of expression being the brain. Module Y is already restricted to the anterior of the embryo by early somite stages (Fig. 5.1, O). Within the brain, module B (EST) is mainly confined to the forebrain (Fig. 5.1, J) whereas the others are more widespread (Fig. 5.1, F, M, P, Q). Modules A, B (EST) and Z have stronger expression in the ventral neural tube than in the dorsal neural tube (Fig. 5.1, G, K, R), although modules B (EST) and Z are also expressed in a subset of neurons present in the dorsal spinal cord (Fig. 5.1, I, Q, T). This is also the case for module B (genomic) (Fig. 5.1, M, N). Additional sites of expression of these transcripts include the trunk mesenchyme, the blood islands for module B (EST) (Fig. 5.1, J) and a few of the cranial ganglia, for module Z (Fig. 5.1, S). The mouse riboprobe used hybridises to modules M and Z not allowing for a direct comparison between the expression of each module in fish and mouse. The expression of zebrafish *pancortin* module Z is the one that most resembles that of mouse *pancortins* -1 and/or -3, with the expression in the cranial ganglia (Fig. 5.1, S and Fig. 3.1, s8129b58).

Zebrafish *calcyphosine* (EST) is maternal and ubiquitously expressed up to late somite stages, when it becomes predominant in the foregut primordium and the brain (Fig. 5.1, U). Unlike in the mouse (Fig. 3.1, m8708a22), *calcyphosine* transcripts were not found to be upregulated in the fish organizer (data not shown).

Two paralogs of mouse *sp120* (*hnrpu*) were found in zebrafish, *sp120* a and b. None appears to be maternally expressed but both are zygotically expressed ubiquitously up to 24 hpf. At this stage, both *sp120* a and *sp120* b become restricted to the brain, with *sp120* b displaying higher levels of expression than *sp120* a (Fig. 5.1, V, W). This expression is similar to that of mouse *sp120* at 8.5 dpc (Fig. 3.1, t7825b42).

Two paralogs of mouse *plu1* were found in zebrafish, *plu1 a* and *b*. Both are maternal and ubiquitously expressed up to 24 hpf, when both transcripts become confined to the brain, foregut primordium and pronephric ducts (Fig. 5.1, X, Z, AA). Overall, *plu1 b* appears to be expressed at lower levels than *plu1 a*. Within the brain, *plu1 b* is more restricted than *plu1 a*, being expressed predominantly in the midbrain. In addition, *plu1 a* is expressed at high levels in the otic vesicles (Fig. 5.1, Y). Like the zebrafish paralogs, mouse *plu1* is expressed in a widespread manner in the early embryo-proper and becomes enhanced in the brain by late somite stages (Fig. 3.1, t8130b26). Mouse *plu1* expression was not detected in the pronephros, however.

Zebrafish *transformer 2 β* is maternal and ubiquitously expressed up to late somite stages, when it becomes restricted mainly to the forebrain (there is weak expression elsewhere in the neural tube) and to the ventral aspect of the somites (Fig. 5.1, AB). This differs from mouse *transformer 2 β*, which was detected in extraembryonic lineages of the early embryo (Fig. 3.1, r8220b09).

Zebrafish *rho GEF 16* is maternal and ubiquitously expressed up to early somite stages, when it becomes downregulated in the ectoderm (Fig. 5.1, AC). By late somite stages transcripts are found in the ventral brain, from fore- to hindbrain, as well as in the foregut primordium and trunk mesenchyme (Fig. 5.1, AD). This is also the case for mouse *rho GEF 16* (Fig. 3.1, w8609b57). The mouse gene, however, has very specific expression in the notochord (Fig. 3.1, w8609b57), which was not observed for the fish counterpart.

Zebrafish *liv-1-related* is maternal and ubiquitously expressed up to 24 hpf, when it becomes strongly restricted to the brain and foregut primordium (Fig. 5.1, AE). Expression of this gene in the brain at late somite stages is much stronger in fish than in mouse (Fig. 5.1, AE and Fig. 3.1, s8609b24).

Zebrafish novel gene *p7822b53* is zygotically ubiquitously expressed up to 24 hpf, when it becomes strongly restricted to the brain (Fig. 5.1, AF). Unlike the mouse orthologue (Fig. 3.1, p7822b53), the zebrafish gene is not upregulated in the organizer (data not shown).

Zebrafish *claudin b* and *claudin-like* genes were found to be ubiquitously expressed at all stages examined (data not shown). The early embryonic expression of zebrafish *ptp(r)* σ has been reported elsewhere (van der Sar *et al.*, 2001).

5.2.3 Early phenotypes of zebrafish morphants screened

The MOs injected into zebrafish embryos and whose phenotype was assessed morphologically for up to 1-2 days were those for *14-3-3 ϵ* , *embigin*, *claudin-b*, *pancortins* containing module A or the module B found in the genomic database, the *calcyphosine* isoform identified in the genomic database, *sp120*, *nsa2* and novel p7822b53 (Table 5.1). Of these, only the module B *pancortin* MO and the *calcyphosine* MO produced no morphologically discernible phenotype by 24 h. The *nsa2* phenotype was studied in some detail and is analysed in the next chapter. I now present the other phenotypes uncovered during this investigation.

Around 50% of zebrafish embryos morphant for *14-3-3 ϵ* present a YSL that is more irregular and that extends further vegetally from the blastoderm than in controls. In a lateral view, YSL nuclei are normally lined up, roughly parallel to the blastoderm leading edge (Fig. 5.2, A), and on a dorsal view they are further away from the leading edge (Fig. 5.2, B). In *14-3-3 ϵ* morphants, in both lateral and dorsal views, YSL nuclei are often less linearly aligned and are further from the leading edge than in controls (Fig. 5.2, G, H). Still, most *14-3-3 ϵ* morphants undergo epiboly at a normal rate. By early somite stages, 50% of the morphants have an elongated yolk cell and embryo relative to controls, which have a round yolk cell and circular embryos (Fig. 5.2, C, I). At 26 hpf most morphants are shorter, and overall delayed in development, present a wavy notochord, irregular somites, and strong oedema in the heart. Fig. 5.2, J – L depicts a severe *14-3-3 ϵ* phenotype at 26 hpf. At 2 days of development all *14-3-3 ϵ* morphants display a clear motility defect whereby their twitches resemble tremors rather than tail flicks (data not shown). Also at this stage of development, a *14-3-3 ϵ* morphants display randomised heart looping (data not shown). This issue is being investigated further.

14-3-3 proteins are phosphoserine/threonine binding proteins that exist in both plants and animals and that have been implicated in a plethora of signalling events and

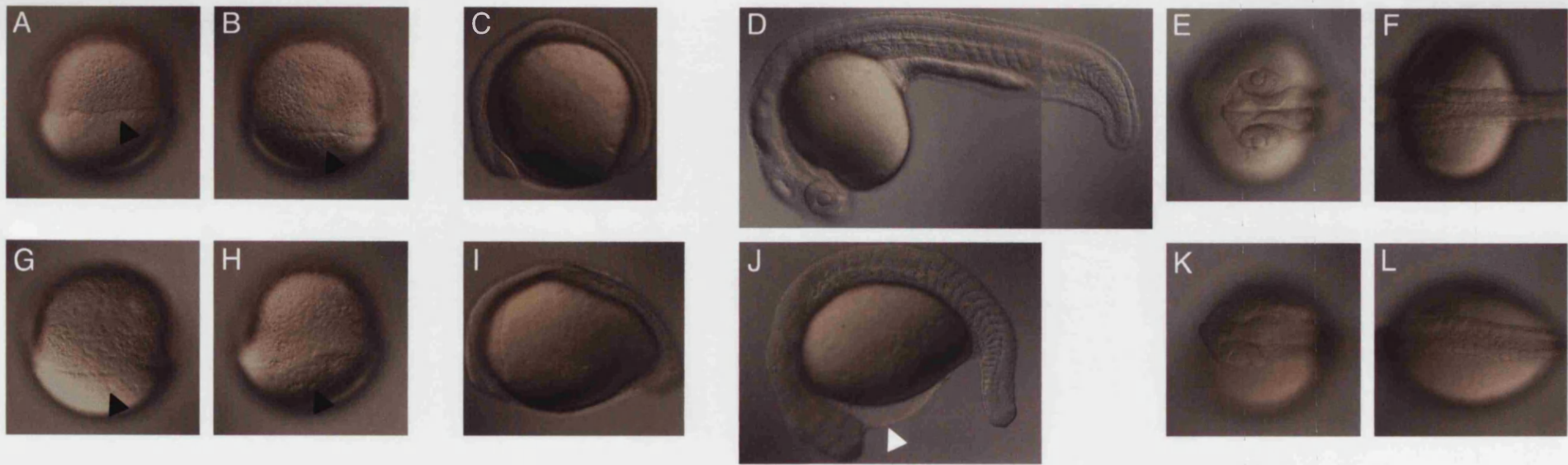


Fig. 5.2 Early phenotype of *14-3-3 ε* zebrafish morphants. A – F, zebrafish embryos injected with 10 ng Control MO; G – L, zebrafish embryos injected with 10 ng *14-3-3 ε* MO. A, B, G, H, embryos at 60% epiboly; C, I, early somite stage embryos; D – F, J – L, 26 hpf embryos. A, C, D, G, I, J are side views; B, H are dorsal views of the embryos depicted in A and G, respectively; E, K are dorsal views of the head of the embryos depicted in D and J, respectively; F, L are dorsal views of the trunk of the embryos depicted in D and J, respectively. **Black arrowheads**, YSL nuclei; **white arrowhead**, oedematous heart.

biological processes, namely cell division and apoptosis (reviewed in Skoulakis and Davis, 1998; Fu *et al.*, 2000; Tzivion *et al.*, 2001; Yaffe, 2002). The literature is vast and the epsilon isoform, analysed here, as well as the others are ascribed pleiotropic roles. There are, however, a few very recent studies that should be mentioned in the context of the results presented here since they provide clues that can be followed up towards a deeper characterisation of the phenotype of 14-3-3 ϵ -depleted fish. Mice deficient in 14-3-3 ϵ have defects in brain development and neuronal migration (Toyooka *et al.*, 2003). A first follow up on the motor phenotype displayed by the morphants could be an assessment of motor-neuron migration and/or axonal projections. The *Drosophila* orthologue of 14-3-3 ϵ (also known as Par-5) has been shown to cooperate with Par-1 in the polarisation of the fly oocyte, which leads to the establishment of the antero-posterior axis of the embryo (Benton *et al.*, 2002). This could be particularly relevant towards understanding the left-right reversal phenotype of 14-3-3 ϵ morphants given that very recent evidence points at a role for 14-3-3 ϵ in the establishment of vertebrate laterality much earlier than previously suspected. Overexpression of *Xenopus laevis* 14-3-3 ϵ leads to trunk laterality reversal (heterotaxia) and this was shown to act upstream of the earliest known left-right asymmetric gene in *Xenopus*, *Xnr-1* (Bunney *et al.*, 2003). Surprisingly, antibodies raised specifically against the epsilon isoform revealed an asymmetric distribution of the protein in the two-cell stage embryo, where 14-3-3 ϵ protein is found in one blastomere and not the other (Bunney *et al.*, 2003). Nonetheless, the plane of the first cleavage in both frog and fish does not usually correlate with the future left-right axis of the embryo. Only a very small percentage of embryos injected in one blastomere at the two-cell stage displays a correlation between the plane of first cleavage and the future left-right axis of the embryo, such that the injected material is seen only on one half of the embryo at later stages.

At 24 hpf, zebrafish embryos morphant for embigin are considerably shorter than controls (Fig. 5.3, A, B). This is at least partly due to undulation of the morphant notochord (Fig., 5.3, B). Furthermore, at this stage there is extensive cell death in the morphant brain, as observed by tissue opaqueness / greyness in the area (Fig. 5.3, B), which is never observed in controls. Embigin is a highly glycosylated transmembrane protein, member of the immunoglobulin superfamily of proteins, that has been implicated in cell-substratum adhesion (Huang *et al.*, 1993). There are very few

functional studies of this protein. Our data suggest it is required for cell survival in the region of the 24 hpf embryo which expresses the transcript most abundantly.



Fig. 5.3 Early phenotype of *embigin* zebrafish morphants. **A**, control embryo at 24 hpf; **B**, morphant embryo at 24 hpf. Both embryos are shown in side views with anterior to the left.

Zebrafish *claudin b* morphants present a morphological phenotype as early as when controls are at 30% epiboly. At this time, the morphant blastoderm is still sitting on top of a flat yolk cell, with no sign of the yolk bulging upward nor of blastoderm epiboly (Fig. 5.4, A, B). By the time control embryos are at shield stage, the yolk cell of morphants does bulge slightly towards the animal pole but less so than a control at 30% epiboly (Fig. 5.4, C, D). At this time, the morphant blastoderm shows sign of radial intercalation in that it is thinner and has a larger surface area than a few hours before, but it only contacts the yolk cell around the periphery and blastoderm epiboly is barely detectable (Fig. 5.4, D). At this stage, in contrast to controls, morphant embryos are radially symmetrical (data not shown). As epiboly progresses, extremely slowly in *claudin b* morphants, radial symmetry is broken in the morphants and the dorsal side of the embryos becomes recognisable as thicker due to greater cell internalisation than in



Fig. 5.4 Early phenotype of *claudin b* zebrafish morphants. All embryos are depicted in side views; C – I, K, L, dorsal is to the right; J, anterior is to the left. A, control at 30% epiboly; B, *claudin b* morphant pictured at the same time as A; C, control at shield stage; D, *claudin b* morphant pictured at the same time as C; E, control at 60% epiboly; F, *claudin b* morphant pictured at the same time as E; G, control at 75% epiboly; H, I two *claudin b* morphants pictured at the same time as G; J, control embryo at the two-somite stage; K – N, four *claudin b* morphants pictured at the same time as J. Arrows point at gap between yolk cell and blastoderm in morphants. Dashed lines outline the blastoderm of two morphants that has detached from the majority of the yolk by 11 hpf. All embryos were cultured in 1x Danieau's solution.

the rest of the margin (Fig. 5.4, E – I). Throughout these stages, the morphant blastoderm only contacts the yolk cell around the periphery and a fluid-filled space is clearly observable between the centre of the blastoderm and the yolk (Fig. 5.4, D, F, H, I, K, L). By the time controls are at the 2-somite stage, that is, at around 11 hpf, approximately half of the *claudin b* morphants have segregated the blastoderm from the majority of the yolk; two distinct masses become visible within a single chorion (Fig. 5.4, M, N). All *claudin b* morphants die by 24 hpf. The above descriptions / phenotypes pertain to *claudin b* morphants reared in 1x Danieau's solution; the phenotype / survival time of these morphants are even more severe / shorter when embryos are reared in Embryo Water (data not shown).

Claudins are transmembrane proteins that are located at the tight junctions of epithelial and endothelial tissues. They are part of a scaffolding complex that links the tight junction components to the actin cytoskeleton. There are at least 18 Claudins in humans and many display restricted expression patterns, which is presumed to underlie differences in permeability among distinct epithelia and endothelia (reviewed in Heiskala *et al.*, 2001). Despite being ubiquitously expressed in the early zebrafish embryo, the phenotype of Claudin b depletion is suggestive of a primordial role for this protein in regulating contact / adhesion between the blastoderm and the yolk cell, more than between blastoderm cells. In the most severely affected embryos, where blastoderm and yolk become segregated, blastoderm cells maintain contacts and round up in a ball (Fig. 5.4, M, N).

Depletion of module A *pancortins* in zebrafish results in epiboly delay, as early as when controls are at 40% epiboly. At this stage, the yolk cell of morphants domes up less than that of controls and the morphant blastoderm has undergone less spreading and thinning over the yolk than that of controls (Fig. 5.5, A, B). By the time controls are at shield stage, that is, when the shield becomes recognisable as a thickening on the dorsal side of the embryo (Fig. 5.5, C, D), morphants are still a little delayed in their epiboly, do not yet present an unequivocal shield, and present an undulating blastoderm (Fig. 5.5, E, F). A little later, when controls are at approximately 60% epiboly, the dorsal side of morphants becomes identifiable, although epiboly is still delayed and the blastoderm is still irregular in appearance (Fig., 5.5, G, I). An animal view of morphant embryos at this stage shows very irregular positioning of the blastoderm cells,

where some bulge out more than others, in contrast to controls embryos, where cells outline a smooth surface (Fig. 5.5, H, J). By early somite stages, morphant embryos have a grossly normal appearance, although with some delay in somitogenesis (approximately 1 somite in delay, that is, 20 min) and less antero-posterior extension (Fig. 5.5, K, M). A closer look at the brains of these embryos reveals signs of cell death in morphants: the brains look slightly grey and cell blebbing is observed (Fig. 5.5, L, N). At 24 hpf, a very severe phenotype is observed in module A *pancortin* morphants. The most obvious features of the phenotype consist of extensive cell death throughout the morphant brain, apparent by black tissue coloration, and very short body axis compares to controls (Fig. 5.5, Q – X). There is also often cell death throughout the neural tube and gut (Fig. 5.5, Q, U, W) and in a few less affected embryos it can be seen that the somites are U rather than chevron shaped (Fig. 5.5, S).

Fig. 5.5 Early phenotype of Module A *pancortin* zebrafish morphants. A, C – D, G – H, K – L, O – P, control embryos; B, E – F, I – J, M – N, Q – X, module A *pancortin* morphants; Picture O in this figure is the same as picture A in Fig. 5.3 since these *embigin* and module A *pancortin* experiments were done in parallel. A, control embryo at 40% epiboly; B, morphant embryo depicted at the same time as A; C – D, control embryo at shield stage; E – F, morphant embryo depicted at the same time as C – D; G – H, control embryo at 60% epiboly; I – J, morphant embryo depicted at the same time as G – H; K – N, embryos at the 1 – 2 somite stage; O – X, embryos at 24 hpf. A, B, C, E, G, I, K, M, O, Q, S, U, W, are side views; D, F, H, J, are animal views of embryos in C, E, G, I, respectively; L, N, P, R, T, V, X, are dorsal views of the brain of embryos in K, M, O, Q, S, U, W, respectively; in C – D, G – J, dorsal is to the right; in K – X, anterior is to the left. **Red arrows** in K and M point at anterior and posterior limits of the embryos depicted; **black arrowhead** in N points at darker coloration of morphant brain, compared to control; **white arrowheads** in N point at cell blebbing in brain; **black arrows** in Q, U, W point at cell death in the neural tube; **white arrows** in Q, U, W point at cell death in the gut region.

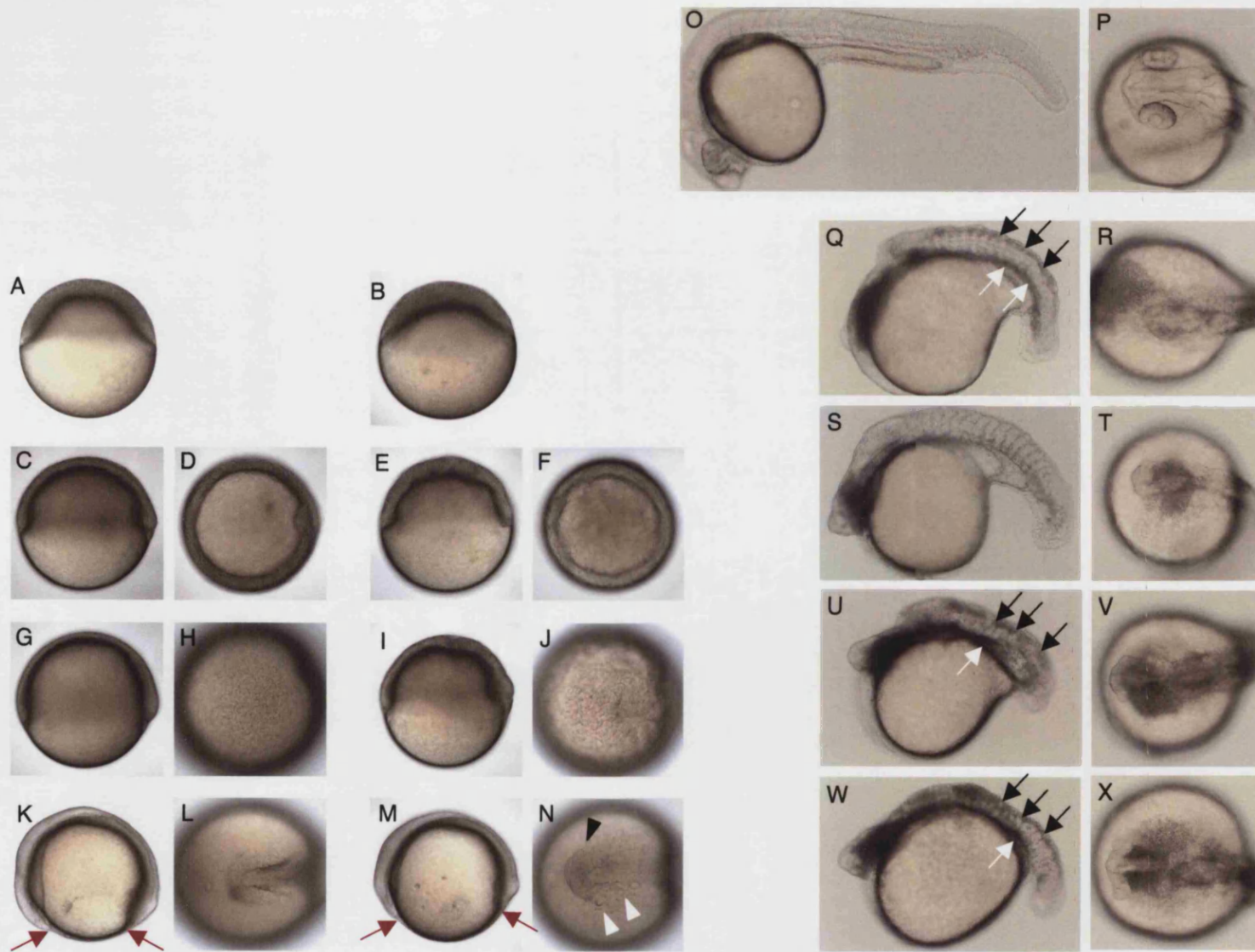


Fig. 5.5

Pancortins belong to the olfactomedin family of proteins, where olfactomedin is a glycoprotein abundantly present in the olfactory epithelium mucous, mostly in a homodimer form (Snyder *et al.*, 1991). Some pancortins are extracellular matrix proteins (this is the case for those containing module Y) while others contain and endoplasmic reticulum localisation signal (this is the case for those containing module Z). While the BMZ isoform has been reported to localise to the Golgi apparatus of rat kidney cells (Kondo *et al.*, 2000), it has been reported to be secreted in chick embryos (Moreno and Bronner-Fraser, 2001). There have been few functional studies of this family of proteins. Overexpression of BMZ / Noelin-1 in the chick causes excess neural crest migration (Barembaum *et al.*, 2000) and is able to induce the neurogenic genes *Xngnr-1* and *XneuroD* in *Xenopus* animal caps (Moreno and Bronner-Fraser, 2001). No loss-of-function experiment has been reported for this family of proteins but our own results implicate it in neuronal survival.

Zebrafish *sp120* a morphants display a morphologically detectable phenotype by early somite stages. At these stages, brain development looks delayed relative to controls (Fig., 5.6, B, J) and the body axis is positioned with a curvature atop the yolk such that the embryos have more yolk to one side than to the other instead of being positioned on the yolk in a bilateral symmetric way like controls (Fig. 5.6, C, K). By 28 hpf the antero-posterior axis of morphants is shorter than that of controls, the tail is more

Fig. 5.6 Early phenotype of *sp120* a zebrafish morphants. A – H, control embryos; I – P, *sp120* a morphants. A – C, I – K, embryos at the 6-somite stage; D – F, L – N, embryos at 28 hpf; G, H, O, P, 2 days old embryos. A, D, G, I, L, O are side views with anterior to the right; B, E, J, M are dorsal views of the heads of the embryos depicted in A, D, I and L, respectively, with anterior to the right; F, H, N, P are frontal views of the embryos depicted in D, G, L, O, respectively, with anterior to the right; C, K are ventral views of the embryos depicted in A and I, respectively, with anterior to the left. **Dashed lines** in C and K illustrate the antero-posterior orientation of the embryos depicted; **arrows** in E and M point at the anterior end of the telencephalon; **arrowhead** in G points at haemoglobin-containing red blood cells in control embryo.

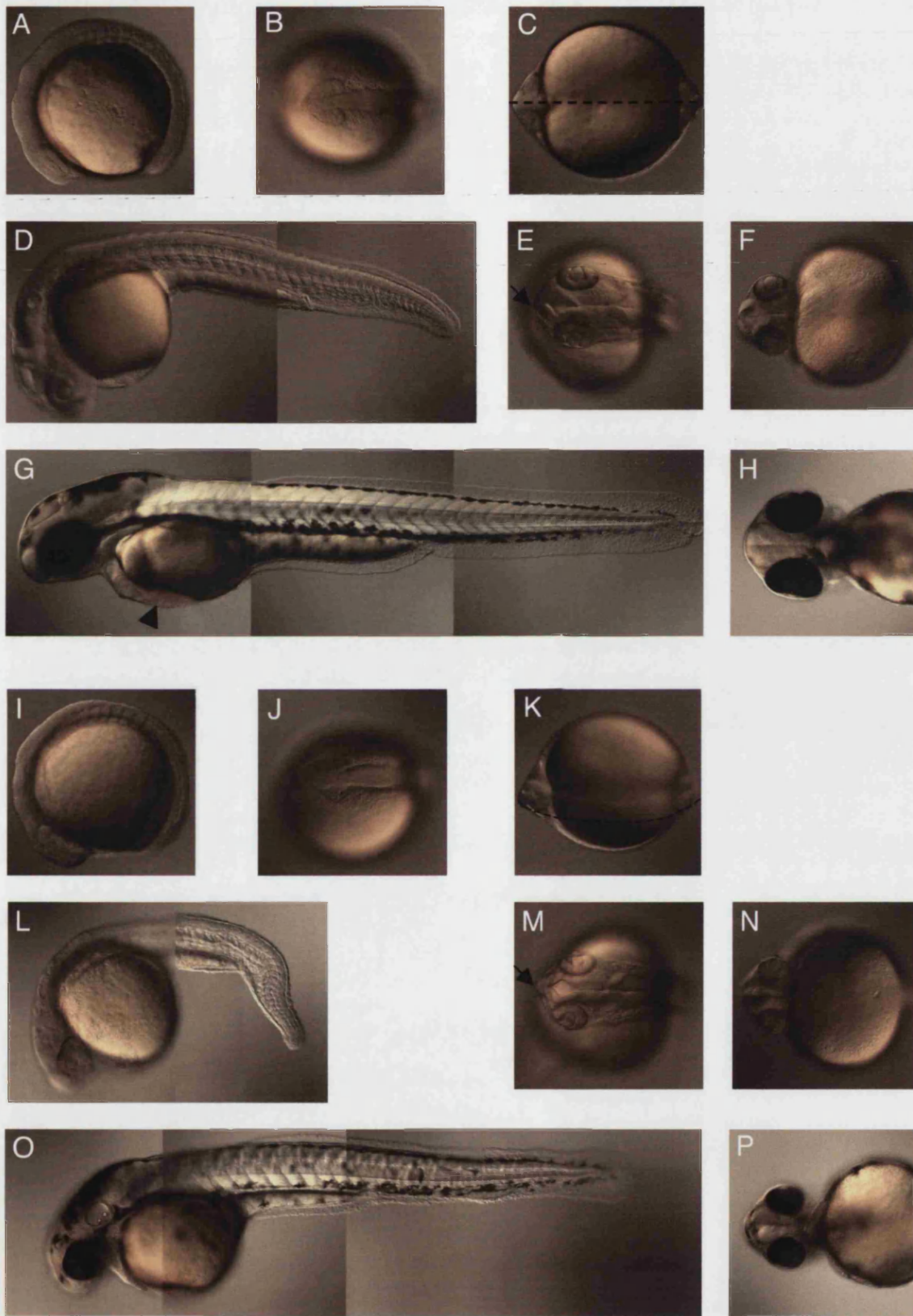


Fig. 5.6

curved downwards than that of controls and the morphant notochord is wavy, unlike in controls (Fig. 5.6, D, L). At this stage, the morphant brain and eyes are smaller and look undeveloped compared to that of controls, namely with the retina being less pigmented (Fig. 5.6, E, F, M, N). Furthermore, the *sp120* morphant telencephalon is protuberant (Fig. 5.6, E, M, arrow). By 30 hpf, few blood cells are visible in these morphants (data not shown). At 2 days of development, the excessive body curvature and notochord waviness of morphants have recovered to a wild-type appearance (Fig. 5.6, G, O) and blood cells are seen circulating throughout the embryo (data not shown). However, at this stage *sp120* morphants are clearly smaller than controls in all dimensions (Fig. 5.6, G, H, O, P) and blood development is at least delayed, since no signs of hemoglobin are visible, unlike in controls (Fig. 5.6, G arrowhead). Furthermore, morphants have impaired yolk extension and ragged fin folds (Fig. 5.6, G, H). Sp120 is a nuclear scaffold protein that binds the matrix attachment region (MAR) stretches of DNA (Tsutsui *et al.*, 1993). To our knowledge, ours is the only functional approach to studying this protein in the context of a whole organism.

At early segmentation stages, zebrafish morphant for the novel gene *p7822b53* present a protuberant telencephalon (Fig. 5.7, A, H) but by 28 hpf telencephalon protuberance is no longer visible in morphants (data not shown). At 28 hpf, the antero-posterior axis of morphants is slightly shorter than that of controls, and this might be attributable to what

Fig. 5.7 Early phenotype of novel gene ‘*p7822b53*’ zebrafish morphants. A – G, control embryos; H – N, *p7822b53* morphants; Pictures E and F in this figure are the same as pictures G and H in Figure 5.6, since these *sp120* and novel *p7822b53* experiments were done in parallel. A, H, embryos at the 6-somite stage; B – D, I – K, embryos at 28 hpf; E – G, L – N, 2 days old embryos. B, E, I, L, are side views with anterior to the right; A, H, are dorsal views of the head, with anterior to the right; C – D, F – G, J – K, M – N, are frontal views of the embryos depicted in B, E, I, L, respectively, with anterior to the right. **White arrowheads** in A and H point at the anterior end of the telencephalon; **arrows** in C and J point at optic recesses; **black arrowheads** in D, G, K, N, point at heart region: heart tube in D; looped heart tube in G, absence of heart tube in K, looping heart tube in N.

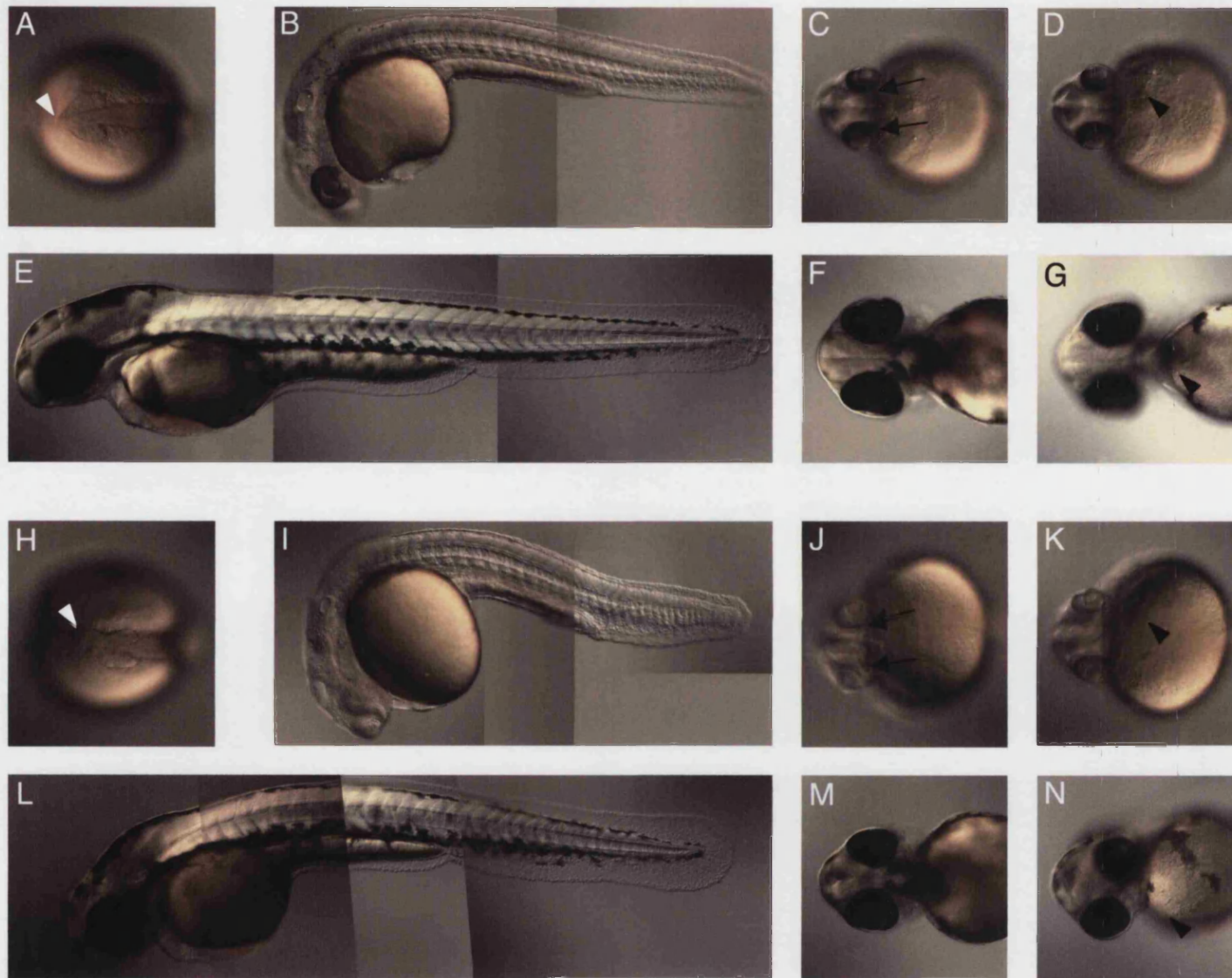


Fig. 5.7

appears to be a compressed tail tip (Fig. 5.7, B, I). In contrast to controls, the morphant retina is not yet pigmented at this stage, and the optic recesses are clearly wider in morphants than in controls (Fig. 5.7, C, J). By 28 hpf, the heart tube is beginning to form in control embryos but not in *p7822b53* morphants (Fig. 5.7, D, K). This could partly explain the observation of greatly reduced circulation in morphants as compared to controls at this stage, both in terms of number and speed of blood cells (data not shown). By 2 days of development, a heart tube has formed in morphants but it is developmentally delayed with respect to that of controls. While the morphant heart is starting to loop, that of control has already undergone looping (Fig. 5.7, G, N). In contrast to what is observed in controls, between 24 and 48 hpf of *p7822b53* morphant development, blood cells pumped in one direction are seen to fall back to where they were pumped from, suggesting impairment in vessel valve function (data not shown). At 2 days of development, morphants are slightly smaller than controls in all dimensions (Fig. 5.7, E, F, L, M). The protein encoded by this gene presents no known motifs.

In this small-scale screen, injection of 7 / 9 MOs targeting zebrafish transcripts resulted in morphologically discernible phenotypes. Due to time restrictions, the phenotypes described were necessarily superficially analysed. This was the nature of our screen: to use MOs as a quick means of functionally screening proteins, from which to select one(s) to study in further detail. With this as an aim, this screen was successful. A few interesting phenotypes could be picked up in this way, and possibly more if a few staining analyses were performed on the morphants. By far the most time-consuming steps in this project were the screening of the incomplete zebrafish genome and transcriptome, both by *in silico* and molecular methods. Once the zebrafish genome is completed, in the near future, studies like this one will be greatly facilitated.

Chapter 6

Functional analysis of zebrafish *nsa2*

Chapter 6

Functional analysis of zebrafish *nsa2*

- 6.1 Introduction to the functional analysis of zebrafish *nsa2*
 - 6.1.1 Nsa2 is required for ribosome biogenesis
 - 6.1.2 Ribosome biogenesis in brief
 - 6.1.3 Mutations in ribosomal proteins lead to the *Minute* phenotype in flies
 - 6.1.4 *Minute* growth rates
 - 6.1.5 Some *Minute* phenotypes arise by maternal effect
 - 6.1.6 *Minute* cell proliferation and cell size
 - 6.1.7 *Minute* morphological defects
 - 6.1.8 Competition between *Minute* and wild-type cells
 - 6.2 Results of the functional analysis of zebrafish *nsa2*
 - 6.2.1 Nsa2 is highly conserved among eukaryotes
 - 6.2.2 In zebrafish as in mouse, *nsa2* is mainly expressed in endodermal and mesodermal derivatives
 - 6.2.3 Depletion of zebrafish Nsa2 slows DEL epiboly
 - 6.2.4 Embryos lacking *nsa2* have patterning defects
 - 6.2.5 The epiboly phenotype of *nsa2* is analogous to that of *Minute* ribosomal proteins
 - 6.2.6 Loss of Nsa2 and *Minute* Rps produce similar morphological defects
 - 6.2.7 Is the fly orthologue of *nsa2* a *Minute*?
 - 6.2.8 Phenotypes of *nsa2* morphant cells
 - 6.2.8.1 Cells morphant for *nsa2* undergo apoptosis
 - 6.2.8.2 TEM study of *nsa2* morphant cells of the epiboly-stage zebrafish embryo
 - 6.3 Discussion of the functional analysis of zebrafish *nsa2*
-

6.1 Introduction to the functional analysis of zebrafish *nsa2*

Depletion of the Nop7 associated protein 2 (Nsa2), causes a gastrulation phenotype in fish. Mutations producing gastrulation defects are rarely observed in zebrafish mutagenesis screens (Driever *et al.*, 1996; Haffter and Nusslein-Volhard, 1996; Golling *et al.*, 2002). As my main interest in the mouse screen was to identify genes important for early development, I focused my efforts on understanding how Nsa2 depletion leads to the gastrulation defects observed.

6.1.1 Nsa2 is required for ribosome biogenesis

Mammalian orthologues of Nsa2 are present in the sequence databases with names that reflect the ways researchers have encountered the protein. The human protein has been

called TINP1, for TGF β -induced nuclear protein 1, or HCLG1, for hairy cell leukaemia gene 1, given that it lies adjacent to a chromosome breakpoint found in this disease (Wu *et al.*, 1999); the mouse protein has been called Lnr42, for L-NAME-related protein 42, where L-NAME is an arginine analogue that blocks nitric oxide synthase. The only functional analysis of this protein published concerns the yeast orthologue, which has been named Nsa2, for Nop7 associated protein 2 (Harnpicharnchai *et al.*, 2001), where Nop7 is a nucleolar protein required for the biogenesis of the 60S (large) ribosomal subunit (Adams *et al.*, 2002). I am using the designation *nsa2* for all the orthologues of this gene and Nsa2 for the proteins they encode.

Yeast *nsa2* is an essential gene (Winzeler *et al.*, 1999) and Nsa2 has been implicated in the biogenesis of the 60S eukaryotic ribosomal particles. A yeast mutant strain lacking Nsa2 has fewer free 60S ribosomal subunits and accumulates 40S subunits stalled at initiation codons, presumably due to the absence of sufficient functional 60S subunits to proceed with translation (Harnpicharnchai *et al.*, 2001). Nsa2 is nuclear, although it is not specifically nucleolar as are many proteins involved in ribosome biogenesis. Given the evolutionary conservation of Nsa2 in eukaryotes, it is likely that Nsa2 is also essential for 60S ribosomal subunit formation in vertebrates.

6.1.2 Ribosome biogenesis in brief

Proliferating eukaryotic cells expend 80% of their energy generating the protein synthesis apparatus (reviewed in Schmidt, 1999). How much a cell invests in generating a functional ribosome has only just been appreciated. In the yeast *Saccharomyces cerevisiae*, systematic gene deletion and the use of the tandem affinity purification protocol (Rigaut *et al.*, 1999) have identified dozens of proteins involved in the process (reviewed in Warner, 2001; Fatica and Tollervey, 2002). Nearly all of these proteins have mammalian counterparts (reviewed in Warner, 2001). Among them, approximately 80 are ribosomal proteins (Rps), part of the mature, functional, ribosome, and twice as many, including Nsa2, are non-Rps, associating transiently with immature ribosomal particles (reviewed in Venema and Tollervey, 1999; Fatica and Tollervey, 2002).

Ribosome synthesis occurs mainly in the nucleolus, where rRNA genes are transcribed.

The proportion of the nucleus occupied by the nucleolus is a good indicator of the level of protein synthesis of a cell and varies greatly reaching up to 25 % in highly synthesising cells (reviewed in Alberts *et al.*, 2002). Nevertheless, there are late maturation steps that occur in the nucleoplasm and cytoplasm. Nsa2 is nuclear but not specifically nucleolar, consistent with a proposed role in late 60S subunit maturation (Harnpicharnchai *et al.*, 2001; reviewed in Fatica and Tollervey, 2002).

The known non-Rps involved in ribosome biogenesis possess several activities. For example, the exosome, which contains at least 11 proteins, has a 3'→5' exoribonuclease activity; an RNA helicase is composed of at least 16 proteins; other proteins covalently modify rRNA and assemble the particles (reviewed in Venema and Tollervey, 1999; Tanner and Linder, 2001; Venema and Tollervey, 1999; Warner, 2001; Fatica and Tollervey, 2002). In addition, many rRNA modifications are performed by numerous small nucleolar RNAs (snoRNAs) of which there are over 100 and which in turn associate with specific proteins (snoRNPs) (reviewed in Venema and Tollervey, 1999).

Only recently has the complexity and highly ordered nature of ribosome synthesis been recognised. Mutational analysis of non-Rp components is an area of intense research. Systematic mutations should reveal the role of each component and tell us how ribosome synthesis is regulated. In crude terms, most of the RNA helicases are essential (reviewed in Venema and Tollervey, 1999) but among other non-Rps recently identified there are both essential and non-essential proteins (Harnpicharnchai *et al.*, 2001).

6.1.3 Mutations in ribosomal proteins lead to the *Minute* phenotype in flies

In *Drosophila*, mutations in 17 of the 53 identified Rps (The FlyBase Consortium, 2003) give rise to the *Minute* phenotype, characterised by frequent dominant small body size of adults (from which the name of the phenotype is derived), dominant slowed larval development, dominant slowed cell cycle, dominant short and thin bristles, and recessive lethality at around the time of egg hatching or early first-instar larva (Schultz, 1929; reviewed in Kay and Jacobs-Lorena, 1987 and Lambertsson, 1998). In addition, many *Minutes* display other dominant morphological phenotypes, such as reduced fertility, reduced viability, rough eyes and etched tergites (reviewed in Kay and Jacobs Lorena, 1987; Lambertsson, 1998). Also, a few atypical *Minutes* are homozygous

viable (Lambertsson, 1998).

Overall, *Minute* phenotypes are nearly identical although they differ in strength (reviewed in Lindsley and Zimm, 1992; Lambertsson, 1998). In general, *Minutes* are non-additive, showing double or triple heterozygous phenotypes that are no more severe than single heterozygotes. This suggests that the *Minute* genes encode functionally similar products (Schultz, 1929, reviewed in Kay and Jacobs-Lorena, 1987; Lambertsson, 1998). There are approximately 55 *Minute* loci and we still do not know the molecular nature of most of the mutations (reviewed in Lambertsson, 1998).

All *Minute* loci identified consist of mutations in Rps (Kongsuwan *et al.*, 1985; Watson *et al.*, 1992; Hart *et al.*, 1993; Melnick *et al.*, 1993; Andersson *et al.*, 1994; Cramton and Laski, 1994; McKim *et al.*, 1996; Schmidt *et al.*, 1996; Saeboe-Larssen and Lambertsson, 1996; Saeboe-Larssen *et al.*, 1997; Reynaud *et al.*, 1997; van Beest *et al.*, 1998; Torok *et al.*, 1999; Kronhamn and Rasmuson-Lestander, 1999; The FlyBase Consortium, 2003) but several *Minute*-like phenotypes have been characterised that consist of mutations in other genes. For example, rRNA deficiencies in the mutants *mini (min)* and *bobbed (bb)* produce a similar phenotype, the severity of which depends on the number of rRNA repeats deleted (reviewed in Lambertsson, 1998) and so do mutations in two enzymes of the polyamine biosynthetic pathway (Larsson and Rasmuson-Lestander, 1997; Larsson and Rasmuson-Lestander, 1998). In all cases, however, there is the common outcome of translation impairment. It is therefore a reasonable notion that essential genes involved in ribosome biogenesis are *Minute* candidates (Kay and Jacobs-Lorena, 1987).

There are at least 53 Rps identified in *Drosophila* (The FlyBase Consortium, 2003). Out of the 36 not already identified as *Minute* loci, there are mutant alleles for only eight. Mutant alleles for four of these Rps have been described as recessive-lethal, one is male and female sterile, and three have no published phenotypic information. It is plausible that detailed phenotypic analysis of these mutants might reveal them to be *Minute* loci. Many Rps map cytologically at or near the sites of uncloned *Minute* loci (reviewed in Lambertsson, 1998), although this could be a consequence of the large number of Rps. The fact that most *Minute* loci are deficiencies could explain the disparity between the number of Rps (~80 in all eukaryotes) and the number of *Minute*

loci. Several *Minute* deficiencies probably encompass more than one Rp, or more than one protein capable of producing a *Minute* phenotype when mutated, not all of which have even been recognised in *Drosophila*. This has hampered the identification of all *Minute* loci through complementation and/or rescue experiments. Also, it is likely that many *Minute* phenotypes have been overlooked, categorized simply as “recessive-lethal” phenotypes.

There is at least one Rp that does not produce a *Minute* phenotype when depleted. The P-element mutation fs(3)02729 disrupts the RpL15 gene, rendering homozygous females nearly sterile (reviewed in Lambertsson, 1998). Two other loci, *rpS14a* and *rpS14b*, which are nearly identical and localised in tandem in the *Drosophila* genome, may be responsible for the *M(1)7C Minute* phenotype. A deletion that removes the two genes, however, does not display any visible phenotype when heterozygous and is lethal when homozygous (Dorer *et al.*, 1991).

In plants, four mutations have been identified in Rp-coding genes. Unlike *Drosophila*, three of these mutations are recessive, but one does show heterozygous growth retardation as well as floral and vascular defects in addition to homozygous embryonic lethality (Van Lijsebettens *et al.*, 1994; Revenkova *et al.*, 1999; Ito *et al.*, 2000; Weijers *et al.*, 2001).

6.1.4 *Minute* growth rates

Most *Minute* mutants develop slower at all stages than wild-type *Drosophila*. For example, *M(1)7C* embryos hatch 2 – 3, 4 and 6 – 8 days later than wild-type embryos, depending on whether they are reared at 29°C, 25°C or 17°C, respectively (Andersson and Lambertsson, 1990). Several homozygous *Minutes* present an embryonic phenotype that consists of slower development of the midgut, with yolk frequently remaining in its lumen, followed by hatching of considerably smaller than normal larvae (Farnsworth, 1957b; Farnsworth, 1957a; reviewed in Kay and Jacobs-Lorena, 1987). Larval development takes 4 days / 96 h at 25 °C in wild-type *Drosophila*. To reach an identical stage to wild-type larvae, *Minute* larvae can take several additional hours or days (Andersson *et al.*, 1994). *M(2)58F¹* larvae reach pupation on average 9.9 h later than wild-types for males, and 13.3 h later for females (Brehme, 1939); *M(3)95A*

heterozygous for a moderate allele of *rpS3*, which causes *rpS3* mRNA levels to be reduced by 30%, have a prolonged larval development by ~16 h whereas heterozygotes for a strong allele, which causes *rpS3* mRNA levels to be reduced by 40%, have a prolonged larval development by ~54 h; when the moderate allele of *M(3)95A* is homozygous, *rpS3* mRNA levels are reduced by 60% and larval development is prolonged by up to 80 h (Farnsworth, 1957a; Saeboe-Larssen *et al.*, 1998). Hence, levels of *rpS3* mRNA and delay in larval development are strongly correlated. The pupal phase of *M(3)95A* mutants lasts 12 - 21 h longer than wild-type (Brehme, 1939).

6.1.5 Some *Minute* phenotypes arise by maternal effect

Most *Minute* phenotypes arise by zygotic effect. In several cases, however, *Minute* females but not *Minute* males show impaired fertility (for example, Schmidt *et al.*, 1996; reviewed in Lindsley and Zimm, 1992) or barely produce *Minute* progeny (for example, Andersson and Lambertsson, 1990). When progeny are produced, mutant phenotypes are observed in both wild-type and mutant offspring. These include smaller eggs, abnormal egg shape, non-hatching and late embryonic lethality, abdominal segmentation defects including fusion and deletion, fused tergites and missing or defective legs and halteres (Farnsworth, 1957a; Kongsuwan *et al.*, 1985; Boring *et al.*, 1989; Andersson and Lambertsson, 1990).

6.1.6 *Minute* cell proliferation and cell size

Minute mutant cells proliferate slower than wild-type cells (Morata and Ripoll, 1975). At least in some of the mutants, the ratio of *Minute* larval developmental time to that of non-*Minute* siblings is similar to the ratio of *Minute* cell proliferation rate to that of non-*Minute* cells in the wing discs (Morata and Ripoll, 1975). Thus, it is possible that a large component of the deceleration in development of *Minute* mutants is due to reduced cell proliferation rate (Morata and Ripoll, 1975).

For several *Minute* mutations, adult mutants reach the same size as their wild-type counterparts. This is paralleled at the cellular level where in most cases *Minute* cells are the same size as wild-type cells (Bryant and Simpson, 1984; Neufeld *et al.*, 1998). This must mean that (slower) cell growth and (slower) cell division are well coupled in these flies. In some cases, however, *Minute* adults are smaller than wild-type (*M(2)21AB*,

M(2)58F¹, *M(3)S35*, *rpS3*). Several experiments suggest that this is caused by a decrease in cell size rather than cell number (Brehme, 1941a; Brehme, 1941b; reviewed in Farnsworth, 1957b; Lindsley and Zimm, 1992; Lambertsson, 1998). Flies deficient in RpS6 kinase (S6K) also show a severely reduced body size, which is attributed to smaller, by ~30%, rather than fewer cells (Montagne *et al.*, 1999). Mice deficient in S6K are smaller than wild-type, especially during embryogenesis but this size difference is largely overcome by adulthood (Shima *et al.*, 1998; reviewed in Kozma, 2002). In *S6K^{-/-}* mutant mice, pancreatic β cells are reduced in size but not in number (Pende *et al.*, 2000).

In mammalian cells RpS6 phosphorylation by S6K is induced by mitotic factors, whereas dephosphorylation occurs when proliferation is arrested (reviewed in Sturgill and Wu, 1991). RpS6 phosphorylation can alter translation patterns (Thomas and Luther, 1981; Palen and Traugh, 1987) and is thought to increase the translation of mRNAs containing terminal oligopyrimidine tracts (5'-TOPs) (reviewed in Thomas and Hall, 1997; Edgar, 1999). These 5'-TOPs are ubiquitous in the mRNAs coding for Rps, are present in many translation factors and are rare in other mRNAs. Therefore, RpS6 phosphorylation favours the production of the translation apparatus (Meyuhas *et al.*, 1996; reviewed in Edgar, 1999; Meyuhas, 2000).

Paradoxically, RpS6 is involved in both the promotion and the inhibition of proliferation. The fly *rpS6* gene was originally named *aberrant immune response 8* (*air8*) because, in addition to strong growth retardation of hemizygotes, larvae display large melanotic tumours that result from increased cell proliferation in some hematopoietic cells. This phenotype is not seen in other *Minute* mutants and suggests that RpS6 may function as a tumour suppressor in addition to its role in protein synthesis.

In addition to proliferation, RpS6 plays a role in the control of cell size. The hematopoietic organs of larvae carrying the *hen* alleles of *rpS6* have abnormally large cells as well as a much greater number of cells (Stewart and Denell, 1993). Similarly, in mice with a conditional null mutation of *rpS6*, livers regenerate to normal size upon partial hepatectomy by cell growth rather than by proliferation as in wild-type livers (Volarevic *et al.*, 2000). Mutant liver cells show decreased proliferation that is thought

not to be a direct consequence of decreased translation given that the translationally-regulated proteins p21^{CIP1} and Cyclin D1 show no difference in levels relative to wild-type cells (Volarevic *et al.*, 2000). In addition, *RpS6* mutant liver cells are able to synthesise proteins and grow extensively (Volarevic *et al.*, 2000). Therefore, the conditional mutation seems to impart a specific failure in a checkpoint that allows cell cycle progression. The failure in cell cycle progression has been attributed to a block in *cyclin A* and *cyclin E* expression (Volarevic *et al.*, 2000), essential for progression between G1 and S phase (Girard *et al.*, 1991; Ohtsubo *et al.*, 1995).

A role for ribosomal dysfunction in cancer has recently been put forward through the study of Dyskeratosis Congenita (DKC), a rare fatal genetic syndrome characterised by premature ageing, severe anaemia due to bone marrow failure, nail dyskeratosis, skin hyperpigmentation and cancer (Ruggero *et al.*, 2003). DKC is caused by mutations in the *DKC1* gene (dyskerin), which is a pseudouridine synthase, an enzyme that mediates post-transcriptional modifications of rRNAs by converting uridine residues into pseudo-uridines, and a component of telomerase. Although dyskerin is involved in telomere regulation, many of the phenotypes of *DKC1*-null mice appear despite telomere length (Ruggero *et al.*, 2003). *DKC1* mutant mice develop tumours during their lifetime in 50% of cases, suggesting that *DKC1* is a tumour-suppressor. Cells derived from *DKC1* mutant mice are hypersensitive to drugs that inhibit translation and undergo apoptosis much more readily than wild-type cells.

6.1.7 Minute morphological defects

Tissue-specific phenotypes observed in *Minute* mutants are generally explained by an exceptional dependence of the tissue on protein synthesis, as with the small bristle phenotype and impaired fertility. Alternatively, the given locus may have a non-ribosomal role in the affected tissues. Several Rps, such as *RpS6*, are known to have extra-ribosomal functions (reviewed in Wool, 1996). Generally, the extra-ribosomal function is related to their ability to bind RNA or DNA but there are notable exceptions. For example, rat P2 is also an iron-binding protein (Furukawa *et al.*, 1992), and *Xenopus laevis* S8, also known as p27, when phosphorylated, becomes associated with the oocyte peripheral membrane as well as with vesicles formed from the nuclear envelope and endoplasmic reticulum during mitosis (Boman *et al.*, 1992).

Furthermore, patterning defects are to be expected if the normal translation rate of a cell is tampered with. The kinetics of translation initiation depends upon the tertiary structure of the mRNA near the initiation codon (Lodish, 1970) as well as the primary structure of the mRNA near this codon (Steitz, 1969). Translation initiation rate can differ more than twenty-fold among distinct mRNAs (Lodish, 1968; Steitz, 1969; Lodish and Robertson, 1969; Lodish, 1970; Steitz, 1973). If one component required for translation initiation becomes limiting, the effect is first noticeable on the mRNAs with lower rate of translation initiation (Lodish, 1974). Thus, translation inhibition will affect distinct proteins differentially. Transcription, processing and degradation of RNA involves a large number of proteins so will undoubtedly be affected by inhibiting translation. For example, inhibition of translation in yeast reduces rRNA transcription by 80%, mRNA transcription by 25% and tRNA transcription by 20% (Shulman *et al.*, 1977). Inhibition of translation alters the expression profile of a cell rather than equally reducing expression levels.

Loss of RpS17 leads to a maternal-effect segmentation defect of larvae, explained by an anomalous pattern of the pair-rule protein Fushi tarazu (Ftz) at embryonic stages (Boring *et al.*, 1989). The primary larval defect consists of single pair segment fusions between the denticle belts of abdominal segments A4 and A5 (occasionally also A6 and A7 fusions) and the anomalous Ftz pattern features narrower than wild-type posterior stripes and inter-stripe domains (Boring *et al.*, 1989). Reduction of protein synthesis causes the anomalous Ftz pattern and segmentation defect. It was estimated that protein synthesis levels were lowered by 30% in the embryos produced by mutant mothers and when this was mimicked by cycloheximide administration to embryos, both the Ftz pattern and segmentation phenotypes were reproduced (Boring *et al.*, 1989). Cycloheximide decreases the half-life of Ftz protein (Edgar *et al.*, 1987) but increases the half-life of *ftz* mRNA (Edgar *et al.*, 1986). In addition, short-lived repressors in the inter-stripe domains, such as Hairy, control *ftz* expression (Edgar *et al.*, 1986; Carroll and Scott, 1986; Howard and Ingham, 1986; Ish-Horowitz and Pinchin, 1987; Carroll *et al.*, 1988). Although the influence of protein synthesis inhibition on Hairy levels and pattern is unknown, it is sensible that reduction of the rate of production of a rapidly degraded transcriptional regulator might significantly affect its target genes. The issue is complex and it reflects how patterning and basic cellular functions have to be

coordinated. If the same molecules controlled both, their coordination would be guaranteed (Martin-Castellanos and Edgar, 2002).

6.1.8 Competition between *Minute* and wild-type cells

The differences in proliferation rates between *Minute* and wild-type cells have been exploited to generate large wild-type clones in *Minute* backgrounds, which was crucial to prove the existence of clonal boundaries between developmental compartments in *Drosophila* (Lawrence *et al.*, 1979). When heterozygous *Minute* clones are generated in wild-type flies, they are out-competed by the faster growing wild-type cells and are eventually eliminated (Morata and Ripoll, 1975). Heterozygous *Minute* cells are only lost in the presence of non-*Minute* cells. If heterozygous *Minute* clones are generated in a homozygous *Minute* background they grow to large sizes as a result of their growth advantage with respect to the surrounding cells. The elimination of *Minute* clones in a non-*Minute* background was recently shown to require the function of *brinker* (*brk*) (Moreno *et al.*, 2002). The gene *brk* is normally repressed by Decapentaplegic (Dpp) signalling and codes for a transcriptional repressor of Dpp signalling (Minami *et al.*, 1999; Jazwinska *et al.*, 1999; Campbell and Tomlinson, 1999). Dpp is a member of the TGF β super-family of proteins. Expression of *brk* is upregulated in heterozygous *Minute* cells, activates the c-Jun amino-terminal kinase pathway, and induces apoptosis (Moreno *et al.*, 2002). It has been proposed *brk* is upregulated in heterozygous *Minute* cells because they are less able to receive or transduce Dpp signals (Moreno *et al.*, 2002).

6.2 Results of the functional analysis of zebrafish *nsa2*

6.2.1 Nsa2 is highly conserved among eukaryotes

All known eukaryotic genomes encode Nsa2 orthologues. These present a high degree of identity and similarity (Fig. 6.1), suggesting that they exert the same function(s) in all eukaryotes. In addition, the prokaryotic family of S8E ribosomal proteins display ~20% identity to Nsa2.

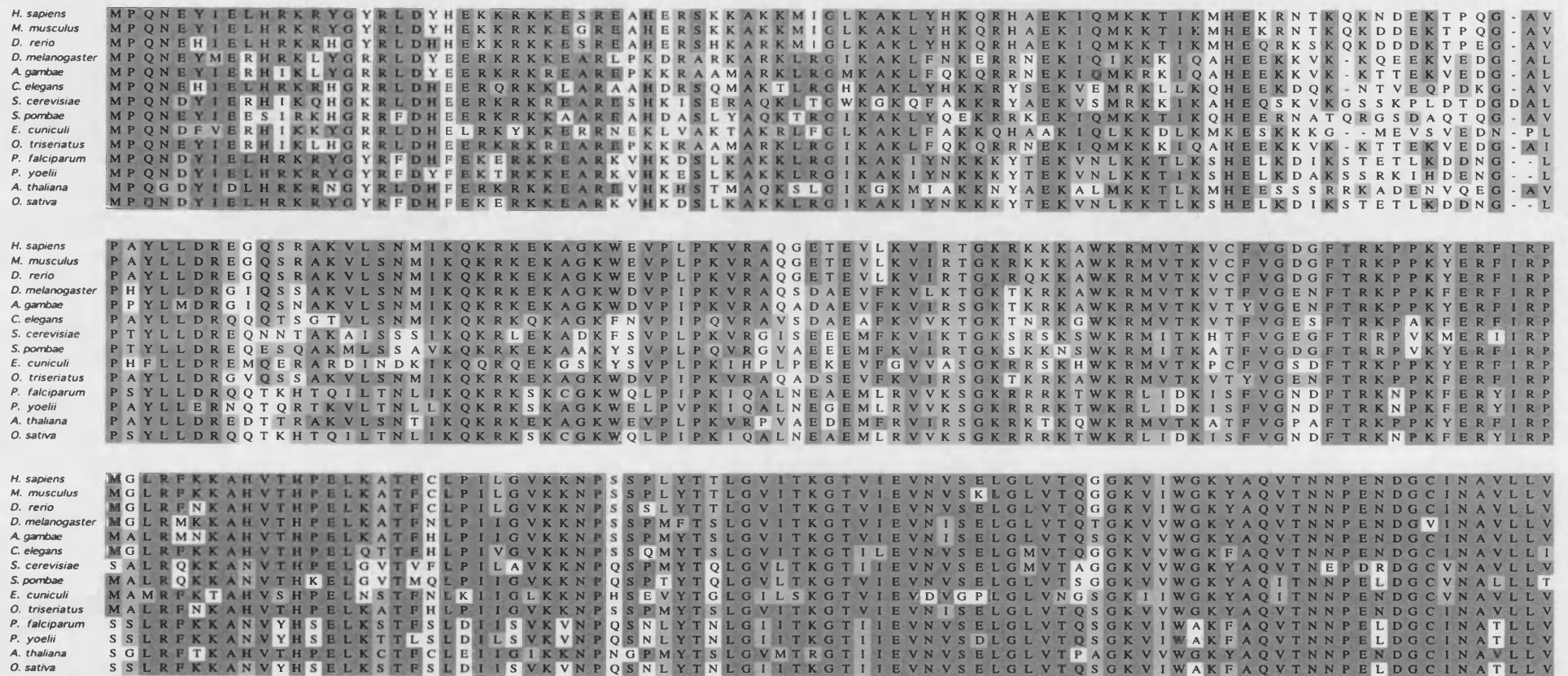


Fig. 6.1 Putative Nsa2 proteins are present throughout the eukaryota. ■ identity; ■ similarity.

6.2.2 In zebrafish as in mouse, *nsa2* is mainly expressed in endodermal and mesodermal derivatives

In both the early mouse and fish embryos, *nsa2* is widely expressed. There are regions of the embryo that express higher levels than others, as seen by whole-mount *in situ* hybridisation. In the mouse, *nsa2* is expressed throughout the epiblast and the extraembryonic ectoderm at 6.5 dpc. At 7.5 dpc it continues to be expressed throughout the internal cell layers of the whole conceptus. At 8.5 dpc expression is strongest in the first branchial arch and in the neural tube, especially in the brain. Low-level expression throughout the lateral mesoderm is also detected. The pattern is largely unchanged by 9.5 dpc. The CNS expression is strongest in the forebrain (Fig. 3.1, k8710a07). In the zebrafish, there is strong and ubiquitous maternal expression of *nsa2* (Fig. 6.2 A). After MBT, *nsa2* is still strongly expressed in all cells of the embryo (Fig. 6.2 B – F) but by somite stages it is down-regulated in the spinal cord, trunk expression being detected mainly in endodermal and mesodermal tissues (Fig. 6.2 E and G). Like in the mouse, *nsa2* expression is highest in the brain (Fig. 6.2, G and H).

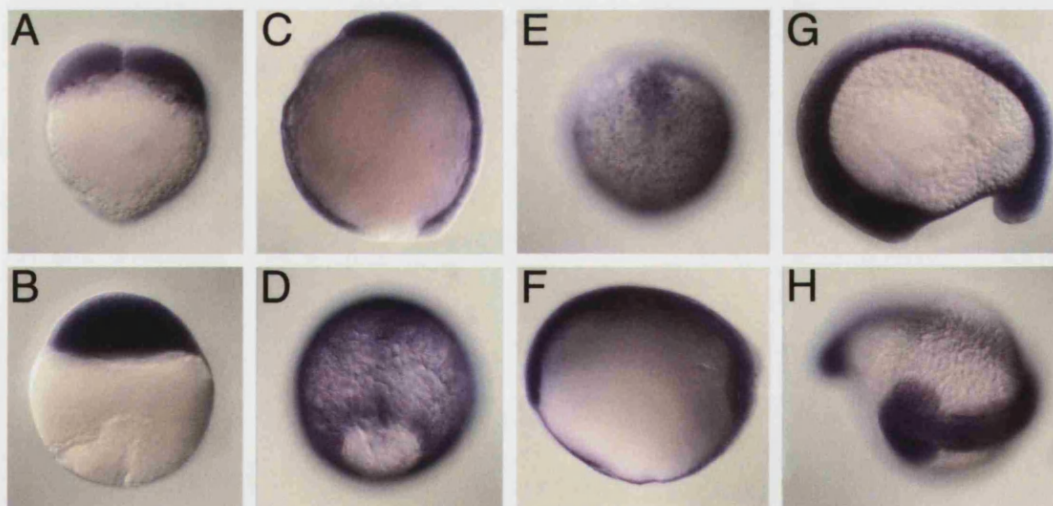


Fig. 6.2 Expression of *nsa2* during early zebrafish development. **A**, side view of 4-cell stage embryo; **B**, side view of sphere stage embryo; **C**, side view of 90% epiboly embryo (dorsal to the right); **D**, vegetal view of 90% epiboly embryo; **E**, dorsal-anterior view of embryo at 90% epiboly; **F**, side view of tailbud stage embryo (anterior to the left); **G**, side view of 15-somite stage embryo (anterior to the left); **H**, dorsal-anterior view of 15-somite stage embryo.




6.2.3 Depletion of zebrafish Nsa2 slows DEL epiboly

I used different MOs to target zebrafish *nsa2* mRNA: MO1 and MO2. MO1 was designed to target what I thought was the start of translation. However, when I compared the sequence of putative Nsa2 proteins across many eukaryotic species I realised the existence of an error in the mouse sequence from which I had extrapolated where the first codon should lie. Therefore, MO1 does not target the first codon of the zebrafish mRNA but a downstream methionine codon (Fig. 6.3, yellow box). I designed MO2 to target the 5'UTR of *nsa2* mRNA (Fig. 6.3, orange box). MO1 resulted in the strongest phenotype and unless otherwise stated, embryos morphant for *nsa2* were always generated by injection of MO1.

```

TACGACTCACTATAGGGGCTCTAAAGAAGAGGCTCTGAGTGAAAAACATCGCGAGCTCGAG
CCACGAATTAACCATCAAAATATCAGAAATAAACACCCGATCGGCGGATTAAACAACACCT
GGTAGCTCCATAAACACTTTAACAACACAGACTTCATCATGCCGCAGAACGAGCACATCGA
GTTACACCGTAAGCGGCATGGCTACCGTCTGGACCACCACGAGAAGAAGAGGAAGAAGGAG
AGCCGTGAAGCCCACGAGCGCTCGCATAAAGCCAGGAAGATGATAGGCCTCAAAGCCAAAC
TCTACCACAAGCAAAGACACGCTGAGAAGATCCAGATGAAGAAGACGATTAAGATGCACGA
ACAGAGGAAGAGCAAACAGAAGGATGACGATAAAACACCAGAAGGGGCGGTGCCTGCTTA
CCTGCTGGACCGAGAGGGCCAATCACGTGCCAAAGTTCTGTCCAATATGATCAAACAGAAG
AGGAAAGAGAAAGCCGAAAGTGGGAGGTTCCCTTTACCGAAGGTTTCGAGCTCAGGGTGAAA
CCGAGGTTCTGAAAGTCATCCGAACAGGAAAGAGACAGAAAAAGGCCTGGAAGAGAATGG
TGACCAAAGTCTGTTTCGTAGGAGACGGTTTCACCCGCAAACCGCCCAAATATGAGCGCTTC
ATCAGACCTATGGGTTTGCGGTTTAACAAGGCACACGTCACCTCACCCTGAACTGAAGGCCAC
ATTCTGTTTGCCCATCCTGGGTGTGAAGAAGAACCCGTCCTCCTCGCTGTACACAACACTCG
GGGTCATCACGAAGGGAACGGTCATCGAGGTCAACGTCAGCGAGCTCGGATTGGTCACACA
GGGCGGAAAGGTCATCTGGGGTAAATACGCCAGGTGACGAATAACCCAGAAAATGATGGC
TGTATTAATGCCGTGTTGCTGGTTTAACGGAGACCCTGAAAGGTTTATTATTGAACTGTGCC
CCGAGTACAGCTGGAAAGTGCTTTTCTYTGAAAACCCCATCATCATCGTCATTATCCAGG
GAATATTGAAATTGCAAAGAAGATTTGAAGACCTCTGATGGAGTTTTGTTTCACCTTGCA
TTCGGATTCACGTGGATCAGAAATAAAGTGCTGTTATTTTCAA

```

Fig. 6.3 Zebrafish *nsa2* cDNA sequence and regions targeted by MOs in this investigation.  ORF;  MO1 target sequence;  MO2 target sequence.

Zebrafish embryos injected with *nsa2* MO1 display uncoupling of DEL epiboly from that of the EVL and YSL (Fig. 6.4) and delay in DEL epiboly (Fig. 6.5). At high blastoderm stage, *nsa2* morphants are indistinguishable from control embryos (Fig. 6.5, A and B) but as early as dome stage, a DEL epiboly delay is observed in all *nsa2* morphants ($n > 500$) (Fig. 6.5, C and D). As epiboly progresses, the difference in DEL epiboly between controls and *nsa2* morphants becomes more apparent (Fig. 6.5, E – L). In large-scale zebrafish mutagenesis screens mutants were found whose DEL epiboly arrests at approximately 70% and is uncoupled from EVL and YSL epiboly.

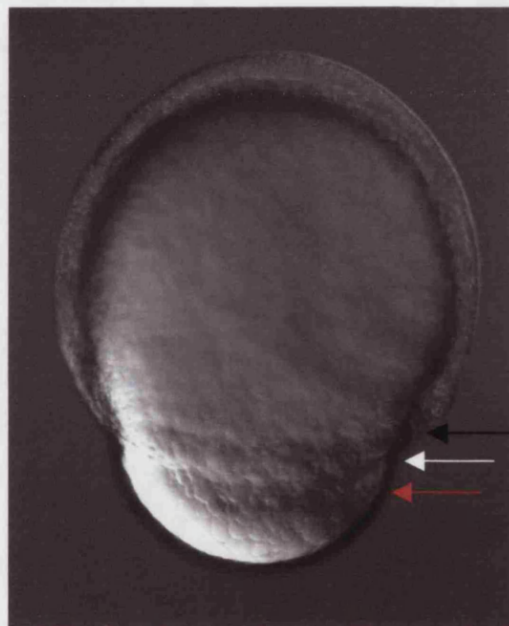


Fig. 6.4 Zebrafish embryos morphant for *nsa2* have uncoupled EVL, DEL and YSL epiboly. Live picture of *nsa2* zebrafish morphant embryo at a stage when controls are at tailbud stage; side view (dorsal to the right). Black arrow points at DEL leading edge; white arrow points at EVL leading edge; red arrow points at row of YSL nuclei. See Fig. 6.5 for control embryos at several extents of epiboly, where this uncoupling is never observed.

Two other phenotypes become apparent in *nsa2* morphant embryos: a frequent phenotype consists of rough appearance of the morphant blastoderm at approximately 50% epiboly (Fig. 6.5, F), in contrast to the smooth blastoderm of controls; less frequently, a gap appears between *nsa2* morphant blastoderms and the YSL, in contrast to controls, where this is never observed (data not shown).

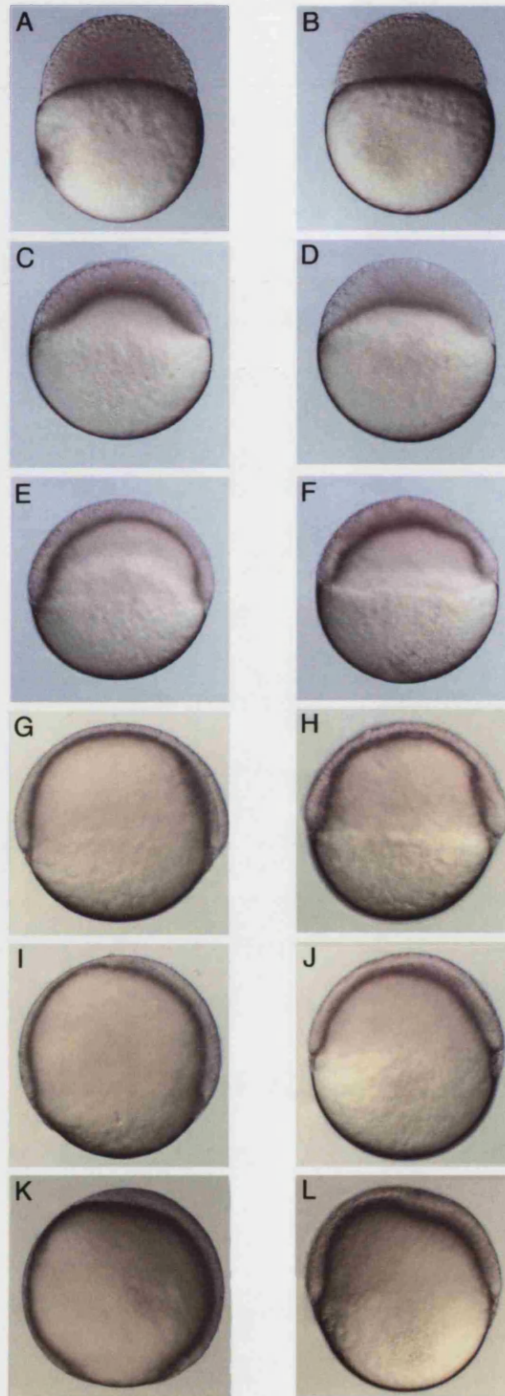


Fig. 6.5 Zebrafish embryos morphant for *nsa2* show DEL epiboly delay relative to controls. Live pictures of tightly-staged control (A, C, E, G, I, K) and *nsa2* morphant (B, D, F, H, J, L) zebrafish embryos. A, high blastoderm stage; B, *nsa2* morphant pictured at the same time as A; C, dome stage; D, *nsa2* morphant pictured at the same time as C; E, 50% epiboly; F, *nsa2* morphant pictured at the same time as E; G, 60% epiboly; H, *nsa2* morphant pictured at the same time as G; I, 70% epiboly; J, *nsa2* morphant pictured at the same time as I; K, 85% epiboly; L, *nsa2* morphant pictured at the same time as K. After shield stage, dorsal is depicted to the right.

At late epiboly stages, the DEL margin is seen lagging behind the YSL nuclei and the EVL margin lags behind that of the DEL (Fig. 6.4). The DEL epiboly phenotype can be described graphically. The black graph in Fig. 6.6 was taken from Kane and Adams, 2002 and data concerning the *nsa2* morphants, in red, was overlaid on it. The DEL epiboly phenotype of zebrafish *nsa2* morphants is distinct from that of the epiboly mutants in that the epiboly of the latter arrests at approximately 70% whereas that of *nsa2* morphants usually carries to completion (Fig. 6.6).

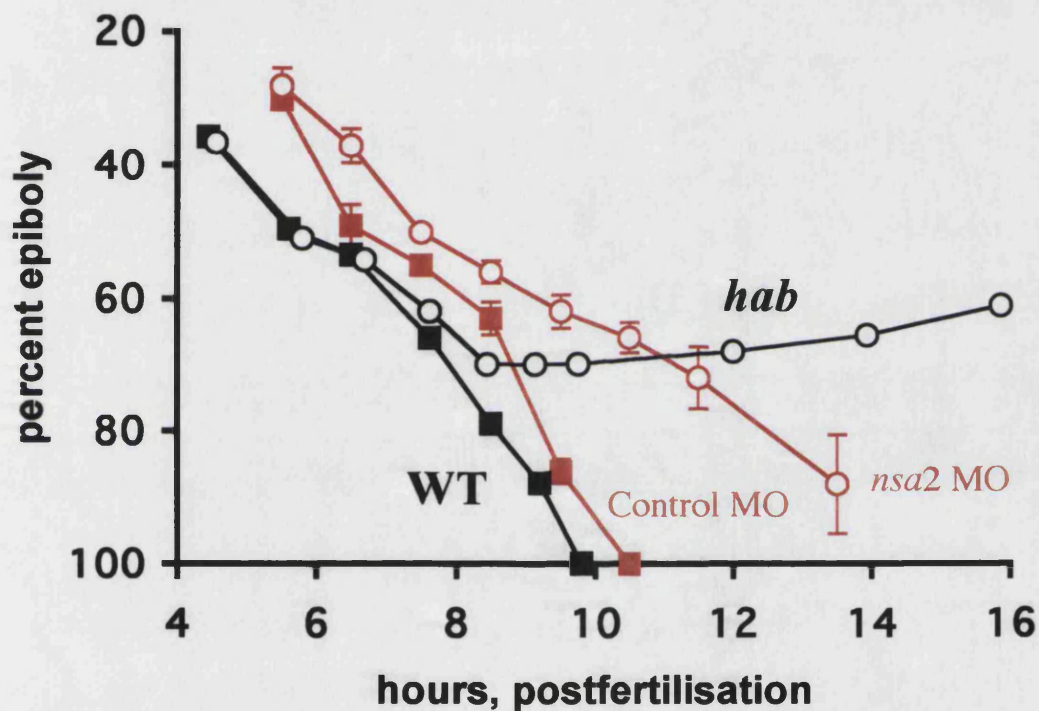


Fig. 6.6 Progression of DEL epiboly of zebrafish embryos morphant for *nsa2* compared with that of epiboly mutants. Red open circles, embryos injected with *nsa2* MO; red squares, sibling embryos injected with control MO; black squares, wild-type embryos; black open circles, *half-baked* (*hab*) mutant embryos. Data for the latter two sets was inferred from Kane *et al.*, 1996. Results in red are expressed as average \pm standard deviation of 12 embryos from one representative experiment.

To test whether the requirement for Nsa2 lay in the YSL, the lineage known to play an active role in epiboly, or in the blastoderm and EVL, thought to be passively towed by the YSL, I injected control and *nsa2* MO specifically into the YSL of embryos at 4 hpf.

The effect on the speed of DEL epiboly is shown graphically in Fig. 6.7. Embryos morphant for *nasa2* specifically in the YSL have slowed epiboly compared with controls but not as slow as that of embryos morphant for *nasa2* in every cell (Fig. 6.7), suggesting that Nsa2 function is required for normal epiboly in the YSL as well as in at least in one of the other two layers, DEL and EVL.

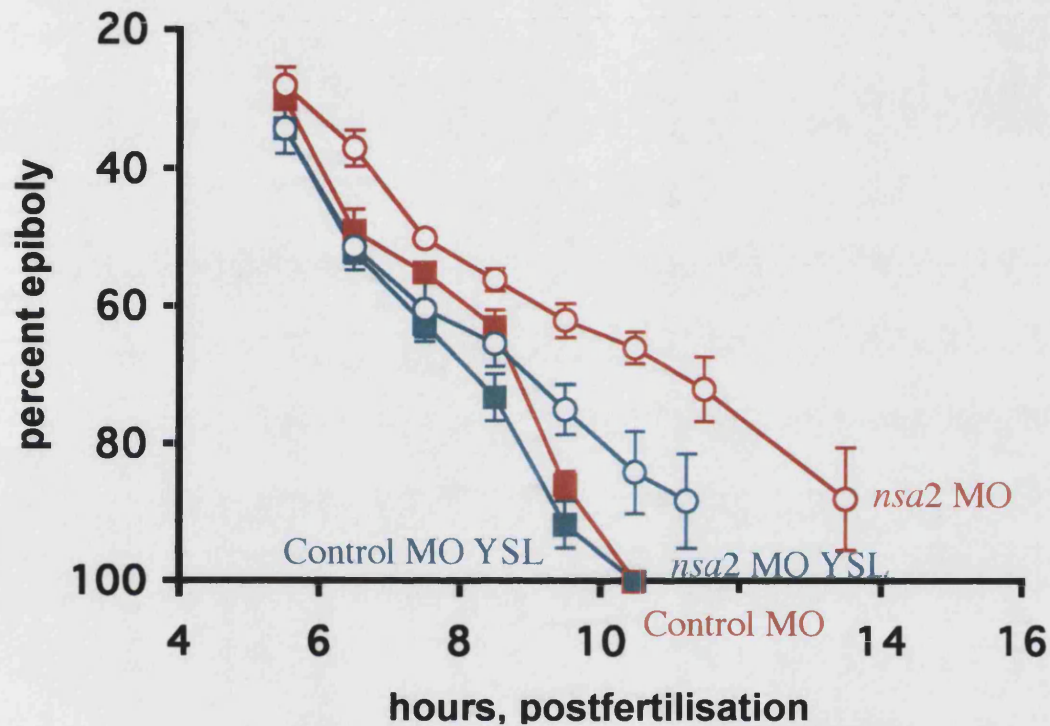


Fig. 6.7 Progression of DEL epiboly of zebrafish embryos morphant for *nasa2* specifically in the YSL compared with that of completely morphant embryos. Red open circles, embryos injected with *nasa2* MO; red squares, sibling embryos injected with control MO; blue open circles, embryos with YSL injected with *nasa2* MO; blue squares, sibling embryos with YSL injected with control MO. Results are expressed as average \pm standard deviation of 12 embryos from one representative experiment.

6.2.4 Embryos lacking *nasa2* have patterning defects

In addition to slower epiboly, *nasa2* morphant embryos develop with a variety of distorted shapes at late gastrulation ($n > 500$) (Fig. 6.8, C – J). The yolk cell is usually elongated relative to controls (Fig. 6.8, C – E; H – J) and the relatively normal internalisation coupled with the epiboly delay often results in accumulation of unusually large masses of the internal germ layers in the head region (Fig. 6.8, F, G). The

chordamesoderm is not straight as it normally would be, as if buckling under compression (Fig. 6.8, H).

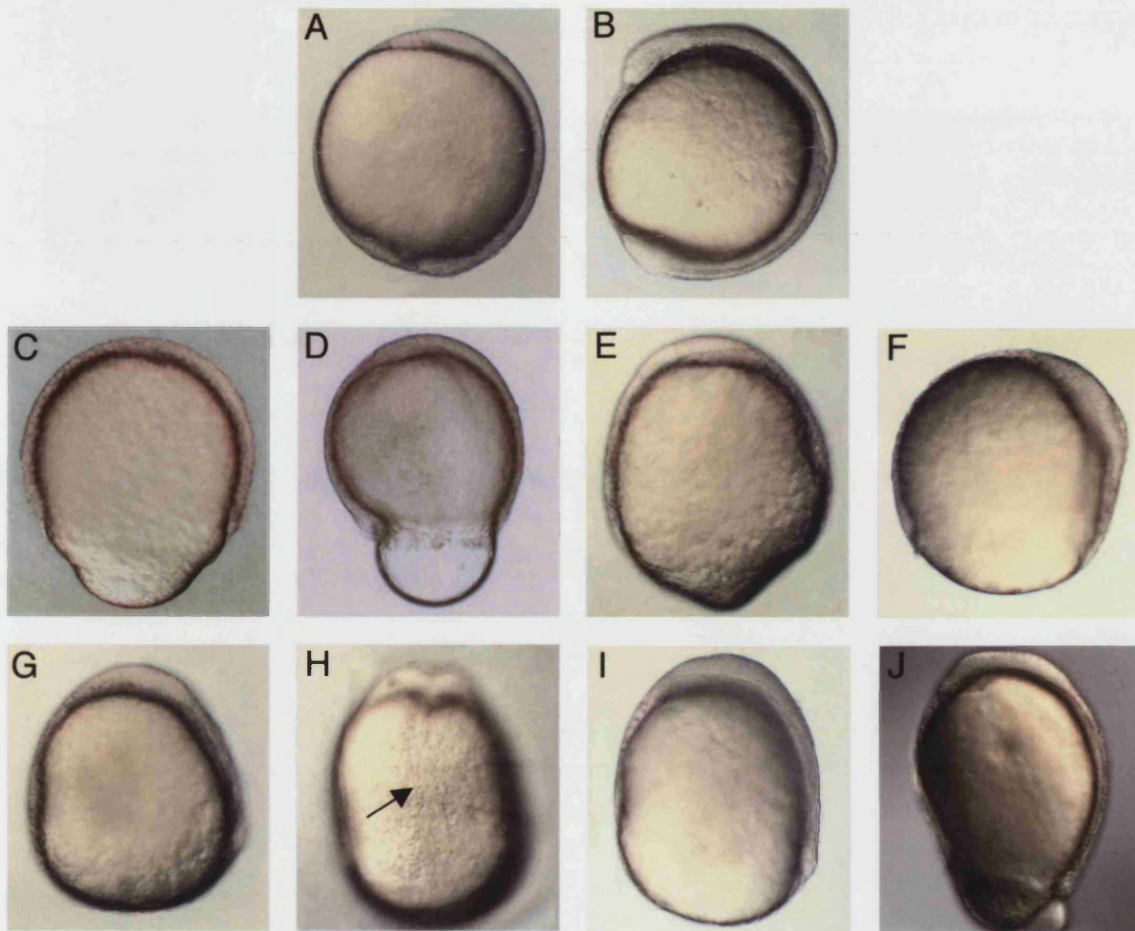


Fig. 6.8 Zebrafish embryos morphant for *nsa2* present a variety of distorted shapes at late gastrulation stages. A, control embryo at bud stage; B, control embryo at the 3 somite stage; C – J, *nsa2* morphants pictured at several times between controls being at bud and the 3 somite stage. All pictures are side views (anterior to the top) except for H, which is a dorsal view (anterior to the top). **Arrow in H** points at chordamesoderm.

Given the morphological patterning defects, I tested whether there were underlying defects in the expression of molecular markers. Since there are not many antibodies available for vertebrate whole-mount immunohistochemistry and because transcription may be reduced as a consequence of impaired translation (Shulman *et al.*, 1977), I examined the mRNA expression of a few regional markers of early development in control and *nsa2* morphant embryos ($n > 50$).

In general, both levels and patterns of expression differ between control and *nsa2* morphant embryos fixed at the same time. The differences, however, can often be accounted for by delayed development in *nsa2* morphants. Thus, a comparison across stages frequently reveals similar patterns of gene expression. This is the case for the presumptive chordamesoderm marker *flh*, which is expressed around the blastoderm margin of the pregastrula zebrafish embryo, enhanced on the future dorsal side, then in the organizer, followed by expression in the notochord (Talbot *et al.*, 1995); the mesodermal marker *fgf 8*, expressed in the gastrula margin, the dorsal organizer and the midbrain-hindbrain boundary (Furthauer *et al.*, 1997); the paraxial mesoderm marker *paraxial protocadherin C (PapC)*, Yamamoto *et al.*, 1998); *pax2b*, a marker of prospective midbrain (that then refines to the midbrain-hindrain boundary), of the otic placodes and spinal cord interneurons (Krauss *et al.*, 1991); and *hatching gland-1 (hgg1)*, an early hatching gland marker, a structure that is derived from the prechordal plate (Thisse *et al.*, 1994) (data not shown).

When comparing across stages so as to compare embryos with equivalent DEL epiboly, there are cases where the levels and domains are slightly lower and/or smaller in *nsa2* morphants than in controls. For example, *gsc*, which is expressed in the organizer hypoblast and prechordal plate (Stachel *et al.*, 1993), is reduced in both levels and number of expressing cells in *nsa2* morphants at all stages analysed (Fig. 6.9). Consistent with this observation, another prechordal plate marker gene, *dbx1a / hlx-1* (Fjose *et al.*, 1994), is reduced in *nsa2* morphants compared to controls (data not shown).

Upregulation of a few marker genes was also observed. Up to late epiboly, the levels of axial mesoderm marker *axial/hnf3 β* (Strahle *et al.*, 1993) are upregulated in *nsa2* morphants relative to controls (Fig. 6.10) as are those of the ventral epiblast marker *eve1* (Joly *et al.*, 1993; data not shown). Expression of the Nodal-responsive gene *bhikhari*, expressed in early mesendodermal cells (Vogel and Gerster, 1999) extends further towards the animal pole in morphants than in controls (Fig. 6.11). The zebrafish *bmp2b / swr* gene contains two domains of expression in the zebrafish gastrula, a ventro-lateral epiblast domain and a small patch of cells in the organizer (Nikaido *et al.*, 1997; Martinez-Barbera *et al.*, 1997; Kishimoto *et al.*, 1997). The first of these domains

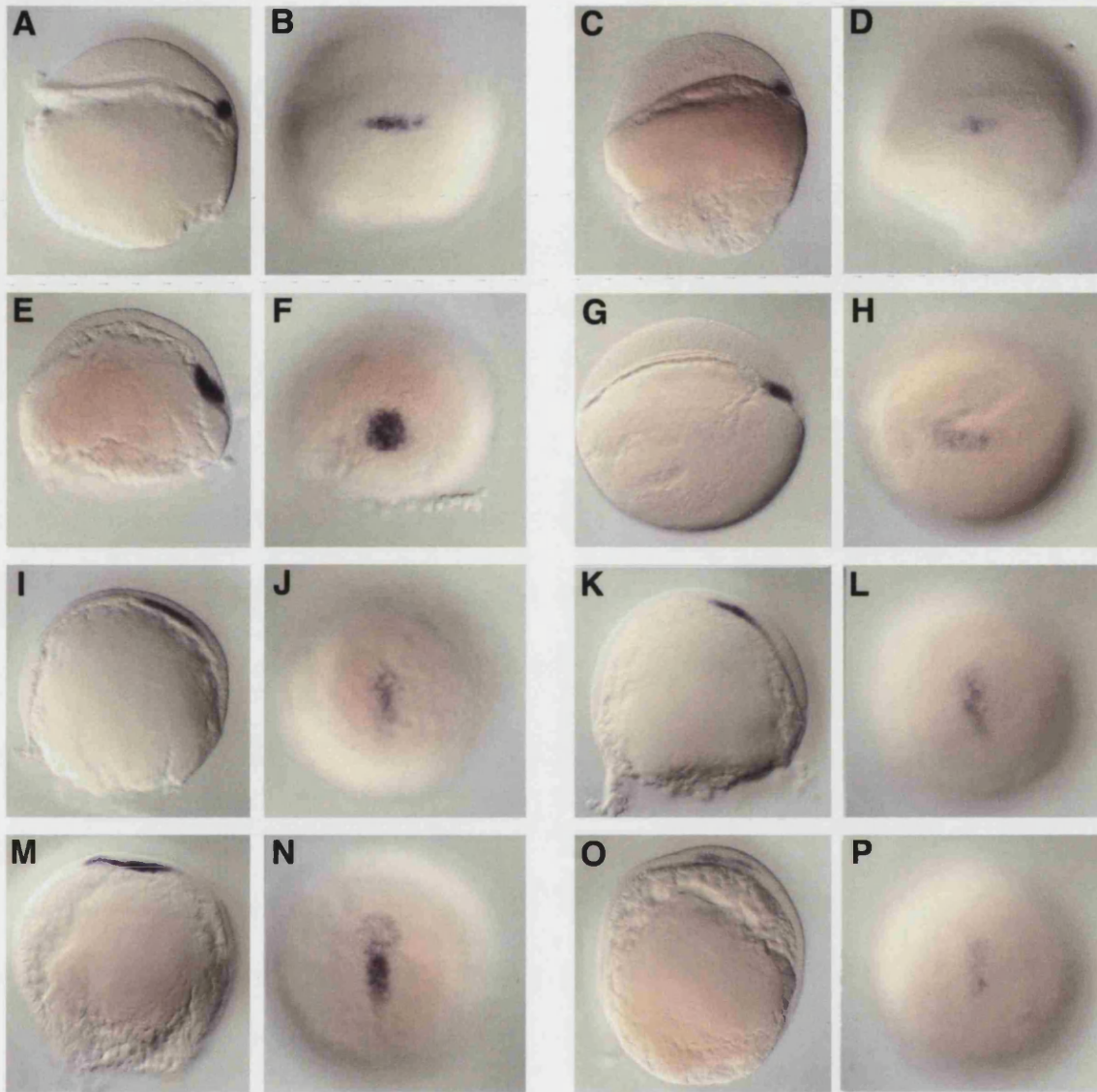


Fig. 6.9 Expression of *gsc* is reduced in *nsa2* morphant embryos relative to controls. Whole-mount *in situ* hybridisation of zebrafish embryos with *gsc* riboprobe. A, C, E, G, I, K, M, O are side views (dorsal to the right), and B, D, F, H, J, L, N, P are dorsal views. A – B, control embryo at dome stage; C – D, *nsa2* morphant pictured at same time as A – B; E – F, control embryo at shield stage; G – H, *nsa2* morphant pictured at same time as E – F; I – J, control embryos at 75% epiboly; K – L, *nsa2* morphant pictured at same time as I – J; M – N, control embryos 90% epiboly; O – P, *nsa2* morphant pictured at same time as M – N.

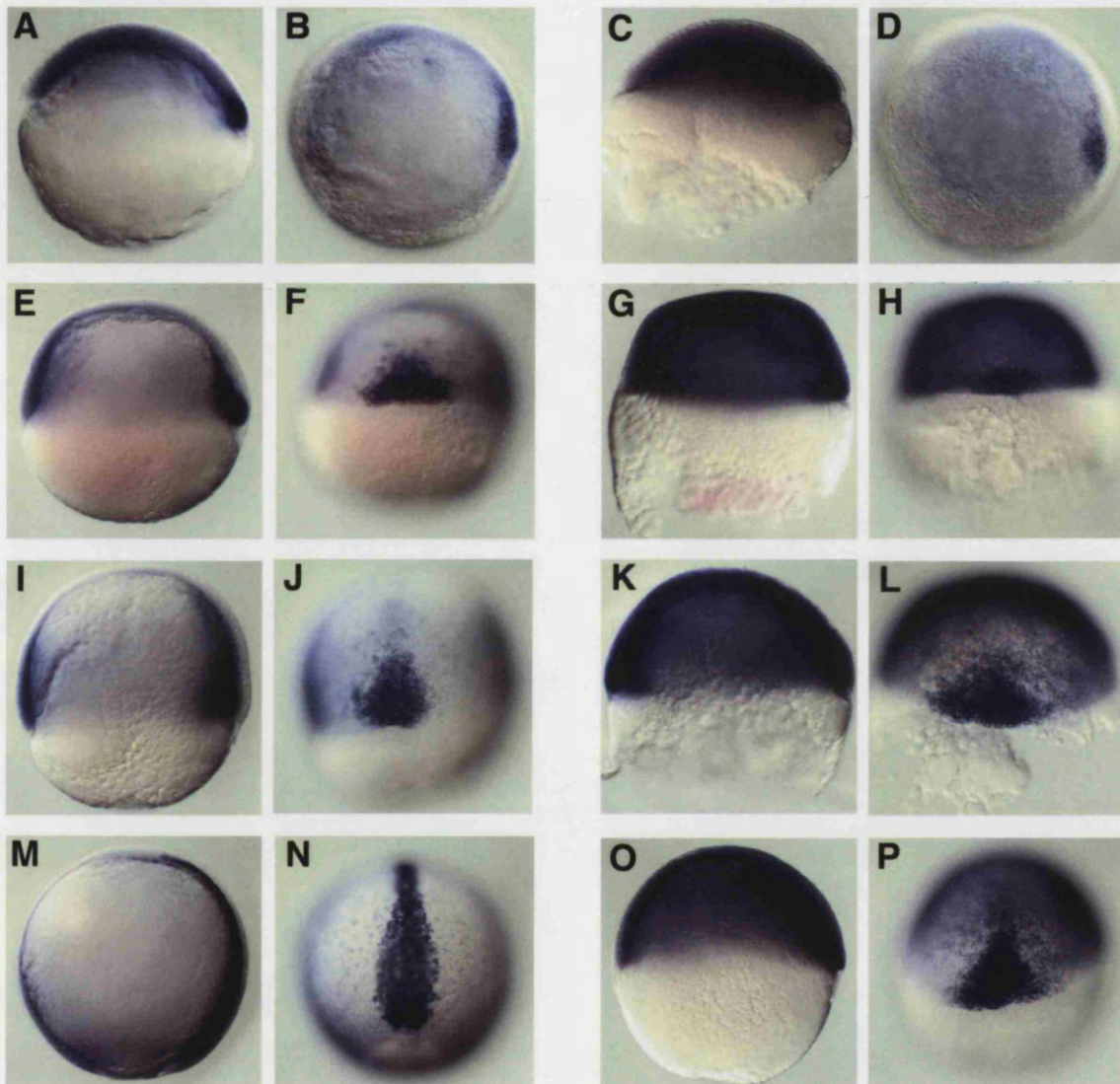


Fig. 6.10 Expression of *axial* is enhanced in *nsa2* morphant embryos relative to controls. Whole-mount *in situ* hybridisation of zebrafish embryos with *axial* riboprobe. A, C, E, G, I, K, M, O are side views (dorsal to the right), B and D are animal views (dorsal to the right), and F, H, J, L, N, P are dorsal views. A – B, control embryos at dome stage; C – D, *nsa2* morphant pictured at same time as A – B; E – F, control embryos at shield stage; G – H, *nsa2* morphant pictured at same time as E – F; I – J, control embryos at 75% epiboly; K – L, *nsa2* morphant pictured at same time as I – J; M – N, control embryos at 90% epiboly; O – P, *nsa2* morphant pictured at same time as M – N.

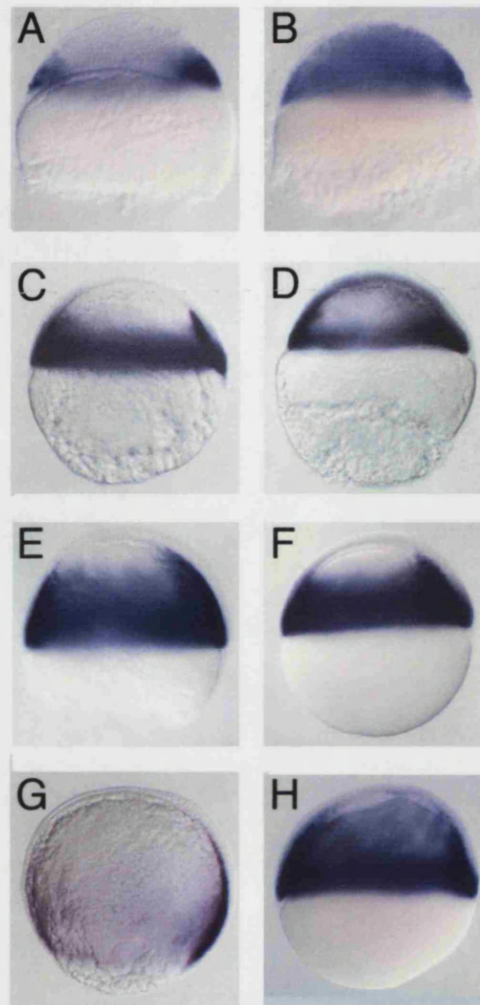


Fig. 6.11 Expression of *bhikhari* extends further anteriorly in *nsa2* morphant embryos than in controls. Whole-mount *in situ* hybridisation of zebrafish embryos with *bhikhari* riboprobe. All pictures are side views (dorsal to the right). **A**, control embryos at dome stage; **B**, *nsa2* morphant pictured at same time as **A**; **C**, control embryos at shield stage; **D**, *nsa2* morphant pictured at same time as **C**; **E**, control embryos at 60% epiboly; **F**, *nsa2* morphant pictured at same time as **E**; **G**, control embryos at 90% epiboly; **H**, *nsa2* morphant pictured at same time as **G**.

is expanded and more intense in *nsa2* morphants while the dorsal domain is normal to reduced in *nsa2* morphants when compared to stage-matched controls (Fig. 6.12).

Finally, there are differences in expression pattern that reflect the disjunction of processes that are normally coupled. Expression of *no tail (ntl) / brachyury*, an early mesodermal marker expressed in the blastoderm margin cells prior to involution and in the axial mesoderm and tail bud (Schulte-Merker *et al.*, 1992), suggests that cell internalisation ends before DEL epiboly is complete in *nsa2* morphants (Fig. 6.13). Up to the stage when controls are at approximately 90% epiboly, the expression of *ntl* in *nsa2* morphants is similar to that of controls at earlier stages (Fig. 6.13, A – H, K – L). However, while *ntl* is still expressed around the margin of 90% epiboly controls (Fig. 6.13, I – J), *nsa2* morphants with approximately 70% DEL epiboly (when controls are at bud stage) do not express *ntl* at the margin and display only axial expression of this gene (Fig. 6.13, O – P). This is consistent with the compressed appearance of the axial mesoderm and the notochord, frequently observed in *nsa2* morphants (Fig. 6.8, H; Fig. 6.16, R).

6.2.5 The epiboly phenotype of *nsa2* is analogous to that of *Minute* ribosomal proteins

To test whether the phenotype of *nsa2* morphants could be explained by impaired ribosome function, I disrupted expression of two ribosomal proteins. Loss-of-function of orthologous proteins in *Drosophila* results in *Minute* phenotypes. RpS5 is a constituent of the small ribosomal subunit and results in a weak *Minute* phenotype; RpL19 is a constituent of the large ribosomal subunit and results in a strong *Minute* phenotype (Morata and Ripoll, 1975). The effect of Rp depletion on the speed of DEL epiboly is shown graphically in Fig. 6.14. Zebrafish embryos morphant for *RpS5* have a subtle delay in DEL epiboly. In contrast, abrogation of RpL19 causes the rate of epiboly to be reduced to one-half of that of control embryos and is indistinguishable from loss of *Nsa2* (Fig. 6.14).

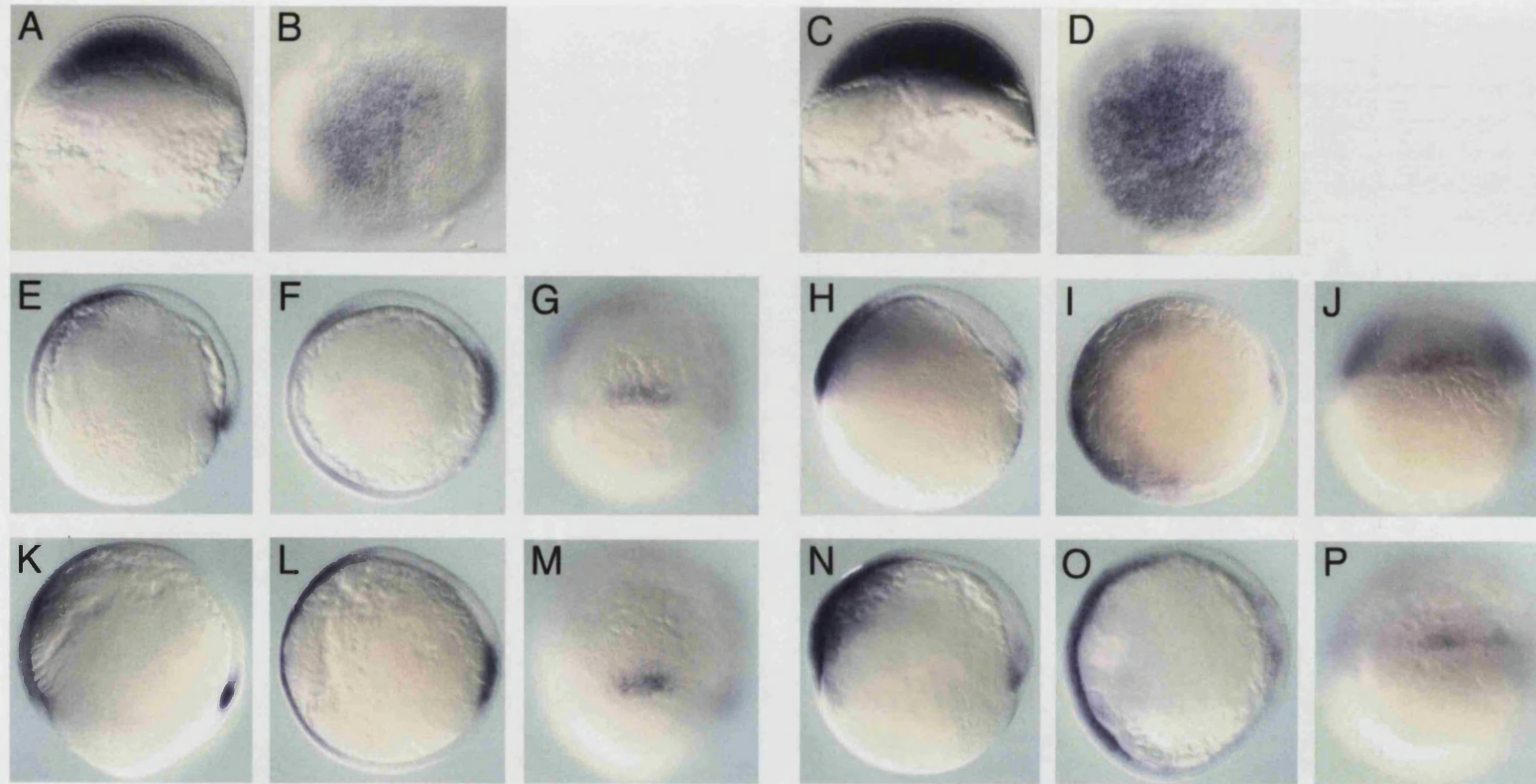


Fig. 6.12 The ventral domain of *swr* expression is upregulated in early *nsa2* morphants whereas the organizer domain of expression is not. Whole-mount *in situ* hybridisation of zebrafish embryos with *swr* riboprobe. A, C, E, H, K, N, are side views (dorsal to the right); B, D, F, I, L, O, are animal views (dorsal to the right); G, J, M, P, are dorsal views. A – B, control embryo at dome stage; C – D, *nsa2* morphant pictured at same time as A – B; E – G, control embryos at 60% epiboly; H – J, *nsa2* morphant pictured at same time as E – G; K – M, control embryos at 75% epiboly; N – P, *nsa2* morphant pictured at same time as K – M.

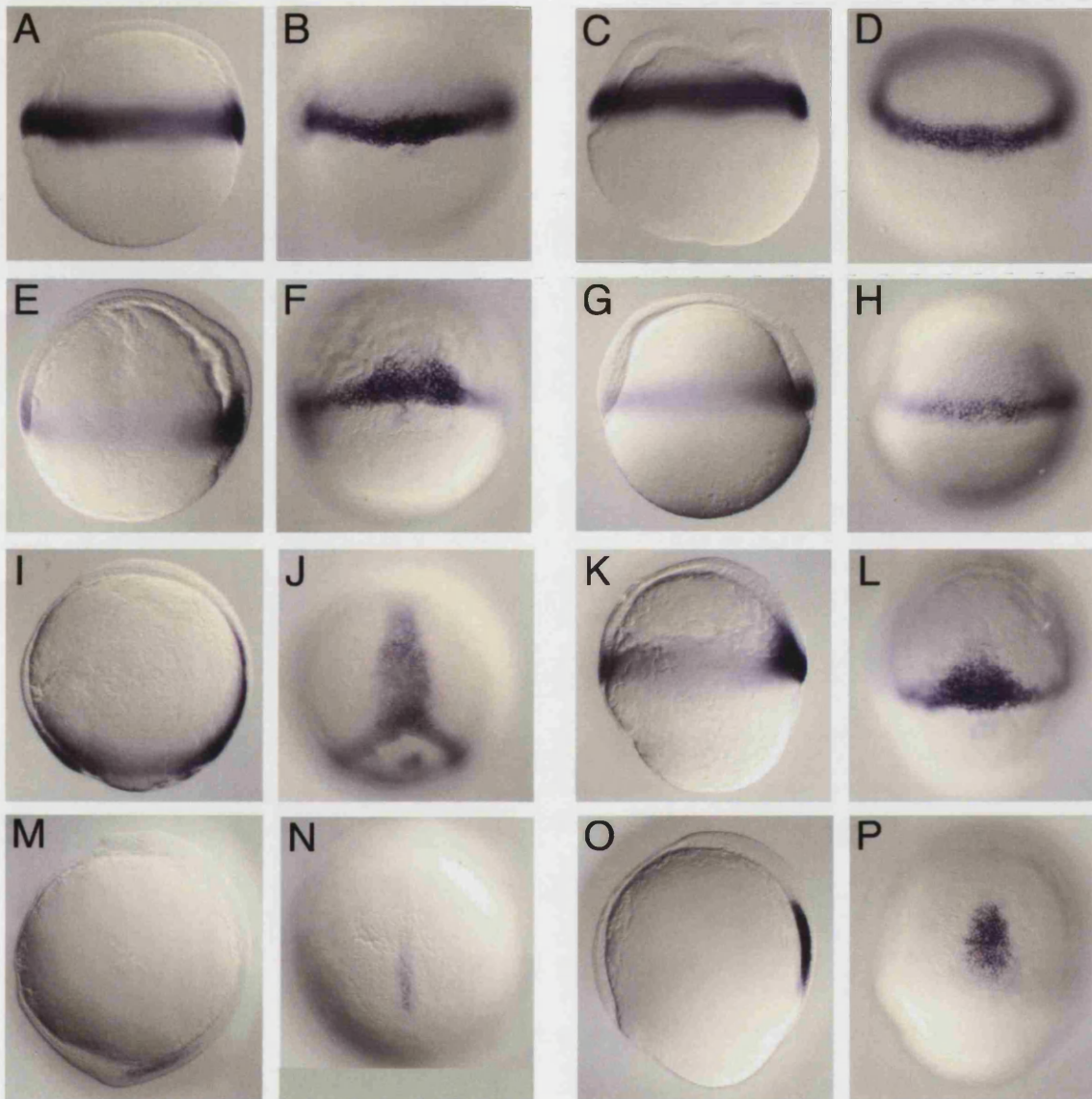
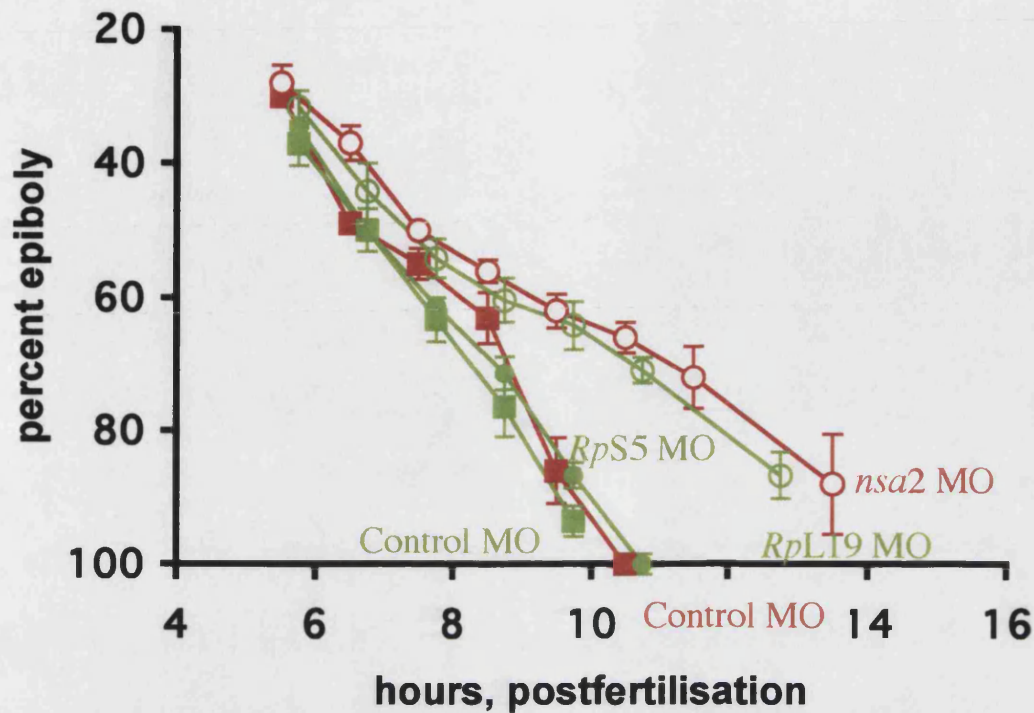


Fig. 6.13 DEL epiboly is more delayed than cell internalisation in *nsa2* morphants. Whole-mount *in situ* hybridisation of zebrafish embryos with *ntl* riboprobe. A, C, E, G, I, K, M, O are side views (dorsal to the right), and B, D, F, H, J, L, N, P are dorsal views. A – B, control embryo at shield stage; C – D, *nsa2* morphant pictured at same time as A – B; E – F, control embryo at 60% epiboly; G – H, *nsa2* morphant pictured at same time as E – F; I – J, control embryos at 90% epiboly; K – L, *nsa2* morphant pictured at same time as I – J; M – N, control embryos bud stage; O – P, *nsa2* morphant pictured at same time as M – N.



F

ig. 6.14 Progression of DEL epiboly of zebrafish embryos morphant for ribosomal proteins compared with that of *nsa2* morphants. Red open circles, embryos injected with *nsa2* MO; red squares, sibling embryos injected with control MO; green open circles, embryos injected with *RpL19* MO; green full circles embryos, injected with *RpS5* MO; green squares, sibling embryos injected with control MO. Red squares are control for *nsa2* MO and green squares are control for *Rp* MOs. Results are expressed as average \pm standard deviation of 12 embryos from one representative experiment.

As a control I tested whether loss of another essential protein, involved in a process other than translation, would produce an epiboly phenotype. Previous work in the lab showed that the *sneezy* locus encodes the Coatamer α subunit ($Cop\alpha$) and that the *sneezy* mutation can be recapitulated by *cop\alpha* MO injection (Coutinho *et al.*, 2003). Coatamer is an essential vesicular coating system involved in retrograde transport from the Golgi to the endoplasmic reticulum (reviewed in Cosson and Letourneur, 1997). The effect of *cop\alpha* MO injection on the speed of DEL epiboly is shown graphically in Fig. 6.15. Depletion of $Cop\alpha$ does not affect the rate of epiboly (Fig. 6.15).

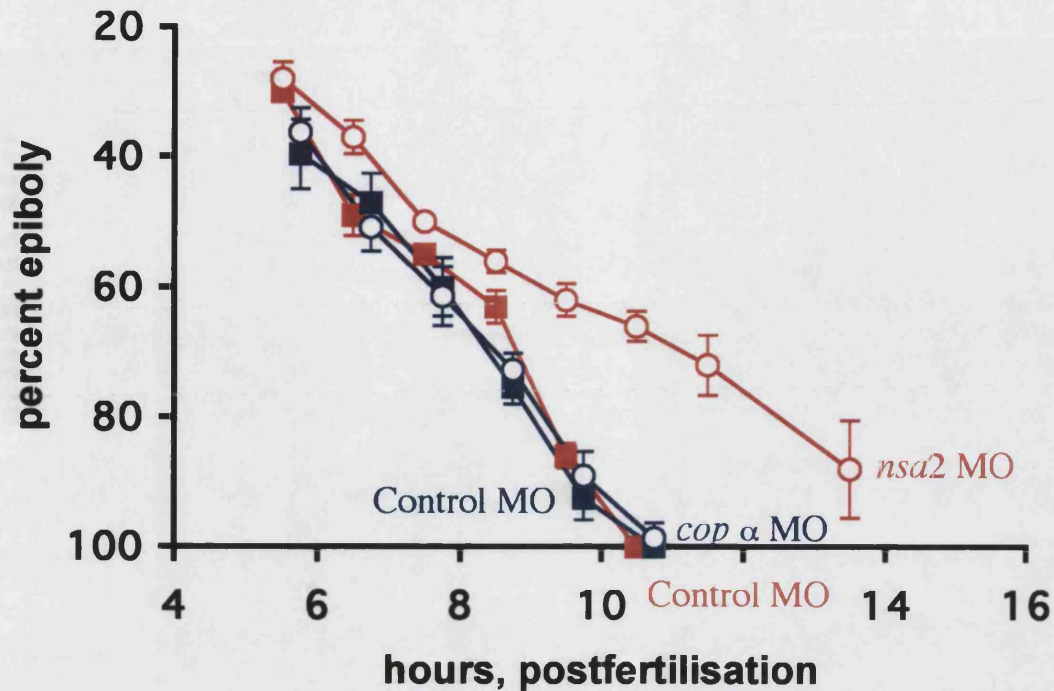
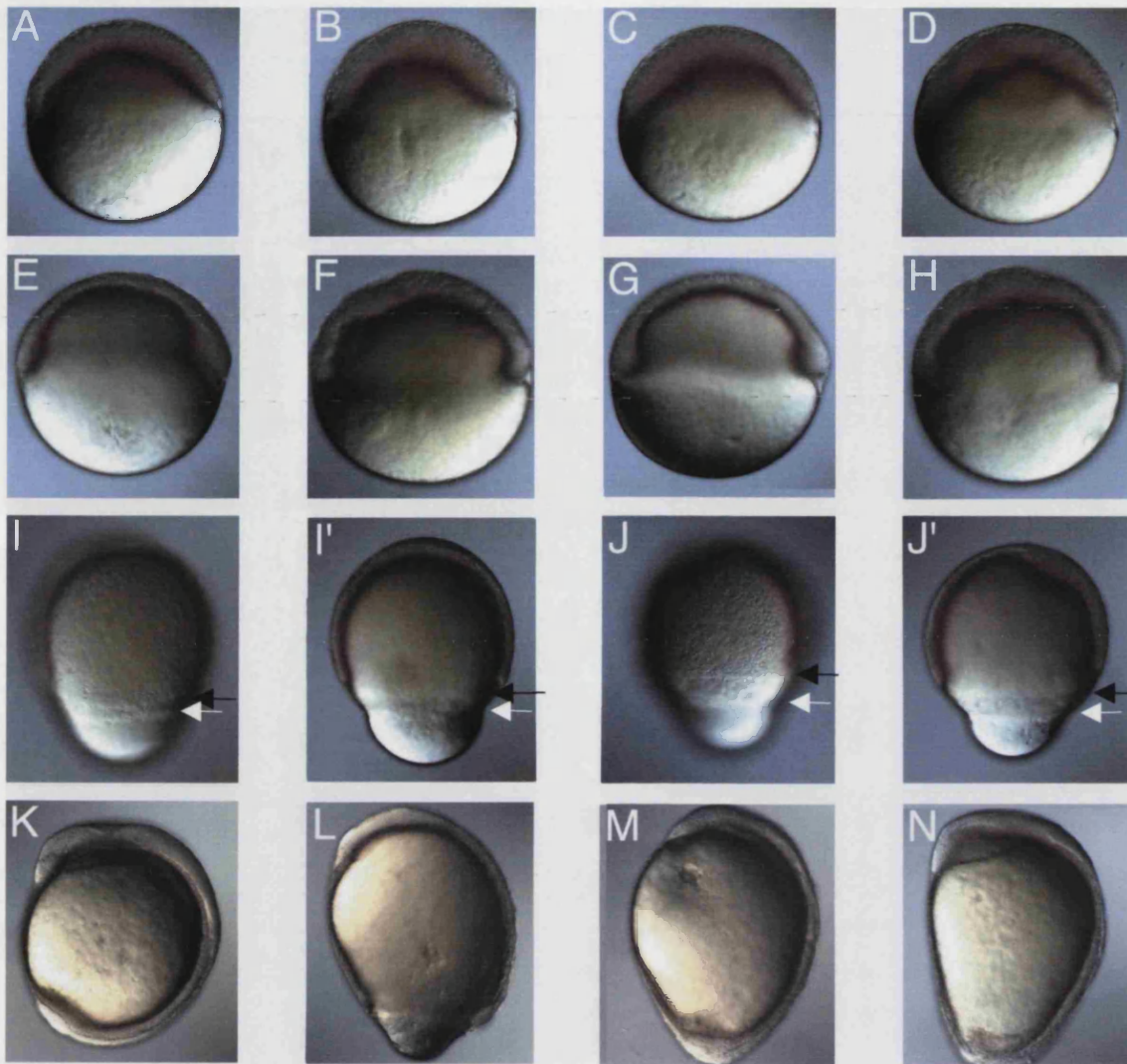


Fig. 6.15 Progression of DEL epiboly of zebrafish embryos morphant for *cop* α compared with that of *nsa2* morphants. Red open circles, embryos injected with *nsa2* MO; red squares, sibling embryos injected with control MO; blue open circles, embryos injected with *cop* α MO; blue squares, sibling embryos injected with control MO. Red squares are control for *nsa2* MO and blue squares are control for *cop* α MO. Results are expressed as average \pm standard deviation of 12 embryos from one representative experiment.

6.2.6 Loss of Nsa2 and Minute Rps produce similar morphological defects

If *nsa2* were to be a vertebrate *Minute* locus it should share loss-of-function phenotypes with *Rp* loci such as *RpS5* and *RpL19*. *RpL19* morphants display all the morphological features characteristic of *nsa2* morphants ($n > 100$) whereas *RpS5* morphants display some of them ($n > 100$). Similarly, the *Drosophila RpS5 Minute* phenotype is less severe than the *RpL19* phenotype. By 30% epiboly, the blastoderm of *nsa2* and *RpL19* morphants often has a rough appearance (Fig. 6.16, B and D) whereas the blastoderm of *RpS5* morphants is indistinguishable from controls (Fig. 6.16, A and C). This is more apparent by ~50% epiboly (Fig. 6.16, E – H). From the stage when DEL epiboly is at ~60%, uncoupling between DEL and EVL epiboly becomes apparent in both *nsa2* and *RpL19*, but not *RpS5*, morphants (Fig. 6.16, I, I', J, J'). Like *nsa2* morphants, both *Minute* morphants have an elongated morphology by late gastrulation (Fig. 6.16, L – N),



(continued on next page)

Fig. 6.16 Zebrafish embryos morphant for *nsa2*, *RpS5* and *RpL19* present analogous morphological phenotypes. A, E, K, O, P, Q, control embryos; B, F, I, I', L, R, S, T, embryos morphant for *nsa2*; C, G, M, U, V, W, embryos morphant for *RpS5*; D, H, J, J', N, X, Y, Z, embryos morphant for *RpL19*. A, side view of control embryo at 30% epiboly; B – D, side views of morphants pictured at the same time as A; E, side view (dorsal to the right) of control embryo at shield stage; F – H, side views (dorsal to the right) of morphants pictured at the same time as E; I, J, side views (dorsal to the right) of morphant embryos where DEL epiboly is 60% – surface focus; I', J', side views (dorsal to the right) of same morphant embryos as in I and I', respectively – optical sections; K, side view (anterior to the top) of control embryo at the 3 somite-stage; L, M, side views (anterior to the top) of morphant embryos pictured at the same time as K; N, side view (anterior to the top) of morphant pictured when controls were at

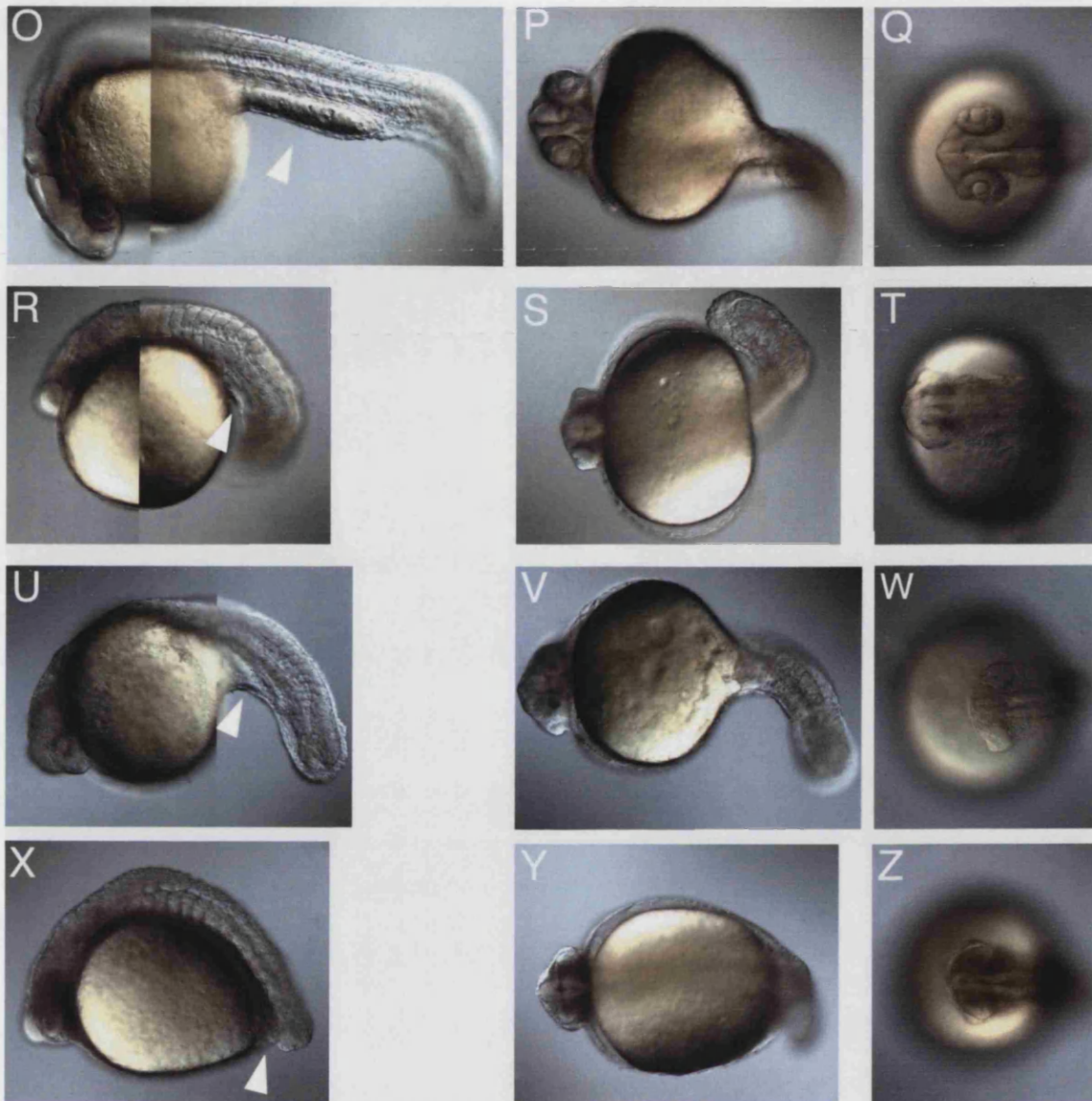


(Fig. 6.16 cont.)

the 7 somite-stage; **O – Q**, control embryo at 28 hpf; **O**, side view (anterior to the left); **P**, frontal view; **Q**, dorsal view of forebrain; **R – T**, *nsa2* morphant at 28 hpf; **R**, side view (anterior to the left); **S**, frontal view; **T**, dorsal view of forebrain; **U – W**, *RpS5* morphant at 28 hpf; **U**, side view (anterior to the left); **V**, frontal view; **W**, dorsal view of forebrain; **X – Z**, *RpL19* morphant at 28 hpf; **X**, side view (anterior to the left); **Y**, frontal view; **Z**, dorsal view of forebrain. In **I, I', J, J'**, **black arrows** point at DEL leading edge and **white arrows** point at EVL leading edge. In **O, R, U, X**, **arrowheads** point at yolk extension or its absence.

although *RpL19* morphants usually adopt this shape later than the other two (Fig. 6.16, K – N). Later, all three morphants have wavy notochords and U-shaped somites (Fig. 6.16, R, U, X), significantly reduced or absent yolk extensions (arrowheads in Fig. 6.16, O, R, U, X) delayed and deficient head patterning as well as massive cell death in the CNS, seen as darkened regions in morphant embryos (Fig. 6.16, R – Z). All three morphants display enhanced cell death in the optic cups (Fig. 6.15, S, T, V, W, Y, Z), suggesting that this region is particularly sensitive to impaired protein synthesis. On the second day of development, survivors of all three morphants are considerably smaller, in all dimensions, than controls (Fig. 6.16, O – Z).

Given that the *Drosophila Minute* phenotypes are usually haploinsufficient (reviewed in Lambertsson, 1998), I used a half dose of MO to, testing whether this would also produce reduced body size in morphants. Zebrafish embryos injected with 5 ng of *nsa2* MO are smaller than controls at 1 day of development (Fig. 6.17, C – D). The same is observed when 10 ng of the less efficient *nsa2* MO2 (Fig. 6.3) were used (data not shown).

Fig. 6.17 Zebrafish embryos injected with 5 ng of *nsa2*, *RpS5* or *RpL19* MO are smaller than controls. A – B, control embryos at 26 hpf; C – D, control embryos at 48 hpf; E – F, embryos injected with 5 ng of *nsa2* MO1, at 26 hpf; G – H, embryos injected with 5 ng of *nsa2* MO1, at 48 hpf; I – J, embryos injected with 5 ng of *RpL19* MO, at 26 hpf; K – L, embryos injected with 5 ng of *RpL19* MO, at 48 hpf; M – N, embryos injected with 5 ng of *RpS5* MO, at 26 hpf; O – P, embryos injected with 5 ng of *RpS5* MO, at 48 hpf. A, C, E, G, I, K, M O are dorsal-anterior views; B, D, F, H, J, L, N, P are side views (anterior to the left). All pictures are at the same magnification.

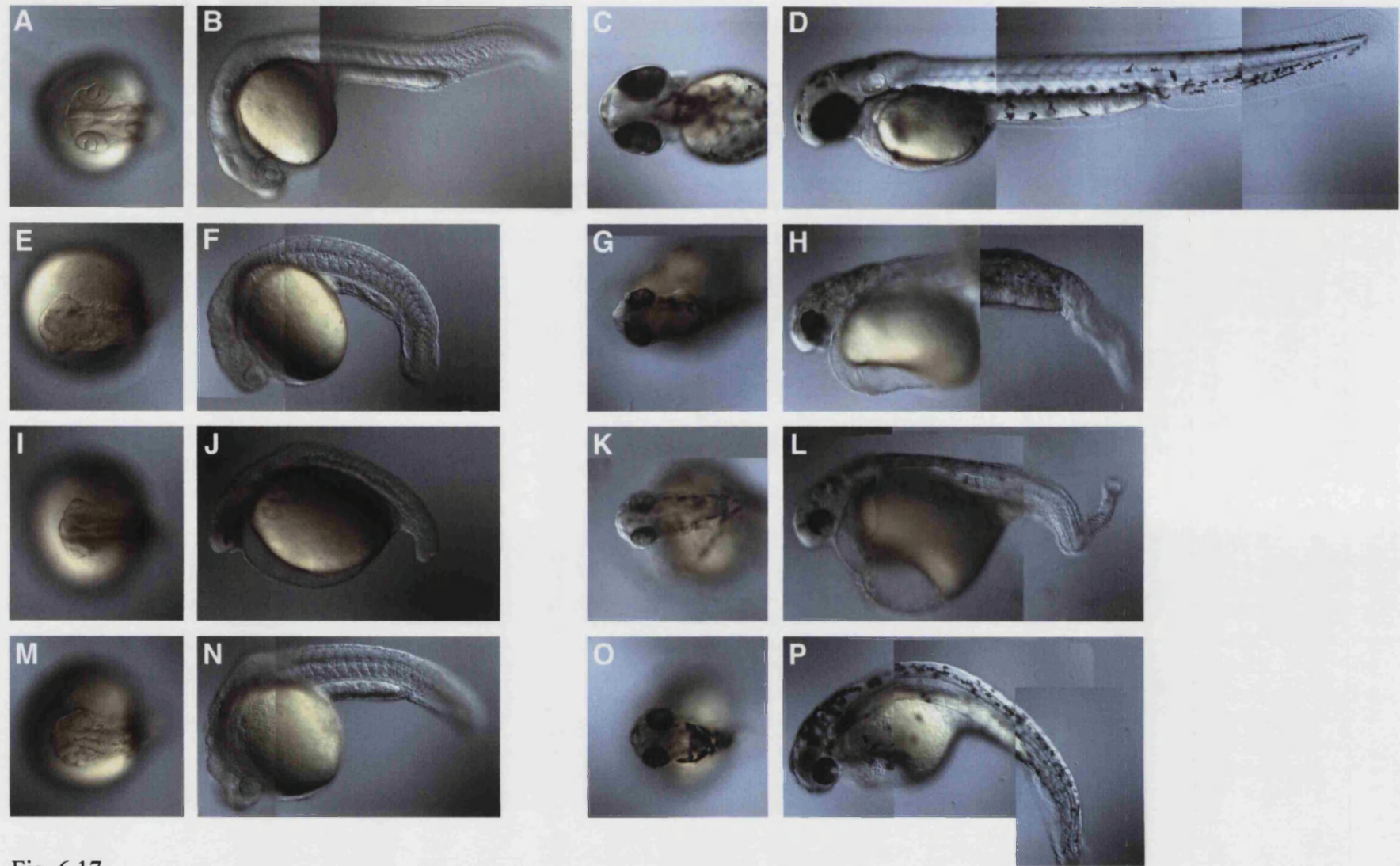


Fig. 6.17

6.2.7 Is the fly orthologue of *nsa2* a *Minute*?

The epiboly phenotype of *nsa2* morphants is strikingly similar to that of a strong *Minute* morphant (*RpL19*). I therefore wanted to test whether loss-of-function of the fly orthologue of *nsa2* would produce a *Drosophila Minute* phenotype. The fly orthologue of *nsa2* (Fig. 6.1), also known as *Ip259*, lies in the region to which an uncloned *Minute*, *M(2)31A*, has been mapped cytogenetically (Fig. 6.18). This is a very gene-rich region of the fly genome (~100 genes within 170 kb) and contains at least two other candidate *Minute* genes, coding for *mRpS7* and *RpS27A*.

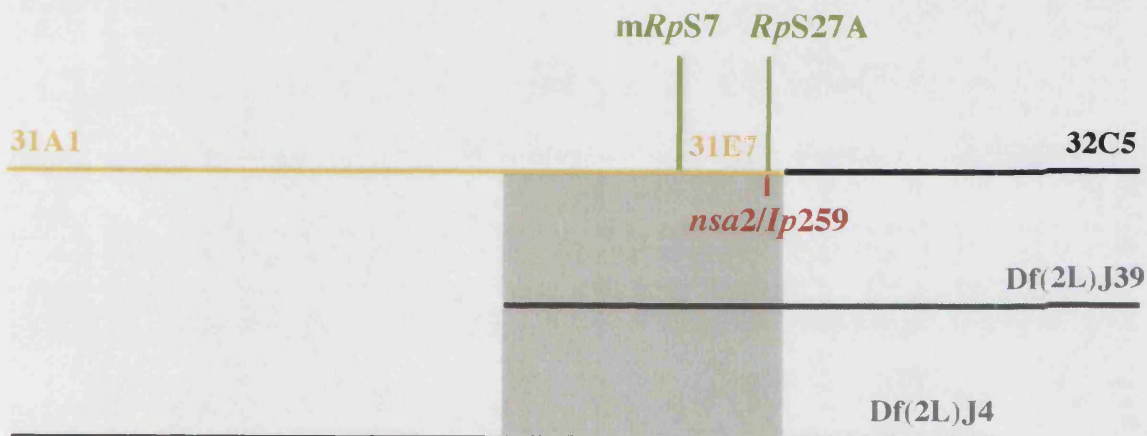


Fig. 6.18 Region of *Drosophila melanogaster* genome to which the *Minute* mutation *M(2)31A* has been mapped. *M(2)31A* has been mapped cytogenetically to zone 31A1 – 31E7, depicted in yellow. There are two deficiencies in this region which uncover the *Minute* phenotype, *Df(2L)J39* and *Df(2L)J4*, depicted in dark grey. The intersection of all three sections is shadowed in green. This intersection region spans 170 kb and contains approximately 100 genes. Three of these, which are good candidates for being mutated in *M(2)31A* are highlighted: *mRpS7* and *RpS27A* encode ribosomal proteins; *nsa2/Ip259* encodes a protein involved in the biogenesis of the 60S ribosome subunit.

I searched for *mRpS7*, *RpS27A* and *nsa2/Ip259* mutant alleles for complementation with the *M(2)31A Minute* mutation. Unfortunately, there are no mutant alleles of

mRpS7. There are, three mutant alleles for *RpS27A*, two of which are specific for this gene (*RpS27A*⁰⁴⁸²⁰ and *RpS27A*^{mf_s31}) and one (*RpS27A*^P) that could also affect the expression of *nsa2/Ip259* (Fig. 6.19). The latter mutant allele is the only one available for *nsa2/Ip259* (*Ip259*^P). This mutation is a P-element insertion 7 bp upstream of the 5'UTR common to both *RpS27A* and *nsa2/Ip259* (Fig. 6.19) and is allelic to *RpS27A*^{mf_s31}. Its effect on *nsa2* transcription, however, has not been assessed. I performed complementation tests between *RpS27A*⁰⁴⁸²⁰, *RpS27A*^{mf_s31}, *RpS27A*^P/*nsa2*^P/*Ip259*^P and *M(2)31A* to address whether the *Minute* phenotype produced by *M(2)31A* could be explained by loss of *RpS27A* or *Nsa2/Ip259* (Table 6.1).

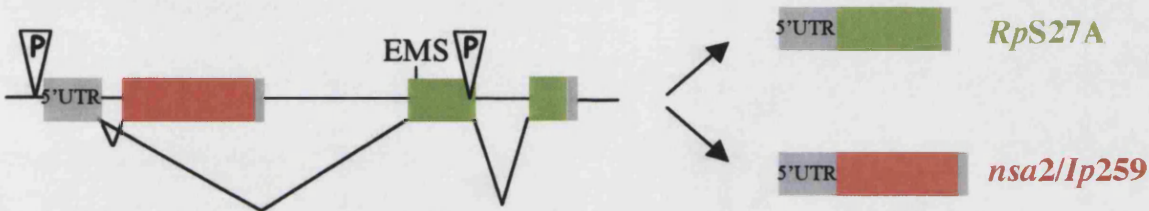


Fig. 6.19 Genomic locus of *Drosophila melanogaster* *RpS27A* and *nsa2/Ip259*.

RpS27A and *nsa2/Ip259* share the same 5' UTR (larger grey box) but no coding sequence. *Nsa2/Ip259* is encoded in an exon (red) that lies within the first intron of the *RpS27A* gene. The coding sequence for *RpS27A* resides in two exons (green). There are two mutations in this locus that specifically disrupt *RpS27A* (represented by ∇ and "EMS", which represent the P-element insertion and ethyl methane-sulfonate mutation, respectively) and one that consists of a P-element insertion 7 bp upstream of the 5'UTR common to the *RpS27A* and *nsa2/Ip259* genes, which possibly disrupts both. The sites of P-element insertion are depicted in the approximately correct position whereas the site of EMS mutation has not been defined but is depicted just for clarity.

As expected, *M(2)31A* over *M(2)31A* results in lethality, and so does *RpS27A*⁰⁴⁸²⁰ over *RpS27A*⁰⁴⁸²⁰. *RpS27A*^{mf_s31} is a hypomorphic mutation since homozygous *RpS27A*^{mf_s31} flies are viable. Homozygous *RpS27A*^{mf_s31} flies do, however, exhibit a *Minute* phenotype. As expected, *RpS27A*⁰⁴⁸²⁰ and *RpS27A*^{mf_s31} fail to complement. *RpS27A*⁰⁴⁸²⁰ and *RpS27A*^{mf_s31} complement the *M(2)31A* *Minute*, indicating that the *M(2)31A*

Table 6.1 Complementation test between *RpS27A*⁰⁴⁸²⁰, *RpS27A*^{mfs31}, *RpS27A*^P/*nsa2*^P/*Ip259*^P and *M(2)31A* in *Drosophila melanogaster*

	<i>M(2)31A</i>	<i>RpS27A</i> ^{mfs31}	<i>RpS27A</i> ⁰⁴⁸²⁰	<i>RpS27A</i> ^P / <i>nsa2</i> ^P / <i>Ip259</i> ^P
<i>M(2)31A</i>	Lethal			
<i>RpS27A</i> ^{mfs31}	Complement	Homozygous <i>Minute</i>		
<i>RpS27A</i> ⁰⁴⁸²⁰	Complement	Fail to complement	Lethal	
<i>RpS27A</i> ^P / <i>nsa2</i> ^P / <i>Ip259</i> ^P	Complement	Fail to complement*	Fail to complement	Lethal

* Mottus *et al.*, 1997

phenotype is not due to disruption of *RpS27A*. As expected, *RpS27A*^P/*nsa2*^P/*Ip259*^P fails to complement *RpS27A*⁰⁴⁸²⁰. However, it too complements *M(2)31A*. Therefore, if the *RpS27A*^P/*nsa2*^P/*Ip259*^P mutation does affect *nsa2* expression, it seems that the *M(2)31A* phenotype is not caused by a mutation in *nsa2*. To test whether *nsa2* expression is affected in *RpS27A*^P/*nsa2*^P/*Ip259*^P embryos, we will perform RT-PCR and Western blot analysis using an antibody raised against the protein (Mottus *et al.*, 1997).

6.2.8 Phenotypes of *nsa2* morphant cells

6.2.8.1 Cells morphant for *nsa2* undergo apoptosis

Loss of *nsa2* in zebrafish leads to massive CNS cell death, especially during somitogenesis stages. To test whether *nsa2* morphant cells undergo apoptosis, I performed TUNEL assays on *nsa2* morphant zebrafish embryos. At 24 hpf there is considerably more TUNEL staining in surviving *nsa2* morphants than in controls (n > 12) (Fig. 6.20). Control embryos have a few stained cells scattered throughout the embryo, especially in the head and tail tip regions (Fig. 6.20, A – B) whereas *nsa2* morphant embryos show heavy staining throughout (Fig. 6.20, C – F). More specific methods for apoptosis detection can be used to further assess whether *nsa2* morphant cells are indeed dying in this way (for example, staining with anti-cleaved caspase-3 antibody).

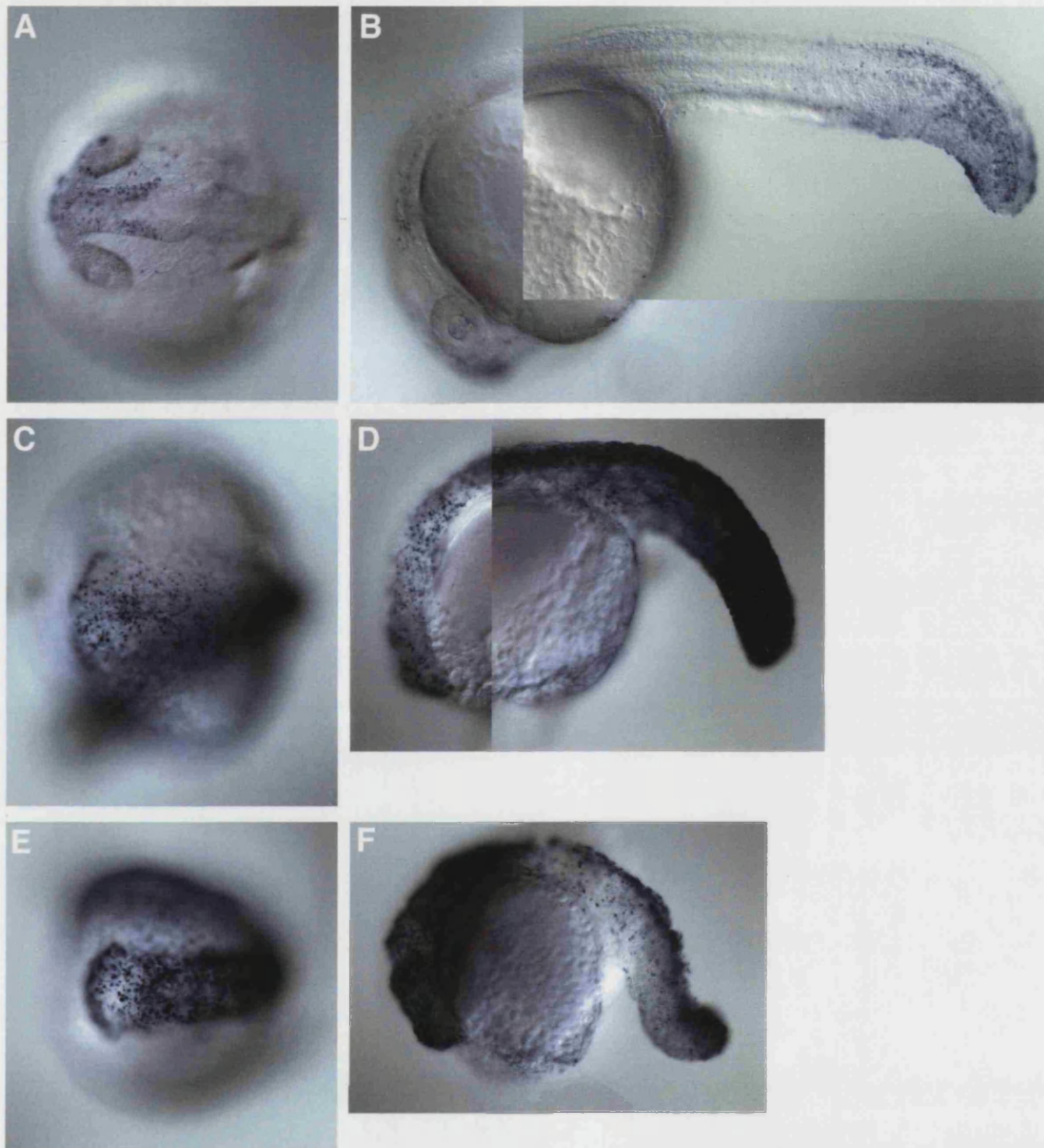


Fig. 6.20 Cells morphant for *nsa2* die by apoptosis. TUNEL staining of 24 hpf embryos. **A – B**, control embryos; **C – D**, **E – F**, two distinct *nsa2* morphant embryos. **A**, **C**, **E** are dorsal-anterior views of the embryos in **B**, **D**, **F**, respectively, which are shown in side views (anterior to the left).

6.2.8.2 TEM study of *nsa2* morphant cells of the epiboly-stage zebrafish embryo

Having observed an apparent detachment of blastoderm cells from the yolk-cell in *nsa2* morphants, I wanted to examine cell-layer interaction at the ultrastructural level. In addition, several aspects of cellular physiology, such as the number and arrangement of ribosomes, might be directly assessed by TEM. 12 morphant and 12 control embryos were processed for TEM. The results described below pertain to close examination of sections performed on 2 morphant and 2 control embryos. Number of embryos should be increased and phenotypes quantified in order to confirm reproducibility of these observations.

A profusion of cell debris is visible in the intercellular spaces of *nsa2* morphant embryos, whereas virtually none are visible in controls. This effect is greatest in the animal region of the embryo, where cell debris were frequently attached to the membranes of living cells and of the YSL (Figs. 6.21 and 6.22), which is unusual, even in other pathological circumstances where abundant cell lysis takes place (Ms Elizabeth Hirst, personal communication). This suggests that the plasma membranes of living *nsa2* morphant cells have altered composition relative to controls.

Contacts between DEL cells and the YSL were not observed in the *nsa2* morphant embryo animal region whereas in the control they were (Fig. 6.22, B). The YSL of control embryos contains a large number of membranous protrusions and a layer of mitochondria (Fig. 6.22, B), suggesting that this structure is highly dynamic. (Fig. 6.22, B). In *nsa2* morphants, YSL mitochondria are frequently degenerated, as judged by their fragmented and/or reduced cristae (Fig. 6.22, C). In addition, an increased number of vesicles is observed in *nsa2* morphant YSL compared to control YSL (Fig. 6.22, C).

At epiboly stages, the DEL cells of the zebrafish embryo present a gradient of orderliness and compactness, which are both enhanced in the lateral regions of the embryo, especially at the margin. The regular arrangement of DEL cells and their close contacts between themselves in the lateral region of the embryo is shown in Fig. 6.23, B. In *nsa2* morphant embryos, the orderly arrangement and large membrane

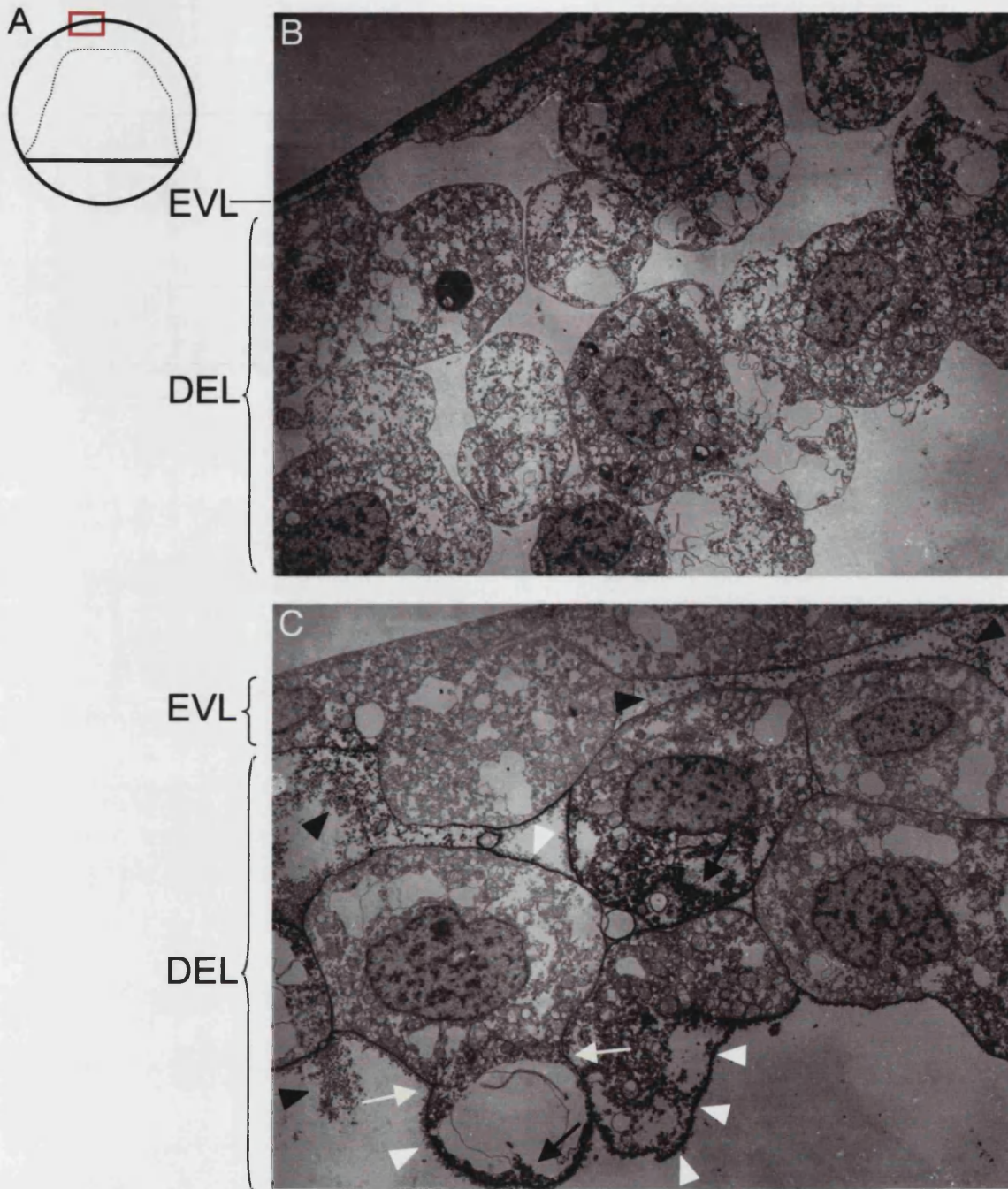


Fig. 6.21 Zebrafish cells morphant for *nsa2* lise and cell debris attach to plasma membrane of living cells. A, Schematic of zebrafish embryo at approximately 85% epiboly, with region depicted in pictures B and C highlighted (red rectangle). B, TEM of control embryo at 85% epiboly; C, TEM of *nsa2* morphant embryo fixed at the same time as B. B and C are at the same magnification. In C, **black arrowheads** point at morphant cell debris in the intercellular space; **white arrowheads** point at morphant cell debris attached to plasma membrane of living cells; **black arrows** point at cytoplasmic debris still inside living cells; **white arrows** point at constriction in living cell presumably trying to exocytose large vacuole and cytoplasmic debris.

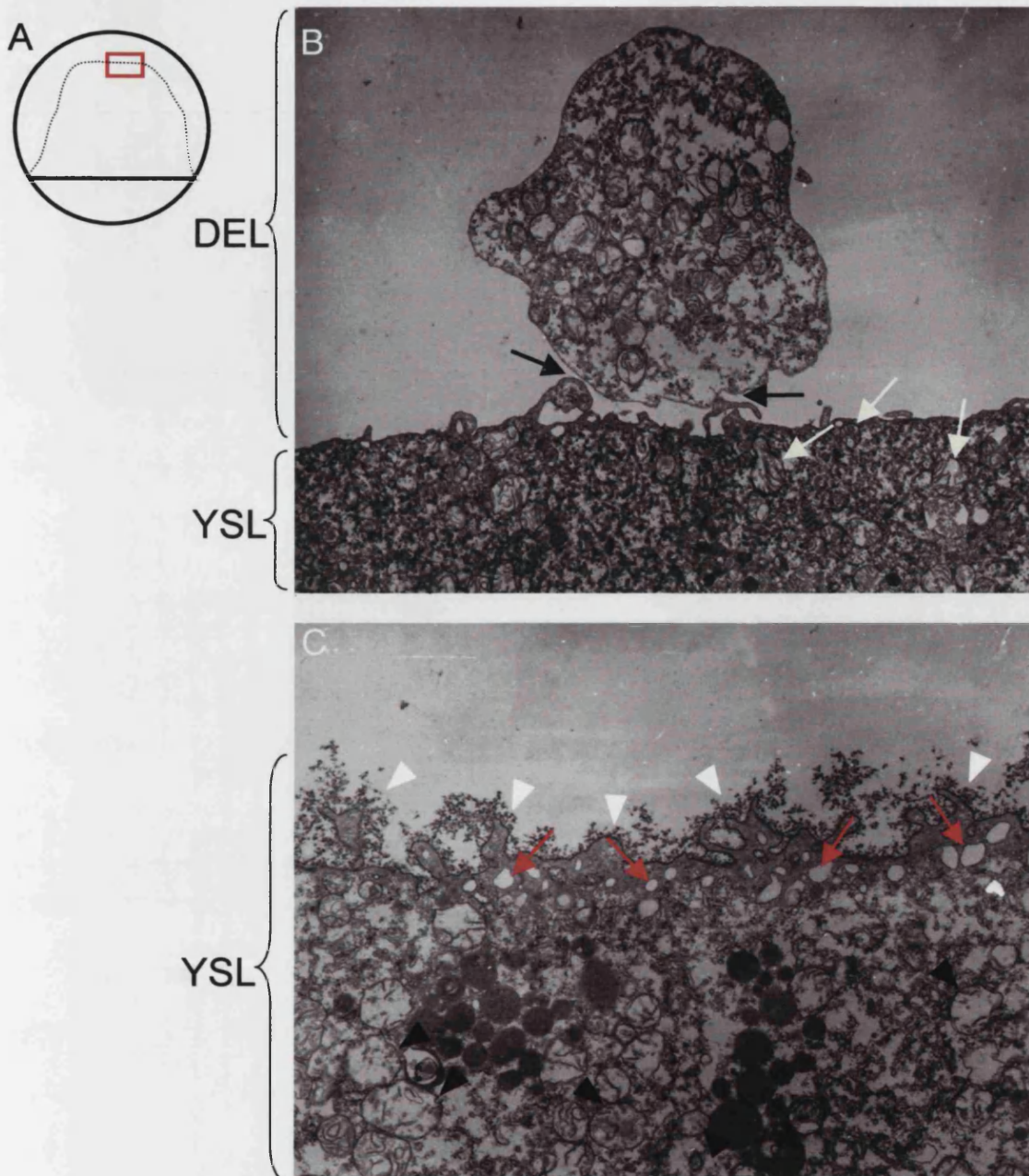


Fig. 6.22 Zebrafish *nsa2* morphant cell debris attach to plasma membrane of the YSL, impairing contact between the DEL and the YSL. **A**, Schematic of zebrafish embryo at approximately 85% epiboly, with region depicted in pictures **B** and **C** highlighted (red rectangle). **B**, TEM of control embryo at 85% epiboly; **C**, TEM of *nsa2* morphant embryo fixed at the same time as **B**. **C** is at 1.5x the magnification of **B**. In **B**, **black arrows** point at contact between control DEL cell and YSL and **white arrows** point at YSL mitochondria; In **C**, **white arrowheads** point at morphant cell debris attached to plasma membrane of YSL, **black arrowheads** point at degenerate mitochondria and **red arrows** point at a few of numerous large vesicles close to plasma membrane.

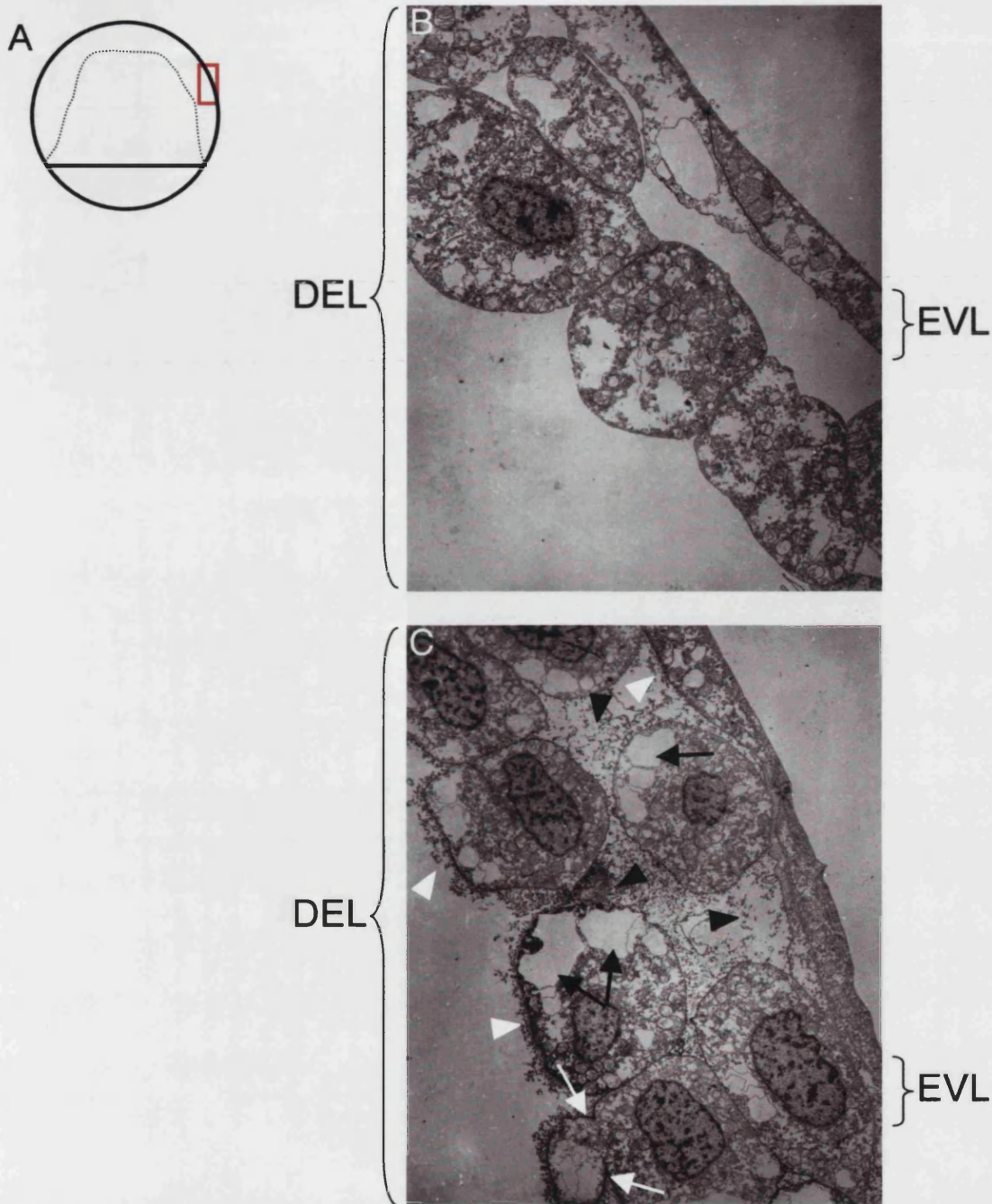


Fig. 6.23 Zebrafish cells morphant for *nsa2* are less orderly arranged in the lateral regions of the embryo and have larger intercellular spaces than controls. **A**, Schematic of zebrafish embryo at approximately 85% epiboly, with region depicted in pictures B and C highlighted (red rectangle). **B**, TEM of control embryo at 85% epiboly; **C**, TEM of *nsa2* morphant embryo fixed at the same time as B. B and C are at the same magnification. In C, **black arrowheads** point at morphant cell debris in the intercellular space; **white arrowheads** point at morphant cell debris attached to plasma membranes; **black arrows** point at large vacuoles found inside morphant cells; **white arrows** point at constriction in living cell presumably trying to exocytose large vacuole and cytoplasmic debris.

contacts between DEL cells are disrupted, with large gaps and debris between cells (Fig. 6.23, C).

Less apparent cell lysis is observed at the margin than in other regions of epiboly-stage *nsa2* morphant embryos. The strength of the *nsa2* cellular phenotype appears to decrease in an animal-to-vegetal direction. Nonetheless, *nsa2* morphant cells at the leading edge are distinct from controls in that they are more vacuolated (Fig. 6.24, B and C). Apparent vacuole exocytosis is observed in *nsa2* morphant cells in the leading edge as well as the remainder of the embryo (Fig. 6.24, C).

High magnification of the DEL cells shows greater detail of intracellular components. Fig. 6.25 illustrates two further features that distinguish *nsa2* morphant cells from controls. First, the ribosomal rosettes, characteristic of embryonic tissues, appear less organised in morphant cells than in controls (Fig. 6.25, C). This would be in accordance with the accumulation of excess 40S ribosomal particles relative to the 60S, whose biogenesis is presumably held up by Nsa2 depletion. Second, *nsa2* morphant membranes are thicker and less well defined than in controls (Fig. 6.25, C). While such membrane appearance can occasionally be observed in controls as a result of the plane of section, the higher frequency in *nsa2* morphant sections suggests it is a genuine morphant phenotype. Finally, the external surface of the yolk is smoothed in *nsa2* morphants when compared to controls, where numerous membrane protrusions are observed (Fig. 6.26, B and C).

6.3 Discussion of the functional analysis of zebrafish *nsa2*

Depletion of Nsa2 from zebrafish embryos results in a severe phenotype that is manifest as early as dome stage, when *nsa2* morphant embryos present an epiboly delay relative to controls. This phenotype is more than a simple developmental delay as by late gastrulation stages embryos are frequently abnormally elongated and present a variety of distorted shapes. Most *nsa2* morphants die by 24 hpf and the remainder die a few hours later.

As Nsa2 is presumably involved in the biogenesis of 60S ribosome subunits (Harnpicharnchai *et al.*, 2001), the phenotype of *nsa2* morphant zebrafish is likely to be

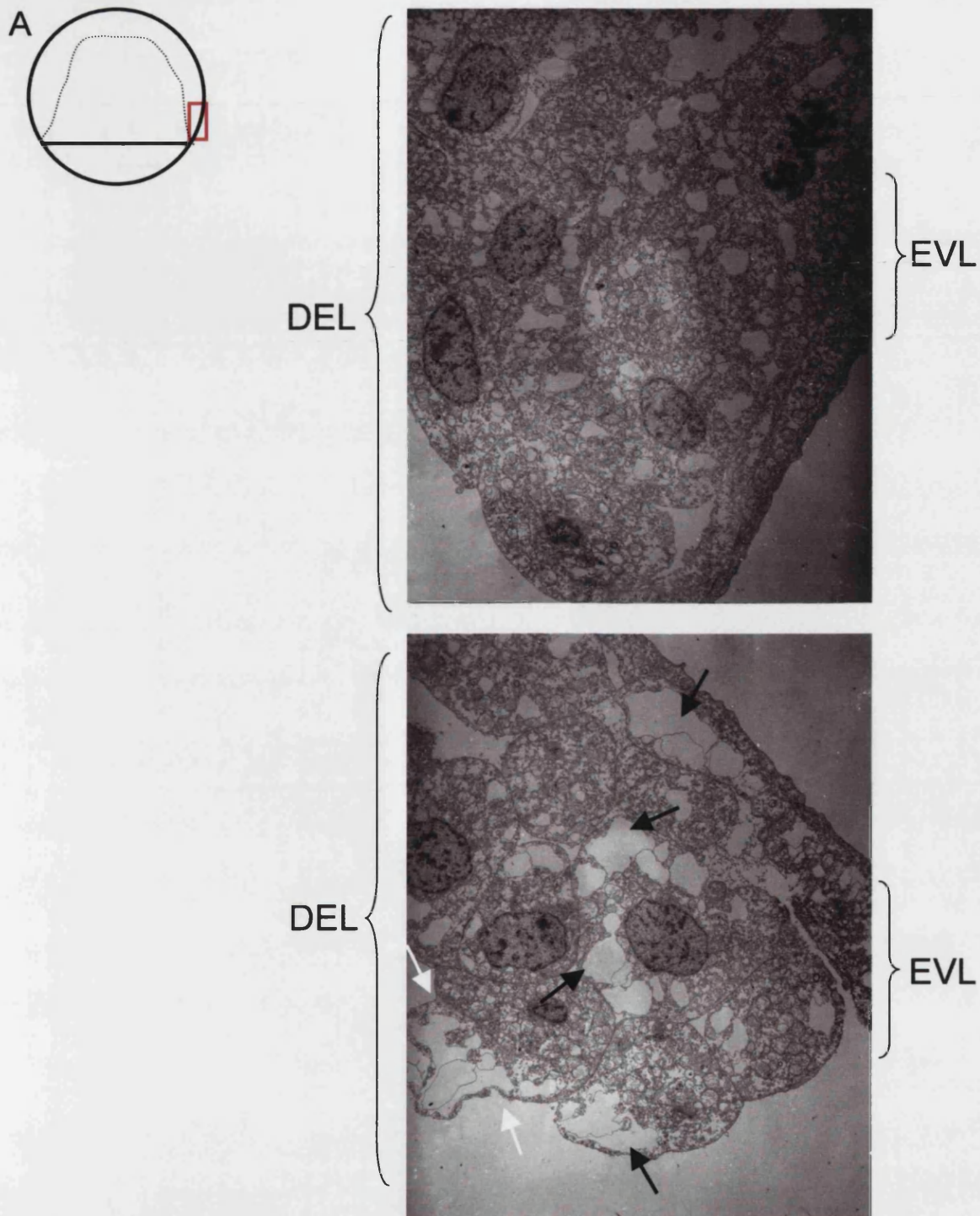


Fig. 6.24 Close to the leading edge of epiboly, less cell lysis of *nsa2* morphant cells is observed relative to other regions of the embryo but cells are highly vacuolated. **A**, Schematic of zebrafish embryo at approximately 85% epiboly, with region depicted in pictures **B** and **C** highlighted (red rectangle). **B**, TEM of control embryo at 85% epiboly; **C**, TEM of *nsa2* morphant embryo fixed at the same time as **B**. **B** and **C** are at the same magnification. In **C**, **black arrows** point at large vacuoles found inside morphant cells; **white arrows** point at constriction in living cell presumably trying to exocytose large vacuole and cytoplasmic debris.

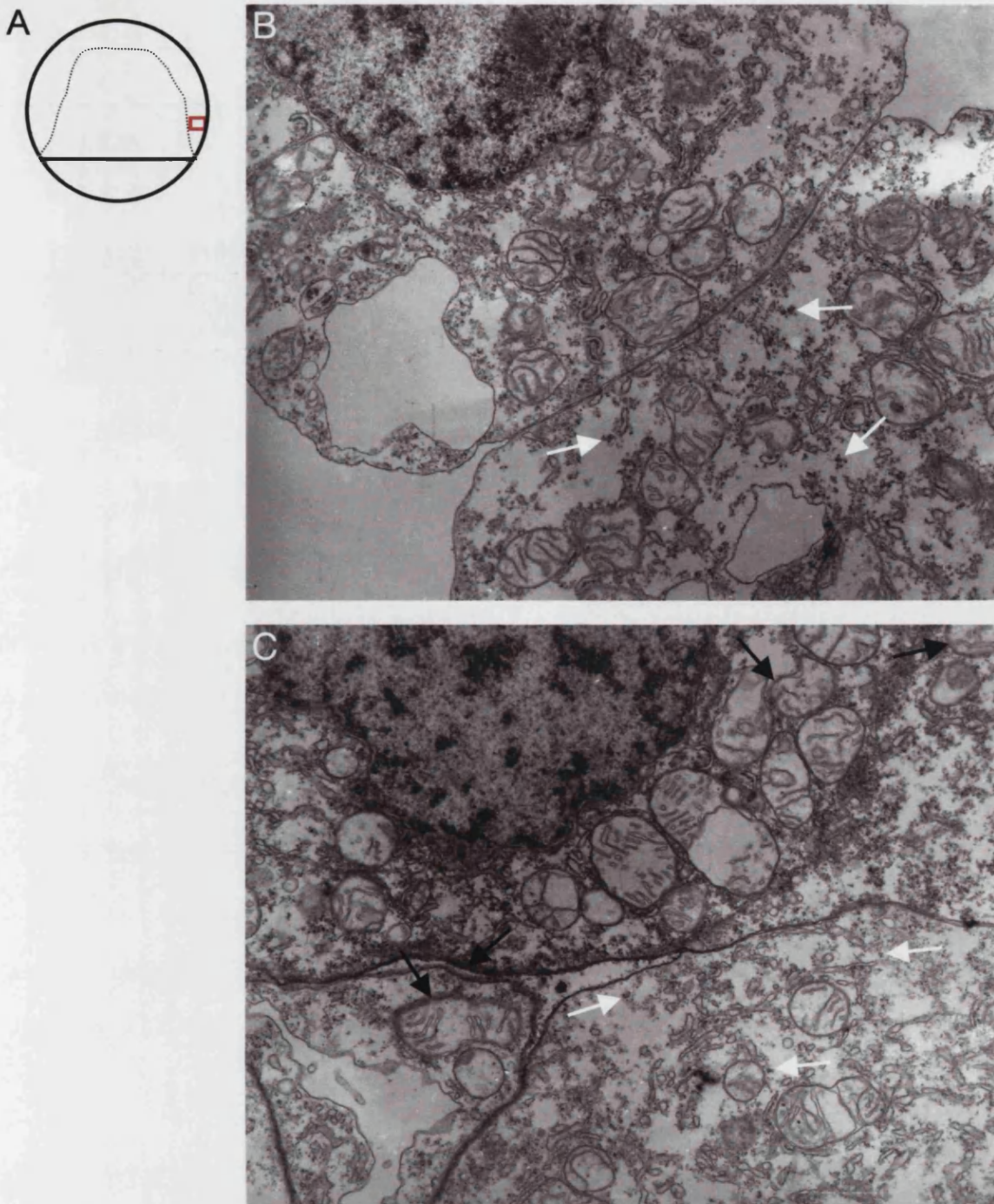


Fig. 6.25 Not only the plasma membranes but also the intracellular membranes of *nsa2* morphant DEL cells have altered appearance relative to controls. **A**, Schematic of zebrafish embryo at approximately 85% epiboly, with region depicted in pictures **B** and **C** highlighted (red rectangle). **B**, TEM of control embryo at 85% epiboly; **C**, TEM of *nsa2* morphant embryo fixed at the same time as **B**. **B** and **C** are at the same magnification. In **B** and **C**, **white arrows** point at ribosomal rosettes; in **C**, **black arrows** point at membranes with wider and fuzzier appearance than controls.

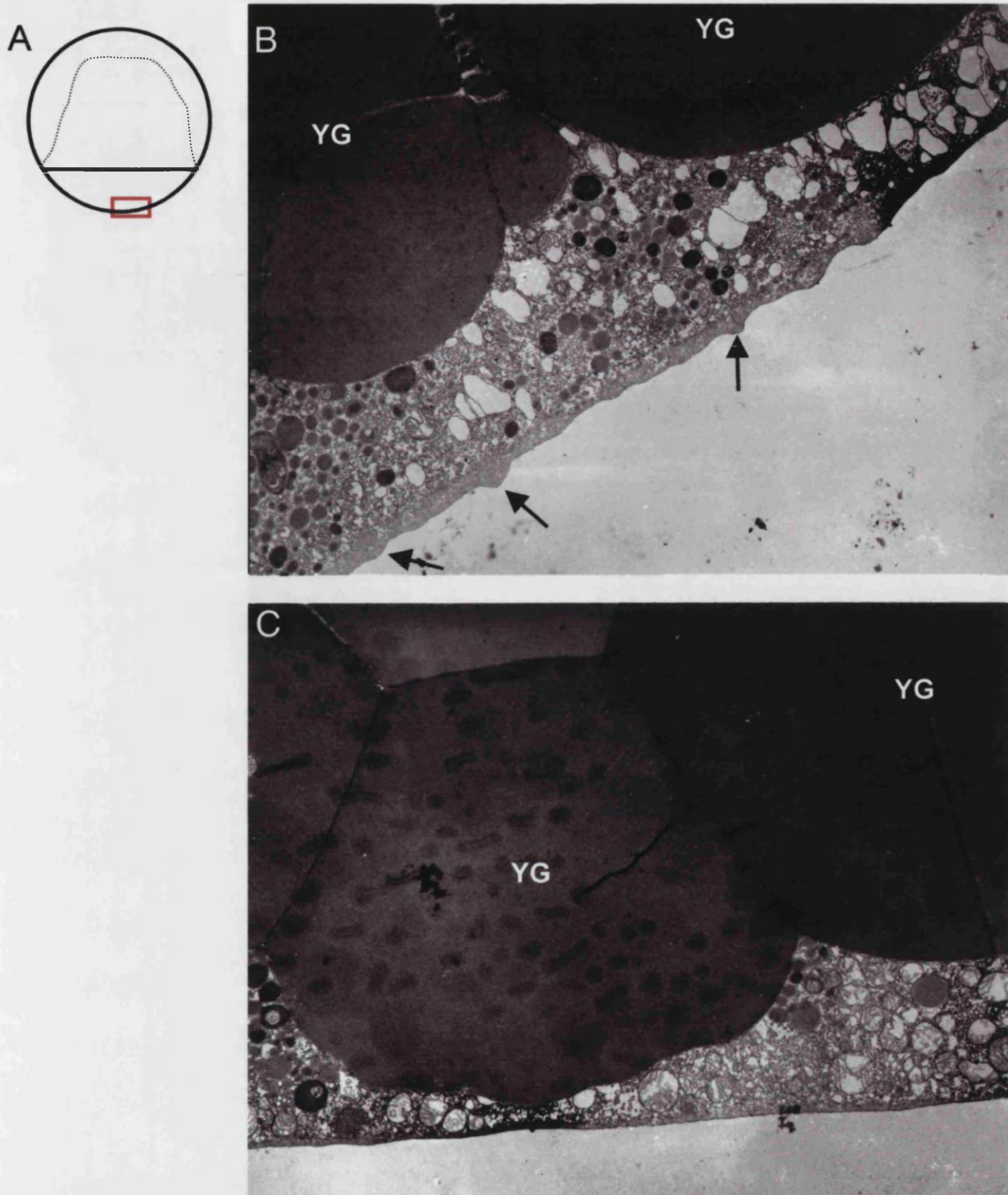


Fig. 6.26 The surface layer of the yolk cell, over which cells migrate during epiboly, is thinner and smoother in *nsa2* morphants than in controls. **A**, Schematic of zebrafish embryo at approximately 85% epiboly, with region depicted in pictures **B** and **C** highlighted (red rectangle). **B**, TEM of control embryo at 85% epiboly; **C**, TEM of *nsa2* morphant embryo fixed at the same time as **B**. **B** and **C** are at the same magnification. In **B**, **black arrows** point at a few of numerous specialisations found in the yolk cell plasma membrane of controls but not of *nsa2* morphants. **YG**, yolk granule.

explained by impaired translation in all cells. The phenotype is not as severe as that of 64- or 128-cell stage embryos treated with 50 $\mu\text{g}/\text{ml}$ of the translation inhibitor cycloheximide, where cleavage is usually arrested by the third cell cycle after treatment (Poulain and Lepage, 2002). However, the epiboly and morphogenetic phenotypes of *nsa2* morphants can be mimicked by treatment of sphere-stage embryos with 2 – 5 $\mu\text{g}/\text{ml}$ cycloheximide (data not shown; a single clutch of embryos treated with the same amount of cycloheximide displays variable phenotypes, among which are the characteristic *nsa2* morphant traits). While it cannot be ruled out that even the strongest MO (MO1, Fig. 6.3) is not completely blocking Nsa2 protein synthesis, a stronger effect is expected of cycloheximide compared to that of completely blocking translation of a factor required for ribosome biogenesis. Cycloheximide inhibits translation directly by inhibiting the translocation reaction on ribosomes, whereas depletion of a factor required for ribosome biogenesis will lead to a gradual decrease in the functional ribosome pool, which in turn will affect different RNAs with distinct kinetics.

Supporting the notion that the *nsa2* defects are due to impaired translation, the same phenotypes are obtained, with varying severity, by targeting RpL19 and RpS5 with MOs. We consider this an indication that all these MOs, plus the weaker *nsa2* MO (MO2), are acting specifically on the targets they were designed for.

At a cellular level, reduced translation results in altered membrane composition, from the plasma membrane to intracellular membranes, including the mitochondrial cristae, which degenerate; intracellular lysis, which leads to excess vacuolation as well as to a greater number of secondary lysosomes (data not shown); and the pulverisation of ribosomal rosettes. At a supra-cellular level, cell-cell contacts are hindered due to excess extracellular space, caused by cell lysis, and possibly also due to the attachment of cellular debris to the plasma membranes of living cells and the YSL. These phenotypes are most severe in the animal region of the epiboly-stage zebrafish embryo and decrease in an animal-to-vegetal direction. Furthermore, the yolk cell surface to which EVL cells attach and onto which DEL cells migrate during epiboly is devoid of the protrusions found in the control.

In yeast, when Nsa2 is placed under the control of a galactose-inducible promoter and shifted from a galactose-containing medium to a glucose-containing one, cells stop

dividing after approximately 25 h (Harnpicharnchai *et al.*, 2001) as observed in other yeast nucleolar protein mutants in similar experiments (Sun and Woolford, 1994). In this time, wild-type yeast undergo approximately 10 cell divisions so the pool of 60S ribosomes is enough for several cell divisions prior to reaching inviable levels. After cleavage stages, the cell cycle of the zebrafish blastomeres lengthens substantially (Kane *et al.*, 1992). By approximately sphere stage, DEL cells undergo their fourteenth cell cycle, which takes ~1.5 h. By extrapolation, there are probably less than 10 cell division cycles between sphere-stage and the 36 hpf embryo in zebrafish.

Given the number of Rps and the number of proteins involved in ribosome biogenesis, the lack of redundancy, apparent in single mutant phenotypes, is remarkable. Moreover, the incidence of haploinsufficient phenotypes suggests that their levels are tightly regulated. Upregulation of many Rps has been detected in several cancers (for example, Yow *et al.*, 1988; Chester *et al.*, 1989; Sharp *et al.*, 1990; Mafune *et al.*, 1991; Pogue-Geile *et al.*, 1991; Barnard *et al.*, 1992; Henry *et al.*, 1993; Kondoh *et al.*, 2001; Cheng *et al.*, 2002; Nadano *et al.*, 2002; Karan *et al.*, 2002; Li *et al.*, 2002), which could be a consequence but also a cause or requirement for uncontrolled cell division. One could imagine that the levels of all Rps or proteins involved in ribosome biogenesis are subject to strict regulation. Alternatively, it might be sufficient to tightly regulate only a few components in order to obtain the desired level of translation in a cell, allowing the others to exist in excess. The difference in severity between the *RpS5* and the *RpL19* morphant phenotype could be due to a longer half-life of the *RpS5* protein relative to *RpL19* and/or by higher levels of maternal *RpS5* relative to maternal *RpL19*. Nonetheless, given that the adult fly *Minute* phenotypes differ in severity in the same way suggests that *RpL19* levels are more limiting for ribosome function than those of *RpS5* and are probably more tightly regulated in the normal situation. Cellular and supracellular physiology are more permissive to variation in the levels of some Rps than others, even if they are cooperatively required for protein synthesis.

It would be interesting to quantify transcription and translation levels in *nsa2* and *Rp* morphants, as well as in embryos treated with cycloheximide. This could demonstrate the distinct effect of translation impairment on individual mRNAs. A qualitative way to address this issue would be to inject zebrafish embryos with either cDNA or mRNA coding for luciferase or GFP into morphants, and assess the effect of the MO on transcription or translation, respectively, over time by the intensity of fluorescence.

This could be refined so as to compare the effect on proteins and mRNAs with different half-lives, since some unstable forms of GFP have been engineered and mRNA stabilising or destabilising elements could be easily built-in. For proper quantification of transcription, RT-PCR could easily be performed on many different transcripts but assessment of protein production in the absence of antibodies would not be as feasible. Relevant patterning molecules could be assessed in this way, as well as candidate molecules that might underlie the altered membrane phenotypes of *nsa2* morphants.

Given the cell-essential function of Nsa2 and that of Rps, the regulative capacity of embryos morphant for these proteins is astonishing. Despite the several phenotypes described (especially apparent during gastrulation and early segmentation stages), these morphants display a relatively normal, albeit smaller, body shape (see Fig. 6.17), shortly before undergoing massive apoptosis and dying. A certain degree of recovery of *nsa2* morphants is already observed by EM between the 50% and 80% DEL epiboly stages, where the latter present less severe cellular phenotype (data not shown). The *nsa2* morphant embryo uses the resources available (reduced protein synthesis, reduced number of cells) to generate a relatively proportionate body. Future studies of invertebrate and now vertebrate *Minutes* might provide a handle on the understudied problem of organism size regulation. The existence of mutations in mouse *Rps* and, very recently, in zebrafish *RpS5* (Golling *et al.*, 2002) should aid the study of the vertebrate *Minute* phenotype.

Other issues, possibly related to that of organism size and developmental regulation, that merit investigation are how cell proliferation and cell size are affected by depletion of Nsa2 or Rps and whether in vertebrates like in the fly imaginal discs there is cell competition between *Minute* and non-*Minute* cells (Moreno *et al.*, 2002). The invertebrate Dpp signalling pathway bears most resemblance to the vertebrate BMP signalling pathway. However, there is no vertebrate brinker-like gene, as judged from the genomes sequenced so far, and there is no molecular evidence for vertebrate cell competition of the kind in operation in *Drosophila*.

I attempted to compare the proliferation rate of *nsa2* and control cells in zebrafish by performing single-cell transplants between morphant donors and control hosts and vice-

versa. In order to make comparisons between undifferentiated cells, given that each differentiated cell type might cycle at different rates or stop cycling altogether when terminally differentiated, I assessed transplants performed at the sphere stage, at the 90% epiboly-stage. However, during this developmental time-window there are only two-three cell divisions so a single cell gives rise to 6-8 progeny (data not shown). This is too small a number to measure differences in cell division rates and so I have not pursued these studies further. I plan to derive primary cultures from MO-injected embryos in order to compare cell proliferation rate, cell size and cell competition, between *nsa2* morphant and control cells, in a system where I should have access to large numbers of uniform cells.

References

Aanstad, P. and Whitaker, M. (1999) "Predictability of dorso-ventral asymmetry in the cleavage stage zebrafish embryo: an analysis using lithium sensitivity as a dorso-ventral marker", *Mech Dev*, **88**(1), 33-41.

Abdelilah, S., Solnica-Krezel, L., Stainier, D. Y. and Driever, W. (1994) "Implications for dorsoventral axis determination from the zebrafish mutation *janus*.PG - 468-71", *Nature* **370**(6489).

Acampora, D., Mazan, S., Lallemand, Y., Avantaggiato, V., Maury, M. and Simeone, A. (1995) "Forebrain and midbrain regions are deleted in *Otx2*^{-/-} mutants due to a defective anterior neuroectoderm specification during gastrulation", *Development* **121**, 3279-90.

Adams, C. C., Jakovljevic, J., Roman, J., Harnpicharnchai, P. and Woolford, J. L., Jr. (2002) "*Saccharomyces cerevisiae* nucleolar protein Nop7p is necessary for biogenesis of 60S ribosomal subunits", *Rna* **8**(2), 150-65.

Adams, M. D., Celniker, S. E., Holt, R. A., Evans, C. A., Gocayne, J. D., Amanatides, P. G., Scherer, S. E., Li, P. W., Hoskins, R. A., Galle, R. F., George, R. A., Lewis, S. E., Richards, S., Ashburner, M., Henderson, S. N., Sutton, G. G., Wortman, J. R., Yandell, M. D., Zhang, Q., Chen, L. X., Brandon, R. C., Rogers, Y. H., Blazej, R. G., Champe, M., Pfeiffer, B. D., Wan, K. H., Doyle, C., Baxter, E. G., Helt, G., Nelson, C. R., Gabor, G. L., Abril, J. F., Agbayani, A., An, H. J., Andrews-Pfannkoch, C., Baldwin, D., Ballew, R. M., Basu, A., Baxendale, J., Bayraktaroglu, L., Beasley, E. M., Beeson, K. Y., Benos, P. V., Berman, B. P., Bhandari, D., Bolshakov, S., Borkova, D., Botchan, M. R., Bouck, J., Brokstein, P., Brottier, P., Burtis, K. C., Busam, D. A., Butler, H., Cadieu, E., Center, A., Chandra, I., Cherry, J. M., Cawley, S., Dahlke, C., Davenport, L. B., Davies, P., de Pablos, B., Delcher, A., Deng, Z., Mays, A. D., Dew, I., Dietz, S. M., Dodson, K., Doup, L. E., Downes, M., Dugan-Rocha, S., Dunkov, B. C., Dunn, P., Durbin, K. J., Evangelista, C. C., Ferraz, C., Ferreira, S., Fleischmann, W., Fosler, C., Gabrielian, A. E., Garg, N. S., Gelbart, W. M., Glasser, K., Glodek, A., Gong, F., Gorrell, J. H., Gu, Z., Guan, P., Harris, M., Harris, N. L., Harvey, D., Heiman, T. J., Hernandez, J. R., Houck, J., Hostin, D., Houston, K. A., Howland, T. J., Wei, M. H., Ibegwam, C., Jalali, M., Kalush, F., Karpen, G. H., Ke, Z., Kennison, J. A., Ketchum, K. A., Kimmel, B. E., Kodira, C. D., Kraft, C., Kravitz, S., Kulp, D., Lai, Z., Lasko, P., Lei, Y., Levitsky, A. A., Li, J., Li, Z., Liang, Y., Lin, X., Liu, X., Mattei, B., McIntosh, T. C., McLeod, M. P., McPherson, D., Merkulov, G., Milshina, N. V., Mobarry, C., Morris, J., Moshrefi, A., Mount, S. M., Moy, M., Murphy, B., Murphy, L., Muzny, D.

- M., Nelson, D. L., Nelson, D. R., Nelson, K. A., Nixon, K., Nusskern, D. R., Pacleb, J. M., Palazzolo, M., Pittman, G. S., Pan, S., Pollard, J., Puri, V., Reese, M. G., Reinert, K., Remington, K., Saunders, R. D., Scheeler, F., Shen, H., Shue, B. C., Siden-Kiamos, I., Simpson, M., Skupski, M. P., Smith, T., Spier, E., Spradling, A. C., Stapleton, M., Strong, R., Sun, E., Svirskas, R., Tector, C., Turner, R., Venter, E., Wang, A. H., Wang, X., Wang, Z. Y., Wassarman, D. A., Weinstock, G. M., Weissenbach, J., Williams, S. M., Woodage, T., Worley, K. C., Wu, D., Yang, S., Yao, Q. A., Ye, J., Yeh, R. F., Zaveri, J. S., Zhan, M., Zhang, G., Zhao, Q., Zheng, L., Zheng, X. H., Zhong, F. N., Zhong, W., Zhou, X., Zhu, S., Zhu, X., Smith, H. O., Gibbs, R. A., Myers, E. W., Rubin, G. M. and Venter, J. C. (2000) "The genome sequence of *Drosophila melanogaster*", *Science* **287**(5461), 2185-95.
- Agathon, A.**, Thisse, B. and Thisse, C. (2001) "Morpholino knock-down of *antivin1* and *antivin2* upregulates nodal signaling", *Genesis* **30**(3), 178-82.
- Alberts, B.**, Johnson, A., Lewis, J., Raff, M., Roberts, K. and Walter, P. (2002) Molecular Biology of the Cell, New York, Garland Science.
- Alexander, J.**, Rothenberg, M., Henry, G. L. and Stainier, D. Y. (1999) "*casanova* plays an early and essential role in endoderm formation in zebrafish", *Dev Biol* **215**(2), 343-57.
- Alexander, J. and Stainier, D. Y.** (1999) "A molecular pathway leading to endoderm formation in zebrafish", *Curr Biol* **9**(20), 1147-57.
- Alliston, T. N.**, Gonzalez-Robayna, I. J., Buse, P., Firestone, G. L. and Richards, J. S. (2000) "Expression and localization of serum/glucocorticoid-induced kinase in the rat ovary: relation to follicular growth and differentiation", *Endocrinology* **141**(1), 385-95.
- Alliston, T. N.**, Maiyar, A. C., Buse, P., Firestone, G. L. and Richards, J. S. (1997) "Follicle stimulating hormone-regulated expression of serum/glucocorticoid-inducible kinase in rat ovarian granulosa cells: a functional role for the Sp1 family in promoter activity", *Mol Endocrinol* **11**(13), 1934-49.
- Altmann, C. R. and Brivanlou, A. H.** (2001) "Neural patterning in the vertebrate embryo", *Int Rev Cytol* **203**:447-82.
- Altschul, S. F.**, Madden, T. L., Schaffer, A. A., Zhang, J., Zhang, Z., Miller, W. and Lipman, D. J. (1997) "Gapped BLAST and PSI-BLAST: a new generation of protein database search programs", *Nucleic Acids Res* **25**(17), 3389-402.
- Alvarez de la Rosa, D.**, Zhang, P., Naray-Fejes-Toth, A., Fejes-Toth, G. and Canessa, C. M. (1999) "The serum and glucocorticoid kinase *Sgk* increases the abundance of

epithelial sodium channels in the plasma membrane of *Xenopus oocytes*", *J Biol Chem* **274**(53), 37834-9.

Amaravadi, L. S., Neff, A. W., Sleeman, J. P. and Smith, R. C. (1997) "Autonomous neural axis formation by ectopic expression of the protooncogene *c-ski*", *Dev Biol* **192**(2), 392-404.

Ancel, P. and Vintemberger, P. (1948) "Recherches sur le déterminisme de la symétrie bilatérale dans l'oeuf des Amphibiens", *Bull Biol Fr Belg* **31 (Suppl)**, 1-182.

Andersson, S. and Lambertsson, A. (1990) "Characterization of a novel *Minute* locus in *Drosophila melanogaster*: a putative ribosomal protein gene", *Heredity* **65 (Pt 1)**, 51-7.

Andersson, S., Saeboe-Larsen, S., Lambertsson, A., Merriam, J. and Jacobs-Lorena, M. (1994) "A *Drosophila* third chromosome *Minute* locus encodes a ribosomal protein", *Genetics* **137**(2), 513-20.

Ang, S.-L., Conlon, R. A., Jin, O. and Rossant, J. (1994) "Positive and negative signals from mesoderm regulate the expression of mouse *Otx2* in ectoderm explants", *Development* **120**(10), 2979-89

Ang, S.-L. and Rossant, J. (1994) "HNF-3 beta is essential for node and notochord formation in mouse development" *Cell*, **78**(4), 561-74.

Aoki, T. O., Mathieu, J., Saint-Etienne, L., Rebagliati, M. R., Peyrieras, N. and Rosa, F. M. (2002) "Regulation of nodal signalling and mesendoderm formation by TARAM-A, a TGFbeta-related type I receptor", *Dev Biol* **241**(2), 273-88.

Aparicio, S., Chapman, J., Stupka, E., Putnam, N., Chia, J. M., Dehal, P., Christoffels, A., Rash, S., Hoon, S., Smit, A., Gelpke, M. D., Roach, J., Oh, T., Ho, I. Y., Wong, M., Detter, C., Verhoef, F., Predki, P., Tay, A., Lucas, S., Richardson, P., Smith, S. F., Clark, M. S., Edwards, Y. J., Doggett, N., Zharkikh, A., Tavtigian, S. V., Pruss, D., Barnstead, M., Evans, C., Baden, H., Powell, J., Glusman, G., Rowen, L., Hood, L., Tan, Y. H., Elgar, G., Hawkins, T., Venkatesh, B., Rokhsar, D. and Brenner, S. (2002) "Whole-genome shotgun assembly and analysis of the genome of *Fugu rubripes*", *Science* **297**(5585), 1301-10.

Arceci, R. J., King, A. A., Simon, M. C., Orkin, S. H. and Wilson, D. B. (1993) "Mouse GATA-4: a retinoic acid-inducible GATA-binding transcription factor expressed in endodermally derived tissues and heart", *Mol Cell Biol* **13**(4), 2235-46.

Arendt, D. and Nubler-Jung, K. (1999) "Rearranging gastrulation in the name of yolk: evolution of gastrulation in yolk-rich amniote eggs", *Mech Dev* **81**(1-2), 3-22.

Bachiller, D., Klingensmith, J., Kemp, C., Belo, J. A., Anderson, R. M., May, S. R.,

- McMahon, J. A., McMahon, A. P., Harland, R. M., Rossant, J. and De Robertis, E. M. (2000) "The organizer factors Chordin and Noggin are required for mouse forebrain development", *Nature* **403**(6770), 658-61.
- Bachvarova, R. F.** (1999) "Establishment of antero-posterior polarity in avian embryos", *Curr Opin Genet Dev* **9**(4), 411-6.
- Balakier, H. and Pedersen, R. A.** (1982) "Allocation of cells to inner cell mass and trophectoderm lineages in preimplantation mouse embryos", *Dev Biol* **90**(2), 352-62.
- Ballabio, A.** (1993) "The rise and fall of positional cloning?" *Nat Genet* **3**(4), 277-9.
- Baltimore, D.** (2001) "Our genome unveiled", *Nature*, **409**(6822), 814-6.
- Barenbaum, M., Moreno, T. A., LaBonne, C., Sechrist, J. and Bronner-Fraser, M.** (2000) "Noelin-1 is a secreted glycoprotein involved in generation of the neural crest", *Nat Cell Biol* **2**(4), 219-25.
- Barnard, G. F., Staniunas, R. J., Bao, S., Mafune, K., Steele, G. D., Jr., Gollan, J. L. and Chen, L. B.** (1992) "Increased expression of human ribosomal phosphoprotein P0 messenger RNA in hepatocellular carcinoma and colon carcinoma", *Cancer Res* **52**(11), 3067-72.
- Batt, J., Asa, S., Fladd, C. and Rotin, D.** (2002) "Pituitary, pancreatic and gut neuroendocrine defects in protein tyrosine phosphatase-sigma-deficient mice", *Mol Endocrinol* **16**(1), 155-69.
- Beddington, R. S.** (1994) "Induction of a second neural axis by the mouse node", *Development* **120**(3), 613-20.
- Beddington, R. S. and Robertson, E. J.** (1989) "An assessment of the developmental potential of embryonic stem cells in the midgestation mouse embryo", *Development* **105**(4), 733-7.
- Beddington, R. S. and Robertson, E. J.** (1998) "Anterior patterning in mouse", *Trends Genet* **14**(7), 277-84.
- Beddington, R. S. and Robertson, E. J.** (1999) "Axis development and early asymmetry in mammals", *Cell* **96**(2), 195-209.
- Behrens, J., von Kries, J., Kuhl, M., Bruhn, L., Wedlich, D., Grosschedl, R. and Birchmeier, W.** (1996) "Functional interaction of b-catenin with the transcription factor LEF-1", *Nature* **382**, 638-42.
- Bell, L. M., Leong, M. L., Kim, B., Wang, E., Park, J., Hemmings, B. A. and Firestone, G. L.** (2000) "Hyperosmotic stress stimulates promoter activity and regulates cellular utilization of the serum- and glucocorticoid-inducible protein kinase (Sgk) by a p38 MAPK-dependent pathway", *J Biol Chem* **275**(33), 25262-72.

- Bellairs, R.** (1993) "Fertilization and early embryonic development in poultry", *Poult Sci* **72**(5), 874-81.
- Bellairs, R. and Osmond, M.** (1998) The Atlas of Chick Development, San Diego, CA, Academic Press.
- Belo, J. A., Bachiller, D., Agius, E., Kemp, C., Borges, A. C., Marques, S., Piccolo, S. and De Robertis, E. M.** (2000) "Cerberus-like is a secreted BMP and nodal antagonist not essential for mouse development", *Genesis* **26**(4), 265-70.
- Belo, J. A., Bouwmeester, T., Leyns, L., Kertesz, N., Gallo, M., Follettie, M. and De Robertis, E. M.** (1997) "Cerberus-like is a secreted factor with neutralizing activity expressed in the anterior primitive endoderm of the mouse gastrula", *Mech Dev* **68**(1-2), 45-57.
- Benton, R., Palacios, I. M., St Johnston, D.** (2002) "Drosophila 14-3-3/PAR-5 is an essential mediator of PAR-1 function in axis formation" *Dev Cell* **3**(5), 659-71.
- Biondi, R. M., Kieloch, A., Currie, R. A., Deak, M. and Alessi, D. R.** (2001) "The PIF-binding pocket in PDK1 is essential for activation of S6K and SGK, but not PKB", *EMBO J* **20**(16), 4380-90.
- Bisgrove, B. W., Essner, J. J. and Yost, H. J.** (1999) "Regulation of midline development by antagonism of lefty and nodal signaling", *Development* **126**(14), 3253-62.
- Black, S. D. and Gerhart, J. C.** (1986) "High-frequency twinning of *Xenopus laevis* embryos from eggs centrifuged before first cleavage", *Dev Biol* **116**(1), 228-40.
- Blum, M., Gaunt, S. J., Cho, K. W., Steinbeisser, H., Blumberg, B., Bittner, D. and De Robertis, E. M.** (1992) "Gastrulation in the mouse: the role of the homeobox gene *goosecoid*", *Cell* **69**(7), 1097-106.
- Blumberg, B., Bolado, J. Jr, Moreno, T. A., Kintner, C., Evans, R. M. and Papalopulu, N.** (1997) "An essential role for retinoid signaling in anteroposterior neural patterning", *Development*, **124**(2), 373-9.
- Boehmer, C., Wilhelm, V., Palmada, M., Wallisch, S., Henke, G., Brinkmeier, H., Cohen, P., Pieske, B. and Lang, F.** (2003) "Serum and glucocorticoid inducible kinases in the regulation of the cardiac sodium channel SCN5A", *Cardiovasc Res* **57**(4), 1079-84.
- Bollag, R. J., Waldman, A. S. and Liskay, R. M.** (1989) "Homologous recombination in mammalian cells", *Annu Rev Genet* **23**, 199-225.

- Boman, A. L., Delannoy, M. R. and Wilson, K. L. (1992)** "GTP hydrolysis is required for vesicle fusion during nuclear envelope assembly in vitro", *J Cell Biol* **116**(2), 281-94.
- Boring, L. F., Sinervo, B. and Schubiger, G. (1989)** "Experimental phenocopy of a *Minute* maternal-effect mutation alters blastoderm determination in embryos of *Drosophila melanogaster*", *Dev Biol* **132**(2), 343-54.
- Bouwmeester, T., Kim, S., Sasai, Y., Lu, B. and De Robertis, E. M. (1996)** "Cerberus is a head-inducing secreted factor expressed in the anterior endoderm of Spemann's organizer", *Nature* **382**(6592), 595-601.
- Brand, M., Heisenberg, C. P., Warga, R. M., Pelegri, F., Karlstrom, R. O., Beuchle, D., Picker, A., Jiang, Y. J., Furutani-Seiki, M., van Eeden, F. J., Granato, M., Haffter, P., Hammerschmidt, M., Kane, D. A., Kelsh, R. N., Mullins, M. C., Odenthal, J. and Nusslein-Volhard, C. (1996)** "Mutations affecting development of the midline and general body shape during zebrafish embryogenesis", *Development* **123**, 129-42.
- Branford, W. W. and Yost, H. J. (2002)** "Lefty-dependent inhibition of nodal- and wnt-responsive organizer gene expression is essential for normal gastrulation", *Curr Biol* **12**(24), 2136-41.
- Brannon, M., Gomperts, M., Sumoy, L., Moon, R. T. and Kimelman, D. (1997)** "A beta-catenin/XTcf-3 complex binds to the *siamois* promoter to regulate dorsal axis specification in *Xenopus*", *Genes Dev* **11**(18), 2359-70.
- Brannon, M. and Kimelman, D. (1996)** "Activation of Siamois by the Wnt pathway", *Dev Biol* **180**(1), 344-7.
- Brazil, D. P. and Hemmings, B. A. (2001)** "Ten years of protein kinase B signalling: a hard Akt to follow", *Trends Biochem Sci* **26**(11), 657-64.
- Brehme, K. S. (1939)** "A study of the effect on development of "*Minute*" mutations in *Drosophila melanogaster*", *Genetics* **24**, 131-61.
- Brehme, K. S. (1941a)** "Development of the *Minute* phenotype in *Drosophila melanogaster*: A comparative study of three *Minute* mutants", *J Exp Zool* **88**, 135-60.
- Brehme, K. S. (1941b)** "The growth of transplanted *Minute* and wild-type optic discs in *Drosophila melanogaster*", *Growth* **5**, 183-95.
- Brennan, F. E. and Fuller, P. J. (2000)** "Rapid upregulation of serum and glucocorticoid-regulated kinase (*sgk*) gene expression by corticosteroids in vivo", *Mol Cell Endocrinol* **166**(2), 129-36.

- Brennan, J., Lu, C. C., Norris, D. P., Rodriguez, T. A., Beddington, R. S. and Robertson, E. J.** (2001) "Nodal signalling in the epiblast patterns the early mouse embryo", *Nature* **411**(6840), 965-9.
- Brickley, D. R., Mikosz, C. A., Hagan, C. R. and Conzen, S. D.** (2002) "Ubiquitin modification of serum and glucocorticoid-induced protein kinase-1 (SGK-1)", *J Biol Chem* **277**(45), 43064-70.
- Brunet, A., Park, J., Tran, H., Hu, L. S., Hemmings, B. A. and Greenberg, M. E.** (2001) "Protein kinase SGK mediates survival signals by phosphorylating the forkhead transcription factor FKHRL1 (FOXO3a)", *Mol Cell Biol* **21**(3), 952-65.
- Bryant, P. J. and Simpson, P.** (1984) "Intrinsic and extrinsic control of growth in developing organs", *Q Rev Biol* **59**(4), 387-415.
- Buck, A., Kispert, A. and Kohlhase, J.** (2001) "Embryonic expression of the murine homologue of *SALL1*, the gene mutated in Townes-Brocks syndrome", *Mech Dev* **104**(1-2), 143-6.
- Bunney, T. D., De Boer, A. H. and Levin, M.** (2003) "Fusicoccin signaling reveals 14-3-3 protein function as a novel step in left-right patterning during amphibian embryogenesis", *Development* **130**(20), 4847-58.
- Burmeister, M., Novak, J., Liang, M.-Y., Basu, S., Ploder, L., Hawes, N. L., Vidgen, D., Hoover, F., Goldman, D., Kalnins, V. I., Roderick, T. H., Taylor, B. A., Hankin, M. H. and McInnes, R. R.** (1996) "Ocular retardation mouse caused by *Chx10* homeobox null allele: impaired retinal progenitor proliferation and bipolar cell differentiation", *Nature Genet* **12**, 376-84.
- Buse, P., Tran, S. H., Luther, E., Phu, P. T., Aponte, G. W. and Firestone, G. L.** (1999) "Cell cycle and hormonal control of nuclear-cytoplasmic localization of the serum- and glucocorticoid-inducible protein kinase, Sgk, in mammary tumor cells. A novel convergence point of anti-proliferative and proliferative cell signaling pathways", *J Biol Chem* **274**(11), 7253-63.
- Busjahn, A., Aydin, A., Uhlmann, R., Krasko, C., Bähring, S., Szelestei, T., Feng, Y., Dahm, S., Sharma, A. M., Luft, F. C. and Lang, F.** (2002) "Serum- and glucocorticoid-regulated kinase (SGK1) gene and blood pressure", *Hypertension* **40**(3), 256-60.
- Callebaut, M.** (1987) "Ooplasmic localization and segregation in quail germs: fate of the four ooplasm", *Arch Biol (Bruxelles)* **98**, 441-73.
- Callebaut, M.** (1993a) "Development of quail germs during and after gravitationally oriented bilateral axialization", *Eur Arch Biol* **104**, 135-40.

- Callebaut, M.** (1993b) "Unequal caudocephalic ooplasmic uptake and eccentric formation of the subgerminal space below unincubated quail blastoderms presenting a Koller's sickle", *Belg J Zool* **123**, 107-12.
- Callebaut, M. and Van Nueten, E.** (1994) "Rauber's (Koller's) sickle: the early gastrulation organizer of the avian blastoderm", *Eur J Morphol* **32**(1), 35-48.
- Campbell, G. and Tomlinson, A.** (1999) "Transducing the Dpp morphogen gradient in the wing of *Drosophila*: regulation of Dpp targets by *brinker*", *Cell* **96**(4), 553-62.
- Cantley, L. C.** (2002) "The phosphoinositide 3-kinase pathway", *Science* **296**(5573), 1655-7.
- Carlton, J. M., Angiuoli, S. V., Suh, B. B., Kooij, T. W., Pertea, M., Silva, J. C., Ermolaeva, M. D., Allen, J. E., Selengut, J. D., Koo, H. L., Peterson, J. D., Pop, M., Kosack, D. S., Shumway, M. F., Bidwell, S. L., Shallom, S. J., van Aken, S. E., Riedmuller, S. B., Feldblyum, T. V., Cho, J. K., Quackenbush, J., Sedegah, M., Shoaibi, A., Cummings, L. M., Florens, L., Yates, J. R., Raine, J. D., Sinden, R. E., Harris, M. A., Cunningham, D. A., Preiser, P. R., Bergman, L. W., Vaidya, A. B., van Lin, L. H., Janse, C. J., Waters, A. P., Smith, H. O., White, O. R., Salzberg, S. L., Venter, J. C., Fraser, C. M., Hoffman, S. L., Gardner, M. J. and Carucci, D. J.** (2002) "Genome sequence and comparative analysis of the model rodent malaria parasite *Plasmodium yoelii yoelii*", *Nature* **419**(6906), 512-9.
- Carmany-Rampey, A. and Schier, A. F.** (2001) "Single-cell internalization during zebrafish gastrulation", *Curr Biol* **11**(16), 1261-5.
- Carnac, G., Kodjabachian, L., Gurdon, J. B. and Lemaire, P.** (1996) "The homeobox gene *Siamois* is a target of the Wnt dorsalisation pathway and triggers organizer activity in the absence of mesoderm", *Development* **122**(10), 3055-65.
- Carreira-Barbosa, F., Concha, M. L., Takeuchi, M., Ueno, N., Wilson, S. W. and Tada, M.** (2003) "Prickle 1 regulates cell movements during gastrulation and neuronal migration in zebrafish", *Development*, **130**, 4037-46.
- Carroll, S. B., Laughon, A. and Thalley, B. S.** (1988) "Expression, function, and regulation of the hairy segmentation protein in the *Drosophila* embryo", *Genes Dev* **2**(7), 883-90.
- Carroll, S. B. and Scott, M. P.** (1986) "Zygotically active genes that affect the spatial expression of the *fushi tarazu* segmentation gene during early *Drosophila* embryogenesis", *Cell* **45**(1), 113-26.

- Casamayor, A.**, Torrance, P. D., Kobayashi, T., Thorner, J. and Alessi, D. R. (1999) "Functional counterparts of mammalian protein kinases PDK1 and SGK in budding yeast", *Curr Biol* **9**(4), 186-97.
- Casellas, R. and Brivanlou, A. H.** (1998) "*Xenopus* Smad7 inhibits both the activin and BMP pathways and acts as a neural inducer", *Dev Biol* **198**(1), 1-12.
- Cebria, F.**, Kobayashi, C., Umesono, Y., Nakazawa, M., Mineta, K., Ikeo, K., Gojobori, T., Itoh, M., Taira, M., Sanchez Alvarado, A. and Agata, K. (2002) "FGFR-related gene *nou-darake* restricts brain tissues to the head region of planarians", *Nature*, **419**(6907), 620-4.
- Chang, C. and Hemmati-Brivanlou, A.** (2000) "A post-mid-blastula transition requirement for TGFbeta signaling in early endodermal specification", *Mech Dev* **90**(2), 227-35.
- Chang, C.**, Wilson, P. A., Mathews, L. S. and Hemmati-Brivanlou, A. (1997) "A *Xenopus* type I activin receptor mediates mesodermal but not neural specification during embryogenesis", *Development* **124**(4), 827-37.
- Chapman, D. L. and Papaioannou, V. E.** (1998) "Three neural tubes in mouse embryos with mutations in the T-box gene *Tbx6*", *Nature* **391**(6668), 695-7.
- Chapman, S. C.**, Schubert, F. R., Schoenwolf, G. C. and Lumsden, A. (2003) "Anterior identity is established in chick epiblast by hypoblast and anterior definitive endoderm", *Development* **130**, 5091-101.
- Chen, P.**, Lee, K. S. and Levin, D. E. (1993) "A pair of putative protein kinase genes (*YPK1* and *YPK2*) is required for cell growth in *Saccharomyces cerevisiae*", *Mol Gen Genet* **236**(2-3), 443-7.
- Chen, S. Y.**, Bhargava, A., Mastroberardino, L., Meijer, O. C., Wang, J., Buse, P., Firestone, G. L., Verrey, F. and Pearce, D. (1999) "Epithelial sodium channel regulated by aldosterone-induced protein *sgk*", *Proc Natl Acad Sci USA* **96**(5), 2514-9.
- Chen, W. S.**, Xu, P. Z., Gottlob, K., Chen, M. L., Sokol, K., Shiyanova, T., Roninson, I., Weng, W., Suzuki, R., Tobe, K., Kadowaki, T. and Hay, N. (2001) "Growth retardation and increased apoptosis in mice with homozygous disruption of the *Akt1* gene", *Genes Dev* **15**(17), 2203-8.
- Chen, X.**, Rubock, M. J. and Whitman, M. (1996) "A transcriptional partner for MAD proteins in TGF-beta signalling", *Nature* **383**(6602), 691-6.
- Chen, Y. and Schier, A. F.** (2001) "The zebrafish Nodal signal *squint* functions as a morphogen", *Nature* **411**(6837), 607-10.

- Cheng, Q.**, Lau, W. M., Chew, S. H., Ho, T. H., Tay, S. K. and Hui, K. M. (2002) "Identification of molecular markers for the early detection of human squamous cell carcinoma of the uterine cervix", *Br J Cancer* **86**(2), 274-81.
- Chester, K. A.**, Robson, L., Begent, R. H., Talbot, I. C., Pringle, J. H., Primrose, L., Macpherson, A. J., Boxer, G., Southall, P. and Malcolm, A. D. (1989) "Identification of a human ribosomal protein mRNA with increased expression in colorectal tumours", *Biochim Biophys Acta* **1009**(3), 297-300.
- Cho, H.**, Mu, J., Kim, J. K., Thorvaldsen, J. L., Chu, Q., Crenshaw, E. B., 3rd, Kaestner, K. H., Bartolomei, M. S., Shulman, G. I. and Birnbaum, M. J. (2001a) "Insulin resistance and a diabetes mellitus-like syndrome in mice lacking the protein kinase Akt2 (PKB beta)", *Science* **292**(5522), 1728-31.
- Cho, H.**, Thorvaldsen, J. L., Chu, Q., Feng, F. and Birnbaum, M. J. (2001b) "Akt1/PKBalpha is required for normal growth but dispensable for maintenance of glucose homeostasis in mice", *J Biol Chem* **276**(42), 38349-52.
- Cho, K. W.**, Blumberg, B., Steinbeisser, H. and De Robertis, E. M. (1991) "Molecular nature of Spemann's organizer: the role of the *Xenopus* homeobox gene goosecoid", *Cell* **67**(6), 1111-20.
- Christiansen, J. H.**, Coles, E. G., Robinson, V., Pasini, A. and Wilkinson, D. G. (2001) "Screening from a subtracted embryonic chick hindbrain cDNA library: identification of genes expressed during hindbrain, midbrain and cranial neural crest development", *Mech Dev* **102**((1-2)), 119-33.
- Chun, J.**, Kwon, T., Lee, E., Suh, P. G., Choi, E. J. and Sun Kang, S. (2002) "The Na(+)/H(+) exchanger regulatory factor 2 mediates phosphorylation of serum- and glucocorticoid-induced protein kinase 1 by 3-phosphoinositide-dependent protein kinase 1", *Biochem Biophys Res Commun* **298**(2), 207-15.
- Clapp, C. M.** (1891) "Some points in the development of the toad-fish", *J Morphol* **5**, 494-501.
- Clements, D.**, Friday, R. V. and Woodland, H. R. (1999) "Mode of action of VegT in mesoderm and endoderm formation", *Development* **126**(21), 4903-11.
- Conlon, F. L.**, Lyons, K. M., Takaesu, N., Barth, K. S., Kispert, A., Herrmann, B. and Robertson, E. J. (1994) "A primary requirement for nodal in the formation and maintenance of the primitive streak in the mouse", *Development* **120**(7), 1919-28.
- Conlon, R. A.** (1995) "Retinoic acid and pattern formation in vertebrates", *Trends Genet*, **11**(8):314-9.

- Cooper, M. S. and D'Amico, L. A.** (1996) "A cluster of noninvoluting endocytic cells at the margin of the zebrafish blastoderm marks the site of embryonic shield formation", *Dev Biol* **180**(1), 184-98.
- Cooper, M. S. and D'Amico, L. A.** (2001) "Morphogenetic Domains in the Yolk Syncytial Layer of Axiating Zebrafish Embryos", *Dev Dyn* **222**, 611-24.
- Coutinho, P., Parsons, M. J., Thomas, K. A., Hirst, E. M. A., Saude, L., Campos, I. and Stemple, D. L.** (2003) "Coatomer mRNA is Regulated by Coatomer Function via Negative Feedback", *submitted*.
- Cosson, P. and Letourneur, F.** (1997) "Coatomer (COPI)-coated vesicles: role in intracellular transport and protein sorting" *Curr Opin Cell Biol* **9**, 484-7.
- Cowling, R. T. and Birnboim, H. C.** (2000) "Expression of serum- and glucocorticoid-regulated kinase (sgk) mRNA is up-regulated by GM-CSF and other proinflammatory mediators in human granulocytes", *J Leukoc Biol* **67**(2), 240-8.
- Cox, W. G. and Hemmati-Brivanlou, A.** (1995) "Caudalization of neural fate by tissue recombination and bFGF", *Development*, **121**(12), 4349-58.
- Cramton, S. E. and Laski, F. A.** (1994) "*string of pearls* encodes *Drosophila* ribosomal protein S2, has Minute-like characteristics, and is required during oogenesis", *Genetics* **137**(4), 1039-48.
- Crossley, P. H. and Martin, G. R.** (1995) "The mouse *Fgf8* gene encodes a family of polypeptides and is expressed in regions that direct outgrowth and patterning in the developing embryo", *Development*, **121**, 439-51.
- Cui, Y., Brown, J. D., Moon, R. T. and Christian, J. L.** (1995) "*Xwnt-8b*: a maternally expressed *Xenopus Wnt* gene with a potential role in establishing the dorsoventral axis", *Development* **121**(7), 2177-86.
- Dale, L., Matthews, G. and Colman, A.** (1993) "Secretion and mesoderm-inducing activity of the TGF-beta-related domain of *Xenopus Vg1*", *EMBO J* **12**(12), 4471-80.
- Dale, L., Matthews, G., Tabe, L. and Colman, A.** (1989) "Developmental expression of the protein product of *Vg1*, a localized maternal mRNA in the frog *Xenopus laevis*", *EMBO J* **8**(4), 1057-65.
- Dale, L. and Slack, J. M.** (1987) "Fate map for the 32-cell stage of *Xenopus laevis*", *Development*. **99**(4), 527-51.
- Daniels, D. L., Eklof Spink, K. and Weis, W. I.** (2001) "beta-catenin: molecular plasticity and drug design", *Trends Biochem Sci* **26**(11), 672-8.
- Danielson, P. E., Forss-Petter, S., Battenberg, E. L., deLecea, L., Bloom, F. E. and Sutcliffe, J. G.** (1994) "Four structurally distinct neuron-specific olfactomedin-related

glycoproteins produced by differential promoter utilization and alternative mRNA splicing from a single gene", *J Neurosci Res* **38**(4), 468-78.

Datto, M. B., Frederick, J. P., Pan, L., Borton, A. J., Zhuang, Y. and Wang, X. F. (1999) "Targeted disruption of Smad3 reveals an essential role in transforming growth factor beta-mediated signal transduction", *Mol Cell Biol* **19**(4), 2495-504.

David, N. B. and Rosa, F. (2001) "Cell autonomous commitment to an endodermal fate and behaviour by activation of Nodal signalling", *Development* **128**(20), 3937-47.

Davies, T. J. and Gardner, R. L. (2002) "The plane of first cleavage is not related to the distribution of sperm components in the mouse", *Hum Reprod* **17**(9), 2368-79.

Debonneville, C., Flores, S. Y., Kamynina, E., Plant, P. J., Tauxe, C., Thomas, M. A., Munster, C., Chraïbi, A., Pratt, J. H., Horisberger, J. D., Pearce, D., Loffing, J. and Staub, O. (2001) "Phosphorylation of Nedd4-2 by Sgk1 regulates epithelial Na(+) channel cell surface expression", *EMBO J* **20**(24), 7052-9.

Dehal, P., Satou, Y., Campbell, R. K., Chapman, J., Degnan, B., De Tomaso, A., Davidson, B., Di Gregorio, A., Gelpke, M., Goodstein, D. M., Harafuji, N., Hastings, K. E., Ho, I., Hotta, K., Huang, W., Kawashima, T., Lemaire, P., Martinez, D., Meinertzhagen, I. A., Necula, S., Nonaka, M., Putnam, N., Rash, S., Saiga, H., Satake, M., Terry, A., Yamada, L., Wang, H. G., Awazu, S., Azumi, K., Boore, J., Branno, M., Chin-Bow, S., DeSantis, R., Doyle, S., Francino, P., Keys, D. N., Haga, S., Hayashi, H., Hino, K., Imai, K. S., Inaba, K., Kano, S., Kobayashi, K., Kobayashi, M., Lee, B. I., Makabe, K. W., Manohar, C., Matassi, G., Medina, M., Mochizuki, Y., Mount, S., Morishita, T., Miura, S., Nakayama, A., Nishizaka, S., Nomoto, H., Ohta, F., Oishi, K., Rigoutsos, I., Sano, M., Sasaki, A., Sasakura, Y., Shoguchi, E., Shin-i, T., Spagnuolo, A., Stainier, D., Suzuki, M. M., Tassy, O., Takatori, N., Tokuoka, M., Yagi, K., Yoshizaki, F., Wada, S., Zhang, C., Hyatt, P. D., Larimer, F., Detter, C., Doggett, N., Glavina, T., Hawkins, T., Richardson, P., Lucas, S., Kohara, Y., Levine, M., Satoh, N. and Rokhsar, D. S. (2002) "The draft genome of *Ciona intestinalis*: insights into chordate and vertebrate origins", *Science* **298**(5601), 2157-67.

deHart, A. K., Schnell, J. D., Allen, D. A. and Hicke, L. (2002) "The conserved Pkh-Ypk kinase cascade is required for endocytosis in yeast", *J Cell Biol* **156**(2), 241-8.

Delmolino, L. M. and Castellot, J. J., Jr. (1997) "Heparin suppresses *sgk*, an early response gene in proliferating vascular smooth muscle cells", *J Cell Physiol* **173**(3), 371-9.

DeRobertis, E. M. and Sasai, Y. (1996) "A common plan for dorsoventral patterning in Bilateria", *Nature* **380**(6569), 37-40.

- Derynck, R.**, Zhang, Y. and Feng, X. H. (1998) "Smads: transcriptional activators of TGF-beta responses", *Cell* **95**(6), 737-40.
- Dick, A.**, Hild, M., Bauer, H., Imai, Y., Maifeld, H., Schier, A. F., Talbot, W. S., Bouwmeester, T. and Hammerschmidt, M. (2000) "Essential role of Bmp7 (snailhouse) and its prodomain in dorsoventral patterning of the zebrafish embryo", *Development* **127**(2), 343-54.
- Dickmeis, T.**, Mourrain, P., Saint-Etienne, L., Fischer, N., Aanstad, P., Clark, M., Strahle, U. and Rosa, F. (2001) "A crucial component of the endoderm formation pathway, CASANOVA, is encoded by a novel *sox*-related gene", *Genes Dev* **15**(12), 1487-92.
- Ding, J.**, Yang, L., Yan, Y. T., Chen, A., Desai, N., Wynshaw-Boris, A. and Shen, M. M. (1998) "Cripto is required for correct orientation of the antero-posterior axis in the mouse embryo", *Nature* **395**(6703), 702-7.
- Domingos, P. M.**, Itasaki, N., Jones, C. M., Mercurio, S., Sargent, M. G., Smith, J. C. and Krumlauf, R. (2001) "The Wnt/beta-catenin pathway posteriorizes neural tissue in *Xenopus* by an indirect mechanism requiring FGF signalling" *Dev Biol*, **239**(1), 148-60.
- Dominguez, I. and Green, J. B.** (2000) "Dorsal downregulation of GSK3beta by a non-Wnt-like mechanism is an early molecular consequence of cortical rotation in early *Xenopus* embryos", *Development* **127**(4), 861-8.
- Dominguez, I.**, Itoh, K. and Sokol, S. Y. (1995) "Role of glycogen synthase kinase 3 beta as a negative regulator of dorsoventral axis formation in *Xenopus* embryos", *Proc Natl Acad Sci USA* **92**(18), 8498-502.
- Donohue, P. J.**, Alberts, G. F., Guo, Y. and Winkles, J. A. (1995) "Identification by targeted differential display of an immediate early gene encoding a putative serine/threonine kinase", *J Biol Chem* **270**(17), 10351-7.
- Dorer, D. R.**, Anane-Firempong, A. and Christensen, A. C. (1991) "Ribosomal protein S14 is not responsible for the *Minute* phenotype associated with the M(1)7C locus in *Drosophila melanogaster*", *Mol Gen Genet* **230**(1-2), 8-11.
- Draper, B. W.**, Morcos, P. A. and Kimmel, C. B. (2001) "Inhibition of zebrafish *fgf8* pre-mRNA splicing with morpholino oligos: a quantifiable method for gene knockdown", *Genesis* **30**(3), 154-6.
- Driever, W.**, Solnica-Krezel, L., Schier, A. F., Neuhauss, S. C., Malicki, J., Stemple, D. L., Stainier, D. Y., Zwartkuis, F., Abdelilah, S., Rangini, Z., Belak, J. and Boggs, C. (1996) "A genetic screen for mutations affecting embryogenesis in zebrafish", *Development* **123**, 37-46.

- Du, S. J., Purcell, S. M., Christian, J. L., McGrew, L. L. and Moon, R. T. (1995)** "Identification of distinct classes and functional domains of Wnts through expression of wild-type and chimeric proteins in *Xenopus* embryos", *Mol Cell Biol* **15**(5), 2625-34.
- Ducibella, T. and Anderson, E. (1975)** "Cell shape and membrane changes in the eight-cell mouse embryo: prerequisites for morphogenesis of the blastocyst", *Dev Biol* **47**(1), 45-58.
- Dufort, D., Schwartz, L., Harpal, K. and Rossant, J. (1998)** "The transcription factor HNF3beta is required in visceral endoderm for normal primitive streak morphogenesis", *Development* **125**(16), 3015-25.
- Dyson, S. and Gurdon, J. B. (1997)** "Activin signalling has a necessary function in *Xenopus* early development", *Curr Biol* **7**(1), 81-4.
- Edgar, B. A. (1999)** "From small flies come big discoveries about size control", *Nat Cell Biol* **1**(8), E191-3.
- Edgar, B. A., Odell, G. M. and Schubiger, G. (1987)** "Cytoarchitecture and the patterning of *fushi tarazu* expression in the *Drosophila* blastoderm", *Genes Dev* **1**(10), 1226-37.
- Edgar, B. A., Weir, M. P., Schubiger, G. and Kornberg, T. (1986)** "Repression and turnover pattern *fushi tarazu* RNA in the early *Drosophila* embryo", *Cell* **47**(5), 747-54.
- Elchebly, M., Wagner, J., Kennedy, T. E., Lanctot, C., Michaliszyn, E., Itie, A., Drouin, J. and Tremblay, M. L. (1999)** "Neuroendocrine dysplasia in mice lacking protein tyrosine phosphatase sigma", *Nat Genet* **21**(3), 330-3.
- Elinson, R. P. and Rowning, B. (1988)** "A transient array of parallel microtubules in frog eggs: potential tracks for a cytoplasmic rotation that specifies the dorso-ventral axis.PG", *Dev Biol* **128**(1).
- Embark, H. M., Bohmer, C., Vallon, V., Luft, F. and Lang, F. (2003)** "Regulation of KCNE1-dependent K(+) current by the serum and glucocorticoid-inducible kinase (SGK) isoforms", *Pflugers Arch* **445**(5), 601-6.
- Episkopou, V., Arkell, R., Timmons, P. M., Walsh, J. J., Andrew, R. L. and Swan, D. (2001)** "Induction of the mammalian node requires Arkadia function in the extraembryonic lineages", *Nature* **410**(6830), 825-30.
- Evsikov, S. V., Morozova, L. M. and Solombko, A. P. (1994)** "Role of ooplasmic segregation in mammalian development", *Roux's Arch Dev Biol* **203**, 199-204.
- Eyal-Giladi, H. (1997)** "Establishment of the axis in chordates: facts and speculations", *Development* **124**(12), 2285-96.

- Eyal-Giladi, H. and Kochav, S.** (1976) "From cleavage to primitive streak formation: a complementary normal table and a new look at the first stages of the development of the chick. I. General morphology", *Dev Biol* **49**(2), 321-37.
- Fagotto, F., Guger, K. and Gumbiner, B. M.** (1997) "Induction of the primary dorsalizing center in *Xenopus* by the Wnt/GSK/beta-catenin signaling pathway, but not by Vg1, Activin or Noggin", *Development* **124**(2), 453-60.
- Fainsod, A., Deissler, K., Yelin, R. Marom, K., Epstein, M., Pillemer, G., Steinbeisser, H. and Blum, M.** (1997) "The dorsalizing and neural inducing gene follistatin is an antagonist of BMP-4", *Mech Dev* **63**, 39-50.
- Faletti, C. J., Perrotti, N., Taylor, S. I. and Blazer-Yost, B. L.** (2002) "sgk: an essential convergence point for peptide and steroid hormone regulation of ENaC-mediated Na⁺ transport", *Am J Physiol Cell Physiol* **282**(3), C494-500.
- Fan, M. J. and Sokol, S. Y.** (1997) "A role for Siamois in Spemann organizer formation", *Development* **124**(13), 2581-9.
- Fan, Q. W., Kadomatsu, K., Uchimura, K. and Muramatsu, T.** (1998) "Embigin/basigin subgroup of the immunoglobulin superfamily: different modes of expression during mouse embryogenesis and correlated expression with carbohydrate antigenic markers", *Dev Growth Differ* **40**(3), 277-86.
- Farman, N., Boulkroun, S. and Courtois-Coutry, N.** (2002) "Sgk: an old enzyme revisited", *J Clin Invest* **110**(9), 1233-4.
- Farnsworth, M. W.** (1957a) "Effects of the homozygous first, second and third chromosome *Minutes* on the development of *Drosophila melanogaster*", *Genetics* **42**, 19-27.
- Farnsworth, M. W.** (1957b) "Effects of the homozygous *Minute-IV* deficiency on the development of *Drosophila melanogaster*", *Genetics* **42**, 7-19.
- Fatica, A. and Tollervey, D.** (2002) "Making ribosomes", *Curr Opin Cell Biol* **14**(3), 313-8.
- Fekany, K., Yamanaka, Y., Leung, T., Sirotkin, H. I., Topczewski, J., Gates, M. A., Hibi, M., Renucci, A., Stemple, D., Radbill, A., Schier, A. F., Driever, W., Hirano, T., Talbot, W. S. and Solnica-Krezel, L.** (1999) "The zebrafish *bozozok* locus encodes Dharma, a homeodomain protein essential for induction of gastrula organizer and dorsoanterior embryonic structures", *Development* **126**(7), 1427-38.
- Fekany-Lee, K., Gonzalez, E., Miller-Bertoglio, V. and Solnica-Krezel, L.** (2000) "The homeobox gene *bozozok* promotes anterior neuroectoderm formation in zebrafish

through negative regulation of BMP2/4 and Wnt pathways", *Development* **127**(11), 2333-45.

Feldman, B., Concha, M. L., Saude, L., Parsons, M. J., Adams, R. J., Wilson, S. W. and Stemple, D. L. (2002) "Lefty antagonism of squint is essential for normal gastrulation", *Curr Biol* **12**(24), 2129-35.

Feldman, B., Gates, M. A., Egan, E. S., Dougan, S. T., Rennebeck, G., Sirotkin, H. I., Schier, A. F. and Talbot, W. S. (1998) "Zebrafish organizer development and germ-layer formation require nodal-related signals", *Nature* **395**(6698), 181-5.

Filosa, S., Rivera-Perez, J. A., Gomez, A. P., Gansmuller, A., Sasaki, H., Behringer, R. R. and Ang, S.-L. (1997) "Goosecoid and HNF-3beta genetically interact to regulate neural tube patterning during mouse embryogenesis", *Development* **124**, 2843-54.

Fine, L. G., Holley, R. W., Nasri, H. and Badie-Dezfooly, B. (1985) "BSC-1 growth inhibitor transforms a mitogenic stimulus into a hypertrophic stimulus for renal proximal tubular cells: relationship to Na⁺/H⁺ antiport activity", *Proc Natl Acad Sci USA* **82**(18), 6163-6.

Firestone, G. L., Giampaolo, J. R. and O'Keeffe, B. A. (2003) "Stimulus-Dependent Regulation of Serum and Glucocorticoid Inducible Protein Kinase (SGK) Transcription, Subcellular Localization and Enzymatic Activity", *Cell Physiol Biochem* **13**(1), 1-12.

Fisher, J. P., Hope, S. A. and Hooper, M. L. (1989) "Factors influencing the differentiation of embryonal carcinoma and embryo-derived stem cells", *Exp Cell Res* **182**(2), 403-14.

Fjose, A., Izpisua-Belmonte, J. C., Fromental-Ramain, C. and Duboule, D. (1994) "Expression of the zebrafish gene *hlx-1* in the prechordal plate and during CNS development", *Development* **120**(1), 71-81.

Fleming, T. P. (1987) "A quantitative analysis of cell allocation to trophectoderm and inner cell mass in the mouse blastocyst", *Dev Biol* **119**(2), 520-31.

Foley, A. C., Skromne, I. and Stern, C. D. (2000) "Reconciling different models of forebrain induction and patterning: a dual role for the hypoblast", *Development* **127**(17), 3839-54.

Foley, A. C. and Stern, C. D. (2001) "Evolution of vertebrate forebrain development: how many different mechanisms?", *J Anat* **199**, 35-52.

Fruttiger, M. (2002) "Development of the mouse retinal vasculature: angiogenesis versus vasculogenesis", *Invest Ophthalmol Vis Sci* **43**(2), 522-7.

Fu, H., Subramanian, R. R. and Masters, S. C. (2000), "14-3-3 proteins: Structure, Function, and Regulation", *Annu Rev Pharmacol Toxicol*, **40**, 617-47.

- Fujimori, T., Kurotaki, Y., Miyazaki, J. and Nabeshima, Y. (2003)** "Analysis of cell lineage in two- and four-cell mouse embryos", *Development*, **130**(21), 5113-22.
- Fujisue, M., Kobayakawa, Y. and Yamana, K. (1993)** "Occurrence of dorsal axis-inducing activity around the vegetal pole of an uncleaved *Xenopus* egg and displacement to the equatorial region by cortical rotation", *Development* **118**, 163-70.
- Funayama, N., Fagotto, F., McCrea, P. and Gumbiner, B. M. (1995)** "Embryonic axis induction by the armadillo repeat domain of beta-catenin: evidence for intracellular signaling", *J Cell Biol* **128**(5), 959-68.
- Fürthauer, M., Thisse, C. and Thisse, B. (1997)** "A role for FGF-8 in the dorsoventral patterning of the zebrafish gastrula" *Development* **124**(21), 4253-64.
- Furukawa, T., Kozac, C. A. and Cepko, C. L. (1997)** "*rax*, a novel paired-type homeobox gene, shows expression in the anterior neural fold and developing retina", *Proc Natl Acad Sci USA* **94**, 3088-93.
- Furukawa, T., Uchiumi, T., Tokunaga, R. and Taketani, S. (1992)** "Ribosomal protein P2, a novel iron-binding protein", *Arch Biochem Biophys* **298**(1), 182-6.
- Gaio, U., Schweickert, A., Fischer, A., Garratt, A. N., Muller, T., Ozcelik, C., Lankes, W., Strehle, M., Britsch, S., Blum, M. and Birchmeier, C. (1999)** "A role of the *cryptic* gene in the correct establishment of the left-right axis", *Curr Biol* **9**(22), 1339-42.
- Gamper, N., Fillon, S., Feng, Y., Friedrich, B., Lang, P. A., Henke, G., Huber, S. M., Kobayashi, T., Cohen, P. and Lang, F. (2002a)** "K(+) channel activation by all three isoforms of serum- and glucocorticoid-dependent protein kinase SGK", *Pflugers Arch* **445**(1), 60-6.
- Gamper, N., Fillon, S., Huber, S. M., Feng, Y., Kobayashi, T., Cohen, P. and Lang, F. (2002b)** "IGF-1 up-regulates K+ channels via PI3-kinase, PDK1 and SGK1", *Pflugers Arch* **443**(4), 625-34.
- Gardner, M. J., Hall, N., Fung, E., White, O., Berriman, M., Hyman, R. W., Carlton, J. M., Pain, A., Nelson, K. E., Bowman, S., Paulsen, I. T., James, K., Eisen, J. A., Rutherford, K., Salzberg, S. L., Craig, A., Kyes, S., Chan, M. S., Nene, V., Shallom, S. J., Suh, B., Peterson, J., Angiuoli, S., Pertea, M., Allen, J., Selengut, J., Haft, D., Mather, M. W., Vaidya, A. B., Martin, D. M., Fairlamb, A. H., Fraunholz, M. J., Roos, D. S., Ralph, S. A., McFadden, G. I., Cummings, L. M., Subramanian, G. M., Mungall, C., Venter, J. C., Carucci, D. J., Hoffman, S. L., Newbold, C., Davis, R. W., Fraser, C. M. and Barrell, B. (2002)** "Genome sequence of the human malaria parasite *Plasmodium falciparum*", *Nature* **419**(6906), 498-511.

- Gardner, R. L.** (1990) Location and orientation of implantation, New York, Serono Symposia Publications, Raven Press.
- Gardner, R. L.** (1997) "The early blastocyst is bilaterally symmetrical and its axis of symmetry is aligned with the animal-vegetal axis of the zygote in the mouse", *Development* **124**(2), 289-301.
- Gardner, R. L.** (1999a) "Polarity in early mammalian development", *Curr Opin Genet Dev* **9**(4), 417-21.
- Gardner, R. L.** (1999b) "Scrambled or bisected mouse eggs and the basis of patterning in mammals", *Bioessays* **21**(4), 271-4.
- Gardner, R. L.** (2001) "Specification of embryonic axes begins before cleavage in normal mouse development", *Development* **128**(6), 839-47.
- Garner, W. and McLaren, A.** (1974) "Cell distribution in chimaeric mouse embryos before implantation", *J Embryol Exp Morphol* **32**(2), 495-503.
- Gawantka, V., Pollet, N., Delius, H., Vingron, M., Pfister, R., Nitsch, R., Blumenstock, C. and Niehrs, C.** (1998) "Gene expression screening in *Xenopus* identifies molecular pathways, predicts gene function and provides a global view of embryonic patterning", *Mech Dev* **77**(2), 95-141.
- Gerhart, J., Danilchik, M., Doniach, T., Roberts, S., Rowning, B. and Stewart, R.** (1989) "Cortical rotation of the *Xenopus* egg: consequences for the anteroposterior pattern of embryonic dorsal development", *Development* **107 Suppl**, 37-51.
- Gerhart, J. and Kirschner, M.** (1997) Cells, embryos and evolution, Malden, MA, Blackwell Science, Inc.
- Gilbert, S. F.** (2000) Developmental Biology, Sunderland, MA, Sinauer Associates Inc.
- Gilbert, S. F. and Raunio, A. M.** (1997) Embryology. Constructing the Organism, Sunderland, MA, Sinauer Associates Inc.
- Gimlich, R. L. and Cooke, J.** (1983) "Cell lineage and the induction of second nervous systems in amphibian development", *Nature* **306**(5942), 471-3.
- Girard, F., Strausfeld, U., Fernandez, A. and Lamb, N. J.** (1991) "Cyclin A is required for the onset of DNA replication in mammalian fibroblasts", *Cell* **67**(6), 1169-79.
- Gitton, Y., Dahmane, N., Baik, S., Ruiz i Altaba, A., Neidhardt, L., Scholze, M., Herrmann, B. G., Kahlem, P., Benkahla, A., Schrunner, S., Yildirimman, R., Herwig, R., Lehrach, H. and Yaspo, M. L.** (2002) "A gene expression map of human chromosome 21 orthologues in the mouse", *Nature* **420**(6915), 586-90.
- Godsave, S. F. and Slack, J. M.** (1991) "Single cell analysis of mesoderm formation in the *Xenopus* embryo", *Development* **111**, 523-30.

- Golling, G.**, Amsterdam, A., Sun, Z., Antonelli, M., Maldonado, E., Chen, W., Burgess, S., Haldi, M., Artzt, K., Farrington, S., Lin, S. Y., Nissen, R. M. and Hopkins, N. (2002) "Insertional mutagenesis in zebrafish rapidly identifies genes essential for early vertebrate development", *Nat Genet* **31**(2), 135-40.
- Gonzalez-Nicolini, V. and McGinty, J. F.** (2002) "Gene expression profile from the striatum of amphetamine-treated rats: a cDNA array and *in situ* hybridisation histochemical study", *Brain Res Gene Expr Patterns* **1**(3-4), 193-8.
- Gonzalez-Robayna, I. J.**, Alliston, T. N., Buse, P., Firestone, G. L. and Richards, J. S. (1999) "Functional and subcellular changes in the A-kinase-signaling pathway: relation to aromatase and *Sgk* expression during the transition of granulosa cells to luteal cells", *Mol Endocrinol* **13**(8), 1318-37.
- Gonzalez-Robayna, I. J.**, Falender, A. E., Ochsner, S., Firestone, G. L. and Richards, J. S. (2000) "Follicle-Stimulating hormone (FSH) stimulates phosphorylation and activation of protein kinase B (PKB/Akt) and serum and glucocorticoid- Induced kinase (*Sgk*): evidence for A kinase-independent signaling by FSH in granulosa cells", *Mol Endocrinol* **14**(8), 1283-300.
- Graham, C. F.** (1971) "The design of the mouse blastocyst", *Symp Soc Exp Biol* **25**, 371-8.
- Graham, C. F. and Deussen, Z. A.** (1978) "Features of cell lineage in preimplantation mouse development", *J Embryol Exp Morphol* **48**, 53-72.
- Griffin, K. J.**, Amacher, S. L., Kimmel, C. B. and Kimelman, D. (1998) "Molecular identification of spadetail: regulation of zebrafish trunk and tail mesoderm formation by T-box genes", *Development* **125**(17), 3379-88.
- Gritsman, K.**, Zhang, J., Cheng, S., Heckscher, E., Talbot, W. S. and Schier, A. F. (1999) "The EGF-CFC protein one-eyed pinhead is essential for nodal signaling", *Cell* **97**(1), 121-32.
- Grose, R.**, Harris, B. S., Cooper, L., Topilko, P. and Martin, P. (2002) "Immediate early genes *krox-24* and *krox-20* are rapidly up-regulated after wounding in the embryonic and adult mouse", *Dev Dyn* **223**(3), 371-8.
- Grunz, H. and Tacke, L.** (1989) "Neural differentiation of *Xenopus laevis* ectoderm takes place after disaggregation and delayed reaggregation without inducer", *Cell Diff Dev* **28**, 211-8.
- Gu, Z.**, Nomura, M., Simpson, B. B., Lei, H., Feijen, A., van den Eijnden-van Raaij, J., Donahoe, P. K. and Li, E. (1998) "The type I activin receptor ActRIB is required for egg cylinder organization and gastrulation in the mouse", *Genes Dev* **12**(6), 844-57.

- Habas, R., Dawid, I. B. and He, X. (2003)** "Coactivation of Rac and Rho by Wnt/Frizzled signaling is required for vertebrate gastrulation" *Genes Dev* **17**(2), 295-309.
- Haegel, H., Larue, L., Ohsugi, M., Fedorov, L., Herrenknecht, K. and Kemler, R. (1995)** "Lack of beta-catenin affects mouse development at gastrulation", *Development* **121**(11), 3529-37.
- Haffter, P. and Nusslein-Volhard, C. (1996)** "Large scale genetics in a small vertebrate, the zebrafish", *Int J Dev Biol* **40**(1), 221-7.
- Haft, C. R., de la Luz Sierra, M., Barr, V. A., Haft, D. H. and Taylor, S. I. (1998)** "Identification of a family of sorting nexin molecules and characterization of their association with receptors", *Mol Cell Biol* **18**(12), 7278-87.
- Hamburger, V. and Hamilton, H. L. (1992)** "A series of normal stages in the development of the chick embryo. 1951", *Dev Dyn* **195**(4), 231-72.
- Hamburger, V. (1988)** The heritage of experimental embryology: Hans Spemann and the organizer, Oxford University Press, Oxford.
- Hanks, S. K., Quinn, A. M. and Hunter, T. (1988)** "The protein kinase family: conserved features and deduced phylogeny of the catalytic domains", *Science* **241**(4861), 42-52.
- Harland, R. and Gerhart, J. (1997)** "Formation and function of Spemann's organizer", *Annu Rev Cell Dev Biol* **13**, 611-67.
- Harnpicharnchai, P., Jakovljevic, J., Horsey, E., Miles, T., Roman, J., Rout, M., Meagher, D., Imai, B., Guo, Y., Brame, C. J., Shabanowitz, J., Hunt, D. F. and Woolford, J. L., Jr. (2001)** "Composition and functional characterization of yeast 66S ribosome assembly intermediates", *Mol Cell* **8**(3), 505-15.
- Harrison, S. M., Dunwoodie, S. L., Arkell, R. M., Lehrach, H. and Beddington, R. S. (1995)** "Isolation of novel tissue-specific genes from cDNA libraries representing the individual tissue constituents of the gastrulating mouse embryo", *Development* **121**(8), 2479-89.
- Hart, A. H., Hartley, L., Sourris, K., Stadler, E. S., Li, R., Stanley, E. G., Tam, P. P., Elefanty, A. G. and Robb, L. (2002)** "Mix11 is required for axial mesendoderm morphogenesis and patterning in the murine embryo", *Development* **129**(15), 3597-608.
- Hart, K., Klein, T. and Wilcox, M. (1993)** "A *Minute* encoding a ribosomal protein enhances wing morphogenesis mutants", *Mech Dev* **43**(2-3), 101-10.

- Hashimoto, H.**, Itoh, M., Yamanaka, Y., Yamashita, S., Shimizu, T., Solnica-Krezel, L., Hibi, M. and Hirano, T. (2000) "Zebrafish Dkk1 functions in forebrain specification and axial mesendoderm formation", *Dev Biol* **217**(1), 138-52.
- Hasty, P.**, Rivera-Perez, J. and Bradley, A. (1992) "The role and fate of DNA ends for homologous recombination in embryonic stem cells", *Mol Cell Biol* **12**(6), 2464-74.
- Hatta, K.**, Kimmel, C. B., Ho, R. K. and Walker, C. (1991) "The *cyclops* mutation blocks specification of the floor plate of the zebrafish central nervous system", *Nature* **350**(6316), 339-41.
- Hatta, K. and Takahashi, Y.** (1996) "Secondary axis induction by heterospecific organizers in zebrafish", *Dev Dyn* **205**(2), 183-95.
- Hawley, S. H. B.**, Wunnenberg-Stapleton, K., Hashimoto, C. Laurent, M. N., Watabe, T. Blumberg, B. W. and Cho, K. W. (1995) "Disruption of BMP signals in embryonic *Xenopus* ectoderm leads to direct neural induction", *Genes Dev* **9**, 2923-35.
- Hayashi, M.**, Tapping, R. I., Chao, T. H., Lo, J. F., King, C. C., Yang, Y. and Lee, J. D. (2001) "BMK1 mediates growth factor-induced cell proliferation through direct cellular activation of serum and glucocorticoid-inducible kinase", *J Biol Chem* **276**(12), 8631-4.
- He, T. C.**, Sparks, A. B., Rago, C., Hermeking, H., Zawel, L., da Costa, L. T., Morin, P. J., Vogelstein, B. and Kinzler, K. W. (1998) "Identification of c-MYC as a target of the APC pathway", *Science* **281**(5382), 1509-12.
- He, X.**, Saint-Jeannet, J. P., Woodgett, J. R., Varmus, H. E. and Dawid, I. B. (1995) "Glycogen synthase kinase-3 and dorsoventral patterning in *Xenopus* embryos", *Nature* **374**(6523), 617-22.
- Heasman, J.** (1997) "Patterning the *Xenopus* blastula", *Development* **124**(21), 4179-91.
- Heasman, J.**, Crawford, A., Goldstone, K., Garner-Hamrick, P., Gumbiner, B., McCrea, P., Kintner, C., Noro, C. Y. and Wylie, C. (1994) "Overexpression of cadherins and underexpression of beta-catenin inhibit dorsal mesoderm induction in early *Xenopus* embryos", *Cell* **79**(5), 791-803.
- Heasman, J.**, Kofron, M. and Wylie, C. (2000) "Beta-catenin signaling activity dissected in the early *Xenopus* embryo: a novel antisense approach", *Dev Biol* **222**(1), 124-34.
- Heasman, J.**, Wessely, O., Llangland, R., Craig, E. J. and Kessler, D. S. (2001) "Vegetal localization of maternal mRNAs is disrupted by VegT depletion", *Dev Biol* **240**(2), 377-86.
- Heisenberg, C. P.**, Houart, C., Take-Uchi, M., Rauch, G. J., Young, N., Coutinho, P., Masai, I., Caneparo, L., Concha, M. L., Geisler, R., Dale, T. C., Wilson, S. W. and

- Stemple, D. L. (2001) "A mutation in the Gsk3-binding domain of zebrafish Masterblind/Axin1 leads to a fate transformation of telencephalon and eyes to diencephalon", *Genes Dev* **15**(11), 1427-34.
- Heisenberg, C. P. and Nusslein-Volhard, C. (1997) "The function of silberblick in the positioning of the eye anlage in the zebrafish embryo", *Dev Biol* **184**(1), 85-94.
- Heisenberg, C. P. and Tada, M. (2002) "Wnt signalling: a moving picture emerges from van gogh", *Curr Biol* **12**(4), R126-8.
- Heisenberg, C. P., Tada, M., Rauch, G. J., Saude, L., Concha, M. L., Geisler, R., Stemple, D. L., Smith, J. C. and Wilson, S. W. (2000) "Silberblick/Wnt11 mediates convergent extension movements during zebrafish gastrulation", *Nature* **405**(6782), 76-81.
- Heiskala, M., Peterson, P. A. and Yang, Y. (2001) "The roles of claudin superfamily proteins in paracellular transport", *Traffic* **2**(2), 93-8.
- Helde, K. A., Wilson, E. T., Cretekos, C. J. and Grunwald, D. J. (1994) "Contribution of early cells to the fate map of the zebrafish gastrula", *Science* **265**(5171), 517-20.
- Hemmati-Brivanlou, A., Kelly, O. G. and Melton, D. A. (1994) "Follistatin, an antagonist of activin, is expressed in the Spemann organizer and displays direct neuralizing activity", *Cell* **77**, 283-95.
- Hemmati-Brivanlou, A. and Melton, D. A. (1992) "A truncated activin receptor inhibits mesoderm induction and formation of axial structures in *Xenopus* embryos", *Nature* **359**(6396), 609-14.
- Hemmati-Brivanlou, A. and Melton, D. A. (1994) "Inhibition of activin receptor signaling promotes neuralization in *Xenopus*", *Cell* **77**(2), 273-81.
- Hemmati-Brivanlou, A. and Melton, D. A. (1997) "Vertebrate embryonic cells will become nerve cells unless told otherwise", *Cell* **88**, 13-7.
- Hemmati-Brivanlou, A. and Thomsen, G. H. (1995) "Ventral mesodermal patterning in *Xenopus* embryos: expression patterns and activities of BMP-2 and BMP-4", *Dev Genet* **17**(1), 78-89.
- Hendzel, M. J., Wei, Y., Mancini, M. A., Van Hooser, A., Ranalli, T., Brinkley, B. R., Bazett-Jones, D. P. and Allis, C. D. (1997) "Mitosis-specific phosphorylation of histone H3 initiates primarily within pericentromeric heterochromatin during G2 and spreads in an ordered fashion coincident with mitotic chromosome condensation", *Chromosoma* **106**(6), 348-60.
- Henry, G. L. and Melton, D. A. (1998) "Mixer, a homeobox gene required for endoderm development", *Science* **281**(5373), 91-6.

- Henry, J. L., Coggin, D. L. and King, C. R.** (1993) "High-level expression of the ribosomal protein L19 in human breast tumors that overexpress erbB-2", *Cancer Res* **53**(6), 1403-8.
- Hildebrand, J. D. and Soriano, P.** (1999) "Shroom, a PDZ domain-containing actin-binding protein, is required for neural tube morphogenesis in mice", *Cell* **99**(5), 485-97.
- Hillman, B., Sherman, M. I. and Graham, C. F.** (1972) "The effect of spatial rearrangement on cell determination during mouse development", *J Embryol Exp Morphol* **28**, 263-78.
- Hoadley, L.** (1928) "On the localization of the developmental potencies in the embryo of *Fundulus heteroclitus*", *J Exp Zool* **227**, 7-44.
- Hogan, H., Beddington, R., Costantini, F. and Lacy, E.** (1994) Manipulating the mouse embryo: A laboratory manual, New York, Cold Spring Harbor Laboratory Press.
- Hollister, R. D., Page, K. J. and Hyman, B. T.** (1997) "Distribution of the messenger RNA for the extracellularly regulated kinases 1, 2 and 3 in rat brain: effects of excitotoxic hippocampal lesions", *Neuroscience* **79**(4), 1111-9.
- Holowacz, T. and Elinson, R. P.** (1993) "Cortical cytoplasm, which induces dorsal axis formation in *Xenopus*, is inactivated by UV irradiation of the oocyte", *Development* **119**(1), 277-85.
- Hoodless, P. A., Pye, M., Chazaud, C., Labbe, E., Attisano, L., Rossant, J. and Wrana, J. L.** (2001) "FoxH1 (Fast) functions to specify the anterior primitive streak in the mouse", *Genes Dev* **15**(10), 1257-71.
- Horb, M. E. and Slack, J. M.** (2001) "Endoderm specification and differentiation in *Xenopus* embryos", *Dev Biol* **236**(2):330-43.
- Horb, M. E. and Thomsen, G. H.** (1997) "A vegetally localized T-box transcription factor in *Xenopus* eggs specifies mesoderm and endoderm and is essential for embryonic mesoderm formation", *Development* **124**(9), 1689-98.
- Horster, M. F., Braun, G. S. and Huber, S. M.** (1999) "Embryonic renal epithelia: induction, nephrogenesis, and cell differentiation", *Physiol Rev* **79**(4), 1157-91.
- Howard, E. W., Newman, L. A., Oleksyn, D. W., Angerer, R. C. and Angerer, L. M.** (2001) "SpKrl: a direct target of beta-catenin regulation required for endoderm differentiation in sea urchin embryos", *Development* **128**(3), 365-75.
- Howard, K. and Ingham, P.** (1986) "Regulatory interactions between the segmentation genes *fushi tarazu*, *hairy*, and *engrailed* in the *Drosophila* blastoderm", *Cell* **44**(6), 949-57.

- Huang, H. C., Murtaugh, L. C., Vize, P. D. and Whitman, M. (1995)** "Identification of a potential regulator of early transcriptional responses to mesoderm inducers in the frog embryo", *EMBO J* **14**(23), 5965-73.
- Huang, R. P., Ozawa, M., Kadomatsu, K. and Muramatsu, T. (1993)** "Embigin, a member of the omminoglobulin superfamily expressed in embryonic cells, enhances cell-substratum adhesion", *Dev Biol* **155**(2), 307-14.
- Huang, W., Lee, S. L., Arnason, S. S. and Sjoquist, M. (1996)** "Dehydration natriuresis in male rats is mediated by oxytocin", *Am J Physiol* **270**(2 Pt 2), R427-33.
- Huber, G. C. (1915)** "The development of the albino rat, *Mus norvegicus*. I. From the pronuclear stage to the stage of the mesoderm anlage: End of the first to the end of the 9th day", *J Morphol* **26**, 247-358.
- Huber, O., Korn, R., McLaughlin, J., Ohsugi, M., Herrmann, B. G. and Kemler, R. (1996)** "Nuclear localization of beta-catenin by interaction with transcription factor LEF-1", *Mech Dev* **59**(1), 3-10.
- Huber, S. M., Friedrich, B., Klingel, K., Lenka, N., Hescheler, J. and Lang, F. (2001)** "Protein and mRNA expression of serum and glucocorticoid-dependent kinase 1 in metanephrogenesis", *Dev Dyn* **221**(4), 464-9.
- Hudziak, R. M., Barofsky, E., Barofsky, D. F., Weller, D. L., Huang, S. B. and Weller, D. D. (1996)** "Resistance of morpholino phosphorodiamidate oligomers to enzymatic degradation", *Antisense Nucleic Acid Drug Dev* **6**(4), 267-72.
- Huelsken, J. and Birchmeier, W. (2001)** "New aspects of Wnt signaling pathways in higher vertebrates", *Curr Opin Genet Dev* **11**(5), 547-53.
- Huelsken, J., Vogel, R., Brinkmann, V., Erdmann, B., Birchmeier, C. and Birchmeier, W. (2000)** "Requirement for beta-catenin in antero-posterior axis formation in mice", *J Cell Biol* **148**(3), 567-78.
- Hug, B., Walter, V. and Grunwald, D. J. (1997)** "*tbx6*, a *Brachyury*-related gene expressed by ventral mesendodermal precursors in the zebrafish embryo", *Dev Biol* **183**(1), 61-73.
- Hyde, C. E. and Old, R. W. (2000)** "Regulation of the early expression of the *Xenopus* nodal-related 1 gene, *Xnr1*", *Development* **127**(6), 1221-9.
- Imai, S., Okayama, N., Shimizu, M. and Itoh, M. (2003)** "Increased intracellular calcium activates serum and glucocorticoid-inducible kinase 1 (SGK1) through a calmodulin-calcium calmodulin dependent kinase kinase pathway in Chinese hamster ovary cells", *Life Sci* **72**(20), 2199-209.

- Imaizumi, K.,** Tsuda, M., Wanaka, A., Tohyama, M. and Takagi, T. (1994) "Differential expression of *sgk* mRNA, a member of the Ser/Thr protein kinase gene family, in rat brain after CNS injury", *Brain Res Mol Brain Res* **26**(1-2), 189-96.
- International Human Genome Sequencing Consortium** (2001) "Initial sequencing and analysis of the human genome", *Nature* **409**, 860-921.
- Ish-Horowicz, D. and Pinchin, S. M.** (1987) "Pattern abnormalities induced by ectopic expression of the *Drosophila* gene *hairy* are associated with repression of *ftz* transcription", *Cell* **51**(3), 405-15.
- Itani, O. A.,** Auerbach, S. D., Husted, R. F., Volk, K. A., Ageloff, S., Knepper, M. A., Stokes, J. B. and Thomas, C. P. (2002a) "Glucocorticoid-stimulated lung epithelial Na(+) transport is associated with regulated ENaC and *sgk1* expression", *Am J Physiol Lung Cell Mol Physiol* **282**(4), L631-41.
- Itani, O. A.,** Liu, K. Z., Cornish, K. L., Campbell, J. R. and Thomas, C. P. (2002b) "Glucocorticoids stimulate human *sgk1* gene expression by activation of a GRE in its 5'-flanking region", *Am J Physiol Endocrinol Metab* **283**(5), E971-9.
- Ito, T.,** Kim, G. T. and Shinozaki, K. (2000) "Disruption of an *Arabidopsis* cytoplasmic ribosomal protein S13-homologous gene by transposon-mediated mutagenesis causes aberrant growth and development", *Plant J* **22**(3), 257-64.
- Izpisua-Belmonte, J. C.,** De Robertis, E. M., Storey, K. G. and Stern, C. D. (1993) "The homeobox gene *gooseoid* and the origin of organizer cells in the early chick blastoderm", *Cell* **74**(4), 645-59.
- Jazwinska, A.,** Kirov, N., Wieschaus, E., Roth, S. and Rushlow, C. (1999) "The *Drosophila* gene *brinker* reveals a novel mechanism of Dpp target gene regulation", *Cell* **96**(4), 563-73.
- Jesuthasan, S. and Stahle, U.** (1997) "Dynamic microtubules and specification of the zebrafish embryonic axis", *Curr Biol* **7**(1), 31-42.
- Johnson, M. H.,** Chisholm, J. C., Fleming, T. P. and Houliston, E. (1986) "A role for cytoplasmic determinants in the development of the mouse early embryo?" *J Embryol Exp Morphol* **97** Suppl, 97-121.
- Johnson, M. H. and Ziomek, C. A.** (1983) "Cell interactions influence the fate of mouse blastomeres undergoing the transition from the 16- to the 32-cell stage", *Dev Biol* **95**(1), 211-8.
- Johnson, W. H.,** Loskutoff, N. M., Plante, Y. and Betteridge, K. J. (1995) "Production of four identical calves by separation of blastomeres from an *in vitro* derived four-cell embryo", *Vet Rec* **137**, 15-6.

- Joly, J. S., Joly, C., Schulte-Merker, S., Boulekbache, H. and Condamine, H. (1993)** "The ventral and posterior expression of the zebrafish homeobox gene *eve1* is perturbed in dorsalized and mutant embryos", *Development* **119**(4), 1261-75.
- Jones, C. M., Broadbent, J., Thomas, P. Q., Smith, J. C. and Beddington, R. S. P. (1999)** "An anterior signalling centre in *Xenopus* revealed by expression of the homeobox gene *XHex*", *Curr Biol* **9**(17), 946-54.
- Joseph, E. M. and Melton, D. A. (1998)** "Mutant Vg1 ligands disrupt endoderm and mesoderm formation in *Xenopus* embryos", *Development* **125**(14), 2677-85.
- Kageura, H. (1990)** "Spatial distribution of the capacity to initiate a secondary embryo in the 32-cell embryo of *Xenopus laevis*", *Dev Biol* **142**(2), 432-8.
- Kageura, H. (1995)** "Three regions of the 32-cell embryo of *Xenopus laevis* essential for formation of a complete tadpole", *Dev Biol* **170**(2), 376-86.
- Kageura, H. (1997)** "Activation of dorsal development by contact between the cortical dorsal determinant and the equatorial core cytoplasm in eggs of *Xenopus laevis*", *Development* **124**(8), 1543-51.
- Kamynina, E. and Staub, O. (2002)** "Concerted action of ENaC, Nedd4-2, and Sgk1 in transepithelial Na(+) transport", *Am J Physiol Renal Physiol* **283**(3), F377-87.
- Kanai-Azuma, M., Kanai, Y., Gad, J. M., Tajima, Y., Taya, C., Kurohmaru, M., Sanai, Y., Yonekawa, H., Yazaki, K., Tam, P. P. and Hayashi, Y. (2002)** "Depletion of definitive gut endoderm in *Sox17*-null mutant mice", *Development* **129**(10), 2367-79.
- Kane, D. A. and Adams, R. J. (2002)** Life at the edge: epiboly and involution in the zebrafish, *Pattern formation in zebrafish*, Solnica-Krezel, L., Berlin, Springer, **40**, 117-35.
- Kane, D. A., Hammerschmidt, M., Mullins, M. C., Maischein, H. M., Brand, M., van Eeden, F. J., Furutani-Seiki, M., Granato, M., Haffter, P., Heisenberg, C. P., Jiang, Y. J., Kelsh, R. N., Odenthal, J., Warga, R. M. and Nusslein-Volhard, C. (1996)** "The zebrafish epiboly mutants", *Development* **123**, 47-55.
- Kane, D. A. and Kimmel, C. B. (1993)** "The zebrafish midblastula transition", *Development* **119**(2), 447-56.
- Kane, D. A., Warga, R. M. and Kimmel, C. B. (1992)** "Mitotic domains in the early embryo of the zebrafish", *Nature* **360**(6406), 735-7.
- Karan, D., Kelly, D. L., Rizzino, A., Lin, M. F. and Batra, S. K. (2002)** "Expression profile of differentially-regulated genes during progression of androgen-independent growth in human prostate cancer cells", *Carcinogenesis* **23**(6), 967-75.

- Kato, Y.**, Tapping, R. I., Huang, S., Watson, M. H., Ulevitch, R. J. and Lee, J. D. (1998) "Bmk1/Erk5 is required for cell proliferation induced by epidermal growth factor", *Nature* **395**(6703), 713-6.
- Kaufman, M. H.** (1992) The atlas of mouse development, Academic Press, London, United Kingdom.
- Kay, M. A. and Jacobs-Lorena, M.** (1987) "Developmental genetics of ribosome synthesis in *Drosophila*", *Trends Genet* **3**(12), 347-51.
- Keller, G.**, Kennedy, M., Papayannopoulou, T. and Wiles, M. V. (1993) "Hematopoietic commitment during embryonic stem cell differentiation in culture", *Mol Cell Biol* **13**(1), 473-86.
- Keller, G. M.** (1995) "In vitro differentiation of embryonic stem cells", *Curr Opin Cell Biol* **7**, 862-9.
- Keller, R. E.** (1980) "The cellular basis of epiboly: an SEM study of deep-cell rearrangement during gastrulation in *Xenopus laevis*", *J Embryol Exp Morphol* **60**, 201-34.
- Keller, R. E.** (1981) "An experimental analysis of the role of bottle cells and the deep marginal zone in gastrulation of *Xenopus laevis*", *J Exp Zool* **216**(1), 81-101.
- Kelley, C.**, Blumberg, H., Zon, L. I. and Evans, T. (1993) "GATA-4 is a novel transcription factor expressed in endocardium of the developing heart", *Development* **118**(3), 817-27.
- Kelly, G. M.**, Erezyilmaz, D. F. and Moon, R. T. (1995) "Induction of a secondary embryonic axis in zebrafish occurs following the overexpression of beta-catenin", *Mech Dev* **53**(2), 261-73.
- Kelly, S. J.**, Mulnard, J. G. and Graham, C. F. (1978) "Cell division and cell allocation in early mouse development", *J Embryol Exp Morphol* **48**, 37-51.
- Kengaku, M. and Okamoto, H.** (1993) "Basic fibroblast growth factor induces differentiation of neural tube and neural crest lineages of cultured ectoderm cells from *Xenopus* gastrula", *Development*, **119**(4), 1067-78.
- Kengaku, M. and Okamoto, H.** (1995) "bFGF as a possible morphogen for the anteroposterior axis of the central nervous system in *Xenopus*", *Development*, **121**(9), 3121-30.
- Kessler, D. S.** (1997) "Siamois is required for formation of Spemann's organizer", *Proc Natl Acad Sci USA* **94**(24), 13017-22.
- Kessler, D. S. and Melton, D. A.** (1995) "Induction of dorsal mesoderm by soluble, mature Vg1 protein", *Development* **121**(7), 2155-64.

- Kettleborough, R.** (2002) The isolation and characterisation of the novel gene C5, Ph.D. Thesis presented to the Department of Anatomy and Developmental Biology, University College London, London, United Kingdom.
- Khaner, O.** (1995) "The rotated hypoblast of the chicken embryo does not initiate an ectopic axis in the epiblast", *Proc Natl Acad Sci USA* **92**(23), 10733-7.
- Kikkawa, M., Takano, K. and Shinagawa, A.** (1996) "Location and behavior of dorsal determinants during first cell cycle in *Xenopus* eggs", *Development* **122**(12), 3687-96.
- Kikuchi, Y., Agathon, A., Alexander, J., Thisse, C., Waldron, S., Yelon, D., Thisse, B. and Stainier, D. Y.** (2001) "*casanova* encodes a novel Sox-related protein necessary and sufficient for early endoderm formation in zebrafish", *Genes Dev* **15**(12), 1493-505.
- Kikuchi, Y., Trinh, L. A., Reiter, J. F., Alexander, J., Yelon, D. and Stainier, D. Y.** (2000) "The zebrafish *bonnie and clyde* gene encodes a Mix family homeodomain protein that regulates the generation of endodermal precursors", *Genes Dev* **14**(10), 1279-89.
- Kim, C. H., Oda, T., Itoh, M., Jiang, D., Artinger, K. B., Chandrasekharappa, S. C., Driever, W. and Chitnis, A. B.** (2000) "Repressor activity of Headless/Tcf3 is essential for vertebrate head formation", *Nature* **407**(6806), 913-6.
- Kimelman, D. and Griffin, K. J.** (1998) "Mesoderm induction: a postmodern view", *Cell* **94**(4), 419-21.
- Kimelman, D. and Kirschner, M.** (1987) "Synergistic induction of mesoderm by FGF and TGF-beta and the identification of an mRNA coding for FGF in the early *Xenopus* embryo", *Cell* **51**(5), 869-77.
- Kimelman, D. and Pierce, S. B.** (1996) "Regulation of dorsal-ventral axis formation in *Xenopus* by intercellular and intracellular signalling", *Biochem Soc Symp* **62**, 13-23.
- Kimelman, D. and Schier, A. F.** (2002) "Mesoderm induction and patterning", *Results Probl Cell Differ* **40**, 15-27.
- Kimmel, C. B., Ballard, W. W., Kimmel, S. R., Ullmann, B. and Schilling, T. F.** (1995) "Stages of embryonic development of the zebrafish", *Dev Dyn* **203**(3), 253-310.
- Kimmel, C. B. and Law, R. D.** (1985a) "Cell lineage of zebrafish blastomeres. I. Cleavage pattern and cytoplasmic bridges between cells", *Dev Biol* **108**(1), 78-85.
- Kimmel, C. B. and Law, R. D.** (1985b) "Cell lineage of zebrafish blastomeres. II. Formation of the yolk syncytial layer", *Dev Biol* **108**(1), 86-93.
- Kimmel, C. B. and Law, R. D.** (1985c) "Cell lineage of zebrafish blastomeres. III. Clonal analyses of the blastula and gastrula stages", *Dev Biol* **108**(1), 94-101.
- Kimmel, C. B. and Warga, R. M.** (1987) "Indeterminate cell lineage of the zebrafish

embryo", *Dev Biol* **124**(1), 269-80.

Kimmel, C. B., Warga, R. M. and Schilling, T. F. (1990) "Origin and organisation of the zebrafish fate map", *Development* **108**, 581-94.

Kintner, C. R. and Dodd, J. (1991) "Hensen's node induces neural tissue in *Xenopus* ectoderm. Implications for the action of the organizer in neural induction", *Development* **113**(4), 1495-505.

Kirschner, M., Gerhart, J. C., Hara, K. and Ubbels, G. A. (1980) "Initiation of the cell cycle and establishment of bilateral symmetry in *Xenopus* eggs", *Symp Soc Develop Biol* **38**, 187-215.

Kishimoto, Y., Lee, K. H., Zon, L., Hammerschmidt, M. and Schulte-Merker, S. (1997) "The molecular nature of zebrafish *swirl*: BMP2 function is essential during early dorsoventral patterning", *Development* **124**(22), 4457-66.

Klingel, K., Warntges, S., Bock, J., Wagner, C. A., Sauter, M., Waldegger, S., Kandolf, R. and Lang, F. (2000) "Expression of cell volume-regulated kinase h-sgk in pancreatic tissue", *Am J Physiol Gastrointest Liver Physiol* **279**(5), G998-G1002.

Klingensmith, J., Ang, S.-L., Bachiller, D. and Rossant, J. (1999) "Neural induction and patterning in the mouse in the absence of the Node and its derivatives", *Dev Biol*, **216**, 535-49.

Knoetgen, H., Teichmann, U., Wittler, L., Viebahn, C. and Kessel, M. (2000) "Anterior neural induction by nodes from rabbits and mice", *Dev Biol* **225**(2), 370-80.

Knoetgen, H., Viebahn, C. and Kessel, M. (1999) "Head induction in the chick by primitive endoderm of mammalian, but not avian origin", *Development* **126**(4), 815-25.

Kobayashi, T. and Cohen, P. (1999) "Activation of serum- and glucocorticoid-regulated protein kinase by agonists that activate phosphatidylinositide 3-kinase is mediated by 3-phosphoinositide-dependent protein kinase-1 (PDK1) and PDK2", *Biochem J* **339** (Pt 2), 319-28.

Kobayashi, T., Deak, M., Morrice, N. and Cohen, P. (1999) "Characterization of the structure and regulation of two novel isoforms of serum- and glucocorticoid-induced protein kinase", *Biochem J* **344** Pt 1, 189-97.

Kochav, S. and Eyal-Giladi, H. (1971) "Bilateral symmetry in chick embryo determination by gravity", *Science* **171**(975), 1027-9.

Kodjabachian, L. and Lemaire, P. (1998) "Embryonic induction: is the Nieuwkoop centre a useful concept?" *Curr Biol* **8**(25), R918-21.

Kofron, M., Demel, T., Xanthos, J., Lohr, J., Sun, B., Sive, H., Osada, S., Wright, C., Wylie, C. and Heasman, J. (1999) "Mesoderm induction in *Xenopus* is a zygotic event

regulated by maternal VegT via TGFbeta growth factors", *Development* **126**(24), 5759-70.

Kohlhase, J., Wischermann, A., Reichenbach, H., Froster, U. and Engel, W. (1998) "Mutations in the SALL1 putative transcription factor gene cause Townes-Brocks syndrome", *Nat Genet* **18**(1), 81-3.

Kollmar, R., Nakamura, S. K., Kappler, J. A. and Hudspeth, A. J. (2001) "Expression and phylogeny of *claudins* in vertebrate primordia", *Proc Natl Acad Sci USA* **98**(18), 10196-201.

Kondo, D., Yamamoto, T., Yaoita, E., Danielson, P. E., Kobayashi, H., Ohshiro, K., Funaki, H., Koyama, Y., Fujinaka, H., Kawasaki, K., Sutcliffe, J. G., Arakawa, M. and Kihara, I. (2000) "Localization of olfactomedin-related glycoprotein isoform (BMZ) in the golgi apparatus of glomerular podocytes in rat kidneys", *J Am Soc Nephrol* **11**(5), 803-13.

Kondoh, N., Shuda, M., Tanaka, K., Wakatsuki, T., Hada, A. and Yamamoto, M. (2001) "Enhanced expression of S8, L12, L23a, L27 and L30 ribosomal protein mRNAs in human hepatocellular carcinoma", *Anticancer Res* **21**(4A), 2429-33.

Kongsuwan, K., Yu, Q., Vincent, A., Frisardi, M. C., Rosbash, M., Lengyel, J. A. and Merriam, J. (1985) "A *Drosophila Minute* gene encodes a ribosomal protein", *Nature* **317**(6037), 555-8.

Koos, D. S. and Ho, R. K. (1998) "The *nieuwkoid* gene characterizes and mediates a Nieuwkoop-center-like activity in the zebrafish", *Curr Biol* **8**(22), 1199-206.

Koos, D. S. and Ho, R. K. (1999) "The *nieuwkoid/dharma* homeobox gene is essential for *bmp2b* repression in the zebrafish pregastrula", *Dev Biol* **215**(2), 190-207.

Kos, R., Reedy, M. V., Johnson, R. L. and Erickson, C. A. (2001) "The winged-helix transcription factor FoxD3 is important for establishing the neural crest lineage and repressing melanogenesis in avian embryos", *Development* **128**(8), 1467-79.

Koshida, S., Shinya, M., Mizuno, T., Kuroiwa, A. and Takeda, H. (1998) "Initial anteroposterior pattern of the zebrafish central nervous system is determined by differential competence of the epiblast", *Development*, **125**, 1957-66.

Koutsourakis, M., Langeveld, A., Patient, R., Beddington, R. and Grosveld, F. (1999) "The transcription factor GATA6 is essential for early extraembryonic development", *Development* **126**(9), 723-32.

Kozak, M. (1987) "At least six nucleotides preceding the AUG initiator codon enhance translation in mammalian cells", *J Mol Biol* **196**(4), 947-50.

- Kozma, S. C. and Thomas, G.** (2002) "Regulation of cell size in growth, development and human disease: PI3K, PKB and S6K", *Bioessays* **24**(1), 65-71.
- Krauss, S., Johansen, T., Korzh, V. and Fjose, A.** (1991) "Expression of the zebrafish paired box gene *pax[zf-b]* during early neurogenesis", *Development* **113**(4), 1193-206.
- Kronhamn, J. and Rasmuson-Lestander, A.** (1999) "Genetic organization of the ci-M-pan region on chromosome IV in *Drosophila melanogaster*", *Genome* **42**(6), 1144-9.
- Kudoh, T., Concha, M. L., Houart, C., Dawid, I. B. and Wilson, S. W.** (2003) "Combinatorial Fgf and Bmp signalling patterns the gastrula ectoderm into prospective neural and epidermal domains", *Development*, in press.
- Kudoh, T., Tsang, M., Hukriede, N. A., Chen, X., Dedekian, M., Clarke, C. J., Kiang, A., Schultz, S., Epstein, J. A., Toyama, R. and Dawid, I. B.** (2001) "A gene expression screen in zebrafish embryogenesis", *Genome Res* **11**(12), 1979-87.
- Kumar, J. M., Brooks, D. P., Olson, B. A. and Laping, N. J.** (1999) "Sgk, a putative serine/threonine kinase, is differentially expressed in the kidney of diabetic mice and humans", *J Am Soc Nephrol* **10**(12), 2488-94.
- Kuo, C. T., Morrissey, E. E., Anandappa, R., Sigrist, K., Lu, M. M., Parmacek, M. S., Soudais, C. and Leiden, J. M.** (1997) "GATA4 transcription factor is required for ventral morphogenesis and heart tube formation", *Genes Dev* **11**(8), 1048-60.
- Labbe, E., Silvestri, C., Hoodless, P. A., Wrana, J. L. and Attisano, L.** (1998) "Smad2 and Smad3 positively and negatively regulate TGF beta-dependent transcription through the forkhead DNA-binding protein FAST2", *Mol Cell* **2**(1), 109-20.
- Lamb, T. M. and Harland, R.** (1995) "Fibroblast growth factor is a direct neural inducer, which combined with noggin generates antero-posterior neural pattern", *Development* **121**, 3627-36.
- Lamb, T. M., Knecht, A. K., Smith, W. C., Stachel, S. E., Economides, A. N., Stahl, N., Yancopolous, G. D. and Harland, R.** (1993) "Neural induction by the secreted polypeptide noggin", *Science* **262**, 713-8.
- Lambertsson, A.** (1998) "The *Minute* genes in *Drosophila* and their molecular functions", *Adv Genet* **38**, 69-134.
- Landesman, Y. and Sokol, S. Y.** (1997) "Xwnt-2b is a novel axis-inducing *Xenopus* Wnt, which is expressed in embryonic brain", *Mech Dev* **63**(2), 199-209.
- Lang, F., Klingel, K., Wagner, C. A., Stegen, C., Warntges, S., Friedrich, B., Lanzendorfer, M., Melzig, J., Moschen, I., Steuer, S., Waldegger, S., Sauter, M., Paulmichl, M., Gerke, V., Risler, T., Gamba, G., Capasso, G., Kandolf, R., Hebert, S. C., Massry, S. G. and Broer, S.** (2000) "Deranged transcriptional regulation of cell-

- volume-sensitive kinase hSGK in diabetic nephropathy", *Proc Natl Acad Sci USA* **97**(14), 8157-62.
- Larabell, C. A., Torres, M., Rowning, B. A., Yost, C., Miller, J. R., Wu, M., Kimelman, D. and Moon, R. T.** (1997) "Establishment of the dorso-ventral axis in *Xenopus* embryos is presaged by early asymmetries in beta-catenin that are modulated by the Wnt signaling pathway", *J Cell Biol* **136**(5), 1123-36.
- Larsson, J. and Rasmuson-Lestander, A.** (1997) "Cloning, mapping and mutational analysis of the *S-adenosylmethionine decarboxylase* gene in *Drosophila melanogaster*", *Mol Gen Genet* **256**(6), 652-60.
- Larsson, J. and Rasmuson-Lestander, A.** (1998) "Somatic and germline clone analysis in mutants of the *S-adenosylmethionine synthetase* encoding gene in *Drosophila melanogaster*", *FEBS Lett* **427**(1), 119-23.
- Launay, C., Fromentoux, V., Shi, D. L. and Boucaut, J. C.** (1996) "A truncated FGF receptor blocks neural induction by endogenous *Xenopus* inducers", *Development* **122**(3), 869-80.
- Laurent, M. N., Blitz, I. L., Hashimoto, C., Rothbacher, U. and Cho, K. W.** (1997) "The *Xenopus* homeobox gene *twin* mediates Wnt induction of *gooseoid* in establishment of Spemann's organizer", *Development* **124**(23), 4905-16.
- Laverriere, A. C., MacNeill, C., Mueller, C., Poelmann, R. E., Burch, J. B. and Evans, T.** (1994) "GATA-4/5/6, a subfamily of three transcription factors transcribed in developing heart and gut", *J Biol Chem* **269**(37), 23177-84.
- Lawrence, P. A., Struhl, G. and Morata, G.** (1979) "Bristle patterns and compartment boundaries in the tarsi of *Drosophila*", *J Embryol Exp Morphol* **51**, 195-208.
- Lawson, A. and Schoenwolf, G. C.** (2001a) "Cell populations and morphogenetic movements underlying formation of the avian primitive streak and organizer", *Genesis* **29**(4), 188-95.
- Lawson, A. and Schoenwolf, G. C.** (2001b) "New insights into critical events of avian gastrulation", *Anat Rec* **262**(3), 238-52.
- Le Menuet, D., Isnard, R., Bichara, M., Viengchareun, S., Muffat-Joly, M., Walker, F., Zennaro, M. C. and Lombes, M.** (2001) "Alteration of cardiac and renal functions in transgenic mice overexpressing human mineralocorticoid receptor", *J Biol Chem* **276**(42), 38911-20.
- Lee, E., Lein, E. S. and Firestone, G. L.** (2001) "Tissue-specific expression of the transcriptionally regulated serum and glucocorticoid-inducible protein kinase (Sgk) during mouse embryogenesis", *Mech Dev* **103**(1-2), 177-81.

- Lemaire, P.,** Garrett, N. and Gurdon, J. B. (1995) "Expression cloning of *Siamois*, a *Xenopus* homeobox gene expressed in dorsal-vegetal cells of blastulae and able to induce a complete secondary axis", *Cell* **81**(1), 85-94.
- Leong, M. L.,** Maiyar, A. C., Kim, B., O'Keeffe, B. A. and Firestone, G. L. (2003) "Expression of the Serum- and Glucocorticoid-inducible Protein Kinase, Sgk, Is a Cell Survival Response to Multiple Types of Environmental Stress Stimuli in Mammary Epithelial Cells", *J Biol Chem* **278**(8), 5871-82.
- Lewis, E. B.** (1978) "A gene complex controlling segmentation in *Drosophila*", *Nature* **276**, 565-70.
- Leyns, L.,** Bouwmeester, T., Kim, S. H., Piccolo, S. and De Robertis, E. M. (1997) "Frzb-1 is a secreted antagonist of Wnt signaling expressed in the Spemann organizer", *Cell* **88**(6), 747-56.
- Li, B.,** Ouyang, B., Pan, H., Reissmann, P. T., Slamon, D. J., Arceci, R., Lu, L. and Dai, W. (1996) "Prk, a cytokine-inducible human protein serine/threonine kinase whose expression appears to be down-regulated in lung carcinomas", *J Biol Chem* **271**(32), 19402-8.
- Li, B.,** Sun, M., He, B., Yu, J., Zhang, Y. D. and Zhang, Y. L. (2002b) "Identification of differentially expressed genes in human uterine leiomyomas using differential display", *Cell Res* **12**(1), 39-45.
- Li, L.,** Keverne, E. B., Aparicio, S. A., Ishino, F., Barton, S. C. and Surani, M. A. (1999) "Regulation of maternal behavior and offspring growth by paternally expressed *Peg3*", *Science* **284**(5412), 330-3.
- Lindsley, D. J. and Zimm, G. G.** (1992) *The Genome of *Drosophila melanogaster**, San Diego, CA, Academic Press.
- Ling, H.,** Vamvakas, S., Busch, G., Dammrich, J., Schramm, L., Lang, F. and Heidland, A. (1995) "Suppressing role of transforming growth factor-beta 1 on cathepsin activity in cultured kidney tubule cells", *Am J Physiol* **269**(6 Pt 2), F911-7.
- Liu, D.,** Yang, X. and Songyang, Z. (2000) "Identification of CISK, a new member of the SGK kinase family that promotes IL-3-dependent survival", *Curr Biol* **10**(19), 1233-6.
- Liu, P.,** Wakamiya, M., Shea, M. J., Albrecht, U., Behringer, R. R. and Bradley, A. (1999) "Requirement for *Wnt3* in vertebrate axis formation", *Nat Genet* **22**(4), 361-5.
- Lodish, H. F.** (1968) "Bacteriophage f2 RNA: control of translation and gene order", *Nature* **220**(165), 345-50.
- Lodish, H. F.** (1970) "Secondary structure of bacteriophage f2 ribonucleic acid and the

- initiation of in vitro protein biosynthesis", *J Mol Biol* **50**(3), 689-702.
- Lodish, H. F. and Robertson, H. D.** (1969) "Regulation of in vitro translation of bacteriophage f2 RNA", *Cold Spring Harb Symp Quant Biol* **34**, 655-73.
- Loffing, J., Zecevic, M., Feraille, E., Kaissling, B., Asher, C., Rossier, B. C., Firestone, G. L., Pearce, D. and Verrey, F.** (2001) "Aldosterone induces rapid apical translocation of ENaC in early portion of renal collecting system: possible role of SGK", *Am J Physiol Renal Physiol* **280**(4), F675-82.
- Long, W. L.** (1983) "The role of the yolk syncytial layer in determination of the plane of bilateral symmetry in the rainbow trout, *Salmo gairdneri* Richardson", *J Exp Zool* **228**, 91-7.
- Lowe, M. and Kreis, T. E.** (1996) "In vivo assembly of coatomer, the COP-I coat precursor", *J Biol Chem* **271**(48), 30725-30.
- Lustig, K. D., Kroll, K. L., Sun, E. E. and Kirschner, M. W.** (1996) "Expression cloning of a *Xenopus* T-related gene (*Xombi*) involved in mesodermal patterning and blastopore lip formation", *Development* **122**(12), 4001-12.
- Mafune, K., Wong, J. M., Staniunas, R. J., Lu, M. L., Ravikumar, T. S., Chen, L. B. and Steele, G. D., Jr.** (1991) "Ubiquitin hybrid protein gene expression during human colon cancer progression", *Arch Surg* **126**(4), 462-6.
- Maiyar, A. C., Huang, A. J., Phu, P. T., Cha, H. H. and Firestone, G. L.** (1996) "p53 stimulates promoter activity of the *sgk. serum/glucocorticoid-inducible serine/threonine protein kinase* gene in rodent mammary epithelial cells", *J Biol Chem* **271**(21), 12414-22.
- Maiyar, A. C., Leong, M. L. and Firestone, G. L.** (2003) "Importin-alpha Mediates the Regulated Nuclear Targeting of Serum- and Glucocorticoid-inducible Protein Kinase (Sgk) by Recognition of a Nuclear Localization Signal in the Kinase Central Domain", *Mol Biol Cell* **14**(3), 1221-39.
- Maiyar, A. C., Phu, P. T., Huang, A. J. and Firestone, G. L.** (1997) "Repression of glucocorticoid receptor transactivation and DNA binding of a glucocorticoid response element within the *serum/glucocorticoid-inducible protein kinase (sgk)* gene promoter by the p53 tumor suppressor protein", *Mol Endocrinol* **11**(3), 312-29.
- Maizels, E. T., Cottom, J., Jones, J. C. and Hunzicker-Dunn, M.** (1998) "Follicle stimulating hormone (FSH) activates the p38 mitogen-activated protein kinase pathway, inducing small heat shock protein phosphorylation and cell rounding in immature rat ovarian granulosa cells", *Endocrinology* **139**(7), 3353-6.

- Mansour, S. L., Thomas, K. R. and Capecchi, M. R. (1988)** "Disruption of the proto-oncogene int-2 in mouse embryo-derived stem cells: a general strategy for targeting mutations to non-selectable genes", *Nature* **336**(6197), 348-52.
- Martin, P. and Cockcroft, D. L. (1999)** "Culture of postimplantation mouse embryos", *Methods in Molecular Biology*, Mason, I., Totowa, N. J., Humana Press Inc., **97** (Molecular Embryology: Methods and Protocols), 7-22.
- Martin-Castellanos, C. and Edgar, B. A. (2002)** "A characterization of the effects of Dpp signaling on cell growth and proliferation in the *Drosophila* wing", *Development* **129**(4), 1003-13.
- Martinez-Barbera, J. P. and Beddington, R. S. P. (2001)** "Getting your head around *Hex* and *Hesx1*: Forebrain formation in mouse", *Int J Dev Biol* **45**(1 (Spec. No.)), 327-36.
- Martinez-Barbera, J. P., Clements, M., Thomas, P., Rodriguez, T., Meloy, D., Kioussis, D. and Beddington, R. S. (2000)** "The homeobox gene *hex* is required in definitive endodermal tissues for normal forebrain, liver and thyroid formation", *Development* **127**(11), 2433-45.
- Martinez-Barbera, J. P., Toresson, H., Da Rocha, S. and Krauss, S. (1997)** "Cloning and expression of three members of the zebrafish Bmp family: *Bmp2a*, *Bmp2b* and *Bmp4*" *Gene* **198**(1-2),
- Massague, J. and Wotton, D. (2000)** "Transcriptional control by the TGF-beta/Smad signaling system", *EMBO J* **19**(8), 1745-54.
- Matzuk, M. M., Kumar, T. R. and Bradley, A. (1995a)** "Different phenotypes for mice deficient in either activins or activin receptor type II", *Nature* **374**(6520), 356-60.
- Matzuk, M. M., Kumar, T. R., Vassalli, A., Bickenbach, J. R., Roop, D. R., Jaenisch, R. and Bradley, A. (1995b)** "Functional analysis of activins during mammalian development", *Nature* **374**(6520), 354-6.
- McDowell, N. and Gurdon, J. B. (1999)** "Activin as a morphogen in *Xenopus* mesoderm induction", *Semin Cell Dev Biol* **10**(3), 311-7.
- McConnell, J. E., Armstrong, J. F., Hodges, P. E. and Bard, J. B. (1995)** "The mouse 14-3-3 epsilon isoform, a kinase regulator whose expression pattern is modulated in mesenchyme and neuronal differentiation", *Dev Biol* **169**(1), 218-28.
- McGrew, L. L., Lai, C. J. and Moon, R. T. (1995)** "Specification of the anteroposterior neural axis through synergistic interaction of the Wnt signaling cascade with noggin and follistatin", *Dev Biol*, **172**(1), 337-42.
- McKendry, R., Hsu, S. C., Harland, R. M. and Grosschedl, R. (1997)** "LEF-1/TCF

- proteins mediate wnt-inducible transcription from the *Xenopus nodal-related 3* promoter", *Dev Biol* **192**(2), 420-31.
- McKim, K. S., Dahmus, J. B. and Hawley, R. S.** (1996) "Cloning of the *Drosophila melanogaster* meiotic recombination gene *mei-218*: a genetic and molecular analysis of interval 15E", *Genetics* **144**(1), 215-28.
- McMahon, A. P. and Moon, R. T.** (1989) "Ectopic expression of the proto-oncogene *int-1* in *Xenopus* embryos leads to duplication of the embryonic axis", *Cell* **58**(6), 1075-84.
- McMahon, J. A., Takada, S., Zimmerman, L. B., Fan, C. M., Harland, R. M. and McMahon, A. P.** (1998) "Noggin-mediated antagonism of BMP signaling is required for growth and patterning of the neural tube and somite", *Genes Dev* **12**, 1438-52.
- Melby, A. E., Beach, C., Mullins, M. and Kimelman, D.** (2000) "Patterning the early zebrafish by the opposing actions of *bozozok* and *vox/vent*", *Dev Biol* **224**(2), 275-85.
- Mellitzer, G., Hallonet, M., Chen, L. and Ang, S. L.** (2002) "Spatial and temporal 'knock down' of gene expression by electroporation of double-stranded RNA and morpholinos into early postimplantation mouse embryos", *Mech Dev* **118**(1-2), 57-63.
- Melnick, M. B., Noll, E. and Perrimon, N.** (1993) "The *Drosophila stubarista* phenotype is associated with a dosage effect of the putative ribosome-associated protein D-p40 on spineless", *Genetics* **135**(2), 553-64.
- Melton, D. A.** (1987) "Translocation of a localized maternal mRNA to the vegetal pole of *Xenopus* oocytes", *Nature* **328**(6125), 80-2.
- Meno, C., Gritsman, K., Ohishi, S., Ohfuji, Y., Heckscher, E., Mochida, K., Shimono, A., Kondoh, H., Talbot, W. S., Robertson, E. J., Schier, A. F. and Hamada, H.** (1999) "Mouse Lefty2 and zebrafish antivin are feedback inhibitors of nodal signaling during vertebrate gastrulation", *Mol Cell* **4**(3), 287-98.
- Meno, C., Shimono, A., Saijoh, Y., Yashiro, K., Mochida, K., Ohishi, S., Noji, S., Kondoh, H. and Hamada, H.** (1998) "lefty-1 is required for left-right determination as a regulator of *lefty-2* and *nodal*", *Cell* **94**(3), 287-97.
- Meyuhas, O.** (2000) "Synthesis of the translational apparatus is regulated at the translational level", *Eur J Biochem* **267**(21), 6321-30.
- Meyuhas, O., Avni, D. and S., S.** (1996), Translational Control, Sonenberg, N., Cold Spring Harbor, Cold Spring Harbor Press, 363-88.
- Mikosz, C. A., Brickley, D. R., Sharkey, M. S., Moran, T. W. and Conzen, S. D.** (2001) "Glucocorticoid receptor-mediated protection from apoptosis is associated with

induction of the *serine/threonine survival kinase* gene, *sgk-1*", *J Biol Chem* **276**(20), 16649-54.

Miller, J. R. and Moon, R. T. (1996) "Signal transduction through beta-catenin and specification of cell fate during embryogenesis", *Genes Dev* **10**(20), 2527-39.

Miller, J. R., Rowning, B. A., Larabell, C. A., Yang-Snyder, J. A., Bates, R. L. and Moon, R. T. (1999) "Establishment of the dorsal-ventral axis in *Xenopus* embryos coincides with the dorsal enrichment of dishevelled that is dependent on cortical rotation", *J Cell Biol* **146**(2), 427-37.

Minami, M., Kinoshita, N., Kamoshida, Y., Tanimoto, H. and Tabata, T. (1999) "*brinker* is a target of Dpp in *Drosophila* that negatively regulates Dpp-dependent genes", *Nature* **398**(6724), 242-6.

Mizuno, H. and Nishida, E. (2001) "The ERK MAP kinase pathway mediates induction of SGK (serum- and glucocorticoid-inducible kinase) by growth factors", *Genes Cells* **6**(3), 261-8.

Mizuno, T., Shinya, M. and Takeda, H. (1999a) "Cell and tissue transplantation in zebrafish embryos", *Methods Mol Biol* **127**, 15-28.

Mizuno, T., Yamaha, E., Kuroiwa, A. and Takeda, H. (1999b) "Removal of vegetal yolk causes dorsal deficiencies and impairs dorsal-inducing ability of the yolk cell in zebrafish. PG - 51-63", *Mech Dev* **81**(1-2).

Mizuno, T., Yamaha, E., Wakahara, M., Kuroiwa, A. and Takeda, H. (1996) "Mesoderm induction in zebrafish", *Nature* **383**, 131-2.

Mizuno, T., Yamaha, E. and Yamazaki, F. (1997) "Localized axis determinant in the early cleavage embryo of the goldfish, *Carassius auratus*", *Dev Genes Evol* **206**, 389-96.

Mohammadi, M., McMahon, G., Sun, L., Tang, C., Hirth, P., Yeh, B. K., Hubbard, S. R. and Schlessinger, J. (1997) "Structures of the tyrosine kinase domain of fibroblast growth factor receptor in complex with inhibitors", *Science*, **276**(5314), 955-60.

Molenaar, M., van de Wetering, M., Oosterwegel, M., Peterson-Maduro, J., Godsave, S., Korinek, V., Roose, J., Destree, O. and Clevers, H. (1996) "XTcf-3 transcription factor mediates beta-catenin-induced axis formation in *Xenopus* embryos", *Cell* **86**(3), 391-9.

Molkentin, J. D., Lin, Q., Duncan, S. A. and Olson, E. N. (1997) "Requirement of the transcription factor GATA4 for heart tube formation and ventral morphogenesis", *Genes Dev* **11**(8), 1061-72.

Molkentin, J. D., Tymitz, K. M., Richardson, J. A. and Olson, E. N. (2000)

- "Abnormalities of the genitourinary tract in female mice lacking GATA5", *Mol Cell Biol* **20**(14), 5256-60.
- Montagne, J., Stewart, M. J., Stocker, H., Hafen, E., Kozma, S. C. and Thomas, G.** (1999) "*Drosophila* S6 kinase: a regulator of cell size", *Science* **285**(5436), 2126-9.
- Montero, J. A., Kilian, B., Chan, J., Bayliss, P. E., Heisenberg, C. P.** (2003) "Phosphoinositide 3-kinase is required for process outgrowth and cell polarization of gastrulating mesendodermal cells", *Curr Biol*, **13**(15), 1279-89.
- Moon, R. T., Brown, J. D., Yang-Snyder, J. A. and Miller, J. R.** (1997) "Structurally related receptors and antagonists compete for secreted Wnt ligands", *Cell* **88**(6), 725-8.
- Moon, R. T. and Kimelman, D.** (1998) "From cortical rotation to organizer gene expression: toward a molecular explanation of axis specification in *Xenopus*", *Bioessays* **20**(7), 536-45.
- Moran, T., Gray, S., Mikosz, C. and Conzen, S.** (2000) "The glucocorticoid receptor mediates a survival signal in human mammary epithelial cells", *Cancer Res* **60**(4), 867-72.
- Morata, G. and Ripoll, P.** (1975) "*Minutes*: mutants of *Drosophila* autonomously affecting cell division rate", *Dev Biol* **42**(2), 211-21.
- Moreno, E., Basler, K. and Morata, G.** (2002) "Cells compete for decapentaplegic survival factor to prevent apoptosis in *Drosophila* wing development", *Nature* **416**(6882), 755-9.
- Moreno, T. A. and Bronner-Fraser, M.** (2001) "The secreted glycoprotein Noelin-1 promotes neurogenesis in *Xenopus*", *Dev Biol* **240**(2), 340-60.
- Moreno, T. A. and Bronner-Fraser, M.** (2002) "Neural expression of mouse *Noelin-1/2* and comparison with other vertebrates", *Mech Dev* **119**(1), 121.
- Morgan, T. H.** (1895) "The formation of the fish embryo", *J Morphol* **10**, 419-72.
- Morrisey, E. E., Ip, H. S., Lu, M. M. and Parmacek, M. S.** (1996) "GATA-6: a zinc finger transcription factor that is expressed in multiple cell lineages derived from lateral mesoderm", *Dev Biol* **177**(1), 309-22.
- Morrisey, E. E., Ip, H. S., Tang, Z., Lu, M. M. and Parmacek, M. S.** (1997) "GATA-5: a transcriptional activator expressed in a novel temporally and spatially-restricted pattern during embryonic development", *Dev Biol* **183**(1), 21-36.
- Morrisey, E. E., Tang, Z., Sigrist, K., Lu, M. M., Jiang, F., Ip, H. S. and Parmacek, M. S.** (1998) "GATA6 regulates HNF4 and is required for differentiation of visceral endoderm in the mouse embryo", *Genes Dev* **12**(22), 3579-90.

- Mortensen, R. M., Conner, D. A., Chao, S., Geisterfer-Lowrance, A. A. and Seidman, J. G.** (1992) "Production of homozygous mutant ES cells with a single targeting construct", *Mol Cell Biol* **12**, 2391-5.
- Mouse Genome Sequencing Consortium** (2002) "Initial sequencing and comparative analysis of the mouse genome", *Nature* **420**, 520-62.
- Moustakas, A., Souchelnytskyi, S. and Heldin, C. H.** (2001) "Smad regulation in TGF-beta signal transduction", *J Cell Sci* **114**(Pt 24), 4359-69.
- Mulnard, J. G. and Puissant, F.** (1984) "Development of mouse embryos after ultracentrifugation at the pronuclei stage", *Arch Biol* **97**, 301-15.
- Nadano, D., Notsu, T., Matsuda, T. and Sato, T.** (2002) "A human gene encoding a protein homologous to ribosomal protein L39 is normally expressed in the testis and derepressed in multiple cancer cells", *Biochim Biophys Acta* **1577**(3), 430-6.
- Nagano, T., Nakamura, A., Mori, Y., Maeda, M., Takami, T., Shiosaka, S., Takagi, H. and Sato, M.** (1998) "Differentially expressed olfactomedin-related glycoproteins (Pancortins) in the brain", *Brain Res Mol Brain Res* **53**(1-2), 13-23.
- Nakayama, T., Snyder, M. A., Grewal, S. S., Tsuneizumi, K., Tabata, T. and Christian, J. L.** (1998) "*Xenopus* Smad8 acts downstream of BMP-4 to modulate its activity during vertebrate embryonic patterning", *Development* **125**(5), 857-67.
- Naray-Fejes-Toth, A., Canessa, C., Cleaveland, E. S., Aldrich, G. and Fejes-Toth, G.** (1999) "sgk is an aldosterone-induced kinase in the renal collecting duct. Effects on epithelial Na⁺ channels", *J Biol Chem* **274**(24), 16973-8.
- Nasevicius, A. and Ekker, S. C.** (2000) "Effective targeted gene 'knockdown' in zebrafish", *Nat Genet* **26**(2), 216-20.
- Neidhardt, L., Gasca, S., Wertz, K., Obermayr, F., Worpenberg, S., Lehrach, H. and Herrmann, B. G.** (2000) "Large-scale screen for genes controlling mammalian embryogenesis, using high-throughput gene expression analysis in mouse embryos", *Mech Dev* **98**(1-2), 77-94.
- Neufeld, T. P., de la Cruz, A. F., Johnston, L. A. and Edgar, B. A.** (1998) "Coordination of growth and cell division in the *Drosophila* wing", *Cell* **93**(7), 1183-93.
- Newport, J. and Kirschner, M.** (1982a) "A major developmental transition in early *Xenopus* embryos: I. characterization and timing of cellular changes at the midblastula stage", *Cell* **30**(3), 675-86.
- Newport, J. and Kirschner, M.** (1982b) "A major developmental transition in early *Xenopus* embryos: II. Control of the onset of transcription", *Cell* **30**(3), 687-96.

- Niehrs, C. and Pollet, N.** (1999) "Synexpression groups in eukaryotes", *Nature* **402**(6761), 483-7.
- Nieuwkoop, P. D.** (1973) "The organization center of the amphibian embryo: its origin, spatial organization, and morphogenetic action", *Adv Morphog* **10**, 1-39.
- Nikaido, M., Tada, M., Saji, T and Ueno, N.** (1997) "Conservation of BMP signaling in zebrafish mesoderm patterning", *Mech Dev* **61** (1), 75-88.
- Nishinakamura, R., Matsumoto, Y., Nakao, K., Nakamura, K., Sato, A., Copeland, N. G., Gilbert, D. J., Jenkins, N. A., Scully, S., Lacey, D. L., Katsuki, M., Asashima, M. and Yokota, T.** (2001) "Murine homolog of *SALL1* is essential for ureteric bud invasion in kidney development", *Development* **128**(16), 3105-15.
- Nishinakamura, R., Matsumoto, Y., Uochi, T., Asashima, M. and Yokota, T.** (1997) "Xenopus FK 506-binding protein homolog induces a secondary axis in frog embryos, which is inhibited by coexisting BMP 4 signaling", *Biochem Biophys Res Commun* **239**(2), 585-91.
- Nomura, M. and Li, E.** (1998) "Smad2 role in mesoderm formation, left-right patterning and craniofacial development", *Nature* **393**(6687), 786-90.
- Nusslein-Volhard, C. and Wieschaus, E.** (1980) "Mutations affecting segment number and polarity in *Drosophila*", *Nature* **287**(5785), 795-801.
- Ober, E. A. and Schulte-Merker, S.** (1999) "Signals from the yolk cell induce mesoderm, neuroectoderm, the trunk organizer, and the notochord in zebrafish.PG - 167-81", *Dev Biol* **215**(2).
- Oh, S. P. and Li, E.** (1997) "The signaling pathway mediated by the type IIB activin receptor controls axial patterning and lateral asymmetry in the mouse", *Genes Dev* **11**(14), 1812-26.
- Oh, S. P., Yeo, C. Y., Lee, Y., Schrewe, H., Whitman, M. and Li, E.** (2002) "Activin type IIA and IIB receptors mediate Gdf11 signaling in axial vertebral patterning", *Genes Dev* **16**(21), 2749-54.
- Ohtsubo, M., Theodoras, A. M., Schumacher, J., Roberts, J. M. and Pagano, M.** (1995) "Human cyclin E, a nuclear protein essential for the G1-to-S phase transition", *Mol Cell Biol* **15**(5), 2612-24.
- Onichtchouk, D., Glinka, A. and Niehrs, C.** (1998) "Requirement for *Xvent-1* and *Xvent-2* gene function in dorsolventral patterning of *Xenopus* mesoderm", *Development* **125**, 1447-56.
- Oppenheimer, J. M.** (1936a) "Processes of localization in developing *Fundulus*", *J Exp Zool* **73**, 405-44.

- Oppenheimer, J. M.** (1936b) "Structures developed in amphibians by implantation of living fish organizer", *Proc Soc Exp Med* **34**, 461-3.
- Oppenheimer, J. M.** (1936c) "Transplantation experiments on developing teleosts (*Fundulus* and *Perca*)", *J Exp Zool* **72**, 377-91.
- Osada, S. I. and Wright, C. V.** (1999) "*Xenopus* nodal-related signaling is essential for mesendodermal patterning during early embryogenesis", *Development* **126**(14), 3229-40.
- Palen, E. and Traugh, J. A.** (1987) "Phosphorylation of ribosomal protein S6 by cAMP-dependent protein kinase and mitogen-stimulated S6 kinase differentially alters translation of globin mRNA", *J Biol Chem* **262**(8), 3518-23.
- Palmeirim, I., Henrique, D., Ish-Horowicz, D. and Pourquie, O.** (1997) "Avian *hairy* gene expression identifies a molecular clock linked to vertebrate segmentation and somitogenesis", *Cell* **91**(5), 639-48.
- Pandolfi, P. P., Roth, M. E., Karis, A., Leonard, M. W., Dzierzak, E., Grosveld, F. G., Engel, J. D. and Lindenbaum, M. H.** (1995) "Targeted disruption of the GATA3 gene causes severe abnormalities in the nervous system and in fetal liver haematopoiesis", *Nat Genet* **11**(1), 40-4.
- Park, J., Leong, M. L., Buse, P., Maiyar, A. C., Firestone, G. L. and Hemmings, B. A.** (1999) "Serum and glucocorticoid-inducible kinase (SGK) is a target of the PI 3-kinase-stimulated signaling pathway", *EMBO J* **18**(11), 3024-33.
- Pearce, J. J. and Evans, M. J.** (1999) "*Mml*, a mouse *Mix*-like gene expressed in the primitive streak", *Mech Dev* **87**(1-2), 189-92.
- Pende, M., Kozma, S. C., Jaquet, M., Oorschot, V., Burcelin, R., Le Marchand-Brustel, Y., Klumperman, J., Thorens, B. and Thomas, G.** (2000) "Hypoinsulinaemia, glucose intolerance and diminished beta-cell size in S6K1-deficient mice", *Nature* **408**(6815), 994-7.
- Perea-Gomez, A., Lawson, K. A., Rhinn, M., Zakin, L., Brulet, P., Mazan, S. and Ang, S.-L.** (2001a) "Otx2 is required for visceral endoderm movement and for the restriction of posterior signals in the epiblast of the mouse embryo", *Development* **128**(5), 753-65.
- Perea-Gomez, A., Rhinn, M., and Ang, S.-L.** (2001b) "Role of the anterior visceral endoderm in restricting posterior signals in the mouse embryo", *Int J Dev Biol* **45**, 311-20.
- Perrotti, N., He, R. A., Phillips, S. A., Haft, C. R. and Taylor, S. I.** (2001) "Activation of serum- and glucocorticoid-induced protein kinase (Sgk) by cyclic AMP and insulin", *J Biol Chem* **276**(12), 9406-12.

- Peterson, R. T. and Schreiber, S. L.** (1999) "Kinase phosphorylation: Keeping it all in the family", *Curr Biol* **9**(14), R521-4.
- Petters, R. M. and Markert, C. L.** (1980) "Production and reproductive performance of hexaparental and octaparental mice", *J Hered* **71**(2), 70-4.
- Pevny, L., Lin, C. S., D'Agati, V., Simon, M. C., Orkin, S. H. and Costantini, F.** (1995) "Development of hematopoietic cells lacking transcription factor GATA-1", *Development* **121**(1), 163-72.
- Pevny, L., Simon, M. C., Robertson, E., Klein, W. H., Tsai, S. F., D'Agati, V., Orkin, S. H. and Costantini, F.** (1991) "Erythroid differentiation in chimaeric mice blocked by a targeted mutation in the gene for transcription factor GATA-1", *Nature* **349**(6306), 257-60.
- Peyrieras, N., Strahle, U. and Rosa, F.** (1998) "Conversion of zebrafish blastomeres to an endodermal fate by TGF-beta-related signaling", *Curr Biol* **8**(13), 783-6.
- Piccolo, S., Agius, E., Leys, L., Bhattacharyya, S., Grunz, H., Bouwmeester, T. and De Robertis, E. M.** (1999) "The head inducer Cerberus is a multifunctional antagonist of Nodal, BMP and Wnt signals", *Nature* **397**(6721), 707-10.
- Piccolo, S., Sasai, Y., Lu, B. and De Robertis, E. M.** (1996) "Dorsoventral patterning in *Xenopus*: inhibition of ventral signals by direct binding of chordin to BMP-4", *Cell* **86**, 589-98.
- Pierce, K. E., Michalopoulos, J., Kiessling, A. A., Seibel, M. M. and Zilberstein, M.** (1997) "Preimplantation development of mouse and human embryos biopsied at cleavage stages using a modified displacement technique", *Hum Reprod* **12**(2), 351-6.
- Pierce, S. B. and Kimelman, D.** (1995) "Regulation of Spemann organizer formation by the intracellular kinase Xgsk-3", *Development* **121**(3), 755-65.
- Piotrowska, K., Wianny, F., Pedersen, R. A. and Zernicka-Goetz, M.** (2001) "Blastomeres arising from the first cleavage division have distinguishable fates in normal mouse development", *Development* **128**(19), 3739-48.
- Piotrowska, K. and Zernicka-Goetz, M.** (2001) "Role for sperm in spatial patterning of the early mouse embryo", *Nature* **409**(6819), 517-21.
- Plusa, B., Grabarek, J. B., Piotrowska, K., Glover, D. M. and Zernicka-Goetz, M.** (2002a) "Site of the previous meiotic division defines cleavage orientation in the mouse embryo", *Nat Cell Biol* **4**(10), 811-5.
- Plusa, B., Piotrowska, K. and Zernicka-Goetz, M.** (2002b) "Sperm entry position provides a surface marker for the first cleavage plane of the mouse zygote", *Genesis* **32**(3), 193-8.

- Pogue-Geile, K., Geiser, J. R., Shu, M., Miller, C., Wool, I. G., Meisler, A. I. and Pipas, J. M.** (1991) "Ribosomal protein genes are overexpressed in colorectal cancer: isolation of a cDNA clone encoding the human S3 ribosomal protein", *Mol Cell Biol* **11**(8), 3842-9.
- Pogoda, H. M., Solnica-Krezel, L., Driever, W. and Meyer, D.** (2000) "The zebrafish forkhead transcription factor FoxH1/Fast1 is a modulator of nodal signaling required for organizer formation", *Curr Biol* **10**(17), 1041-9.
- Polakis, P.** (1999) "The oncogenic activation of beta-catenin", *Curr Opin Genet Dev* **9**(1), 15-21.
- Poulain, M. and Lepage, T.** (2002) "Mezzo, a paired-like homeobox protein is an immediate target of Nodal signalling and regulates endoderm specification in zebrafish", *Development* **129**(21), 4901-14.
- Psychoyos, D. and Stern, C. D.** (1996) "Fates and migratory routes of primitive streak cells in the chick embryo" *Development* **122**(5), 1523-34.
- Rana, A.** (2003) Targeted deletion of mouse dynein 2 light intermediate chain disrupts formation of the body axes, Ph.D. Thesis presented to the Department of Anatomy and Developmental Biology University College London, London, United Kingdom.
- Rands, G. F.** (1986) "Size regulation in the mouse embryo. I. The development of quadruple aggregates", *J Embryol Exp Morphol* **94**, 139-48.
- Reiter, J. F., Alexander, J., Rodaway, A., Yelon, D., Patient, R., Holder, N. and Stainier, D. Y.** (1999) "Gata5 is required for the development of the heart and endoderm in zebrafish", *Genes Dev* **13**(22), 2983-95.
- Reiter, J. F., Kikuchi, Y. and Stainier, D. Y.** (2001) "Multiple roles for Gata5 in zebrafish endoderm formation", *Development* **128**(1), 125-35.
- Renucci, A., Lemarchandel, V. and Rosa, F.** (1996) "An activated form of type I serine/threonine kinase receptor TARAM-A reveals a specific signalling pathway involved in fish head organizer formation", *Development* **122**(12), 3735-43.
- Revenkova, E., Masson, J., Koncz, C., Afsar, K., Jakovleva, L. and Paszkowski, J.** (1999) "Involvement of *Arabidopsis thaliana* ribosomal protein S27 in mRNA degradation triggered by genotoxic stress", *EMBO J* **18**(2), 490-9.
- Reymond, A., Marigo, V., Yaylaoglu, M. B., Leoni, A., Ucla, C., Scamuffa, N., Caccioppoli, C., Dermitzakis, E. T., Lyle, R., Banfi, S., Eichele, G., Antonarakis, S. E. and Ballabio, A.** (2002) "Human chromosome 21 gene expression atlas in the mouse", *Nature* **420**(6915), 582-6.

- Reynaud, E., Bolshakov, V. N., Barajas, V., Kafatos, F. C. and Zurita, M. (1997)** "Antisense suppression of the putative ribosomal protein S3A gene disrupts ovarian development in *Drosophila melanogaster*", *Mol Gen Genet* **256**(4), 462-7.
- Rhinn, M., Dierich, A., Shawlot, W., Behringer, R. R., Le Meur, M. and Ang, S. L. (1998)** "Sequential roles for Otx2 in visceral endoderm and neuroectoderm for forebrain and midbrain induction and specification", *Development* **125**(5), 845-56.
- Rhumbler, L. (1902)** "Zur Mechanik des Gastrulationsvorganges, insbesondere der Invagination. Eine entwicklungsmechanische Studie", *Wilhelm Roux' Arch Entwicklungsmech Org*, **14**, 401-76.
- Richards, J. S. (1994)** "Hormonal control of gene expression in the ovary", *Endocr Rev* **15**(6), 725-51.
- Richardson, M. K., Hanken, J., Gooneratne, M. L., Pieau, C., Raynaud, A., Selwood, L. and Wright, G. M. (1997)** "There is no conserved embryonic stage in the vertebrates: implications for current theories of evolution and development", *Anat Embryol* **196**(2):91-106.
- Rigaut, G., Shevchenko, A., Rutz, B., Wilm, M., Mann, M. and Seraphin, B. (1999)** "A generic protein purification method for protein complex characterization and proteome exploration", *Nat Biotechnol* **17**(10), 1030-2.
- Risau, W. and Flamme, I. (1995)** "Vasculogenesis", *Annu Rev Cell Dev Biol* **11**, 73-91.
- Robb, L., Hartley, L., Begley, C. G., Brodnicki, T. C., Copeland, N. G., Gilbert, D. J., Jenkins, N. A. and Elefanty, A. G. (2000)** "Cloning, expression analysis, and chromosomal localization of murine and human homologues of a *Xenopus mix* gene", *Dev Dyn* **219**(4), 497-504.
- Robertson, E. J. (1987)**, Teratocarcinomas and Embryonic Stem Cells: A Practical Approach, Robertson, E. J., Oxford and Washington D.C., IRL Press, p. 71.
- Roeser, T., Stein, S. and Kessel, M. (1999)** "Nuclear beta-catenin and the development of bilateral symmetry in normal and LiCl-exposed chick embryos", *Development* **126**(13), 2955-65.
- Rosen, B. and Beddington, R. S. P. (1993)** "Whole-mount *in situ* hybridisation in the mouse embryo: gene expression in three dimensions", *Trends in Genetics* **9**, 162-7.
- Rosenquist, T. A. and Martin, G. R. (1995)** "Visceral endoderm-1 (VE-1): an antigen marker that distinguishes anterior from posterior embryonic visceral endoderm in the early post-implantation mouse embryo", *Mech Dev* **49**(1-2), 117-21.

- Rossant, J.** (1976) "Postimplantation development of blastomeres isolated from 4- and 8-cell mouse eggs", *J Embryol Exp Morphol* **36**(2), 283-90.
- Rowning, B. A., Wells, J., Wu, M., Gerhart, J. C., Moon, R. T. and Larabell, C. A.** (1997) "Microtubule-mediated transport of organelles and localization of beta-catenin to the future dorsal side of *Xenopus* eggs", *Proc Natl Acad Sci USA* **94**(4), 1224-9.
- Rozansky, D. J., Wang, J., Doan, N., Purdy, T., Faulk, T., Bhargava, A., Dawson, K. and Pearce, D.** (2002) "Hypotonic induction of SGK1 and Na⁺ transport in A6 cells", *Am J Physiol Renal Physiol* **283**(1), F105-13.
- Rozen, S. and Skaletsky, H. J.** (2000) "Primer3 on the WWW for general users and for biologist programmers", in Krawetz, S. and Misener, S., eds., *Bioinformatics Methods and Protocols: Methods in Molecular Biology*, Humana Press, Totowa, NJ, pp 365-386.
- Ruggero, D., Grisendi, S., Piazza, F., Rego, E., Mari, F., Rao, P. H., Cordon-Cardo, C. and Pandolfi, P. P.** (2003) "Dyskeratosis congenita and cancer in mice deficient in ribosomal RNA modification", *Science* **299**(5604), 259-62.
- Ruiz i Altaba, A., Placzek, M., Baldassare, M., Dodd, J. and Jessell, T. M.** (1995) "Early stages of notochord and floor plate development in the chick embryo defined by normal and induced expression of HNF-3 beta", *Dev Biol* **170**(2), 299-313.
- Russ, A. P., Wattler, S., Colledge, W. H., Aparicio, S. A., Carlton, M. B., Pearce, J. J., Barton, S. C., Surani, M. A., Ryan, K., Nehls, M. C., Wilson, V. and Evans, M. J.** (2000) "Eomesodermin is required for mouse trophoblast development and mesoderm formation", *Nature* **404**(6773), 95-9.
- Ruvinsky, I., Silver, L. M. and Ho, R. K.** (1998) "Characterization of the zebrafish *tbx16* gene and evolution of the vertebrate T-box family", *Dev Genes Evol* **208**(2), 94-9.
- Ryan, K., Garrett, N., Mitchell, A. and Gurdon, J. B.** (1996) "*Eomesodermin*, a key early gene in *Xenopus* mesoderm differentiation", *Cell* **87**(6), 989-1000.
- Ryu, S. L., Fujii, R., Yamanaka, Y., Shimizu, T., Yabe, T., Hirata, T., Hibi, M. and Hirano, T.** (2001) "Regulation of dharma/bozozok by the Wnt pathway", *Dev Biol* **231**(2), 397-409.
- Saeboe-Larssen, S. and Lambertsson, A.** (1996) "A novel *Drosophila Minute* locus encodes ribosomal protein S13", *Genetics* **143**(2), 877-85.
- Saeboe-Larssen, S., Lyamouri, M., Merriam, J., Oksvold, M. P. and Lambertsson, A.** (1998) "Ribosomal protein insufficiency and the *Minute* syndrome in *Drosophila*: a dose-response relationship", *Genetics* **148**(3), 1215-24.
- Saeboe-Larssen, S., Urbanczyk Mohebi, B. and Lambertsson, A.** (1997) "The *Drosophila* ribosomal protein L14-encoding gene, identified by a novel *Minute*

- mutation in a dense cluster of previously undescribed genes in cytogenetic region 66D", *Mol Gen Genet* **255**(2), 141-51.
- Sakaguchi, T.**, Kuroiwa, A. and Takeda, H. (2001) "A novel sox gene, 226D7, acts downstream of Nodal signaling to specify endoderm precursors in zebrafish", *Mech Dev* **107**(1-2), 25-38.
- Sakaguchi, T.**, Mizuno, T. and Takeda, H. (2002) Formation and patterning roles of the yolk syncytial layer, *Pattern formation in zebrafish*, Solnica-Krezel, L., Berlin, Springer, **40**, 1-14.
- Sakai, M.** (1996) "The vegetal determinants required for the Spemann organizer move equatorially during the first cell cycle", *Development* **122**(7), 2207-14.
- Salamov, A. A. and Solovyev, V. V.** (2000) "Ab initio Gene Finding in *Drosophila* Genomic DNA", *Genome Res* **10** (4), 516-22.
- Sampath, K.**, Rubinstein, A. L., Cheng, A. M., Liang, J. O., Fekany, K., Solnica-Krezel, L., Korzh, V., Halpern, M. E. and Wright, C. V. (1998) "Induction of the zebrafish ventral brain and floorplate requires cyclops/nodal signalling", *Nature* **395**(6698), 185-9.
- Sander, K.** (1983) The evolution of patterning mechanisms: gleanings from insect embryogenesis and spermatogenesis, *Development and Evolution*, Goodwin., B. C., Holder, N. and Wylie C. C., Cambridge, Cambridge University Press, 124-37.
- Sasai, Y. and De Robertis, E. M.** (1997) "Ectodermal patterning in vertebrate embryos" *Dev Biol*, **182**(1), 5-20.
- Sasai, Y.**, Lu, B., Piccolo, S. and De Robertis, E. M. (1996) "Endoderm induction by the organizer-secreted factors chordin and noggin in *Xenopus* animal caps", *EMBO J* **15**(17), 4547-55.
- Sasai, Y.**, Lu, B., Steinbeisser, H. and De Robertis, E. M. (1995) "Regulation of neural induction by the Chd and Bmp-4 antagonistic patterning signals in *Xenopus*", *Nature* **376**, 333-6.
- Sasai, Y.**, Lu, B., Steinbeisser, H., Geissert, D., Gont, L. K. and De Robertis, E. M. (1994) "Xenopus chordin: a novel dorsalizing factor activated by organizer-specific homeobox genes", *Cell*, **79**(5), 779-90.
- Sasaki, H. and Hogan, B. L.** (1993) "Differential expression of multiple fork head related genes during gastrulation and axial pattern formation in the mouse embryo", *Development* **118**(1), 47-59.
- Sato, S. M. and Sargent, T. M.** (1989) "Development of neural inducing capacity in dissociated *Xenopus* embryos", *Dev Biol* **134**, 263-6.

- Saude, L., Woolley, K., Martin, P., Driever, W. and Stemple, D. (2000) "Axis inducing activity and cell fates of the zebrafish organizer", *Development* **127**, 3407-17.
- Sawicki, J. A., Magnuson, T. and Epstein, C. J. (1982) "Evidence for the expression of the paternal genome in the two-cell mouse embryo", *Nature* **294**, 450-1.
- Scharf, S. R. and Gerhart, J. C. (1980) "Determination of the dorsal-ventral axis in eggs of *Xenopus laevis*: complete rescue of uv-impaired eggs by oblique orientation before first cleavage", *Dev Biol* **79**(1), 181-98.
- Scharf, S. R., Lieberman, M. B. and Cande, W. Z. (1986) "Determination of dorsoventral polarity in the *Xenopus* egg requires microtubules.PG - 345-8", *Prog Clin Biol Res* **217B**.
- Scharf, S. R., Rowning, B., Wu, M. and Gerhart, J. C. (1989) "Hyperdorsoanterior embryos from *Xenopus* eggs treated with D₂O", *Dev Biol* **134**(1), 175-88.
- Schier, A. F. (2001) "Axis formation and patterning in zebrafish", *Curr Opin Genet Dev* **11**(4), 393-404.
- Schier, A. F., Neuhauss, S. C., Helde, K. A., Talbot, W. S. and Driever, W. (1997) "The *one-eyed pinhead* gene functions in mesoderm and endoderm formation in zebrafish and interacts with *no tail*", *Development* **124**(2), 327-42.
- Schmidt, A., Hollmann, M. and Schafer, U. (1996) "A newly identified *Minute* locus, M(2)32D, encodes the ribosomal protein L9 in *Drosophila melanogaster*", *Mol Gen Genet* **251**(3), 381-7.
- Schmidt, E. V. (1999) "The role of c-myc in cellular growth control", *Oncogene* **18**(19), 2988-96.
- Schneider, S., Steinbeisser, H., Warga, R. M. and Hausen, P. (1996) "Beta-catenin translocation into nuclei demarcates the dorsalizing centers in frog and fish embryos", *Mech Dev* **57**(2), 191-8.
- Schoenwolf, G. C., Garcia-Martinez, V. and Dias, M. S. (1992) "Mesoderm movement and fate during avian gastrulation and neurulation", *Dev Dyn* **193**, 235-48.
- Schulte-Merker, S., Ho, R. K., Herrmann, B. G. and Nusslein-Volhard, C. (1992) "The protein product of the zebrafish homologue of the mouse *T* gene is expressed in nuclei of the germ ring and the notochord of the early embryo", *Development* **116**(4), 1021-32.
- Schulte-Merker, S., Lee, K. J., McMahon, A. P. and Hammerschmidt, M. (1997) "The zebrafish organizer requires chordino", *Nature* **387**(6636), 862-3.
- Schulte-Merker, S., Smith, J. C. and Dale, L. (1994) "Effects of truncated activin and FGF receptors and of follistatin on the inducing activities of BVg1 and activin: does activin play a role in mesoderm induction?" *EMBO J* **13**(15), 3533-41.

- Schultz, J.** (1929) "The *Minute* reaction in the development of *Drosophila melanogaster*", *Genetics* **14**, 366-419.
- Seleiro, E. A., Connolly, D. J. and Cooke, J.** (1996) "Early developmental expression and experimental axis determination by the chicken *Vg1* gene", *Curr Biol* **6**(11), 1476-86.
- Setiawan, I., Henke, G., Feng, Y., Bohmer, C., Vasilets, L. A., Schwarz, W. and Lang, F.** (2002) "Stimulation of *Xenopus* oocyte Na(+),K(+)ATPase by the serum and glucocorticoid-dependent kinase sgk1", *Pflugers Arch* **444**(3), 426-31.
- Shah, S. B., Skromne, I., Hume, C. R., Kessler, D. S., Lee, K. J., Stern, C. D. and Dodd, J.** (1997) "Misexpression of chick *Vg1* in the marginal zone induces primitive streak formation", *Development* **124**(24), 5127-38.
- Sharma, K., Jin, Y., Guo, J. and Ziyadeh, F. N.** (1996) "Neutralization of TGF-beta by anti-TGF-beta antibody attenuates kidney hypertrophy and the enhanced extracellular matrix gene expression in STZ-induced diabetic mice", *Diabetes* **45**(4), 522-30.
- Sharp, M. G., Adams, S. M., Elvin, P., Walker, R. A., Brammar, W. J. and Varley, J. M.** (1990) "A sequence previously identified as metastasis-related encodes an acidic ribosomal phosphoprotein, P2", *Br J Cancer* **61**(1), 83-8.
- Shawlot, W. and Behringer, R. R.** (1995) "Requirement for *Lim1* in head-organizer function", *Nature* **374**(6521), 425-30.
- Shawlot, W., Min Deng, J., Wakamiya, M. and Behringer, R. R.** (2000) "The *cerberus*-related gene, *Cerr1*, is not essential for mouse head formation", *Genesis* **26**(4), 253-8.
- Shawlot, W., Wakamiya, M., Kwan, K. M., Kania, A., Jessell, T. M. and Behringer, R. R.** (1999) "*Lim1* is required in both primitive streak-derived tissues and visceral endoderm for head formation in the mouse", *Development* **126**(22), 4925-32.
- Shelly, C. and Herrera, R.** (2002) "Activation of SGK1 by HGF, Rac1 and integrin-mediated cell adhesion in MDCK cells: PI-3K-dependent and -independent pathways", *J Cell Sci* **115**(Pt 9), 1985-93.
- Shen, M. M., Wang, H. and Leder, P.** (1997) "A differential display strategy identifies *Cryptic*, a novel EGF-related gene expressed in the axial and lateral mesoderm during mouse gastrulation", *Development* **124**(2), 429-42.
- Sheppard, K. E. and Autelitano, D. J.** (2002) "11Beta-hydroxysteroid dehydrogenase 1 transforms 11-dehydrocorticosterone into transcriptionally active glucocorticoid in neonatal rat heart", *Endocrinology* **143**(1), 198-204.

- Shigaev, A., Asher, C., Latter, H., Garty, H. and Reuveny, E. (2000)** "Regulation of sgk by aldosterone and its effects on the epithelial Na(+) channel", *Am J Physiol Renal Physiol* **278**(4), F613-9.
- Shih, J. and Fraser, S. E. (1996)** "Characterizing the zebrafish organizer: microsurgical analysis at the early-shield stage", *Development* **122**(4), 1313-22.
- Shima, H., Pende, M., Chen, Y., Fumagalli, S., Thomas, G. and Kozma, S. C. (1998)** "Disruption of the *p70(s6k)/p85(s6k)* gene reveals a small mouse phenotype and a new functional S6 kinase", *EMBO J* **17**(22), 6649-59.
- Shimizu, T., Yamanaka, Y., Ryu, S. L., Hashimoto, H., Yabe, T., Hirata, T., Bae, Y. K., Hibi, M. and Hirano, T. (2000)** "Cooperative roles of Bozozok/Dharma and Nodal-related proteins in the formation of the dorsal organizer in zebrafish", *Mech Dev* **91**(1-2), 293-303.
- Shimono, A. and Behringer, R. R. (1999)** "Isolation of novel cDNAs by subtractions between the anterior mesendoderm of single mouse gastrula stage embryos", *Dev Biol* **209**(2), 369-80.
- Shivdasani, R. A. (2002)** "Molecular regulation of vertebrate early endoderm development", *Dev Biol* **249**(2), 191-203.
- Shivdasani, R. A., Fujiwara, Y., McDevitt, M. A. and Orkin, S. H. (1997)** "A lineage-selective knockout establishes the critical role of transcription factor GATA-1 in megakaryocyte growth and platelet development", *EMBO J* **16**(13), 3965-73.
- Shulman, R. W., Sripati, C. E. and Warner, J. R. (1977)** "Noncoordinated transcription in the absence of protein synthesis in yeast", *J Biol Chem* **252**(4), 1344-9.
- Siddall, L. S., Barcroft, L. C. and Watson, A. J. (2002)** "Targeting gene expression in the preimplantation mouse embryo using morpholino antisense oligonucleotides", *Mol Reprod Dev* **63**(4), 413-21.
- Simeone, A., Acampora, D., Mallamaci, A., Stornaiuolo, A., D'Apice, M. R., Nigro, V. and Boncinelli, E. (1993)** "A vertebrate gene related to orthodenticle contains a homeodomain of the bicoid class and demarcates anterior neuroectoderm in the gastrulating mouse embryo", *EMBO J* **12**(7), 2735-47.
- Simmons, D. L., Neel, B. G., Stevens, R., Evett, G. and Erikson, R. L. (1992)** "Identification of an early-growth-response gene encoding a novel putative protein kinase", *Mol Cell Biol* **12**(9), 4164-9.
- Simpson, E. H., Johnson, D. K., Hunsicker, P., Suffolk, R., Jordan, S. A. and Jackson, I. J. (1999)** "The mouse *Cer1* (*Cerberus* related or homologue) gene is not required for anterior pattern formation", *Dev Biol* **213**(1), 202-6.

- Sirard, C.**, de la Pompa, J. L., Elia, A., Itie, A., Mirtsos, C., Cheung, A., Hahn, S., Wakeham, A., Schwartz, L., Kern, S. E., Rossant, J. and Mak, T. W. (1998) "The tumor suppressor gene *Smad4/Dpc4* is required for gastrulation and later for anterior development of the mouse embryo", *Genes Dev* **12**(1), 107-19.
- Sirotkin, H. I.**, Dougan, S. T., Schier, A. F. and Talbot, W. S. (2000a) "bozozok and squint act in parallel to specify dorsal mesoderm and anterior neuroectoderm in zebrafish", *Development* **127**(12), 2583-92.
- Sirotkin, H. I.**, Gates, M. A., Kelly, P. D., Schier, A. F. and Talbot, W. S. (2000b) "Fast1 is required for the development of dorsal axial structures in zebrafish", *Curr Biol* **10**(17), 1051-4.
- Sive, H. L.**, Grainger, R. M. and M., H. R. (2000) Early development of *Xenopus laevis*: a laboratory manual, New York, Cold Spring Harbor Laboratory Press.
- Skoulakis, E. M. and Davis, R. L.** (1998) "14-3-3 proteins in neuronal development and function", *Mol Neurobiol*, **16**(3), 269-84.
- Skromne, I. and Stern, C. D.** (2001) "Interactions between Wnt and Vg1 signalling pathways initiate primitive streak formation in the chick embryo", *Development* **128**(15), 2915-27.
- Slack, J. M.**, Darlington, B. G., Heath, J. K. and Godsave, S. F. (1987) "Mesoderm induction in early *Xenopus* embryos by heparin-binding growth factors", *Nature* **326**(6109), 197-200.
- Smith, J. C.**, Price, B. M., Van Nimmen, K. and Huylebroeck, D. (1990) "Identification of a potent *Xenopus* mesoderm-inducing factor as a homologue of activin A", *Nature* **345**(6277), 729-31.
- Smith, J. C. and Slack, J. M.** (1983) "Dorsalization and neural induction: properties of the organizer in *Xenopus laevis*", *J Embryol Exp Morphol* **78**, 299-317.
- Smith, L. J.** (1980) "Embryonic axis orientation in the mouse and its correlation with blastocyst relationships to the uterus. Part 1. Relationships between 82 hours and 4 1/4 days", *J Embryol Exp Morphol* **55**, 257-77.
- Smith, W. C. and Harland, R. M.** (1991) "Injected *Xwnt-8* RNA acts early in *Xenopus* embryos to promote formation of a vegetal dorsalizing center", *Cell* **67**(4), 753-65.
- Smith, W. C. and Harland, R. M.** (1992) "Expression cloning of noggin, a new dorsalizing factor localized to the Spemann organizer in *Xenopus* embryos", *Cell* **70**(5), 829-40.

- Snyder, D. A., Rivers, A. M., Yokoe, H., Menco, B. P. and Anholt, R. R. (1991)** "Olfactomedin: purification, characterization, and localization of a novel olfactory glycoprotein" *Biochemistry* **30**(38), 9143-53.
- Snyder, P. M., Olson, D. R. and Thomas, B. C. (2002)** "Serum and glucocorticoid-regulated kinase modulates Nedd4-2-mediated inhibition of the epithelial Na⁺ channel", *J Biol Chem* **277**(1), 5-8.
- Sokol, S., Christian, J. L., Moon, R. T. and Melton, D. A. (1991)** "Injected *Wnt* RNA induces a complete body axis in *Xenopus* embryos", *Cell* **67**(4), 741-52.
- Sokol, S. Y. (1996)** "Analysis of Dishevelled signalling pathways during *Xenopus* development", *Curr Biol* **6**(11), 1456-67.
- Sokol, S. Y., Klingensmith, J., Perrimon, N. and Itoh, K. (1995)** "Dorsalizing and neuralizing properties of *Xdsh*, a maternally expressed *Xenopus* homolog of dishevelled", *Development* **121**(10), 3487.
- Solnica-Krezel, L. and Cooper, M. S. (2002)** Cellular and genetic mechanisms of convergence and extension, *Pattern formation in zebrafish*, Solnica-Krezel, L., Berlin, Springer, **40**, 136-65.
- Solnica-Krezel, L. and Driever, W. (1994)** "Microtubule arrays of the zebrafish yolk cell: organization and function during epiboly", *Development* **120**(9), 2443-55.
- Solnica-Krezel, L. and Driever, W. (2001)** "The role of the homeodomain protein *Bozozok* in zebrafish axis formation", *Int J Dev Biol* **45**(1 Spec No), 299-310.
- Solnica-Krezel, L., Stemple, D. L. and Driever, W. (1995)** "Transparent things: cell fates and cell movements during early embryogenesis of zebrafish", *Bioessays* **17**(11), 931-9.
- Solnica-Krezel, L., Stemple, D. L., Mountcastle-Shah, E., Rangini, Z., Neuhauss, S. C., Malicki, J., Schier, A. F., Stainier, D. Y., Zwartkuis, F., Abdelilah, S. and Driever, W. (1996)** "Mutations affecting cell fates and cellular rearrangements during gastrulation in zebrafish", *Development* **123**, 67-80.
- Song, J., Oh, S. P., Schrewe, H., Nomura, M., Lei, H., Okano, M., Gridley, T. and Li, E. (1999)** "The type II activin receptors are essential for egg cylinder growth, gastrulation, and rostral head development in mice", *Dev Biol* **213**(1), 157-69.
- Spemann, H. (1931)** "Uber den anteil von implantat und wirtskeim an der orientierung und beschaffenheit der induzierten embryonalanlage", *Roux's Arch Entw Mech Org* **123**, 399-517.

- Spemann, H. and Mangold, H.** (1924) "Uber Induktion von Embryonalanlagen durch Implantation artfremder Organisatoren", *W Roux Arch Entwicklungsmech Organ* **100**, 599-638. (Reprinted in *Int. J. Dev. Biol.*, **45**,13-38 (2001).
- Spratt, N. T. and Haas, H.** (1960) "Integrative mechanisms in development of the early chick blastoderm. I. Regulative potentiality of separated parts", *J Exp Zool* **33**, 97-137.
- Srinivas, S., Rodriguez, T. A., Clements, M., Smith, J. C. and Beddington, R. S.** (2004) "Active cell migration drives the unilateral movements of the anterior visceral endoderm", *Development*, **131**(5), 1157-64.
- Stachel, S. E., Grunwald, D. J. and Myers, P. Z.** (1993) "Lithium perturbation and *gooseoid* expression identify a dorsal specification pathway in the pregastrula zebrafish" *Development* **117**, 1261-74.
- Stein, D., Foster, E., Huang, S. B., Weller, D. and Summerton, J.** (1997) "A specificity comparison of four antisense types: morpholino, 2'-O-methyl RNA, DNA, and phosphorothioate DNA", *Antisense Nucleic Acid Drug Dev* **7**(3), 151-7.
- Steitz, J. A.** (1969) "Polypeptide chain initiation: nucleotide sequences of the three ribosomal binding sites in bacteriophage R17 RNA", *Nature* **224**(223), 957-64.
- Steitz, J. A.** (1973) "Discriminatory ribosome rebinding of isolated regions of protein synthesis initiation from the ribonucleic acid of bacteriophage R17", *Proc Natl Acad Sci USA* **70**(9), 2605-9.
- Stennard, F., Carnac, G. and Gurdon, J. B.** (1996) "The *Xenopus* T-box gene, *Antipodean*, encodes a vegetally localised maternal mRNA and can trigger mesoderm formation", *Development* **122**(12), 4179-88.
- Stern, C. D.** (1990) "The marginal zone and its contribution to the hypoblast and primitive streak of the chick embryo", *Development* **109**(3), 667-82.
- Stern, C. D. and Canning, D. R.** (1990) "Origin of cells giving rise to mesoderm and endoderm in chick embryo", *Nature* **343**(6255), 273-5.
- Stewart, M. J. and Denell, R.** (1993) "Mutations in the *Drosophila* gene encoding ribosomal protein S6 cause tissue overgrowth", *Mol Cell Biol* **13**(4), 2524-35.
- Storey, K. G., Crossley, J. M., De Robertis, E. M., Norris, W. E. and Stern, C. D.** (1992) "Neural induction and regionalisation in the chick embryo", *Development* **114**(3), 729-41.
- Storz, P. and Toker, A.** (2002) "3'-phosphoinositide-dependent kinase-1 (PDK-1) in PI 3-kinase signaling", *Front Biosci* **7**, d886-902.

- Strahle, U. and Jesuthasan, S.** (1993) "Ultraviolet irradiation impairs epiboly in zebrafish embryos: evidence for a microtubule-dependent mechanism of epiboly", *Development* **119**(3), 909-19.
- Strahle, U., Blader, P. Henrique, D. and Ingham, P. W.** (1993) "Axial, a zebrafish gene expressed along the developing body axis, shows altered expression in cyclops mutant embryos" *Genes Dev* **7**, 1436-46.
- Streit, A., Berliner, A. J., Papanayotou, C., Sirulnik, A. and Stern, C. D.** (2000) "Initiation of neural induction by FGF signalling before gastrulation", *Nature* **406**(6791), 74-8.
- Streit, A., Lee, K. J., Woo, I., Roberts, C., Jessell, T. M. and Stern, C. D.** (1998) "Chordin regulates primitive streak development and the stability of induced neural cells, but is not sufficient for neural induction in the chick embryo", *Development* **125**(3), 507-19.
- Sturgill, T. W. and Wu, J.** (1991) "Recent progress in characterization of protein kinase cascades for phosphorylation of ribosomal protein S6", *Biochim Biophys Acta* **1092**(3), 350-7.
- Su, L. K., Vogelstein, B. and Kinzler, K. W.** (1993) "Association of the APC tumor suppressor protein with catenins", *Science* **262**(5140), 1734-7.
- Summerton, J.** (1999) "Morpholino antisense oligomers: the case for an RNase H-independent structural type", *Biochim Biophys Acta* **1489**(1), 141-58.
- Summerton, J. and Weller, D.** (1997) "Morpholino antisense oligomers: design, preparation, and properties", *Antisense Nucleic Acid Drug Dev* **7**(3), 187-95.
- Sumoy, L., Kiefer, J. and Kimelman, D.** (1999) "Conservation of intracellular Wnt signaling components in dorsal-ventral axis formation in zebrafish", *Dev Genes Evol* **209**(1), 48-58.
- Sun, C. and Woolford, J. L., Jr.** (1994) "The yeast NOP4 gene product is an essential nucleolar protein required for pre-rRNA processing and accumulation of 60S ribosomal subunits", *EMBO J* **13**(13), 3127-35.
- Sun, Y., Taniguchi, R., Tanoue, D., Yamaji, T., Takematsu, H., Mori, K., Fujita, T., Kawasaki, T. and Kozutsumi, Y.** (2000) "Sli2 (Ypk1), a homologue of mammalian protein kinase SGK, is a downstream kinase in the sphingolipid-mediated signaling pathway of yeast", *Mol Cell Biol* **20**(12), 4411-9.
- Sun, X., Meyers, E. N., Lewandoski, M. and Martin G. R.** (1999) "Targeted disruption of Fgf8 causes failure of cell migration in the gastrulating mouse embryo", *Genes Dev*, **13**(14), 1834-46.

- Surani, M. A. and Barton, S. C.** (1984) "Spatial distribution of blastomeres is dependent on cell division order and interactions in mouse morulae", *Dev Biol* **102**(2), 335-43.
- Suzuki, A., Kanedo, E. Ueno, N. and Hemmati-Brivanlou, A.** (1997) "Regulation of epidermal induction by BMP2 and BMP7 signalling", *Dev Biol* **189**, 112-22.
- Suzuki, A., Shioda, N. and Ueno, N.** (1995) "Bone morphogenetic protein acts as a ventral mesoderm modifier in early *Xenopus* embryos", *Dev Growth Differ* **37**, 581-88.
- Tada, M., Concha, M. L. and Heisenberg, C. P.** (2002) "Non-canonical Wnt signalling and regulation of gastrulation movements", *Semin Cell Dev Biol* **13**(3), 251-60.
- Tada, M. and Smith, J. C.** (2000) "*Xwnt11* is a target of *Xenopus* Brachyury: regulation of gastrulation movements via Dishevelled, but not through the canonical Wnt pathway", *Development* **127**(10), 2227-38.
- Talbot, W. S., Trevarrow, B., Halpern, M. E., Melby, A. E., Farr, G., Postlethwait, J. H., Jowett, T., Kimmel, C. B. and Kimelman, D.** (1995) "A homeobox gene essential for zebrafish notochord development", *Nature* **378**(6553), 150-7.
- Tam, P. P. and Beddington, R. S.** (1987) "The formation of mesodermal tissues in the mouse embryo during gastrulation and early organogenesis", *Development* **99**(1), 109-26.
- Tam, P. P. and Quinlan, G. A.** (1996) "Mapping vertebrate embryos", *Curr Biol* **6**(2), 104-6.
- Tam, P. P. and Steiner, K. A.** (1999) "Anterior patterning by synergistic activity of the early gastrula organizer and the anterior germ layer tissues of the mouse embryo", *Development* **126**(22), 5171-9.
- Tam, P. P., Steiner, K. A., Zhou, S. X. and Quinlan, G. A.** (1997) "Lineage and functional analyses of the mouse organizer", *Cold Spring Harbor Symposia on Quantitative Biology* **62**, 135-44.
- Tannahill, D. and Melton, D. A.** (1989) "Localized synthesis of the Vg1 protein during early *Xenopus* development", *Development* **106**(4), 775-85.
- Tanner, N. K. and Linder, P.** (2001) "DEXD/H box RNA helicases: from generic motors to specific dissociation functions", *Mol Cell* **8**(2), 251-62.
- Tarkowski, A. K.** (1959) "Experiments on the development of isolated blastomeres of mouse eggs", *Nature* **184**, 1286-7.
- Tarkowski, A. K. and Wroblewska, J.** (1967) "Development of blastomeres of mouse eggs isolated at the 4- and 8-cell stage", *J Embryol Exp Morphol* **18**(1), 155-80.

- Tetsu, O. and McCormick, F.** (1999) "Beta-catenin regulates expression of cyclin D1 in colon carcinoma cells", *Nature* **398**(6726), 422-6.
- The *C. elegans* genome consortium** (1998) "Genome sequence of the nematode *C. elegans*: a platform for investigating biology. The *C. elegans* Sequencing Consortium", *Science* **282**(5396), 2012-8.
- The FANTOM Consortium and the RIKEN Genome Exploration Research Group Phase I & II Team** (2002) "Analysis of the mouse transcriptome based on functional annotation of 60,770 full-length cDNAs", *Nature* **420**(6915), 563-73.
- The FlyBase Consortium** (2003) "The FlyBase database of the *Drosophila* genome projects and community literature", *Nucleic Acids Res* **31**, 172-5. <http://flybase.org/>.
- Thisse, B., Wright, C. V. and Thisse, C.** (2000) "Activin- and Nodal-related factors control antero-posterior patterning of the zebrafish embryo", *Nature* **403**(6768), 425-8.
- Thisse, C. and Thisse, B.** (1998) "High resolution whole-mount *in situ* hybridisation", *Zebrafish Sci Mon* **5**, 8-9.
- Thisse, C. and Thisse, B.** (1999) "Activin, a novel and divergent member of the TGFbeta superfamily, negatively regulates mesoderm induction", *Development* **126**(2), 229-40.
- Thisse, C., Thisse, B., Halpern, M. E. and Postlethwait, J. H.** (1994) "*Gooseoid* expression in neurectoderm and mesendoderm is disrupted in zebrafish *cyclops* gastrulas", *Dev Biol* **164**(2), 420-9.
- Thomas, G. and Hall, M. N.** (1997) "TOR signalling and control of cell growth", *Curr Opin Cell Biol* **9**(6), 782-7.
- Thomas, G. and Luther, H.** (1981) "Transcriptional and translational control of cytoplasmic proteins after serum stimulation of quiescent Swiss 3T3 cells", *Proc Natl Acad Sci USA* **78**(9), 5712-6.
- Thomas, P. and Beddington, R.** (1996) "Anterior primitive endoderm may be responsible for patterning the anterior neural plate in the mouse embryo", *Current Biology* **6**(11), 1487-96.
- Thomas, P., Brickman, J. M., Popperl, H., Krumlauf, R. and Beddington, R. S.** (1997) "Axis duplication and anterior identity in the mouse embryo", *Cold Spring Harbor Symposia on Quantitative Biology* **62**, 115-25.
- Thomas, P., Brown, A. and Beddington, R. S. P.** (1998) "*Hex*: a homeobox gene revealing peri-implantation asymmetry in the mouse embryo and an early transient marker of endothelial cell precursors", *Development* **125**, 85-94.

- Thomsen, G., Woolf, T., Whitman, M., Sokol, S., Vaughan, J., Vale, W. and Melton, D. A.** (1990) "Activins are expressed early in *Xenopus* embryogenesis and can induce axial mesoderm and anterior structures", *Cell* **63**(3), 485-93.
- Thomsen, G. H. and Melton, D. A.** (1993) "Processed Vg1 protein is an axial mesoderm inducer in *Xenopus*", *Cell* **74**(3), 433-41.
- Ting, C. N., Olson, M. C., Barton, K. P. and Leiden, J. M.** (1996) "Transcription factor GATA-3 is required for development of the T-cell lineage", *Nature* **384**(6608), 474-8.
- Tojo, H. and Ogita, Z.** (1984) "An improved method for destroying mouse blastomeres electrically inside the *zona pellucida* and the *in vitro* development of the surviving blastomeres", *J Exp Zool* **229**(3), 475-80.
- Torok, I., Herrmann-Horle, D., Kiss, I., Tick, G., Speer, G., Schmitt, R. and Mechler, B. M.** (1999) "Down-regulation of RpS21, a putative translation initiation factor interacting with P40, produces viable minute imagos and larval lethality with overgrown hematopoietic organs and imaginal discs", *Mol Cell Biol* **19**(3), 2308-21.
- Torres, R. M. and Kuhn, R.** (1995) *The Cologne Guide to Gene Targeting*. Cologne.
- Toyo-oka, K., Shionoya, A., Gambello, M. J., Cardoso, C., Leventer, R., Ward, H. L., Ayala, R., Tsai, L. H., Dobyns, W., Ledbetter, D., Hirotsune, S. and Wynshaw-Boris, A.** (2003) "14-3-3epsilon is important for neuronal migration by binding to NUDEL: a molecular explanation for Miller-Dieker syndrome", *Nat Genet* **34**(3), 274-85.
- Trinkaus, J. P.** (1951) "A study of the mechanism of epiboly in the egg of *Fundulus heteroclitus*", *J Exp Zool* **118**, 269-320.
- Tropepe, V., Hitoshi, S., Sirard, C., Mak, T. W., Rossant, J. and van der Kooy, D.** (2001) "Direct neural fate specification from embryonic stem cells: a primitive mammalian neural stem cell stage acquired through a default mechanism", *Neuron* **30**(1), 65-78.
- Tsai, F. Y., Keller, G., Kuo, F. C., Weiss, M., Chen, J., Rosenblatt, M., Alt, F. W. and Orkin, S. H.** (1994) "An early haematopoietic defect in mice lacking the transcription factor GATA-2", *Nature* **371**(6494), 221-6.
- Tsai, K. J., Chen, S. K., Ma, Y. L., Hsu, W. L. and Lee, E. H.** (2002) "*Sgk*, a primary glucocorticoid-induced gene, facilitates memory consolidation of spatial learning in rats", *Proc Natl Acad Sci USA* **99**(6), 3990-5.
- Tsutsui, K., Tsutsui, K., Okada, S., Watarai, S., Seki, S., Yasuda, T. and Shohmori, T.** (1993) "Identification and characterization of a nuclear scaffold protein that binds the matrix attachment region DNA", *J Biol Chem* **268**(17), 12886-94.

- Tung, T. C., Chan, C. Y. and Tung, Y. F. Y. (1945)** "Experiments on the developmental potencies of blastoderms and fragments of teleostean eggs separated latitudinally", *Proc Zool Soc Lond* **115**, 175-89.
- Tzivion, G., Shen, Y. H. and Zhu, J. (2001)** "14-3-3 proteins: bringing new definitions to scaffolding", *Oncogene*, **20**(44), 6331-8.
- Ubbels, G. A. (1977)** "Symmetrization of the fertilized egg of *Xenopus laevis* (studied by cytological, cytochemical, and ultrastructural methods)", *Mém Soc Zool France, Symp L Gallien* **41**, 103-16.
- Uchiyama, H., Kobayashi, T., Yamashita, A., Ohno, S. and Yabe, S. (2001)** "Cloning and characterization of the T-box gene *Tbx6* in *Xenopus laevis*", *Dev Growth Differ* **43**(6), 657-69.
- Ulrich, F., Concha, M. L., Heid, P. J., Voss, E., Witzel, S., Roehl, H., Tada, M., Wilson, S. W., Adams, R. J., Soll, D. R., Heisenberg, C.-P. (2003)** "Slb/Wnt11 controls hypoblast cell migration and morphogenesis at the onset of zebrafish gastrulation", *Development*, in press.
- van Beest, M., Mortin, M. and Clevers, H. (1998)** "*Drosophila* RpS3a, a novel *Minute* gene situated between the segment polarity genes *scubitus interruptus* and *dTCF*", *Nucleic Acids Res* **26**(19), 4471-5.
- van den Eijnden-Van Raaij, A. J., van Zoelent, E. J., van Nimmen K., Koster C.H., Snoek G.T., Durston A.J. and D., H. (1990)** "Activin-like factor from a *Xenopus laevis* cell line responsible for mesoderm induction." *Nature* **345**(6277), 732-4.
- van der Sar, A., Betist, M., de Fockert, J., Overvoorde, J., Zivkovic, D. and den Hertog, J. (2001)** "Expression of receptor protein-tyrosine phosphatase alpha, sigma and LAR during development of the zebrafish embryo", *Mech Dev* **109**(2), 423-6.
- Van Lijsebettens, M., Vanderhaeghen, R., De Block, M., Bauw, G., Villarroel, R. and Van Montagu, M. (1994)** "An S18 ribosomal protein gene copy at the *Arabidopsis* PFL locus affects plant development by its specific expression in meristems", *EMBO J* **13**(14), 3378-88.
- Varlet, I., Collignon, J. and Robertson, E. J. (1997)** "*nodal* expression in the primitive endoderm is required for specification of the anterior axis during mouse gastrulation", *Development* **124**(5), 1033-44.
- Venema, J. and Tollervey, D. (1999)** "Ribosome synthesis in *Saccharomyces cerevisiae*", *Annu Rev Genet* **33**, 261-311.
- Venter, J. C., Adams, M. D., Myers, E. W., Li, P. W., Mural, R. J., Sutton, G. G., Smith, H. O., Yandell, M., Evans, C. A., Holt, R. A., Gocayne, J. D., Amanatides, P.,**

Ballew, R. M., Huson, D. H., Wortman, J. R., Zhang, Q., Kodira, C. D., Zheng, X. H., Chen, L., Skupski, M., Subramanian, G., Thomas, P. D., Zhang, J., Gabor Miklos, G. L., Nelson, C., Broder, S., Clark, A. G., Nadeau, J., McKusick, V. A., Zinder, N., Levine, A. J., Roberts, R. J., Simon, M., Slayman, C., Hunkapiller, M., Bolanos, R., Delcher, A., Dew, I., Fasulo, D., Flanigan, M., Florea, L., Halpern, A., Hannenhalli, S., Kravitz, S., Levy, S., Mobarry, C., Reinert, K., Remington, K., Abu-Threideh, J., Beasley, E., Biddick, K., Bonazzi, V., Brandon, R., Cargill, M., Chandramouliswaran, I., Charlab, R., Chaturvedi, K., Deng, Z., Di Francesco, V., Dunn, P., Eilbeck, K., Evangelista, C., Gabrielian, A. E., Gan, W., Ge, W., Gong, F., Gu, Z., Guan, P., Heiman, T. J., Higgins, M. E., Ji, R. R., Ke, Z., Ketchum, K. A., Lai, Z., Lei, Y., Li, Z., Li, J., Liang, Y., Lin, X., Lu, F., Merkulov, G. V., Milshina, N., Moore, H. M., Naik, A. K., Narayan, V. A., Neelam, B., Nusskern, D., Rusch, D. B., Salzberg, S., Shao, W., Shue, B., Sun, J., Wang, Z., Wang, A., Wang, X., Wang, J., Wei, M., Wides, R., Xiao, C., Yan, C., Yao, A., Ye, J., Zhan, M., Zhang, W., Zhang, H., Zhao, Q., Zheng, L., Zhong, F., Zhong, W., Zhu, S., Zhao, S., Gilbert, D., Baumhueter, S., Spier, G., Carter, C., Cravchik, A., Woodage, T., Ali, F., An, H., Awe, A., Baldwin, D., Baden, H., Barnstead, M., Barrow, I., Beeson, K., Busam, D., Carver, A., Center, A., Cheng, M. L., Curry, L., Danaher, S., Davenport, L., Desilets, R., Dietz, S., Dodson, K., Doup, L., Ferriera, S., Garg, N., Gluecksmann, A., Hart, B., Haynes, J., Haynes, C., Heiner, C., Hladun, S., Hostin, D., Houck, J., Howland, T., Ibegwam, C., Johnson, J., Kalush, F., Kline, L., Koduru, S., Love, A., Mann, F., May, D., McCawley, S., McIntosh, T., McMullen, I., Moy, M., Moy, L., Murphy, B., Nelson, K., Pfannkoch, C., Pratts, E., Puri, V., Qureshi, H., Reardon, M., Rodriguez, R., Rogers, Y. H., Romblad, D., Ruhfel, B., Scott, R., Sitter, C., Smallwood, M., Stewart, E., Strong, R., Suh, E., Thomas, R., Tint, N. N., Tse, S., Vech, C., Wang, G., Wetter, J., Williams, S., Williams, M., Windsor, S., Winn-Deen, E., Wolfe, K., Zaveri, J., Zaveri, K., Abril, J. F., Guigo, R., Campbell, M. J., Sjolander, K. V., Karlak, B., Kejariwal, A., Mi, H., Lazareva, B., Hatton, T., Narechania, A., Diemer, K., Muruganujan, A., Guo, N., Sato, S., Bafna, V., Istrail, S., Lippert, R., Schwartz, R., Walenz, B., Yooseph, S., Allen, D., Basu, A., Baxendale, J., Blick, L., Caminha, M., Carnes-Stine, J., Caulk, P., Chiang, Y. H., Coyne, M., Dahlke, C., Mays, A., Dombroski, M., Donnelly, M., Ely, D., Esparham, S., Fosler, C., Gire, H., Glanowski, S., Glasser, K., Glodek, A., Gorokhov, M., Graham, K., Gropman, B., Harris, M., Heil, J., Henderson, S., Hoover, J., Jennings, D., Jordan, C., Jordan, J., Kasha, J., Kagan, L., Kraft, C., Levitsky, A., Lewis, M., Liu, X., Lopez, J., Ma, D., Majoros, W., McDaniel, J., Murphy, S., Newman, M., Nguyen, T., Nguyen, N.,

- Nodell, M., Pan, S., Peck, J., Peterson, M., Rowe, W., Sanders, R., Scott, J., Simpson, M., Smith, T., Sprague, A., Stockwell, T., Turner, R., Venter, E., Wang, M., Wen, M., Wu, D., Wu, M., Xia, A., Zandieh, A. and Zhu, X. (2001) "The sequence of the human genome", *Science* **291**(5507), 1304-51.
- Vincent, J. P. and Gerhart, J. C. (1987) "Subcortical rotation in *Xenopus* eggs: an early step in embryonic axis specification", *Dev Biol* **123**(2), 526-39.
- Vincent, J. P., Oster, G. F. and Gerhart, J. C. (1986) "Kinematics of gray crescent formation in *Xenopus* eggs: the displacement of subcortical cytoplasm relative to the egg surface", *Dev Biol* **113**(2), 484-500.
- Vintemberger, P. and Clavert, J. (1960) "Sur le determinisme de la symetrie bilaterale chez les Oiseaux. XIII. Les facteurs de l'orientation de l'embryon par rapport à l'axe de l'oeuf et la règle de von Baer, à la lumiere de nos experiences d'orientation dirigée sur l'oeuf de Poule extrait de l'uterus", *Comptes Rendus Societé de Biologie, Paris* **154**(5), 1072-6.
- Virbasius, J. V., Song, X., Pomerleau, D. P., Zhan, Y., Zhou, G. W. and Czech, M. P. (2001) "Activation of the Akt-related cytokine-independent survival kinase requires interaction of its phox domain with endosomal phosphatidylinositol 3-phosphate", *Proc Natl Acad Sci USA* **98**(23), 12908-13.
- Vittet, D., Prandini, M. H., Berthier, R., Schweitzer, A., Martin-Sisteron, H., Uzan, G. and Dejana, E. (1996) "Embryonic stem cells differentiate in vitro to endothelial cells through successive maturation steps", *Blood* **88**(9), 3424-31.
- Vogel, A. M. and Gerster, T. (1999) "Promoter activity of the zebrafish *bhikhari* retroelement requires an intact activin signaling pathway" *Mech Dev* **85**(1-2), 133-46.
- Volarevic, S., Stewart, M. J., Ledermann, B., Zilberman, F., Terracciano, L., Montini, E., Grompe, M., Kozma, S. C. and Thomas, G. (2000) "Proliferation, but not growth, blocked by conditional deletion of 40S ribosomal protein S6", *Science* **288**(5473), 2045-7.
- Vuagniaux, G., Vallet, V., Jaeger, N. F., Hummler, E. and Rossier, B. C. (2002) "Synergistic activation of ENaC by three membrane-bound channel-activating serine proteases (mCAP1, mCAP2, and mCAP3) and serum- and glucocorticoid-regulated kinase (Sgk1) in *Xenopus* Oocytes", *J Gen Physiol* **120**(2), 191-201.
- Wacker, S., Herrmann, K. and Berking, S. (1994) "The orientation of the dorsal-ventral axis of zebrafish is influenced by gravitation", *Roux's Arch Dev Biol* **203**, 281-3.
- Waddington, C. H. (1932) "Experiments on the development of chick and duck embryos, cultivated *in vitro*", *Phil Trans R Soc London (B)* **211**, 179-230.

- Wagner, C. A., Broer, A., Albers, A., Gamper, N., Lang, F. and Broer, S. (2000)** "The heterodimeric amino acid transporter 4F2hc/LAT1 is associated in *Xenopus* oocytes with a non-selective cation channel that is regulated by the serine/threonine kinase sgk-1", *J Physiol* **526 Pt 1**, 35-46.
- Wagner, C. A., Ott, M., Klingel, K., Beck, S., Melzig, J., Friedrich, B., Wild, K. N., Broer, S., Moschen, I., Albers, A., Waldegger, S., Tummler, B., Egan, M. E., Geibel, J. P., Kandolf, R. and Lang, F. (2001)** "Effects of the serine/threonine kinase SGK1 on the epithelial Na(+) channel (ENaC) and CFTR: implications for cystic fibrosis", *Cell Physiol Biochem* **11(4)**, 209-18.
- Wakamiya, M., Rivera-Perez, J. A., Baldini, A. and Behringer, R. R. (1997)** "Goosecoid and goosecoid-related genes in mouse embryogenesis", *Cold Spring Harb Symp Quant Biol* **62**, 145-9.
- Walbot, V. and Holder, N. (1987)** *Developmental Biology*, Random House Inc., New York.
- Waldegger, S., Barth, P., Forrest, J. N., Jr., Greger, R. and Lang, F. (1998)** "Cloning of *sgk* serine-threonine protein kinase from shark rectal gland - a gene induced by hypertonicity and secretagogues", *Pflugers Arch* **436(4)**, 575-80.
- Waldegger, S., Barth, P., Raber, G. and Lang, F. (1997)** "Cloning and characterization of a putative human serine/threonine protein kinase transcriptionally modified during anisotonic and isotonic alterations of cell volume", *Proc Natl Acad Sci USA* **94(9)**, 4440-5.
- Waldegger, S., Gabrysch, S., Barth, P., Fillon, S. and Lang, F. (2000)** "*h-sgk* serine-threonine protein kinase as transcriptional target of p38/MAP kinase pathway in HepG2 human hepatoma cells", *Cell Physiol Biochem* **10(4)**, 203-8.
- Waldegger, S., Klingel, K., Barth, P., Sauter, M., Rfer, M. L., Kandolf, R. and Lang, F. (1999)** "*h-sgk* Serine-Threonine Protein Kinase Gene as Transcriptional Target of Transforming Growth Factor b in Human Intestine", *Gastroenterology* **116(5)**, 1081-8.
- Waldrip, W. R., Bikoff, E. K., Hoodless, P. A., Wrana, J. L. and Robertson, E. J. (1998)** "Smad2 signaling in extraembryonic tissues determines antero-posterior polarity of the early mouse embryo", *Cell* **92(6)**, 797-808.
- Wallace, M. J., Batt, J., Fladd, C. A., Henderson, J. T., Skarnes, W. and Rotin, D. (1999)** "Neuronal defects and posterior pituitary hypoplasia in mice lacking the receptor tyrosine phosphatase PTPsigma", *Nat Genet* **21(3)**, 334-8.

- Wallingford, J. B., Fraser, S. E. and Harland, R. M. (2002)** "Convergent extension: the molecular control of polarized cell movement during embryonic development", *Dev Cell* **2**(6), 695-706.
- Wang, S., Krinks, M., Lin, K., Luyten, F. P. and Moos, M., Jr. (1997)** "Frzb, a secreted protein expressed in the Spemann organizer, binds and inhibits Wnt-8", *Cell* **88**(6), 757-66.
- Warga, R. M. and Kimmel, C. B. (1990)** "Cell movements during epiboly and gastrulation in zebrafish", *Development* **108**(4), 569-80.
- Warga, R. M. and Nusslein-Volhard, C. (1999)** "Origin and development of the zebrafish endoderm", *Development* **126**(4), 827-38.
- Warga, R. M. and Stainier, D. Y. (2002)** "The guts of endoderm formation", *Results Probl Cell Differ* **40**, 28-47.
- Warner, J. R. (2001)** "Nascent ribosomes", *Cell* **107**(2), 133-6.
- Warntges, S., Friedrich, B., Henke, G., Duranton, C., Lang, P. A., Waldegger, S., Meyermann, R., Kuhl, D., Speckmann, E. J., Obermuller, N., Witzgall, R., Mack, A. F., Wagner, H. J., Wagner, A., Broer, S. and Lang, F. (2002)** "Cerebral localization and regulation of the cell volume-sensitive serum- and glucocorticoid-dependent kinase SGK1", *Pflugers Arch* **443**(4), 617-24.
- Watson, K. L., Konrad, K. D., Woods, D. F. and Bryant, P. J. (1992)** "*Drosophila* homolog of the human S6 ribosomal protein is required for tumor suppression in the hematopoietic system", *Proc Natl Acad Sci USA* **89**(23), 11302-6.
- Weber, R. J., Pedersen, R. A., Wianny, F., Evans, M. J. and Zernicka-Goetz, M. (1999)** "Polarity of the mouse embryo is anticipated before implantation", *Development* **126**(24), 5591-8.
- Webster, M. K., Goya, L. and Firestone, G. L. (1993a)** "Immediate-early transcriptional regulation and rapid mRNA turnover of a putative serine/threonine protein kinase", *J Biol Chem* **268**(16), 11482-5.
- Webster, M. K., Goya, L., Ge, Y., Maiyar, A. C. and Firestone, G. L. (1993b)** "Characterization of *sgk*, a novel member of the serine/threonine protein kinase gene family which is transcriptionally induced by glucocorticoids and serum", *Mol Cell Biol* **13**(4), 2031-40.
- Weijers, D., Franke-van Dijk, M., Vencken, R. J., Quint, A., Hooykaas, P. and Offringa, R. (2001)** "An *Arabidopsis Minute*-like phenotype caused by a semi-dominant mutation in a RIBOSOMAL PROTEIN S5 gene", *Development* **128**(21), 4289-99.

- Weinstein, D. C. and Hemmati-Brivanlou, A.** (1999) "Neural induction", *Annu Rev Cell Dev Biol* **15**, 411-33.
- Weinstein, D. C., Ruiz i Altaba, A., Chen, W. S., Hoodless, P., Prezioso, V. R., Jessell, T. M., Darnell, J. E. Jr.** (1994) "The winged-helix transcription factor HNF-3 beta is required for notochord development in the mouse embryo" *Cell*, **78**(4), 575-88.
- Weinstein, M., Yang, X., Li, C., Xu, X., Gotay, J. and Deng, C. X.** (1998) "Failure of egg cylinder elongation and mesoderm induction in mouse embryos lacking the tumor suppressor smad2", *Proc Natl Acad Sci USA* **95**(16), 9378-83.
- Wetts, R. and Fraser, S. E.** (1989) "Slow intermixing of cells during *Xenopus* embryogenesis contributes to the consistency of the blastomere fate map", *Development* **105**(1), 9-15.
- Whitman, M.** (2001) "Nodal signaling in early vertebrate embryos: themes and variations", *Dev Cell* **1**(5), 605-17.
- Wijnholds, J., Chowdhury, K., Wehr, R. and Gruss, P.** (1995) "Segment-specific expression of the neuronatin gene during early hindbrain development", *Dev Biol* **171**(1), 73-84.
- Wiles, M.V. and Johansson, B. M.** (1999) "Embryonic stem cell development in a chemically defined medium", *Exp Cell Res* **247**(1), 241-8.
- Wilkinson, D. G., Bhatt, S. and Herrmann B. G.** (1990) "Expression pattern of the mouse *T* gene and its role in mesoderm formation" *Nature* **343**(6259), 657-9.
- Wilkinson, D. G.** (1992) Whole-mount *in situ* hybridisation of vertebrate embryos, *In Situ Hybridisation*, Wilkinson, D. G., Oxford, IRL Press, 75-83.
- Wilson, I. B., Bolton, E. and Cuttler, R. H.** (1972) "Preimplantation differentiation in the mouse egg as revealed by microinjection of vital markers", *J Embryol Exp Morphol* **27**(2), 467-9.
- Wilson, P. A. and Hemmati-Brivanlou, A.** (1995) "Induction of epidermis and inhibition of neural fate by Bmp-4", *Nature* **376**, 331-3.
- Wilson, S. I., Graziano, E., Harland, R., Jessell, T. M. and Edlund, T.** (2000) "An early requirement for FGF signalling in the acquisition of neural cell fate in the chick embryo", *Curr Biol* **10**(8), 421-9.
- Winzler, E. A., Shoemaker, D. D., Astromoff, A., Liang, H., Anderson, K., Andre, B., Bangham, R., Benito, R., Boeke, J. D., Bussey, H., Chu, A. M., Connelly, C., Davis, K., Dietrich, F., Dow, S. W., El Bakkoury, M., Foury, F., Friend, S. H., Gentalen, E., Giaever, G., Hegemann, J. H., Jones, T., Laub, M., Liao, H., Davis, R. W. and et al.**

- (1999) "Functional characterization of the *S. cerevisiae* genome by gene deletion and parallel analysis", *Science* **285**(5429), 901-6.
- Withington, S.**, Beddington, R. and Cooke, J. (2001) "Foregut endoderm is required at head process stages for anteriormost neural patterning in chick", *Development*, **128**, 309-20.
- Wittbrodt, J. and Rosa, F. M.** (1994) "Disruption of mesoderm and axis formation in fish by ectopic expression of activin variants: the role of maternal activin", *Genes Dev* **8**(12), 1448-62.
- Wolpert, L.**, Beddington, R., Brockes, J., Jessell, T., Lawrence, P. and Meyerowitz, E. (1998) Principles of Development, New York, Oxford Univ. Press Inc..
- Woo, K. and Fraser, S. E.** (1997) "Specification of the zebrafish nervous system by nonaxial signals", *Science*, **277**(5323), 254-7.
- Wool, I. G.** (1996) "Extraribosomal functions of ribosomal proteins", *Trends Biochem Sci* **21**(5), 164-5.
- Wu, X.**, Ivanova, G., Merup, M., Jansson, M., Stellan, B., Grander, D., Zabarovsky, E., Gahrton, G. and Einhorn, S. (1999) "Molecular analysis of the human chromosome 5q13.3 region in patients with hairy cell leukemia and identification of tumor suppressor gene candidates", *Genomics* **60**(2), 161-71.
- Wulff, P.**, Vallon, V., Huang, D. Y., Volkl, H., Yu, F., Richter, K., Jansen, M., Schlunz, M., Klingel, K., Loffing, J., Kauselmann, G., Bosl, M. R., Lang, F. and Kuhl, D. (2002) "Impaired renal Na(+) retention in the *sgk1*-knockout mouse", *J Clin Invest* **110**(9), 1263-8.
- Wylie, C.**, Kofron, M., Payne, C., Anderson, R., Hosobuchi, M., Joseph, E. and Heasman, J. (1996) "Maternal beta-catenin establishes a 'dorsal signal' in early *Xenopus* embryos", *Development* **122**(10), 2987-96.
- Wylie, C. C.** (1972) "The appearance and quantitation of cytoplasmic ribonucleic acid in the early chick embryo", *J Embryol Exp Morphol* **28**(2), 367-84.
- Xanthos, J. B.**, Kofron, M., Wylie, C. and Heasman, J. (2001) "Maternal VegT is the initiator of a molecular network specifying endoderm in *Xenopus laevis*", *Development* **128**(2), 167-80.
- Xu, J.**, Liu, D., Gill, G. and Songyang, Z. (2001) "Regulation of cytokine-independent survival kinase (CISK) by the Phox homology domain and phosphoinositides", *J Cell Biol* **154**(4), 699-705.

- Xu, R. H., Kim, J., Taira, M., Zhan, S., Sredni, D. and Kung, H. F. (1995)** "A dominant-negative bone morphogenetic protein 4 receptor causes neuralization in *Xenopus* ectoderm", *Biochem Biophys Res Commun* **212**, 212-9.
- Yaffe, M. B. (2002)** "How do 14-3-3 proteins work? – Gatekeeper phosphorylation and the molecular anvil hypothesis", *FEBS Letters*, 513, 53-7.
- Yamaha, E., Mizuno, T., Hasebe, Y., Takeda, H. and Yamazaki, F. (1998)** "Dorsal specification in blastoderm at the blastula stage in the goldfish, *Carassius auratus*.PG - 267-75", *Dev Growth Differ* **40**(3).
- Yamamoto, A., Amacher, S. L., Kim, S. H., Geissert, D., Kimmel, C. B. and De Robertis, E.M. (1998)** "Zebrafish paraxial *protocadherin* is a downstream target of *spadetail* involved in morphogenesis of gastrula mesoderm" *Development* **125**(17), 3389-97.
- Yamanaka, Y., Mizuno, T., Sasai, Y., Kishi, M., Takeda, H., Kim, C. H., Hibi, M. and Hirano, T. (1998)** "A novel homeobox gene, *dharm*, can induce the organizer in a non-cell-autonomous manner", *Genes Dev* **12**(15), 2345-53.
- Yamashita, H., ten Dijke, P., Huylebroeck, D., Sampath, T. K., Andries, M., Smith, J. C., Heldin, C. H. and Miyazono, K. (1995)** "Osteogenic protein-1 binds to activin type II receptors and induces certain activin-like effects", *J Cell Biol* **130**(1), 217-26.
- Yamashita S., Miyagi, C., Carmany-Rampey, A., Shimizu, T., Fujii, R., Schier, A. F., Hirano, T. (2002)** "Stat3 Controls Cell Movements during Zebrafish Gastrulation", *Dev Cell*, **2**(3), 363-75.
- Yasuo, H. and Lemaire, P. (1999)** "A two-step model for the fate determination of presumptive endodermal blastomeres in *Xenopus* embryos", *Curr Biol* **9**(16), 869-79.
- Yatskievych, T. A., Pascoe, S. and Antin, P. B. (1999)** "Expression of the homeobox gene *Hex* during early stages of chick embryo development", *Mech Dev* **80**(1), 107-9.
- Yeo, C. and Whitman, M. (2001)** "Nodal signals to Smads through Cripto-dependent and Cripto-independent mechanisms", *Mol Cell* **7**(5), 949-57.
- Yeo, C. Y., Chen, X. and Whitman, M. (1999)** "The role of FAST-1 and Smads in transcriptional regulation by activin during early *Xenopus* embryogenesis", *J Biol Chem* **274**(37), 26584-90.
- Yeo, S.Y., Little, M. H., Yamada, T., Miyashita, T., Halloran, M. C., Kuwada, J. Y., Huh, T. L., Okamoto, H. (2001)** "Overexpression of a slit homologue impairs convergent extension of the mesoderm and causes cyclopia in embryonic zebrafish" *Dev Biol*, **230**(1), 1-17.

- Ying, Q. L.,** Stavridis, M., Griffiths, D., Li, M. and Smith, A. (2003) "Conversion of embryonic stem cells into neuroectodermal precursors in adherent monoculture", *Nat Biotechnol* **21**(2), 183-6.
- Yoo, D.,** Kim, B. Y., Campo, C. K., Nance, L., King, A., Maouyo, D. and Welling, P. A. (2003) "Cell surface expression of the ROMK (Kir 1.1) channel is regulated by the aldosterone-induced kinase, SGK-1 and PKA", *J Biol Chem.* **278**(25), 23066-75.
- Yow, H. K.,** Wong, J. M., Chen, H. S., Lee, C. G., Davis, S., Steele, G. D., Jr. and Chen, L. B. (1988) "Increased mRNA expression of a laminin-binding protein in human colon carcinoma: complete sequence of a full-length cDNA encoding the protein", *Proc Natl Acad Sci USA* **85**(17), 6394-8.
- Yuge, M.,** Kobayakawa, Y., Fujisue, M. and Yamana, K. (1990) "A cytoplasmic determinant for dorsal axis formation in an early embryo of *Xenopus laevis*", *Development* **110**(4), 1051-6.
- Yun, C. C.,** Chen, Y. and Lang, F. (2002) "Glucocorticoid activation of Na(+)/H(+) exchanger isoform 3 revisited. The roles of SGK1 and NHERF2", *J Biol Chem* **277**(10), 7676-83.
- Zeng, L.,** Fagotto, F., Zhang, T., Hsu, W., Vasicek, T. J., Perry, W. L., 3rd, Lee, J. J., Tilghman, S. M., Gumbiner, B. M. and Costantini, F. (1997) "The mouse *Fused* locus encodes Axin, an inhibitor of the Wnt signaling pathway that regulates embryonic axis formation", *Cell* **90**(1), 181-92.
- Zernicka-Goetz, M.** (1998) "Fertile offspring derived from mammalian eggs lacking either animal or vegetal poles.PG - 4803-8", *Development* **125**(23).
- Zhang, B. H.,** Tang, E. D., Zhu, T., Greenberg, M. E., Vojtek, A. B. and Guan, K. L. (2001) "Serum- and glucocorticoid-inducible kinase SGK phosphorylates and negatively regulates B-Raf", *J Biol Chem* **276**(34), 31620-6.
- Zhang, J.,** Houston, D. W., King, M. L., Payne, C., Wylie, C. and Heasman, J. (1998a) "The role of maternal VegT in establishing the primary germ layers in *Xenopus* embryos", *Cell* **94**(4), 515-24.
- Zhang, J. and King, M. L.** (1996) "Xenopus VegT RNA is localized to the vegetal cortex during oogenesis and encodes a novel T-box transcription factor involved in mesodermal patterning", *Development* **122**(12), 4119-29.
- Zhang, J.,** Talbot, W. S. and Schier, A. F. (1998b) "Positional cloning identifies zebrafish one-eyed pinhead as a permissive EGF-related ligand required during gastrulation", *Cell* **92**(2), 241-51.

-
- Zhou, X., Sasaki, H., Lowe, L., Hogan, B. L. and Kuehn, M. R. (1993)** "*Nodal* is a novel TGF-beta-like gene expressed in the mouse node during gastrulation", *Nature* **361**(6412), 543-7.
- Zhu, Y., Richardson, J. A., Parada, L. F. and Graff, J. M. (1998)** "Smad3 mutant mice develop metastatic colorectal cancer", *Cell* **94**(6), 703-14.
- Zimmerman, L. B., De Jesus-Escobar, J. M. and Harland, R. M. (1996)** "The Spemann organizer signal noggin binds and inactivates bone morphogenetic protein 4", *Cell* **86**, 599-606.
- Ziomek, C. A., Johnson, M. H. and Handyside, A. H. (1982)** "The developmental potential of mouse 16-cell blastomeres", *J Exp Zool* **221**(3), 345-55.
- Zorn, A. M., Butler, K. and Gurdon, J. B. (1999)** "Anterior endomesoderm specification in *Xenopus* by Wnt/beta-catenin and TGF-beta signalling pathways", *Dev Biol* **209**(2), 282-9.

Appendices

Appendix 1 Widespread and ubiquitous mouse endoderm library clones

Table A.1 Identity of endoderm library cDNAs with widespread or ubiquitous expression

Sequence ID	Frequency	Expression	Representative ID	Description
r8224b38	1	W	ENSMUST00000001452	Tcp-1
k8220b04	1	W		Potentially novel
k8311b33	1	W		Potentially novel
r8316a43	4	W	TC451582	
t8708a52		W		
t8708a58		W		
k8417b60	4	W	ENSMUSG00000032294	Pyruvate kinase, M2 isozyme (EC 2.7.1.40)
t8219b01	1	W		Potentially novel
r8220b48	4	W	TC461859	
r8316a38	1	W	ENSMUSG00000029538	Splicing factor, arginine/serine rich 9 (25 kDa)
r8319a26	1	W		Potentially novel
r8710a01	1	W	ENSMUSG00000022400	Ring-box protein 1
m8708a53	1	W	ENSMUSG00000001424	Staphylococcal nuclease domain-containing protein 1; p100 co-activator
t8708a13		W		
m8220b33	2	W	ENSMUSG00000001416	T-complex protein 1, gamma subunit (Tcp-1-gamma)

k8225b50	1	W	ENSMUSG00000001847	Ras-related C3 Botulinum toxin substrate 1 (p21-Rac1) / Ras-like protein Tc25
m8708a04	1	W	ENSMUSG00000002812	Flightless I (<i>Drosophila</i>) homolog
k8225b28	3	W	ENSMUSG00000002835	Chromatin assembly factor 1 subunit a (Chromatin assembly factor I p150 subunit)
r8313b48	1	W	ENSMUSG000000018235	Putative transcription factor Alf-4
s8408b38	7	W	ENSMUSG000000020372	Guanine nucleotide-binding protein, beta subunit-like protein 12.3
k8710a21	2	W	ENSMUSG000000022400	Ring-box 1
s8408b20	1	W	ENSMUSG000000022570	GDP-fucose synthetase (FX protein) (Red cell NADP(H)-binding protein)
v8130b15	1	W	ENSMUSG000000023286	Ubiquitin conjugating enzyme 6
w8609b47	1	W	ENSMUSG000000024392	Large proline-rich protein Bat3 (Hla-b-associated transcript 3)
s7827b59	1	W	ENSMUSG000000024844	Barrier-to-autointegration factor (breakpoint cluster region protein 1)
r8220b44	2	W	ENSMUSG000000026726	Cubilin (fragment)
r8220b07	2	W	ENSMUSG000000027129	Hypothetical 26.3 kDa protein
r8313b19	2	W	ENSMUSG000000027170	Similar to dendritic cell protein
k8417b21	4	W	ENSMUSG000000027405	Nucleolar protein Nop56
v8130b56	2	W	ENSMUSG000000029063	Putative inorganic polyphosphate/ATP-NAD kinase (EC 2.7.1.23)
r8316a38	1	W	ENSMUSG000000029538	Splicing factor, arginine/serine rich 9 (25 kDa)
v8130b42	1	W	ENSMUSG000000031591	Acid ceramidase precursor (EC 3.5.1.23) (Acylsphingosine deacylase)
p8129b33	1	W	ENSMUSG000000031996	Amyloid-like protein 2 precursor (CDEI-box binding protein) (CDE-BP)
t8609b46	1	W	ENSMUSG000000032582	RNA binding motif protein 6

k8225b47	2	W	ENSMUSG00000034256	Forkhead box protein J1, (Hepatocyte nuclear factor 3 forkhead homolog 4)
r8220b18	3	W	ENSMUSG00000035320	Tumor necrosis factor receptor superfamily, member 19/20
t8609b35	1	W	ENSMUSG00000037149	Similar to DEAD/H (asp-glu-ala-asp/his) box polypeptide 1
t8130b25	2	W	ENSMUSG00000039231	Similar to suppressor of variegation 3-9 homolog 1
k8311b18	2	W	TC506388	Rho family GTPase RhoA; <i>Aplysia</i> Ras-related homolog A2
v8130b63	1	W	TC451697	Similarity (11%) to mouse Nedd-4 protein (EC 6.3.2.-)
t8219b23	1	W	TC501496	Similarity (26%) to thyroid hormone receptor-associated protein complex component TRAP 150 1
t8219b03	1	W	TC532000	Similarity (53%) to Poly(A) polymerase alpha (EC 2.7.7.19)
p8224a64	1	W	TC537418	Similarity (67%) to Echinoderm microtubule-associated protein-like 1
m8220b34	1	W	ENSMUSG00000016921	Splicing factor, arginine/serine rich 5 pre mRNA splicing factor srp40 family
k8224b13	2	W	ENSMUSG00000021037	c14orf3 protein family member
r8319a64	3	W	ENSMUSG00000021676	Ras GTPase activating like protein
k8710a08	1	W	ENSMUSG00000033285	WD repeat protein
t8609b43	1	W	ENSMUSG00000034673	Pre b cell leukemia transcription factor (homeobox-containing)
r8319a50	1	W	ENSMUSG00000035073	Zinc finger protein
w8609b44	1	W	ENSMUSG00000039923	80 kDa nuclear cap binding protein
r8224b43	2	W	ENSMUSG00000032361	Transcription factor-like protein, MORF-related gene
k8225b19	2	W	BB533367	

k8130b51	1	W	ENSMUSG00000022350	
t8219b05	1	W	ENSMUSG00000028863	
k8225b11	2	W	ENSMUSG00000039322	
k8220b21	1	W	ENSMUSG00000040771	
r8313b15	1	W	TC478679	
p8224a33	3	W	TC481831	
t8130b57	1	W	TC482831	
m8708a05	1	W	TC487192	
r8224b37	1	W	TC514478	
k8225b12	1	W	TC521606	
r8316a46	1	U	ENSMUSG00000001833	Septin 7 (Cdc10 protein homolog)
r8319a47	2	U	ENSMUSG00000003687	Elongation factor 1-gamma (ef-1-gamma)
k8225b31	1	U	ENSMUSG00000003759	Seta binding protein 1
k8417b28	1	U	ENSMUSG00000003779	Rab kinesin-6 (Rab 6-interacting kinesin-like protein)
s8408b07	4	U	ENSMUSG00000003814	Calreticulin precursor (crp55) (Calregulin)
t8219b06	1	U	ENSMUSG00000004897	Hepatoma-derived growth factor (HDGF)
s8130b40	1	U	ENSMUSG00000020236	Similar to cg2245 gene product
m8220b56	1	U	ENSMUSG00000021953	cDNA sequence AF134346; l-threonine 3-dehydrogenase
p8224a38	1	U	ENSMUSG00000021998	l-plastin (Lymphocyte cytosolic protein 1)
s8408b52	2	U	ENSMUSG00000024006	Similar to serine threonine protein kinase
t8609b21	1	U	ENSMUSG00000024474	Red protein (Rer protein)

v8608b25	1	U	ENSMUSG00000028438	Kinesin superfamily protein 24 (fragment)
r8220b21	1	U	ENSMUSG00000028964	DJ-1 protein; RNA-binding protein regulatory subunit
m8220b54	2	U	ENSMUSG00000029062	Cell division cycle 2 homolog (<i>S. pombe</i>)-like 2
v8130b46	1	U	ENSMUSG00000030654	Arl-6 interacting protein-1 (aip-1) (Tbx2 protein)
p8224a43	1	U	ENSMUSG00000030796	Transcriptional enhancer factor Tef-4 (embryonic TEA domain-containing factor)
t7825b20	1	U	ENSMUSG00000035078	Myotubularin-related protein 3 (fragment)
p7822b59	3	U	ENSMUSG00000040731	Eukaryotic translation initiation factor 4h (eif-4h)
k8224b04	1	U	ENSMUSG00000041059	High mobility group protein HMG-y
m8220b46	1	U	TC467769	p53-regulated Dda3
k8220b58	1	U	TC511443	Cdv-3b, Carnitine deficiency-associated protein, cdv3b
k8709a15	1	U	TC531846	Ras-related GTP-binding protein 4b
v8130b60	1	U	TC446791	Similar to Human Dj222e13.3 (novel protein)
r8223b47	1	U	TC448255	Similar (12%) to Human Kiaa0423
t8130b48		U	TC457725	Similar to putative Human prostate cancer tumor suppressor
k8225b43	1	U	ENSMUSG00000021484	Vesicular integral membrane protein, Vip36, precursor-family
t8219b14	1	U	ENSMUSG00000023010	Bax inhibitor 1 bi 1 testis enhanced gene family
r8316a20	2	U	ENSMUSG00000026965	Anaphase promoting complex subunit 2 family
k8225b03	1	U	ENSMUSG00000027828	Translocon associated protein
r8707a46	1	U	ENSMUSG00000031843	M phase phosphoprotein
k8224b30	3	U	ENSMUSG00000035618	Nuclease sensitive element binding protein 1, Y box binding protein

k8417b20	1	U	ENSMUSG00000037197	Splicing factor
m8220b58	1	U	ENSMUSG00000040914	WD repeat protein
k8311b01	1	U	ENSMUSG00000042097	Zinc finger protein
k8225b27	1	U	AL023012	
r8223b48	1	U	AL023075	
v8608b33	1	U	ENSMUSG00000000759	
k8417b15	1	U		Potentially novel
r8223b37	1	U		Potentially novel
v8608b22	1	U		Potentially novel
w8408b10	1	U	ENSMUSG00000032902	
t7821b51	1	U		Potentially novel
r8710a50		U		
t8708a28		U		
v8130b12	1	U		Potentially novel
r8220b16	1	U	ENSMUSG00000002486	
k8220b25	1	U	ENSMUSG00000020608	
p8610b17	3	U	ENSMUSG00000021486	
v8130b02	3	U	ENSMUSG00000021905	
k8130b38	2	U	ENSMUSG00000025421	
p8224a40	1	U	ENSMUSG00000031756	
v8130b61	2	U	ENSMUSG00000037278	

w8609b14	1	U	ENSMUSG00000037677
r8220b40	1	U	ENSMUSG00000039575
t8219b16	1	U	ENSMUSG00000042307
p8224a36	1	U	TC447493
t8130b60	1	U	TC456825
t8130b62	1	U	TC469437
k8225b01	1	U	TC472673
r8319a55	1	U	TC481995
k8130b43	1	U	TC497372
k8220b41	1	U	TC497498
r8710a27	1	U	TC501233
r8313b62	2	U	ENSMUSG00000003660
r8710a06	1	X	ENSMUSG00000018581 Dynein, axon, heavy chain 11; <i>situs inversus</i> viscerum
v8130b28		X	ENSMUSG00000042720 Reduced expression 3
m8220b60	1	X	TC473104
k8220b27	1	X	TC526797
k8220b28	1	X	TC522924

cDNAs are categorised according to their expression patterns: Widespread (W), Ubiquitous (U) and not detected (X). Within each of these categories, cDNA clones are further grouped as: known genes', similar to known genes, containing known protein domains, and not annotated. Headings represent (i) the sequence identification number; (ii) the number of times the sequence was isolated; (iii) the ENSEMBL gene number of the cDNA or its TIGR Cluster number; (iv) gene family.

Appendix 2 Protocol for differentiation of ES cells into endothelial cells

Foreword

The endothelial-specific conditions defined in Vittet *et al.*, 1996 were combined with the protocol for ES cell differentiation into hematopoietic lineages established by Dr. G. Keller (Keller *et al.*, 1993). The resultant protocol presented here is adequate for feeder-independent ES cells and is accomplished via the formation of embryoid bodies.

Iscove's Modified Dulbecco's Medium (IMDM) is used for blood stem cell cultures. Culturing embryoid bodies (EBs) in this medium increases the frequency of appearance of blood islands relative to that obtained in the more common Dulbecco's Modified Eagle Medium (DMEM) (Doetschman *et al.*, 1985).

All FCS batches should be tested for their ability to support normal ES cell growth at clonal densities (Robertson, 1987). The selected ES Quality (ESQ) batches should then be tested for their capacity in supporting EB formation and consequent cell differentiation (ESQD). Approximately 1/4 of FCS batches support excellent hematopoietic differentiation (Wiles, 1993).

All water used must be ultrapure and sterile. Use autoclaved *Millipore* water, which can be stored at 4 °C.

Media and solutions

2x IMDM (500 ml)

Add 500 ml of water to IMDM powder provided for 1 l.

Sterilise in tissue-culture hood by filtering through 0.20 µm pore membrane.

Save 250 ml to prepare 2% methylcellulose (MC)-IMDM and aliquot the rest into 50 ml aliquots. Store aliquots at – 20 °C.

Used for preparing 2 % MC-IMDM and IMDM ES.

IMDM ES (100 ml)

50 ml 2x IMDM

35 ml water

0.3024 g NaHCO₃

12.4 µl fresh 1/10 dilution of monothioglycerol (MTG) in water (MTG is very viscous so pipette at least 100 µl)

Sterilise in tissue-culture hood by filtering through 0.20 µm pore membrane and add LIF so that final concentration is 10³ U/ml, and 15 ml ESQ.

Used for last ES cell passage prior to differentiation.

IMDM (100 ml)

Similar to IMDM ES except, importantly, with no LIF.

Used for washing and counting cells prior to differentiation as well as for medium change prior to seeding in differentiation medium.

2% MC-IMDM (500 ml)

Weigh autoclaved *Schott* bottle containing magnetic stirrer.

Rinse with water to remove any residual detergent.

Add 235 ml water and boil on hotplate for 5-10 min.

Slowly add 10 g MC while stirring.

Let it come to a boil 3 times without letting it boil over. Swirl vigorously between boils until no lumps are found in the slurry.

Sterilise by boiling another 10-12 min. Meanwhile prepare fresh 2x IMDM.

To 250 ml fresh 2x IMDM add 3.024 g NaHCO₃ and 124 µl fresh 1/10 MTG in water.

Sterilise in tissue-culture hood by filtering through 0.20 µm pore membrane and aliquot into 50 ml aliquots. If stored at 4 °C, aliquots can be used for at least 1 month; if stored at -20 °C, aliquots can be used for longer.

Allow slurry to cool below 40 °C and add 250 ml of 2x IMDM.

Stir rapidly for a few min in order to mix and remove any lumps. At this stage the medium will still appear cloudy and moderately thin.

Weigh everything again. Weight of media should be very close to 500 g; adjust it to 500 g with water.

Leave medium at 4 °C O/N.

Remove 1-2 ml of medium and incubate at 37 °C for several days to check for

contamination, and aliquot the rest into a maximum of 13.5 ml / 50 ml tube (volume adequate for 12 cultures of 1 ml each). This stock solution is extremely thick so use a syringe fitted with a 16 or 18-G blunt-ended needle for all its manipulations.

Store at -20 °C. Only following a freezing and thawing cycle will the medium appear as a transparent viscous liquid.

MC medium should not be refrozen. Working stocks can be maintained at 4 °C for 1 month.

Used to make MC-IMDM.

MC-IMDM – make FRESH (100 ml)

MC-IMDM is composed of 1% MC-IMDM, 15% ESQ and 450 µM MTG.

Dilute fresh 26 µl MTG / 2 ml IMDM.

Mix 42.5 ml 2% MC-IMDM, 42.5 ml 2x IMDM, 15 ml ESQD and 300 µl diluted MTG.

Used for plating ES cells for differentiation.

Differentiation factors stock solutions

Prepare 7.5% BSA carrier solution by dissolving 0.75 g BSA in 10 ml sterile PBS.

Sterilise in tissue-culture hood by filtering through 0.20 µm pore low protein binding membrane.

Reconstitute vascular endothelial growth factor (VEGF), erythropoietin (EPO), human basic FGF (hbFGF) and interleukin 6 (IL-6) lyophilates/solutions as following:

VEGF (Peprotech 100-20): Recommended stock is 100 µg/ml in water. Add 100 µl water to 10 g vial.

EPO (Roche 1 276 964): No recommended stock concentration but solvent suggested is PBS containing BSA. Add 9 ml PBS and 133.3 µl 7.5% BSA carrier solution to 500 U vial. Stock will be 50 U/ml.

hbFGF-2 (R&D 233-FB-025): Recommended stock is 10 µg/ml in PBS, 0.1 % BSA, 1 mM DTT. Add 2.5 ml sterile PBS, 33.3 µl 7.5% BSA carrier solution and 25 µl sterile 100 mM DTT to 25 µg vial. Can be stored at 4 °C for 1 month or at -70 °C to -20 °C for 3 months.

IL-6 (R&D 406-ML-005): Recommended stock is 1 µg/ml in PBS, 0.1% BSA. Add 5 ml sterile PBS and 66.7 µl 7.5% BSA carrier solution to 5 µg vial. Can be stored at 4 °C for 1 month or at -70 °C to -20 °C for 3 months.

Aliquot all stocks and store at -20 °C. Avoid repeated freeze-thawing of stocks.

Used to supplement MC-IMCM in order to make Endothelial Differentiation medium.

Endothelial Differentiation medium

MC-IMDM supplemented with the following angiogenic growth factors:

50 ng/ml VEGF \Rightarrow Dilute stock 2000x \Rightarrow 40 μ l stock / 80 ml medium

2 U/ml EPO \Rightarrow Dilute stock 25x \Rightarrow 3.2 ml stock / 80 ml medium

100 ng/ml hbFGF-2 \Rightarrow Dilute stock 100x \Rightarrow 800 μ l stock / 80 ml medium

10 ng/ml IL-6 \Rightarrow Dilute stock 100x \Rightarrow 800 μ l stock / 80 ml medium

Add factors to MC-IMDM, vortex vigorously, spin down quickly and allow 10-15 min for air bubbles to dissipate.

Trypsin/EDTA

0.25% Trypsin, 1 mM Na₂EDTA in PBS (pH 7.5)

Testing ESQ capacity to support EB differentiation

Seed ES cells in MC-IMDM. The criteria for assessing desirable ESQ promotion of EB differentiation are:

- 1) EBs should be observed after 3 days;
- 2) After 10 days, at least 40% of EBs should show overt globinisation, meaning they will be distinctly red.

Differentiation parameters decline after approximately Day 11 (blood cell parameters do so earlier than those of endothelial cells) (Wang *et al.*, 1992).

Protocol for differentiating ES into endothelial cells

Day -2

Two days prior to differentiation initiation, split ES cells into IMDM ES medium. This one passage into IMDM prior to differentiation should greatly enhance the efficiency of the subsequent differentiation. Plate 2 dilutions (for example, 1/10 and 1/20), aiming for 25 – 50 % confluence in 2 days.

ES cells grow much faster in IMDM as compared to DMEM. Make sure they are in good condition before starting the differentiation: few or no dead cells, media should

not be too acidic, few if any differentiated cells.

Day 0

Remove old medium with suction pump and replace it with new IMDM.

Incubate cells in new medium for for 1-3 h (this medium change prior to change into differentiation medium enhances the consistency of results).

Remove medium and wash cells once with 1.5 ml of Trypsin/EDTA.

Remove this Trypsin/EDTA and add an additional 1 ml of new Trypsin/EDTA. Make sure it covers the bottom of the flask and let it act for 5 min at RT (or 37 °C).

Confirm under the microscope that a single-cell suspension is obtained.

Add 10 ml of IMDM and transfer the cell suspension to a 14 ml screw cap tube.

Spin at 150 x g for 5 min at 4 °C and wash cells twice in IMDM:

Carefully remove supernatant with suction pump and resuspend cells in 1 ml of IMDM.

Add 5 ml more of IMDM and spin again.

Repeat the wash and resuspend the cells in 1.0 ml of IMDM.

Count cells in a hemocytometer and determine their viability, which should be greater than 95%:

Dilute cells 5x by mixing 160 µl Trypan Blue with 40 µl cell suspension, vortex and count (around 200 cells should be counted for a statistically accurate determination of cell concentration): $\text{no. cells / ml} = \text{average no. of cells / square} \times 5 \times 10^4$.

Prepare at least 1.2 times the desired amount of Differentiation Medium:

2 ml medium is used / 35-mm dish; the no. dishes / experiment is 2 x 15 (duplicates for 15 days) = 30. Prepare 80 ml.

To a 50 ml tube add 1.2 times the number of cells necessary to obtain the desired final concentration for all dishes (1.25 or 2.5×10^3 cells / dish). The desired result is 50 – 100 EBs / dish. As a first step it may be necessary to perform a dose curve to determine the optimal number of cells required: score the number of EBs obtained, which should be directly proportional to the number of cells plated.

Using a syringe fitted with a blunt-ended 16-G needle, add the Differentiation Medium to the cells, vortex vigorously, spin down quickly and allow 10 - 15 min for air bubbles to dissipate. It is important to add the cells first.

Plate cells in 35-mm bacterial grade petri dishes: 2 ml / dish. Swirl dish gently to ensure that the suspension is evenly distributed on the bottom of the dish without touching the lid.

Place the dishes in a clean plastic box together with a 35-mm dish containing autoclaved water and incubate without further feeding for the time required (3 - 11 days) at 37 °C, 5 % CO₂.

Days 1 – 11

Collect the EB-containing medium from culture dishes into 15 ml Falcon tubes.

Wash dish with 1 ml of PBS and add this to the tube to ensure all EBs are collected.

Mix and let EBs settle for 10 - 15 min.

Carefully remove supernatant and proceed to next analysis (for example, quick-freeze and store at – 80 °C for subsequent RNA purification).





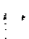
References

- Doetschman, T. C., Eistetter, H., Katz, M., Schmidt, W. and Kemler, R. (1985) "The *in vitro* development of blastocyst-derived embryonic stem cell lines: formation of visceral yolk sac, blood islands and myocardium", *J Embryol Exp Morphol* **87**, 27-45.
- Keller, G., Kennedy, M., Papayannopoulou, T. and Wiles, M. V. (1993) "Hematopoietic commitment during embryonic stem cell differentiation in culture", *Mol Cell Biol* **13**(1), 473-86.
- Robertson, E. J. (1987), Teratocarcinomas and Embryonic Stem Cells: A Practical Approach, Robertson, E. J., Oxford and Washington D.C., IRL Press, p. 71.
- Vittet, D., Prandini, M. H., Berthier, R., Schweitzer, A., Martin-Sisteron, H., Uzan, G. and Dejana, E. (1996) "Embryonic stem cells differentiate *in vitro* to endothelial cells through successive maturation steps", *Blood* **88**(9), 3424-31.
- Wang, R., Clark, R. and Bautch, V. L. (1992) "Embryonic stem cell-derived cystic embryoid bodies form vascular channels: an *in vitro* model of blood vessel development", *Development* **114**(2), 303-16.
- Wiles, M. V. (1993) "Embryonic stem cell differentiation *in vitro*", *Methods Enzymol* **225**, 900-18.
- Wilkinson, D. G., Bhatt, S. and Herrmann, B. G. (1990) "Expression pattern of the mouse T gene and its role in mesoderm formation", *Nature*, **343**, 657-9.

Appendix 3 cDNA and protein sequences of zebrafish orthologues of selected restricted mouse endoderm genes

When possible, full-length sequence of the zebrafish cDNA was assembled *in silico* through EST alignment, my own sequencing of the insert of ordered ESTs and/or 5' RACE sequence. Sequences thus assembled are surely expressed. However, in some cases, expressed sequence was complemented by genomic sequence in an attempt to assemble the complete cDNA and protein sequences.

The ORF is indicated on each of the cDNAs, as well as the region of the mRNA targeted by a MO, used for functional analysis of the corresponding proteins in zebrafish embryonic development. Only cDNAs not available in the public databases are shown. Incomplete cDNA sequences obtained for zebrafish *sp120 b*, *plu1 a* and *b*, *rho GEF 16* and *liv-1*-related are not shown. In the cases where 5' RACE was used to obtain 5' sequence, the region where RACE was initiated is also indicated. Protein sequences were obtained by translating the assembled cDNAs. The following code was used to highlight the relevant regions on the sequences presented:

-  ORF outline
-  MO target sequence
-  5' RACE primers (shown in sense strand)
-  Identical amino acid residues
-  Similar amino acid residues

Zebrafish *sgk-1* cDNA a

MO1 | MO2

GCGGTCGGTCCGGATTCCCGGGATGTTTTGGTCTCGGGCCAGAGTGGAAAACACTACAGCCAT
 GACAATCCAAACGGAGACGAGCGTTTCAGCTCCAGACTTGACCTACTCTAAAACAAGAGGA
 CTAGTAGCTAATCTGAGTGCTTTTTATGAAGCAGAGAAAGATGGGACTGAATGACTTCATCCA
 GAAGCTTTCTGCAAACCTCCTATGCATGCAAGCATCCTGAGGTTGAGTCCATCCTAAACCTGA
 CACCACCACAAGATGTGGAGCTAATGAACAGCAACCCTTCCCCTCCGCCAAGTCCCTCTCAG
 CAGATCAACCTCGGCCCTTCTCAAACCCACCGCCAAACCATCAGACTTCGACTTTCTGAA
 AGTCATCGGAAAGGGTAGCTTCGGCAAGGTTCTCCTGGCACGMCACCGGAGCGATGAGAAG
 TTTTATGCTGTGAAGGTGCTTCAGAAGAAAGCCATCTTAAAGAAAAAAGAGGAGAAACACA
 TTATGTCAGAGCGCAAYGTGTTACTGAAGAATGTCAAGCATCCATTCCTTGTGGCCTGCAT
 TACTCTTCCAGACCACTGATAAACTCTACTTCGACTGGACTACATCAATGGAGGAGAGCT
 GTTTTATCACTTGCAAAGAGAGCGATGCTTTCTGGAGCCGCGCGCTCGCTTCTATGCAGCAG
 AGATTGCCAGTGCTTTGGGTTACCTGCATTCCTGAAACATCGTCTATCGAGACCTGAAGCCC
 GAGAACATTCTGCTGGATTCTCAAGGGCACATCATTTGACTGACTTTGGCCTGTGCAAAGA
 GAACATCGAGCCCAATGGAACGACGTCAACCTTCTGTGGGACGCCAGAGTATTTGGCACCG
 GAGGTGTTACACAAGCAGCCGTATGACCGAACGGTGGACTGGTGGTGTGTTGGGCGCAGTGC
 TGTATGAAATGTTATATGGCCTGCCTCCGTTCTACAGTCGTAACACAGCAGAGATGTACGAT
 AACATTTTGAACAAGCCACTGCAGCTGAAACCGAACATCTCCAACGCTGCCAGACACCTGCT
 GGAGGGCCTGCTGCAAAAAGACAGAACCAAAAAGGCTGGGCTTCACTGATGACTTTACTGAA
 ATCAAGAACCACATGTTCTTCTCTCCCATCAACTGGGACGATCTGAATGCCAAGAAGCTTAC
 GCCACCATCAACCCCAATGTGACGGGGCCTAACGACTTGCACACTTTGACCCTGAGTTCA
 CCGATGAGCCAGTGCCGAATTCAATCGGCTGCTCGCCGGACAGCGCTCTGGTCACGTCCAGC
 ATCACTGAAGCGACCGAGGCTTTCCTGGGCTTCTCTTACGCCCTGCTATGGACTCCTACCTG
 TAGCCCATCCCTAGAAAACGCCATCCCATGGACTCCTACCTGTAGCTCATTACCAGGGAAA
 TGCTGTCCCATGGAATCTCACCTGTAGTGCATCACTATGAGAAAAGCAAACCCCGTCTCATT
 TCCCTGCCTCCAGATCGGGGGCATTTGCACATGGCGTACGGCAGCTCGAAAGGCCTTTATTG
 AAAGGCCTGAGTTTTACACGTTAAAGAAGAAGACTTTCCTCTTCATCCAAATGCACGATTT
 CTCCTCCGCTTTCACCCTGGGTTGTGACAGATGGGGAAAAAGAGAGAGAAGATTGATGCTG
 ATGGACGTTTATGTA TAGATTTATTTCAAAGCTTACTTGCCTTTCATTTTTTAGACATCATA
 GTTTTGGATGGATTGAATGCTTGTGTTGTGGGTGCGTGTGTGTGTATGTGCCTTCATTTAACA
 CCCCTGTTCAAATGTTTGTAGTCTAAATCATGTGATCTGGCATGTCAGTCCATGTCAGGTA
 TAAACAGTCAACGTGACACTAAAACCACTAAAATATATCAGCATCTGATGTTTTTGTGACCT
 TTCAGTTACGCATCTGGGATCAAATTTTTTGCACATTTATCTTCCTAAATTAAGAGCACTTC
 CTTAATGCTTTTTTTTTYCTTGTATGACTTGAGCAGAAGGTGCTAGAAGGATGTGCTGCT
 AATGTGTGTAGAAATGCTCACTTTAGTCTTCCAGCCTCCTTGGATGTACAGTAATCCAGAAA
 CGGGCCAGTCTGTCTCAGCAACACATTCCATTGAACAAGACTGTATGGTTATTTAAGTTTGT
 ATATTTGAGGTCTTCTGTGTTAGTTTTAATGTATATGGAACAAAACTTAAAAGGGTATGCT
 TATATGTA ACTATAAATGTA CTGTA AAAATTGTA AAAATGTTTGAATTATGTGACCTTGTGGT
 TCGCAATAAAACTTTATGGTTATTTTTCCCCTAAAAA AAAAA

Zebrafish *sgk-1* cDNA b

CGTGCCGCACCCGACAGCCTGGCATCTCAGTCCAGTAGTGCGCTTCAACAAGCGGTTTAGAA
 CGGGAGATCAGCGCGCTCTGAAGGAATACACTCCTCCTGTGGATTTAWACTTCTTAAAYAA
 GTGATGGCAGTTACTCAGGCTGGATGTGATTTGACATACTGCAAGATGAGAGGAATCGTGTG
 TGTTCTTGCCGCTTTTATTAAAGAAAGGAAGATGGGCTTGAACGACTTCATCCAAAGGCTTG
 TCTCCAACCCTCCCATCTGTCAACATGCTGATGTTGGTTCCTTTCTAAAAATTGATGAGAACC
 AGAATGAGGAAGTGGATGAGAATCTTCTGTGTTGACCCATCCTAGGAGCTCTTTGGCTGAG
 GAGACTCAGATCAAACCTCAGATTTTGACTACTTAAAGATCATCGGCAAGGGGAGCTTTGG
 GAAGGTTCTGCTTGCGCGGCACAAGGAAAACGAACTCTACTATGCTGTGAAGGTGCTTCAGA
 AGAAAATCATTATGAAAAAGAAAGAGCAAAAGCATATCATGGCAGAAAGGAGTGTACTAAT
 GAAAAATATCAAACATCCATTCCTGGTGGGTCTGCACTACTCTTTCCAAACCACAGACAAAC
 TGTATTTTCGTGCTASACTACGTCAATGGAGGCGAGCTGTTTTACCACCTCCATCGTGAGAGA
 GTGTTTTTGGAGCCCAGACCGAGGTTTTATGCTGCTGAAATCTCTAGTGCACCTGGTTACCTT
 CACTCTCTGCACATAGTTTACAGAGACTGGAAGCCAGAGAACATCCTCTTGGACTCTCAAGG
 CCACATTGTGCTGACACATTTCCGTCTATGCAAAGAGGGACTGCATCCCAACGGCTCAACCA
 CTACATTTTGTGGAACCTCTGAGTACCTAGCACCCGAAGTACTCCAGAAACAGGCCTATGAT
 CGTACAGTAGACTGGTGGTGTCTGGGATCAGTACTGTTTGAGATGCTGTATGGACTGCCTCC
 ATTCTACAGTCGCAACACAGCCGAGATGTACAACAACATTCTACACAAGCCTCTTGTCTGA
 AGCCTAATGTGTCCAATGCTGGCCGTGACCTGCTAGAGGGCTTGCTGCACAAAGACCGTACC
 AAGAGACTGGGGTCCAAGGATGATTTTTTGAATTGAAGTTTACAGCTTCTTCTCTCCCATC
 AACTGGGACGATCTCATGGCCAAAAGGATTGTGCCTCCATTGTTTCTACAGTACTGGTCC
 TACTGACCTCCGGCACTTTGATCCAGAGTTACCCACCTTCTGTGTCGACCTCTCTATGCAA
 CACCGATAACCTGCACGTGACCAGCAGCGTGCAGAAAGCAGCCGGAGCGTTCCCTGGTTTTT
 CCTACGGTCCCTCCATCTGATGCCTTCCAGTAATGGCACCTTCCAAGACACCTTCCATTCCAGC
 ATCAGTAGAAGCAATGTGACAGAAGTAGGACCACAAGACGGGACACTTAGCTCTTCCAATT
 TATTTTGATGTACGACCTCACAGCACAATGGACACTCGTGCATGTCTGAGATGAATGCGGA
 AACTGTAGGAAAGAGACTACAATAAAAACTTCCAGAAAACGTGAATTGTGTGCCAACGGA
 TGCAGAGGACCTGAGCTCATCGAAGAAAGAGCTTAGAAGTGCCTRAGAGATTATTTGTGGG
 GGAAACAAACAAGCAAATTTCTATAAACAGACAATGGTTTGCCCGAGTTATGAAGATGGC
 ACCAGCTATTGGGCGAAATGCCTTCTGTGATCGTTACATTTGATCAACTTGTCAATTGAATGAT
 GTTTTGTTAATTGTATTTTTTTCATGCATCGTTGCACAGTGAAGGTGAAGGATCAAGAAAAGT
 AAAAAATATATGGATAGTCATTAAAAAAGGGGTTGTTATGTCATCAACCCCATCACAGGA
 TACACAGGCTGTCCGACTCAAATATCAATACATTTTTAGAGCATATGTTAATATCTTCTCC
 TATTGACAAATGTTAATTTAATAACTGCATTATTTATCATTTTAGTGTGGTTTGAATGAACTC
 TTCTWAAARCTTTGTGAACGGTAGTAAGACATTAGGTTTATATTAGAAGACAAACTAGTTA
 GATAACGCAACCAAAAAGGATTTTATCTGTGACTATTTGTCTGAATCAGTAGAAGACATCCTG
 TGTTCTCCTAAAATGAATGTTTTGTCTTACAAGTACTTCTTTCTTTTCTTTTCTCCAATGC
 CAGCACTTTTACAAAATATGCCAGACACTGTGTTTCTTGAAAAGTCATGTTCTTTTGTGATA
 CAGGTAGTGAGATTGATGTATATTTATACATTGTTGTTATCTGAAGCGACTGTTGTACTG
 CAAAAACAGCATGTTGATTAGATTGTAAGTACTGAAACCATTTGCATCATGTACAGACGTTATATA
 TATAGTAGCCCGAAGGAACCGTGTCTTTATTTTGTTCAAATTGTGCCTGTTTCAGCTAATTTA

TGTATGTTGTGATACATTTCCACATGTGTCTATCATTCTGTCTGTATCATTGTGGGTTGGAC
 AGGGATATGGAATGCTGTGCAATAGAAATGATGACTTGGGTACGATGTGAACAGTTTGTTCAT
 CATTGGGACGAATGAGCGGTATCGGCTTAATGAAGGAGAGAGGTTTGGATGCCCTCATGAA
 AAGCATCCCTATTTTAACTGTAATATATTTTCATATCATTGGACCAATAATGTGCTATACGTCG
 TTCTTTAGATAACTACGAACATGGCAATATGGATAAAGTTTATTTTCTCCATTTTCGGAAGT
 CATTACATATATGGTTTTATATTTTTCCATGTATATTTATTTACATGTCACATATATTACCTC
 TAATGATCAGAGTGTTAAATTCATAGAATGATGAAATGTTGGACAATGATCTATATGAATGC
 TAATAAATATTTAATAATAAAAAA

Zebrafish 14-3-3e cDNA

TTGTTTCGCGCAGGGCCTGCCGGTGAACCTCACACTCCTCCTTTACTCCAATCGCTCACGAAAC
 ACGTCCTGCGCGCTCTCCAACATGGGTGACCGGGAGGATTTGGTGTACCAAGCCAAACTCG
 CCGAGCAGGCAGAGATATGACGAAATGGTCGACTCCATGAAGAAAGTGGCTGGGATGGA
 TGTTGAGCTAACGGTGGAGGAGAGAAACCTGCTCTCAGTGGCTTACAAGAACGTTATTGGG
 GCGAGAAGAGCATCCTGGAGGATAATCAGTAGTATTGAGCAGAAAGAGGAGAATAAGGGT
 GGAGAGGACAAACTGAAAATGATTCGGGAATACAGGCAAACGGTTGAGAATGAGTTGAAAT
 CAATCTGCAATGACATCCTTGATGTATTGGACAAGCATTTAATCCCAGCTGCAAATTCAGGA
 GAATCCAAGGTCTTCTACTACAAAATGAAGGGCGATTACCACAGGTATCTCGCTGAGTTTGC
 CACAGGAAACGACAGGAAGGAGGCTGCAGAAAACAGTTTGGTTGCTTACAAAGCTGCTAGT
 GATATTGCAATGACAGACCTTCAGCCCACACACCCTATTCGCTTGGGTCTGGCTCTTAACTTC
 TCTGTATTCTATTATGAAATCCTCAACTCTCCGGACCGTGCGTGCAGGTTGGCAAAGGCGGC
 ATTTGACGATGCTATCGCTGAACTGGACACATTGAGTGAAGAAAGCTACAAGGACTCGACG
 CTCATCATGCAATTGTTACGTGATAACCTGACACTATGGACTTCAGATATGCAGGGAGATGG
 TGAGGAACAGAATAAAGAGGGCGCTGCAAGATGTGGAGGATGAAAACCAATGAGACAACAC
 CGCCAATATGAGACTCCACCCACCCCCCTCCCCTT

Zebrafish and mouse 14-3-3ε protein alignment

M. musculus M D D R E D L V Y Q A K L A E Q A E R Y D E M V E S M K K V A G M D V E L T V E
D. rerio M G D R E D L V Y Q A K L A E Q A E R Y D E M V D S M K K V A G M D V E L T V E

M. musculus E R N L L S V A Y K N V I G A R R A S W R I I S S I E Q K E E N K G G E D K L K
D. rerio E R N L L S V A Y K N V I G A R R A S W R I I S S I E Q K E E N K G G E D K L K

M. musculus M I R E Y R Q M V E T E L K L I C C D I L D V L D K H L I P A A N T G E S K V F
D. rerio M I R E Y R Q T V E N E L K S I C N D I L D V L D K H L I P A A N S G E S K V F

M. musculus Y Y K M K G D Y H R Y L A E F A T G N D R K E A A E N S L V A Y K A A S D I A M
D. rerio Y Y K M K G D Y H R Y L A E F A T G N D R K E A A E N S L V A Y K A A S D I A M

M. musculus T E L P P T H P I R L G L A L N F S V F Y Y E I L N S P D R A C R L A K A A F D
D. rerio T D L Q P T H P I R L G L A L N F S V F Y Y E I L N S P D R A C R L A K A A F D

M. musculus D A I A E L D T L S E E S Y K D S T L I M Q L L R D N L T L W T S D M Q G D G E
D. rerio D A I A E L D T L S E E S Y K D S T L I M Q L L R D N L T L W T S D M Q G D G E

M. musculus E Q N K E A L Q D V E D E N Q
D. rerio E Q N K E A L Q D V E D E N Q

Zebrafish *gp-70/embigin* cDNA

ACTTGCATAACTATCTCCAATTGGTTAACCCTCTTCATGCCCATCCTCAAACGTTCTGTTTTA
 ATCAGAATTGCTTTCAGAAGCTCAGCAACACAGCARGAGGAGCTGAAAGCGAACACCAGTC
 CTGCTAAGTCACCAATGGCTGCAGTGAGGAGAGGCTGTCCCTGTGGACCTGCTTCACCTCAGT
 CCTCCAGTACAACACTGCAGGCAGACATGGCGAAATACATGGCTAAAACCTGTCCTGCTGCTG
 CTCTTCTGTCAGGGGATCCACGCAGATACTACAACCTTCTCCAGAGTCTGATCCTGTAGTTACA
 ACTCGGAAAGCTGCACCCAAAGGTC AAGGTCAGGTCATTATGAAGAGYTTTCAATCCTGAC
 ACCCAATATATTGAGCTCTTATGCAACCTCACCGATATACCAAACAACCCTCCATACATGA
 CTGGCTATTGGACTAAAGRTGGAAAAGAAATCGAAAACCTCTGAAGAACTATAAAAYAGAAA
 CAATGCACAGTATATCCTTAAAAAGACTTTCAGCATA CAGGCCAGAGATCTGGGAAATTATT
 CGTGTGCTTTCAGAGAAAATGATGCACGAGTGACGTTTGTGTTTACAAGTTCCTGTGATGAAG
 GACAAACGGGACAAGCCTGTGGTGAGCTACATGGAGATT CAGTTGTA CTGGTGTGTAAACT
 CAAACACATGCTCAACACCTGGAACTGGTACAAGGCTAACAACACYGAAAAGGAGCTCATC
 AATGTTACCGCGGACCCCTCTRAAGTACAAGATCCTTCTGAATGGAAATGAAACCAAACCTGAC
 AGTGCTGAATCTGACCGAGGCTCAGTCTGGAAAGTACATCTGCAGTGCTGAGTTTGACATTA
 AAGCCAGCGAGTCTCAGGTGGAGCTGAAGGTGCTGTCGTACACTGAGCCTCTCAAACCCTTC
 GTGGCCATCGTGGCTGAAGTCCTGCTGCTCGTCACGCTCATCTGTTGTGGkAGAAATGCAGC
 AAACCCAAACACAGCAGCTCTACTGCAGATGATGTGTACTCTGAACATACCAGCAAACCTCAC
 TCCATtGATtGAGAaGCAATGGAGTtGGATAACAACACAACAAGACAAAGAAAGCTGGAGCAC
 TGAGATCTCTTCTGTTTTTCAGGAGCAGCACTGAACACATTGCCTTTATAGTCTGGCTGCAATC
 ACATAATGAGCAA TAATGTTTTGCTAAACCTGTT CAGCAATATAACATATATTTACTGTATAT
 TCAATATTTACATtCTCAATATTAAGTACTGAAAGTATGAGGAATGTTTTCCAAGCCTCCAGT

ATAGTGTACTGAGATCAGTTCAAGTCTGACATTTTTCTGTTTCAGTCACATGTTTATTTTAA
 TCATTGAATTCTCATGCATATTTATTTTATTCTAATGGAGAAGCTGTCTAAAATACCCTTG
 TAAGTGCTTCTTTTATCACTCTTTATTAATCTGTGTTAATGTAATCAAGACACTGCAGAGTAT
 AATAAAATATATTATTACATTAATAAAAA

Zebrafish and mouse Gp-70 / Embigin protein alignment

M. musculus M R S H T G L R A L V A P G Y P L L L L C L L A A T R P D P A E G D P T D P T F
D. rerio M A A V R R G C P C G P A S P Q S S S T T L Q A D M A K Y M A K T V L L L L F

M. musculus T S L P V R E E M M A K Y S N L S L K S C N I S V T E K S N V S V E E N V I L E
D. rerio C Q G I H A D T T T S P E S D P V V T T R K A A P K G Q G Q V I I E E X X I L T

M. musculus K P S H V E L K C V Y T A T K D L N - L M N V T W K K D D E P L E T T G D F N T
D. rerio - P Q Y I E L L C N L T D I P N N P P Y M T G Y W T K X G K E I E N S - - E E T

M. musculus T K M G N T L T S Q Y R F I V F N S K Q L G K Y S C V F G E K E L R G T F N I H
D. rerio I N R N N A Q Y I L K K T F S I Q A R D L G N Y S C V F R E N D A R V T F V L Q

M. musculus V P Q S S W E K - K S L I A Y V G D S T V L K C V C Q D C L P L N W T W Y M G N
D. rerio V P V M K D K R D K P V V S Y I G D S V V L V C K L K H - M P N T W N W Y K A N

M. musculus E T A Q V P I D A H S N E K Y I I N G S H A N E T R L K I K H L L E E D G G S Y
D. rerio N T E K E L I N V T A D P L K Y K I L L N G N E T K L T V L N L T E A Q S G K Y

M. musculus W C R A T F Q L G E S E E Q N E L V V L S F L V P L K P F L A I L A E V I L L V
D. rerio I C S A E F D I K A S E S Q V E L K V L S Y T E P L K P F V A I V A E V L L L V

M. musculus A I I L L C - - - - - - - - - - E V Y - T H K K K N G P D A G K E F E Q
D. rerio T L I C L W X K C S K P K H S S S T A D D V Y S E H T S K L T P L I E K Q W S W

M. musculus I E Q L K S D D S N G I E N N V P R Y R K T D S A D Q
D. rerio I T T Q Q D K E S W S T E I S S V F R S S T E H I A F I V W L Q S H N E Q

Zebrafish *lzf-1* cDNA

CGAGCCTGTTGGCCTCTGGACGTTAGTGTGTCGGCTCCTCCCTAGACGTCTATGGCTTATACA
 CAGCAGCTWGAAGAAATGTTGTGGAATTGTTATTAACGTACATTTTCATAATATTATTTTCAGT
 TTTATAATATCAGCGAGTTAAAATTGAAAAATTACGACTGMWATTATGCGATTGGATTATTG
 CAAACCGTAGCARATGATAAATACACTTGTGGTAACGTTAGGTCGTCAGATTTAAAGGTAM
 CGCTAAGATTGTAAACACTAATCTTTWAGKCAATATGATTTAGAATCTTGATGATCCCGAAG
 CAAATCAAACGTCTAGAAAACATGGAAGTACATTAATATTCGTCGTAAACCTGGCTCITTAG
 TAGGACAAAGCCACCTCGGATGTAAATTGAAATGTCATGGTTTCCTGGAGCCATGTCTTGTA
 GTCTAAAGTGGCTCCCAGTGTGGATTTTGACCACAGCTGCTCTGACAGTGTGAATATCTAA
 CACTCAACTTCGGGCCTTTTCGAGACTGTCCACCGCTGGAGAAGGCTGCCGCCGTGCGATGAG
 TTTGTGGGTGCAAGGCGTAGCAAGCATACCGTTGTGGCATAACAGGGATGCCATATATGTCTT
 TGGAGGAGACAATGGCAAGAACATGCTTAATGACCTGTTGCGGTTTGACGTGAAGGATTGCT
 CATGGTGTGCGGCGTTTACTACTGGCACCCACCAGCGCCGAGATATCACCACTCTGCWGT
 GTGTATGGAAGCAGCATGTTTGTGTTTGGTGGCTACACTGGAGACATCTATTCAAACCTCTAA
 CTTAAAAACAAGAACGACCTTTTTGAGTACAAGTTGCCACCGGACAGTGGACAGAATGG
 AAAGTGAAGGACGTTTGGTAGCCAGATCAGCTCATGGAGCCACGGTTTACAATGACAAAC
 TCTGGATTTTGTGCTGGATATGATGGAAATGCCAGGCTGAATGATATGTGGACCATCGGTCTT
 CAGGATCGTGAACAGGCATATTGGGAAGAGATTGAACAAAGTGGTGAAATCCCACCCTCT
 GTTGTAACCTCCCAGTAGCCGTATGCTGGGATAAGATGYTTGTCTTCTCCGGCCAAAGTGGA
 GCCAAGATTACCAACAACCTGTTTCAGTTTGAATTCAAAGGCCACATATGGACACGTATCCC
 GACAGAGCACCTGCTGCGTGGCTCACCTCCACCCCTCAAAGACGCTACGGACACACTATGG
 TGGCGTTTGACCGTCACCTGTATGTGTTTGGAGGGGCAGCAGACAACACTCTGCCCAATGAA
 CTGCACTGCTACGACGTAGACTCGCAGACATGGGAGGTCATCCAGCCCAGCACAGACAGCG
 AGATGCCAAGTGGAAAGCTGTTCCATGCAGCAGCTGTTATCCACGATGCCATGTACATCTTT
 GGAGGAACAGTTGACAATAATGTACGCAGTGGAGAAATGTACAGATTCCAGTTTTCTTGTTA
 TCCAAAGTGCACCCTTCATGAGGACTATGGCAAACCTGTGGGAGAACCGTCAGTTCTGTGATG
 TCGAGTTTATCTTGGGGGAGAGGGAGGAGAAGGTCCTGGGTCATATTGCCATAGTAACGGCT
 CGCTGTAAGTGGCTCCGTAAGAAGATTCTACAAGCAAGAGATAGACAGAAACAGAAGAGTA
 AACTGGAATGTAATGAGGARAGTGATGAGTCTGGTTCAGGCAGTCAGAAGGACTGCTCTGG
 AAGGTCCTCAAGGGTCCCTCTTTATTAGAAGTGTCAATCAGAGAAGCAGACGCTCAACCAT
 TTGAGGTTTTGATGCAGTTTCTGTACACAGACAAGATACAGTACCCACGTAGAGGTCATGTC
 CAGGATGTGCTGTTGATAATGGACGTTTATAAACTTGCTCTGAGTTTTAACTGTCCAGACTG
 GAGCAGCTCTGGGTCAGTACATTTAAGGCTGAGTGGATCTGCAGAACGTCCTGAGTGTGTG
 TGAATAATGCAGACAAACTTCAGCTGGACCAGCTCAAGGAACATTGTCTGAACTTCGTGGTGA
 AGGAAAGTCACTTTAACCAGGTGATCATGACTAAAGAGTTTGAACACCTGTCCACTCCGCTC
 ATTGTGGAGATCGTGAGACGCAAACAGCAGCCACCTCCCAGAGTCTATTTCAGATCAGCCGGT
 GGACATAGGCACATCTCTGGTGCAGGACATGAAGGCTTATCTGGAAGGGGCGGGGCATGAG
 TTCTGTGACATCATCTTTTGTAGATGGTTCATCCACGTCCTGCTCATAAGGCCATACTGGCT
 GCTCGCTCCAGTTATTTGAGGCCATGTTTCGCTCCTTCATGCCAGAGGATGGGCAGGTGAA
 CATTTCTATAGGAGAGATGGTTCCTAGTACACAGGCCTTTGAGTCCATGCTGCGYTACATTT

ACTATGGGGACGTCGACATGCCTCCAGAGGACTCACTATACCTCTTTGCTGCACCTTATTACT
ATGGTTTCTCCAACAACAGACTGCAGGCTTACTGCAAGCAAAATCTGGAGATGAACGTTACT
GTAGAGAATGTCTTGCAGATCTTGGAAAGCGGCTGATAAACTCAAGCTCTGGACATGAAGA
AACACTGCCTGCATATTATAGTGCATCAGTTCACCAAGGTTTCCAAGCTCCCCAACCTGCGA
TCGCTCAGCCAACCGCTGCTGTTGGACATCATTGACTCGCTGGCATCCACATATCAGACAA
ACAGTGCCTGAGATGAGCTCTGATATTAGACTCTCCTTCCCTTTCACGTCCCATCCTATCT
TTTATGAGCTTTTTCTTAATTTATGCTTCCACTCCATATCCTTCCCTTTTCATCCAGCACCTCC
TCCCAACCTATTTAATCCTGCTYCACACCCGTCTACAATGAGATTGAGTCTACAATGAGATTR
AGTCATCACTAGATTTTATTTACCCAATTGTTTGTA AAAAATGCTGCTTGTACATTTTAATGA
AGCTTCGATTTGTTGCATTTGCAGATAGTTTTGCGTACATCAAATCACTTGACGGCCTAAGTA
TAATTAGGCATGTGTCCCAGACGTAATGAAAAGTGGTGT TTTCAAAGCTTTTCATATAAAAAAC
CCAAAGAAAACAATTGATGTAGTGCAGCTCTTCTGTATATATAATCTATTCCACTTTTGTGCTT
AACTAAAAGCATTGCAACAAC TAGTACAAATATGATCATCCAACATCTATAAATAACTTTTT
TTTTACTCTACATACATTAATAAGAAATATCAAATATTGATTTYGGCGATTTAAAAAATGACCTG
GACGTGACTTTCTGCACTTTACGAATACATCAGTAAATATTTATACCTGAACCGTAGTGACTC
TATGCTGCTGTTGTTATCCTGATTTATGTCAGTGT TTTGCCATTATGTAATAATATAGTTATATG
AGCAGATAATCACAGCAACAGTCAATGTTAAGACTCGTGTATGCTTTACTGTAATTGTTGAG
CAGTGTTCGTGGCCCTGTGGGCACTATGCCTTAATAAACTGTCCACCATCAAAAAAAAAAA
AAAAAAAAAAAAAAAAAAAAAAAAAAGGGCGGCCGCTCTAGAGTATCCCTCGAGGGGCCCAA
GCTTACGCGTACCCAGCTTTTCTTGTACGAAGTGGTCCCTATAGGAG

Zebrafish and mouse Lztr-1 protein alignment

M. musculus M A G S G G P I G S G A L T G G V R S K V A P S V D F D H S C S D S V E Y L T L
D. rerio M S W F P G - - - - - A M S C K S K V A P S V D F D H S C S D S V E Y L T L

M. musculus N F G P P F E T V H R W R R L P P C D E F V G A R R S K H T V V A Y K D A I Y V F
D. rerio N F G P P F E T V H R W R R L P P C D E F V G A R R S K H T V V A Y R D A I Y V F

M. musculus G G D G K T L L N L L R F D V K C S W C R A T T G T P P A P R Y H H S A
D. rerio G G D N G K N M L N D L L R F D V K D C S W C R A F T T G T P P A P R Y H H S A

M. musculus V V Y G S S M F V F G G Y T G D I Y S N S N L K N K N D L F E Y K F A T G Q W T
D. rerio V V Y G S S M F V F G G Y T G D I Y S N S N L K N K N D L F E Y K F A T G Q W T

M. musculus E W K I E G R L P V A R S A H G A T V Y S D K L W I F A G Y D G N A R L N D M W
D. rerio E W K V E G R L - V A R S A H G A T V Y N D K L W I F A G Y D G N A R L N D M W

M. musculus T I G L Q D R E L T C W E E V A Q S G E I P P S C C N F P V A V C R D K M F V F
D. rerio T I G L Q D R E Q A Y W E E I E Q S G E I P P S C C N F P V A V C W D K M X V F

M. musculus I I Q S G A K I T N N L F Q F F F D K T W T R I P T E H L L R G S P P P P Q R
D. rerio S G Q S G A K I T N N L F Q F E F K G H I W T R I P T E H L L R G S P P P P Q R

M. musculus R Y G H T M V A F D R H L Y V F G G A A D N T L P N E L H C Y D V D F Q T W E V
D. rerio R Y G H T M V A F D R H L Y V F G G A A D N T L P N E L H C Y D V D S Q T W E V

M. musculus V Q P S S D S E V G G A E M P E R A S S S E D A S T L T S E E R S S F K K S R D
D. rerio I Q P S T D S - - - - -

M. musculus V F G L D F G T T S A K Q P V H L A S E L P S G R L F H A A A V I S D A M Y I F
D. rerio - - - - - E M P S G R L F H A A A V I H D A M Y I F

M. musculus G G T V D N N I R S G E M Y R F Q F S C Y P K C T L H E D Y G R L W E G R Q F C
D. rerio G G T V D N N V R S G E M Y R F Q F S C Y P K C T L H E D Y G K L W E N R Q F C

M. musculus D V E F V L G E K E E C V Q G H V A I V T A R S R W L R R K I V Q A Q E W L A Q
D. rerio D V E F I L G E R E E K V L G H I A I V T A R C K W L R K K I L Q A R D R Q K Q

M. musculus K L E E D G A L A P K E A P G - - - P A V G R A R - - P P L L R V A I R E A E
D. rerio K S K L E C N E E S D E S G S G S Q K D C S G R S S R G P P L L E V S I R E A D

M. musculus A R P F E V L M Q F L Y T D K I K Y P R K H V E D V L L I M D V Y K L A L S F
D. rerio A Q P F E V L M Q F L Y T D K I Q Y P R R G H V Q D V L L I M D V Y K L A L S F

M. musculus Q L C R L E Q L C R Q Y I E A S V D L Q N V L V V C E S A A R L Q L G Q L K E H
D. rerio K L S R L E Q L C V Q Y I E A S V D L Q N V L S V C E N A D K L Q L D Q L K E H

M. musculus C L N F I V K E S H F N Q V I M M L E F F R L S S P L I V E I V R R K Q Q P P P
D. rerio C L N F V V K E S H F N Q V I M T K E F E H L S T P L I V E I V R R K Q Q P P P

M. musculus R T P S D Q P V D I G T S L I Q D M K A Y L E G A G S E F C D I T L L L D G Q P
D. rerio R V Y S D Q P V D I G T S L V Q D M K A Y L E A G H E F C D I I L L L D G H P

M. musculus R P A H K A I L A A R S S Y F E A M F R S F M P E D G Q V N I S I G E M V P S R
D. rerio R P A H K A I L A A R S S Y F E A M F R S F M P E D G Q V N I S I G E M V P S T

M. musculus Q A F E S M L R Y I Y Y G E V N M P P E D S L Y L F A A P Y Y Y G F Y N N R L Q
D. rerio Q A F E S M L R Y I Y Y G D V D M P P E D S L Y L F A A P Y Y Y G S N N R L Q

M. musculus A Y C K Q N L E M N V T V Q N V L Q I L E A A D K T Q A L D M K R H C L H I I V
D. rerio A Y C K Q N L E M N V T V E N V L Q I L E A A D K T Q A L D M K K H C L H I I V

M. musculus H Q F T K V S K L P T L R L L S Q Q L L L D I I D S L A S H I S D K Q C A E L G
D. rerio H Q F T K V S K L P N L R S L S Q P L L L D I I D S L A S H I S D K Q C T E M S

M. musculus A D I
D. rerio S D I

Zebrafish claudin b cDNA

```

CCACCAACCAACCAACAAGGAAAACGAAAAAGCATGGCATCAACCGGCCTACAGATGCTGG
GCATCGCCCTGGCCATCTTTGGGTGGATCGGAGTCATTGTGCTCTGCGCACTCCCCATGTGG
AAAGTCACAGCCTTCATCGGCGCCAACATTGTCACTTCACAGACATCCTGGGAAGGAATTTG
GATGAGCTGCGTGGTTCAAAGCACCGGACAGATGCAGTGTAAGGTCTACGACTCCATGCTG
GCTCTCCTCAGATATTC AAGCCGCTCGAGCTCTCACCGTCATCTCCATCGTGATCGGAGTC
ATGGGAATCATGCTGTCGATGGCTGGTGGAAAATGCACCAACTGCATCGAGGAGGAGAGCT
CCAAAGCCAAGGTTGGGATCACGGCAGGTGTGATTTTCATCATCTCTGGGGTGCTATGTCTG
GTCCCGGTGTGCTGGACGGCTAACGCTATCATCCAGGACTTCTACAACCCGCTAGTGGTCCA
GGCACAGAAGAGGGAGATTGGAGCGTCACTGTACATCGGCTGGGGTGCCTCAGCTCTGTTG
ATCATTGGTGGAAGTCTGCTCTGTTGCCACTGCCCGAAAAATCAGACAGCGGAAAATACAC
AGCTAAATACAACGCAACCCCTCGCTCTGAAGCCTCTGCACCCTCCGGAAAGAAGCTTTGTGT
AAATGATCAACTCAGGAAAATGGACTCTACAATGTTTACGGTCTTAGTTTGTGGACATTGA
GGCTCAAAATGAGTTTGCAGGACTTGAAAAGCAGATGCTGAATGTTTTTTTTTTTTTTTTTTT
TTACCAATATATATGCAAAACAAACAAAGAAAATGGGGAACCACGTTTGAAACAGCCTCTG
CAGTTAAAGGAGGTTAACCTGAAAATTATTTTTGCTTAAGTTTGGTCAAATGTTCTTTTGTAC
CGTGGTCATTATAAAAGTGTTCACTTTTGTATGTTTTCAAGTATGATTTTGTAAATATTAGCA
TTTTTGTACAGCCTAAGTACAGTTTTTCTACAACTTTGTACAGTTTTATTTCTTGATATATGT
TTAAAGGAATTAATAAATAAATACATTTTGTAAATATC

```

Zebrafish Claudin b and Claudin-like, and mouse Claudin-6 protein alignment

```

M. musculus Claudin-6 M A S T G L Q I L G I V L T L L G W V N A L V S C A L P M W K V T A F I G N S I
D. rerio Claudin b M A S T G L Q M L G I A L A I F G W I G V I V L C A L P M W K V T A F I G A N I
D. rerio Claudin-like M S T G L Q L L G T T L G T L G W L G I I I S C A I P L W R V T A F I G N N I

```

```

M. musculus Claudin-6 V V A Q M V W E G L W M S C V V Q S T G Q M Q C K V Y D S L L A L P Q D L Q A A
D. rerio Claudin b V T S Q T S W E G I W M S C V V Q S T G Q M Q C K V Y D S M L A L S S D I Q A A
D. rerio Claudin-like V T A Q T M W E G L W M S C V V Q S T G Q M Q C K V Y D S M L A L A Q D L Q A S

```

```

M. musculus Claudin-6 R A L C V V T L L I V L L G L L V Y L A G A K C T T C V E D R N S K S R L V L I
D. rerio Claudin b R A L T V I S I V I G V M G I M L S M A G G K C T N C I E E E S S K A K V G I T
D. rerio Claudin-like R A I L V I S A I V G L I A M F A S F A G G K C T N C L A D N S A K A L V A T T

```

```

M. musculus Claudin-6 S G I I F V I S G V L T L I P V C W T A H S I I Q D F Y N P L V A D A Q K R E L
D. rerio Claudin b A G V I F I I S G V L C L V P V C W T A N A I I Q D F Y N P L V V Q A Q K R E I
D. rerio Claudin-like G G V A F I I A G I L G L V P P S W T A N T I I R D F Y N P L V A E A Q K R E F

```

```

M. musculus Claudin-6 G A S L Y L G W A A S G L L L L G G G L L C C A C S S G G T Q G P R H Y M A C Y
D. rerio Claudin b G A S L Y I G W G A S A L L I I G G S L L C C H C P E K S D S G - K Y T X K Y N
D. rerio Claudin-like G A A I F I C W G A A V L L V I G G G L L C S S Y P K G R T S S - - - R - G R Y

```

```

M. musculus Claudin-6 S T S V P H S R G P S E Y P T K N Y V
D. rerio Claudin b A T P R S E A S A P S - - - G K N F V
D. rerio Claudin-like T P A S Q N G R E R S - - - - E Y V

```

**Zebrafish *pancortin* cDNAs shown as modules A, B, M, Y, Z
(Isoforms AMY, BMY, AMY, BMZ are present in the mouse but several more
modules and isoforms exist in mouse as well as in fish)**

Module A

```
CTGCGTGACGCTCATCTAACGGGGACGGGAGACGTCGGGAGGCGGAGAGACACACGGGAG
AAACCGCGACGAGGCACCGCGCGGAGATGCCAGAGAAGGCTGCGCGAGACCGACTTGTG
TTTCTCTGTCAATCCGTTGCTGAGAGGAGAGAGAAACGAGAGGGAGAGATAGAGAGAGAGA
GATACCGGGGACAGAGGAGAGCGAGGAGTGAGCACCGAGCACCGACGAGCGGCTCTGACC
GAGGCACCGGACCGAATCTGCATGCCCAGCGAGCGGGCGCGAGATGCAGCGCGTGCAC
AAGCTCTTGAGTCTCATCGTGCTGGTGCTGATGGGCACGGA ACTCACGCAA
```

Module B from genomic sequence

```
ACACCAGACGGGACCAGCGCGGAGCAGACTGCTCGGTTTTCACTTCAAACACACCGG
ACTCCGTTGAACCTCAAGATGAGCACCCCTGAGACCGTTCGAACCGGGACCTTTAGTGGAGAT
GATGCGGATGATGGAGATGCACGAGGCGCGCACGGGCAGCGATGCTTGCCGTTACGGTTCC
CCGATGGCTTTTGTAGAATGAGAGTTTGGGTAAGCGCGCAGAGATGTCGGTGCCTTTGCTGA
AGATCGGTGTGGTGCTCAGCACCATGGCCATGATCACCAACTGGATGTCCCAGACTCTGCCA
TCACTAGTGGGACTCAACACCACCAA ACTGACCGCGGCGCAGGGCGGCTATCCGGACCGGA
GTATAGGA
```

Module B from ESTs

```
TGGACTCTGTGTGTGTA ACTCCTCCATCTCTCTGTCAGGGTGTGTGTGTGTTTGGACTATCC
TCCTCCATCTCTCCGTCAGATCAGCGTGTGTGTGTGTGTGTGTGTGTGGTGCATGAGTGCTGCT
CTGCTGAAGCTCGGGGCGGTGTTGAGCACTATGGTCCTCATCAGTAACTGGATGTCCCAGAA
TCTGCCGCGCTGGTGGGACTGGACCAACACACCGCTGCACCCGGCACCTCCGAGAAGATC
ATCAGC
```

Module M

GTTTTACCCGCTAACCCAGAGGAGTCCTGGCAAGTGTACAGCTCGGCTCAGGACAGCGAGG
 GCAGATGTGTGTGTACAGTCGTGGCACCTCAGCAGACCATGTGCTCGAGAGATGCCCCGACC
 AAACAACCTGCGCCAACTACTGGAGAAGGTGCAAAACATGACGCAATCAATCCAAGTATTGG
 ACCAGCGGACCCAGAGGGACCTGCAGTACGTGGTAAAGATGGAGGATCAACTCCGTGGCCT
 GGAGACCAAATTCAGACAGGTGGAAGAGAACCACAAACAAAACATCGCCAAGCAATACAA
 G

Module Y

GGCTAACTATAAAGACATGATAGGAGAGCCAGAGGCCAGAAGAAGCAGGTCTAACCCACG
 ATTGGCTGAAGTGGGCGTCAGTCACGCTGTTTATGTCACGATTCTCATATTCTATACGACATT
 AGCTGTAAGAAACACCCTCCCCCCTTTTCCTTACCAACCACCAATCAGATCTCCTCCTGCAT
 GCTACTCTAAAGAATTATTATTGTTACGTTTTATTTATATGAACTACATTATTAAGTTCATT
 GATATATATTGCTATTATTATTAGTAGTATTTCTACCATTATTATTCTCATCTTTGCTAGT
 ATTGCTTAAGTTTTTTTTTATGATTTGTCACTATGAATCTCATGTTTTTGAAGTAATATGCGTT
 TACTTTGGAAGTCAAGAATTCAATCTTAACATCACATTGTTGTATGTGAGTTGTAATTTCAGC
 ATGTGTCCCTTTCTGCTGTTGCATTCTAAACGATAAACTAATAAAGTCTTTTTCCCAATTGTT
 AAAAAAAAAAAAAAAAAA

Module Z

GGCATAAAGGCAAAAATGGCAGAGCTGCGTCCGCTAATCCCCGTCCTGGAGGAGTACAAAG
 CTGACGCTCGACTGGTCCAGCAGTTTAAGGAGGAGGTGCAGAATCTGACTGCGAGTCTCGGC
 CTCCTCCAGCAGGAGATGGGAGCTTATGACTATGATGACCTGCACTCCCGCGTGGTCAGTCT
 GGAGGAGCGGCTGCGAGCATGCATGCAGAACTCGCATGTGGTAAACTGACCGGCATTAGT
 GATGCAATCACTATTAACAATCCGGGTCCCGCTTCGGATCCTGGATGACGGATCCTCTCGC
 TCCTGAAGGAGACACTAGGGTGTGGTACATGGACGGTTATCATAACAACCGATTTGTGCGGG
 AGTACAAATCCATGGCGGACTTCATGACGTCGGACAACCTTCACGTCCCACCGGCTCCCGCAC
 CCCTGGTCTGGAACGGGTGAGGTGGTCTACAACGGCTCCATCTACTTCAACAAGTTCAGAG
 CAACATGATCATCAAGTTCGACTTCAAAACCTCCACCATGAGTAAATCCCAGCGACTGGACA
 ACGCCGGCTTCAGCAACACCTACCACTACGCTTGGGGCGGACACTCCGACATCGACCTCATG
 GTCGACGAGGGCGGGCTGTGGGCCGTCTATGCCACCAATCAGAACGCGGGAAACATCGTCA
 TCAGCAAGCTCCACCAATCACCTGCACATCATCCAGTCCTGGACCACCAATCATCCGAGG
 CGCAGTGCTGGGGAGTCTTTATGATTTGCGGGACGCTGTACGTGACCAACGGCTACTCGGG
 AGGGACAAAAGTCTACTACGCCTACCACACCAACTCCTCCACATATGAGTACATCGATATCG
 TTCTGCAAAAAGTACTCGCATATCTCCATGTTGACTATAACCCGCGGGATCGAGCACTG
 TATGCTTGAATAACGGACATCAGGTCTGTACAACGTTACGCTTTTTYCATGTCATCCGCTCG
 GAGCAGCTGTAAACGCTGAGGATTTCAATTTGGAGCTTCAAAAAAATAAATAAAAATGGAAC
 AAGACCATCCTTTGGAATGTCTTTCAACAGATTGTTACACAAAAAAAAAAAAAAAAA

Zebrafish and mouse Pancortin protein alignments shown as modules A, B, M, Y, Z

Module A

M. musculus M Q P A R K L L S L L V L L V M G T E L T Q
D. rerio M Q R V H K L L S L I V L V L M G T E L T Q

Module B from genomic sequence

M. musculus M S V P L L K I G V V L S T M A M I T N W M S Q T L P S L V G L N T T R L S A A
D. rerio M S V P L L K I G V V L S T M A M I T N W M S Q T L P S L V G L N T T K L T A A

M. musculus S G G T L D R S T G
D. rerio Q G G Y P D R S I G

Module B from ESTs

M. musculus M S V P L L K I G V V L S T M A M I T N W M S Q T L P S L V G L N T T R L S A A
D. rerio M S A A L L K L G A V L S T M V L I S N W M S Q N L P A L V G L D Q H - - - T A

M. musculus S G G T L D R S T G
D. rerio A P G T S E K I I S

Module M

M. musculus V L P T N P E E S W Q V Y S S A Q D S E G R C I C T V V A P Q Q T M C S R D A R
D. rerio V L P A N P E E S W Q V Y S S A Q D S E G R C V C T V V A P Q Q T M C S R D A R

M. musculus T K Q L R Q L L E K V Q N M S Q S I E V L D R R T Q R D L Q Y V E K M E N Q M K
D. rerio T K Q L R Q L L E K V Q N M T Q S I Q V L D Q R T Q R D L Q Y V V K M E D Q L R

M. musculus G L E T K F K Q V E E S H K Q H L A R Q F K
D. rerio G L E T K F R Q V E E N H K Q N I A K Q Y K

Module Y

M. musculus G
D. rerio G

Module Z

M. musculus A I K A K M D E L R P L I P V L E E Y K A D A K L V L Q F K E E V Q N L T S V L
D. rerio G I K A K M A E L R P L I P V L E E Y K A D A R L V Q Q F K E E V Q N L T A S L

M. musculus N E L Q E E I G A Y D Y D E L Q S R V S N L E E R L R A C M Q K L A C G K L T G
D. rerio G L L Q Q E M G A Y D Y D D L H S R V V S L E E R L R A C M Q K L A C G K L T G

M. musculus I S D P V T V K T S G S R F G S W M T D P L A P E G D N R V W Y M D G Y H N N R
D. rerio I S D A I T I K T S G S R F G S W M T D P L A P E G D T R V W Y M D G Y H N N R

M. musculus F V R E Y K S M V D F M N T D N F T S H R L P H P W S G T G Q V V Y N G S I Y F
D. rerio F V R E Y K S M A D F M T S D N F T S H R L P H P W S G T G Q V V Y N G S I Y F

M. musculus N K F Q S H I I I R F D L K T E A I L K T R S L D Y A G Y N N M Y H Y A W G G H
D. rerio N K F Q S N M I I K F D F K T S T M S K S Q R L D N A G F S N T Y H Y A W G G H

M. musculus S D I D L M V D E N G L W A V Y A T N Q N A G N I V I S K L D P V S L Q I L Q T
D. rerio S D I D L M V D E G G L W A V Y A T N Q N A G N I V I S K L H P I T L H I I Q S

M. musculus W N T S Y P K R S A G E A F I I C G T L Y V T N G Y S G G T K V H Y A Y Q T N A
D. rerio W T T N H P R R S A G E S F M I C G T L Y V T N G Y S G G T K V Y Y A Y H T N S

M. musculus S T Y E Y I D I P F Q N K Y S H I S M L D Y N P K D R A L Y A W N N G H Q T L Y
D. rerio S T Y E Y I D I V L Q N K Y S H I S M L D Y N P R D R A L Y A W N N G H Q V L Y

M. musculus N V T L F H V I R S D E L
D. rerio N V T L F H V I R S E Q L

Zebrafish *calcyphosine* cDNA**From genomic sequence (putative first exon):**

TAGAGGATCCCAAACAACCTTGTCAGAAAATCTGTATGAAAGTCACTGACAAGCATACCAA
 ACTACACTCAAGTGAAGCAATACATTGTTTCTAATTGATACAACCAAGAACATGAAAGCAGT
 AGCTTTATATTTCTCTATCATTTAAAAATGGTATTGTCATTTAAAGAGCTTCATGTGATTGTA
 GTTCTTTCCCTCATAAAGTAGAGTTTGTGTCATGACTCTCTTCTTAGCGTTTTGACCAGTAGACA
 GCAGATGTGTATATACATTTGAATAAAAACCCATGCATATGTTATCTTGTGAGCTTTAGATCAG
 ATAGGTGGAGGATGGCAGGTACATCGCGACATAATCGAGAAATGATGATCAATGCCAAAAA
 GCAGCTGGCTGAGTGTTCCAGACCCCAATTGAGCGTCTGCGGCTGCAGTGTTTGTCCCGAGGGT
 GTGCGGGCATCAAGGGACTGGGCAGGT

From ESTs (ORF beginning missing):

```

GCAGACGCTTTGCAGGATCTCCGACAGCAGTGCCTCAGCCGAGGAGCCGCGGGAATCAAGG
GTCTTGGAAAGGATGTTTCGCAGTATGGACGACGACGGCAGTAAATCTCTCGACTTCCAGGAG
TTTGTGACAGAGGTCTGCAGGATTATGGCGTGTCTGTGGGGAGAGATCAAGCGCAGCAGATCTT
CGCCATGATGGACAAAGATGGAAGTGGCAGCATCAACTTCGACGAGTTTCTGGAGAAATTA
AGACCACCCATGTCGAGCACACGGATGCAGGTCATCAGACAGGCTTCCAGAAGTTTGATA
AGAGCGGAGACGGCGTCGTGACCGTGGAGGATCTGCAGGGTGTTTACAACAGCAAACATCA
CCCCAAATACAAGAGCGGCGAGTGGACAGAAACACAAGTCTTCCACTCTTTCCTCGACAGCT
TTGACTCTCCGCATGACAAAGATGGAAAGGTGACCCCTGGAGGAGTTTGTGAATTACTACAGC
GGCGTCAGCGCTTCTGTGACAGTGACGAGTACTTCATCTCCATGATGAAGAGCGCATGGAA
GCTGTAGGCTTTTTCATTTGTCATTAGAAAATCAGATTGGAACCTGCAATATTTACATGTAGAA
ATCATGTCTCATTAAAGGTCTTTGATTTAAAAAAAAAAAAAAAAAAGGGCGGCCGCTCTAGA
GGATCCAAGCTTACGTACGCGTGCATGCGACGTCATAGCTCTTGG

```

Zebrafish and mouse Calcyplosine protein alignment

```

M. musculus      MAGTARHDREMAIQSKKKLS TATDPIERLRLQCLARGSAG
D. rerio (from ESTs)  ADALQDLRQQCLSRGAAG
D. rerio (from genomic) MAGTSRHNRREMMINAKKQLAECS DPIERLRLQCLSRGCAG

```

```

M. musculus      IKGLGRVFRIMDDNNNR TLDLFKEFLKGLNDYAVVMEKEEA
D. rerio (from ESTs) IKGLGRMFRSMDDDGSKSLDFQEFVRGLQDYGVSVGRDQA
D. rerio (from genomic) IKGLGR

```

```

M. musculus      EELFQRFDRDGS GTIDFNEFLLT LRPPMSRARKEVIMKAF
D. rerio (from ESTs) QQIFAMMDKDGSGSIN FDEFL EKLRPPMSSTRMQVIRQAF

```

```

M. musculus      RKLDKTGDGVITIEDLRE VYN AKHHPKYQNGEWTEE QVFR
D. rerio (from ESTs) QKFDKSGDGVVTVEDLQG VYNSKHHPKYKSGEWTEET QVFH

```

```

M. musculus      KFLDNFDSPLYDKDGLVTP EEFMNY YAGV SASIDTDVYFI I
D. rerio (from ESTs) SFLDSFDSPHDKDGLVTL EEFVNY YSGV SASVDSDEYFIS

```

```

M. musculus      MMTTAWKL
D. rerio (from ESTs) MMKS AWKL

```


Zebrafish *sp120 a / hnrpu a* cDNA

TGAATTGTTTTGCCGGTGGACAGACGCAGAATCACCGCGGCTGTGTGCAACTCACAGAAGCG
 AAGCGGCCGTCGGCTCCCCTGCATTGCTATATTCAAACAACCGAGTCTCTCTGTTTTTATTAG
 ACCATCTACGCTAAATCGACAAGATGAGTGAAATCAACGTGAAAAAGCTTAAGGTGAACGA
 GCTGAAGGACGAGCTAAAGAAGCGGCAGCTCTCTGACAAGGGGTGAAGGCCGAGCTCATG
 GAGCGTCTGCAGGCCGCGCTCGACGCAGAGGCCAGGCCAAGAGGAAGAAACGACCGCG
 CCAGGGACTACAGAAGGAAACGATGCCGATGGAAACGGCGTTGCAGCCGAACAAGAAGGT
 ACGGGTGAAGAAGAGCCGGAGGGGGAAAACATGGAGGCCGAGGAGCAGAATGGGGAAGG
 AGATGAAGCCGCCAGTCAGGACGACGAAATGGGAGAGGAGGAGGAGGAGGAGGACGACGA
 CGCCGGGGAGGAAATAGACAAAGCCTTAGACGATGAAGATGATGAAGAAGACGATATCATT
 GACAAAATCGACGTTGAAGACGGGGATGCGGACAAAGACAGCAGTGTGATCAGAAGAAT
 AAGAAGGGTGTAAAGAGACGCCGAGAGGATCATGGAAGGGGCTACTTTGAATTTATTGAAG
 AAAGCAAATACAGCCGGACCAAGTCTCCTCAGCCGCCTTTGGAGGAAGTGGATGAAGAGTT
 TGATGACACCCCTGGTCTGCTTGGATCCATACAATTGTGACCTTCACTTCAAAGTGTCCCGGA
 ACCGTTACAGTGCCTCCTCTCTTACCATGGAGAGTTTTGCTCACCTTTGGGCAGGTGGCCGTG
 CATCTTATGGTGTAAACAAGGGCAAAGTCTGCTTTGAAATGAAGGTCACTGAGAAAACCC
 AATCAAGCATTAAACAGCAAATCATGGACTTCCATGATGTCCATATTGGCTGGTCTCTGG
 CTAATGGGTGTCTGTCACTAGGTGAGGAGGAGTTTTCTTACTCCTATTCTGACAAAGGGAAG
 AAGGCTTCAAAGTGTGTGACTGAAGACTACGGGGAGGGCTTTGATGAAAATGATGTCATCG
 GCTGCTTCATTAATTTTCGAGGCTGATGAAGTGGAGATTTCTTTTCTAAAAATGGCAATGAC
 CTTGGTGTGGCTTTCAAGGTCAATAAGGAGTCGTTGGCTGACAGAGCCCTGTTCCCCCATGT
 TCTTTGTCACAAGTGTACTGTTGAGTTCAATTTTGGTCAGAACGAGACTCCGTTCTTCCCTAA
 GTTGGAGGACTTACCTTCATGCAGCAGATTCCTCTGGAAGAGCGTATCAGAGGACCCAAAG
 GACCTGTGGCCAAGAAAGACTGCGAGGTGATTGTGATGGTCGGCCTTCTGGATCTGGAAAA
 ACTACCTGGGTAGTTAAACATGTTGAAGAAAACCTGGGAAGTACAACATCCTCAGCACCA
 ACACHGTCTTGGAGAAATTGATGATTAACAGCGTAAAGAGGGCAAAAATAAAGACATAACAAA
 ACTCATGGCCATTTCCAGCGTGTTCCTTTTTACCTGGGCAAGTTGATTGAAAATTGCTGCCCC
 CAAAAAAGACACTATATTTTGGACCAGACGAACGTCTTTCAGCAGCCCAAAGAAGGAAG
 ATGTGTCTGTTTGTGGTTTCCAGCGCAAAGCCGTGGTGGTCTTTCCACAGATGAGAACTTA
 AAGGAGAGAGCGCAGAAGAAGGCAGAAGCGGATGGTAAAGATATACCCGAGCACGCCCTA
 CTCAAATGAAAGCTCTCTACACGCTTCCAGAACAAGGGGACTGCTTTTTCAGAGGTACCTA
 TGTTGAGCTGCAGAAGGACGAGGCCCTCAAGCTTTTTGGAGAAGTACAAGGAAGAGAGTAAG
 AATGCTTTGCCTCCAGAGAAGAAGCCCAACCAGGGACCCCAACTCCCAAACGGGGATCCC
 GCCGAGGMAGAGGGCAAAGAACCAGTTCAACAGGAGTGGTGGTGGTGGTGGTGGTGGTGGT
 GTCAAGGCAACCGTGGAGGCAGGGGTGGATTCAGCCCCGAGGAAACTACAGAGCGTTGCT
 TGCACCACCTCGTGTGAGCGGATTTGATCGTCGCCCCGCGGGTTACATTCTGCCACCTCCAC
 CACCACCACAGTCTACCGAGGTTATCCTAGCAGAGACGGTTACAACAGAGGAGGGTCTGG

TGGAATGCAGAGTAGAGGAATGTCTCCACGCGGTGGACAAATGAGGGGCAACATGGCCAGC
AGAGGTGGTGAATGAGCCGTGGAGGACATGCCAACAGAGGAGGAAACATGCACCGCGGA
GGTGGACAAGGTGGTCCCAACCACAGAGGACACTACCAGCAGAAATTCCACGGCAGAGGAG
GCCACCAGCAGAATCGTGGAGGATATGGCAACAAGAACGGCTCTTTTGCCCAAGCCTCAA
CCAGAGCTGGCAACAAGGGTTCTGGAACCAGAAGCCATGGAATCAACAGTACCATCCAGGA
TATTATTTGAATGCACATTTGTATTAAGACTCGTGGCCTGTGGTGTGCAGCCACTGAAAAAA
AAAAAAAAAAACCATCCACTTTTATGGTCCTTGTTTAAAATAATTTTTTTAAAAAGATAGTC
CATTTTTAAATAWGAGAAGCAAGTGGCAAACAAACATTCCGCCTCTGAAGTAAACAGTCTA
CGTTCAACGGATGTGTGATGGCTTCACGCTCAGATTTTTTCGTAGAAAGGTTTTCTTCCCCT
TTATTTTTCTATCACAGCTTTGATTGATATTGTTCTATCACTGCATTTCTTGTGCGAGTGAT
GCTTTRAATTTCAAGGTTGTGCATTTTTATTCTGTAAAATGTCATTTTTTTTACACAATGTAAA
TTATTATTTATTATTTGTCAAGATTTTTTTGTGCAAGACTTGTGTTCTAGTGTGAAAGAATCC
ATATATAGTCTTTTTGAGGCTTTTGTCAATTAATCATTAAATGCAGCAACTTCATGTTTAGTGCA
GGAGTGAAAATATTGTTCTCGATTTTTACTTTTTACTGTTTGTTTAAGCCCAGACTGTAACGG
TACTTCATAGGTTTGCAATAAATGACGTGCTTGCTTTTCTAAAAAAAAAAAA

Zebrafish Sp120 a and mouse Sp120 / Hnrpu protein alignment

M. musculus M S S S P V N V K K L K V S E L K E E L K K R R L S D K G L K A D L M D R L Q A
D. rerio (a) M S E I N V K K L K V N E L K D E L K K R Q L S D K G L K A E L M E R L Q A

M. musculus A L D N E A G G R P A M E P G N G S L D L G G D A A G R S G A G L E Q E A A A G
D. rerio (a) A L D A E A Q A Q - E E E T T A P G T T E G N D A D G - N G V A A E Q E G T G -

M. musculus T E D D E E E E G I S A L D G D Q M E L G E E N G A A G A A D A G A M E E E E A
D. rerio (a) - - - - E E E P - - - - E G E N M E A E E Q N - - - G E G D E A A S Q D D E M

M. musculus A S E D E N G D D Q G F Q E G E D E L G D E E E G A G D E N G H G E Q Q S Q P H
D. rerio (a) G E E E E E D D D A G E E I D K A L D D E D - - - - D E - - - - - - - - - -

M. musculus S A Q Q Q P S Q Q R G A G K E A A G K S S A P T S L F A V T V A P P G A R Q G Q
D. rerio (a) - - - - - - - - - - - - - - E D D - - - - - - - - - - I I D K I D V E D - - G D

M. musculus Q Q A G G D G K T E Q K G G D K K R G V K R P R E D H G R G Y F E Y I E E N K Y
D. rerio (a) - - A D K D S S A D Q K N - - K K G V K R R R E D H G R G Y F E F I E E S K Y

M. musculus S R A K S P Q P P V E E E D E H F D D T V V C L D T Y N C D L H F K I S R D R L
D. rerio (a) S R T K S P Q P P L E E V D E E F D D T L V C L D P Y N C D L H F K V S R N R Y

M. musculus S A S S L T M E S F A F L W A G G R A S Y G V S K G K V C F E M K V T E K I P V
D. rerio (a) S A S S L T M E S F A H L W A G G R A S Y G V N K G K V C F E M K V T E K T P I

M. musculus R H L Y T K D I D I H E V R I G W S L T T S G M L L G E E E F S Y G Y S L K G I
D. rerio (a) K H L N S K I M D F H D V H I G W S L A N G C L S L G E E E F S Y S Y S D K G K

M. musculus K T C N C E T E D Y G E K F D E N D V I T C F A N F E T D E V E L S Y A K N G Q
D. rerio (a) K A S N C V T E D Y G E G F D E N D V I G C F I N F E A D E V E I S F S K N G N

M. musculus D L G V A F K I S K E V L A D R P L F P H V L C H N C A V E F N F G Q K E K P Y
D. rerio (a) D L G V A F K V N K E S L A D R A L F P H V L C H N C T V E F N F G Q N E T P F

M. musculus F P I P E D C T F I Q N V P L E D R V R G P K G P E E K K D C E V V M M I G L P
D. rerio (a) F P K L E D F T F M Q Q I P L E E R I R G P K G P V A K K D C E V I V M V G L P

M. musculus G A G K T T W V T K H A A E N P G K Y N I L G T N T I M D K M M V A G F K K Q M
D. rerio (a) G S G K T T W V V K H V E E N P G K Y N I L S T N T V L E K L M I N S V K R Q N

M. musculus A D T G K L N T L L Q R A P Q C L G K F I E I A A R K K R N F I L D Q T N V S A
D. rerio (a) K D I T K L M A I S Q R V P F Y L G K L I E I A A R K K R H Y I L D Q T N V S S

M. musculus A A Q R R K M C L F A G F Q R K A V V V C P K D E D Y K Q R T Q K K A E V E G K
D. rerio (a) A A Q R R K M C L F A G F Q R K A V V V F P T D E N L K E R A Q K K A E A D G K

M. musculus D L P E H A V L K M K G N F T L F E V A E C F D E I T Y V E L Q K E E A Q K L L
D. rerio (a) D I P E H A L L K M K A L Y T L P E Q G D C F S E V T Y V E L Q K D E A S K L L

M. musculus E Q Y K E E S K K A L P P E K K Q N T G S - - - K K S N K N K S G - K N Q F N R
D. rerio (a) E K Y K E E S K N A L P P E K K P N Q G P P T P K R G S R R G R G Q K N Q F N R

M. musculus - G G G - - - - - - H R G - R G G F N M R G G N F R G G A P G N R G G Y N R R
D. rerio (a) S G G G G G G G G Q G N R G G R G G F Q P R G N Y R A L L A P P R V S G F D R R

M. musculus G N - - - - - - - - - - - M P Q R G G G - - G G S G G I G - - Y P Y P R
D. rerio (a) P R G Y I L P P P P P P V Y R G Y P S R D G Y N R G G S G G M Q S R G M S P R

M. musculus G P V F P G - - - - - - - R G G Y S N R G - N Y N R G G - - - M P - N R G
D. rerio (a) G G Q M R G N M A S R G G G M S R G G H A N R G G N M H R G G G Q G G P N H R G

M. musculus N Y N Q N F R G R G - - - N N R G - Y K N Q S - - - Q G Y N Q - W Q Q G Q F W
D. rerio (a) H Y Q Q K F H G R G G H Q Q N R G G Y G N K N G S F A Q A F N Q S W Q Q G - F W

M. musculus G Q K P W S Q H Y H Q G Y Y
D. rerio (a) N Q K P W N Q Q Y H P G Y Y

Zebrafish *transformer-2* β cDNA

CATTTACAGACGTCTGGTTTGTGTGTGCGTTTGTGAGCACTAATTGTGTGTTGTCCTAATCATT
CTCTTGCATTGTAATTATTGCAGCATATTACAAACTAAACAAAAATGAGTGACGCCGAGAAG
GAATTCGTGGAGCGGGAGTCTCGTTCAGCCTCTAGGAGCGCAAGTCCTAGAGGATCTGCCAA
GTCCGGCAGTCGCTCAGCYGAACGCTCGCCTGCTCATTCCAAAGAGAGGTCCCATCATTCCC
GCTCAAARTCCCGCTCGCGCTCCCGTTCCAAGACCAGGTCTCGTTCCCATCGAAGTTCTCGA
AGACATTACAGTCGATCACGTTACGCTCTTATTCTCGCCGAAGACGTTCRCGCAGCCGCTC
ATACAGCAGTGAATATCACCGCCGCCGAGCAGTCACAGTCACTCTCCCATGTCCAACCGCA
GACGACATATTGGTGACCGGGCAAATCCAGACCCAAACTGCTGCCTGGGAGTGTTCCGATTG
AGCCTGTACACCACAGAGAGAGACCTGAGGGAGGTCTTCTCTAAATATGGCCCTCTGAGTGA
TGTGTGCATTGTGTACGACCAGCAGTCACGGCGCTCCAGGGGTTTTGCTTTTGTCTACTTTGA
GAACAGAGAAGATTCAAAAGAGGCWAAAGAGCGTGCAAATGGTATGGAGCTTGATGGCCG
AAGAATCAGRGTAGACTaCTCCATTACCAAGAGGCCACACaCACCTACTCCTGGAATATATAT
GGGCAGACCAACATATGGTGGTGGGCCAAGTGTAAGCCGTCGGCGGGATAGCTATGATCGA
GGGTATGAACGTGGATATGATCGCTATGAAGACAGAGACTACTACAACAACAGGAGAAGAT
CCCCGTCTCCTTACTACAGCCGAGGACCGTACAGGTCAAGATCACGCTCTCGCTCTTACTCTC
CTCGTCATTATTTGAAGTGAAGTTCAGCTCCTCTCTTGAAGATGACTACAATATTGTTGATGAC
GTAGATGTTTATTTCTGGTGGCATGAGTCTCGATGTACTTTTCTTCGATTTTCTTGCCATAAG
GTTTCATGTGTCTTTGACTGATCTGGATGTTTCATTAGTGGGATGAATATTTTGCCTGTTGT
TGAGTTTTTGTTCATTTTTTTTTTTTTTCGTTCCCGATCTGATGCTAAACTTGCGTTTGTAT
AATATGATGAAGTGTTCCGGCTCACATCCCCGTATGCTTTTTTCGCATTTAAGCTTAGCAGTGGT
CTTGCAATAAACTGCTTTAaCCTCC

Zebrafish and mouse Transformer-2 β protein alignment

M. musculus MS D S G E Q N Y G E R E S R S A S R S G S A H G S G K S - - - A R H T P A R
D. rerio MS D - A E K E F V E R E S R S A S R S A S P R G S A K S G S R S A E R S P A H

M. musculus S R S K E D S R R S R S K S R S R S E S R S R S R R S S R R H Y T R S R S R S R
D. rerio S K E R S H H S R S K S R S R S R S K T R S R S H R S S R R H Y S R S R S R S Y

M. musculus S H R R - S R S R S Y S R D Y R R R H S - H S H S P M S T R R R H V G N R A N P
D. rerio S R R R R S R S R S Y S S E Y H R R R S S H S H S P M S N R R R H I G D R A N P

M. musculus D P N C C L G V F G L S L Y T T E R D L R E V F S K Y G P I A D V S I V Y D Q Q
D. rerio D P N C C L G V F G L S L Y T T E R D L R E V F S K Y G P L S D V C I V Y D Q Q

M. musculus S R R S R G F A F V Y F E N V D D A K E A K E R A N G M E L D G R R I R V D F S
D. rerio S R R S R G F A F V Y F E N R E D S K E A K E R A N G M E L D G R R I R V D Y S

M. musculus I T K R P H T P T P G I Y M G R P T Y G S - - - S R R R D Y Y D R G Y D R G Y
D. rerio I T K R P H T P T P G I Y M G R P T Y G G G P S V S R R R D S Y D R G Y E R G Y

M. musculus D D R D Y Y S R S Y R G G G G G G G W R A A Q D R D Q I Y R R R S P S P Y Y S
D. rerio D R - - Y E D R D Y Y N N - - - - - - - - - - - - - - - R R R S P S P Y Y S

M. musculus R G G Y R S R S R S R S Y S P R R Y
D. rerio R G P Y R S R S R S R S Y S P R H Y

Zebrafish “novel p7822b53” cDNA

GGACTGACATGGACTGAAGGAGTAGAAAGTAATGACAGGCCTCTAACACACAGGAGCAG
 CAGAGCCACGTAAACGTGCGATGACGTCCTGCGAAGAAATGTGCTGTTACTTCCTGGGCT
 TCACTTCACTTTCACAAGCAGTCTTCTGCTGATCCAGTGAGCCATTTCATCTGCTGATGTTGGT
 AAGCAGCTTTAGATTGAAGGTGTCATGGATTCTGGTGAGGATGGAGGTTGTGTTGGAGGTCC
 ATCAGGGGATGAAAACACTTCCAGGGCTACACCTTCACTGATCGCTCCCATTCCAGCCGTG
 TTGTGAAGAGCATCATGGACTTGTGCCTGGAGGACGGGCTGTTTGCAGACGTCATTGTGACT
 GTGGACAGTAAAGAGTCCAGCTTCCAGCTTCCAGCTTCCAGCTTCCAGCTTCCAGCTTCCAG
 GTCCATGTTCACTCAAACCTCAGAGAGGCTTATGACCGTAATATTGAGCTGAAGGACGTC
 GTGCAACTGTCTTCCAGTCACTGGTGGACTACATCTACCATGGGATGATCAAGCTGAGGGTT
 GAAGATCTGCAGGACACCTATGAAATGGCCGATATGTATCAGCTCACCGCTCTGTTTGAGGA
 GTGCTCCCGCTTCTGTACGGACTGTGGATGTTAGGAACTGCCTTCAGGTGATGTGGTTGGC
 GGACAGACACAGTGACCAGGAGGTGTATACAGCTGCCAAGCACTGTGCAAAGATACACCTG
 GTTCAGCTGCACCAGACAGATGAGTTTCTGAATTTGCCATTGTGCCTTCTCATGGACATCATT
 AAAGATGGTGTGCCAAGCTCACAAAATCCAACCGCAGCTATTGAATCTTGGATCAATCACAA
 CAAAGTGGAGCGAGAGGAGTATTCTGATATGCTTCTTGACAGCCTAAAGGAAATTGGTGAA
 AAAGTGCACATATACCTAATTGGAAAGGAAGACACACGCACACACTCACTAGCAGTGTCTC
 TTCATTGTGATGAGGACCACGCCATTAGTGTGAGCGGCCAGAACAGTCTGTGCCACCAGATC
 ACGGCTGCCTGCAAACATGGGGCGGATCTATATGTTGTAGGAGGCTCCATACCGCGACGCAT
 GTGGAAATGCAACATGCACACGATGGACTGGGAACGCTGCGCCCCTCTGCCCGGGACCGT
 CTCCACCACACGCTAGTGTCCGTGTCCACAGAGGACGCCATATACTCATTGGGAGGCAAAAC
 CCTTCAGGACACTCTCTCAAACGCCGTCAATTTGCTACACCGTAAAGGACAACATATGGAAAG
 AGACCACTCAGCTAGACACGGCAGTATCAGGTGCAGCCGGAGTCAATTTGGGAGGTACCAT
 TTACCTTTTGGGTGGAGAAGAAAATGACATGGACTTCTTTACCAAGCCTTCTCGCCTTATACA
 GTGCTTTGAGACTGCCACCCAGAGGTGCCAGACCAAGCCCTACATGCTGCCTTTTGTGCTGGAT
 GCATGCATGCCACCGCTCATAAGGACCTTATTTTTGTGGTGGCAGAGGGCGACTCTTTGGTG
 TGTTATAACCCACTGCTGGACAGTTTACGAGGTTGCGCTTCCCTGAAGTTTGGAGCTGTGTG
 CCATCTTTATGGAAAGTGGCCAGCTGCAATGGGTGCATTTATGTTTTTLAGGGACAAATGCAA
 GAAAGGCGATGCGAACACTTTGAAGTTGAACCCTGCCACATCTGTGGTCTCTGTAATCAAGG
 GAATCAAATCCTGCTCACGAACTGGCAGTTCGACTGGCCGTGAGATGTTTGATGTAATGCA
 TGGGACCATAATAAATGTACT

Zebrafish and mouse “novel p7822b53” protein alignment

D. rerio M D S G - - E D G G C V G G P - - - - S G D E N Y F Q G Y T F T D R
M. musculus M K G G I A D S W Q R E K L A T M E S P E E P G A S M D E N Y F V N Y T F K D R

D. rerio S H S S R V V K S I M D L C L E D G L F A D V I V T V D S K E F Q L H R L V L S
M. musculus S H S G R V A Q G I M K L C L E E E L F A D V T I S V E G R E F Q L H R L V L S

D. rerio A Q S S F F R S M F T S N L R E A Y D R N I E L K D V S A T V F Q S L V D Y I Y
M. musculus A Q S C F F R S M F T S N L K E A H N R V I V L Q D V S E S V F Q L L V D Y I Y

D. rerio H G M I K L R V E D L Q D T Y E M A D M Y Q L T A L F E E C S R F L S R T V D V
M. musculus H G T V K L R A D E L Q E I Y E V S D M Y Q L T S L F E E C S R F L A R T V Q V

D. rerio R N C L Q V M W L A D R H S D Q E V Y T A A K H C A K I H L V Q L H Q T D E F L
M. musculus G N C L Q V M W L A D R H S D P E L Y T A A K H C A K T H L A Q L Q S T E E F L

D. rerio N L P L C L L M D I I K D G V P S S Q N P T A A I E S W I N H N K V E R E E Y S
M. musculus H L P H H L L T D I I S D G V P C S Q N P T E A I E A W I N F N K E E R E A F A

D. rerio D M L L D S L K E I G E K V H I Y L I G K E D T R T H S L A V S L H C D E D H A
M. musculus E S L R T S L K E I G E N V H I Y L I G K E S S R T H S L A V S L H C A E D D S

D. rerio I S V S G Q N S L C H Q I T A A C K H G A D L Y V V G G S I P R R M W K C N M H
M. musculus I S V S G Q N S L C H Q I T A A C K H G G D L Y V V G G S I P R R M W K C N N A

D. rerio T M D W E R C A P L P R D R L H H T L V S V S T E D A I Y S L G G K T L Q D T L
M. musculus T V D W E W C A P L P R D R L Q H T L V S V P G K D A I Y S L G G K T L Q D T L

D. rerio S N A V I C Y T V K D N I W K E T T Q L D T A V S G A A G V N L G G T I Y L L G
M. musculus S N A V I Y Y R V G D N V W T E T T Q L E V A V S G A A G A N L N G I I Y L L G

D. rerio G E E N D M D F F T K P S R L I Q C F E T A T Q R C Q T K P Y M L P F A G C M H
M. musculus G E E N D L D F F T K P S R L I Q C F D T E T D K C H V K P Y V L P F A G R M H

D. rerio A T A H K D L I F V V A E G D S L V C Y N P L L D S F T R L R F P E V W S C V P
M. musculus A A V H K D L V F I V A E G D S L V C Y N P L L D S F T R L C L P E A W S S A P

D. rerio S L W K V A S C N G C I Y V F R D K C K K G D A N T L K L N P A T S V V S V I K
M. musculus S L W K I A S C N G S I Y V F R D R Y K K K G D A N T Y K L D P A T S A V T V T R

D. rerio G I K I L L T N W Q F V L A
M. musculus G I K V L L T N L Q F V L A

A radiation hybrid transcript map of the mouse genome

Philip Avner^{1,2}, Thomas Bruls¹, Isabelle Poras¹, Lorraine Eley³, Shahinaz Gas¹, Patricia Ruiz⁴, Michael V. Wiles^{5,10}, Rita Sousa-Nunes⁶, Ross Kettleborough⁶, Amer Rana⁶, Jean Morissette⁴, Liz Bentley³, Michelle Goldsworthy³, Alison Haynes³, Eifion Herbert³, Lorraine Southam³, Hans Lehrach⁵, Jean Weissenbach¹, Giacomo Manenti⁷, Patricia Rodriguez-Tome^{8,10}, Rosa Beddington*, Sally Dunwoodie^{6,9} & Roger D. Cox³

Expressed-sequence tag (EST) maps are an adjunct to sequence-based analytical methods of gene detection and localization for those species for which such data are available, and provide anchors for high-density homology and orthology mapping in species for which large-scale sequencing has yet to be done¹. Species for which radiation hybrid-based transcript maps have been established include human², rat³⁻⁵, mouse⁶, dog⁷, cat⁸ and

zebrafish^{9,10}. We have established a comprehensive first-generation–placement radiation hybrid map of the mouse consisting of 5,904 mapped markers (3,993 ESTs and 1,911 sequence-tagged sites (STSs)). The mapped ESTs, which often originate from small-EST clusters, are enriched for genes expressed during early mouse embryogenesis and are probably different from those localized in humans. We have confirmed by *in situ* hybridization that even singleton ESTs, which are usually not retained for mapping studies, may represent *bona fide* transcribed sequences. Our studies on mouse chromosomes 12 and 14 orthologous to human chromosome 14 show the power of our radiation hybrid map as a predictive tool for orthology mapping in humans.

To ensure the mapping of novel embryonic transcripts, we sequenced the Beddington endoderm cDNA library derived from a 7.5–days *post coitum* (dpc) gastrulating embryo. Some 4,000 EST sequences from this library and 200 sequences from a previously analyzed embryonic library^{11,12} were examined by clustering homologous sequences into groups corresponding to putative single genes and determining their expression profile by computational analysis. Approximately 18% were novel; after clustering, 108 sequences remained as unique single sequences (singletons). Although singletons are often considered to be DNA contaminants and omitted from EST mapping programs, they may be transcripts expressed at low levels, or transcripts that are poorly represented in the nucleotide database because they are specific to a cell type or are poor substrates for reverse transcriptase. To address the biological significance of these singletons, we generated probes for *in situ* hybridization from six of the EST-sequence

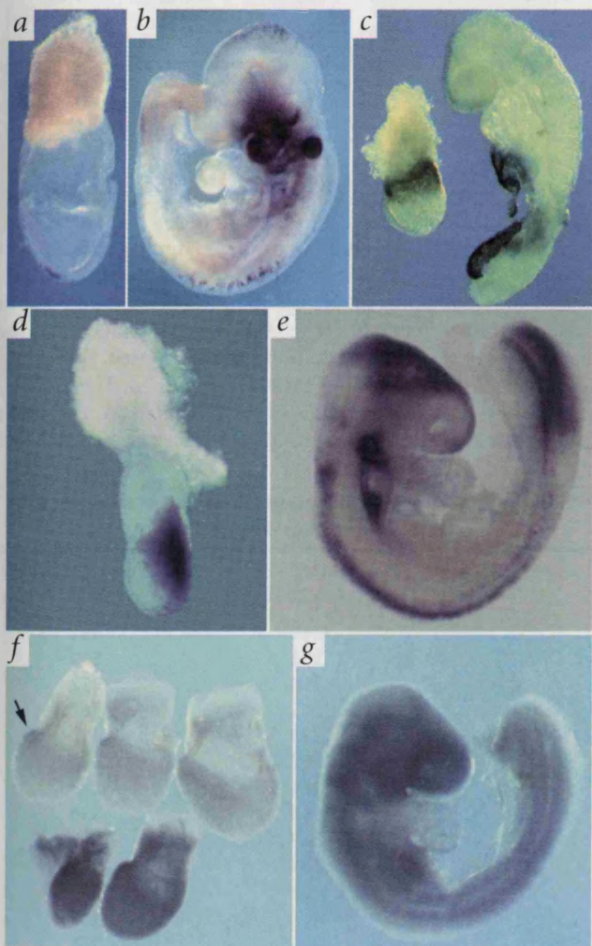


Fig. 1 Whole-mount *in situ* hybridization: singletons represent *bona fide* gene transcripts. Whole-mount RNA *in situ* hybridization of mouse embryos (lateral view) using probes generated from ESTs (a,b) AL022911 (c) AL023051 (d,e) AL033345, and (f,g) AL034928. Singletons represent *bona fide* transcripts. a, At 7.5 dpc, AL022911 transcripts are localized to the head process. b, At 9.5 dpc, they are found in the otic vesicle, the branchial arches and isolated cells in the midbrain, ventral to the heart and adjacent to the neural tube. c, At 7.5 dpc (left), AL023051 transcripts are restricted to the visceral endoderm, and at 9.5 dpc (right) to its descendant, the yolk sac. d, At 7.5 dpc, AL03334 transcripts are restricted to the nascent mesoderm and primitive streak. e, At 9.5 dpc, they are localized to the midbrain, dorsal neural tube, pharyngeal pouches and pre-somitic mesoderm. f, EST genes with restricted patterns of expression 7–7.5-dpc embryos show widespread but non-ubiquitous localization of AL034928 transcripts. Embryos developed for a short time show expression in the anterior visceral endoderm (arrow), whereas those developed for longer (bottom) show the extent of gene expression. g, At 9.5 dpc, AL034928 transcript localization is widespread but is absent from the heart, yolk sac and neuroepithelium.

¹Genoscope, Centre National de Séquençage and CNRS UMR 8030, CP 5706, 91057 Evry Cedex, France. ²Unité de Génétique Moléculaire Murine, Institut Pasteur, Paris, France. ³Mammalian Genetics Unit, Medical Research Council, Harwell, UK. ⁴Centre de Recherche du CHUL ⁵Max-Planck Institute of Molecular Genetics, Ihnestrasse, Berlin, Germany. ⁶Laboratory of Mammalian Development, National Institute for Medical Research, The Ridgeway, Mill Hill, London, UK. ⁷Ste-Foy, Quebec, Canada. ⁸Instituto Nazionale Tumori, Division of Oncology, Milano, Italy. ⁹The European Bioinformatics Institute, European Molecular Biology Laboratory Outstation, European Bioinformatics Institute, Wellcome Trust Genome Campus, Hinxton, Cambridge, UK. ¹⁰The Victor Chang Cardiac Research Institute, Darlinghurst, Sydney, Australia. ¹¹Present addresses: Deltagen Inc., Menlo Park, California, USA (M.V.M.); Geneva Proteomics Inc., Meyring, Switzerland (P.R.-T.). *Deceased. Correspondence should be addressed to P.A. (e-mail: pavner@pasteur.fr).

cDNAs and examined their expression in the early embryo. Three of the ESTs (AL023051, AL033345, AL022911) show highly restricted patterns of hybridization, one (AL034928) is relatively widespread in its expression and two (AL023012, AL023075) show ubiquitous hybridization (Fig. 1). These findings suggest that many of the singletons that remain after clustering are likely to be *bona fide* cDNAs. *In situ* hybridization of a larger sample of 350 cDNAs from the embryonic libraries shows that 80% have widespread or ubiquitous patterns of expression in the 7.5-dpc embryo.

For high-throughput radiation hybrid marker typing in a 96-well plate format, we selected 90 radiation hybrids from the original panel of 94 (ref. 13) to permit inclusion of appropriate control DNAs. We selected more than 2,800 SSLP

markers for the framework map from the MIT (96 meiosis F2 intercross) and EUCIB (1,000 progeny backcross) mouse genetic maps^{14,15}, of which 2,230 yielded valid panel typings. The observed average marker retention frequency of 30.5% is consistent with previously published results for the T31 radiation hybrid panel^{6,13,16}.

The X chromosome shows the lowest retention frequency (expected because the male donor cell line that was irradiated contained a single copy of the X chromosome) and chromosome 19, the smallest chromosome, shows the highest (Table 1). Construction of the framework map resulted in a series of extended framework maps that comprise 1,238 markers.

We produced comprehensive EST placement maps by mapping chromosome-assigned ESTs and STSs against the framework-map intervals by multipoint maximum likelihood analysis. This resulted in a placement map of 3,446 markers. We also produced a map using the traveling-salesman problem (TSP) approach. Chromosome maps produced in this way generally contained fewer markers, as the reordering algorithm caused the more error-prone markers to be discarded from the map. The maps produced with the two approaches, however, are highly consistent (Fig. 2), indicating that data quality and not algorithmic approach is the critical factor in producing high-quality maps. Of the markers on the maximum likelihood map (Fig. 2) with odds higher than 1:1,000 that are also on the TSP map, 87% show the same relative order on both maps. Typically, about 80% of other chromosomes also show the same relative order. Overall, using our build criteria, we were unable to assign about 7% of validated vector scores to a chromosome, and among the markers assigned, we were unable to precisely localize 15%. Of the assigned markers, we found that 40% were localized to both ends of the chromosomes, and eliminated these as potentially error-prone vector scores. This build contains 1,803 ESTs and 1,643 STSs. Many of the mapped ESTs included in the comprehensive map are derived from small EST sequence clusters, compatible with their being derived from genes that have both a restricted transcriptional profile and low copy number in the cell (data not shown).

Table 1 • Summary of radiation hybrid map data

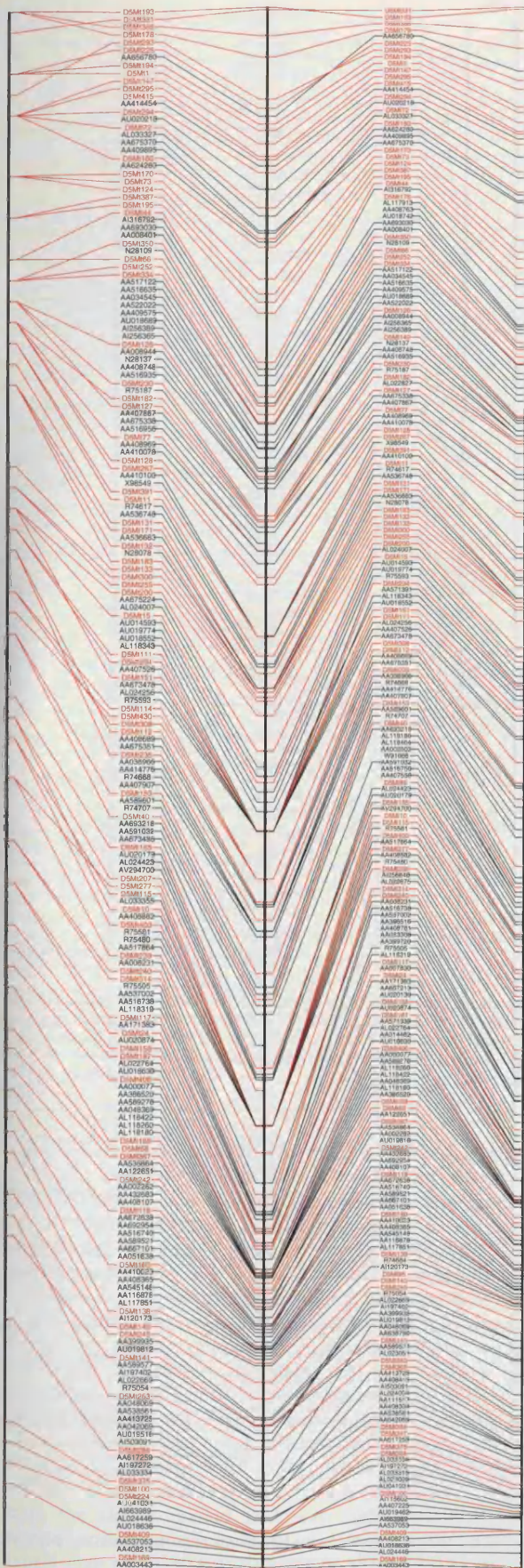
Chr	Mb	cR	kb/cR	Fw	HOM	LOM	cRperMark	Av. ret
1	216.00	5,579.80	38.71	73	148	87	23.74	0.29
2	208.50	6,003.00	34.73	92	208	103	19.30	0.28
3	179.70	5,066.70	35.47	72	154	51	24.72	0.33
4	176.70	5,398.00	32.73	76	151	58	25.83	0.27
5	170.40	4,886.00	34.88	68	132	103	20.79	0.28
6	165.90	5,234.30	31.69	81	117	102	23.90	0.27
7	155.70	4,296.50	36.24	57	129	58	22.98	0.27
8	149.10	4,366.50	34.15	64	113	92	21.30	0.31
9	143.70	4,290.40	33.49	49	109	60	25.39	0.30
10	144.90	2,514.30	57.63	58	83	9	27.33	0.32
11	141.60	5,185.80	27.31	72	190	13	25.55	0.31
12	146.40	2,255.20	64.92	44	75	3	28.91	0.35
13	131.40	3,864.30	34.00	48	108	4	34.50	0.31
14	133.80	3,624.00	36.92	56	110	30	25.89	0.28
15	121.50	2,797.80	43.43	53	109	12	23.12	0.32
16	114.00	3,594.20	31.72	51	137	9	24.62	0.34
17	115.50	5,175.70	22.32	57	139	11	34.50	0.33
18	116.40	2,979.70	39.06	44	100	3	28.93	0.32
19	81.90	2,523.40	32.46	50	113	31	17.52	0.38
X	186.90	3,682.30	50.76	73	119	63	20.23	0.23
tot	3,000.00	83,317.90	36.01	1,238	2,544	902	24.18	0.30

Av. ret, average retention rate; chr, chromosome; cRperMark, average number of centiray per marker; HOM, high-ordered marker (framework markers and markers whose first placement interval is at least 1,000 times more likely than the second placement interval); kb, kilobase; LOM, low-ordered marker (markers whose first placement interval is less than 1,000 times more likely than the second placement interval); Mb, megabase; tot, total.

Since the first build of the comprehensive placement maps reported here, a further 2,190 ESTs and 268 STSs have been localized on the placement map using a mapping criterion that requires the two top-ranking intervals to be adjacent if the odds of the top ranking interval are less than 1,000:1 compared to the second placement interval. If the slightly more stringent requirements used in the first-release build had been used, some 2,384 additional placements would have been obtained. The locations of these new ESTs relative to the framework map are available at <http://www.genoscope.cns.fr>. In all, 5,904 markers (3,993 ESTs

Table 2 • Chromosome distribution of EST markers in first placement map (Feb. 1, 2001)

Chr	Total ESTs Feb 2001	Total markers Feb 2001
1	262	391
2	352	500
3	228	332
4	265	367
5	321	410
6	202	336
7	245	333
8	243	330
9	268	357
10	111	188
11	258	356
12	102	161
13	116	185
14	131	222
15	166	257
16	144	229
17	186	271
18	106	172
19	153	227
X	134	280
total	3,993	5,904



plus 1,911 WI-MIT markers) have been localized as of the 1 February 2001 map build, of which 4,032 are high-confidence markers that allow the precise positioning of any newly typed marker (Table 2).

Figure 3 shows an example of this map built for mouse chromosome 2. In order to validate our EST localizations and estimate the potential error rates, we tested a subset of ESTs localizing to chromosomes 3, 6 and 12 against a corresponding monochromosomal hybrid¹⁷. Of the 145 ESTs tested, 94% (136) gave unambiguous positive results on the corresponding monochromosomal hybrid. This rate is close to that found for the human Genebridge 4 panel¹⁸ and confirms that the criteria we have adopted for assignment are appropriate.

Our radiation hybrid framework map was constructed in a different manner from the WI-MIT radiation hybrid map and would appear to be a useful update to the previously published mouse radiation hybrid framework map⁶. The concatenation step in particular should improve the accuracy of the framework map. The 1,066 markers common to both maps will facilitate comparison between them, increasing the value of the overall EST dataset. Assuming an average retention frequency of 30% and a mean size of the radiation-induced fragments of 5–10 Mb, the theoretical resolution limit that can be achieved with our 90 hybrid lines is about 300 kb, corresponding to the mapping of some 10,000 uniformly distributed markers. It is likely that the resolution obtained using the non-redundant set of markers mapped by the joint efforts of the WI-MIT group¹⁹ and the EU consortium will therefore approach that of the T31 panel.

We initially attempted a global cross-species orthology search based on BLAST analysis between the mapped mouse and human EST-cluster consensus sequences. This approach confirmed 63 known regions of homology and defined 17 putative new regions of homology that were, however, supported only by single clusters (data not shown). We did a pilot comparative human/mouse gene localization study in which EST markers that we had radiation hybrid mapped were compared with sequence data from human chromosome 14. This chromosome shows conserved gene orthology with mouse chromosomes 12 and 14 (ref. 20). Conversely, a 15-cM region between the centromere and the Tpo marker of mouse chromosome 12 is orthologous to human chromosome 2p, whereas a genetic segment extending from 15 cM from the centromere to around 23 cM is orthologous to parts of human chromosome 7. The rest of the chromosome is thought to be orthologous with human 14q. Mouse chromosome 14 has previously been shown to have conserved linkages or conserved orthologies involving human chromosomes 3, 8, 10, 13 and 14 as well as the X and Y chromosomes. Our approach combined information from the following sources: (i) the genomic sequence corresponding to a clone-tiling path covering 99% of human chromosome 14; (ii) consensus sequences for the EST clusters produced at the EBI and for which a representative had been RH-mapped; (iii) orthologous relationships between human and mouse genes computed at the Jackson Laboratory (<http://www.jax.org>) and (iv) orthologous relationships predicted at the National Center for Biotechnology Information from sequence alignment using the megablast algorithm between the mouse and human UniGene sets (<http://www.ncbi.nlm.nih.gov/Homology/>). Because our initial attempts at aligning single short-pass mouse EST sequences against human chromosome 14 genomic sequences

Fig. 2 Placement maps for chromosome 5. Comparison of maps established using the maxlik program²⁸ (right-hand bar) and the traveling-salesman program (TSP) approach (middle bar), as well as the MIT genetic map (left-hand bar).

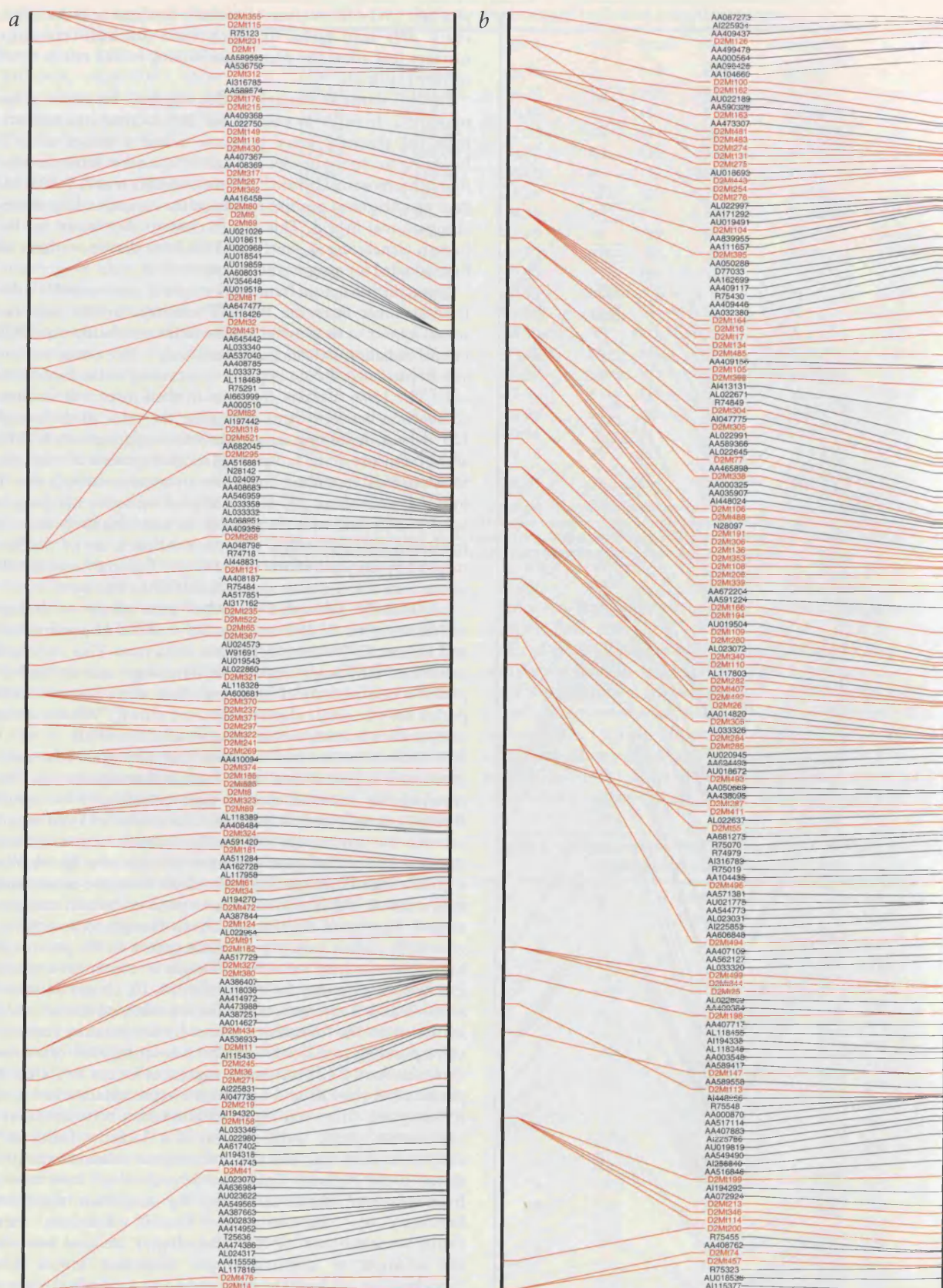


Fig. 3 Comprehensive radiation hybrid map of mouse chromosome 2. Left-hand bar: genetic localizations taken from the MIT genetic map. Right-hand bar: position on the radiation hybrid map. a, Top corresponds to the centromere of chromosome 2. b, Bottom corresponds to the telomere of chromosome 2.

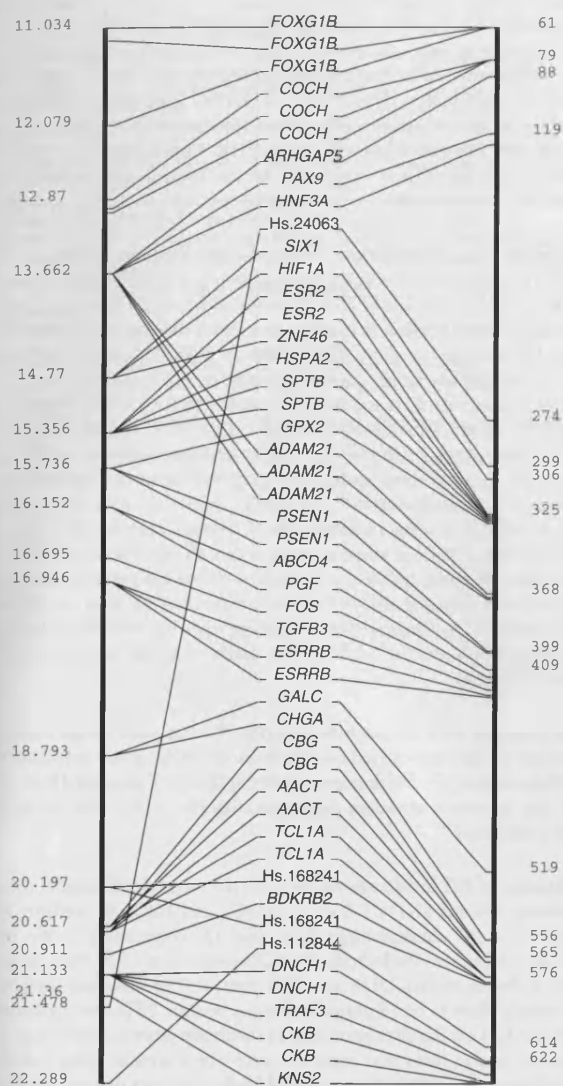


Fig. 4 Orthologous relationships between mouse ESTs mapping to mouse chromosome 12 and human chromosome 14, showing positions on the radiation hybrid map of mouse chromosome 12 (left-hand bar) and human chromosome 14 (right-hand bars). The numbers on the right identify the relevant human BAC on the minimal-tiling path³¹.

using tblastx were considered unreliable, we derived longer transcript sequences for each EST from either the EGI or UniGene EST cluster databases. We then either directly aligned the longest mouse transcript or consensus sequence against the human chromosome 14 genomic sequence using the blastn and tblastx algorithms, or used this transcript to retrieve putative orthologs in the human UniGene set, which we then aligned against the genomic sequence by blastn analysis. To increase the number of potential points of orthology, we integrated previously known orthologs genetically mapped in the mouse but absent from the set of radiation hybrid-mapped ESTs in the first build of our placement radiation hybrid map. We indirectly localized these orthologous relationships on the radiation hybrid map by identifying, from the genetic coordinates on the Mouse Genome Informatics integrated genetic map, the closest marker that was both radiation hybrid mapped and genetically mapped, and assigning the radiation hybrid map position of this marker to the orthologous gene.

We used the correspondence between the mouse and human Unigene sets available through NCBI's Homologene project (<http://www.ncbi.nlm.nih.gov/Homology/>) to provide further cross-species links. Using these combined approaches, we anchored 100 ESTs onto the sequence map of human chromosome 14. The orthology relationships between ESTs mapped on mouse chromosome 12 and human chromosome 14 are shown in Fig. 4. Using this map, we were able to localize ESTs that had been assigned to mouse chromosome 12, but whose localization remained ambiguous (under the criteria that both the highest and next highest allocations must be in neighboring intervals), with greater confidence by reference to the orthology and linkage relationships based on the sequence of human chromosome 14.

We have constructed a radiation hybrid map of the mouse genome that contains some 6,000 markers, of which over 4,000 are ordered at high odds. ESTs extracted from this map should be useful in identifying the many mutants being generated by phenotype-driven ENU mutagenesis. For example, the 500 new ENU-induced mouse mutants reported by Nolan and colleagues²¹, of which 30 were initially mapped, or the 182 mutants identified by de Angelis and colleagues²² can be tackled most efficiently at the gene level using a candidate-gene approach. The usefulness of our radiation hybrid map as a predictive tool for candidate-gene cloning is indicated by our studies of the Delta3 gene and pudgy mutations^{11,23}. Likewise, mapped ESTs will be useful for characterizing the genetic basis underlying quantitative traits once these have been refined by congenic/and or BAC transgenesis studies. This map is an important resource for cross-referencing of mammalian genomes, positional cloning of mouse genes through candidate gene approaches, and anchoring and orientation of current draft sequencing efforts.

Methods

Radiation hybrids. We obtained DNAs corresponding to the T31 radiation hybrid panel¹³ from Research Genetics. A list of the subset of 90 hybrids used in our experiments is available at www.genoscope.cns.fr.

Sequencing of cDNA clones. We sequenced the 7.5-dpc endoderm library of Beddington and colleagues¹² using standard methods. We submitted approximately 4,000 clones that yielded high-quality sequence data to the EMBL database and subjected them to cluster analysis (see below); their accession numbers are listed at www.genoscope.cns.fr.

Cluster analysis. To identify and group transcribed sequences derived from a single gene, we processed EST sequences extracted from the EMBL database to remove or mask redundant repetitive sequences, contaminating vector sequences and low-quality sequences that could confound the analysis, then carried out cluster analysis on the basis of sequence homology using the JESAM packages²⁴ and tools available at <http://corba.ebi.ac.uk/EST/egi.html>. This was done at the European Bioinformatics Institute (EBI). Each cluster of homologous and aligned sequences, and the consensus sequence derived from them, corresponds—subject to certain important caveats—to an individual gene²⁴.

SSLP marker development. We selected STS markers from the MIT and EUCIB mouse genetic map^{14,15}. We obtained EST markers either from our internal sequencing program or from cDNA sequences obtained from the dbEST EBI site after clustering²⁴. We used endoderm-derived sequences systematically for EST derivation if they corresponded to unallocated sequences; otherwise, we derived ESTs from clusters in the database composed of two or more sequences of which at least 30% were derived from early-embryonic libraries (that is, earlier than 10.5 dpc). The list of retained libraries can be consulted on the [genoscope.server](http://www.genoscope.cns.fr). We modified these criteria in the case of the mouse urogenital ridge (NMUR library 144; see the library browser at <http://www.ncbi.nlm.nih.gov/UniGene/>) and the mouse eight-cell-stage embryo (library 150), in that we sometimes used sequence clusters from these libraries without regard for the overall proportion of

embryonic-derived sequences and some singleton sequences were selected. We selected primer sequences using the Primer 3 program (http://www.genome.wi.mit.edu/genome_software/other/primer3.html). We tested both STS and EST markers for their specificity against mouse, Chinese hamster and human DNAs before typing them on the radiation hybrid panel. We carried out all tests in duplicate. All primer sequences have been submitted to RHdb (ref. 25 and <http://www.ebi.ac.uk/RHdb>) and are available on the RHdb and Genoscope websites.

Radiation hybrid assays. We carried out polymerase chain reaction (PCR) amplification of EST fragments from radiation hybrid DNAs in 96-well plates containing the 90 radiation hybrid, control mouse and Chinese hamster DNAs in duplicate. PCR conditions and gel electrophoresis were as described at www.genoscope.cns.fr. We analyzed PCR products by agarose gel electrophoresis, detected them by ethidium bromide staining, and used a semi-automated method to score for the presence or absence of PCR products of the expected size by comparison with molecular standards. The data were recorded as a string of 0 (no amplification of a mouse fragment), 1 (amplification of a mouse fragment) or 2 (ambiguous or unknown) vector scores corresponding to the radiation hybrid DNA order. All loci were scored in duplicate.

Framework map construction. In constructing the framework map, we started with the 1,066 genetic markers typed in common at the Genoscope and at the Whitehead Institute–Massachusetts Institute of Technology⁶. Because of differences in the scoring methods used by the two centers, we considered the typing of a radiation hybrid at each center as two independent assays and joined the vectors (radiation hybrid scores) into a single vector string (concatenated Genoscope–WI-MIT) to increase the overall marker information content and map accuracy. Vectors from both centers were concatenated only if the original vectors contained fewer than 5 unresolved positions and if the marker retention rate was between 14% and 47% (with the exception of chromosomes 11 and 19, for which the ranges were 14–60% and 14–55%, respectively). We removed markers that were too close to each other (as measured by the number of obligate chromosomal breaks) and ordered the remaining markers by analogy to the well-studied traveling-salesman problem (TSP), for which powerful computational tools are available^{26,27}. We translated the radiation hybrid problem into 5 slightly differing versions of the TSP problem that were characterized by minor variations of the objective function. We solved these TSP instances with the Lin–Kernighan (LK) heuristic from the 'CONCORDE' package²⁷ (<http://www.caam.rice.edu/keck/concorde.html>) and compared the resulting marker orders to identify segments conserved in all solutions. We then checked the relative ordering of these conserved segments for consistency against the WI-MIT genetic map¹⁵. The initial framework maps resulting from this process contained 814 markers. We used these markers and 1,369 additional genetic markers that had been typed at the Genoscope to produce extended framework maps. We converted typing data corresponding to the pooled 2,183 genetic markers into TSP instances and solved these using the concorde LK heuristic to obtain temporary comprehensive maps. We then determined the most likely framework interval for each of the 1,369 non-framework markers using a maximum likelihood criterion, and recorded the associated lod score. We submitted this information, along with the previously computed framework maps, to a global reordering algorithm²⁶ that reorders and consolidates the comprehensive maps. We discarded markers with order discordancies under different TSP solutions by applying the algorithm of the longest-common-subsequence problem (LCSP)²⁸. This yielded extended framework maps comprising 1,821 genetic markers.

Because the TSP transformations are strictly valid only for haploid, error-free data, we re-evaluated the map likelihoods and inter-marker distances with the radiation hybrid maxlik program²⁹ under a diploid model. We then applied a pruning routine to the extended framework maps, both to ensure that adjacent markers were not too close to each other and to favor the inclusion of markers with the highest associated lod scores. We discarded 752 markers in this pruning step.

To further extend the new framework maps, we mapped ESTs and non-framework genetic markers typed at Genoscope against the framework maps by multipoint maximum-likelihood analysis. We considered additional markers for inclusion into intervals defined by adjacent framework markers separated by a breakage probability of 0.5 or more. We retained two types of markers for this step: 86 STS markers assigned to such intervals with a lod score of at least 2, and showing a placement consistent with

both the genetic map and the WI-MIT radiation hybrid map⁶; and 79 ESTs that mapped to these intervals and for which all alternative placement intervals were at least 1,000 times less likely. When more than one candidate framework marker was available for a given interval, we applied the following integrating criteria: first, we sorted candidate markers were according to the average difference between their retention rate and that of the adjacent framework marker ones; second, among markers with small retention-rate differences, we selected the marker with the smallest number of ambiguous positions in its typing vector.

Placement map construction. We used both framework markers and genetic markers discarded in the pruning step as reference markers for the chromosomal assignment of ESTs. We considered an EST assigned if it was linked to at least 2 reference markers on a given chromosome with a two-point lod score of 7 or more and showed no linkage above this threshold with a reference marker for another chromosome. The use of a very dense map of reference markers and the imposition of a positive threshold cut-off to at least two reference markers markedly reduces the chances of detecting such linkage purely by chance. Once ESTs had been assigned to chromosomes, we mapped them against the framework intervals by multipoint maximum likelihood analysis²⁹. We ordered markers binned into the same interval according to the radiation hybrid distance from the upper framework marker. For each marker, we recorded all placement intervals for which the odds were higher than 1:1,000 with the top-ranking placement interval; we considered markers for which these intervals were not adjacent to be unreliable, and removed these from the map. We discarded 640 markers through this process, leaving 3,446 markers on the first build of the placement maps.

Whole-mount RNA *in situ* hybridization. We collected mouse embryos from 5.5–9.5 dpc and carried out whole-mount RNA *in situ* hybridization on these embryos¹². We linearized pSPORT1-cDNA plasmid DNA with *Sall* and generated antisense digoxigenin-labeled riboprobes using SP6 RNA polymerase³⁰.

Validation of EST localizations. We used the monochromosomal mouse × human hybrids SN11C5-3/sc1.3, N12C1 and N2C1 to confirm EST localizations to chromosomes 3, 6 and 12, respectively¹⁷. We used genomic DNA from the hybrids for PCR screening of ESTs. We systematically included human DNA as a PCR control. The observed confirmation rate is likely to be a minimal estimate, because ESTs that produced a PCR product on the corresponding monochromosomal hybrid that was different in size from that expected were not scored as being positive, even though these size differences could reflect the fact that control DNA of the mouse parent of the hybrids was not available to us and was replaced by 129/Sv DNA.

Acknowledgments

We dedicate this article to our friend and colleague Rosa Beddington (March 23, 1956–May 18, 2001), a scientist of great biological insight. This work was supported by EEC Contract PL 962414. We thank B. Gorick and the Human Genome Mapping Project at Hinxton, UK, for help with the replication of the 7.5-dpc mouse endoderm library; A.M. Mallon and S. Greenaway of the informatics group at the Medical Research Council, Harwell; and V. Taghavi and E. Sartory for technical assistance in marker typing at MRC Harwell.

Received 12 April; accepted 17 July 2001.

1. Yang, Y.P. & Womack, J.E. Parallel radiation hybrid mapping: a powerful tool for high-resolution genomic comparison. *Genome Res.* **8**, 731–736 (1998).
2. Deloukas, P. *et al.* A physical map of 30,000 human genes. *Science* **282**, 744–746 (1998).
3. Watanabe, T.K. *et al.* A radiation hybrid map of the rat genome containing 5,255 markers. *Nature Genet.* **22**, 27–36 (1999).
4. Steen, R.G. *et al.* A high-density integrated genetic linkage and radiation hybrid map of the laboratory rat. *Genome Res.* **9**, AP1–8 (1999).
5. Scheetz, T.E. *et al.* Generation of a high-density rat EST map. *Genome Res.* **11**, 497–502 (2001).
6. Van Etten, W.J. *et al.* Radiation hybrid map of the mouse genome. *Nature Genet.* **22**, 384–387 (1999).
7. Mellersh, C.S. *et al.* An integrated linkage–radiation hybrid map of the canine genome. *Mamm. Genome* **11**, 120–130 (2000).
8. Murphy, W.J. *et al.* A radiation hybrid map of the cat genome: implications for comparative mapping. *Genome Res.* **10**, 691–702 (2000).
9. Geisler, R. *et al.* A radiation hybrid map of the zebrafish genome. *Nature Genet.*

- 23, 86–89 (1999).
10. Hukriede, N.A. *et al.* Radiation hybrid mapping of the zebrafish genome. *Proc. Natl Acad. Sci. USA* **96**, 9745–9750 (1999).
 11. Dunwoodie, S.L., Henrique, D., Harrison, S.M. & Beddington, R.S.P. Mouse Dll3: a novel divergent Delta gene which may complement the function of other Delta homologues during early pattern formation in the mouse embryo. *Development* **124**, 3065–3076 (1997).
 12. Harrison, S.M., Dunwoodie, S.L., Arkell, R.M., Lehrach, H. & Beddington, R.S.P. Isolation of novel tissue-specific genes from cDNA libraries representing the individual tissue constituents of the gastrulating mouse embryo. *Development* **121**, 2479–2489 (1995).
 13. McCarthy, L.C. *et al.* A first generation whole genome-radiation hybrid map spanning the mouse genome. *Genome Res.* **7**, 1153–1161 (1997).
 14. Breen, M. *et al.* Towards high resolution maps of the mouse and human genomes—a facility for ordering markers to 0.1 cM resolution. *Hum. Mol. Genet.* **3**, 621–627 (1994).
 15. Dietrich, W. F. *et al.* A comprehensive genetic map of the mouse genome. *Nature* **380**, 149–152 (1996).
 16. Elliott, R.W., Manly, K.F. & Hohman, C. A radiation hybrid map of mouse chromosome 13. *Genomics* **57**, 365–370 (1999).
 17. Sabile, A., Poras, I., Cherif, D., Goodfellow, P. & Avner, P. Isolation of monochromosomal hybrids for mouse chromosomes 3, 6, 10, 12, 14 and 18. *Mamm. Genome* **8**, 81–85 (1997).
 18. Gyapay, G. *et al.* A radiation hybrid map of the human genome. *Hum. Mol. Genet.* **5**, 339–46 (1996).
 19. Hudson, T.J. *et al.* A radiation hybrid map of mouse genes. *Nature Genet.* **27**, 201–205.
 20. DeBry, R.W. & Seldin, M.F. Human/mouse homology relationships. *Genomics* **33**, 337–351 (1996).
 21. Nolan, P.M. *et al.* A systematic, genome-wide, phenotype-driven mutagenesis programme for gene function studies in the mouse. *Nature Genet.* **25**, 440–443 (2000).
 22. Hrabe de Angelis, M.H. *et al.* Genome-wide, large-scale production of mutant mice by ENU mutagenesis. *Nature Genet.* **25**, 444–447 (2000).
 23. Kusumi, K. *et al.* The mouse pudgy mutation disrupts Delta homologue Dll3 and initiation of early somite boundaries. *Nature Genet.* **19**, 274–278 (1998).
 24. Parsons, J.D. & Rodriguez-Tome, P. JESAM: CORBA software components to create and publish EST alignments and clusters. *Bioinformatics* **16**, 313–325 (2000).
 25. Rodriguez-Tome, P. & Lijnzaad, P. RHdb: the Radiation Hybrid Database. *Nucleic Acids Res.* **28**, 146–147 (2000).
 26. Agarwala, R., Applegate, D.L., Maglott, D., Schuler, G.D. & Schaffer, A.A. A fast and scalable radiation hybrid map construction and integration strategy. *Genome Res.* **10**, 350–364 (2000).
 27. Applegate, D., Bixby, R., Chvatal, V. & Cook, W. On the solution of traveling salesman problems. *Documenta Mathematica Journal der Deutschen Mathematiker-Vereinigung International Congress of Mathematics III*, 645–656 (1998).
 28. Gusfield, D. Algorithms on strings, trees, and sequences: computer science & computational biology (Cambridge University Press, Cambridge, UK, 1997).
 29. Boehnke, M., Lange, K. & Cox, D.R. Statistical methods for multipoint radiation hybrid mapping. *Am. J. Hum. Genet.* **49**, 1174–1188 (1991).
 30. Wilkinson, D.G. Whole-mount *in situ* hybridisation of vertebrate embryos. in *In Situ Hybridisation* (ed. Wilkinson, D.G.) 75–83 (Oxford University Press, Oxford, UK, 1992).
 31. Bruls, T. *et al.* A physical map of human chromosome 14. *Nature* **409**, 947–948 (2001).

ISSN 1088-9051

December 2003

GENOME RESEARCH

Volume 13 Number 12

Mouse Embryonic Gene Expression ♦ Human Genome
Pseudogenes ♦ Honey Bee Defense Behavior Genetics ♦ Zebrafish
Mutagenesis ♦ Sugarcane Gene Annotation

Cold Spring Harbor
Laboratory Press



Can You Compare?



Our Universal Reference RNA sets the standard for microarray analysis, enabling comparison across multiple sets of data. Pooled from cell lines, our collection of human, mouse, and rat reference RNA provides high-quality total RNA for microarray gene-expression profiling.



- *Human, mouse, rat RNA*
- *Diverse gene representation*
- *High-quality total human, mouse and rat RNA*
- *Industrial lots for long-range experiments*



For more information, please visit www.stratagene.com/microarrays.

Universal Reference RNA

**THE STANDARD FOR
MICROARRAY RESEARCH**

STRATAGENE USA and CANADA
ORDER: (800) 424-5444 x3
TECHNICAL SERVICES: (800) 894-1304

STRATAGENE EUROPE
ORDER: 00800 7000 7000
TECHNICAL SERVICES: 00800 7400 7400
FAX: 00800 7001 7001
MAIN OFFICE PHONE: +31 (0)20 312 5600
MAIN OFFICE FAX: +31 (0)20 312 5700

www.stratagene.com

Universal Human Reference RNA	400 µg	740000
Universal Mouse Reference RNA	400 µg	740100
Universal Rat Reference RNA	400 µg	740200



Characterizing Embryonic Gene Expression Patterns in the Mouse Using Nonredundant Sequence-Based Selection

Rita Sousa-Nunes,^{1,10} Amer Ahmed Rana,^{1,10,7} Ross Kettleborough,^{1,10}
Joshua M. Brickman,^{1,8} Melanie Clements,¹ Alistair Forrest,² Sean Grimmond,²
Philip Avner,³ James C. Smith,^{4,11} Sally L. Dunwoodie,^{1,5,6,11}
and Rosa S.P. Beddington^{1,9}

¹Division of Mammalian Development, National Institute for Medical Research, The Ridgeway, London NW7 1AA, United Kingdom; ²Institute of Molecular Bioscience, University of Queensland, 4072 Australia; ³Unité Génétique Moléculaire Murine, Institut Pasteur, 75015 Paris, France; ⁴Wellcome Trust/Cancer Research UK Institute and Department of Zoology, University of Cambridge, Cambridge CB2 1QR, United Kingdom; ⁵Developmental Biology Program, Victor Chang Cardiac Research Institute, Darlinghurst, 2010, Australia; ⁶Department of Biotechnology and Biomolecular Sciences, University of New South Wales, Kensington, NSW 2033, Australia

This article investigates the expression patterns of 160 genes that are expressed during early mouse development. The cDNAs were isolated from 7.5 d postcoitum (dpc) endoderm, a region that comprises visceral endoderm (VE), definitive endoderm, and the node-tissues that are required for the initial steps of axial specification and tissue patterning in the mouse. To avoid examining the same gene more than once, and to exclude potentially ubiquitously expressed housekeeping genes, cDNA sequence was derived from 1978 clones of the *Endoderm* library. These yielded 1440 distinct cDNAs, of which 123 proved to be novel in the mouse. In situ hybridization analysis was carried out on 160 of the cDNAs, and of these, 29 (18%) proved to have restricted expression patterns.

[Supplemental material is available online at www.genome.org.]

The genomic sequences of many animals are now known, including *C. elegans*, human, mouse, and *Drosophila* (The *C. elegans* genome consortium 1998; Adams et al. 2000; Lander et al. 2001; Venter et al. 2001; Aparicio et al. 2002; Carlton et al. 2002; Dehal et al. 2002; Gardner et al. 2002; Waterston et al. 2002), and the sequences of others will be available very soon. The task now facing biologists is to discover the functions of the genes that have been identified through these sequencing projects. For some organisms, such as *C. elegans*, it is possible to adopt a systematic approach to ablating gene function (Fraser et al. 2000; Kamath et al. 2003). For vertebrates, and especially mammals, a systematic approach of this sort is a daunting prospect, but a widespread analysis of gene function is nevertheless essential for a proper understanding of development and disease.

The most tractable mammalian species for such an analysis is the mouse, in which it is possible to mutate gene function randomly, by using γ -irradiation, chemical mutagenesis or gene traps (Stanford et al. 2001), or a directed fashion by means of homologous recombination in embryonic stem cells (Doetschman et al. 1987; Thomas and Capecchi 1987). Mutagenesis has proved a very useful approach, but it is limited in some

respects because redundancy or compensation may mask functional requirements and because early lethality may conceal later roles of some genes. The necessity to maintain large numbers of mutant strains also presents practical difficulties.

Homologous recombination overcomes these problems by allowing the ablation of specific genes at particular times in development and in a tissue-specific manner. It is not yet feasible, however, to contemplate targeting the entire proteome in this way, so it is necessary to decide which genes to target first. Work from several species indicates that one criterion might be based on gene expression patterns. In situ hybridization analyses of random clones from unmodified, normalized, or subtracted cDNA libraries has identified many genes with restricted expression patterns that hint at particular embryonic functions (Gawantka et al. 1998; Neidhardt et al. 2000; Christiansen et al. 2001; Kudoh et al. 2001). In addition, the results have allowed the definition of "synexpression groups," the members of which are expressed in similar patterns and may be regulated in similar ways and act in the same molecular pathways (Gawantka et al. 1998; Niehrs and Pollet 1999).

In this article we refine this approach by using sequence comparisons to reduce cDNA library complexity and to remove unwanted molecules (see below). We use a cDNA library constructed from 7.5 d postcoitum (dpc) endoderm (Harrison et al. 1995), a region that comprises VE, definitive endoderm, and the node-tissues that are required for the initial steps of axial specification and tissue patterning in the mouse embryo (Beddington and Robertson 1999; Lu et al. 2001; Hamada et al. 2002). This *Endoderm* library, together with four others (whole *Embryonic Region*, *Ectoderm*, *Mesoderm*, and *Primitive Streak*), has already proved its worth in subtractive and differential hybridization experi-

Present addresses: ⁷Wellcome Trust/Cancer Research UK Institute, Cambridge CB2 1QR, UK; ⁸Institute for Stem Cell Research, The University of Edinburgh, Edinburgh EH9 3JQ, UK.

⁹Deceased May 18, 2001.

¹⁰These authors contributed equally to the work described.

¹¹Corresponding authors.

E-MAIL jim@welc.cam.ac.uk; FAX 44-1223-33413.

E-MAIL s.dunwoodie@victorchang.unsw.edu.au; FAX: 61-02-9295-8501.

Article and publication are at <http://www.genome.org/cgi/doi/10.1101/gr.1362303>. Article published online before print in November 2003.

Table 1. Summary of Endoderm Sequence Analysis

cDNA clones selected for sequencing	3072
Successful single pass sequence	2635
Masked sequences >199 base pairs in length	1978
Sequences matching ENSEMBL genes	1355
Sequences matching TIGR-TC EST clusters only	496
Novel sequences	127
Nonredundant clones matching mouse ESTs	1317
Nonredundant novel clones	123

ments that have identified regionally expressed genes that are required for normal development (Harrison et al. 1995, 2000; Dunwoodie et al. 1997, 1998, 2002; Dunwoodie and Beddington 2002; Martinez Barbera et al. 2002).

Analysis of 1978 sequences derived from the endoderm library identified 1440 different cDNAs, of which 123 proved to be novel in the mouse. In situ hybridization analysis was carried out on 160 of the cDNAs, and of these, 18% proved to have restricted expression. This work provides valuable information about the repertoire of gene expression in the endoderm of the mouse embryo and may supply pointers as to which genes merit further investigation concerning their roles in development and disease (Anderson and Beddington 1997).

RESULTS

Sequence Analyses

cDNA clones (3072) were selected at random from the *Endoderm* library, and 2635 sequence tags were generated by single-pass 3'

sequencing (Avner et al. 2001). Repetitive and poor-quality sequence was masked, and any sequence tag of <199 nucleotides after masking was discarded. Analysis of the remaining 1978 sequences is presented in Table 1. Each sequence was compared by using BLASTN with mouse expressed sequence tag (EST) clusters (TIGR Tentative Consensus sequences or TCs version 8.0, June 1, 2002; <http://www.tigr.org/tdb/tgi/mgi>) and with predicted mouse transcripts in ENSEMBL (version 8.3c.1, July 12, 2002; http://www.ensembl.org/Mus_musculus/). Sequence matches were considered significant if alignment of >50 nucleotides was observed and the significance value was less than e^{-30} . All remaining sequences were considered novel.

Of the 1978 sequences, 1851 clones matched a defined EST (TIGR-TC) cluster, an ENSEMBL gene or transcript, or both. The remaining 127 clones matched neither data set and are classified as novel. Clustering of the 1851 sequences that matched the TIGR-TC or EMSEMBL databases generated a non-redundant set of 1317 known cDNAs. The 127 novel sequences were compared with each other by using BLASTN, using significance limits similar to those described above. This procedure reduced the number of novel cDNAs to 123. All sequences described in this article are available in GenBank, and cDNAs can be obtained from the UK Human Genome Mapping Project Resource Centre (http://www.hgmp.mrc.ac.uk/geneservice/reagents/products/cdna_resources/index.shtml).

Expression Analysis

Of the 1978 cDNAs described above, 160 were chosen for expression analysis. Clones were selected so as to exclude housekeeping genes and genes previously studied in a developmental context,

Table 2. Sequence Analysis of cDNA Clones With Restricted Expression

Sequence ID	Frequency	Representative ID	Description
t8219b01	1		
t7822b10	2	ENSMUSG00000013236	Protein-tyrosine phosphatase, receptor-type (Ptp9; EC 3.1.3.48)
r8220b29	1	TC469486	
s8609b60	2	ENSMUSG00000019970	Serum and glucocorticoid-regulated kinase (Sgk; EC 2.7.1)
m8708a09	4	ENSMUSG00000021728	Embigin precursor, also known as Teratocarcinoma glycoprotein 70 (GP-70)
v8130b53	9	TC461859	Solute carrier family 2 (facilitated glucose transporter) member 3 (Slc2a3)
t7825b42	3	TCS11260	Sp120 (Hnrpu)
s8609b24	1	ENSMUSG00000039878	Similar to LIV-1, estrogen-regulated
r8316a33	1	ENSMUSG00000024253	Dynein 2 light intermediate chain (mD2LIC)
v8130b25	1	ENSMUSG00000028162	
r8707a53	3	ENSMUSG00000023906	Claudin-6
m8708a22	1	ENSMUSG00000039676	Calcyphosine
p7822b53	1	ENSMUSG00000005505	Weakly similar to ring canal protein; contains BTB/POZ domain
t8130b59	1	TC503400	
t8417b56	1	ENSMUSG0000002764	Neuronatin, also known as Peg5 (isoform 2)
t8219b25	1	TC488224	Similar (16%) to KIAA0802 protein (<i>Homo sapiens</i>)
w8609b57	1	ENSMUSG00000029032	Neuroblastoma; similar to Rho GEF 16;
t7822b19	1	ENSMUSG00000021681	Paternally expressed gene 3 (Peg3)
k8709a24	1	ENSMUSG00000031665	Sal-like 1 (Sall1)
r8220b09	1	TCS01397	Silica-induced gene 41 (Silg41); similar to arg/ser-rich splicing factor (transformer2)
t8130b26	1	ENSMUSG00000042142	Rb-binding protein 2 (Rb-BP2); also known as Plu-1
m8708a39	1	ENSMUSG00000022761	Leucine-zipper-like transcriptional regulator 1 (Lztr1)
s8129b58	1	ENSMUSG00000026833	Pancortins 1 and/or 3
k8220b03	1	ENSMUSG00000029381	Shroom (actin binding protein) (Shrm)
r8220b57	1	ENSMUSG00000005566	Transcription intermediary factor 1- β (Tif1- β)
r8319a44	2		14-3-3 protein σ
k8709a20	2	ENSMUSG00000020849	14-3-3 protein ϵ (protein kinase C inhibitor protein-1)
k8710a07	1	ENSMUSG00000021667	Nop seven associated protein 2 (Nsa2p); also known as Lnr42, TINP1 or HCLG1
t8219b26	1	ENSMUSG00000032376	Ubiquitin-specific protease 3 (Ubp7)

The table shows 29 cDNAs with restricted patterns of expression. The clones are shown in the same order as in Figure 1, with the first three being members of the visceral endoderm synexpression group. Headings represent (1) the sequence identification number, (2) the number of times the sequence was isolated, (3) the ENSEMBL gene number of the cDNA or its TIGR Cluster number, and (4) gene name or family. Genes for which no description is appended bear no resemblance to any other in the databases.

A

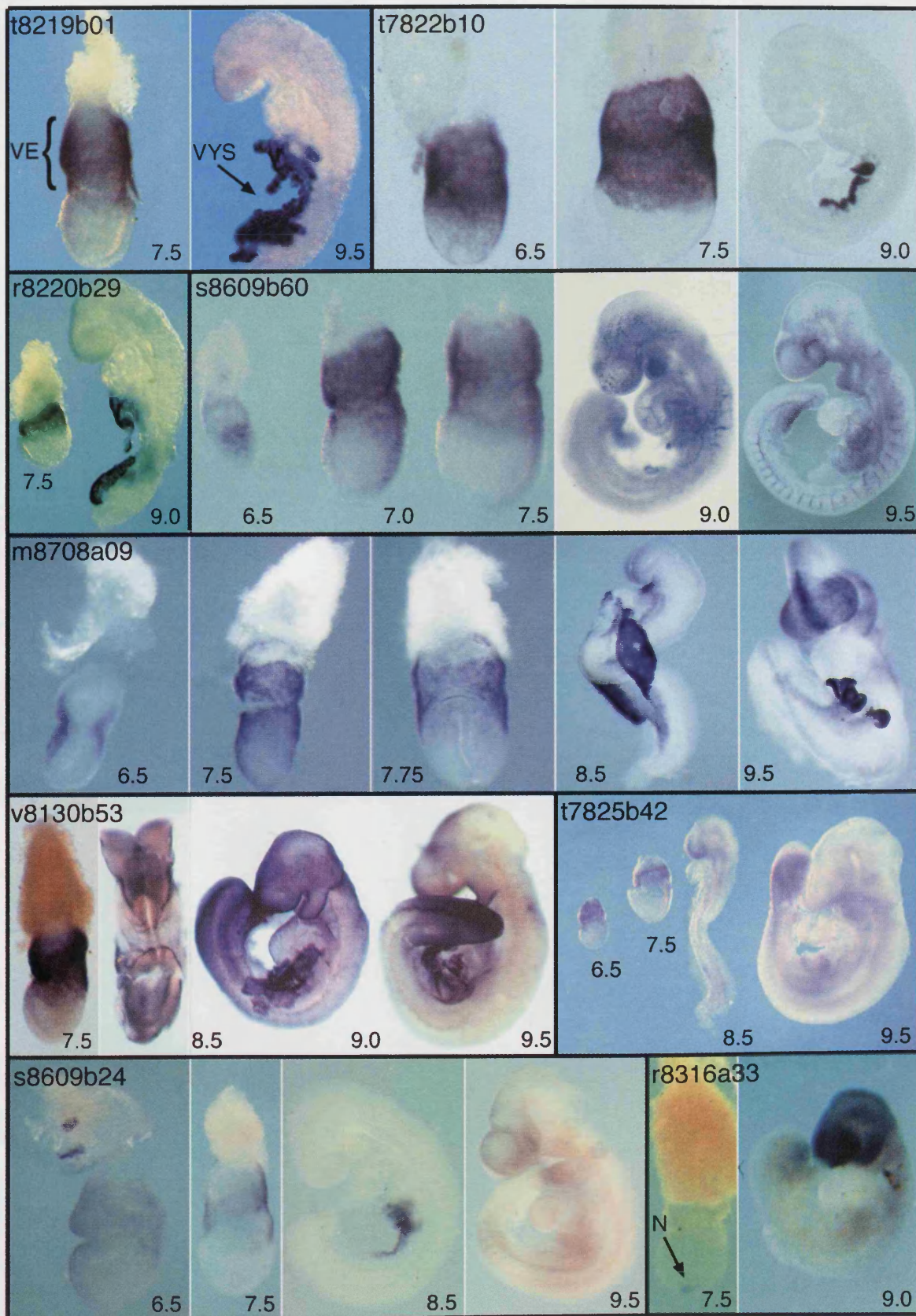


Figure 1 (Continued on next page)

B

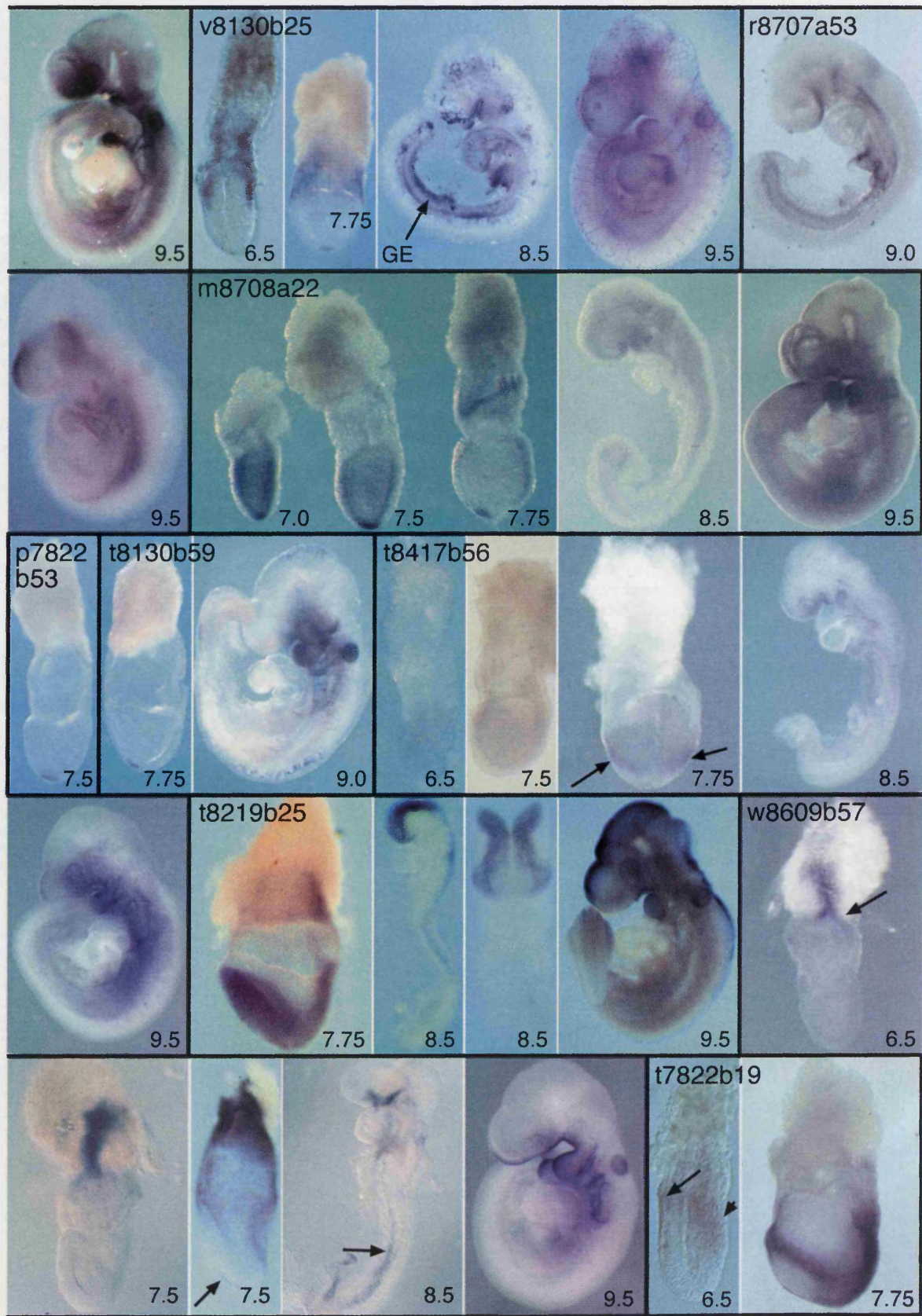


Figure 1 (Continued on next page)

C

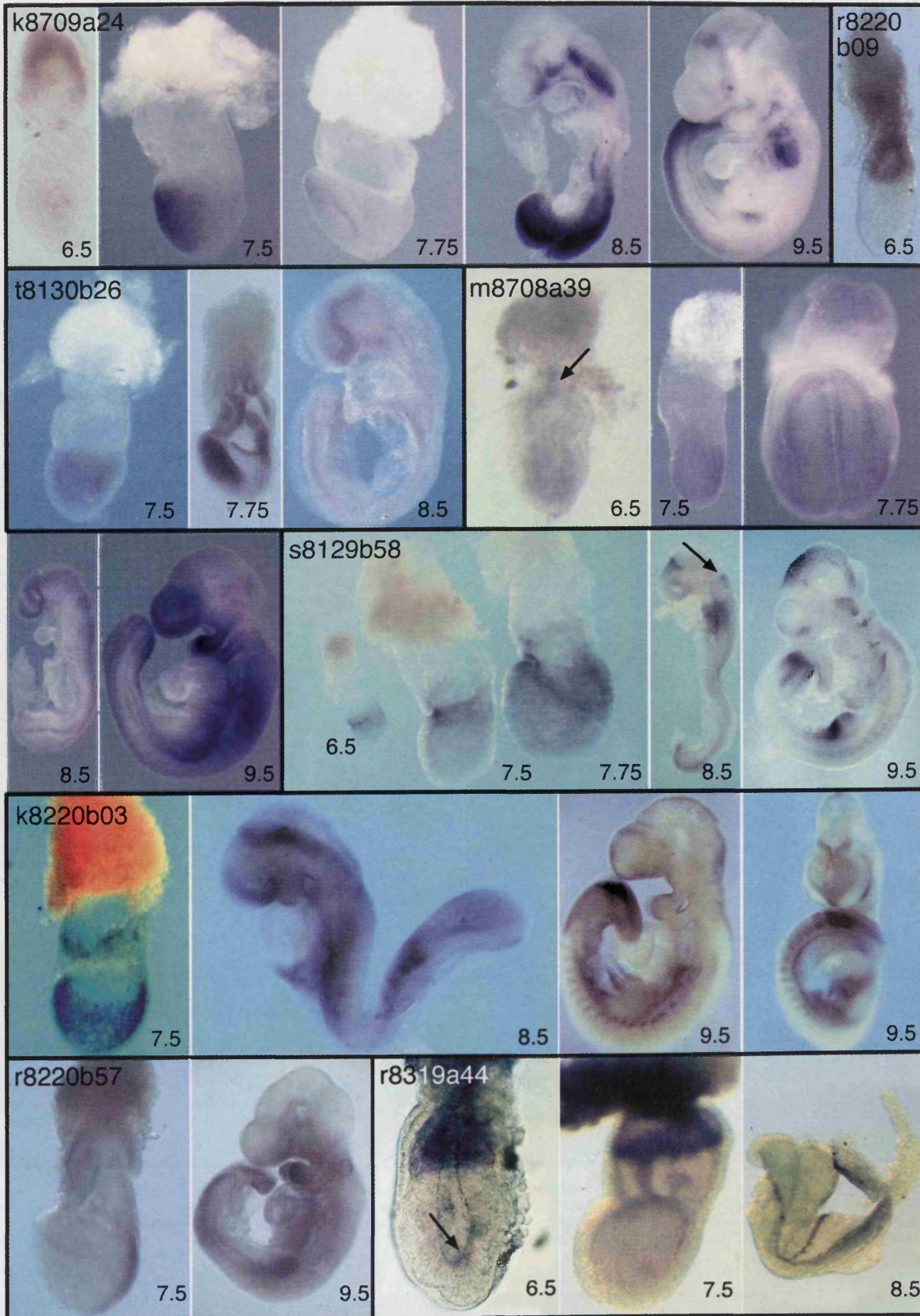


Figure 1 (Continued on next page)

D

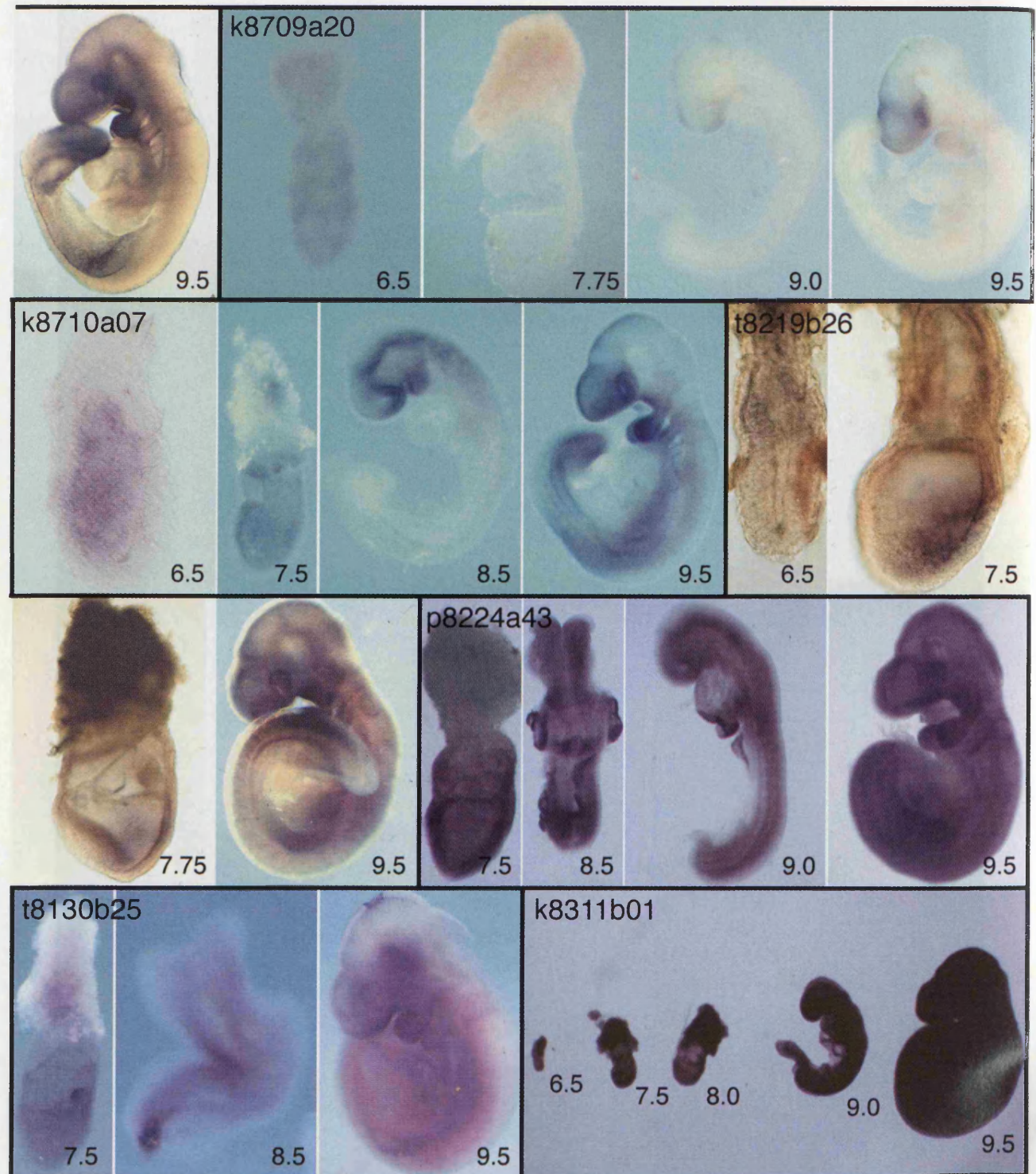


Figure 1 Images of the expression patterns of all the "restricted" genes (beginning with the three genes in the synexpression group), two of the widespread cDNAs, and one ubiquitously expressed sequence. Images representing individual clones are enclosed by black lines; sequence identifiers and other information are indicated on the figures. A more detailed description of the expression patterns, together with explanations of the annotations, is provided in the Appendix. The restricted genes are listed in the same order as in Table 2.

but to include completely novel sequences, previously unknown sequences that had also been identified in other organisms, cDNAs encoding putative transcriptional regulators, splicing fac-

tors, signaling molecules, cell-cycle regulators, cytoskeletal proteins, and cDNAs encoding homologs of proteins implicated in human disease (for examples, see Table 2).

Table 3. Coexpression Groups

Coexpression group	Clones
Visceral endoderm	s8609b60, m8708a09, v8130b53, t7825b42, s8609b24, v8130b25
Node	v8130b25, r8316a33, m8708a22, p7822b53, t8130b59
Gut endoderm	v8130b25, r8707a53

The three coexpression groups are based on the constituent tissues of the 7.5-dpc mouse embryo. Only genes with restricted expression patterns are included.

Expression patterns were categorized subjectively as "ubiquitous" (64; 40%) if similar levels of expression were observed in all tissues, as "widespread" (57; 36%) if expression was observed in several but not all tissues (frequently with different levels in different tissues), as "restricted" (29; 18%) if transcripts were localized to just a few regions in at least one of the stages examined, and as "undetectable" (10; 6%). The expression patterns of all the restricted cDNAs and of one ubiquitous and two widespread clones are illustrated in Figure 1 and described in the Appendix. Details of the restricted cDNAs are summarized in Table 2, which lists the clones in the same order as in Figure 1, with the first three being members of the visceral endoderm synexpression group (see below). A Supplement to Table 2 (available online at www.genome.org) lists the cDNAs with widespread and ubiquitous expression.

Of the 29 restricted expression patterns identified, 22 are expressed in the tissues from which the library was made, of which three (t8219b01, t7822b10, and r8220b29) are exclusively expressed in these tissues. Seven genes were not expressed at detectable levels in the source tissues (w8609b57, r8220b09, t8130b26, m8708a39, r8220b57, r8319a44, t8219b26). Examination of the restricted expression patterns revealed just one group of genes with a similar expression pattern at all stages examined (6.5–9.5 dpc). This synexpression group (Niehrs and Pollet 1999) comprises the three clones, t8219b01, t7822b10, and r8220b29, that are expressed exclusively in the tissues from which the *Endoderm* library was constructed. All three are expressed in VE at 6.5 and 7.5 dpc and in the yolk sac at 8.5 and 9.5 dpc (Fig. 1). Of the three, only t7822b10 has been described previously. It en-

codes a receptor-type protein tyrosine phosphatase termed *Ptpt9*, the loss of function of which causes abnormalities of the central and peripheral nervous systems and of the neuroendocrine system (Elchebly et al. 1999; Wallace et al. 1999; Batt et al. 2002). We do not know whether the three genes have related functions, because no known motifs have been identified in t8219b01 or r8220b29. *Ptpt9* maps to chromosome 17 (54.5Mb), whereas t8219b01 maps to chromosome 8 (60.6Mb) and r8220b29 to chromosome 5 (127.4Mb). The coordinated expression of the three genes is therefore unlikely to be a consequence of their genomic organization.

In addition to this single synexpression group, we have also identified three "coexpression groups," all members of which are expressed in the same tissue at a particular stage of development and therefore may cooperate in the specification of that tissue in which they are expressed. Members of a coexpression group may also be expressed in other regions, and their expression patterns at earlier and later stages may also diverge. In defining these groups, we omit the ubiquitously expressed and widespread clones (which are likely to have housekeeping functions), and focus particularly on the signaling centers in the 7.5-dpc embryo from which the *Endoderm* library was derived. Thus, Table 3 lists the clones expressed in the VE coexpression group (the largest) and the node and definitive endoderm coexpression groups.

DISCUSSION

Endoderm cDNA Sequence Analysis

At 7.5 dpc, the endoderm that surrounds the embryonic region of the mouse conceptus, from which the endoderm library is derived, is a single layer of ~700 cells (Snow 1977). This tissue comprises the node (which is required to establish the anterior-posterior, dorso-ventral, and left-right axes of the embryo), VE (which is important for nutrient exchange and for initiating anterior patterning), and the definitive endoderm (which is also involved in anterior patterning; Anderson and Beddington 1997; Beddington and Robertson 1999; Bielinska et al. 1999; Lu et al. 2001; Hamada et al. 2002). The node, VE, and definitive endoderm go on to form the notochord and floor plate of the neural tube, yolk sac endoderm, and gut endoderm (GE) respectively.

Although the mouse genome has been almost completely sequenced (Waterston et al. 2002), our data indicate that transcript identification is incomplete. Indeed, sequencing of just

Table 4. Frequency of Selection of Restricted cDNAs in Different Expression Screens

Reference	Species	Stages screened	cDNA library	Library type	Number of clones screened	Restricted cDNAs
This study	Mouse	6.5–9.5 dpc	7.5-dpc endoderm	Parent	160	18%
Neidhardt et al. 2000	Mouse	9.5 dpc	9.5-dpc embryo	Parent	989	6%
Neidhardt et al. 2000	Mouse	9.5 dpc	9.5-dpc embryo	Subtracted	3737	7%
Neidhardt et al. 2000	Mouse	9.5 dpc	9.5-dpc embryo	Normalized	622	18%
Reymond et al. 2002	Mouse	9.5 dpc	Orthologues of human chromosome 21 genes	—	158	21%
Reymond et al. 2002	Mouse	10.5 dpc	idem	—	158	28%
Reymond et al. 2002	Mouse	14.5 dpc (sections)	idem	—	158	42%
Gitton et al. 2002	Mouse	9.5 dpc	idem	—	158	21%
Christiansen et al. 2001	Chick	HH* 9–12	Hindbrain HH* 10–11 ^a	Subtracted	445	8%
Kudoh et al. 2001	Zebrafish	Shield, 3 somites, 15 somites, 24 hpf	Early somitogenesis embryo	Normalized	2765	13%
Gawantka et al. 1998	<i>X. laevis</i>	Stages 10+, 13, 30	Neurula stage embryo	Parent	1765	25% ^b

^aStage according to Hamburger and Hamilton (1951).

^bThis figure is reduced to 16% if one considers only unique cDNAs with a restricted expression pattern.

1978 clones of the *Endoderm* library has identified no fewer than 123 novel cDNAs. Therefore, our work provides a valuable source of ESTs, which will be useful in functional genomic projects and expression profiling. Further sequencing of the library will be required to draw conclusions about the complexity of gene expression in the endoderm, but we note that two-thirds of the 1978 sequences analyzed were represented only once, indicating that many more transcripts remain to be isolated from the original 5.8×10^5 independent clones (Harrison et al. 1995).

Endoderm cDNA Expression Analysis

In this article we have studied the expression patterns of 160 cDNAs derived from a mouse endoderm cDNA library. Our screen differs from related screens (Gawantka et al. 1998; Neidhardt et al. 2000; Christiansen et al. 2001; Kudoh et al. 2001) because cDNAs were sequenced and clustered before carrying out expression analyses. This ensured that each transcript was studied only once, an important issue when analyzing mouse development because obtaining mouse embryos at the appropriate stages is more costly and time-consuming than doing the same in chicken, frog, or fish.

Many transcripts proved to have ubiquitous or widespread expression patterns, but the expression of 29 (18%) was restricted to particular tissues at least in one of the time points examined. Such cDNAs are of interest because they may provide useful molecular markers for those tissues and because their expression patterns may provide hints as to their developmental functions.

A sequence-based approach such as that taken here may assist in the identification of cDNAs with restricted expression patterns. In addressing this point, it is difficult to make direct comparisons with other screens because definitions of "restricted" may vary, because other screens have used different species at different stages, and because of the way in which cDNA clones were selected. Nevertheless, screens that have selected cDNAs at random, whether using parent libraries or even subtracted cDNA libraries, have tended to obtain lower proportions of restricted expression patterns than those described in this article (Table 4; Neidhardt et al. 2000; Christiansen et al. 2001; Kudoh et al. 2001). In contrast, a screen making use of a library normalized by colony hybridization rather than by sequence analysis (Neidhardt et al. 2000) obtained a very similar proportion to that reported here, emphasizing the importance of normalization in screens of this sort, especially when material might be limiting. We opted to use of the parent cDNA library rather than a subtracted version so as to avoid the loss of rare clones. Interestingly, a similar percentage of restricted patterns at 9.5 dpc was obtained in an expression analysis of murine orthologs of all genes on human chromosome 21 (Gitton et al. 2002; Raymond et al. 2002).

One benefit of a screen such as this is that it enables the definition of sets of coregulated genes, or "synexpression groups" (Niehrs and Pollet 1999) as well as coexpression groups. In defining such groups, we omit widespread and ubiquitous clones so as to exclude "housekeeping" genes. As described above, we found a single synexpression group, which comprises genes expressed in the VE at 6.5 and 7.5 dpc and in the yolk sac at 8.5 and 9.5 dpc. In addition, we defined coexpression groups for VE, node, and GE. Each coexpression group contains the genes that are expressed in the tissue in question at 7.5 dpc (Table 3), with the VE group containing six clones; the node group, five clones; and the definitive gut group, two clones. Members of a coexpression group may cooperate in the specification or function of the tissue in question.

METHODS

Endoderm cDNA Sequence Analysis

Clones from the *Endoderm* library were randomly picked and gridded into 384-well plates (Genetix Ltd) using an automated colony picker (Meier-Ewert et al. 1993). They were sequenced from the 3' end, vector sequence was removed, and repeats and regions of poor quality were masked by using PHRED (<http://www.phrap.org/phrap.docs/phred.html>). Sequences containing <200 nucleotides were not analyzed further. Sequence data have been submitted to the EMBL database.

BLASTN (NCBI: <ftp://ftp.ncbi.nih.gov/blast/executables/>) was used to compare each sequence with two publicly available mouse gene data sets: the ENSEMBL gene predictions for mouse (version 8.3c.1, July 12, 2002; http://www.ensembl.org/Mus_musculus) and the TIGR Gene Index (TIGR-Tentative Consensus sequences or TCs version 8.0, June 1, 2002; <http://www.tigr.org/tdb/tgi/mgi/>). Alignments were inspected manually, and possible homology or novelty was further investigated by using BLASTP (NCBI: <ftp://ftp.ncbi.nih.gov/blast/executables/>). Sequences that failed to match an ENSEMBL gene or a TIGR TC were considered as potentially novel. To determine redundancy within the clone set, sequences that mapped to the same ENSEMBL predicted gene were considered redundant. Similarly, sequences that lacked an ENSEMBL mapping but shared the same TIGR TC were considered redundant. Sequences that failed to map to an ENSEMBL prediction or a TIGR TC were considered nonredundant.

RNA In Situ Hybridization

Mouse embryos were collected from CBA/Ca \times C57B110 or C57BL6 \times C57BL6 matings at 6.5, 7.5, 8.5, and 9.5 dpc. Extra-embryonic membranes were removed in M2 medium (Hogan et al. 1994) containing 10% fetal calf serum. Embryos were fixed overnight in 4% paraformaldehyde (PFA) in phosphate buffered saline (PBS) at 4°C, after which they were dehydrated in increasing concentrations of methanol in PBS and stored in 100% methanol at -20°C until use. Antisense RNA probes were generated as described (Harrison et al. 1995) and whole-mount RNA in situ hybridization (WISH) was performed according to the method of Wilkinson (1992). Hybridization conditions were those of Rosen and Beddington (1993), except that embryo powder was omitted from the procedure, and treatment with 10 mg/mL proteinase K was 5 min for embryos at 6.5 to 7.5 dpc and 12 min for embryos at 8.5 to 9.5 dpc. Embryos were processed in 12-well plates (Costar) in 12- μm mesh nets for embryos at ≤ 7.5 dpc, and 74- μm mesh nets for embryos at ≥ 8.5 dpc. At least three embryos of each stage were examined for each probe, and restricted expression patterns were confirmed by an independent set of hybridizations. After stopping the staining reaction, embryos were postfixed in 4% PFA, 0.1% glutaraldehyde in PBS for 1 h at room temperature and stored in 0.4% PFA at 4°C. Photographs were taken by using a dissecting microscope (Nikon) and tungsten film (Kodak 64T). Images were digitized by using a Polaroid SprintScan 35 scanner.

ACKNOWLEDGMENTS

Dedicated to the memory of Rosa Beddington (March 23, 1956 to May 18, 2001).

This work was supported by an MRC Special Project Grant (G9118913) and EEC Contract PL 962414. S.G. is an NHMRC RD Wright Fellow. R.S.-N. is a Gulbenkian PhD Program in Biology and Medicine student and was funded by the Portuguese Foundation for Science and Technology. J.M.B. was supported by a Human Frontier Science Programme Long Term Fellowship. S.L.D. is a Pharmacia Foundation of Australia Senior Research Fellow. We are grateful to B. Gorick and the Human Genome Mapping Project at Hinxtton UK for help with replication of the 7.5-dpc mouse endoderm library, and to Michael Wiles and Patricia Ruiz for initial sequence analysis. We also thank Simon Bullock, Juan Pedro Martinez Barbera, and Tristan Rodriguez for

their help and advice throughout the course of this work and their comments on the manuscript. "Restricted" expression patterns have been submitted to the Mouse Gene Expression database (GXD) <http://www.informatics.jax.org/mgihome/GXD/aboutGXD.shtml>.

The publication costs of this article were defrayed in part by payment of page charges. This article must therefore be hereby marked "advertisement" in accordance with 18 USC section 1734 solely to indicate this fact.

APPENDIX

Expression Patterns of "Restricted" cDNAs

t8219b01

At the mid streak stage, expression of clone *t8219b01* is detected in the VE. Expression at later stages is restricted to the visceral yolk sac (VYS).

t7822b10

At 6.0 dpc, *Ptpt9* expression is restricted to the VE and later to the VYS. Loss of function of this gene has been reported to cause abnormalities of the central and peripheral nervous systems and of the neuroendocrine system (Elchebly et al. 1999; Wallace et al. 1999; Batt et al. 2002).

r8220b29

At the mid streak stage, clone *r8220b29* expression is detected in the VE (7.5 dpc). Expression at later stages (9.0 dpc) is restricted to the VYS.

s8609b60

At the onset of gastrulation, *Sgk* is strongly expressed in the VE overlying the nascent mesodermal wings and, more weakly, in the mesoderm itself. Transcripts are also detected in the VE overlying the extra-embryonic ectoderm. As gastrulation proceeds, the latter domain of expression becomes more robust, and in the embryo proper, it is strongest in the regions juxtaposing the primitive streak. At 8.5 and 9.5 dpc, *Sgk* transcripts are found in the vasculature as well as in the eye and branchial arches. Loss of function of this gene reduces the ability of mice to reduce Na⁺ excretion when subjected to dietary NaCl restriction (Wulff et al. 2002). The expression pattern of *Sgk* has been described by Lee and colleagues (2001).

m8708a09

At 6.5 dpc, *Embigin* is strongly expressed in the VE at the junction between extra-embryonic and embryonic portions of the conceptus. By 7.5 dpc, expression occurs throughout the VE and, more weakly, in the definitive endoderm. At head-fold stages, *Embigin* transcription occurs in anterior definitive endoderm, with strong expression also detectable in the VE. At 8.5 dpc, transcripts are present in the forebrain neuroepithelium, the foregut diverticulum, and the yolk sac. By 9.5 dpc, expression is strong in forebrain neuroepithelium (especially in the dorsal midline) and also occurs in the mid- and hindbrain. Transcripts are also detectable in branchial arches and the nephrogenic cord. The early expression pattern of this gene has been described by Shimono and Behringer (1999); later stages, by Fan and colleagues (1998).

v8130b53

At the late gastrula stage, strong expression of *Slc2a3* is detected in the VE (7.5 dpc). Later, expression is seen in the surface ectoderm (8.5 and 9.0 dpc) and the VYS. As development proceeds, expression in surface ectoderm persists but decreases anteriorly. Expression in the yolk sac is still detectable at 9.5 and 10.5 dpc (data not shown).

t7825b42

At egg cylinder stages, mouse *Sp120* is most strongly expressed in the extra-embryonic half of the conceptus, with only weak expression in the embryonic half, mostly in the primitive streak. At

8.5 and 9.5 dpc, robust expression is seen in the tailbud and presomitic mesoderm, when transcripts are also present in ventral forebrain, branchial arches, and the limb buds.

s8609b24

At egg cylinder stages, expression of *s8609b24* occurs in the VE overlying the extra-embryonic portion of the conceptus and the most proximal region of the epiblast. At 6.5 dpc, VE expression covers most of the conceptus, although it is weaker distally and completely absent from the most proximal region. At 7.5 dpc, expression persists in the progeny of the VE cells, coming to lie over the extra-embryonic ectoderm; transcripts are still absent from the most proximal VE. By 8.5 dpc, expression is confined to the yolk sac, but at 9.5 dpc, there is widespread, albeit weak, expression in the embryo proper, particularly in the forebrain, anterior midbrain, branchial arches, and gut.

r8316a33

mD2LIC expression is first detected in the node at the mid to late streak stage. Expression persists in the node at the late neural plate/early head-fold stage, but is reduced by the eight-somite stage when widespread expression is detectable throughout the embryo (data not shown). This widespread expression persists and becomes stronger in the 25-somite stage embryo. By 11 dpc, expression is detected in GE and the heart (data not shown).

v8130b25

At 6.5 dpc, expression of *v8130b25* is restricted to the VE overlying the embryonic and extra-embryonic ectoderm. By 7.5 dpc, expression is observed in the node, and at 8.5 dpc, this gene is strongly expressed in the VYS, GE, and developing blood cells. By 9.5 dpc, expression is associated with the vasculature, heart, branchial arch, and brain.

r8707a53

Expression of *Claudin-6* is detectable in the forebrain, in the VYS, and throughout the GE from 9.0 dpc. At 9.0 dpc, expression in the forebrain is predominantly ventral, whereas at 9.5 dpc, it is mainly dorsal.

m8708a22

Calcyphosine is weakly expressed in extra-embryonic ectoderm at 6.5 dpc (data not shown). At 7.0 dpc, expression occurs throughout the extra-embryonic ectoderm and the epiblast, with maximal expression in the node. During elongation of the streak, highest expression is seen in the node. At 8.5 and 9.5 dpc, expression is ubiquitous.

p7822b53

Expression of *p7822b53* is restricted to the node of the gastrulating embryo.

t8130b59

Expression of clone *t8130b59* is detectable in the node at 7.5 dpc and in the branchial arches and otic vesicles at 9.5 dpc.

t8417b56

At 6.5 dpc, *Neuronatin* is expressed weakly in the embryonic half of the conceptus. By 7.0 dpc, transcripts are present throughout the mesoderm and ectoderm, and maximal expression is then seen in the posterior head-folds (arrows). At 8.5 to 9.5 dpc, *Neuronatin* expression is detectable in the ventral forebrain, branchial arches, and foregut diverticulum. Forebrain expression is more widespread at this time, and expression also occurs throughout the trunk mesoderm. Expression of *neuronatin* at 8.5 and 9.5 dpc has also been described by Wijnholds et al. (1995), who detected expression in rhombomeres 3 and 5 of the hind-brain.

t8219b25

Before gastrulation, weak transcription of *t8219b25* occurs throughout the epiblast, and this widespread embryonic expres-

sion persists until the late head-fold stage (8.0 dpc). By 8.5 to 9.0 dpc, expression is detected in the diencephalon and midbrain, with weaker expression in the hindbrain and spinal cord. At 9.5 dpc, expression occurs in the roofplate and first branchial arch, with elevated expression detected in the hindbrain and anterior spinal cord.

w8609b57

At the onset of gastrulation, *Neuroblastoma* is strongly expressed in a single domain comprising the most proximal region of the egg cylinder and a proximo-distal stripe within the ectoplacental cone (arrow). This domain persists during head-fold stages, when the gene becomes weakly expressed throughout the VE and more strongly in the head-fold pocket, and notochord (7.5 dpc; arrow). At 8.5 dpc, expression is strong in notochord and ventral forebrain, with weak activation in the foregut diverticulum. By 9.5 dpc, epithelial expression extends from the ventral forebrain to the fourth branchial arch, with transcription also occurring in the otic vesicle.

t7822b19

At 6.5 dpc, *Peg3* expression occurs in the anterior VE (long arrow) and the primitive streak (short arrow). By 7.5 dpc, expression is widespread in embryonic mesoderm and allantois. Loss of function of *Peg3* causes growth retardation and an impairment of maternal behavior that frequently results in death of the offspring (Li et al. 1999).

k8709a24

At egg cylinder stages, *Sall1* is expressed in the anterior and, more weakly, in the posterior epiblast. At head-fold stages, transcripts become restricted to anterior neural folds, and at 8.5 dpc, this expression resolves into ventral neural plate and neural groove. Weak expression is also seen in the branchial arch region and posterior trunk. At 9.5 dpc, *Sall1* is expressed in the ventral forebrain, anterior midbrain, the midbrain/hindbrain boundary, branchial arch ectoderm, posterior trunk, and, most prominently, mesonephros and presomitic mesoderm and somites. *SALL1* is implicated in Townes-Brooks syndrome (Kohlhase et al. 1998), and loss of function of *Sall1* indicates that the gene is required for ureteric bud invasion during kidney development (Nishinakamura et al. 2001). Expression of *Sall1* at 7.5, 8.5, and 9.5 dpc has been reported by Buck and colleagues (2001).

r8220b09

Expression of *Silg41* occurs in the extra-embryonic ectoderm before and at the onset of gastrulation, at 6.0 to 6.5 dpc.

t8130b26

Rb-BP2 expression is restricted to the embryonic ectoderm from 6.0–7.5 dpc. By 7.75 dpc, transcripts are strongly detectable in the anterior definitive endoderm as well as in the chorion and allantois. By 8.5 dpc, expression is restricted to the forebrain.

m8708a39

At 6.5 dpc, *Lztr-1* is expressed in the epiblast and in extraembryonic ectoderm and/or endoderm adjacent to the ectoplacental cone (arrow). At 7.5 dpc, although expression is widespread in the embryonic region, it is stronger posteriorly and down-regulated in the node. At head-fold stages, *Lztr-1* expression is most prominent in the neural folds and nascent neural tube. At 9.5 dpc, expression is high in the forebrain, branchial arches, and limb buds.

s8129b58

At the onset of gastrulation, *Pancortin-1* and/or -3 is expressed at the junction between embryonic and extra-embryonic portions of the conceptus, with higher levels anteriorly. As gastrulation proceeds, expression occurs in the amnion and chorion and becomes widespread within the embryo proper. During somatogenesis (8.5 dpc), expression becomes restricted to rhombomere 4 (arrow), to the junction between the diencephalon and mesen-

cephalon, and to anterior and posterior portions of trunk mesenchyme. At 9.5 dpc, spotty expression is detectable in the midbrain in the earliest differentiating neurons. Expression also occurs in the olfactory placodes and in some cranial ganglia. Expression in the limb buds is initially widespread but becomes restricted to posterior regions as development proceeds. Expression of the closely related genes *Noelin 1* and *2* at 10.5 dpc has been described by Moreno and Bronner-Fraser (2002). The expression pattern they describe is similar, although not identical, to that described in this article at 9.5 dpc.

k8220b03

At 7.5 dpc, *Shrm* expression is detected throughout all embryonic tissues. Particularly strong expression occurs in the rostral region of presomitic mesoderm and later in the most posterior somites. Weaker expression is detected in the neural epithelium at 8.5 dpc. Somitic expression persists in older embryos, particularly in cells giving rise to ventral sclerotome. At 9.5 dpc, there is weak expression in the brain. Loss-of-function experiments indicate that Shroom, an actin-binding protein, is required for neural tube morphogenesis (Hildebrand and Soriano 1999).

r8220b57

Expression of *Tif-1* β is restricted to the advancing primitive streak at 7.5 dpc, and later at 9.0 dpc, it is strongest in the tailbud, presomitic mesoderm, nascent somites, branchial arches, and limb buds.

r8319a44

Expression of *14-3-3* σ is detected at the onset of gastrulation (6.5 dpc) and up to late streak stages (7.5 dpc) in the extra-embryonic ectoderm and ectoplacental cone. At the onset of gastrulation, transcripts are localized to the apical surface of cells (arrow). At somites stages (8.5, 9.5 dpc), expression occurs in surface ectoderm precursors along the distal edges of the neural folds and then, briefly, in a thin line above the neural tube. Expression is observed in branchial arches.

k8709a20

14-3-3 ϵ is ubiquitously expressed at 6.5 dpc but is then down-regulated such that by 7.5 dpc, transcripts are barely detectable. At 8.5 dpc, weak expression occurs in the forebrain and heart. At 9.5 dpc, forebrain expression is prominent, together with strong expression in the midbrain and branchial arches. These observations complement work by McConnell and colleagues (1995), which has analyzed expression of *14-3-3* ϵ from 8.5 dpc and found that expression is high in neural tissue by 12.5 dpc.

k8710a07

Nsa2p is expressed throughout the epiblast and extraembryonic ectoderm at 6.5 dpc. At 7.5 dpc, it continues to be expressed in all internal cell layers of the conceptus. By 8.5 and 9.5 dpc, expression is strongest in the branchial arches, neural tube, and, particularly, the forebrain. Low-level expression also occurs throughout the lateral mesoderm.

t8219b26

Expression of *Ubp7* is detected in the extra-embryonic ectoderm at the onset of gastrulation (6.5 dpc) and in the primitive streak and emerging mesoderm during gastrulation (7.5 dpc). At 7.75 and 9.5 dpc, widespread expression occurs in some mesodermal derivatives.

p8224a43

An example of a "widespread" cDNA. Expression is ubiquitous but occurs at different levels in different tissues.

t8130b25

An example of a "widespread" cDNA. Expression is ubiquitous but occurs at different levels in different tissues.

k831/b01

An example of a "ubiquitous" cDNA Expression is completely ubiquitous in both embryonic and extra-embryonic tissues.

REFERENCES

- Adams, M.D., Celniker, S.E., Holt, R.A., Evans, C.A., Gocayne, J.D., Amanatides, P.G., Scherer, S.E., Li, P.W., Hoskins, R.A., Galle, R.F., et al. 2000. The genome sequence of *Drosophila melanogaster*. *Science* **287**: 2185–2195.
- Anderson, K. and Beddington, R. 1997. Pattern formation and developmental mechanisms. *Curr. Opin. Genet. Dev.* **7**: 455–458.
- Aparicio, S., Chapman, J., Stupka, E., Putnam, N., Chia, J.M., Dehal, P., Christoffels, A., Rash, S., Hoon, S., Smit, A., et al. 2002. A radiation hybrid transcript map of the mouse genome. *Nat. Genet.* **29**: 194–200.
- Avner, P., Bruls, T., Poras, I., Eley, L., Gas, S., Ruiz, P., Wiles, M.V., Sousa-Nunes, R., Kettleborough, R., Rana, A. 2001. A radiation hybrid transcript map of the mouse genome. *Nat. Genet.* **29**: 194–200.
- Batt, J., Asa, S., Fladd, C., and Rotin, D. 2002. Pituitary, pancreatic and gut neuroendocrine defects in protein tyrosine phosphatase-sigma-deficient mice. *Mol. Endocrinol.* **16**: 155–169.
- Beddington, R.S.P. and Robertson, E.J. 1999. Axis development and early asymmetry in mammals. *Cell* **96**: 195–209.
- Bielinska, M., Narita, N., and Wilson, D.B. 1999. Distinct roles for visceral endoderm during embryonic mouse development. *Int. J. Dev. Biol.* **43**: 183–205.
- Buck, A., Kispert, A., and Kohlhase, J. 2001. Embryonic expression of the murine homologue of SALL1, the gene mutated in Townes-Brocks syndrome. *Mech. Dev.* **104**: 143–146.
- The *C. elegans* genome consortium. 1998. Genome sequence of the nematode *C. elegans*: A platform for investigating biology. The *C. elegans* Sequencing Consortium. *Science* **282**: 2012–2018.
- Carlton, J.M., Angiuoli, S.V., Suh, B.B., Kooij, T.W., Perlea, M., Silva, J.C., Ermolaeva, M.D., Allen, J.E., Selengut, J.D., Koo, H.L., et al. 2002. Genome sequence and comparative analysis of the model rodent malaria parasite *Plasmodium yoelii yoelii*. *Nature* **419**: 512–519.
- Christiansen, J.H., Coles, E.G., Robinson, V., Pasini, A., and Wilkinson, D.G. 2001. Screening from a subtracted embryonic chick hindbrain cDNA library: Identification of genes expressed during hindbrain, midbrain and cranial neural crest development. *Mech. Dev.* **102**: 119–133.
- Dehal, P., Satou, Y., Campbell, R.K., Chapman, J., Degnan, B., De Tomaso, A., Davidson, B., Di Gregorio, A., Gelpke, M., Goodstein, D.M., et al. 2002. The draft genome of *Ciona intestinalis*: Insights into chordate and vertebrate origins. *Science* **298**: 2157–2167.
- Doetschman, T., Gregg, R.G., Maeda, N., Hooper, M.L., Melton, D.W., Thompson, S., and Smithies, O. 1987. Targeted correction of a mutant HPRT gene in mouse embryonic stem cells. *Nature* **330**: 576–578.
- Dunwoodie, S.L. and Beddington, R.S.P. 2002. The expression of the imprinted gene *Ipl* is restricted to extra-embryonic tissues and embryonic lateral mesoderm during early mouse development. *Int. J. Dev. Biol.* **46**: 459–466.
- Dunwoodie, S.L., Henrique, D., Harrison, S.M., and Beddington, R.S.P. 1997. Mouse *Dil3*: A novel divergent Δ gene which may complement the function of other Δ homologues during early pattern formation in the mouse embryo. *Development* **124**: 3065–3076.
- Dunwoodie, S.L., Rodriguez, T.A., and Beddington, R.S.P. 1998. *Msg1* and *Mrg1*, founding members of a gene family, show distinct patterns of gene expression during mouse embryogenesis. *Mech. Dev.* **72**: 27–40.
- Dunwoodie, S.L., Clements, M., Sparrow, D.B., Sa, X., Conlon, R.A., and Beddington, R.S.P. 2002. Axial skeletal defects caused by mutation in the spondylocostal dysplasia/pudgy gene *Dil3* are associated with disruption of the segmentation clock within the presomitic mesoderm. *Development* **129**: 1795–1806.
- Elchebly, M., Wagner, J., Kennedy, T.E., Lancot, C., Michaliszyn, E., Itie, A., Drouin, J., and Tremblay, M.L. 1999. Neuroendocrine dysplasia in mice lacking protein tyrosine phosphatase sigma. *Nat. Genet.* **21**: 330–333.
- Fan, Q.W., Kadomatsu, K., Uchimura, K., and Muramatsu, T. 1998. Embigin/basigin subgroup of the immunoglobulin superfamily: Different modes of expression during mouse embryogenesis and correlated expression with carbohydrate antigenic markers. *Dev. Growth Diff.* **40**: 277–286.
- Fraser, A.G., Kamath, R.S., Zipperlen, P., Martinez-Campos, M., Sohmann, M., and Ahringer, J. 2000. Functional genomic analysis of *C. elegans* chromosome 1 by systematic RNA interference. *Nature* **408**: 325–330.
- Gardner, M.J., Hall, N., Fung, E., White, O., Berriman, M., Hyman, R.W., Carlton, J.M., Pain, A., Nelson, K.E., Bowman, S., et al. 2002. Genome sequence of the human malaria parasite *Plasmodium falciparum*. *Nature* **419**: 498–511.
- Gawantka, V., Pollet, N., Delius, H., Vingron, M., Pfister, R., Nitsch, R., Blumenstock, C., and Niehrs, C. 1998. Gene expression screening in *Xenopus* identifies molecular pathways, predicts gene function and provides a global view of embryonic patterning. *Mech. Dev.* **77**: 95–141.
- Gitton, Y., Dahmane, N., Baik, S., Ruiz i Altaba, A., Neidhardt, L., Scholze, M., Herrmann, B.G., Kahlem, P., Benkahl, A., Schrinner, S., et al. 2002. A gene expression map of human chromosome 21 orthologues in the mouse. *Nature* **420**: 586–590.
- Hamada, H., Meno, C., Watanabe, D., and Saijoh, Y. 2002. Establishment of vertebrate left-right asymmetry. *Nat. Rev. Genet.* **3**: 103–113.
- Hamburger, V. and Hamilton, H.L. 1951. A series of normal stages in the development of the chick embryo. *J. Morphol.* **88**: 49–92.
- Harrison, S.M., Dunwoodie, S.L., Arkell, R.M., Lehrach, H., and Beddington, R.S.P. 1995. Isolation of novel tissue-specific genes from cDNA libraries representing the individual tissue constituents of the gastrulating mouse embryo. *Development* **121**: 2479–2489.
- Harrison, S.M., Houzelstein, D., Dunwoodie, S.L., and Beddington, R.S.P. 2000. Sp5, a new member of the Sp1 family, is dynamically expressed during development and genetically interacts with Brachyury. *Dev. Biol.* **227**: 358–372.
- Hildebrand, J.D. and Soriano, P. 1999. Shroom, a PDZ domain-containing actin-binding protein, is required for neural tube morphogenesis in mice. *Cell* **99**: 485–497.
- Hogan, B., Beddington, R., Costantini, F., and Lacy, E. 1994. *Manipulating the mouse embryo: A laboratory manual*. Cold Spring Harbor Laboratory Press, Cold Spring Harbor, NY.
- Kamath, R.S., Fraser, A.G., Dong, Y., Poulin, G., Durbin, R., Gotta, M., Kanapin, A., Le Bot, N., Moreno, S., Sohrmann, M., et al. 2003. Systematic functional analysis of the *Caenorhabditis elegans* genome using RNAi. *Nature* **421**: 231–237.
- Kohlhase, J., Wischermann, A., Reichenbach, H., Froster, U., and Engel, W. 1998. Mutations in the SALL1 putative transcription factor gene cause Townes-Brocks syndrome. *Nat. Genet.* **18**: 81–83.
- Kudoh, T., Tsang, M., Hukriede, N.A., Chen, X., Dedekian, M., Clarke, C.J., Kiang, A., Schultz, S., Epstein, J.A., Toyama, R., et al. 2001. A gene expression screen in zebrafish embryogenesis. *Genome Res.* **11**: 1979–1987.
- Lander, E.S., Linton, L.M., Birren, B., Nusbaum, C., Zody, M.C., Baldwin, J., Devon, K., Dewar, K., Doyle, M., FitzHugh, W., et al. 2001. Initial sequencing and analysis of the human genome. *Nature* **409**: 860–921.
- Lee, E., Lein, E.S., and Firestone, G.L. 2001. Tissue-specific expression of the transcriptionally regulated serum and glucocorticoid-inducible protein kinase (Sgk) during mouse embryogenesis. *Mech. Dev.* **103**: 177–181.
- Li, L., Keverne, E.B., Aparicio, S.A., Ishino, F., Barton, S.C., and Surani, M.A. 1999. Regulation of maternal behavior and offspring growth by paternally expressed *Peg3*. *Science* **284**: 330–333.
- Lu, C.C., Brennan, J., and Robertson, E.J. 2001. From fertilization to gastrulation: Axis formation in the mouse embryo. *Curr. Opin. Genet. Dev.* **11**: 384–392.
- Martinez Barbera, J.P., Rodriguez, T.A., Greene, N.D., Weninger, W.J., Simeone, A., Copp, A.J., Beddington, R.S.P., and Dunwoodie, S. 2002. Folic acid prevents exencephaly in *Cited2* deficient mice. *Hum. Mol. Genet.* **11**: 283–293.
- McConnell, J.E., Armstrong, J.F., Hodges, P.E., and Bard, J.B. 1995. The mouse 14-3-3 epsilon isoform, a kinase regulator whose expression pattern is modulated in mesenchyme and neuronal differentiation. *Dev. Biol.* **169**: 218–228.
- Meier-Ewert, S., Maier, E., Ahmadi, A., Curtis, J., and Lehrach, H. 1993. An automated approach to generating expressed sequence catalogues. *Nature* **361**: 375–376.
- Moreno, T.A. and Bronner-Fraser, M. 2002. Neural expression of mouse *Noelin-1/2* and comparison with other vertebrates. *Mech. Dev.* **119**: 121.
- Neidhardt, L., Gasca, S., Wertz, K., Obermayr, F., Wopenberg, S., Lehrach, H., and Herrmann, B.G. 2000. Large-scale screen for genes controlling mammalian embryogenesis, using high-throughput gene expression analysis in mouse embryos. *Mech. Dev.* **98**: 77–94.
- Niehrs, C. and Pollet, N. 1999. Synexpression groups in eukaryotes. *Nature* **402**: 483–487.
- Nishinakamura, R., Matsumoto, Y., Nakao, K., Nakamura, K., Sato, A., Copeland, N.G., Gilbert, D.J., Jenkins, N.A., Scully, S., Lacey, D.L., et al. 2001. Murine homolog of SALL1 is essential for ureteric bud invasion in kidney development. *Development* **128**: 3105–3115.

- Reymond, A., Marigo, V., Yaylaoglu, M.B., Leoni, A., Ucla, C., Scamuffa, N., Caccioppoli, C., Dermitzakis, E.T., Lyle, R., Banfi, S., et al. 2002. Human chromosome 21 gene expression atlas in the mouse. *Nature* **420**: 582–586.
- Rosen, B. and Beddington, R.S.P. 1993. Whole-mount in situ hybridization in the mouse embryo: Gene expression in three dimensions. *Trends Genet.* **9**: 162–167.
- Shimono, A. and Behringer, R.R. 1999. Isolation of novel cDNAs by subtractions between the anterior mesoderm of single mouse gastrula stage embryos. *Dev. Biol.* **209**: 369–380.
- Snow, M.H.L. 1977. Gastrulation in the mouse: Growth and regionalization of the epiblast. *J. Embryol. Exp. Morph.* **42**: 293–303.
- Stanford, W.L., Cohn, J.B., and Cordes, S.P. 2001. Gene-trap mutagenesis: Past, present and beyond. *Nat. Rev. Genet.* **2**: 756–768.
- Thomas, K.R. and Capecchi, M.R. 1987. Site-directed mutagenesis by gene targeting in mouse embryo-derived stem cells. *Cell* **51**: 503–512.
- Venter, J.C., Adams, M.D., Myers, E.W., Li, P.W., Mural, R.J., Sutton, G.G., Smith, H.O., Yandell, M., Evans, C.A., Holt, R.A., et al. 2001. The sequence of the human genome. *Science* **291**: 1304–1351.
- Wallace, M.J., Batt, J., Fladd, C.A., Henderson, J.T., Skarnes, W., and Rotin, D. 1999. Neuronal defects and posterior pituitary hypoplasia in mice lacking the receptor tyrosine phosphatase PTP σ . *Nat. Genet.* **21**: 334–338.
- Waterston, R.H., Lindblad-Toh, K., Birney, E., Rogers, J., Abril, J.F., Agarwal, P., Agarwala, R., Ainscough, R., Alexandersson, M., An, P., et al. 2002. Initial sequencing and comparative analysis of the mouse genome. *Nature* **420**: 520–562.
- Wijnholds, J., Chowdhury, K., Wehr, R., and Gruss, P. 1995. Segment-specific expression of the neuronatin gene during early hindbrain development. *Dev. Biol.* **171**: 73–84.
- Wilkinson, D.G. 1992. Whole mount in situ hybridisation of vertebrate embryos. In *In situ hybridisation*, pp. 75–83. IRL Press, Oxford, UK.
- Wulff, P., Vallon, V., Huang, D.Y., Volkl, H., Yu, F., Richter, K., Jansen, M., Schlunz, M., Klingel, K., Loffing, J., et al. 2002. Impaired renal Na⁺ retention in the sgk1-knockout mouse. *J. Clin. Invest.* **110**: 1263–1268.

WEB SITE REFERENCES

- <http://www.tigr.org/tdb/tgi/mgi/>; TIGR Tentative Consensus sequences, version 8.0.
- http://www.ensembl.org/Mus_musculus/; predicted mouse transcripts in ENSEMBL.
- http://www.hgmp.mrc.ac.uk/geneservice/reagents/products/cdna_resources/index.shtml; the UK Human Genome Mapping Project Resource Centre.
- <http://www.phrap.org/phrap.docs/phred.html>; PHRED.
- <ftp://ftp.ncbi.nih.gov/blast/executables/>; BLASTN and BLASTP.
- <http://www.tigr.org/tdb/tgi/mgi/>; TIGR Gene Index.

Received March 24, 2003; accepted in revised form September 18, 2003.